JOHANNES GUTENBERG UNIVERSITÄT MAINZ

Max-Planck-Institut für Polymerforschung

Max Planck Institute for Polymer Research

Living Anionic Polymerization of Activated Aziridines

Dissertation

zur Erlangung des akademischen Grades eines

“Doctor rerum naturalium (Dr. rer. nat.)“

des Fachbereiches Chemie, Pharmazie und Geowissenschaften (FB 09)

der Johannes Gutenberg-Universität Mainz

vorgelegt von

Dipl.-Chem. Elisabeth Rieger

geboren in Rosenheim

Mainz, Februar 2018

Die vorliegende Arbeit wurde im Zeitraum von Dezember 2014 bis Februar 2018 am Max-Planck-Institut für Polymerforschung im Arbeitskreis von Prof. Dr. Katharina Landfester unter der Betreuung von Priv.-Doz. Dr. habil. Frederik Wurm angefertigt.

1. Gutachter: Priv.-Doz. Dr. habil. Frederik Wurm

2. Gutachter: Prof. Dr. Pol Besenius

Erklärung

Hiermit versichere ich, die vorliegende Arbeit selbstständig und ohne Benutzung anderer als der angegebenen Hilfsmittel angefertigt zu haben. Alle Stellen, die wörtlich oder sinngemäß aus Veröffentlichungen oder anderen Quellen entnommen sind, wurden als solche eindeutig kenntlich gemacht. Diese Arbeit ist in gleicher oder ähnlicher Form noch nicht veröffentlicht und auch keiner anderen Prüfungsbehörde vorgelegt worden.

Elisabeth Rieger

Mainz, Februar 2018

Für meine Familie

”Nothing has really happened until it has been recorded”

Virginia Woolf

Danksagung

Mein besonderer Dank gilt PD Dr. habil. Frederik Wurm für die Möglichkeit, in seiner Arbeitsgruppe das Thema der erfolgreichen Diplomarbeit als Dissertation unter seiner Betreuung fortsetzen zu können. Dank zahlreicher offener und ehrlicher Diskussionen, für die er jederzeit verfügbar war, konnten viele Projekte innerhalb dieser Arbeit mit großem Erfolg ausgeführt werden.

Bei Prof. Dr. Katharina Landfester bedanke ich mich für die Mitbetreuung meiner Doktorarbeit und besonders für die Möglichkeit, diese in ihrem Arbeitskreis durchzuführen. Neben den wissenschaftlichen Diskussionen danke ich beiden auch für die persönliche Förderung, die es mir ermöglichte, Konferenzen und Seminare zu besuchen, die mich wissenschaftlich, aber auch persönlich weitergebracht haben.

Den perfekten Arbeitspartner und einen guten Freund habe ich in Tassilo Gleede gefunden. Neben stundenlangen und sehr produktiven Diskussionen war das gemeinsame Arbeiten im Labor ein Traum, weil alles problemlos Hand in Hand ging. Seine uneingeschränkte und selbstlose Hilfsbereitschaft, wie man sie selten findet, hat bleibenden Eindruck bei mir hinterlassen. Ich danke ihm für seinen großen Anteil am Fortschritt der Forschung und auch für die Sicherheit und Unterstützung, die er mir gegeben hat.

Große Geduld und viel Durchhaltevermögen hat Angelika Manhart bewiesen, die großen Anteil an meinem zügigen Fortschritt hatte, indem sie mir mit ihrer großen synthetischen Erfahrung viel Arbeit abgenommen hat, wofür ich zutiefst dankbar bin und meine besondere Wertschätzung ausdrücken möchte.

Besonders bedanken möchte ich mich bei Dr. Manfred Wagner und Stefan Spang, die immer bereit waren, mir für die vielen, teils auch nervenaufreibenden NMR-Kinetiken, das Gerät und ihre Zeit zur Verfügung zu stellen. Vielen Dank für die vielen Stunden am NMR, die mir immer wie eine kleine, entschleunigte Auszeit vorkamen.

Dr. Anke Kaltbeitzel bin ich dankbar, dass sie unermüdlichen Ehrgeiz bei der Erstellung schöner cLSM-Aufnahmen gezeigt hat. Ebenso möchte ich Beate Müller danken, dass sie so viel Geduld in langwierige HPLC-Messungen gesteckt hat, die zu tollen Resultaten geführt haben.

Für eine wunderbare, sich perfekt ergänzende Zusammenarbeit für das erfolgreiche Droplet-Paper, möchte ich mich bei Jan Blankenburg und Eduard Grune bedanken.

Vielen Dank auch an Katja Weber für ihre große synthetische Hilfe im Labor. Ihr, Joachim Pfuhl und Dennis Unthan möchte ich für die Zusammenarbeit im Rahmen ihrer Bachelorarbeiten und bei Tatjana Homann-Müller im Rahmen ihrer Masterarbeit danken.

Für die synthetische Unterstützung im Labor bedanke ich mich herzlich bei Sabrina Brand, Maximilian Lorenian, Nina Bürkle und Tizian Passow.

Stefan Schuhmacher danke ich ebenfalls für seine akribische Geduld, mit der er wunderschöne Blender-Bilder erstellt, sowie für die Unterstützung bei meinen eigenen Bildern.

Dr. Laura Thomi danke ich für die Einarbeitung in die anionische Polymerisation und den damit verbundenen Diskussionen. Mein Dank gilt ebenso Dr. Arda Alkan, Dr. Daniel Leibig und Dr. Adrian Natalello für die Einweisung in die NMR-Kinetiken.

Für die vielen GPC-Messungen bedanke ich mich bei Sandra Seywald, Ute Heinz, Christine Rosenauer, Monika Schmelzer und Regina Holm. Des Weiteren danke ich Petra Räder für die DSC- und TGA-Messungen, Elke Muth für die Oberflächenspannungs- und die IR-Messungen. Bei Dr. Elene Berger-Nicoletti, Camille Bakkali-Hassani und ganz besonders Markus Lamla möchte ich mich für die vielen gemessenen MALDI-TOF-Spektren bedanken.

Für gelungene und sehr ergiebige Kooperationen bedanke ich mich bei Camille Bakkali-Hassani, Dr. Joan Vignolle, Prof. Dr. Stéphane Carlotti, Prof. Dr. Daniel Taton (Bordeaux), sowie bei Dr. Lei Liu, Dr. Denis Andrienko (MPI-P) und bei Louis Chip Reisman, Pierre Canisius Mbarushimana, Prof. Paul A. Rupar (Alabama, USA). Ebenso bedanke ich mich bei Barbara Riehl und Prof. Dr. Siegfried R. Waldvogel für die elektrochemischen Experimente.

Für zukunftsweisende Unterstützung bedanke ich mich herzlich bei meinem Mentor Dr. Gunter Scharfenberger.

Ein besonderer Dank geht an die Freunde/Kollegen, Benny Zwietasch und die Band of 5, die mir geholfen haben das Lady Nano-Video so professionell zu gestalten und mit denen ich viel Spaß dabei hatte. Der Videodreh und die Live-Auftritte werden zu den außergewöhnlichsten und unvergesslichsten Erlebnissen meiner Zeit am MPI-P gehören.

Mein großer Dank geht an meine Freunde, die ich am MPI fürs Leben gewonnen habe, meine (auch ehemaligen) Labor- und Bürokollegen, sowie den Mitgliedern der Arbeitsgruppe, die eine tolle Arbeitsatmosphäre geschaffen haben und mit denen ich viele schöne Stunden erleben durfte. Dank meiner Freunde (auch außerhalb des MPIs), konnte ich mein Leben auch fern der Arbeit genießen. Ihnen allen danke ich für schöne Erinnerungen, ihre große Unterstützung und ein immer offenes Ohr.

Mein größter Dank gilt meinen Eltern, die mich immer in jeglicher Hinsicht, auch in den schwierigsten Phasen unterstützt haben und auf die ich immer vertrauen konnte. Am meisten Kraft konnte ich dank Diego schöpfen, der mir unerschütterlich und bedingungslos in jeder Situation zur Seite stand, viel Verständnis gezeigt hat und dem ich es verdanke, bis heute durchhalten zu können.

Table of Contents

Motivation and Objectives

Aziridine is a three-membered ring consisting of one nitrogen and two carbon atoms. It has been labeled as the "ugly cousin" of the epoxide, its oxygen-containing counterpart. Aziridines have been long under the shadow of epoxides, especially regarding their ability to undergo anionic ring-opening polymerization (AROP). The polymeric product of epoxides, polyethylene glycol (PEG), is an important part of our daily life. PEG derivatives are extensively employed in food, medicine and cosmetic products. The nitrogen-analog of PEG, hyperbranched or linear polyethylene imine (*hb*- or LPEI), is widely used for water waste treatment, paper industry and as a non-viral gene transfection agent.

To date, PEI can be prepared exclusively *via* cationic polymerization. In contrast to the cationic mechanism, the so-called "living" anionic polymerization (LAP), also used to produce PEG, is the polymerization technique with the highest control over the polymer architecture, end-group fidelity and narrow molecular weight distributions. This thesis will present strategies to establish and to control the LAP for aziridines.

In contrast to the well-known carb- and oxyanionic polymerization techniques, azaanionic polymerization had been discovered in 2005 and was revisited by our group. The development of azaanionic ring-opening polymerization was possible using a sulfonamide group (acting as activating group) at the nitrogen. The so-called polyaziridines (PAz), to emphasize their origin from aziridines, give access to a novel variety of polyamines, with new interesting properties and a range of potential applications.

The objective of this thesis is therefore the establishment of azaanionic polymerization along with the traditional oxy- and carbanionic counterparts. By extensive investigation of the characteristics of azaanionic polymerization, we aim to create a new polymer class, with novel functionalities and properties

To demonstrate the potential of azaanionic polymerization, the available monomer family was expanded within this work. Most of the monomers are produced *via* convenient and efficient one- to three-step synthesis protocols. The monomer family also includes new functionalities as acetal-protected aziridines, to obtain polyhydroxypolyamines ("polyamino-polyols") in a facile fashion.

The establishment of a new polymerization technique requires the understanding of the involved mechanism. Therefore, different azaanionic polymerizations were monitored by *in situ* ^{1}H NMR spectroscopy. With this analytical tool the polymerization kinetics towards polyaziridines were studied. To understand and categorize this polymerization technique, different reaction conditions were investigated. For example, the performance of typical solvents for anionic polymerization and the influence of counter ions was of special interest. Our findings allowed us

to make a parallel with the well-known carb- and oxyanionic polymerization, remarking the advantages of the azaanionic system over the other techniques.

As the nucleophilicity is the crucial factor for anionic polymerization, the usual limits of anionic polymerization (especially protic impurities) were tested. Anionic polymerization is an experimentally demanding technique, since it has to be performed under dry and inert conditions. Hence, an anionic technique showing tolerance against protic impurities is of high interest for further industrial applications. Carbanionic polymerization with the strongest nucleophilic character is directly terminated in the presence of minuscule amounts of protic impurities, whereas oxyanionic polymerization can still proceed, when tiny amounts are present, due to the very fast proton exchange or additional initiation. For azaanionic polymerization, the effect of protic impurities like water and different alcohols was studied. Impurities were added to the polymerization mixture without seriously affecting its living character, even at two orders of magnitude higher than the amount of initiator. Besides kinetic investigations, DFT-calculations demonstrated the influence comparing the nucleophilicities of the azaanion at the growing chain end next to the alkoxides, generated from the added solvents, and the pK_a-values thereof. This represents another advantage of the novel azaanionic polymerization over the traditional techniques.

A major challenge in current research is to establish methods for sequence-control in macromolecules. Therefore, we focused on the investigation of copolymerizations, namely the order of incorporation of monomers. As the variety of different activating groups exhibits different reactivities, the simultaneous copolymerization of up to five monomers was monitored using real-time NMR spectroscopy as well. As this was achieved in a closed-system one-pot reaction, the different reactivities offer a higher freedom of sequence control, which is not possible by other polymerization methods. The scope of adjustable monomer incorporation was further expanded to physically separated monomer components. The different solubility profile of constituting monomers was thus used as an external handle to tune their copolymerization behavior on demand. The concept of compartmentalization within a closed-system was tested on a monomer pair, which undergoes an ideal random copolymerization in solution and was forced to produce gradient to even block-like structures in emulsion.

Primarily, polyaziridines can be regarded as PEI-analogues for similar applications. This is especially important in the field of gene transfection, where the need of a better alternative to LPEI is still latent. As already mentioned, the standard LPEI is produced *via* cationic polymerization of oxazolines, albeit lacking a controlled and modular synthetic approach that could even broaden their application or increase their efficiency. It is noticeable that the vast majority of PEI derivatives are obtained by modifying commercially available PEI. Conversely, more functionalities are easily introduced in the azaanionic polymerization, a feature that might

help to overcome the toxicity of LPEI without compromising its efficiency. Thus, the pathway *via* the AROP to obtain polyaziridines and subsequent desulfonylation offers a promising alternative. Consequently, investigations on the removal of the activating group was the necessary step into this direction. In classic organic synthesis, the tosyl group is widely used as a protection group and several removal strategies are reported in literature. Polymeric structures are not as easily transformed as low-molecular sulfonamides, thus several desulfonylation methods were examined for PAz until satisfying conversions were obtained. Nevertheless, the demands on polymers in terms of uniformity and purity are extraordinary for any kind of biomedical application. Hence, the azaanionic polymerization has the capability to stand out due to its unique characteristics.

Abstract

More than sixty years have passed after the discovery of living anionic polymerization (LAP). However, to date it is still the polymerization technique to access well-defined polymers. Carbanionic and oxyanionic LAP techniques have been extensively studied and are essential for industrial polymer production; they are used on a multi ton scale to manufacture various daily-life products.

In strong contrast, the azaanionic polymerization of aziridines was first discovered in 2005 and by then forgotten. Our group retrieved this strategy in 2013 with this thesis as the first complete PhD thesis solely focusing on anionic polymerization of aziridines. A unique type of polyamines / polyamides with a wider range of functionalities is obtained, the so-called polyaziridines, opening the possibility to novel exciting applications by a new building block for complex macromolecular architectures.

N-Sulfonamide groups activate the aziridine for nucleophilic attack. These activating groups also replace the acidic *N*-proton, whereby the polymerization can proceed *via* living anionic mechanism efficiently. The growing aziridine monomer family includes several functionalities and the monomers are mostly produced by efficient one- to three-step synthetic procedures.

The polymerization kinetics for homo- and copolymerizations were studied by *in situ* ^{1}H NMR spectroscopy. This methodology allows the real-time monitoring of the incorporation of monomer units into the growing polymer chains. Several solvents, counter ions and initiators were studied to reveal DMF and DMSO as the most suitable solvents. In contrast to oxyanionic, where lithium inhibits any chain growth, all counter ions, originated from alkali salts, were found to be appropriate. Different initiators, including a bifunctional one and the commercially available butyllithium were successfully tested.

The novel azaanionic polymerization exhibited narrow monomodal molecular weight distributions in all cases and was proven to be living for several reaction conditions. Furthermore, it shows an enormous tolerance against protic impurities, like water and alcohols. Concentrations of these solvents, which would inhibit the other living anionic polymerizations immediately, were found to have almost no influence on the azaanionic polymerization. The secondary initiation by these impurities was below 10% in most cases, which is within the same range for controlled radical polymerization techniques. The nucleophilicity of the anions (chain ends and alkoxides) in reversed interaction with their pK_a-values are considered as the main influencing factors, evaluated by DFT-calculations. These unique characteristics make the azaanionic polymerization highly promising for industrial applications due to its simpler handling and excellent control.

The great variety of the different monomers has a big impact on a special feature of azaanionic polymerization, not achievable in other anionic polymerization to the same extent: sequence

control in one-pot reactions. As the activating groups exhibit different electron withdrawing effects, they dominate the monomer reactivity. The ring-substituents, in turn, only show a negligible impact on the reaction kinetics, due to steric hindrance. The stronger the electron withdrawing effect of the activating group, the faster it reacts, which is reflected in the determined electrophilicity indices. This offers new possibilities to tune the final microstructure of copolymers, as tailored random, gradient and block copolymers are afforded in a closed system one-pot reaction, without further monomer addition. These copolymerizations were also monitored using real-time NMR-spectroscopy, allowing the simultaneous copolymerization of up to five monomers for the first time. This allows the precise installation of functional groups along the polymer backbone (sequence control), just by the selection of different starting monomers with respective reactivities.

Next to the intrinsic reactivity of the monomers, also their physical properties, such as their different solubility profiles, offers another strategy to alter the copolymerization behavior. A monomer pair with identical activating groups but ring-substituents of different hydrophobicity exhibit the same chemical reactivity and lead to an ideal random copolymer in solution. However, these two monomers can be physically separated in an emulsion system, where the hydrophobic monomer prefers the continuous cyclohexane phase over the dispersed DMSO-phase, which contains mainly the hydrophilic monomer. As the copolymerization is exclusively constricted to the DMSO-phase (compartments), the random monomer pair is forced to produce gradient to block-like structures, just by simple separation and respective dilution of the continuous phase, which adjusts the strength of the gradient.

As the application of polyaziridines themselves is still in its very early stages, their manifest value lies in the use of their desulfonylated version as polyamines. Among this class of polymers, mainly linear polyethyleneimine (LPEI) stands out as the gold standard for non-viral gene delivery. LPEI is to date the most efficient transfection agent, but it is also very toxic. Consequently, the research on alternatives continues and polyaziridines represent a potential new option. Polyoxazolines (produced via cationic polymerization) are the usual precursor to obtain LPEI. Nevertheless, the use of polyaziridines as LPEI precursors is particularly advantageous because of their better polymerization control. Moreover, the deprotection methods currently used for polyoxazolines suffer of low efficacy. Therefore, two deprotection strategies for the desulfonylation of polyaziridines are presented within this work, to reveal new alternatives for LPEI and its applications as a polyelectrolyte.

In summary, this is the first thesis focusing solely on the living anionic polymerization of aziridines, which proves them as powerful building blocks for future macromolecular architectures. Tuning functional group density along a polyamide/polyamine backbone provides a wide range of new materials with manifold functionalities and properties.

Zusammenfassung

Mehr als sechzig Jahre sind seit Entdeckung der lebenden anionischen Polymerisation (LAP) vergangen. Bis heute gilt diese als die beste Polymerisationstechnik für die Herstellung hoch definierter Polymere. Carbanionische und oxyanionische LAPs-Techniken wurden bereits ausgiebig untersucht und sind essentiell für die industrielle Polymerproduktion; sie werden für verschiedenste Produkte des täglichen Lebens im Tonnenmaßstab umgesetzt.

Im Gegensatz dazu wurde die azaanionische Polymerisation von Aziridinen erst 2005 entdeckt, wurde jedoch zunächst nicht weiter erforscht. Mit der vorliegenden Arbeit, als erster vollständiger Doktorarbeit, die sich ausschließlich auf die anionische Polymerisation von Aziridinen konzentriert, hat unsere Gruppe diese Forschung im Jahr 2013 wieder aufgegriffen. Diese sogenannten Polyaziridine ermöglichen den Zugang zu neuartigen Polyamin- / Polyamid-Strukturen, mit einem breiten Spektrum an neuen, hochinteressanten Anwendungen dank neuer Bausteine für komplexe makromolekulare Architekturen.

N-Sulfonamidgruppen aktivieren den Aziridinring für einen nukleophilen Angriff. Diese aktivierenden Gruppen ersetzen auch das acide *N*-Proton, wodurch die lebende anionische Polymerisation der Aziridine erst ermöglicht wird. Seit 2013 hat unsere Gruppe sich mit der Synthese neuer Monomere für die anionische Polymerisation beschäftigt um verschiedene Funktionalitäten in die Polyaziridine einzubauen.

Die zugrunde liegenden Kinetiken für Homo- und Copolymerisationen wurden mittels *in situ* ^{1}H-NMR-Spektroskopie untersucht. Diese Methode ermöglicht die Echtzeit-Überwachung des Einbaus von Monomereinheiten in die wachsende Polymerkette. Mehrere Lösungsmittel, Gegenionen und Initiatoren wurden hinsichtlich deren Einfluss auf die Polymerisation untersucht, mit dem Ergebnis, dass es sich bei DMF und DMSO um die am besten geeigneten Lösungsmittel handelt. Im Gegensatz zur Oxyanionik, bei der Lithium jegliches Kettenwachstum hemmt, erlaubt die Azaanionik alle Gegenionen aus ersten Hauptgruppe. Verschiedene Initiatoren, einschließlich eines bifunktionellen und des kommerziell erhältlichen Butyllithiums, wurden ebenfalls erfolgreich getestet.

Üblicherweise ermöglicht die azaanionische Polymerisation in allen Fällen enge, monomodale Molekulargewichtsverteilungen. Ihr lebender Charakter konnte für eine Vielzahl an Reaktionsbedingungen nachgewiesen werden. Zudem zeigt sie eine außergewöhnliche Toleranz gegenüber protischen Verunreinigungen wie Wasser und Alkohole. Konzentrationen dieser Lösungsmittel, die die anderen lebenden anionischen Polymerisationen sofort inhibieren würden, haben einen geringen Einfluss auf die azaanionische Polymerisation. Die sekundäre Initiierung durch diese Verunreinigungen lag in den meisten Fällen unter 10%, dies ist vergleichbar mit radikalischen Polymerisationstechniken. Als entscheidende Faktoren werden die Nucleophilie der

Anionen (Kettenenden und Alkoxide) im Zusammenspiel mit ihren gegenläufigen pK_s-Werten angesehen, die durch DFT-Berechnungen ermittelt wurden. Diese einzigartigen Charakteristika machen die azaanionische Polymerisation aufgrund ihrer einfacheren Handhabung und ausgezeichneten Kontrolle sehr attraktiv für industrielle Anwendungen.

Die große Vielfalt an unterschiedlichen Monomere ist verantwortlich für eine weitere Besonderheit der azaanionischen Polymerisation, die bei anderer anionischer Polymerisation nicht in gleichem Maße erreichbar ist: Sequenzkontrolle in Eintopfreaktionen. Die aktivierenden Gruppen, die unterschiedliche elektronenziehende Effekte aufweisen, dominieren die Monomerreaktivitäten. Die Ring-Substituenten wiederum besitzen weder elektronenziehende noch -schiebende Effekte; ihr sterischer Einfluss ist für die Reaktionskinetik vernachlässigbar. Je stärker die elektronenziehende Wirkung der aktivierenden Gruppe ist, desto schneller polymerisiert das Momoner, was sich in den ermittelten Elektrophilie-Indizes widerspiegelt. Dies eröffnet neue Optionen, um die Mikrostruktur von Copolymeren einzustellen, da maßgeschneiderte Statistische, Gradienten- und Blockcopolymere in einer geschlossenen Eintopfreaktion ohne weitere Monomerzugabe realisierbar sind. Diese Copolymerisationen wurden ebenfalls mittels Echtzeit-NMR-Spektroskopie verfolgt, so dass erstmals bis zu fünf Monomere gleichzeitig copolymerisiert werden konnten. Dies ermöglicht die präzise Verteilung von funktionellen Gruppen entlang des Polymerrückgrats (Sequenzkontrolle), allein durch die Auswahl verschiedener Ausgangsmonomere mit entsprechenden Reaktivitäten.

Neben der intrinsischen Reaktivität der Monomere bieten auch ihre physikalischen Eigenschaften, wie ihre unterschiedlichen Löslichkeitsprofile, eine weitere Strategie, um das Copolymerisationsverhalten zu verändern. Ein Monomerpaar mit identischen Aktivierungsgruppen, aber Ringsubstituenten unterschiedlicher Hydrophobie zeigt die gleiche chemische Reaktivität, was in Lösung zu einem idealen statistischen Copolymer führt. Diese zwei Monomere können jedoch in einem Emulsionssystem physikalisch voneinander getrennt werden, wobei das hydrophobe Monomer die kontinuierliche Cyclohexan-phase gegenüber der dispergierten DMSO-Phase bevorzugt, die wiederum hauptsächlich das hydrophile Monomer enthält. Da die Copolymerisation ausschließlich auf die DMSO-Phase (Kompartimente) beschränkt ist, werden Gradienten- bis zu blockartigen Strukturen erhalten, welche durch entsprechende Verdünnung der kontinuierlichen Phase einstellbar sind.

Da sich die Anwendung von Polyaziridinen selbst noch im Anfangsstadium befindet, liegt ihr offenkundiger Wert in der Verwendung ihrer desulfonylierten Version als Polyamine. Innerhalb dieser Polymerklasse zeichnet sich vor allem lineares Polyethylenimin (LPEI) als Goldstandard für die nicht-virale Transfektion von Fremdgenen aus. LPEI ist bis heute das wirksamste Transfektionsmittel, zeichnet sich aber auch durch seine hohe Toxizität aus. Folglich dauert die Forschung für andere Optionen an und Polyaziridine stellen eine potentielle Alternative dar.

Polyoxazoline (hergestellt durch kationische Polymerisation) sind die üblichen Vorstufen, um LPEI zu erhalten. Die Verwendung von Polyaziridinen als LPEI-Vorstufen erscheint wegen der höheren Polymerisationskontrolle besonders vorteilhaft. Zudem mangelt es den derzeit für Polyoxazoline verwendeten Entschützungsmethoden noch an ausreichender Effizienz. Daher werden im Rahmen dieser Arbeit zwei Entschützungsstrategien für die Desulfonylierung von Polyaziridinen vorgestellt, um neue Alternativen für LPEI und seine Anwendungen als Polyelektrolyt aufzuzeigen.

Zusammenfassend ist dies die erste Arbeit, die sich ausschließlich auf die lebende anionische Polymerisation von Aziridinen fokussiert und ihr Potential als leistungsfähige Bausteine für zukünftige makromolekulare Architekturen darstellt. Die exakte Einstellbarkeit der Abfolge/des Anteils funktioneller Gruppen entlang eines Polyamid- / Polyamin-Rückgrats bietet eine breite Palette neuartiger Materialien mit vielseitigen Funktionalitäten und Eigenschaften.

Graphical Abstract

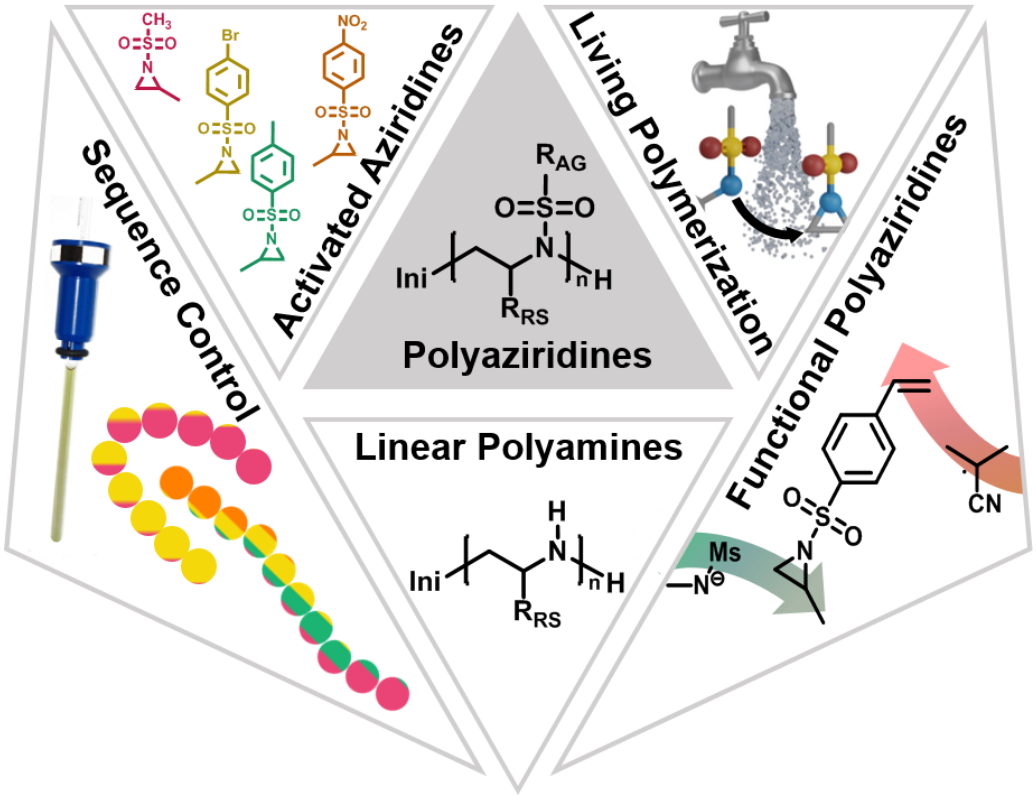

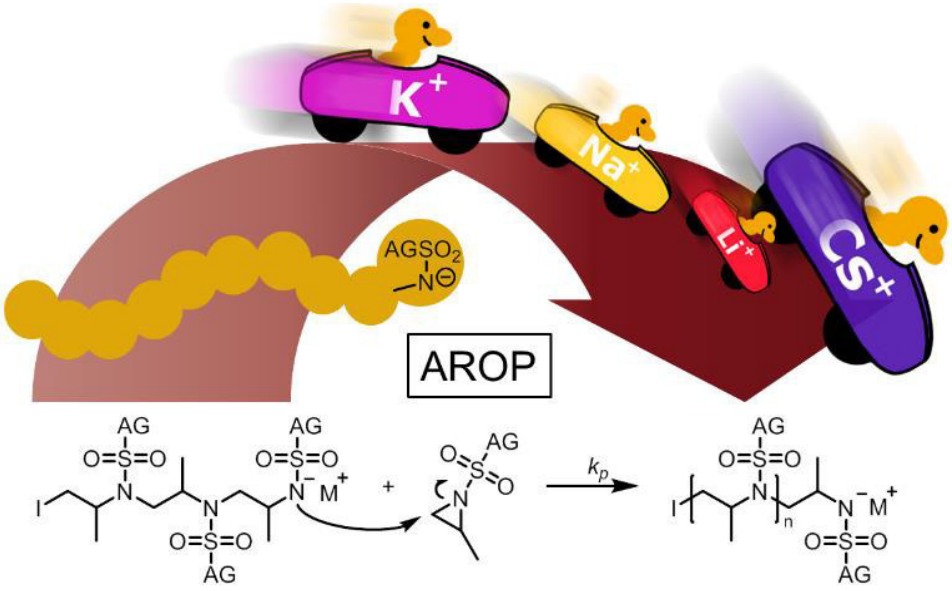

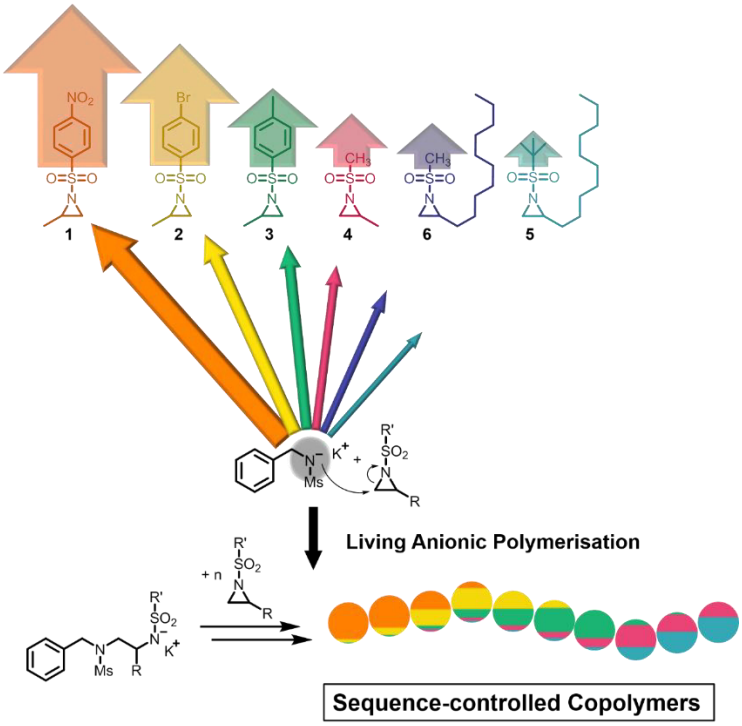

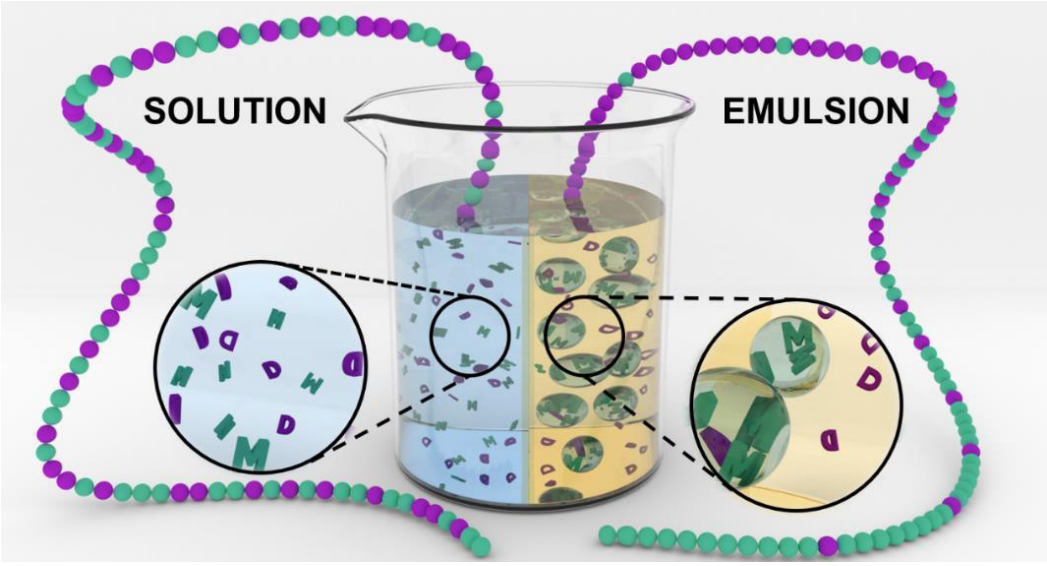

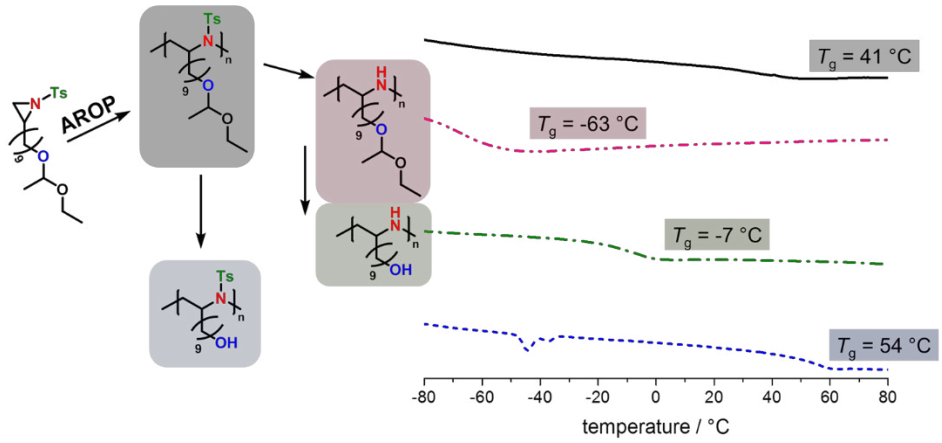

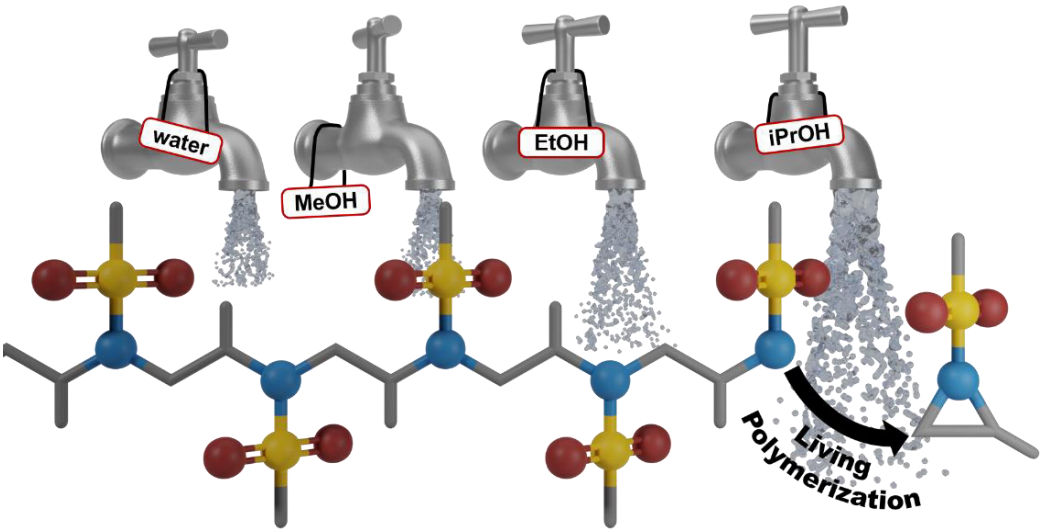

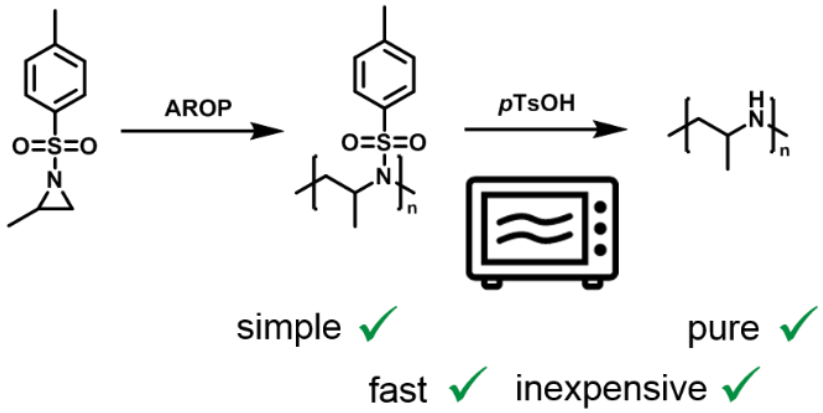

1. Introduction

Elisabeth Rieger,[1] Tassilo Gleede,[1] Canisius P. Mbarushimana,[2] Louis Reisman,[2] Paul A. Rupar,[2] Frederik R. Wurm[1]

[1]*Max Planck Institute for Polymer Research, Ackermannweg 10, 55128 Mainz, Germany*
[2]*Department of Chemistry, The University of Alabama, Tuscaloosa, Alabama, 35487-0336, United States of America*

The introduction is part of an unpublished review.

Tassilo Gleede wrote the Chapters Monomers and OROP and Canisius P. Mbarushimana wrote the Chapter about Applications of PEI.

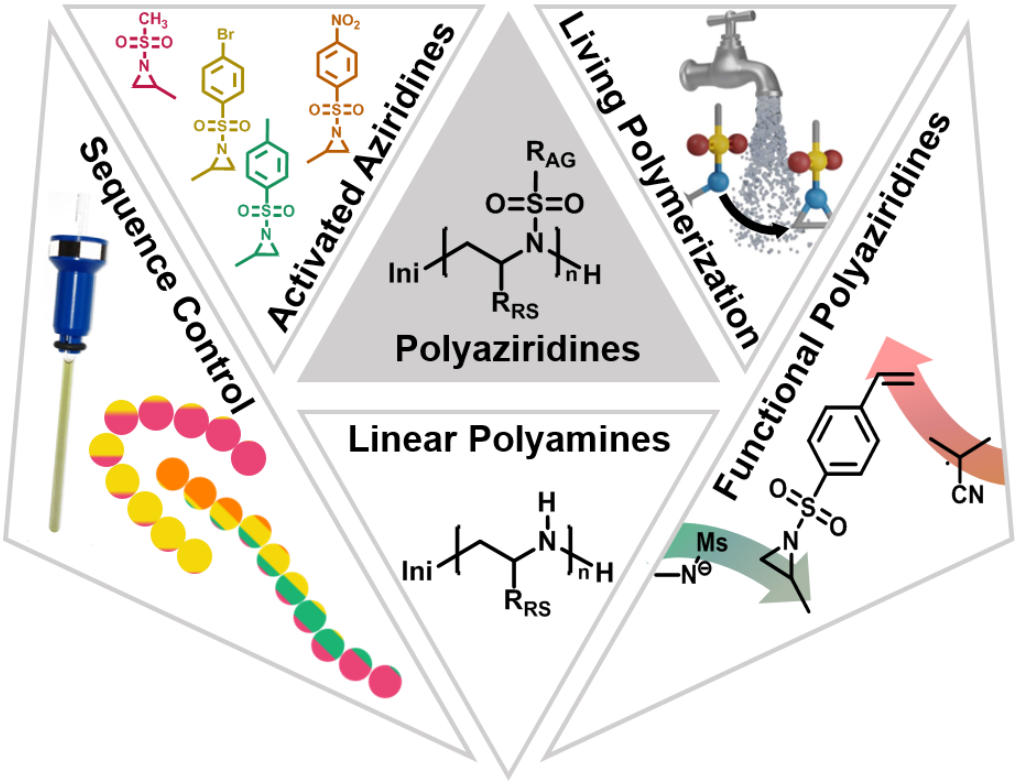

1.1 Living Anionic Polymerization

Living anionic polymerization (LAP) is, even 60 years after its discovery,[1] still the polymerization technique with the best control over molecular weight and dispersity.[2-4] Its establishment as a standard polymerization technique greatly affected modern polymer science. Many different monomer classes were thus developed for anionic polymerization, such as classic vinyl-monomers for carbanionic polymerization and heterocyclic monomers for anionic ring-opening polymerization (AROP) (see Scheme 1.1).[5] These materials are indispensable to industry, e.g. like well-known poly(ethylene glycol) (PEG) and derivatives (like Pluronics®), are commodities in bio-related applications (in medicine, food, cosmetics) or as surfactants.[6-8]

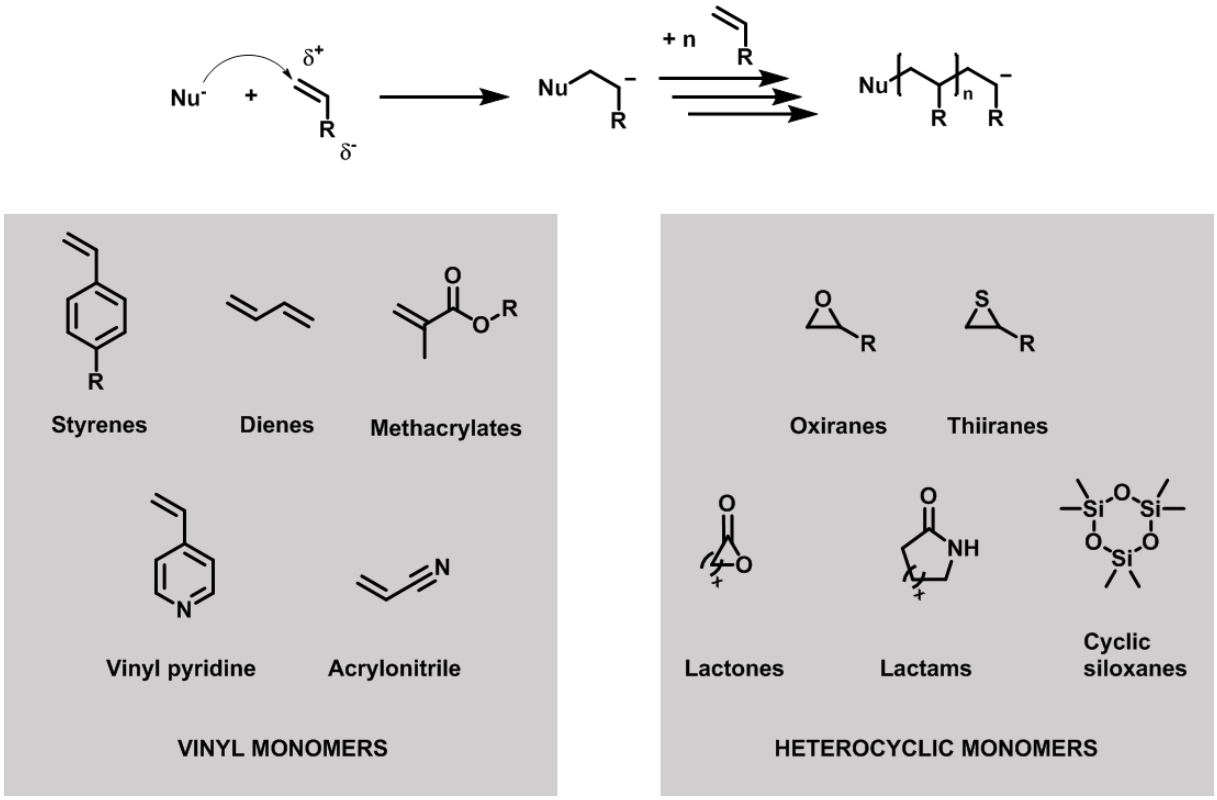

Scheme 1.1. Mechanism of living anionic polymerization. Selection of vinyl monomers for carbanionic polymerization on the left and heterocyclic monomers for anionic ring-opening polymerization on the right.

As a prerequisite for anionic polymerization, potential monomers must not bear any acidic protons, and need substituents able to stabilize the emerging anion by electron delocalization (mainly electron withdrawing (EWD) groups). Anionic polymerization can be a living polymerization, as long as no termination occurs and no protic impurities are present. Therefore, the negatively charged chain end remains active after addition of new monomers, continuing with the propagation (Scheme 1.1). In contrast to radical polymerization techniques, no termination

via recombination is possible and chain transfer is suppressed in LAP. Since anionic polymerization is based on a nucleophilic mechanism, only electrophilic substances – including water– can terminate the polymerization (for carbanions) or act as transfer agents (for oxyanions).[9] This makes LAP experimentally demanding, as it is highly important to work under inert conditions and with carefully dried solvents.[10-11] Suitable solvents for anionic polymerization are either polar solvents such as tetrahydrofuran (THF), *N,N*-dimethylformamide (DMF) and dimethylsulfoxide (DMSO), or nonpolar aliphatic or aromatic hydrocarbons. When the initiation step is faster than the propagation step, all chains start to grow simultaneously and yield highly defined polymer strands with narrow molecular weight distributions ($Đ \leq 1.1$). Therefore, the design of complex architectures is feasible, as it is easy to get block copolymers and specific end groups with high conversions. This high degree of control over the polymerization is highly important for biological or materials science applications.[2-3, 12]

Thus, it became highly desirable to exert such control over already well-established chain-growth polymerization techniques.[13] In the last decades, different methods were developed to control those techniques by minimizing side-reactions as much as possible. For radical polymerization several different methods were developed, including ATRP, NMP and RAFT,[14] also called controlled/living radical polymerization (CLRP). Those controlled radical polymerization techniques are more popular today as the reaction conditions are usually much milder, tolerating many other functional groups.[14] However, the very high control of molecular weight and molecular weight dispersity, without the use of a heavy metal catalyst or additional ligands makes anionic polymerization superior to other controlled polymerization techniques, especially when it comes to bio-applications.

1.2 Living Anionic Polymerization of Activated Aziridines – Poly(aziridine)s (PAz)

In contrast to the already well-established carb- and oxyanionic polymerization methods (see Scheme 1.1), the azaanionic polymerization was recently discovered by Bergman and Toste in 2005.[15] Until then, polymerization of aziridines were carried out exclusively by a cationic mechanism (Scheme 1.2A) leading to ill-defined, hyperbranched poly(ethyleneimine) (*hb*PEI).[16] Aziridines possess an acidic proton, which prevented their use in anionic polymerization. Linear PEI (LPEI) is only produced via cationic ring-opening polymerization (CROP) of oxazolines, with subsequent acidic hydrolysis (Scheme 1.2B).

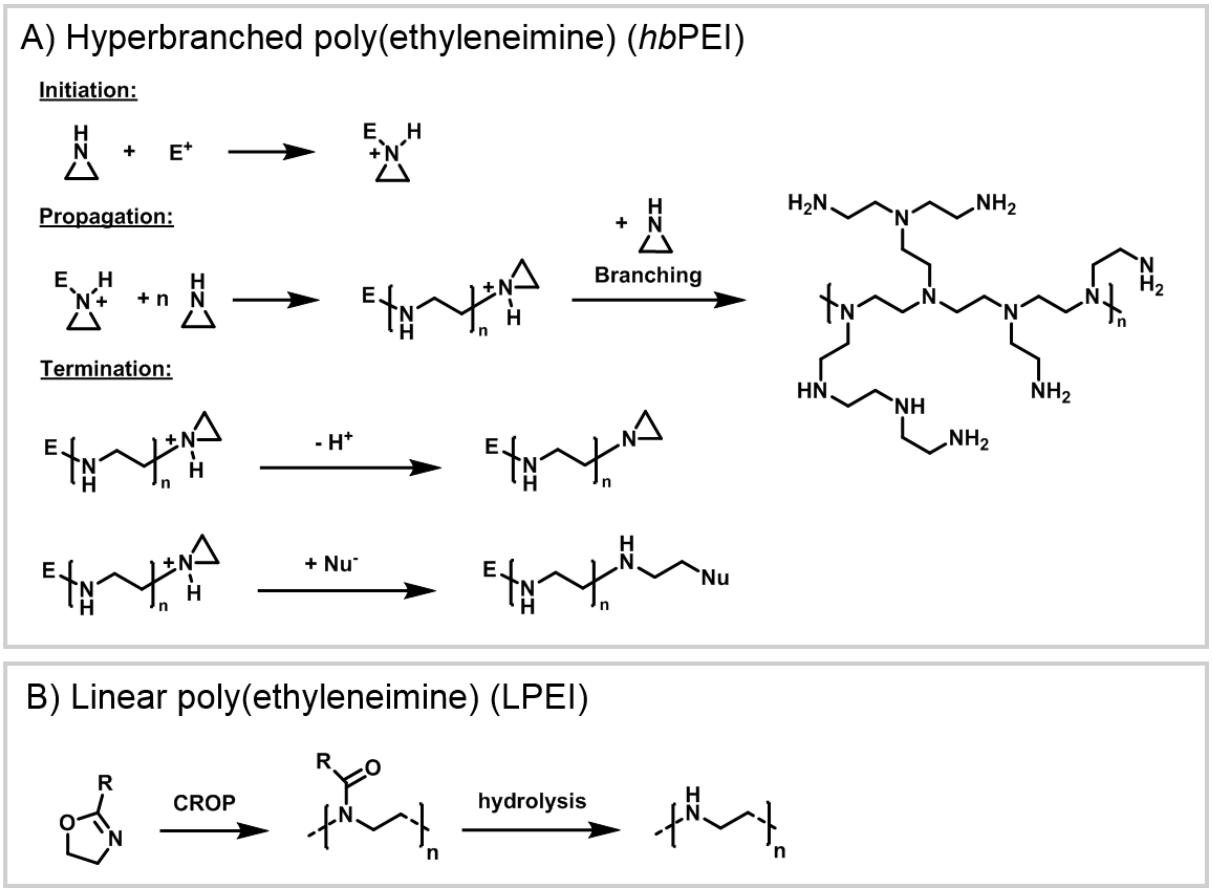

Scheme 1.2. A) Mechanism of cationic ring-opening polymerization (CROP) of aziridines to obtain branched *hb*PEI. B) CROP of oxazolines to obtain LPEI after hydrolysis.

When investigating the reactivity of a nucleophilic transition metal complex, Bergman, Toste and coworkers unexpectedly observed ring-opening polymerization of enantiopure (+)-2-benzyl-*N*-tosylaziridine in their initial work.[15] Instead of an acidic proton, this molecule is activated at the ring-nitrogen by a sulfonamide, enabling the nucleophilic attack at the aziridine ring in the 2-position. The electron withdrawing effect of the sulfonyl group further stabilizes the evolving azaanion at the growing chain end by delocalization, and propagation continues as long as the monomer is still available (Scheme 1.3). Different activating groups have been investigated, such as diphenylphosphinyl, acetyl and ethylcarbamoyl substituents, but exclusively the sulfonamide-aziridines were suitable for azaanionic polymerization.[15] In 2005, this was the first example of linear poly(sulfonamide)s, also called poly(aziridine)s, prepared by the so-called azaanionic polymerization.

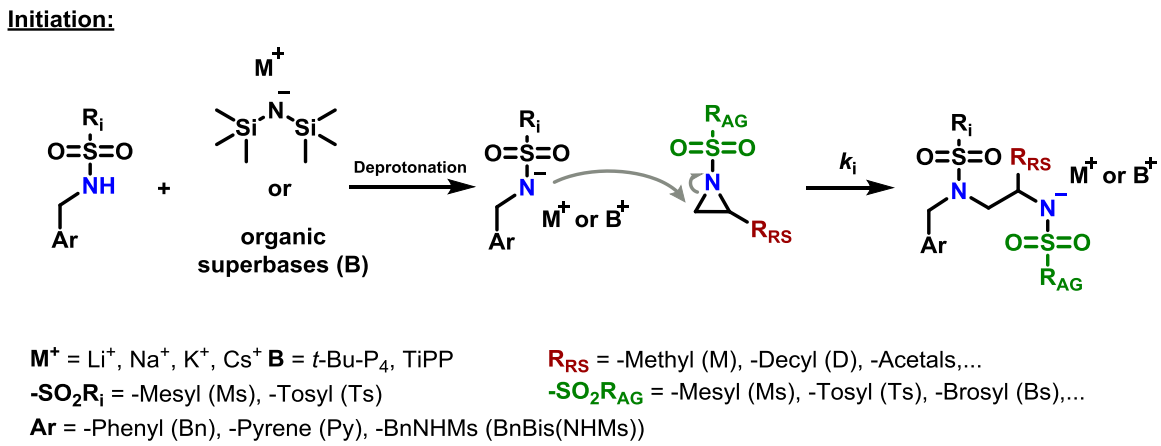

Scheme 1.3. Mechanism of living anionic ring-opening polymerization of activated aziridines.

The originally employed enantiopure monomer (+)-2-benzyl-*N*-tosylaziridine produced insoluble oligomers only. Therefore, Bergman and Toste studied three different monomers as racemic mixtures and were able to reach degrees of polymerization (D_P) of up to 200 (about M_n = 20000 g mol^{-1}) and polydispersities below 1.10.[15] Their protocol is still used as a standard procedure for the preparation of well-defined poly(sulfonamide)s. Prior to polymerization the initiator *N*-benzyl-methanesulfonamide (BnNHMs) is deprotonated with the strong (but not nucleophilic) base potassium bis(trimethylsilyl)amide (KHMDS), creating BnNKMs in dry DMF solution, and then added to the monomer solution in dry DMF (refer to Scheme 1.3). All steps are carried out in a glovebox or under Schlenk conditions to ensure inert atmosphere. A typical polymerization is usually done between 45 to 55 °C for several hours, depending on the monomer of choice. Upon initiation, the solution turns yellow to orange, indicating the generation of the delocalized azaanion at the active chain end.[17-18] Usually, resulting polymers are terminated with acidic methanol, precipitated and further washed in methanol. Following this protocol, linear polyaziridines with low polydispersities are available, so far with a maximum of 200 repeating

units,[15, 19-20] but this should not be regarded as the upper limit. Furthermore, Bergman and Toste examined the kinetics of the first azaanionic polymerization and proved, that its polymerization kinetics follow a first order mechanism. The kinetic dependence of the initiator was also found to be of first order, further proof for a living anionic mechanism.

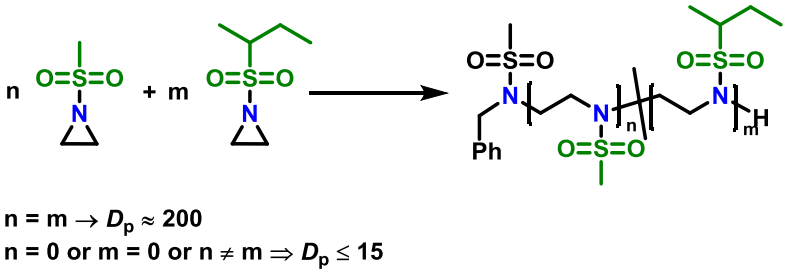

n = m → D_p ≈ 200
n = 0 or m = 0 or n ≠ m ⇒ D_p ≤ 15

Scheme 1.4. Azaanionic copolymerization of unsubstituted aziridines. High degree of polymerization only obtained, when the monomers were used in a 1:1 ratio (n = m).[20]

Solubility issues were also encountered when activated aziridines, without ring-substitution, were used for azaanionic polymerization. The first publication of the group of Wurm revealed that mainly insoluble oligomers were obtained when polymerizing TsAz, probably due to interchain packing.[18] Rupar and coworkers found a very elegant method to overcome this problem by copolymerizing two ethylene imine-derivatives, namely MsAz and ^{s}BusAz with D_P = 200, as they aimed for LPEI (Scheme 1.4).[20] Interestingly, this worked only in a 1:1 ratio of both monomers, ratios of 1:3 and 3:1 gave insoluble oligomers similarly to their corresponding homopolymers.

1.3 Tolerance of Azaanionic Polymerization towards Impurities

The crucial factor for anionic polymerization is basicity or nucleophilicity.[10, 21] Carbanions are highly basic/nucleophilic species. Therefore, strong bases (also strong nucleophiles) like butyllithium (BuLi) (pK_a ≈ 50) are necessary, to initiate the polymerization. Hence, any kind of electrophilic impurity must be avoided, otherwise irreversible termination will inhibit any further chain growth (Scheme 1.5A). On the other hand, oxyanions are less basic/nucleophilic, hence can be initiated by alkali alkoxides (pK_a ≈ 16). Thus, electrophilic impurities, like water, will not terminate the polymerization but will be also deprotonated and might initiate a secondary polymer species.[6] As a very fast proton exchange between hydroxyl groups and alkoxides is present in oxyanionic polymerization, the polymerization can continue and narrow molecular weight distributions are obtained (Scheme 1.5B).[6, 22]

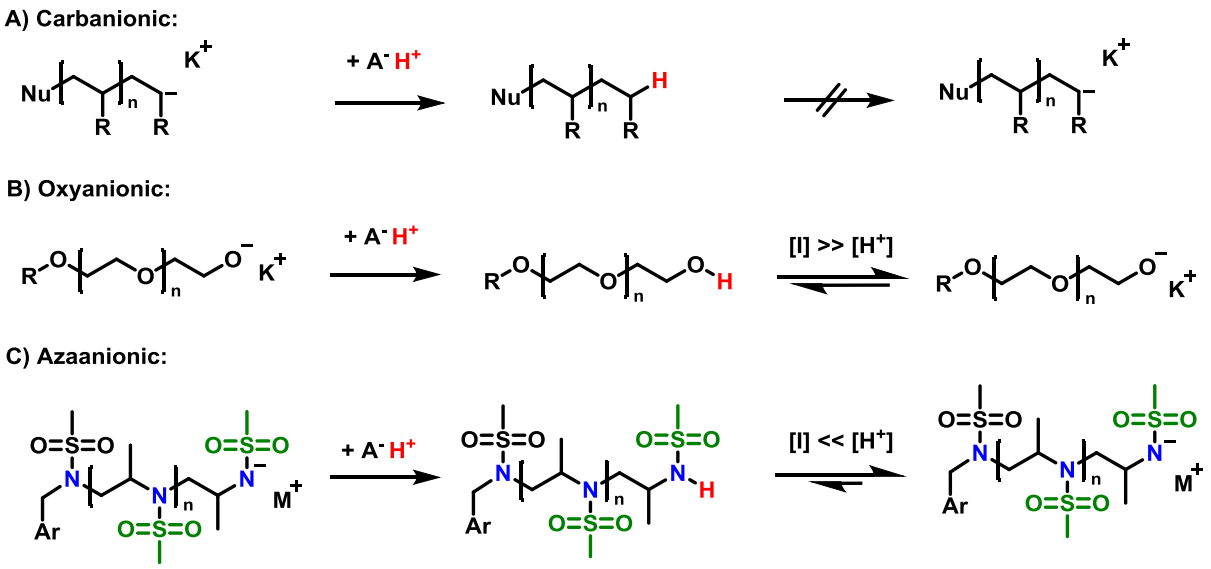

Scheme 1.5. The effect of protic additives (A^-H^+) on different living anionic polymerizations. A) Carbanionic polymerization is inhibited immediately. B) Oxyanionic polymerization can continue, if the amount of protons is much smaller than the growing chain ends. C) Azaanionic polymerization can tolerate protic impurities in much higher concentrations than the initiator.

Azaanionic was carried out as well under inert, dry conditions, as known from the other living anionic polymerizations and naturally, the necessity of those conditions was hypothesized in the first publications. However, azaanionic polymerization turned out to be exceptionally robust regarding impurities, especially protic solvents (see Scheme 1.5C) like water, methanol (MeOH), ethanol (EtOH) and isopropanol (iPrOH). In Chapter 6 it was proven that azaanionic polymerization can tolerate those solvents in amounts up to two orders of magnitude with respect to the initiator (in DMF). Moreover, the polymerization can be performed in open vials and retains its living characteristics. As further demonstrated *via* MALDI-TOF and ^{13}C NMR spectra, when the alcohols were added as ^{13}C-labeled species, a second initiation of the solvents as alkoxides up to 10% (in most cases) is observed. In all cases narrow polydispersities were obtained, however, they slightly increased with the acidity of the solvent (maximum of 1.25), with slightly reduced molecular weights due to initiation by the additives. As additionally computed by DFT-calculations, the basicity of the propagating azaanion is decreased by the activating group of the sulfonamide, but still remains highly nucleophilic, enabling the nucleophilic attack towards monomers. Remarkably, the basicity of the deprotonated alkoxides, originated from the impurities, is higher than the basicity of the growing chain end. Consequently, the alkoxides are expected to react with monomers, before the azaanion does. However, since the polymerization is performed in DMF, the degree of deprotonation of those solvents is very low, as their pK_a-values are magnitudes higher than the chain ends in DMF. Hence, the concentration of alkoxides is very low (compare Chapter 6), which also keeps the amount of second initiated polymers low. Furthermore, the speed of initiation is slower, as the resulting molecular weights are significantly

smaller than the ones afforded from the impurity-free initiated polymers. Therefore, the azaanionic ring-opening polymerization (A-AROP) can be handled under non inert conditions, similar to controlled radical polymerization, where also a certain degree of differently initiated polymers is typically accepted,[23-25] but in contrast no “dead” chains occur in the A-AROP. This also allows the use of unprotected hydroxyl monomers to undergo a well-controlled A-AROP, a fast access to polyols. This represents an important advantage and make them a promising material for future industrial production, as its handling is as easy as in controlled radical polymerizations.

1.4 Initiators for the Polymerization of Activated Aziridines

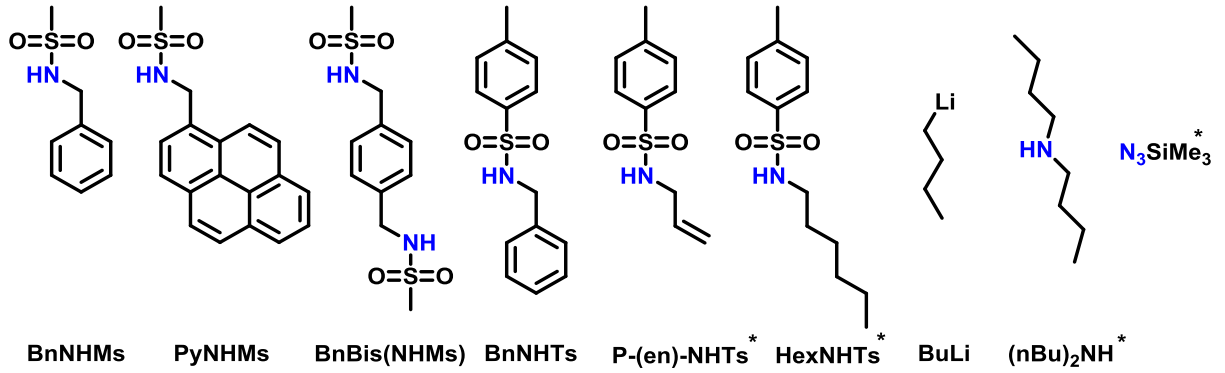

Scheme 1.6. Different initiators for azaanionic polymerization. Initiators, only reported for OROP are labeled with a star *.

BnNHMs is to date the most used initiator for the azaanionic ring-opening polymerization (A-AROP) of sulfonyl aziridines, however, various initiators have been employed for azaanionic polymerization (Scheme 1.6). Further secondary *N*-sulfonamide-initiators are *N*-benzyl-4-methylbenzenesulfonamide (BnNHTs),[19] and the fluorescent *N*-pyrene-methanesulfonamide (PyNHMs).[15, 17, 26] The first bifunctional initiator *N,N'*-(1,4-phenylenebis(methylene))dimethane-sulfonamide (BnBis(NHMs)), which allows the preparation of ABA-triblock copolymers, was introduced in 2017.[27] Besides the sulfonamides, also commercially available BuLi was used successfully to initiate the ring-opening polymerization (ROP) of sulfonyl aziridines.[18, 27] In all cases, MALDI-TOF spectra proved the incorporation of the respective initiator, rendering the A-AROP of sulfonyl aziridines a powerful method to prepare α-functionalized PEI-derivatives. To date, the standard protocol uses mainly KHMDS or other alkali bis(trimethylsilyl)amide salts to deprotonate the sulfonamide-initiators.[27] Since, KHMDS is a very strong base, but not a strong nucleophile, it creates the highly nucleophilic sulfonamide, which is able to attack the aziridine-monomer. Wurm and coworkers also used KHMDS without an initiator, and was able to obtain polymeric structures, which showed a bimodal molecular weight distribution.[17, 28] We believe that

the range of initiators for the azaanionic polymerization will be expanded in the future, allowing access to a variety of functional PAz and derivatives.

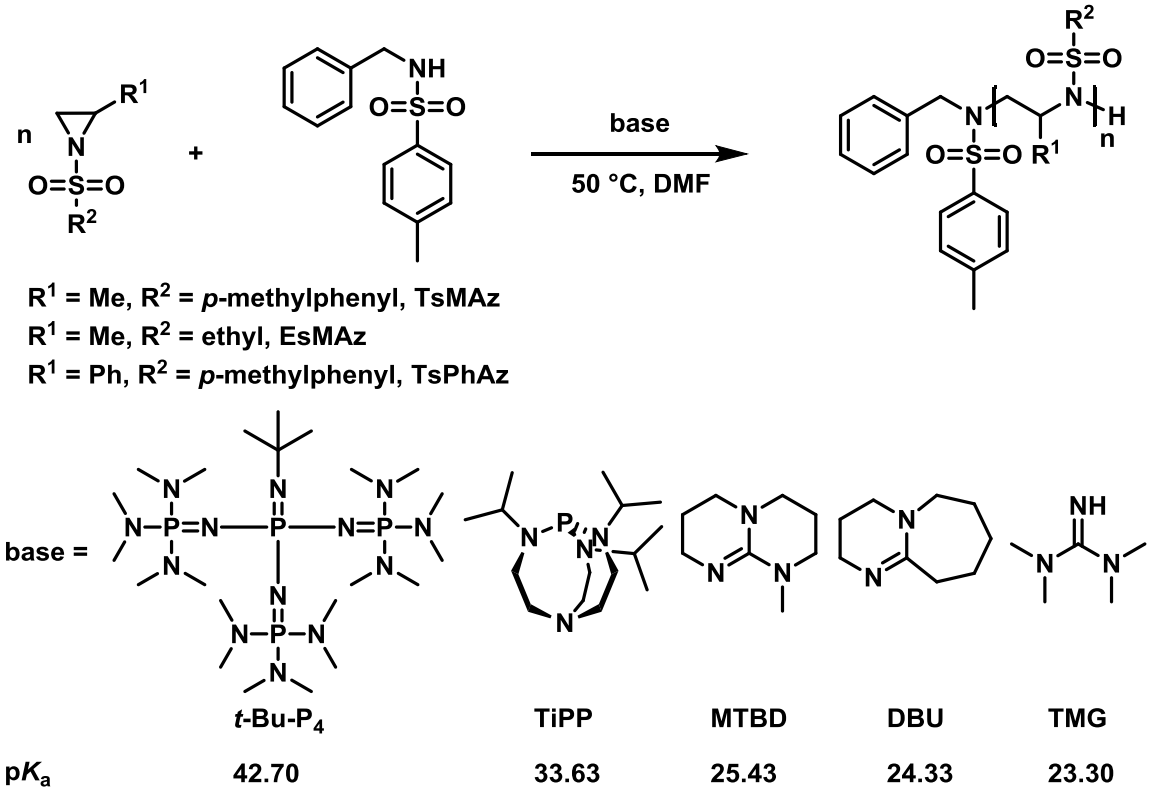

Scheme 1.7. Anionic ring-opening polymerization of 2-alkyl-*N*-sulfonyl aziridines catalyzed with various organic bases as presented by *Wang et al.* Copyright @ 2017 The American Chemical Society. Reprinted with permission from ACS Macro Letters.[19]

Recently, the first metal-free azaanionic polymerizations of sulfonyl aziridines were reported (Scheme 1.7),[19] when screening five different organic superbases, namely TMG, DBU, MTBD, TiPP and *t*-Bu-P_4. The basicity (pK_a-values of the conjugated acids) of these compounds increases in the order TMG < DBU < MTBD < TiPP < *t*-Bu-P_4 and correlates with their increasing catalytic activity. The organocatalyzed AROP performed best (regarding reaction time (20 min), conversion, and dispersity ($Đ$ = 1.05)) using the most basic phosphazene (*t*-Bu-P_4) (but with low nucleophilicity). Also, TiPP showed satisfactory results. The remaining three bases were found acceptable, showing higher polydispersities ($Đ$ up to 1.4), due to their increased nucleophilicity. Overall, the strongest bases had the best catalytic activity. Moreover, the amount of catalyst could be lowered to 0.05% respect to the initiator, which indicates a very fast proton exchange, similarly to the already exploited method for oxyanionic polymerization to reduce the activating agent. Additionally, using lower amounts of catalyst resulted in final molecular weights closer to the

theoretical molecular weight. Consequently, the molecular weight distribution was narrower and the reaction time was longer.

1.5 Monomers

Aziridines are, in direct analogy to epoxides, saturated three membered ring compounds with one nitrogen. The ring-strain of 26.7 kcal mol^{-1} is very similar to its oxygen analog (ethylene oxide (EO) = 26.3 kcal mol^{-1}). As base (pK_a (of conjug. acid) = 7.98)) with a more pronounced dipole moment and a stronger hydrogen bonding, its boiling point is with 55 °C around 45 degrees higher than that of EO. Aziridines are miscible with most organic liquids and water. The industrial production of ethylene imine monomer is around 9000 t/a (2006) of high industrial relevance. Due to its toxicity, the monomer is usually directly converted into its nontoxic intermediates and polymers.[29] Nevertheless, the relevant synthesis strategies can be easily adopted to lab scale and taking into account todays safety protocol for toxic chemicals, synthesis of such compounds can be conducted reliably.

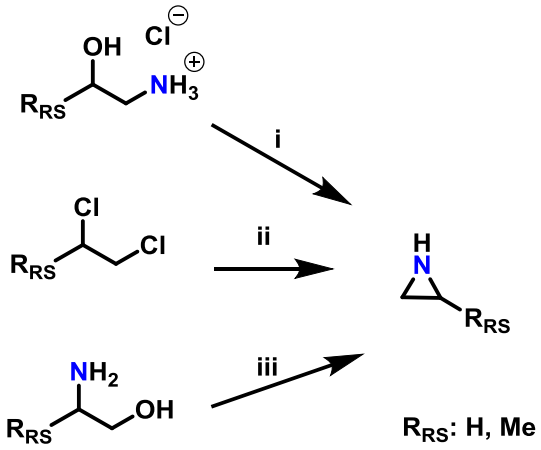

Scheme 1.8. Synthesis of aziridines with and without a ring substituent (RS) by i: the β chloroethylamine process, ii: The Dow Process, iii: The Wenker Synthesis.

In Scheme 1.8 the following reactions are depicted: (i) The *β*-chloroethylamine process uses vicinal chloro amine hydrochloride salts with sodium hydroxide. Because hydrochloric acid (HCl) is released if the process is not conducted under optimal conditions, making CROP of the product a possibility, and the fact that HCl is corrosive, this process lost industrial relevance in 1963.[29] The Dow Process in Scheme 1.8, ii was used in industrial scale since 1978; it was stopped due to drawbacks like high corrosion rates and waste stream disposal. Per one equivalent starting material three equivalents ammonia are necessary, which gives the Dow Process a low atom economy.[29] A large-scale process of still industrial relevance is the Wenker Synthesis

(Scheme 1.8, iii). It is considered to be the most efficient and convenient method for the synthesis of aziridine. This two-step process starts originally with 2-aminoethanol or other vicinal amino alcohols. Total yields of 90% are obtained with ease.[29] Significant waste disposal problems can be avoided through good atom economy and nontoxic side products. Aziridine is usually obtained as pure product, therefore, amino alcohols and sulfuric acid or, under more efficient conditions with chlorosulfuric acid replacing sulfuric acid and diethylether as solvent,[30] a sulfate is formed at ambient temperatures. For laboratory scales, sulfates can be purified by filtration and washing with an excess of ether. After esterification, the sulfates are treated with 5-6 equivalents of sodium hydroxide or saturated sodium carbonate solution to give the aziridine after a nucleophilic cyclization. Low molecular weight aziridines such as 2-methyl aziridine can be further purified by azeotrope distillation, by using e.g. CaH_2 as a drying agent. If stored longer, alkali hydroxide in the receiver flask stabilizes the aziridine against spontaneous cationic polymerization. Synthesis of *N*-substituted aziridines can be obtained if secondary amines are used as starting material.[31-32]

Monomer preparation for anionic polymerization of aziridines.

Since LAP requires proton free conditions and further electron-withdrawing *N*-substituents or activation groups (AG) that polarize the aziridine moiety and allow AROP, the *N*-hydrogen needs to be replaced by a sulfonyl group. In analogy to the Hinsberg reaction,[33] secondary amines react with chorosulfuric acids (Scheme 1.9, ii), to conveniently convert aziridines to sulfonyl aziridines. Scheme 1.9 illustrates several pathways to the monomer class of activated aziridines.

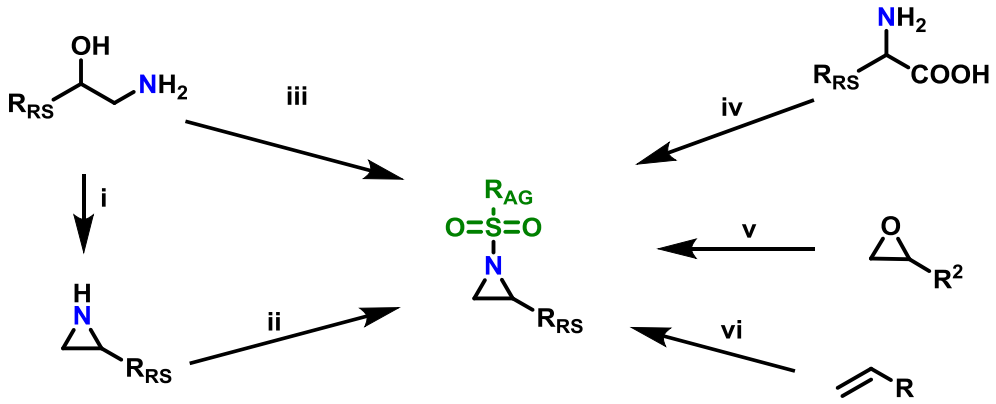

Scheme 1.9. Synthesis of aziridine monomers suitable for the azaanionic polymerization: i: Wenker synthesis of aziridine: 1) vicinal amino alcohol derivate, Sulfuric acid or sulfuric acid chloride 2) NaOH (*aq.*); ii: Sulfonyl chloride, TEA, DCM; iii: Sulfonic chloride, DCM, DMAP or K_2CO_3 (Microwave, 400 W); iv: 1) Amino acid, NaOH (*aq.*), 0 °C, TsCl. 2) THF dry, BH_3-SMe_2, reflux. 3) DCM, TsCl, DMAP, Py; v: RSO_2NH_2, K_2CO_3, $BnEt_3N^+Cl^-$, Dioxane, 90 °C, MsCl, DCM, 0 °C to reflux; vi-1: Chloramine salts, ACN, PTAB, 12 h; vi-2: IPrCu(DBM), PhI=O, RSO_2-NH_2, Chlorobenzene, r.t., 25 h; vi-3: $Rh_2(cap)_4$, $TsNH_2$, NBS, K_2CO_3.

Besides route (i) and (ii) in Scheme 1.9, other efficient strategies to synthesize aziridines are possible. Starting directly from amino alcohols (iii), alkenes (vi), epoxides (v) or amino acids (iv) also leads to sulfonyl aziridines. Due to high yields (up to 93%), simple synthesis routes, beneficial starting materials and other advantages, these different monomer synthesis are explained in detail.

H. Xu *et al.*[34] showed an efficient microwave-assisted one-pot reaction (iii) for sulfonyl aziridines, using valinol, *L*-phenylalaninol, *L*-leucinol, *L*-alaninol and *L*-serine methylester as aminoalcohol compound and methyl-, phenyl- and 4-methoxyphenyl-sulfonic chlorides as co-reactants. Potential solvents for this strategy were diethylether, THF, Acetonitrile (MeCN), and dichloromethane (DCM). Bases such as alkali carbonates and hydroxides are used with DMAP as catalyst. The advantage of this strategy is the short reaction time of only 30 min, while maintaining a high monomer yield of 84%-93%. However, the aziridines prepared by H. Xu. and coworkers have not yet been tested for polymerization.

Synthesis (iv) shows, that the sulfonyl aziridines can also be obtained from amino acids. This reaction demonstrates that a variety of different potential monomers can be obtained from natural products. In a three-step procedure M. B. Berry and D. Craig synthesized *N*-tosylaziridines from different amino acids (Scheme 1.10).[35] Their method involves the *N*-tosylation of the amino acids followed by reduction to *N*-tosyl-2-amino alcohols and *O*-tosylation with an *in situ* ring closure reaction. Particularly interesting is that this method does not require any purification of intermediates. Starting from amino acids represents a step towards a greener synthesis of aziridines suitable for the AROP.

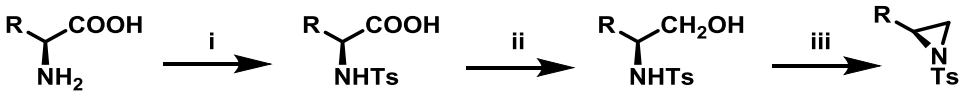

R= $HOCH_2$, Me, ^{i}Pr, ^{i}Bu, $PhCH_2$, $MeS(CH_2)_2$

Scheme 1.10. i: Preparation of *N*-tosyl-2-aminoacids via *N*-Tosylation with TsCl; ii: Preparation of *N*-tosyl-2-aminoalcohols reduction of the carbonyl group; iii: Preparation of 2-substituted *N*-tosylaziridines.

Route (vi) in Scheme 1.9 allows the synthesis of aziridine monomers with terminal alkenes as a starting material. Sulfonyl aziridines with varying lengths of alkyl chains can be produced in a catalytic one step synthesis. Functional side groups, such as alcohols and ethers are tolerated during the reaction. An important advantage of this strategy is that the potentially toxic aziridine (with NH) intermediate is avoided and the activated sulfonyl aziridines are obtained directly. Usually the conversion of non-functionalized alkenes to aziridines has high yields of 95% with

rhodium catalyst and up to 93% with PTAB as catalyst, however, the yields vary depending on the side groups. Catalysts are either commercially available or can be prepared with ease.[36-38]

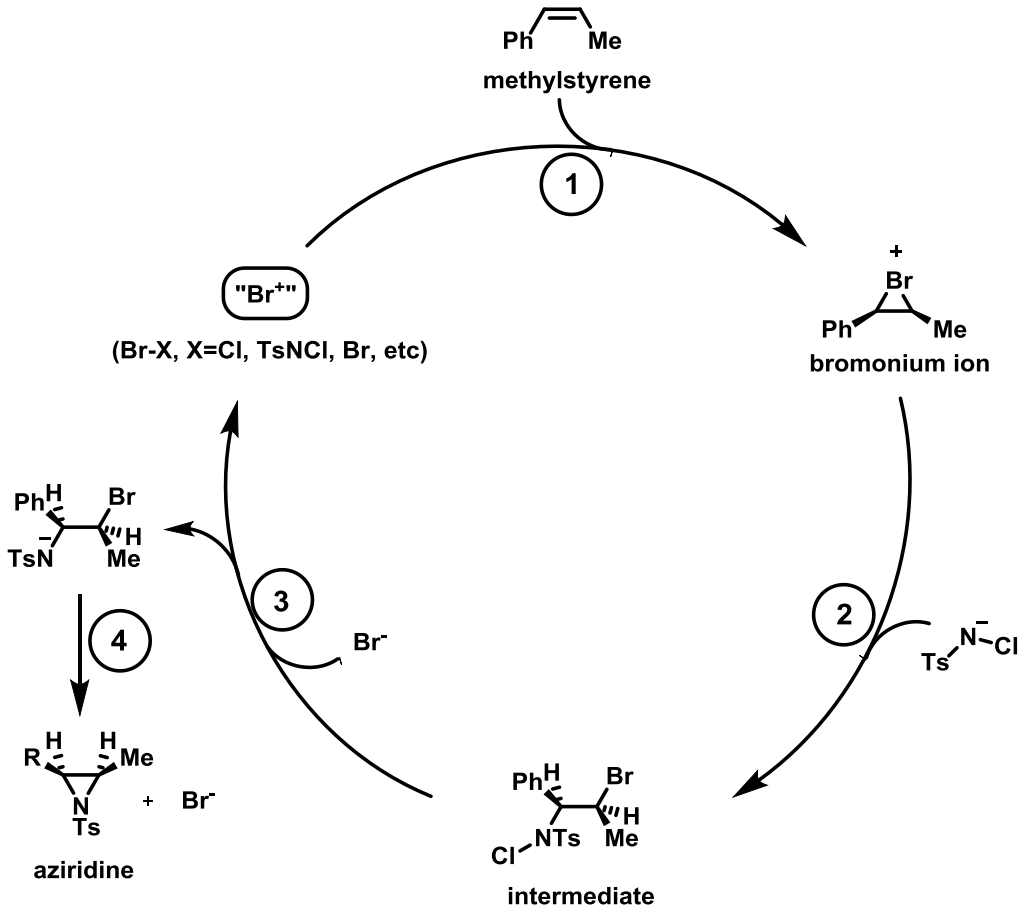

Scheme 1.11. Catalytic cycle of the PTAB catalyzed aziridination of olefins, adopted from previous work of Sharpless. Copyright @ 1998 The American Chemical Society. Reprinted with permission from Journal of the American Chemical Society.[38]

The proposed pathway for this bromine-catalyzed aziridination process of Sharpless and coworkers is shown in Scheme 1.11 for cis-*α*-methylstyrene as an example. In the first step, the olefin reacts with a Br^+ source, given by PTAB. The bromonium ion is then subjected to a benzylic opening by nucleophilic attack of $TsNCl^-$, to form the *α*-bromo-*N*-chloro-*N*-toluenesulfonamide (Step 2). Attack of the bromide anion (Br^-) (or $TsNCl^-$) on the N-Cl group of the intermediate generates the anion and a Br-X species (Step 3). Expulsion of Br^- from the anion finally yields the aziridine and the regenerated Br-X species (Step 4). The formed Br^+ source is ready to initiate another turn of the catalytic cycle.[38] This synthesis route was also successfully used for monomer synthesis by the group of Wurm by using chloramine-T and chloramine–M to synthesize MsDAz (49%) and TsDAz (47%)[39] and acetal functionalized aziridine monomers (17%-30%).[17]

Synthesizing the monomer for polysulfonamides from epoxides is also possible[15, 40]. Since many epoxides are commercially available, epoxides build a good platform for the synthesis of activated aziridines. The method of P. O`Brien[41] is a convenient and high yielding two-step synthesis (see Scheme 1.12). For example the synthesis of 2-Benzyl-1-(2,4,6-triisopropylbenzene-sulfonyl)aziridine involves, as first step, a ring-opening reaction of 2-benzyloxirane with the primary sulfonamide (2,4,6-$^{i}Pr_3C_6H_2SO_2NH_2$). This reaction requires 0.1 eq of potassium carbonate and $BnNEt_3^+Cl^-$ as catalyst in dioxane (73% yield). The subsequent mesylation-cyclization of the hydroxy sulfonamide requires mesyl chloride to activate the hydroxy group basic conditions for the cyclization (86% yield). This route is particularly amenable to variation of the *N*-sulfonyl substituent.

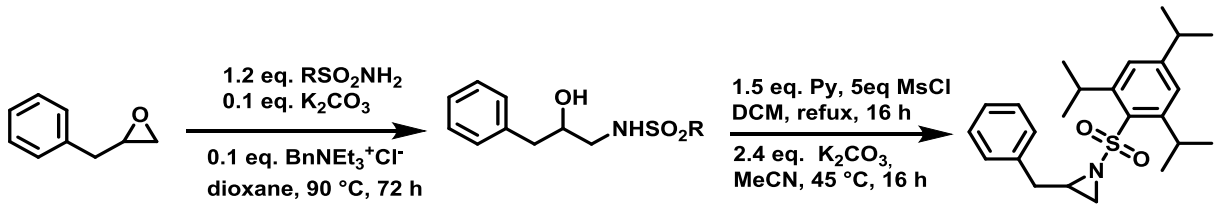

Scheme 1.12. Synthesis of 2-Benzyl-1-(2,4,6-triisopropylbenzenesulfonyl)aziridine from 2-benzyloxirane, R=2,4,6-$^{i}Pr_3C_6H_2$.

Another route, starting from epoxides was used by Bergman and Toste,[42] they synthesized 2-*n*-Decyl-*N*-methanesulfonyl aziridine (MsDAz). Thomi and Wurm[40] followed this procedure to synthesize functional aziridine monomers, namely 2-(oct-7-en-1-yl)-*N*-mesylaziridine. This procedure involves three steps; first the epoxide is ring-opened with sodium azide to give the azido-hydroxyalkane as intermediate, which is converted in the second step, by a ring closure reaction to the corresponding alkyl aziridine. To activate the obtained aziridine for anionic polymerization mesylchloride is used to replace the *N*-terminal hydrogen in the third step.

Scheme 1.13 shows activated aziridines, which were successfully polymerized *via* azaanionic polymerization to this day.

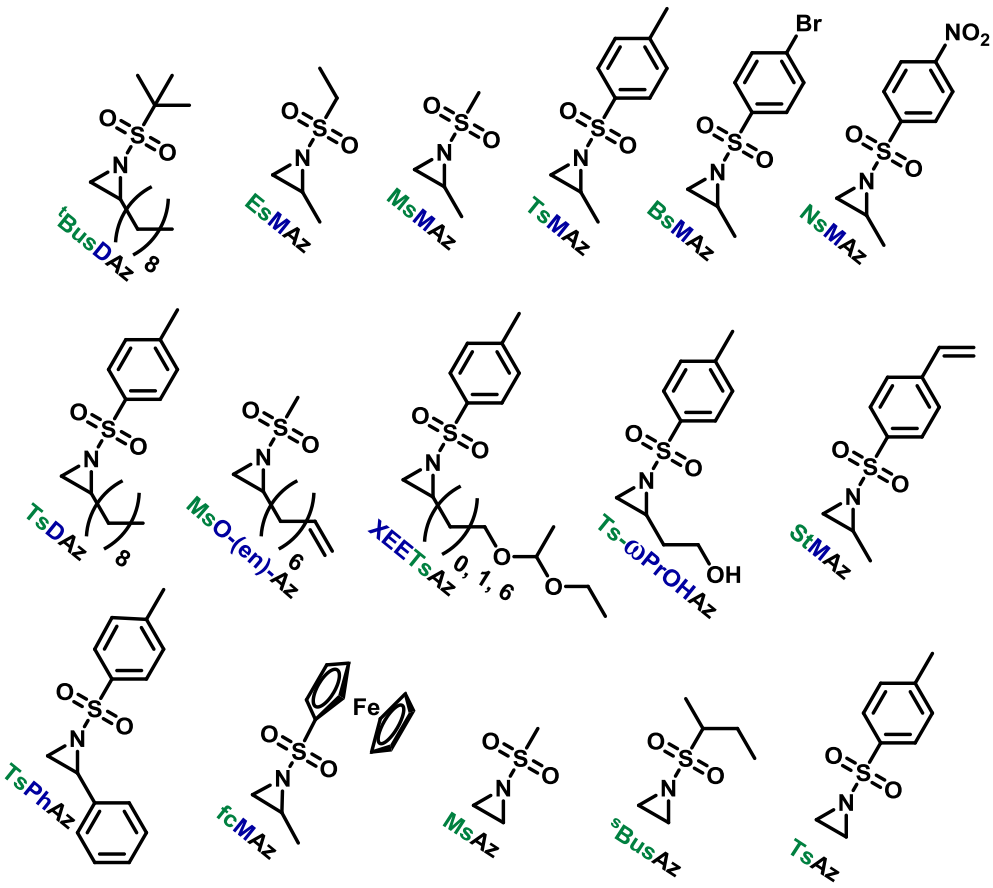

Scheme 1.13. Activated aziridines which were successfully tested for A-AROP.

1.6 Organocatalytic Ring-Opening Polymerization (OROP) of Activated Aziridines

N-heterocyclic carbenes (NHC), such as 1,3-bis(isopropyl)-4,5(dimethyl)imidazole-2-ylidene, are powerful catalysts in many types of polymerizations. Their near unlimited structural diversity, their inherent high Bronsted-basicity and nucleophilicity makes NHCs powerful organocatalysts.[43-44] Examples of applications of NHCs include some of the most important commercial monomers in the step-growth polymerization of terephthalaldehyde[45], the group transfer polymerization of methacrylic monomers[46] and the zwitterionic ring-opening polymerization (ZROP) of ethylene oxide (EO)[47], which was discovered in 2009 by Taton and coworkers. As activated aziridines polymerize with nucleophilic bases (similar to EO) *via* AROP, it was of interest if organocatalytic ring-opening polymerization (OROP) can also be successfully performed with this new monomer class. The first living OROP of 2-alkyl-*N*-sulfonyl aziridines was presented by Carlotti, Taton and coworkers in 2016 (see Scheme 1.14).[48] The ring-opening polymerization of *N*-tosylaziridines in the presence of 1,3-bis(isopropyl)-4,5(dimethyl)imidazole-2-ylidene as a sterically hindered organocatalyst and activated secondary *N*-tosyl amine as the initiator. This mechanism offers a mild and metal-free route for the polymerization of activated

aziridines to obtain identical polyaziridines, as from AROP, with narrow molecular weight distributions ($1.04 < Đ < 1.15$) and molecular weights up to 21,000 g mol^{-1}. Depending on the steric hindrance of the ring-substituent, the reaction time to full conversion varies between 1 and 5 days at 50 °C in THF.

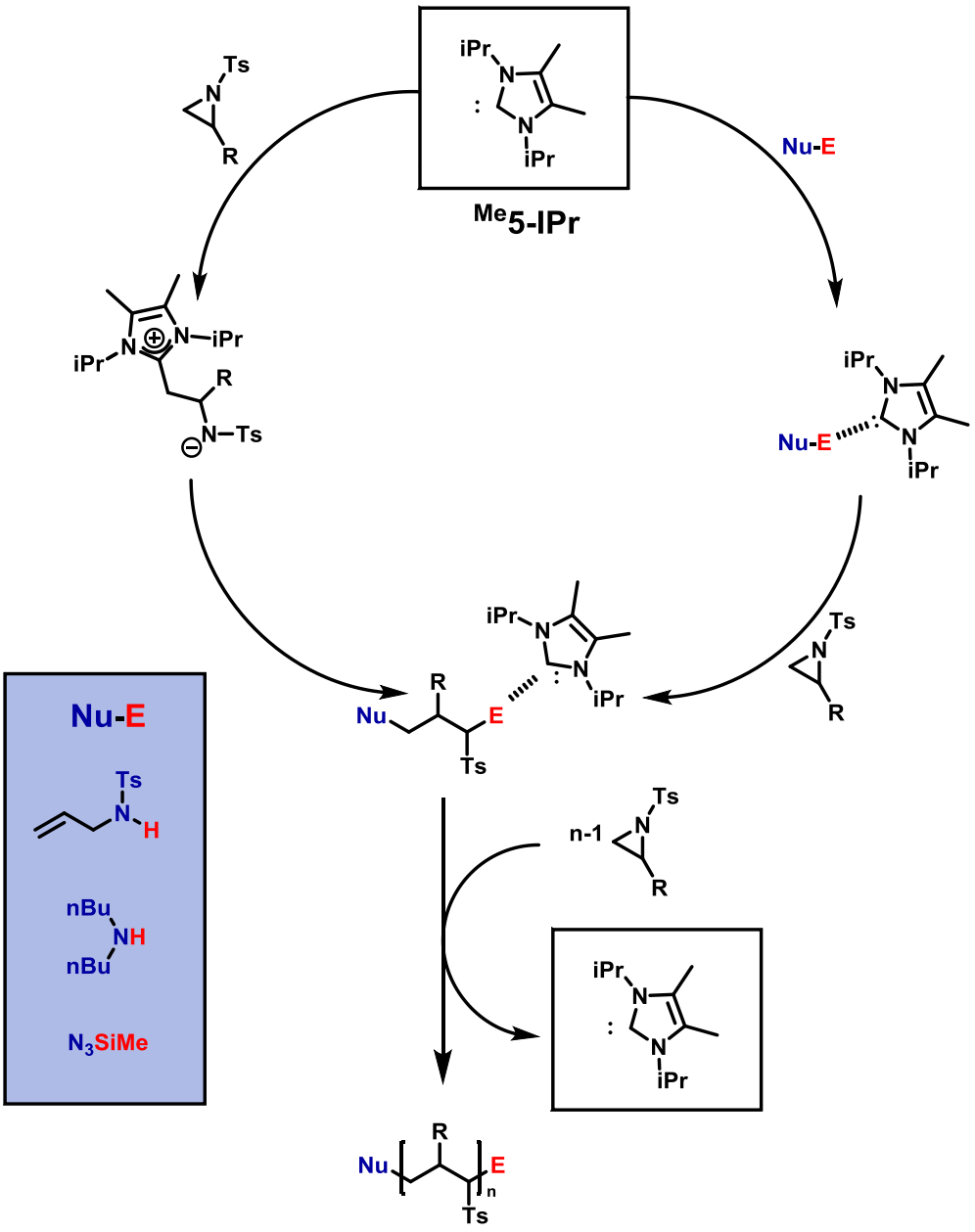

Scheme 1.14. Possible mechanism for the NHC-OROP of 2-alkyl *N*-*p*-toluenesulfonyl aziridines initiated by *N*-allyl *N*-*p*-toluenesulfonyl amine, di-*n*-butylamine and trimethylsilyl azide. Copyright @ 2017 Elsevier. Reprinted with permission from European Polymer Journal.[49]

Depending on the nature of the monomers, the NHCs either react as nucleophilic initiators or behave as organic catalysts and activate the monomer for nucleophilic attack of the initiator/active chain end. MALDI-TOF spectrometry clearly demonstrated the incorporation of the initiator (secondary *N*-tosyl amines) into the polymer, without showing a polymer fraction with NHCs

covalently bond to the polymer. The scope of practicable initiators was expanded, when non-activated amines were investigated, which allow further post-modification of the poly(aziridine)s.[49]

1.7 Functional Poly(aziridine)s

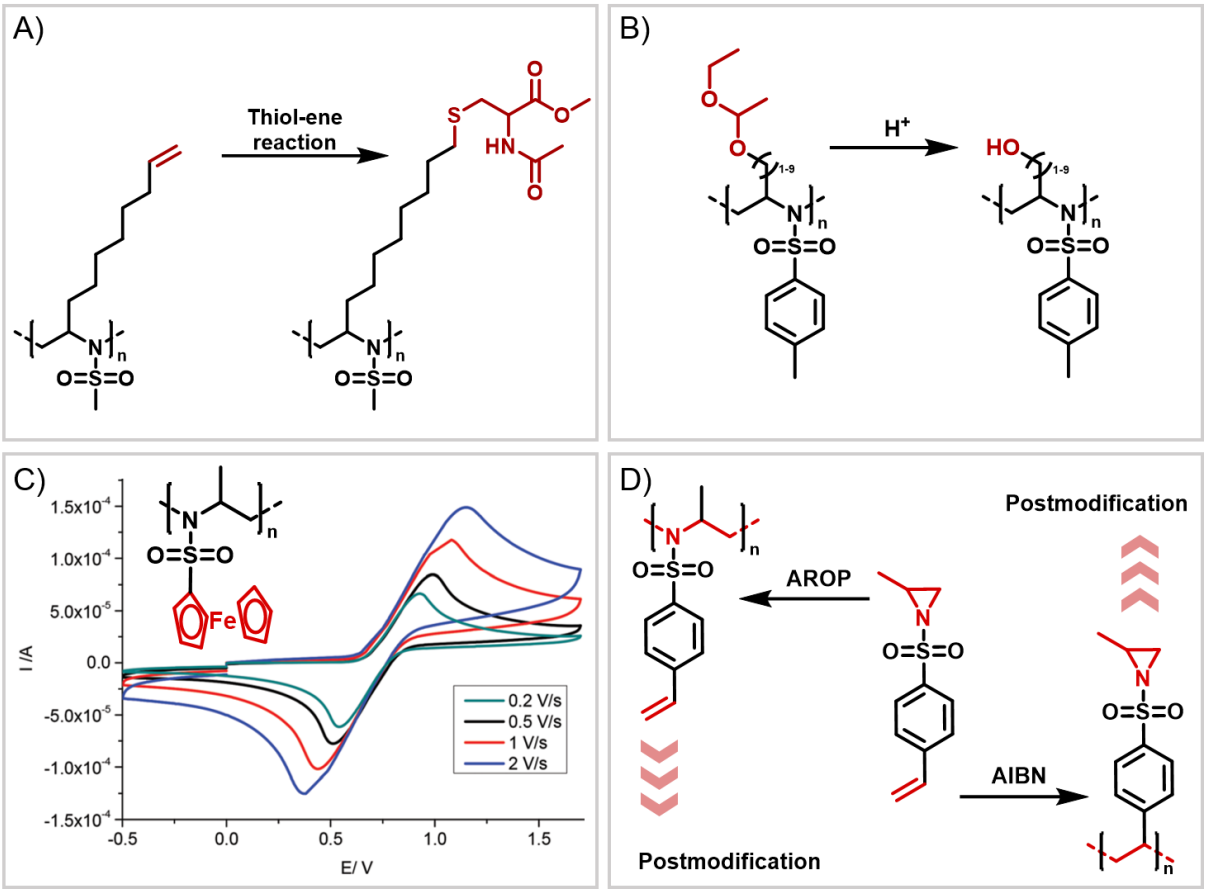

Figure 1.1. Functional polyaziridines: A) Terminal double bond can be converted *via* thiol-ene reaction. B). Acetal-protected polyaziridines yield hydroxyl functionalities. C) Ferrocene-containing polyaziridines are redox-responsible. D) Orthogonal aziridine allows anionic and radical polymerization.

Functional groups can be installed as substituents at the activating group (R_{AG}) or at the ring (R_S; see Scheme 1.3 and Scheme 1.13). The first orthogonal functionality in PAz prepared by AROP was a terminal olefin: 2-Octenyl-*N*-mesylaziridine (MsO-(en)-Az) (Figure 1.1A) carries a terminal double bond and was homo- and copolymerized *via* AROP. The olefins were post-modified by a radical thiol-ene reaction with *N*-acetyl-L-cysteine methyl ester providing quantitative conversion (Figure 1.1A).[40]

Also, polyols have been prepared by the AROP of sulfonyl aziridines. In analogy to ethoxy ethyl glycidyl ether (EEGE), the well-known precursor in oxyanionic polymerization to obtain linear poly(glycerol) (linPG),[6, 50] acetal-protected *N*-tosyl-activated aziridines were introduced in 2016

(see Figure 1.1B) as masked hydroxyl monomers.[17] Three different acetal-protected monomers with variable alkyl chain lengths were prepared and polymerized under living conditions. The hydroxyl groups were released by acidic hydrolysis, without touching the sulfonamides. Removal of the sulfonyl groups resulted in polyamine-polyols. Such materials can be regarded as double-protected precursors to polyhydroxyl-PEI-derivatives, which can be selectively and/or consecutively deprotected.[17]

Also inspired by oxyanionic polymerizations,[51] the first redox-responsive ferrocene-containing aziridine *N*-ferrocenylsulfonyl-2-methylaziridine (fcMAz) was added to the growing monomer-family.[28] Homopolymerization resulted in insoluble organometallic poly(sulfonamide)s, however, solid state NMR (ssNMR) and MALDI-TOF spectra proved clearly the polymeric structure. In addition, copolymerization with TsMAz or MsMAz resulted in soluble copolymers with rather narrow dispersities (<1.4), and even chain extension experiments proved the living nature of the polymerization. Further, the ferrocene-containing PAz proved a reversible oxidation/reduction by cyclic voltammetry (see Figure 1.1C). Redox-responsive materials based on polyamine-structures, expand the range of possible applications of these novel polymers

Several chemical functionalities can also be installed into the activating group. The orthogonally-polymerizable monomer, 2-methyl-*N*-(4-styrenesulfonyl)aziridine (StMAz) (Figure 1.1D)[52] allows polymerization by azaanionic ROP or by radical polymerization of the vinyl bond, keeping the aziridine-ring intact. Thermal characterization revealed a high char yield after TGA-measurements, for both kinds of polymers. Post-modification was demonstrated by thiol-ene addition of mercaptoethanol or mercaptopropionic acid to the styrenic double bond. The aziridine-ring itself is suitable for further nucleophilic modifications, as already described for some polymer systems with aziridines as a side group.[53-56] This is one of the few examples of an orthogonal monomer, which can be polymerized chemoselectively by different mechanisms without affecting the other polymerizable group.[57-59]

The PAz prepared by anionic ROP inherently carry a reactive secondary sulfonamide end group. In addition, it was the first report by Rupar who introduced the first telechelic poly(aziridine)s by termination of the A-AROP with propargyl bromide, which allows further modifications by click chemistry.[20]

1.8 Polymerization Kinetics

Real-time ^{1}H NMR spectroscopy is a powerful technique to monitor polymerization kinetics at every time-point of the reaction *in situ*. It is especially interesting for copolymerizations, allowing direct monitoring of the growing microstructure at any point of the polymerization and thus gives the reactivity parameters quickly. The *in situ* NMR technique was established eight years ago for

oxy-[60-62] and carbanionic[63-66] polymerizations. In most cases a solution (co)polymerization was monitored by ^{1}H NMR, but we recently also used ^{13}C NMR spectroscopy in bulk[67] or ^{31}P NMR spectroscopy.[68] As in a living polymerization, no side reactions occur and monomer consumption is equivalent to monomer incorporation into the growing polymer chain. Therefore, integration of the monomer resonances (usually sharp signals) can be used to determine each monomer conversion. Further requirements for *in situ* kinetics are well-separated/distinguishable monomer signals for integration and reaction times in the range of minutes to several hours (to allow spectra collection). The real-time kinetics of the homopolymerization of MsMAz is exemplified in Figure 1.2. The ring-protons appear as two doublets with a $^{3}J_{HH}$-coupling of 7.0 Hz with the vicinal proton between 2 and 3 ppm (labeled a (*cis*-configuration) and b (*trans*-configuration) in red in Figure 1.2B) and one multiplet at ca 2.7 ppm. During the polymerization, the monomer signals vanish and the evolution of the polymer backbone can be detected (highlighted in green, Figure 1.2A) as broad signals between 3.5 and 4.5 ppm.

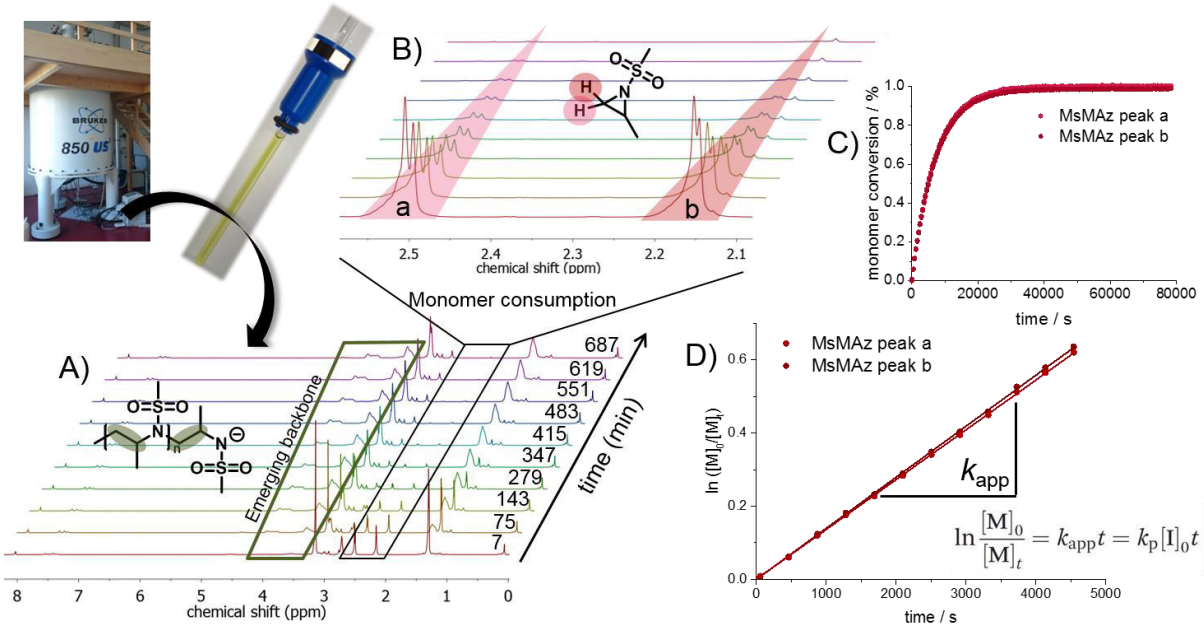

Figure 1.2. A) Real-time ^{1}H NMR kinetic characterization of azaanionic polymerization of MsMAz. B) The time-dependent decrease in intensity of the signals of the ring-protons (a and b) allows calculation of (C) monomer conversion *versus* time and (D) apparent propagation rate (k_{app}). Copyright @ 2017 The Royal Society of Chemistry. Reprinted with permission from Polymer Chemistry.[27]

Integration of the monomer signals over time, followed by normalization to the amount of unreacted monomer, allows calculation of k_{app} (Figure 1.2C, D). As initiation proceeds very fast, the slope follows first-order kinetics, suggesting a living polymerization mechanism. Therefore, all chains are initiated simultaneously and the concentration of the growing polymer chains

[P$^-$] is equal to the initiator concentration [I], as shown in equation (1). The independent propagation rate (k_p) is then obtained by dividing the slope from the kinetic plot of $\ln([M]_0/[M]_t)$ *vs.* time by the initiator-concentration (equation 2).

$$\frac{-\mathrm{d}[\mathrm{M}]}{\mathrm{d}t} = k_\mathrm{p}[\mathrm{P}^-][\mathrm{M}] = k_\mathrm{p}[\mathrm{I}][\mathrm{M}] \qquad (1)$$

$$\ln\frac{[\mathrm{M}]_0}{[\mathrm{M}]_t} = k_\mathrm{app}t = k_\mathrm{p}[\mathrm{I}]_0 t \qquad (2)$$

In anionic polymerizations, reaction parameters like counter ion and solvent have a strong influence on the reaction kinetics.[9-10, 12] Hence, a systematic investigation of the effect of different reaction conditions on azaanionic polymerization was published by our group.[27] Importantly, we found that the polymerization of MsMAz retained its living character up to a reaction temperature of 100 °C (Figure 1.3A). The polymerization proceeds in several hours in solvents such as DMSO and DMF at 50°C (Figure 1.3B). Such polar solvents efficiently separate the cation from the growing chain end and thus increase the propagation rates. In contrast, THF and benzene exhibited very slow reaction kinetics.

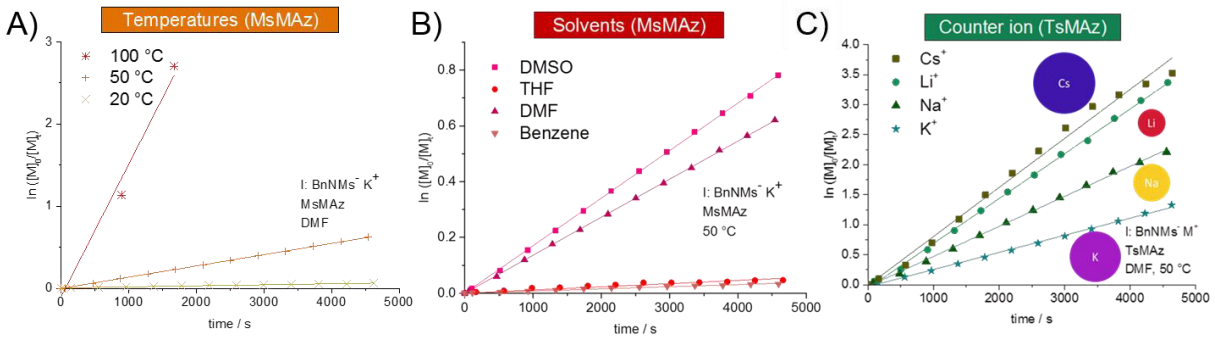

Figure 1.3. Kinetic plots of $\ln([M]_0/[M]_t)$ *vs.* time for the azaanionic polymerization of A) MsMAz at different temperatures in DMF. B) MsMAz in different solvents at 50 °C. C) TsMAz in DMF at 50 °C with different counter ions. Copyright @ 2017 The Royal Society of Chemistry. Reprinted with permission from Polymer Chemistry.[27]

To examine the influence of different counter ions, the respective hexamethyldisilazide lithium, sodium, potassium, and cesium salts were used to form the sulfonamide initiator. Importantly, lithium can be used as a counter ion for azaanionic polymerization, while the oxyanionic polymerization with lithium as counter ions is too slow to be relevant.[6, 10, 18, 69] According to the Pearson HSAB theory (charge to size ratio),[70-71] oxygen and lithium are very hard ions, hampering propagation in oxyanionic polymerization. The rate of polymerization increases thus concomitantly with increasing size of the counter ion.[6, 10, 69] For azaanionic polymerization, on the other hand, propagation takes place independent of which counter ion is employed (Figure 1.3C).[27] The azaanion, with the negative charge distributed over the whole sulfonamide-

structure, is considerably softer than the oxyanion. The propagation rates of activated aziridines are only slightly affected by the nature of the counter ion, proving the versatility of the azaanionic polymerization of aziridines under different reaction conditions.

1.9 Reactivity Ratios

In copolymerizations, the reactivity of each comonomer is described by the reactivity ratios. The reactivity ratios are listed for many comonomer pairs and are useful parameters for radical copolymerizations. They describe the probability of monomer-incorporation and can be calculated for different monomer combinations.[9, 72]

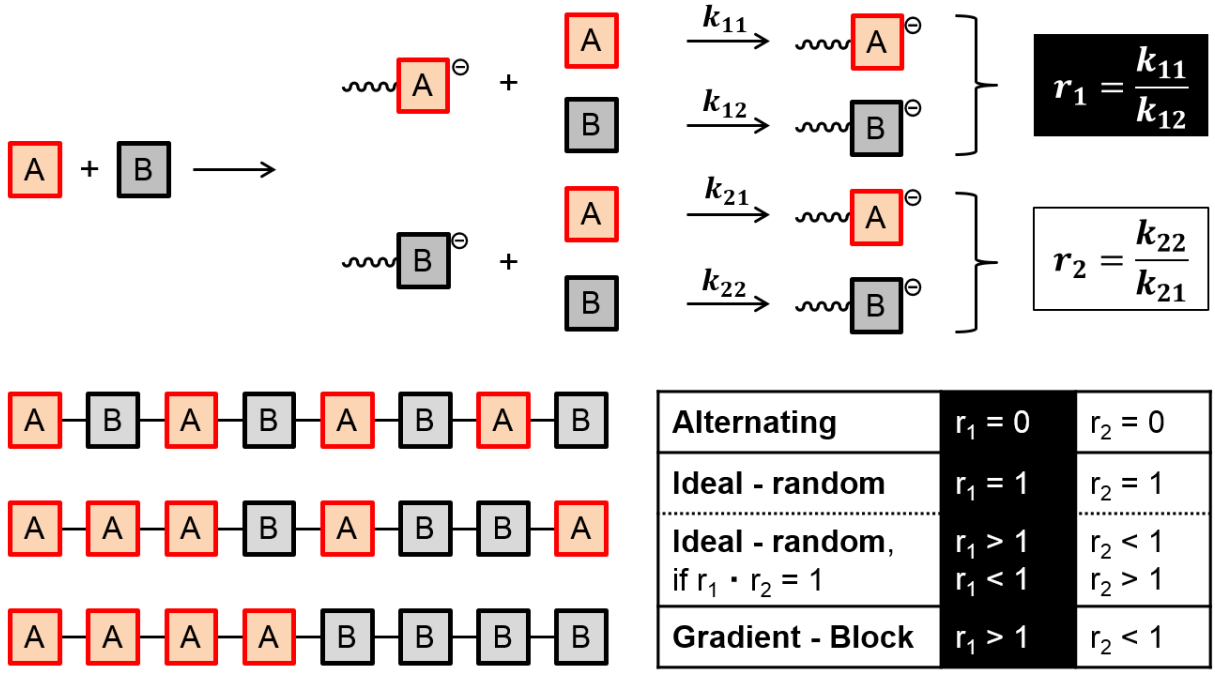

Figure 1.4. The relation between propagation rates and reactivity ratios for all possible copolymerizations in anionic polymerization.

As depicted in Figure 1.4, two monomers, A and B, can react in four different ways with each other, depending on which monomer is present at the growing chain ends. For those four possibilities, four different propagation rates (k_{11}, k_{12}, k_{21} and k_{22}) can be determined. The reactivity ratios are the correlations within the rates of the same monomer, also called *r*-parameters (r_1 and r_2). If both values are close to zero, alternating copolymers are obtained, as every monomer prefers the other monomer over itself ($k_{12} >> k_{11}$). If both monomers do not have any preference, random – also called ideal – copolymers are the result, exhibiting reactivity ratios (or their product) around one ($k_{12} \approx k_{11}$). Finally, if one monomer favors itself, its *r*-parameter is

greater than one ($k_{11} >> k_{12}$). If additionally, the other monomer prefers the first monomer, with the reactivity ratio smaller than one ($k_{21} >> k_{22}$), gradient to even block-like structures are obtained (Figure 1.4).[9, 72]

Compared to radical polymerizations, in anionic polymerizations the counter ion and the solvent can change the monomer incorporation significantly. Therefore, reactivity ratios in LAP are always specified for the whole system. Nevertheless, reactivity ratios are also gaining interest for anionic polymerizations and several publications already list values of well-known techniques, like carb- and oxyanionic polymerizations.[61, 65, 73-74] As the mechanism of anionic polymerization differs from radical polymerization, the complete conversion time is taken into account, not only the first five percent of conversion. To determine reactivity ratios for LAP, several copolymerizations with different monomer ratios of only two monomers are carried out and are evaluated by different methods.[26, 75-77]

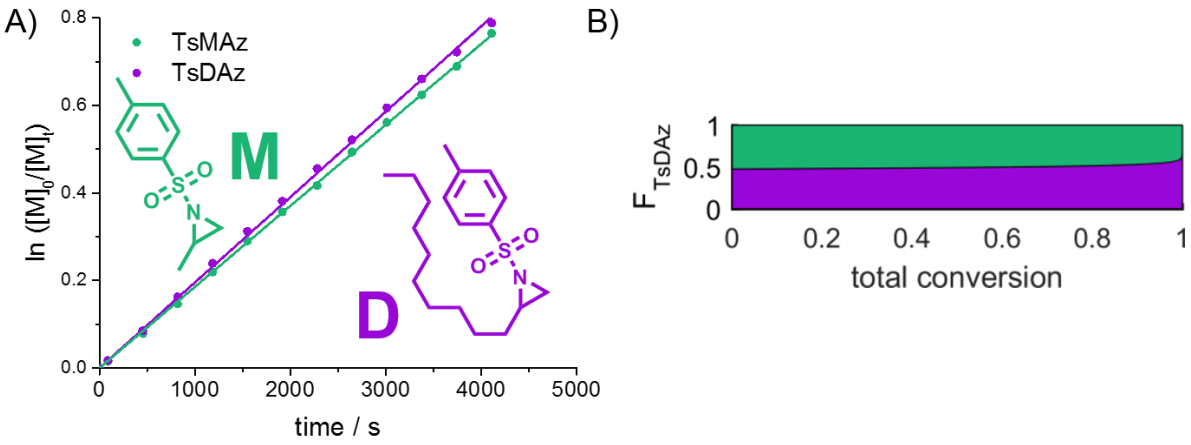

Figure 1.5. A) Kinetic plots of $\ln([M]_0/[M]_t)$ *vs.* time for the azaanionic copolymerization of TsMAz (M) and TsDAz (D). C) Incorporation probability of TsDAz (F_{TsDAz}) *vs.* total conversion: Final microstructure of the random copolymer. Copyright @ 2018 WILEY-VCH Verlag GmbH & Co. KGaA. Reprinted with permission from Angewandte Chemie International Edition.[26]

For the azaanionic polymerization the reactivity ratios of TsMAz (M, green) and TsDAz (D, purple) were determined *via in situ* ^{1}H NMR kinetics in different ratios (monomer ratio of 50:50 in Figure 1.5A). Their ideal random copolymerization was proven with r(TsMAz) = 1.08 and r(TsDAz) = 0.98 and their product r(TsMAz) · r(TsDAz) = 1.05 (Kelen-Tüdös).[26] Additionally the final microstructure (comonomer distribution along the polymer chain) was analyzed (Figure 1.5B).[78-79] Consequently, the influence of the activating group surpasses the ring-substituents drastically. The minuscule deviation is justified by the steric hindrance of the decyl-chain, slightly decreasing its *r*-parameter.

1.10 Controlling the Microstructure by Monomer Reactivity

Monomer sequence distribution is important for the materials properties of copolymers. A random or a gradient distribution of comonomers along the polymer backbone can influence mechanical and thermal properties. In ionic polymerizations care must be taken to ensure that the combination of comonomers still allows a copolymerization of both monomers and does not lead to termination of the chain growth (due to the chain end reactivity). As mentioned above, the electron-withdrawing effect of the activating sulfonyl group influences the reactivity of the aziridine ring with respect to nucleophilic attack. The chemical shift of the ring-protons of sulfonyl aziridines are a direct measure for the comonomer reactivity, due to the electron withdrawing effect of the substituents, which influence the electrophilicity of the monomers. Also, ^{15}N NMR-spectra prove the changing electrophilicity of the monomers directly. This effect was recently used by our group to prepare multi-gradient copolymers by the copolymerization of up to five monomers and proven by real-time ^{1}H NMR spectroscopy in one-pot reactions.[39] This fine-tuning of comonomer reactivities is rarely found in ionic polymerizations, as the reactivity of the monomers change by the choice of the sulfonyl aziridine, but all of the reported monomers still undergo copolymerization. In contrast, styrene derivatives that carry different electron withdrawing groups do not offer such a diversity regarding one-pot multi-block synthesis. Thus, the monomer combination allows access to random, gradient or almost block-like structures based on sulfonyl aziridines (Figure 1.6).[39]

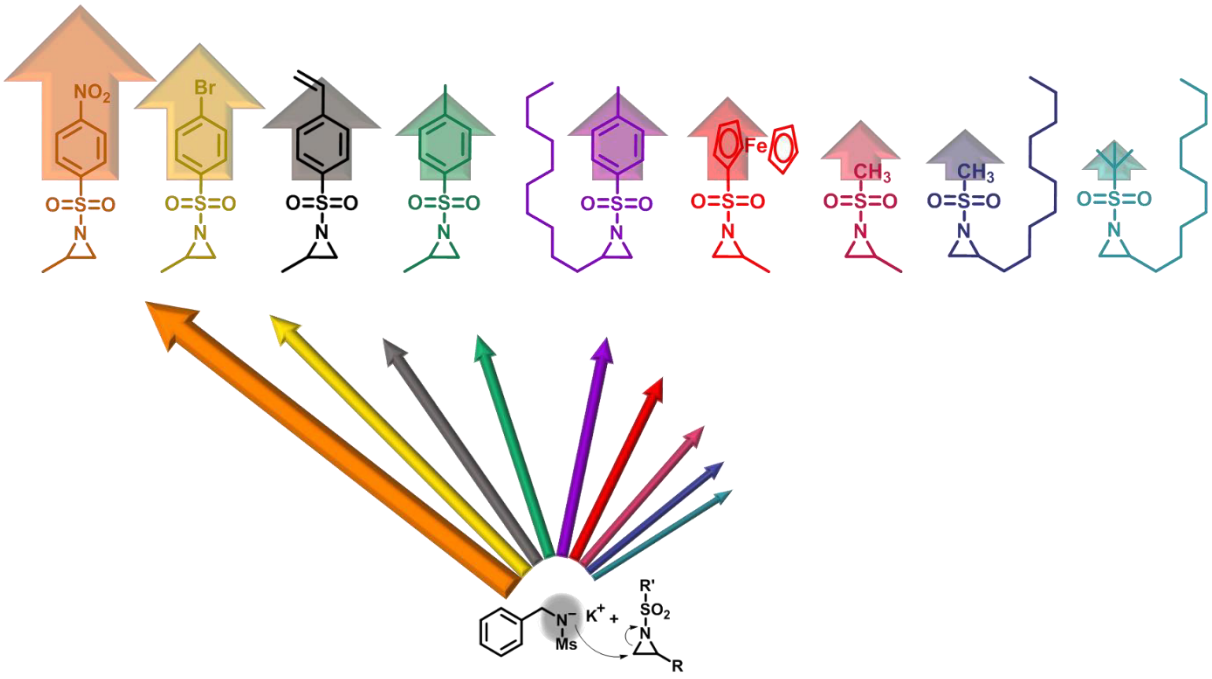

Figure 1.6. Order of reactivity of the examined monomers from NMR-kinetics. Copyright @ 2018 WILEY-VCH Verlag GmbH & Co. KGaA. Reprinted with permission from Macromolecular Rapid Communications.[39]

The copolymerization studies clearly show that the incorporation is mainly affected by the electron withdrawing effect of the activating group (represented in the size of the arrows in Figure 1.6). The stronger this effect, the faster the polymerization kinetics, and the more it is incorporated at the beginning of the growing copolymer. Interestingly, the substituent at the aziridine-ring has an almost negligible influence on the propagation rates (for *n*-alkyl chains). The trend allows making predictions of the copolymerization behavior of two (or more) monomers, while keeping the polydispersities low. For copolymers prepared from a copolymerization of BsMAz and MsMAz, two glass transition temperatures were detected in the DSC, proving a phase separation in the bulk, due to the block-like monomer distribution. DFT-calculations of the electrophilicity indices (ω^+) supports these empirically determined comonomer reactivities, with BsMAz (2.22 eV) > TsMAz (1.98 eV) > MsMAz (1.25 eV). Contrarily, the nucleophilicity (ω^-) of the azaanion at the growing chain end changes only *ca*. 0.14 eV, proving that the crucial factor which determines the incorporation rate is the monomer reactivity, and not the azaanion nucleophilicity.

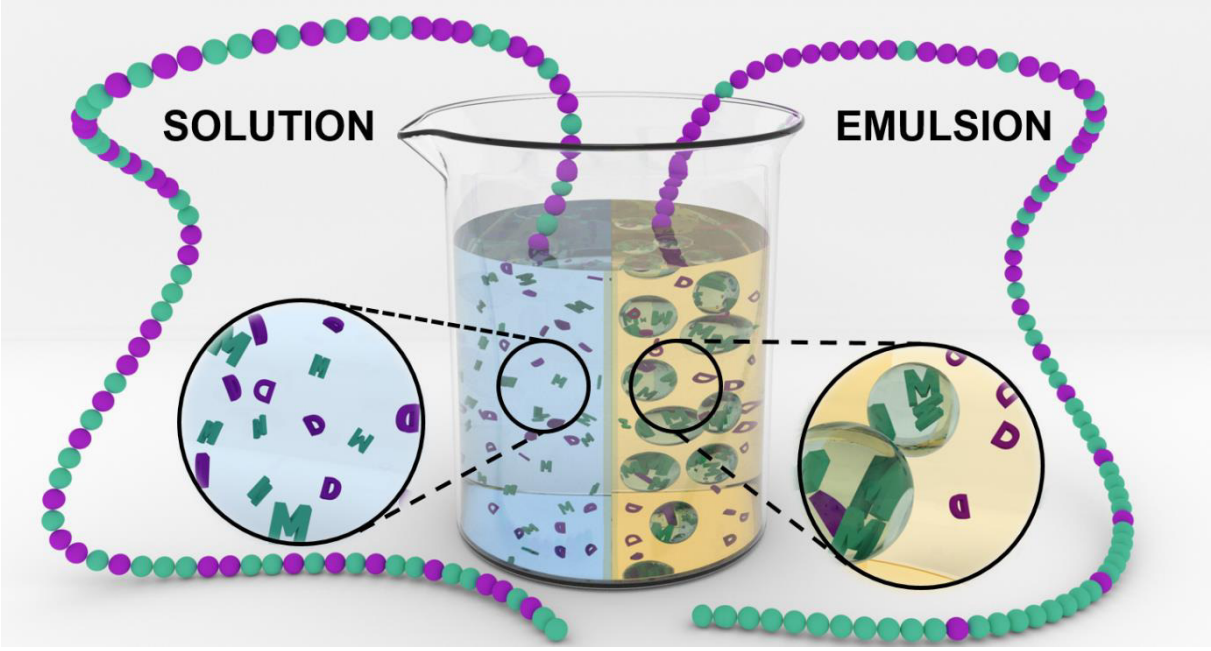

Figure 1.7. The selective solubility of two monomers in a DMSO/cyclohexane emulsion forces the production of controllable gradient copolymers. Copyright @ 2018 WILEY-VCH Verlag GmbH & Co. KGaA. Reprinted with permission from Angewandte Chemie International Edition.[26]

Besides the electrophilicity adjustment of comonomers to control their propagation rates, also a physical approach by selected solubilities was recently presented by our group. As a proof of a general concept for living copolymerizations, we chose the already mentioned *N*-tosylated monomers, TsMAz (M, green) and TsDAz (D, purple), differing only in their ring-substituent, which undergo an ideal random copolymerization in solution. When separated from each other by an

emulsion consisting of DMSO-droplets (blue) – to dissolve TsMAz - in cyclohexane (yellow) – to dissolve TsDAz - as the continuous phase (Figure 1.7 on the right).[26] The initiator and the growing poly(aziridine) chains are exclusively soluble in the DMSO compartments.[26-27] Therefore, the monomer feed is only determined by the monomers inside the DMSO-compartments leading to gradient copolymers from the copolymerization in emulsion, in contrast to the ideal random copolymers obtained in solution (see Figure 1.7, on the left and Figure 1.5).[26] In addition, the distribution gradient was adjusted by variation of continuous to dispersed phase. This is represented in apparent reactivity ratios, which are r_{app}(TsMAz) = 4.98 and r_{app}(TsDAz) = 0.20 in case of a 1:20-DMSO/cyclohexane emulsion, revealing the formation of strong gradient copolymers.[74, 77, 80] Their copolymerization behavior was once more monitored with real-time ^{1}H NMR-spectroscopy and evaluated by the numerical solution of the differential Mayo-Lewis equation to depict the microstructure.[74, 79] This is the first example (especially for LAP) where copolymerization behavior was changed by compartmentalization in an emulsion.

1.11 Poly(ethyleneimine)-Derivatives (Desulfonylation of PAz)

The deprotection of poly(aziridine)s to obtain the respective poly(amine)s is of high interest, for applications like gene transfection or the use as polyelectrolytes.[81] LPEI is produced from poly(oxazoline) (POx) (see Scheme 1.2), but the CROP of oxazolines lacks the degree of control achieved for PAz, and additionally suffers from an incomplete acidic hydrolysis afterwards to reveal LPEI.[82-85]

In contrast, poly(sulfonamide)s are accessible in large chemical variety *via* LAP. However, few papers describe the desulfonylation in detail, in spite of many published strategies for low molecular weight sulfonamides.[86-87] The major challenge for desulfonylation of PAz to the respective poly(amine)s is the change of solubility. The (mostly) hydrophobic poly(sulfonamide)s are transferred into (mostly very) hydrophilic poly(amine)s, making the choice of solvent crucial. Since many desulfonylation reactions need harsh conditions, chain scission might occur, which would ruin any sophisticated macromolecular architecture.

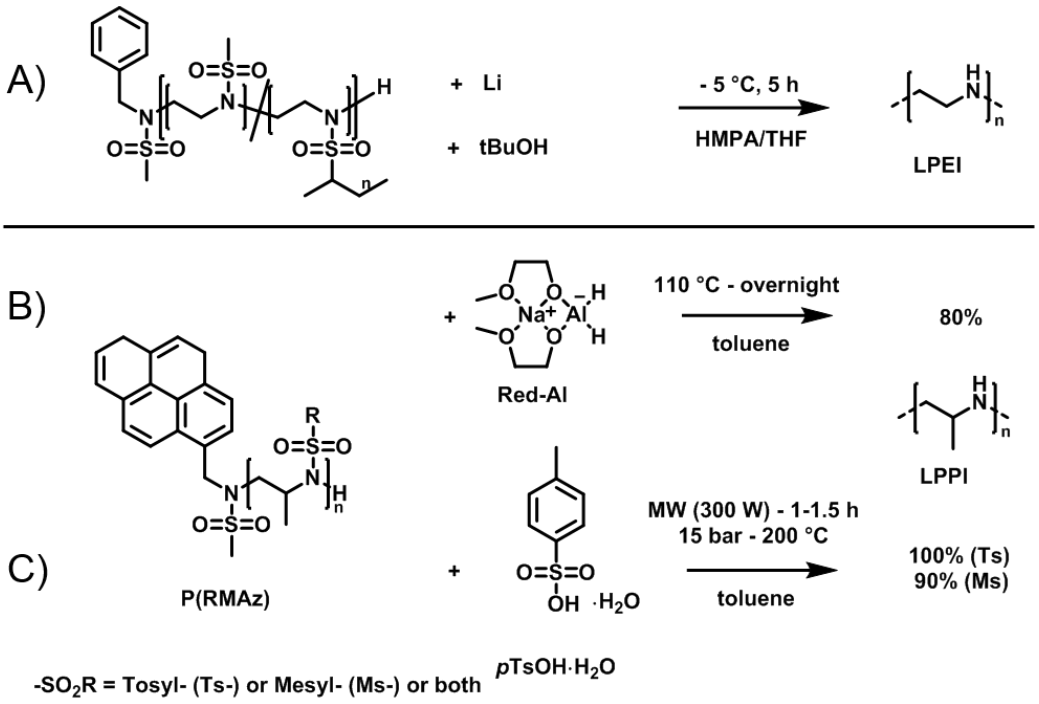

Scheme 1.15. Deprotection methods for PAz: A) Reductive deprotection, using elemental lithium in HMPA/THF. B) Reductive deprotection, using Red-Al in toluene. C) Acidic hydrolysis, using *p*TsOH in toluene under microwave irradiation.

As discussed in Chapter 7, promising deprotection methods such as electrolysis,[87] sodium naphathalenide (NaNp)[86-87] and samarium(II) iodide (SmI_2)[86-91] did not yield the desired desulfonylated PAz, so far. According to Bergman and Toste, a successful desulfonylation was achieved by LiNp.[15] However, no spectral analyses or molecular weight distributions of the obtained structures were given. In another approach from our group, tosylamides were cleaved by acidic hydrolysis with hydrobromic acid (HBr) and phenol.[18] In spite of the harsh reaction conditions, the method was reported to be successful. Later, we were able to remove tosylamides with sodium bis(2-methoxyethoxy)aluminiumhydride (Red-Al) to ca 80% (Scheme 1.15B, Chapter 7).[17] Rupar and coworkers were able to prepare LPEI under reductive conditions, using elemental lithium (Li), with *tert*-butanol (*t*-BuOH) in hexamethylphosphoramide (HMPA) and THF at low temperatures. (Scheme 1.15A).[20] As mentioned before, solubility issues are challenging and therefore complete characterization was not feasible, especially for longer polymers. We recently proved a much simpler approach for desulfonylation by adapting a protocol for the acidic hydrolysis of poly(oxazoline)s under microwave irradiation.[87, 92] With this method, deprotection of P(TsMAz) produced 100% desulfonylated LPPI, while for P(MsMAz) about 90% deprotection was achieved (Scheme 1.15C, Chapter 7). The solubility problems were bypassed by using *p*-toluenesulfonic acid (as monohydrate) (*p*TsOH), suspended in toluene along with the polymer. As no more additives were involved, purification was achieved by filtration over an ion exchange resin. This represents a fast and easy deprotection procedure without involving any toxic

substances (including metals). However, chain scission cannot be completely ruled out and still needs further investigation. In general, LPEI-alternatives derived from poly(sulfonamide)s are promising materials for a variety of applications, as they can be easily combined with other anionic techniques to obtain a variety of copolymers and functionalities.[18]

1.12 Applications of PEI

Over the last few decades, PEI has received tremendous attention by researchers due to their extensive application in gene delivery and CO_2 capture. PEIs are interesting mainly due to their high amine density, which enables them to complex with and condense the negatively charged DNA and RNA and to maintain a high affinity to carbon dioxide.

In gene delivery, PEI is used to deliver nucleic acids, such as DNA, and nucleic acids drugs into the host cell where they can be multiplied and studied further or used for therapeutic purposes. PEI, which is fully protonated under physiological conditions (pH 7.3), complexes with and envelops the anionic charge of nucleic acid drugs *via* electrostatic interactions to form nanoparticles referred to as polyplexes (Figure 1.8).[84-85, 93-106] Depending on the structure of the PEI polymer used (i.e. molar mass, degree of branching), these polyplexes show varied transfection efficiencies, resistance against degrading nucleases during circulation in blood, and endosomal release.[85, 107-110] It has been reported that the higher the molar mass and cationic charge density, the stronger the electrostatic interactions between PEI and nucleic acid drugs, and thus the more stable the polyplexes and higher transfection efficiencies.[109] Although PEI has shown different levels of cytotoxicity depending on the characteristics of the polymer, PEI offers a much safer and cheaper alternative to the virus-mediated and physical transfection methods.[97, 111] To date, linear PEI is clinically preferred over branched PEI due to its relatively low cytotoxicity, and acceptable biocompatibility. Moreover, LPEI can be easily conjugated to and/or functionalized with other moieties to adopt additional properties.[84, 112]

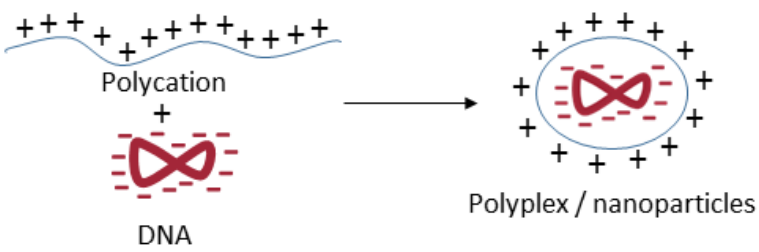

Figure 1.8. PEI-DNA polyplex formation.

Several functionalizations and modifications have been performed on PEI to alleviate its cytotoxicity, and to improve its biocompatibility and gene transfection efficiency.[95, 101, 113-118] Wang and coworkers prepared low molecular weight PEI conjugated pluronic copolymers using pluronics (PEO-PPO-PEO triblock copolymer) of different molecular weights and hydrophilic-lipophilic balance (HLB), and studied their gene transfection efficiency in C2C12 myoblasts and CHO cells *in vitro,* and in dystrophic *mdx* mice *in vivo.*[119] They showed that PEI conjugated pluronic copolymers prepared from 2000 to 5000 Da molecular weight pluronics with intermediate HLB (12-23) and low molecular weight PEI had enhanced gene transfection efficiency and lower cytotoxicity compared to PEI 25k. In the same light, Yoon and coworkers synthesized a ternary complex consisting of DNA, degradable disulfide cross-linked PEI and sodium hyaluronate, and showed that the formed complex had a high transfection efficiency comparable, if not higher, to that of Lipofectamine 2000, a common commercially available transfection reagent.[120]

Recent literature has focused on the use of PEI in various cancer therapies. [95, 121-122] Oupicky and coworkers have recently developed a cyclam-modified PEI (PEI-C) by functionalizing PEI with a CXCR4-binding cyclam derivative. CXCR4 is a chemokine receptor that significantly influences cancer cell invasion and metastasis. After being tested both *in vitro* and *in vivo*, PEI-C showed efficient anticancer activity against metastatic breast cancer.[122] Equally noteworthy, Luo and coworkers reported a non-toxic and efficient PEI system to deliver siRNA molecules into the heart (Figure 1.9).[123] After neutralizing PEI by replacing the primary amino groups of PEI with neutral hydrazide (HYD) groups, Luo and coworkers successfully utilized it to cross-link and deliver siRNA molecules in a heart of a zebrafish with notable biocompatibility *in vitro,* and a remarkable tissue uptake and gene silencing efficiency *in vivo*.

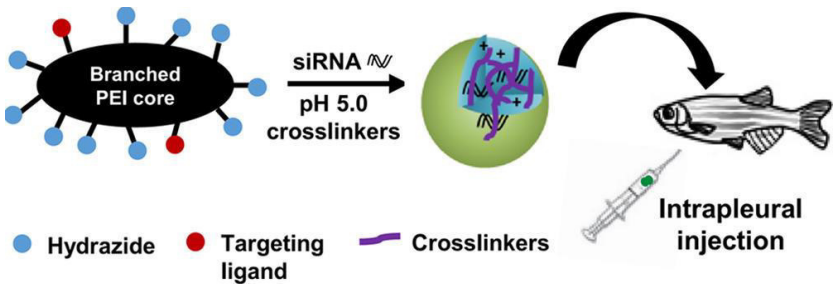

Figure 1.9. PEI-HYD-siRNA nanoparticles delivery in the adult zebrafish heart. Copyright @ 2016 The American Chemical Society. Reprinted with permission from ACS Applied Materials & Interfaces.[123]

In addition to being used in various cancer therapies, quaternized PEI has also been reported to have antimicrobial/antiviral properties.[117, 124-130] It was first hypothesized that poly (quaternized amine) deactivated and killed bacteria via the leaching mechanism, where the quarternary oniums

(ammonium and pyridium) displaced the bacteria cell wall countercations (i.e. Mg^{2+}, Ca^{2+}) and interrupted its phospholipid bilayer structure to disintegrate the cell.[129] On the other hand, Bieser and coworkers later proposed the phospholipid sponge effect mechanism, which showed that anionic phospholipids of a bacteria cell wall could be drawn and trapped into the polymer matrix, thus exposing and killing the bacteria cell. The later hypothesis was recently further evidenced by Jason and coworkers who synthesized a series of benzophenone substituted quaternized PEI thin films with varied cross-linking densities and studied their respective antimicrobial activity (Figure 1.10).[125] In support of the phospholipid sponge effect, highly cross-linked PEI thin films showed reduced antimicrobial activity due to their reduced porosity, surface charge density, and hydrophobicity.

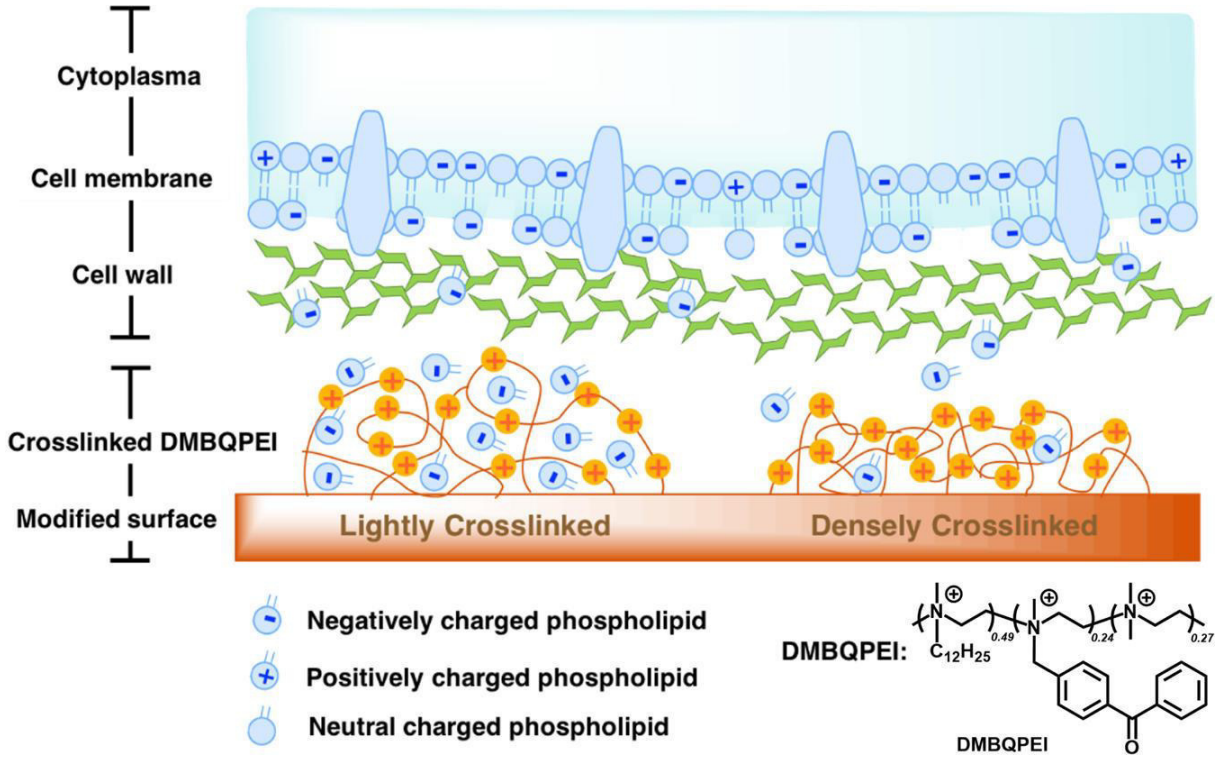

Figure 1.10. The phospholipid sponge effect illustration (DMBQPEI = Quaternized PEI). Copyright @ 2017 The American Chemical Society. Reprinted with permission from ACS Applied Materials & Interfaces [125]

PEI is also used in CO_2 capture, where it is impregnated into or covalently tethered on a mesoporous matrix surface to increase the adsorption capacity of CO_2.[131-140] Historically, PEI was first used to prepare a solid sorbent that can remove CO_2 from space shuttles by NASA.[133, 141] PEI-based solid adsorbents are more preferable to the previously used lithium hydroxide (LiOH) based adsorbents as they are easily regenerated, reducing storage occupation as well as the space shuttle's launch weight. Moreover, these solid PEI adsorbents also have a high advantage

over membrane and liquid amine solution CO_2 separation as they are relatively cheap to make, do not require the pressurization of CO_2-rich streams, and facilitate the disposal of the resulting corrosive carbamates. More recently, Jones and coworkers synthesized hyperbranched aminosilica (HAS) adsorbents with different amine loadings via the ring-opening polymerization of aziridine in presence of a mesoporous silica support (Scheme 1.16), and showed that the higher the PEI loading on the adsorbent, the higher the capacity of that adsorbent to capture CO_2.

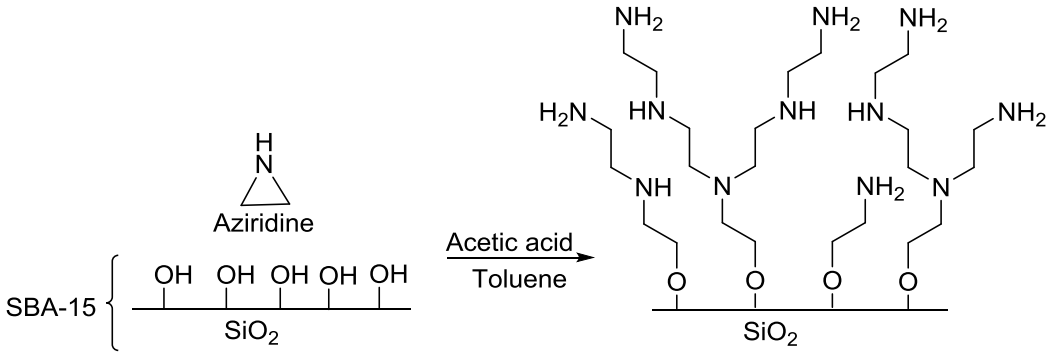

Scheme 1.16. Hyperbranched aminosilica synthesis.[142]

Besides gene delivery and CO_2 capture, PEIs find applications in several other and industrial processes such as the flocculation of negatively charged fibers in paper-making industries,[143-145] metal chelation in waste water treatments,[146] and as additives for inkjet paper production,[84] and as electron injection layers in organic light-emitting diodes.[147-148]

1.13 List of Abbreviations

A-AROP	Azaanionic ring-opening polymerization
ACN	Acetonitrile
AG	Activation group
AROP	Anionic ring-opening polymerization
ARTP	Atom-transfer radical-polymerization
BnBis(NHMs)	*N,N'*-(1,4-Phenylenebis(methylene))dimethanesulfonamide
BH_3-SMe_2	Borane dimethyl sulfide complex
BnNHMs	*N*-Benzyl-methanesulfonamide
BnNHTs	*N*-Benzyl-4-methylbenzenesulfonamide
$BnEt_3N^+Cl^-$	Benzyltriethylammoniumchloride
BsMAz	2-Methyl-*N*-brosylaziridine
BuLi	Butyllithium
CLRP	Controlled/living radical polymerization
CROP	Cationic ring-opening polymerization
DBU	1,8-Diazabicyclo[5.4.0]undec-7-ene
DCM	Dichloromethane
DFT-calculations	Density functional theory-calculations
DMF	*N,N*-Dimethylformamide
DMAP	4-(Dimethylamino)-pyridin
DMBQPEI	Quaternized PEI
DMSO	Dimethylsulfoxide
DNA	Deoxyribonulceic acid
D_p	Degree of polymerization
DSC	Differential scanning calorimetry
EEETsAz	2-((1-Ethoxyethoxy)ethyl)-*N*-tosylaziridine
EEGE	Ethoxy ethyl glycidyl ether
EO	Ethylene oxide
EsMAz	2-Methyl-*N*-esylaziridine = 2-Methyl-*N*-(ethylsulfonyl)aziridine
EtOH	Ethanol
EWD	Electron withdrawing
fcMAz	2-Methyl-*N*-(ferrocenylsulfonyl)aziridine
HAS	hyperbranched aminosilica
*hb*PEI	Hyperbranched poly(ethyleneimine)
HBr	Hydrobromic acid
HCl	Hydrochloride acid

HLB	Hydrophilic lipophilic balance
HMPA	Hexamethylphosphoramide
HSAB	Hard and soft (Lewis) acids and bases
HYD	Hydrazide
^{i}Bu	Isobutyl
iPrOH	Isopropanol
^{i}Pr	isopropyl
KHMDS	Potassium bis(trimethylsilyl)amide
K_2CO_3	Potassium carbonate
LAP	Living anionic polymerization
linPG	Linear poly(glycerol)
LiOH	Lithium hydroxide
LPEI	Linear poly(ethyleneimine)
MALDI-TOF	Matrix-assisted laser desorption/ionization-Time of flight
MeCN	Acetonitrile
MEETsAz	2-((1-Ethoxyethoxy)methyl)-*N*-tosylaziridine
MeOH	Methanol
MsAz	*N*-Mesylaziridine
MsCl	Mesylchloride
MsDAz	2-Decyl-*N*-mesylaziridine
MsMAz	2-Methyl-*N*-mesylaziridine
MsO-(en)-Az	2-Octenyl-*N*-mesylaziridine
MTBD	7-Methyl-1,5,7-triazabicyclo[4.4.0]dec-5-ene
NaOH	Sodium hydroxide
NaNp	Sodium naphathalenide
NBS	*N*-Bromsuccinimid
NEETsAz	2-((1-Ethoxyethoxy)nonyl)-*N*-tosylaziridine
NHC	*N*-Heterocyclic carbenes
NMP	Nitroxide mediated radical polymerization
NMR-spectroscopy	Nuclear magnetic resonance spectroscopy
NsMAz	2-Methyl-*N*-nosylaziridine
OROP	Organocatalytic ring-opening polymerization
PAz	Poly(aziridine)
PEG	Poly(ethylene glycol)
PEI	Poly(ethyleneimine)
POx	Poly(oxazoline)
Py	Pyridine

PTAB	Trimethylphenylammonium tribromide
*p*TsOH	*p*-Toluenesulfonic acid
PyNHMs	*N*-Pyrene-methanesulfonamide
RAFT	Reversible addition-fragmentation chain transfer
Red-Al	Sodium bis(2-methoxyethoxy)aluminiumhydride
RNA	Ribonucleic acid
ROP	Ring-opening polymerization
^{s}BusAz	*N*-*sec*-Busylaziridine = *N*-(*sec*-Butylsulfonyl)aziridine
SEC	Size-exclusion chromatography
siRNA	small interfering RNA
SmI_2	Samarium(II) iodide
ssNMR	solid state NMR
StMAz	2-Methyl-*N*-(4-styrenesulfonyl)aziridine
t-BuOH	*tert*-Butanol
t-Bu-P_4	1-*tert*-Butyl-4,4,4-tris-(dimethylamino)-2,2-bis[tris-(dimethylamino)phos-phoranylidenamino]-2Λ^5,4Λ^5-catenadi(phosphazene)
^{t}BusDAz	2-Decyl-*N*-*tert*-busylaziridine
TEA	Triethylamine
TGA	Thermogravimetric analysis
THF	Tetrahydrofuran
TiPP	Verkade's base proazaphosphatrane (P(*i*-PrNCH$_2$CH$_2$)$_3$N)
TMG	*N,N,N',N'*-Tetramethylguanidine
TsAz	*N*-Tosylaziridine
TsCl	Tosylchloride
TsDAz	2-Decyl-*N*-tosylaziridine
TsMAz	2-Methyl-*N*-tosylaziridine
$TsNH_2$	*p*-Toluenesulfonamide
TsPhAz	2-Phenyl-*N*-tosylaziridine
Ts-ωPrOHAz	2-*ω*-propanol-*N*-tosylaziridine
ZROP	Zwitterionic ring-opening polymerization

1.14 References

1. Szwarc, M., *Nature* **1956,** *178*, 1168.
2. Hirao, A.; Goseki, R.; Ishizone, T., *Macromolecules* **2014,** *47* (6), 1883-1905.
3. Frey, H.; Ishizone, T., *Macromolecular Chemistry and Physics* **2017,** *218* (12), 1700217
4. Leibig, D.; Morsbach, J.; Grune, E.; Herzberger, J.; Müller, A. H. E.; Frey, H., *Chemie in unserer Zeit* **2017,** *51* (4), 254-263.
5. Nuyken, O.; Pask, S., *Polymers* **2013,** *5* (2), 361-403.
6. Herzberger, J.; Niederer, K.; Pohlit, H.; Seiwert, J.; Worm, M.; Wurm, F. R.; Frey, H., *Chemical Reviews* **2016,** *116* (4), 2170-2243.
7. Bijlard, A. C.; Wald, S.; Crespy, D.; Taden, A.; Wurm, F. R.; Landfester, K., *Advanced Materials Interfaces* **2017,** *4* (1).
8. Scharfenberg, M.; Wald, S.; Wurm, F. R.; Frey, H., *Polymers* **2017,** *9* (9), 422.
9. Odian, G., *Principles of Polymerization*. 4. ed.; John Wiley & Sons, Inc. : Hoboken, New Jersey, USA, **2004**.
10. Hadjichristidis, N.; Hirao, A., *Anionic Polymerization*. Springer Japan: Japan, **2015**; p 1082.
11. Hadjichristidis, N.; Iatrou, H.; Pispas, S.; Pitsikalis, M., *Journal of Polymer Science Part A: Polymer Chemistry* **2000,** *38* (18), 3211-3234.
12. Szwarc, M., Living polymers and mechanisms of anionic polymerization. In *Living Polymers and Mechanisms of Anionic Polymerization*, Springer: **1983**; pp 1-177.
13. Matyjaszewski, K.; Müller, A. H. E., *Controlled and Living Polymerizations: From Mechanisms to Applications*. John Wiley & Sons: Weinheim, Germany, **2009**; p 634.
14. Braunecker, W. A.; Matyjaszewski, K., *Progress in Polymer Science* **2007,** *32* (1), 93-146.
15. Stewart, I. C.; Lee, C. C.; Bergman, R. G.; Toste, F. D., *Journal of the American Chemical Society* **2005,** *127* (50), 17616-17617.
16. Jones, G. D.; Langsjoen, A.; NEUMANN, S. M. M. C.; Zomlefer, J., *The Journal of Organic Chemistry* **1944,** *9* (2), 125-147.
17. Rieger, E.; Manhart, A.; Wurm, F. R., *ACS Macro Letters* **2016,** *5* (2), 195-198.
18. Thomi, L.; Wurm, F. R., *Macromolecular Rapid Communications* **2014,** *35* (5), 585-589.
19. Wang, X.; Liu, Y.; Li, Z.; Wang, H.; Gebru, H.; Chen, S.; Zhu, H.; Wei, F.; Guo, K., *ACS Macro Letters* **2017,** *6* (12), 1331-1336.
20. Reisman, L.; Mbarushimana, C. P.; Cassidy, S. J.; Rupar, P. A., *ACS Macro Letters* **2016,** *5* (10), 1137-1140.
21. Hsieh, H.; Quirk, R. P., *Anionic polymerization: principles and practical applications*. CRC Press: **1996**.

22. Asami, R.; Khanna, S.; Levy, M.; Szwarc, M., *Transactions of the Faraday Society* **1962,** *58*, 1821-1826.
23. Li, Y.; Schadler, L.; Benicewicz, B.; Barner-Kowollik, C., *Handbook of RAFT Polymerization.* Wiley-VCH: Weinheim: **2008**.
24. Matyjaszewski, K., *Macromolecules* **2012,** *45* (10), 4015-4039.
25. Perrier, S. b., *Macromolecules* **2017,** *50* (19), 7433-7447.
26. Rieger, E.; Blankenburg, J.; Grune, E.; Wagner, M.; Landfester, K.; Wurm, F. R., *Angewandte Chemie International Edition* **2018,** *57*, DOI:10.1002/anie.201710417.
27. Rieger, E.; Gleede, T.; Weber, K.; Manhart, A.; Wagner, M.; Wurm, F. R., *Polym. Chem.* **2017,** *8* (18), 2824-2832.
28. Homann-Müller, T.; Rieger, E.; Alkan, A.; Wurm, F. R., *Polym. Chem.* **2016,** *7* (35), 5501-5506.
29. Steuerle, U.; Feuerhake, R., *Ullmann's Encyclopedia of Industrial Chemistry* **2001**.
30. Xu, J.; Li, X.; Chen, N., *Synthesis* **2010,** *2010* (20), 3423-3428.
31. Lin, Z.; Lu, P.; Hsu, C.-H.; Sun, J.; Zhou, Y.; Huang, M.; Yue, K.; Ni, B.; Dong, X.-H.; Li, X.; Zhang, W.-B.; Yu, X.; Cheng, S. Z. D., *Macromolecules* **2015,** *48* (16), 5496-5503.
32. Goethals, E.; Schacht, E.; Bruggeman, P.; Bossaer, P., Cationic polymerization of cyclic amines. ACS Publications: **1977**.
33. Wang, Z., *Hinsberg Reaction. Comprehensive Organic Name Reactions and Reagents*. John Wiley & Sons, **2010**; Vol. 316.
34. Xu, H.; Tian, H.; Zheng, L.; Liu, Q.; Wang, L.; Zhang, S., *Tetrahedron Letters* **2011,** *52* (22), 2873-2875.
35. Berry, M. B.; Craig, D., *Synlett* **1992,** *1992* (01), 41-44.
36. Catino, A. J.; Nichols, J. M.; Forslund, R. E.; Doyle, M. P., *Org Lett* **2005,** *7* (13), 2787-90.
37. Gontcharov, A. V.; Liu, H.; Sharpless, K. B., *Organic Letters* **1999,** *1* (5), 783-786.
38. Jeong, J. U.; Tao, B.; Sagasser, I.; Henniges, H.; Sharpless, K. B., *Journal of the American Chemical Society* **1998,** *120* (27), 6844-6845.
39. Rieger, E.; Alkan, A.; Manhart, A.; Wagner, M.; Wurm, F. R., *Macromolecular Rapid Communications* **2016,** *37* (10), 833-839.
40. Thomi, L.; Wurm, F. R., *Macromolecular Symposia* **2015,** *349* (1), 51-56.
41. O'Brien, P.; Huang, J., *Synthesis* **2006,** (3), 425-434.
42. Zhao, Y.; Sakai, F.; Su, L.; Liu, Y.; Wei, K.; Chen, G.; Jiang, M., *Advanced Materials* **2013,** (37), 5215-5256.
43. Kiesewetter, M. K.; Shin, E. J.; Hedrick, J. L.; Waymouth, R. M., *Macromolecules* **2010,** *43* (5), 2093-2107.
44. Naumann, S.; Dove, A. P., *Polymer Chemistry* **2015,** *6* (17), 3185-3200.

45. Pinaud, J.; Vijayakrishna, K.; Taton, D.; Gnanou, Y., *Macromolecules* **2009,** *42* (14), 4932-4936.
46. Raynaud, J.; Gnanou, Y.; Taton, D., *Macromolecules* **2009,** *42* (16), 5996-6005.
47. Raynaud, J.; Absalon, C.; Gnanou, Y.; Taton, D., *Journal of the American Chemical Society* **2009,** *131* (9), 3201-3209.
48. Bakkali-Hassani, C.; Rieger, E.; Vignolle, J.; Wurm, F. R.; Carlotti, S.; Taton, D., *Chem. Commun. (Camb)* **2016,** *52* (62), 9719-9722.
49. Bakkali-Hassani, C.; Rieger, E.; Vignolle, J.; Wurm, F. R.; Carlotti, S.; Taton, D., *European Polymer Journal* **2017,** *95*, 746-755.
50. Thomas, A.; Muller, S. S.; Frey, H., *Biomacromolecules* **2014,** *15* (6), 1935-54.
51. Alkan, A.; Klein, R.; Shylin, S. I.; Kemmer-Jonas, U.; Frey, H.; Wurm, F. R., *Polymer Chemistry* **2015,** *6* (40), 7112-7118.
52. Gleede, T.; Rieger, E.; Homann-Müller, T.; Wurm, F. R., *Macromolecular Chemistry and Physics* **2017**, 1700145.
53. McLeod, D. C.; Tsarevsky, N. V., *Macromol Rapid Commun* **2016,** *37* (20), 1694-1700.
54. Jang, H.-J.; Lee, J. T.; Yoon, H. J., *Polymer Chemistry* **2015,** *6* (18), 3387-3391.
55. Moon, H. K.; Kang, S.; Yoon, H. J., *Polym. Chem.* **2017,** *8* (15), 2287-2291.
56. Suzuki, T.; Kusakabe, J.-i.; Kitazawa, K.; Nakagawa, T.; Kawauchi, S.; Ishizone, T., *Macromolecules* **2010,** *43* (1), 107-116.
57. Ishizone, T.; Takata, T.; Kobayashi, M., *Journal of Polymer Science Part A: Polymer Chemistry* **2003,** *41* (9), 1335-1340.
58. Luo, D.; Li, P.; Li, Y.; Yang, M., *Journal of applied polymer science* **2010,** *118* (3), 1527-1533.
59. Alkan, A.; Thomi, L.; Gleede, T.; Wurm, F. R., *Polymer Chemistry* **2015,** *6* (19), 3617-3624.
60. Herzberger, J.; Leibig, D.; Liermann, J. C.; Frey, H., *ACS Macro Letters* **2016,** *5* (11), 1206-1211.
61. Leibig, D.; Seiwert, J.; Liermann, J. C.; Frey, H., *Macromolecules* **2016,** *49* (20), 7767-7776.
62. Obermeier, B.; Wurm, F.; Frey, H., *Macromolecules* **2010,** *43* (5), 2244-2251.
63. Natalello, A.; Werre, M.; Alkan, A.; Frey, H., *Macromolecules* **2013,** *46* (21), 8467-8471.
64. Leibig, D.; Lange, A.-K.; Birke, A.; Frey, H., *Macromolecular Chemistry and Physics* **2017,** *218* (12), 1600553.
65. Natalello, A.; Alkan, A.; von Tiedemann, P.; Wurm, F. R.; Frey, H., *ACS Macro Letters* **2014,** *3* (6), 560-564.
66. Natalello, A.; Hall, J. N.; Eccles, E. A.; Kimani, S. M.; Hutchings, L. R., *Macromol. Rapid Commun.* **2011,** *32* (2), 233-237.

67. Alkan, A.; Natalello, A.; Wagner, M.; Frey, H.; Wurm, F. R., *Macromolecules* **2014,** *47* (7), 2242-2249.
68. Becker, G.; Deng, Z.; Zober, M.; Wagner, M.; Lienkamp, K.; Wurm, F. R., *Polymer Chemistry* **2018,** *9* (3), 315-326.
69. Brocas, A.-L.; Mantzaridis, C.; Tunc, D.; Carlotti, S., *Progress in polymer science* **2013,** *38* (6), 845-873.
70. Holleman, A. F. W., E., *Lehrbuch der Anorganischen Chemie*. 34. ed. ed.; Walter de Gruyter Co.: Berlin, Germany, **1995**; Vol. 101.
71. Pearson, R. G., *Journal of the American Chemical Society* **1963,** *85* (22), 3533-3539.
72. Young, R. J.; Lovell, P. A., *Introduction to polymers*. CRC press: 2011.
73. Lee, B. F.; Wolffs, M.; Delaney, K. T.; Sprafke, J. K.; Leibfarth, F. A.; Hawker, C. J.; Lynd, N. A., *Macromolecules* **2012,** *45* (9), 3722-3731.
74. Blankenburg, J.; Wagner, M.; Frey, H., *Macromolecules* **2017,** *50* (22), 8885-8893.
75. Fineman, M.; Ross, S. D., *Journal of Polymer Science Part A: Polymer Chemistry* **1950,** *5* (2), 259-262.
76. Kelen, T.; Tüdös, F., *Journal of Macromolecular Science: Part A - Chemistry* **1975,** *9* (1), 1-27.
77. Jaacks, V., *Angewandte Chemie* **1967,** *79* (9), 419.
78. Mayo, F. R.; Lewis, F. M., *Journal of the American Chemical Society* **1944,** *66* (9), 1594-1601.
79. Skeist, I., *Journal of the American Chemical Society* **1946,** *68* (9), 1781-1784.
80. Wall, F. T., *J Am Chem Soc* **1941,** *63*, 1862-1866.
81. Taranejoo, S.; Liu, J.; Verma, P.; Hourigan, K., *Journal of Applied Polymer Science* **2015,** *132* (25), n/a-n/a.
82. Perevyazko, I.; Gubarev, A. S.; Tauhardt, L.; Dobrodumov, A.; Pavlov, G. M.; Schubert, U. S., *Polymer Chemistry* **2017,** *8* (46), 7169-7179.
83. Akinc, A.; Thomas, M.; Klibanov, A. M.; Langer, R., *J Gene Med* **2005,** *7* (5), 657-663.
84. Jaeger, M.; Schubert, S.; Ochrimenko, S.; Fischer, D.; Schubert, U. S., *Chemical Society Reviews* **2012,** *41* (13), 4755-4767.
85. Boussif, O.; Lezoualc'h, F.; Zanta, M. A.; Mergny, M. D.; Scherman, D.; Demeneix, B.; Behr, J.-P., *Proceedings of the National Academy of Sciences* **1995,** *92* (16), 7297-7301.
86. Alonso, D. A.; Andersson, P. G., *The Journal of Organic Chemistry* **1998,** *63* (25), 9455-9461.
87. Senboku, H.; Nakahara, K.; Fukuhara, T.; Hara, S., *Tetrahedron Letters* **2010,** *51* (2), 435-438.
88. Knowles, H. S.; Parsons, A. F.; Pettifer, R. M.; Rickling, S., *Tetrahedron* **2000,** *56* (7), 979-988.

89. Szostak, M.; Spain, M.; Procter, D. J., *Chemical Society Reviews* **2013,** *42* (23), 9155-9183.
90. Vedejs, E.; Lin, S., *The Journal of Organic Chemistry* **1994,** *59* (7), 1602-1603.
91. Goulaouic-Dubois, C.; Guggisberg, A.; Hesse, M., *The Journal of Organic Chemistry* **1995,** *60* (18), 5969-5972.
92. Kubrakova, I. V.; Formanovsky, A. A.; Mikhura, I. V., *Mendeleev Communications* **1999,** *9* (2), 65-66.
93. Li, T.; Wu, L.; Zhang, J.; Xi, G.; Pang, Y.; Wang, X.; Chen, T., *ACS applied materials & interfaces* **2016,** *8* (45), 31311-31320.
94. Pan, J.; Lyu, Z.; Jiang, W.; Wang, H.; Liu, Q.; Tan, M.; Yuan, L.; Chen, H., *ACS applied materials & interfaces* **2014,** *6* (16), 14391-14398.
95. Ding, X.; Wang, W.; Wang, Y.; Bao, X.; Wang, Y.; Wang, C.; Chen, J.; Zhang, F.; Zhou, J., *Molecular pharmaceutics* **2014,** *11* (10), 3307-3321.
96. Lo, Y.-L.; Sung, K.-H.; Chiu, C.-C.; Wang, L.-F., *Molecular pharmaceutics* **2013,** *10* (2), 664-676.
97. De Smedt, S. C.; Demeester, J.; Hennink, W. E., *Pharmaceutical research* **2000,** *17* (2), 113-126.
98. Pack, D. W.; Hoffman, A. S.; Pun, S.; Stayton, P. S., *Nature reviews Drug discovery* **2005,** *4* (7), 581.
99. de Ilarduya, C. T.; Sun, Y.; Düzgüneş, N., *European journal of pharmaceutical sciences* **2010,** *40* (3), 159-170.
100. Giron-Gonzalez, M. D.; Salto-Gonzalez, R.; Lopez-Jaramillo, F. J.; Salinas-Castillo, A.; Jodar-Reyes, A. B.; Ortega-Muñoz, M.; Hernandez-Mateo, F.; Santoyo-Gonzalez, F., *Bioconjugate chemistry* **2016,** *27* (3), 549-561.
101. Mintzer, M. A.; Simanek, E. E., *Chemical reviews* **2008,** *109* (2), 259-302.
102. Neu, M.; Fischer, D.; Kissel, T., *The journal of gene medicine* **2005,** *7* (8), 992-1009.
103. Raymond, C.; Tom, R.; Perret, S.; Moussouami, P.; L'Abbé, D.; St-Laurent, G.; Durocher, Y., *Methods* **2011,** *55* (1), 44-51.
104. Altuntaş, E.; Knop, K.; Tauhardt, L.; Kempe, K.; Crecelius, A. C.; Jäger, M.; Hager, M. D.; Schubert, U. S., *Journal of Mass Spectrometry* **2012,** *47* (1), 105-114.
105. Moghimi, S. M.; Symonds, P.; Murray, J. C.; Hunter, A. C.; Debska, G.; Szewczyk, A., *Molecular Therapy* **2005,** *11* (6), 990-995.
106. Thomas, M.; Klibanov, A. M., *Proceedings of the National Academy of Sciences* **2003,** *100* (16), 9138-9143.
107. Shim, M. S.; Kwon, Y. J., *Bioconjugate chemistry* **2009,** *20* (3), 488-499.
108. Bonnet, M.-E.; Erbacher, P.; Bolcato-Bellemin, A.-L., *Pharmaceutical research* **2008,** *25* (12), 2972.

109. Wightman, L.; Kircheis, R.; Rössler, V.; Carotta, S.; Ruzicka, R.; Kursa, M.; Wagner, E., *The journal of gene medicine* **2001,** *3* (4), 362-372.
110. Yin, H.; Kanasty, R. L.; Eltoukhy, A. A.; Vegas, A. J.; Dorkin, J. R.; Anderson, D. G., *Nature Reviews Genetics* **2014,** *15* (8), 541.
111. Kim, T. K.; Eberwine, J. H., *Analytical and bioanalytical chemistry* **2010,** *397* (8), 3173-3178.
112. Tauhardt, L.; Kempe, K.; Knop, K.; Altuntaş, E.; Jäger, M.; Schubert, S.; Fischer, D.; Schubert, U. S., *Macromolecular Chemistry and Physics* **2011,** *212* (17), 1918-1924.
113. Xie, L.; Tan, Y.; Wang, Z.; Liu, H.; Zhang, N.; Zou, C.; Liu, X.; Liu, G.; Lu, J.; Zheng, H., *ACS applied materials & interfaces* **2016,** *8* (43), 29261-29269.
114. Nguyen, H.; Lemieux, P.; Vinogradov, S.; Gebhart, C.; Guerin, N.; Paradis, G.; Bronich, T.; Alakhov, V.; Kabanov, A., *Gene Therapy* **2000,** *7* (2), 126.
115. Petersen, H.; Fechner, P. M.; Martin, A. L.; Kunath, K.; Stolnik, S.; Roberts, C. J.; Fischer, D.; Davies, M. C.; Kissel, T., *Bioconjugate chemistry* **2002,** *13* (4), 845-854.
116. Breunig, M.; Lungwitz, U.; Liebl, R.; Goepferich, A., *Proceedings of the National Academy of Sciences* **2007,** *104* (36), 14454-14459.
117. Milović, N. M.; Wang, J.; Lewis, K.; Klibanov, A. M., *Biotechnology and bioengineering* **2005,** *90* (6), 715-722.
118. Thomas, M.; Klibanov, A. M., *Proceedings of the National Academy of Sciences* **2002,** *99* (23), 14640-14645.
119. Wang, M.; Lu, P.; Wu, B.; Tucker, J. D.; Cloer, C.; Lu, Q., *Journal of Materials Chemistry* **2012,** *22* (13), 6038-6046.
120. Xu, P.; Quick, G. K.; Yeo, Y., *Biomaterials* **2009,** *30* (29), 5834-5843.
121. Kim, B.-K.; Kim, D.; Kwak, G.; Yhee, J. Y.; Kwon, I.-C.; Kim, S. H.; Yeo, Y., *ACS Biomaterials Science & Engineering* **2017,** *3* (6), 990-999.
122. Zhou, Y.; Yu, F.; Zhang, F.; Chen, G.; Wang, K.; Sun, M.; Li, J.; Oupický, D., *Biomacromolecules* **2018**.
123. Wang, F.; Gao, L.; Meng, L.-Y.; Xie, J.-M.; Xiong, J.-W.; Luo, Y., *ACS applied materials & interfaces* **2016,** *8* (49), 33529-33538.
124. Dhende, V. P.; Samanta, S.; Jones, D. M.; Hardin, I. R.; Locklin, J., *ACS applied materials & interfaces* **2011,** *3* (8), 2830-2837.
125. Gao, J.; White, E. M.; Liu, Q.; Locklin, J., *ACS applied materials & interfaces* **2017,** *9* (8), 7745-7751.
126. Haldar, J.; An, D.; de Cienfuegos, L. A.; Chen, J.; Klibanov, A. M., *Proceedings of the National Academy of Sciences* **2006,** *103* (47), 17667-17671.
127. Bieser, A. M.; Tiller, J. C., *Macromolecular bioscience* **2011,** *11* (4), 526-534.
128. Koplin, S. A.; Lin, S.; Domanski, T., *Biotechnology progress* **2008,** *24* (5), 1160-1165.

129. Kügler, R.; Bouloussa, O.; Rondelez, F., *Microbiology* **2005,** *151* (5), 1341-1348.
130. Lin, J.; Tiller, J. C.; Lee, S. B.; Lewis, K.; Klibanov, A. M., *Biotechnology Letters* **2002,** *24* (10), 801-805.
131. Choi, S.; Drese, J. H.; Jones, C. W., *ChemSusChem* **2009,** *2* (9), 796-854.
132. Hicks, J. C.; Drese, J. H.; Fauth, D. J.; Gray, M. L.; Qi, G.; Jones, C. W., *Journal of the American Chemical Society* **2008,** *130* (10), 2902-2903.
133. Li, P.; Ge, B.; Zhang, S.; Chen, S.; Zhang, Q.; Zhao, Y., *Langmuir* **2008,** *24* (13), 6567-6574.
134. Liu, F.-Q.; Wang, L.; Huang, Z.-G.; Li, C.-Q.; Li, W.; Li, R.-X.; Li, W.-H., *ACS applied materials & interfaces* **2014,** *6* (6), 4371-4381.
135. Wang, Q.; Luo, J.; Zhong, Z.; Borgna, A., *Energy & Environmental Science* **2011,** *4* (1), 42-55.
136. Xu, X.; Song, C.; Miller, B. G.; Scaroni, A. W., *Fuel processing technology* **2005,** *86* (14-15), 1457-1472.
137. Chaikittisilp, W.; Khunsupat, R.; Chen, T. T.; Jones, C. W., *Industrial & Engineering Chemistry Research* **2011,** *50* (24), 14203-14210.
138. MacDowell, N.; Florin, N.; Buchard, A.; Hallett, J.; Galindo, A.; Jackson, G.; Adjiman, C. S.; Williams, C. K.; Shah, N.; Fennell, P., *Energy & Environmental Science* **2010,** *3* (11), 1645-1669.
139. Sanz, R.; Calleja, G.; Arencibia, A.; Sanz-Pérez, E. S., *Journal of Materials Chemistry A* **2013,** *1* (6), 1956-1962.
140. Xu, X.; Song, C.; Andresen, J. M.; Miller, B. G.; Scaroni, A. W., *Energy & Fuels* **2002,** *16* (6), 1463-1469.
141. Satyapal, S.; Filburn, T.; Trela, J.; Strange, J., *Energy & Fuels* **2001,** *15* (2), 250-255.
142. Drese, J. H.; Choi, S.; Lively, R. P.; Koros, W. J.; Fauth, D. J.; Gray, M. L.; Jones, C. W., *Advanced Functional Materials* **2009,** *19* (23), 3821-3832.
143. Bayer, E.; Spivakov, B. Y.; Geckeler, K., *Polymer Bulletin* **1985,** *13* (4), 307-311.
144. Kobayashi, S.; Hiroishi, K.; Tokunoh, M.; Saegusa, T., *Macromolecules* **1987,** *20* (7), 1496-1500.
145. Von Zelewsky, A.; Barbosa, L.; Schläpfer, C., *Coordination chemistry reviews* **1993,** *123* (1-2), 229-246.
146. Bolto, B. A., *Progress in Polymer Science* **1995,** *20* (6), 987-1041.
147. Chen, H.-C.; Lin, S.-W.; Jiang, J.-M.; Su, Y.-W.; Wei, K.-H., *ACS applied materials & interfaces* **2015,** *7* (11), 6273-6281.
148. Stolz, S.; Zhang, Y.; Lemmer, U.; Hernandez-Sosa, G.; Aziz, H., *ACS applied materials & interfaces* **2017,** *9* (3), 2776-2785.

2. The Living Anionic Polymerization of Activated Aziridines: Systematic Study of Reaction Conditions and Kinetics

Elisabeth Rieger, Tassilo Gleede, Katja Weber, Angelika Manhart, Manfred Wagner, Frederik R. Wurm

Max Planck Institute for Polymer Research, Ackermannweg 10, 55128 Mainz, Germany

Parts of the kinetic measurements and the synthesis of the CsHMDS were performed by Tassilo Gleede. Parts of the kinetic measurements and chain extensions, the synthesis of BnBis(NHMs) and parts of the monomer syntheses were performed by Katja Weber. Parts of the monomers were synthesized by Angelika Manhart. NMR kinetic measurements were performed in collaboration with Manfred Wagner.

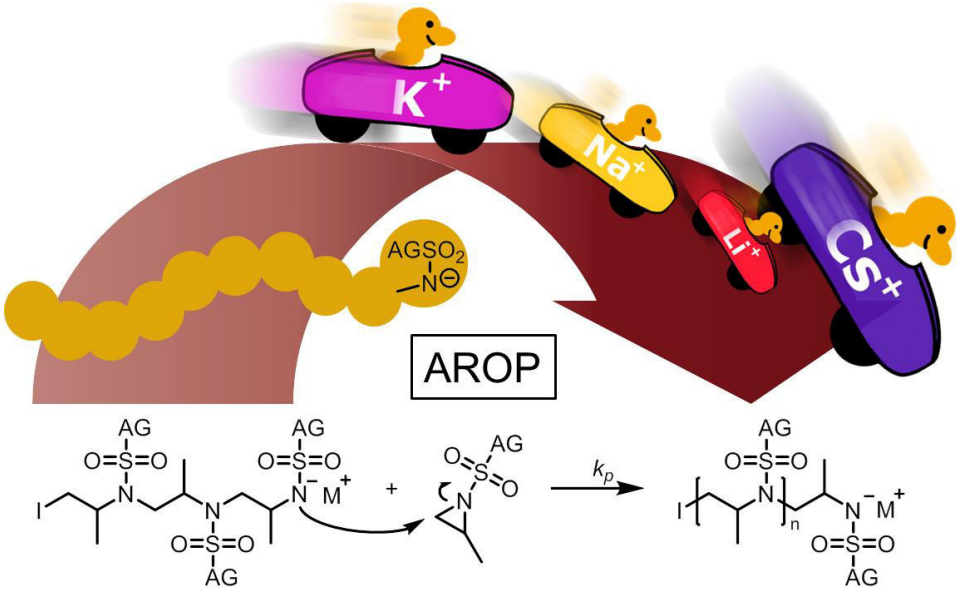

Keywords: Anionic Polymerization, Aziridine, Sulfonamide, Ring-Opening Polymerization, Azaanionic.

2.1 Abstract

"*A living race*" – polymerization kinetics of anionic polymerizations depends strongly on the solvent polarity and reactivity of the growing chain end. Both the carb- and oxyanionic polymerization is under control at the university lab and on the industrial level, however, no information for the *aza*-anionic polymerization of aziridines has been reported systematically. This work studies the polymerization of two activated aziridines (2-methyl-*N*-mesylaziridine (MsMAz) and 2-methyl-*N*-tosylaziridine (TsMAz)) by real-time ^{1}H NMR spectroscopy. This technique allows monitoring the consumption of the monomer precisely during the polymerization under different conditions (temperature, solvent, initiator and counter-ion variation). From the experimental data, propagation rate constants (k_p) were calculated and analyzed. The polymerization of MsMAz was monitored at different temperatures (20, 50 and100 °C). The increase of temperature increases the speed of polymerization, but keeps the living behavior. Furthermore, the influence of different solvents on the polymerization speed was examined, proving solvating solvents such as DMSO and DMF as the fastest solvents. Two different initiators, the potassium salts of *N,N'*-(1,4-phenylenebis(methylene))dimethanesulfonamide (BnBis(NHMs)), the first bifunctional initiator for the AROP of aziridines, and of *N*-benzyl-sulfonamide (BnNHMs) were compared. The variation of the counter ions Li^+, Na^+, K^+ and Cs^+ (generated from the respective bis(trimethylsilyl)amide salts) proved successful polymerization of both monomers with all counter ions. Slight variations have been detected in the order: $Cs^+ > Li^+ > Na^+ > K^+$, which is in strong contrast for the AROP of epoxides shows a strong gegeniondependent kinetic profile. This allows the use of commercially available initiators, such as BuLi for the synthesis of PAz. With these results in hand, the azaanionic polymerization can be used as a valuable tool in the family of anionic polymerization for the preparation of structurally diverse polysulfonamides and polyamines under a broad variety of conditions, while maintaining the living behavior.

2.2 Introduction

The knowledge of polymerization kinetics allows us to construct complex polymeric architectures by different polymerization techniques. 60 years after the discovery of the living anionic polymerization, their solvent, counter ion and temperature dependencies are taught in introductory polymer classes. Conditions are known for the carb- and oxyanionic polymerization.[1-3]

However, such detailed and fundamental investigations are missing for the living anionic ring-opening polymerization (AROP) of aziridines and will be presented in this work.

The azaanionic polymerization of activated aziridines was recently established.[4-9] To enable anionic polymerization of aziridines, the acidic proton at the nitrogen needs to be substituted by an activating group, *e.g.* a sulfonamide group (Scheme 2.1). To date, only such activated aziridines undergo anionic polymerization, but also a few other aziridine-containing polymers have been prepared and studied as functional polymers for postmodification.[10-14]

The AROP of aziridines allows us to prepare well-defined poly(ethylene imine) derivatives.[4, 9] We have developed new monomers and initiator-systems during the last few years, expanding this still rather unexplored approach to polysulfonamides and amines.[5-8, 15-16]

With a similar ring-strain of 111 kJ mol^{-1} for ethylene imine as for ethylene oxide (114 kJ mol^{-1}), the anionic ring-opening polymerization should be feasible.[17-18] In contrast to unsubstituted ethylene imine, which can only be polymerized *via* a cationic mechanism, leading to branched PEI (poly(ethylene imine)),[19] *N*-protected aziridines can also be polymerized anionically, due to their activating group. The sulfonamide substitutes the acidic proton at the aziridine and acts as an electron-withdrawing group. This results not only in the general possibility for anionic AROP, but further in different reactivities of the monomers, leading to sequential incorporation.[7]

Herein, 2-**m**ethyl-*N*-**m**e**s**yl-**az**iridine (MsMAz, **1**) and 2-**m**ethyl-*N*-**t**o**s**yl**az**iridine (TsMAz, **2**) were used to elucidate the polymerization kinetics under different conditions. The results from this study will allow us to use activated aziridines for the preparation of well-defined polymer architectures by anionic polymerization in the future.

2.3 Experimental Section

General procedure for the azaanionic polymerization. All Schlenk flasks were flame dried *in vacuo* at least three times, using the Schlenk technique, as for the following steps. All reactants (except the bis(trimethylsilyl)amide salts) were freeze-dried from benzene *in vacuo* for at least 4 h. The monomers and the initiator were dissolved in 2 and 1 mL anhydrous *N,N*-dimethylformamide (DMF). The bis(trimethylsilyl)amide salt was added quickly in argon-counter flow to the initiator-solution. From the initiator-solution the appropriate volume was added to the monomer solution. The mixture was stirred at the desired temperature and over the desired time (to ensure complete reaction: 18 h reaction time at 50 °C). The polymers were obtained as colorless powders after precipitation of the reaction mixture into 30 mL methanol and drying at reduced pressure. For chain extension experiments the polymerizations were carried out in analogy to the conventional procedure. After stirring the mixtures for at least 18 h, a 100 µL-sample was taken out for further analyses and the second monomer, in 1 mL DMF, was added

and stirred for further 24 h at the same temperature (SEC traces are summarized in the Supporting Information).

Monitoring polymerizations by real-time ^{1}H NMR spectroscopy. All polymerizations were carried out in analogy to the conventional procedure in a Schlenk-flask. Inside a glove box under a nitrogen-atmosphere the respective monomer was dissolved as a ca. 10 wt% solution in a total volume of 0.7 mL of the respective deuterated solvent, calculated for a monomer to initiator of $[M]_0 : [I]_0 = 30 : 1$, if not otherwise stated. The initiator-solution in 1 mL deuterated solvent was prepared separately (exemplarily for the polymerization of MsMAz (**1**) (70 mg) in 0.7 mL DMF-d_7 and the initiator-system: BnNHMs (**3**) ((32.0 mg), potassium bis(trimethylsilyl)-amide (KHMDS) (34.4 mg) in 1 mL DMF-d_7). A conventional NMR-tube was filled with the reaction mixture and sealed with a rubberseptum. Prior to initiation, the pure monomer-solvent mixture was measured at 50 °C. From the stock solution of the initiator 100 µL were added to the monomer mixture, mixed quickly and inserted into the spectrometer. All ^{1}H NMR kinetics were recorded using a Bruker Avance III 700. All spectra were referenced internally to residual proton signals of the deuterated solvent dimethylformamide-d_7 at 8.03 ppm, dimethylsulfoxide-d_6 at 2.50 ppm, tetrahydrofuran-d_8 at 3.58 ppm, benzene-d_6 7.16 ppm, and cyclohexane-d_{12} at 1.38 ppm. The π/2-pulse for the proton measurements was 13.1 µs. The spectra of the polymerizations were recorded at 700 MHz with 32 scans (equal to 404 s (acquisition time of 2.595 s and a relaxation time of 10 s after every pulse)) over a period of at least 3 h. No B-field optimizing routine was used over the kinetic measurement time. The spin-lattice relaxation rate (T1) of the ring-protons, which are used afterwards for integration, was measured before the kinetic run with the inversion recovery method.[20]

2.4 Results and Discussion

The AROP of *N*-activated aziridines can be initiated by a deprotonated secondary sulfonamide, which can be formed *in situ e.g.* by the use of bis(trimethylsilyl)amides. This freshly prepared nucleophile opens the ring most likely at its less substituted side and thus forms the propagating sulfonamide anion.[4] Propagation occurs via nucleophilic attack of this azaanion at the next monomer and it continues, as long as the monomer is available. As it is a living polymerization, no termination occurs, in the absence of impurities, and controlled termination by adding an electrophile is possible (Scheme 2.1).[4, 7]

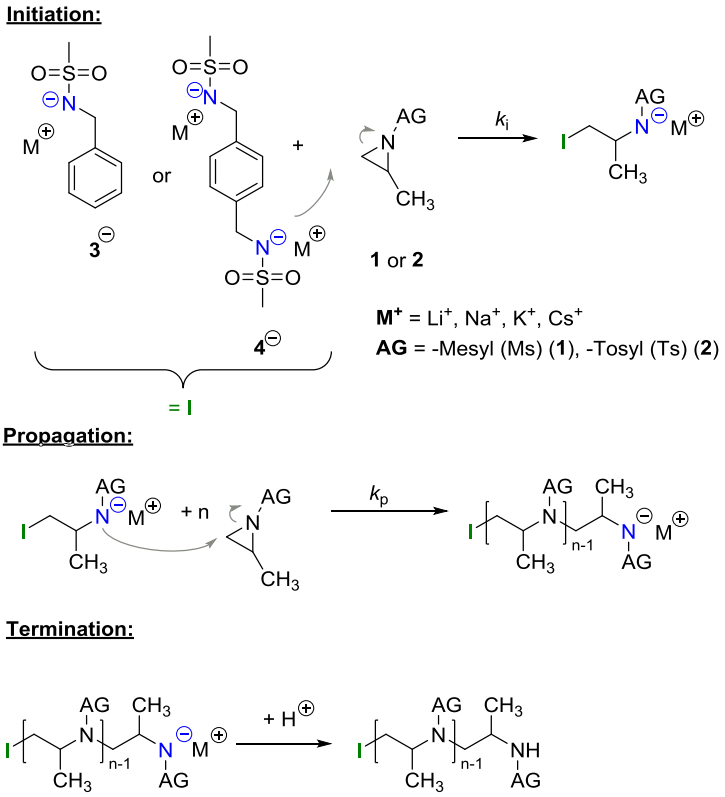

Scheme 2.1. Mechanism of the living anionic ring-opening polymerization of activated aziridines (AG = activation group).

All propagation rates are calculated from the linear first-order kinetic plots, using the equations, shown below for living polymerizations (eq. I, II). Equation I shows the reduction of the monomer concentration [M] over time, [P^-] stands for the number of growing chains and is equivalent to the initiator concentration [I], because in the living anionic polymerization (LAP) each initiating site starts a growing polymer chain ([P^-] = [I]). Integration gives the linear equation II, therefore plotting $\ln([M]_0/[M]_t)$ *versus* time results in a straight line, where the slope (k_{app}) gives the propagation rate (k_p), when divided by the original initiator concentration $[I]_0$. First-order kinetics, which are required for simplification of the equation, are evidenced if $\ln([M]_0/[M]_t)$ increases linearly and has already been reported for the LAP of some sulfonyl aziridines.[2, 4]

$$\frac{-\mathrm{d}[\mathrm{M}]}{\mathrm{d}t} = k_\mathrm{p}[\mathrm{P}^-][\mathrm{M}] = k_\mathrm{p}[\mathrm{I}][\mathrm{M}] \qquad \text{(I)}$$

$$\ln\frac{[\mathrm{M}]_0}{[\mathrm{M}]_t} = k_\mathrm{app}t = k_\mathrm{p}[\mathrm{I}]_0 t \qquad \text{(II)}$$

However, a systematic kinetic investigation of the AROP has not been reported to date. Here we chose 2-methyl-*N*-mesylaziridine (MsMAz, **1**) and 2-methyl-*N*-tosyl-aziridine (TsMAz, **2**) as

two monomers with different activating groups that alter the monomer reactivity, to study the polymerization in different solvents, namely dimethylsulfoxide (DMSO-d_6), dimethylformamide (DMF-d_7), tetrahydrofuran (THF-d_8), benzene-d_6 and cyclohexane-d_{12} (CyHex) at a constant temperature of 50 °C. In DMF-d_7 also different temperatures (20, 50, 100 °C) were investigated. Two sulfonamide-based initiators were used and the influence of the counter ions on propagation rates was studied. *N*-Benzyl methanesulfonamide (BnNHMs, **3**), deprotonated by lithium (LiMDS), sodium (NaMDS), potassium (KMDS) and cesium (CsMDS) bis(trimethylsilyl)amide, was used as a monofunctional initiator. *N,N'*-(1,4-Phenylenebis(methylene))dimethanesulfonamide (BnBis(NHMs), **4**) was designed as a novel bifunctional initiator for the AROP and also deprotonated with KMDS, which will allow the preparation of ABA triblock copolymers and is currently under investigation in our lab.

Real-time ^{1}H NMR spectroscopy was used to monitor the polymerization under these different conditions.[21-22] Requirements for this method are reaction times in the range of minutes to hours and reagents with distinguishable resonances in their spectrum (Figure 2.1). In *N*-sulfonyl-aziridines, the three ring-protons are detected as two doublets (CH_2) and one multiplet (CH) in the region from 3 to 2 ppm of the ^{1}H NMR spectrum (Figure 2.1A). These chemical shifts are sensitive probes for the monomer reactivity: the more they are shifted downfield in the spectrum, the stronger the activation, *i.e.* the electron-withdrawing effect of the sulfonamide. This allowed us to use the different monomer reactivities and to prepare sequenced copolymers.[7] As the monomer is consumed during the polymerization, the monomer signals vanish and simultaneously the growing polymer-backbone emerges between 3.5 and 4.5 ppm (Figure 2.1B). By integration of the well-separated monomer peaks over time and normalization to the amount of unreacted monomer, plotting of the monomer conversion *vs.* the reaction time or the total conversion is possible (Figure 2.1C and D).

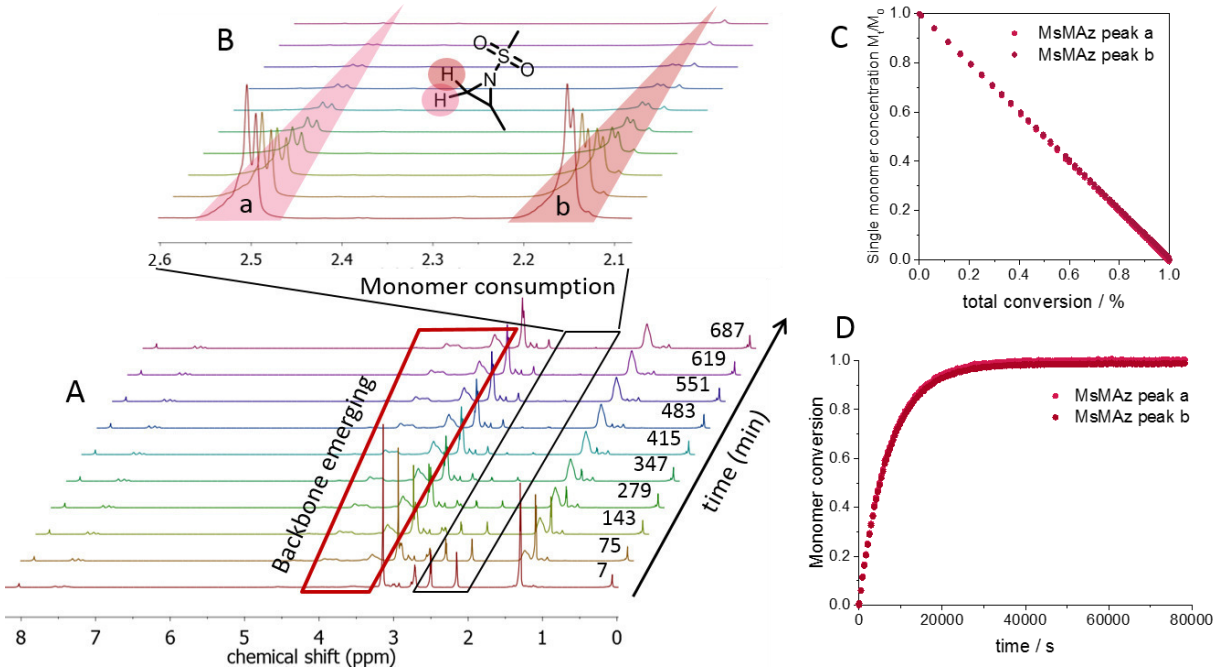

Figure 2.1. (A) Selection of ^{1}H NMR spectra of the azaanionic polymerization of MsMAz (**1**) with BnNKMs (**3**) as initiator in DMF-d_7, at 50 °C. (B) Relevant signals of the monomer ring-protons, showing the consumption of the monomer. (C) Normalized monomer concentration *versus* total conversion. (D) Monomer conversion *versus* reaction time.

The azaanionic polymerization proceeds in a living manner which was proven by chain extension experiments. Both the formation of diblock copolymers of **1** and **2**, and the chain extension of **2** resulted in a complete shift of the molecular weight distributions in SEC experiments and thus underlines the living character of the chain ends (Figures S2.15-S2.18).

The propagation rate constants k_p were calculated from the integrals of the monomer signals of the first 13 spectra (ca. 1.5 h reaction time). For “fast” polymerizations (100 % conversion in less than 1 h) only the first 4 values were used for the determination of the slope (equivalent to the apparent propagation rate constant (k_{app})) of the linear fits. Division of k_{app} with the initial initiator-concentration reveals the initiator-independent propagation rate coefficient k_p.

From every reaction in the NMR tube a small aliquot was taken and analyzed by size exclusion chromatography (SEC). All polymers exhibited monomodal and narrow molecular weight distributions ($Đ$ typically < 1.1, Tables 2.1-2.4 and Supporting Information) and reached full monomer conversion in most cases (see below). The molecular weights of the PAz determined from SEC are underestimated on our setup compared to the absolute values calculated from NMR by end group analysis (Tables 2.1-2.4). Since for all SEC analyses PEO-standards were used for conventional calibration, the molecular weights calculated from NMR-data should be considered for comparisons.

Temperature variation. The polymerization of MsMAz (**1**) was initiated with BnNHMs (**3**)/ KMDS in DMF-d_7 at 20, 50 and 100 °C (Table 2.1; note: under these conditions 1 eq. hexamethyldisilazane (HMDS) is present as an inherent additive in the polymerization mixture, its influence will be discussed later on). At 20 °C after 17 hours the conversion reached 60% with a propagation rate of k_p = 0.98 x 10^{-3} L mol^{-1} s^{-1}. At 50 °C full conversion was achieved after ca. 8 hours, revealing a k_p of 10.53 x 10^{-3} L mol^{-1} s^{-1}, which is ca. ten times higher compared to 20°C. When the polymerization was performed at 100 °C, full conversion was achieved after 30 min with a k_p-value of ca. 123.85 x 10^{-3} L mol^{-1} s^{-1} (Figure 2.2). At all temperatures, the polymerization remains living, and the addition of new monomer allows the formation of block copolymers.[7-8, 15]

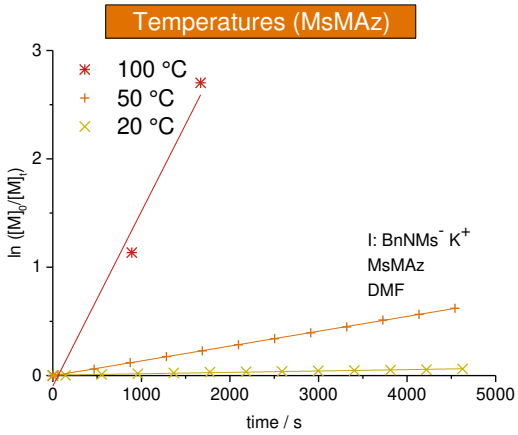

Figure 2.2. Kinetic Plots of ln($[M]_0/[M]_t$) *vs.* time for the azaanionic polymerization of MsMAz (**1**), BnNKMs (**3**, initiator) in DMF-d_7 at different temperatures. (also compare Table 2.1).

Table 2.1. Overview of the performed anionic polymerization of 2-methyl-*N*-mesyl-aziridine at different temperatures in *N,N*-dimethylformamide.

Initiator	BnNKMs (3-K)	BnNKMs (3-K)	BnNKMs (3-K)
Ratio [I]:[M]	01:30	01:30	01:30
Monomer	MsMAz (1)	MsMAz (1)	MsMAz (1)
Additive	HMDS	HMDS	HMDS
Solvent	DMF-d_7	DMF-d_7	DMF-d_7
T **/ °C**	**100**	**50**	**20**
k_p **/ 10^{-3} L mol^{-1} s^{-1}**	**123.85**	**10.53**	**0.98**
M_n[a] / g mol^{-1}	2000	2200	2000
M_n[b] / g mol^{-1}	4000	3600	2200
$Đ$[a]	1.08	1.06	1.08
Reaction time / h	0.50	8.00	17.00
Conversion / %	>99	>99	60

[a] Number-average molecular weight and molecular weight dispersity determined *via* SEC in DMF (*vs.* PEO standards). [b] Number-average molecular weight determined by NMR analyses.

Solvent variation. The solvent polarity and the solvation of the living chain ends have a tremendous influence on the propagation rate in ionic polymerizations.[2-3, 23] For the azaanionic ROP of MsMAz (**1**) at 50°C, polar solvents such as DMSO-d_6 (k_p = 13.17 ± 0.7 x 10^{-3} L mol^{-1} s^{-1} (mean value from repeated measurements I and II)) and DMF-d_7 (10.53 x 10^{-3} L mol^{-1} s^{-1}) are the suitable solvents and reach full conversion after ca. 8 hours and with narrow molecular weight distributions (Figure 2.3 and Table 2.2).

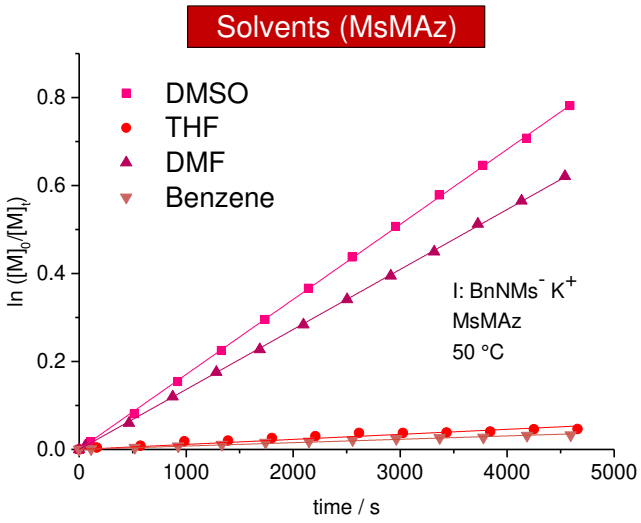

Figure 2.3. Kinetic Plots of $\ln([M]_0/[M]_t)$ *vs.* time of MsMAz (**1**), BnNKMs (**3**) at 50 °C in different solvents (data listed in Table 2.2).

The polymerization in THF-d_8 was remarkably slower with k_p = 0.76 ± 0.11 x 10^{-3} L mol^{-1} s^{-1} (mean value from repeated measurements I and II). Also in benzene-d_6 only slow propagation was detected (k_p = 0.56 x 10^{-3} L mol^{-1} s^{-1}). After 17 h a conversion of 30% was reached. Cyclohexane-d_{12}, a typical solvent for carbanionic polymerization, did not result in chain growth. This trend directly reflects the solvation of the living chains and reveals aprotic polar solvents such as DMSO and DMF as the solvents of choice for the AROP of sulfonyl aziridines. However, also in the other solvents the polymerizations remain living and might be considered for special monomers.

Table 2.2. Overview of the performed anionic polymerizations of 2-methyl-*N*-mesyl-aziridine in different solvents.

Initiator	BnNKMs (3-K)	BnNKMs (3-K)	BnNKMs (3-K)	BnNKMs (3-K)	BnNKMs (3-K)	BnNKMs (3-K)	BnNKMs (3-K)
Ratio [I]:[M]	01:30	01:30	01:30	01:30	01:30	01:30	01:30
Monomer	MsMAz (1)	MsMAz (1)	MsMAz (1)	MsMAz (1)	MsMAz (1)	MsMAz (1)	MsMAz (1)
Additive	HMDS	HMDS	HMDS	HMDS	HMDS	HMDS	HMDS
Solvent[a]	**DMSO-d_6-I[a]**	**DMSO-d_6-II[a]**	**DMF-d_7**	**THF-d_8-I[a]**	**THF-d_8-II[a]**	**Benzene-d_6**	**CyHex-d_{12}**
T / °C	50	50	50	50	50	50	50
k_p / 10^{-3} L mol^{-1} s^{-1}	**13.87**	**12.46**	**10.53**	**0.87**	**0.65**	**0.56**	**---**
M_n[b] / g mol^{-1}	2100	2500	2200	1600	1500	700	---
M_n[c] / g mol^{-1}	4100	5100	3600	1500[d]	1700[d]	---[d]	---[d]
$Đ$[b]	1.11	1.09	1.06	1.09	1.09	1.17	---
Reaction time / h	8.00	8.00	8.00	> 17	> 17	> 17	>17
Conversion / %	>99	>99	>99	30	n.d.	n.d.	n.d.

[a] Two identical polymerization mixtures (I or II). [b] Number-average molecular weight and molecular weight dispersity determined *via* SEC in DMF (*vs.* PEO standards). [c] Number-average molecular weight determined by NMR analyses. [d] Samples taken after 17 h reaction, no full conversion.

Initiator variation. Deprotonated sulfonamides are used as the initiators for the azaanionic ROP of activated aziridines. KMDS was previously used for this series of experiments at 50 °C in DMF-d_7 (Table 2.3). It has to be noted, that in all cases an equimolar amount of HMDS is produced during the initiator formation (*also compare sections below*).

Comparing different sulfonamide initiators, (Fig. 2.4) the potassium salt of *N*-benzyl methanesulfonamide (BnNKMs, **3**) (k_p = 10.53 x 10^{-3} L mol^{-1} s^{-1}) and the novel bifunctional initiator (BnBis(NKMs), **4**) exhibit a propagation constant of k_p (BnBis(NKMs)) = 9.02 x 10^{-3} L mol^{-1} s^{-1}. MALDI-ToF mass spectrometry of the polymers prepared with both initiators proves their successful incorporation in the polymer chain and the absence of any additional distribution (Figures S2.9 & S2.10). This allows the synthesis of ABA triblock-copolymers based on aziridines which is currently under investigation.

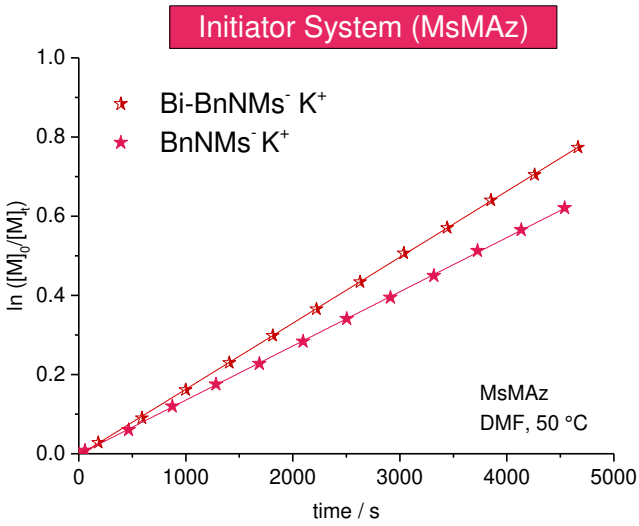

Figure 2.4. Kinetic Plots of $\ln([M]_0/[M]_t)$ *vs.* time for the azaanionic polymerization of MsMAz (**1**) with different initiators at 50 °C (data listed in Table 2.3).

As the studies with different counter ions revealed (*see below*) that also lithium cations can propagate the AROP of aziridines, *n*-butyllithium (*n*-BuLi) was tested as a commercially available initiator for the AROP of MsMAz (**1**) which demonstrated the fastest reaction rate under these conditions (k_p = 18.08 x 10^{-3} L mol^{-1} s^{-1}, cf. Fig. S2.3 and discussion for counter ions). MALDI-ToF mass spectrometry proved the incorporation of the butyl chain and shows a single mass distribution (Figure S2.12).

Table 2.3. Overview of the performed anionic polymerizations of 2-methyl-*N*-mesyl-aziridine using different initiators.

Initiator	**BnNKMs (3-K)**	**BnBi(NKMs) (4-K)**	**BuLi**
Ratio [I]:[M]	01:30	01:50	01:30
Monomer	MsMAz (1)	MsMAz (1)	MsMAz (1)
Additive	HMDS	HMDS	-
Solvent	DMF-d_7	DMF-d_7	DMF-d_7
T / °C	50	50	50
k_p / 10^{-3} L mol^{-1} s^{-1}	**10.53**	**9.02**	**18.08**
M_n[a] / g mol^{-1}	2200	2700	2200
M_n[b] / g mol^{-1}	3600	3700	n.d.
$Đ$[a]	1.06	1.09	1.08
Reaction time / h	8	6	5
Conversion / %	99	>99	>99

[a] Number-average molecular weight and molecular weight dispersity determined *via* SEC in DMF (*vs.* PEO standards). [b] Number-average molecular weight determined by NMR analyses.

Influence of counter-ions. It is known from ionic polymerizations that the solvation of the growing chain and the respective counter ion plays an important role in the polymerization kinetics: the stronger the binding between the growing chain and the counter ion (and the lower the solvation efficiency of the solvent), the slower the propagation. For the anionic polymerization of styrene, for example, lithium counter ions show an increase of the polymerization kinetics compared to sodium counter ions. For epoxides, typically potassium and cesium show the highest propagation rates, while lithium alkoxides do not or only very slowly propagate, as they coordinate strongly to the Pearson-hard alkoxide.[2, 24-31] In the case of sulfonamide anions such studies had not been performed; in previous work, potassium salts proved to be efficient. We studied the polymerization of **1** and **2** (DMF-d_7, 50°C, BnNHMs (**3**) as the initiator) with different counter ions by deprotonating **3** with different bis(trimethylsilyl)amide salts (lithium, sodium, potassium salts are commercially available, CsMDS was prepared according to the literature[4, 32]). For both monomers, propagation with all counter ions was observed (Figures 2.5 and S2.1 and Table 2.4), probably due to the rather soft nature of the propagating anion. Under these conditions the order of $Cs^+ > Li^+ > Na^+ > K^+$ was found for both monomers (Figure 2.5A).

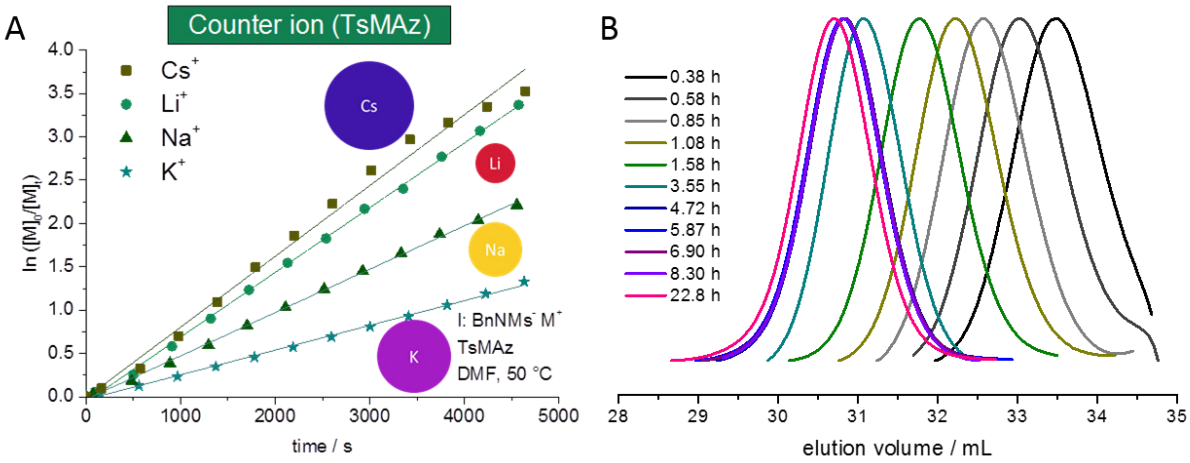

Figure 2.5. (A) Kinetic Plots of $\ln([M]_0/[M]_t)$ *vs.* time for the azaanionic polymerization of TsMAz (**2**) with BnNHMs (**3**, initiator) in DMF-d7 at 50 °C with different bis(trimethlsilyl)amide-salts. (B) SEC-kinetics of MsMAz (**1**), BnNKMs (**3**) at 50 °C in DMF (RI-signal, PEO-standard), (Table 2.4).

Table 2.4. Overview of the performed anionic polymerizations of 2-methyl-*N*-tosyl-aziridine in *N,N*-dimethylformamide with different gegenions.

Initiator	BnNLiMs (**3-Li**)	BnNNaMs (**3-Na**)	BnNKMs (**3-K**)	BnNCsMs (**3-Cs**)
Ratio [I]:[M]	01:30	01:30	01:30	01:30
Monomer	TsMAz (2)	TsMAz (2)	TsMAz (2)	TsMAz (2)
Additive	**HMDS**	**HMDS**	**HMDS**	**HMDS**
Solvent	DMF-d_7	DMF-d_7	DMF-d_7	DMF-d_7
T / °C	50	50	50	50
k_p / 10^{-3} L mol^{-1} s^{-1}	**90.30**	**60.91**	**39.79**	**98.69**
M_n[a] / g mol^{-1}	3000	2900	2300	2800
M_n[b] / g mol^{-1}	n.d.	n.d.	n.d.	n.d.
$Đ$[a]	1.09	1.09	1.09	1.06
Reaction time / h	8	8	8	8

[a] Number-average molecular weight and molecular weight dispersity determined *via* SEC in DMF (*vs*. PEO standards). [b] Number-average molecular weight determined by NMR analyses.

For MsMAz (**1**) as a less reactive monomer the same trend was observed ($Cs^+ > Li^+ > Na^+ > K^+$), however, the differences were less pronounced (Figure S2.1, Table 2.5). Noteworthily, in all cases living polymerization with reasonable polymerization rates of the activated aziridines is observed (cf. Figure 2.5B and Figures S2.13, S2.14). This indicates a higher solvation of the propagating azaanion chains under these conditions, in contrast to the epoxide polymerization, where hardly propagation is observed with lithium as a counter ion, also in very solvating solvents.

Also the cation dependence on the polymerization kinetics, which does not follow the cation size can be explained by the Pearson acid base concept[33] that the sulfonamide anion is weakly coordinated by its respective cation compared to an alkoxide, which strongly binds to lithium cations also on polar organic solvents as mentioned above. The “softer” sulfonamide anion exhibits higher binding to intermediate sized cations sodium and potassium, but less binding to the hard lithium and soft cesium cations. In addition, comparing the two monomers **1** and **2**, with the smaller electron withdrawing effect of the mesyl-group in MsMAz (**1**) compared to the tosyl-group in **2**, a more nucleophilic growing chain end is produced. This leads to the less expressed trend in the propagation rate of the different counter ions, as the interaction between the azaanion at the chain and the cationic counter ion is stronger.

Table 2.5. Overview of the performed anionic polymerizations of 2-methyl-*N*-mesyl-aziridine with different gegenions and amounts of hexamethyldisilazane.

Initiator	BnNLiMs (3-Li)	BnNNaMs (3-Na)	BnNKMs (3-K)	BnNCsMs (3-Cs)	BnNKMs[c] (3-K)	BnNKMs (3-K)
Ratio[I]:[M]	01:30	01:30	01:30	01:30	01:30	01:30
Monomer	MsMAz (1)	MsMAz (1)	MsMAz (1)	MsMAz (1)	MsMAz (1)	MsMAz (1)
Additive	**HMDS**	**HMDS**	**HMDS**	**HMDS**	**-**	**2 eq. HMDS**
Solvent	DMF-d_7	DMF-d_7	DMF-d_7	DMF-d_7	DMF-d_7	DMF-d_7
T / °C	50	50	50	50	50	50
k_p / 10^{-3} L mol^{-1} s^{-1}	**15.39**	**11.66**	**10.53**	**15.74**	**11.19**	**8.45**
M_n[a] / g mol^{-1}	2400	2400	2200	2100	2200	2000
M_n[b] / g mol^{-1}	4000	3900	3600	3800	3700	4000
$Đ$[a]	1.07	1.06	1.06	1.08	1.07	1.10
Reaction time / h	8.00	7.00	8.00	7.00	8.00	9.00
Conversion / %	>99	>99	97	>99	98	>99

[a] Number-average molecular weight and molecular weight dispersity determined *via* SEC in DMF (*vs.* PEO standards). [b] Number-average molecular weight determined by NMR analyses. [c] Prepared by deprotonation with KOH.

To identify the influence of the inherent additive hexamethyldisilazane (HMDS), which is generated in a molar amount after the deprotonation of BnHMs (**3**) by the bis(trimethylsilyl)amide salt, on the chain end reactivity, polymerizations of **1** with different amounts of HMDS were performed (note: MALDI-ToF mass spectrometry revealed that only polymers, initiated by **3** are produced under these conditions, cf. SI).

To study the influence of HMDS on the polymerization kinetics, several experiments were conducted: (i) (**3**) was deprotonated with KMDS (*i.e.* one equivalent of HMDS is produced with respect to the initiator); (ii) to exclude HMDS in the polymerization, BnNHMs (**3**) was deprotonated with potassium hydroxide (KOH) and dried by azeotropic removal of the emerging water with benzene before adding the monomers; (iii) another polymerization was conducted under the same conditions, however with two equivalents of HMDS with respect to the initiator. Comparing the propagation rate constants of these three polymerizations in the presence of 1 or 2 eq. or without HMDS, a decrease of the polymerization kinetics with an increasing amount of HMDS was detected (BnNKMs in DMF (no HMDS) at 50 °C k_p = 11.19 x 10^{-3} L mol^{-1} s^{-1}, BnNKMs, 1 eq. HMDS in DMF at 50 °C k_p = 10.53 x 10^{-3} L mol^{-1} s^{-1}, BnNKMs, 2 eq. HMDS in DMF at 50 °C k_p = 8.45 x 10^{-3} L mol^{-1} s^{-1}). These results prove that HMDS influences the polymerization kinetics, probably due to coordination to the anionic chain end and the formation of a complex. The same trend was observed for the polymerization of **1** with lithium as the counter ion: for MsMAz, 50°C, DMF, BuLi (no HMDS) a k_p = 18.1 x 10^{-3} L mol^{-1} s^{-1} was determined (Table 2.3),

while the presence of HMDS in the system reduced the k_p to 15.4 x 10^{-3} L mol^{-1} s^{-1} (Table 2.5 first entry, MsMAz, 50°C, DMF, BnNLiMs, HMDS).

To examine the influence of DMF as a highly solvating solvent, polymerizations with lithium, potassium and cesium, with the "standard procedure", *i.e.* BnNHMs (**3**), the respective bis(trimethylsilyl)amide salt, at 50 °C, were carried out in THF. In all cases the polymerization proceeds much slower in THF compared to DMF, irrespective of which counter ion was used (Table 2.6, Figure S2.2). This indicates a lower solvation of the living chain ends in THF, reducing the polymerization kinetics (at least by a factor of 10). In contrast, the conventional oxyanionic polymerization and the recently reported organocatalytic ring-opening polymerization of sulfonyl-aziridines,[16] proceed smoothly in THF and reach full conversion in the course of several hours.

With these results in hand, the combination of the azaanionic polymerization with other ionic polymerization techniques will be used to produce various macromolecular architectures and the use of commercially available lithium-based initiators (*e.g.* butyllithium).

Table 2.6. Overview of the performed anionic polymerizations of 2-methyl-*N*-mesyl-aziridine with different gegenions in tetrahydrofuran.

Initiator	BnNLiMs (3-Li)	BnNKMs (3-K)	BnNKMs (3-K)	BnNCsMs (3-Cs)
Ratio [I]:[M]	01:30	01:30	01:30	01:30
Monomer	MsMAz (1)	MsMAz (1)	MsMAz (1)	MsMAz (1)
Additive[a]	**HMDS**	**HMDS-I**	**HMDS-II**	**HMDS**
Solvent	THF-d_8	THF-d_8	THF-d_8	THF-d_8
T / °C	50	50	50	50
k_p / 10^{-3} L mol^{-1} s^{-1}	**0.72**	**0.87**	**0.65**	**1.36**
M_n[b] / g mol^{-1}	700	1600	1500	1400
M_n[c] / g mol^{-1}	1300 [d]	1500 [d]	1700 [d]	2500[d]
$Đ$[a]	1.17	1.09	1.09	1.08
Reaction time / h	> 24	> 17	> 17	> 18
Conversion / %	33	38	43	63

[a] In the case of KMDS the measurements were repeated and are marked with I, respectively II. [b] Number-average molecular weight and molecular weight dispersity determined *via* SEC in DMF (*vs.* PEO standards). [c] Number-average molecular weight determined by NMR analyses. [c] Prepared by deprotonation with KOH. [d] Samples taken after minimum 17 h reaction, no full conversion.

2.5 Summary

We report on the systematic polymerization kinetics of the living anionic polymerization of *N*-activated aziridines, exemplary with MsMAz and TsMAz, two activated aziridines of different reactivities, by real-time ^{1}H NMR spectroscopy. We found that their polymerization follows living conditions at temperatures between 20 and 100 °C. The comparison of different solvents for the polymerization proved that polar aprotic solvents exhibit the fastest polymerization kinetics with the order of DMSO ≥ DMF >> THF ≥ benzene, and no propagation in cyclohexane, depending on the solvation of the living chain end. The use of different initiators, namely sulfonamides BnNHMs and a novel bifunctional sulfonamide (BnBis(NHMs)) were compared with each other and we additionally identified *n*-butyllithium as a potent commercial alternative.

However, the sulfonamide initiators are ideal to study the influence of the counter ion on the polymerization kinetics. The sulfonamide initiator was deprotonated with the respective metal bis(trimethylsilyl)amide (Li, Na, K, or Cs). In all cases fast propagation of the anionic polymerization was observed, which is in strong contrast to epoxide polymerization, where lithium alkoxides show only very slow propagation rate constants. For activated aziridines the following trend was observed: $Cs^+ > Li^+ > Na^+ > K^+$ with reasonable k_p values in all cases in DMF, indicating a high solvation of all propagating azaanions in DMF, with a less pronounced effect of the counter ion compared to alkoxide chains. In contrast, in THF only a weak counter ion dependency and low reaction kinetics have been observed.

We believe that this fundamental work will help to further understand and foster the field of the anionic polymerization of aziridines. In particular, the less pronounced counter ion effect compared to the well-known anionic polymerization of epoxide makes the AROP of sulfonylaziridines easy and switching for example from carb- to aza-anionic polymerization or the use of simple commercially available butyllithium. *N*-Sulfonyl-activated aziridines undergo AROP under various conditions producing well-defined polysulfonamides and –amines after hydrolysis. This defined access to such structures was not possible to date and we believe, that aziridines will become a valuable tool for combinations with other anionic polymerizations for diverse applications, for example as well-defined alternative for branched poly(ethylene imine)s.

2.6 Acknowledgments

The authors thank the Deutsche Forschungsgemeinschaft (DFG WU750/ 7-1) for support. The authors thank Stefan Spang for the NMR measurements and Dr. Elena Berger-Nicoletti for the MALDI-ToF-spectra. E.R. thanks the BMBF/MPG network MaxSynBio.

2.7 Supporting Information

The Supporting Information contains additional synthetic procedures, characterization data for monomers, polymers and kinetic measurements.

Content

2.7.1 Materials and Methods.

Materials.

All solvents and reagents were purchased from Sigma-Aldrich, Acros Organics or Fluka and used as received unless otherwise mentioned. All deuterated solvents were purchased from Deutero GmbH and were distilled from CaH_2 or sodium and stored in a glovebox prior to use. All monomers and initiators were dried extensively by azeotropic distillation with benzene prior to polymerization. Cesium bis(trimethylsilyl)amide was synthesized according to literature protocol.[4, 32] 2-methyl-*N*-mesyl-aziridine (MsMAz, **1**), 2-methyl-*N*-tosylaziridine (TsMAz, **2**) and *N*-benzyl methanesulfonamide (BnNHMs, **3**) were synthesized to our previously published protocol.[7] The synthesis of the bifunctional initiator (BnBis(NHMs), **4**) can be found below.

Instrumentation and Characterization Techniques.

NMR. ^{1}H NMR spectra were recorded using a Bruker Avance III 250, a Bruker Avance 300, a Bruker Avance III 500 or a Bruker Avance III 700. All spectra were referenced internally to residual proton signals of the deuterated solvent.

SEC. Size exclusion chromatography (SEC) measurements of standard polymers were performed in DMF (1 g L^{-1} LiBr added) at 60°C and a flow rate of 1 mL min^{-1} with an PSS SECcurity as an integrated instrument, including a PSS GRAM 100-1000 column and a refractive index (RI) detector. Calibration was carried out using poly(ethylene glycol) standards provided by Polymer Standards Service. For polymers from the NMR-kinetics size exclusion chromatography measurements were performed in DMF (containing 0.25 g L^{-1} of lithium bromide as an additive) with an Agilent 1100 Series as an integrated instrument, including a PSS HEMA column (106/105/104 g mol^{-1}), a UV detector (275 nm), and a RI detector at a flow rate of 1 mL min^{-1} at 50 °C. Calibration was carried out using PEO standards provided by Polymer Standards Service.

MALDI-TOF. Matrix-assisted laser desorption/ionization time-of-flight (MALDI-ToF) measurements were performed using a Shimadzu Axima CFR MALDI-TOF mass spectrometer, employing DCTB (trans-2-[3-(4-tert-butylphenyl)-2-methyl-2-propenylidene] malononitrile) as a matrix (5 mg mL^{-1} in THF).

2.7.2 Kinetic data of counter Ion (MsMAz (1)).

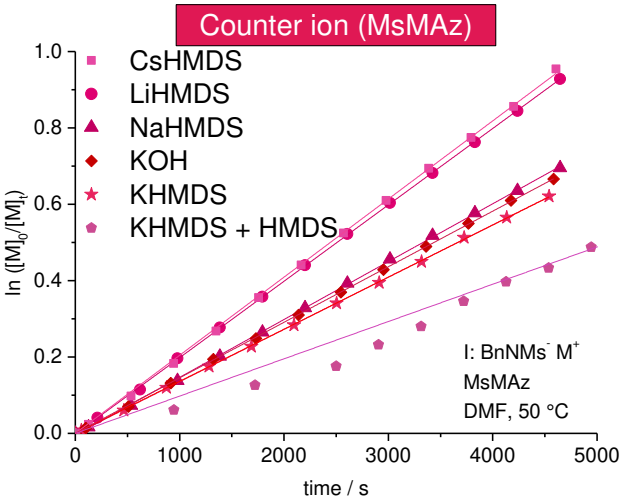

Figure S2.1. Kinetic Plots of $\ln([M]_0/[M]_t)$ *vs.* time for the azaanionic polymerization of MsMAz (**1**), BnNHMs (**3**, initiator) in DMF-d_7 at 50 °C with different counter ions (also compare Table 2.5).

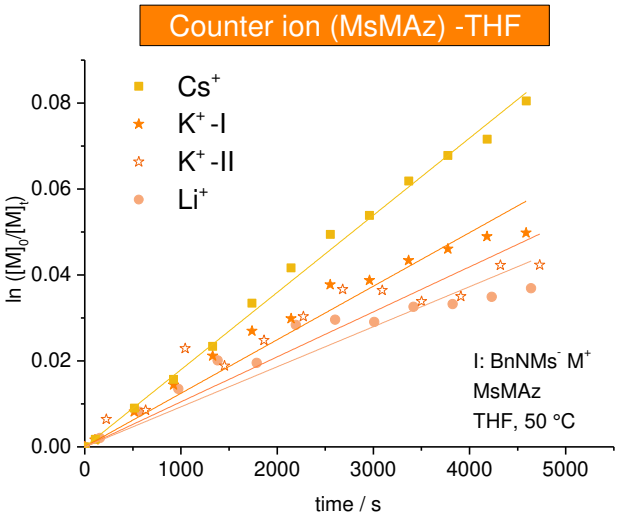

Figure S2.2. Kinetic Plots of $\ln([M]_0/[M]_t)$ *vs.* time for the azaanionic polymerization of MsMAz (**1**), BnNHMs (**3**, initiator) in DMF-d_7 at 50 °C with different counter ions. All data are listed in Table 2.6. In case potassium the measurements were repeated and are marked with I, respectively II.

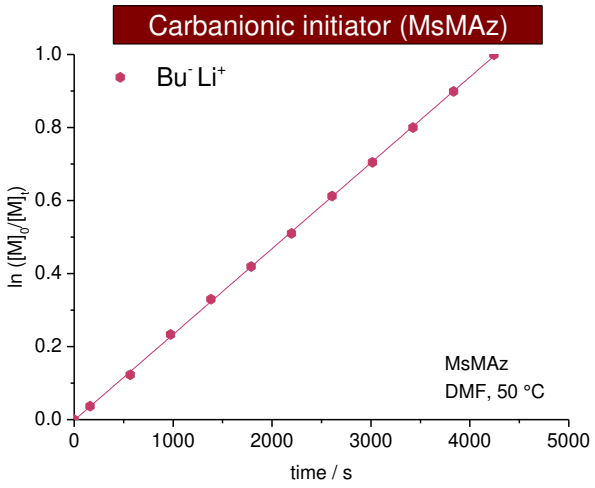

Figure S2.3. Kinetic Plots of $\ln([M]_0/[M]_t)$ *vs.* time for the azaanionic polymerization of MsMAz (**1**) with *n*-butyllithium in DMF-d_7 at 50 °C. All data are listed in Table 2.3.

2.7.3 Initiator.

N,N'-(1,4-phenylenebis(methylene))dimethanesulfonamide (BnBis(NHMs),5)

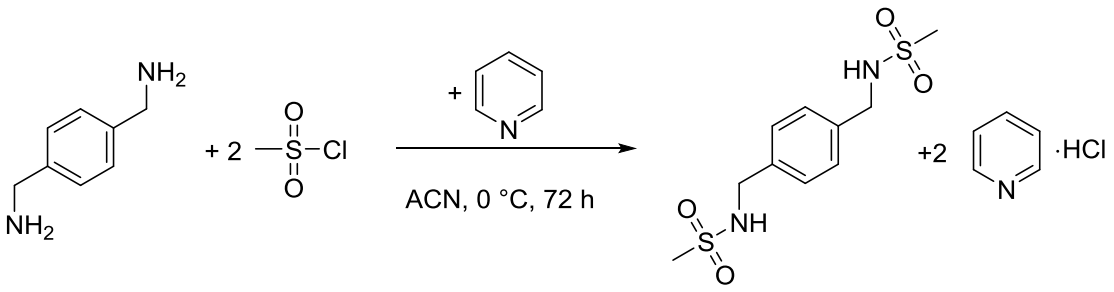

The compound was synthesized following to literature procedures.[234] 1,4-bis(amino-methyl)-benzene (4.50 g, 33.0 mmol) and pyridine (13.3 mL, 165 mmol) were dissolved in anhydrous ACN (100 mL). The solution was cooled down to 0 °C and methanesulfonylchloride (5.1 mL, 66.1 mmol) was added dropwise over ten minutes. The reaction mixture turned yellow and was stirred for 72 h. The precipitation was filtered and the solvent was removed at reduced pressure. The residue was recrystallized twice from H_2O/EtOH (1:1) and yielded the product as yellowish, needle-shaped crystals (1.32 g, 4.51 mmol, 14%) ^{1}H NMR (250 MHz, 297 K, DMSO-d_6): δ [ppm] = 7.55 (t, 2H, b), 7.32 (s, 4H, b), 4.14 (d, 4H, c), 2.73 (s, 6H, d). ^{13}C NMR (176 MHz, 297 K, DMSO-d_6): δ [ppm] = 137.25, 127.70, 45.77, 39.96. Analysis (calcd., found for $C_{10}H_{16}N_2O_4S_2$): C (41.05, 41.27), H (5.43, 5,66), N (9.45, 9,70), S (21.81, 21.99).

2.7.4 NMR spectra of polymers prepared in the NMR-kinetic experiments.

Bn-P(MsMAz)

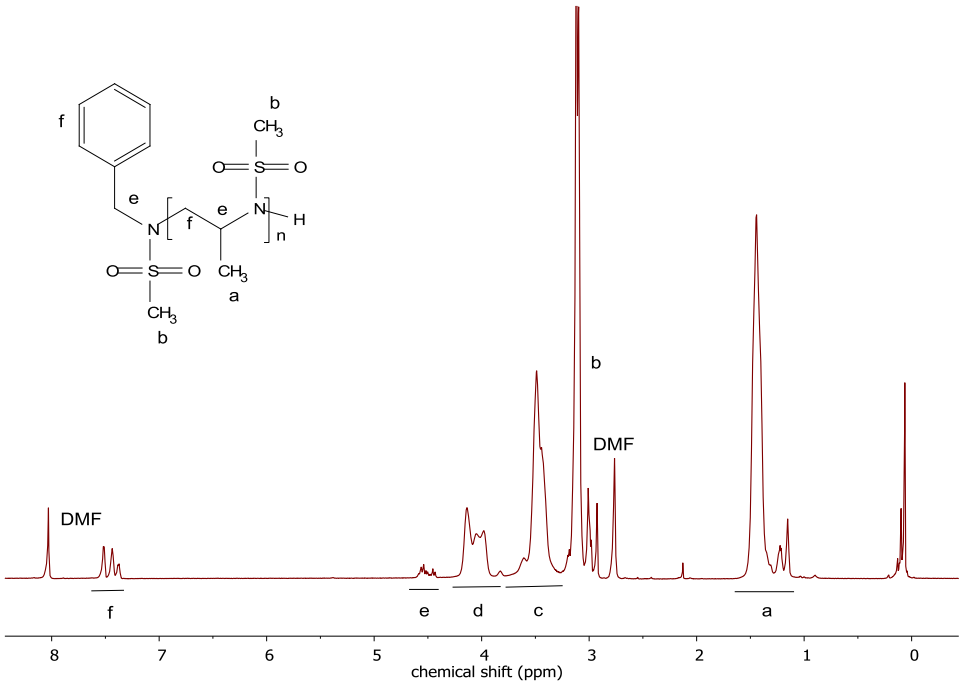

Figure S2.4. ^{1}H NMR (700 MHz, 323 K, DMF-d_7) of Bn-P(MsMAz).

BiBn-P(MsMAz)

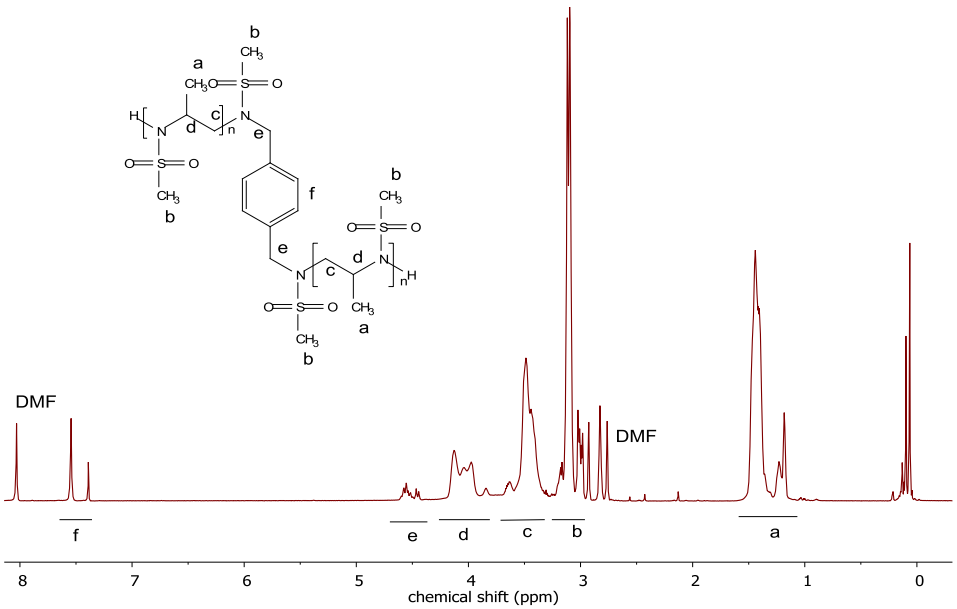

Figure S2.5. ^{1}H NMR (700 MHz, 323 K, DMF-d_7) of BiBn-P(MsMAz).

Bu-P(MsMAz)

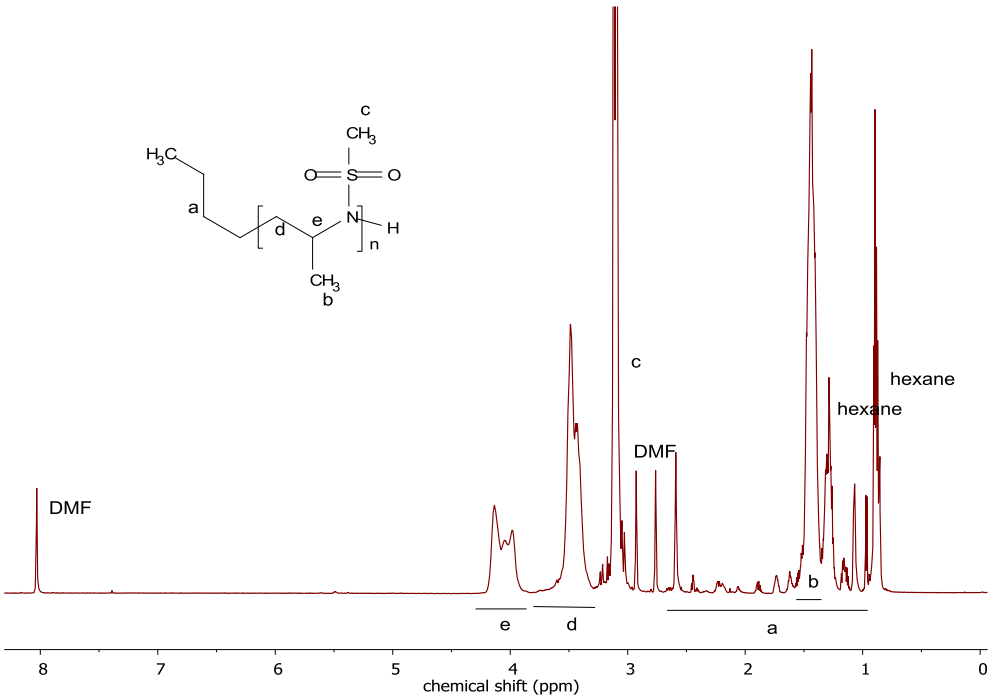

Figure S2.6. ^{1}H NMR (700 MHz, 323 K, DMF-d_7) of Bu-P(MsMAz).

Bn-P(TsMAz)

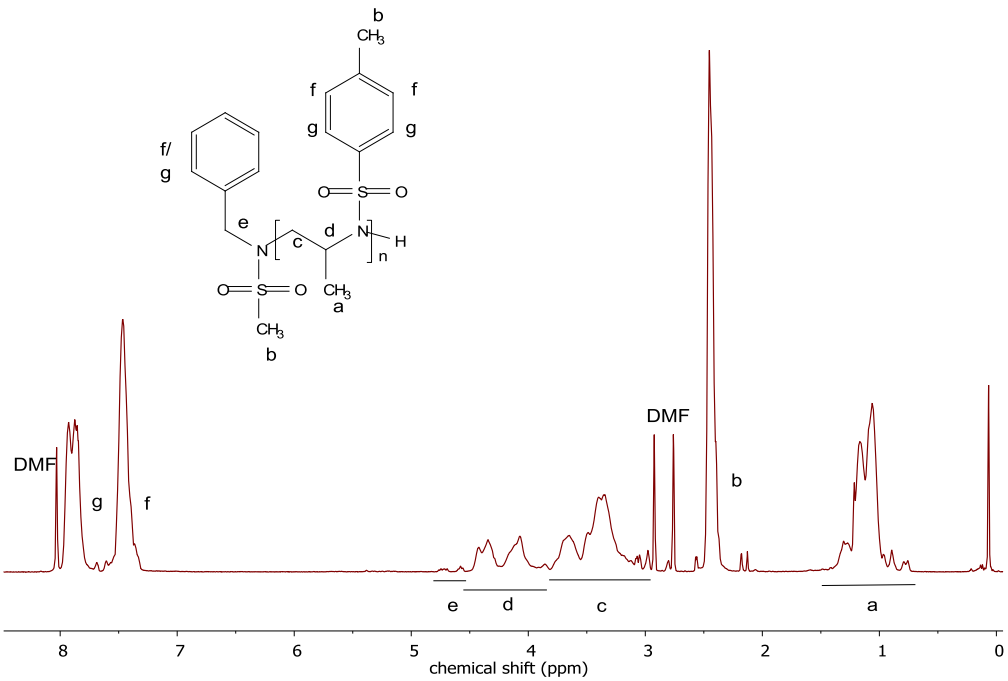

Figure S2.7. ^{1}H NMR (700 MHz, 323 K, DMF-d_7) of Bn-P(TsMAz).

Bu-P(TsMAz)

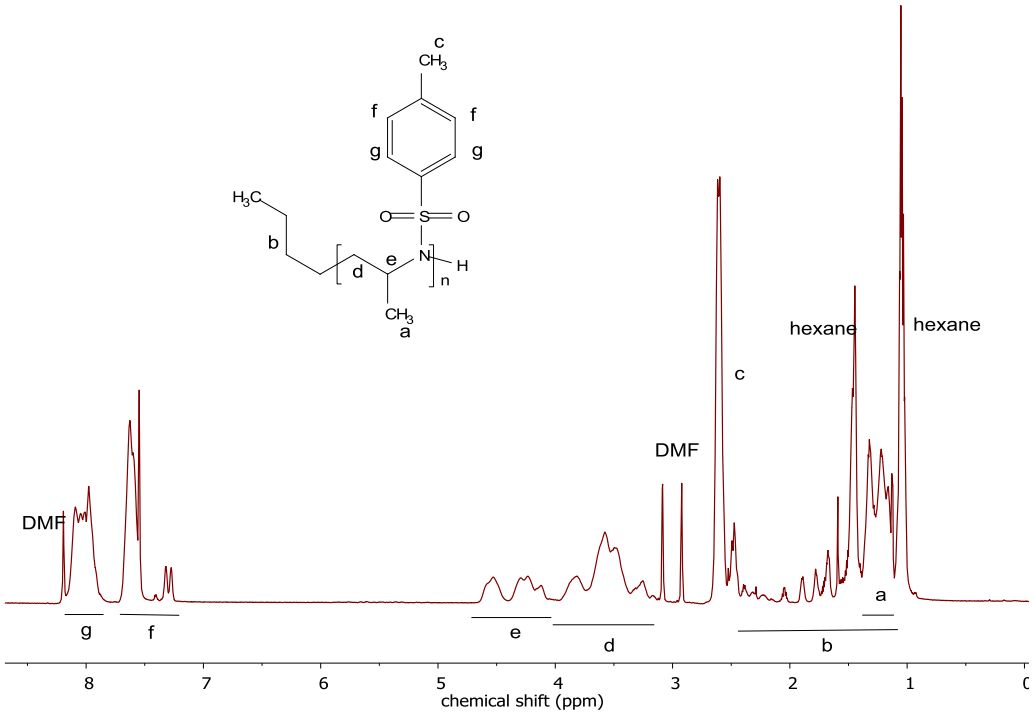

Figure S2.8. ^{1}H NMR (700 MHz, 323 K, DMF-d_7) of Bu-P(TsMAz).

2.7.5 MALDI ToF mass spectra.

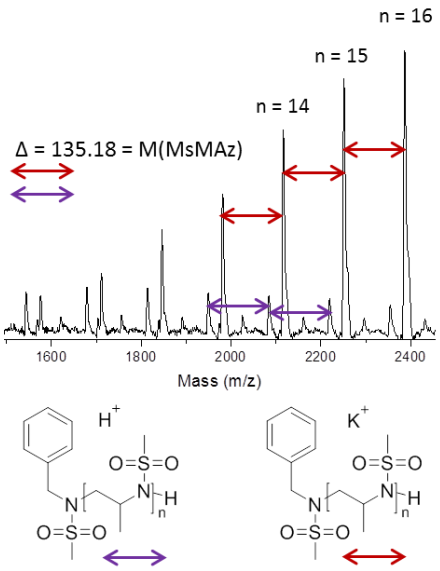

Figure S2.9. Zoom into the MALDI ToF mass spectrum of Bn-P(MsMAz).

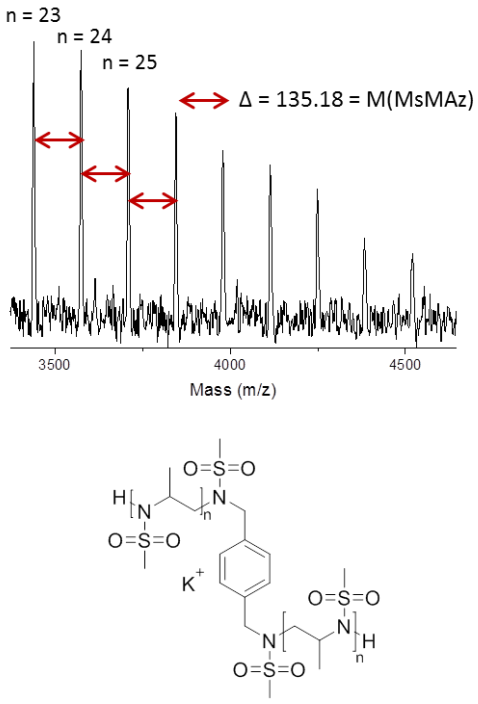

Figure S2.10. Zoom into the MALDI ToF mass spectrum of BiBn-P(MsMAz).

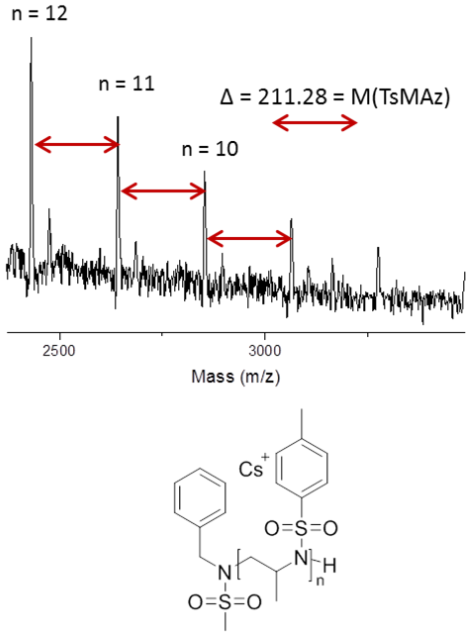

Figure S2.11. Zoom into the MALDI ToF mass spectrum of Bn-P(TsMAz).

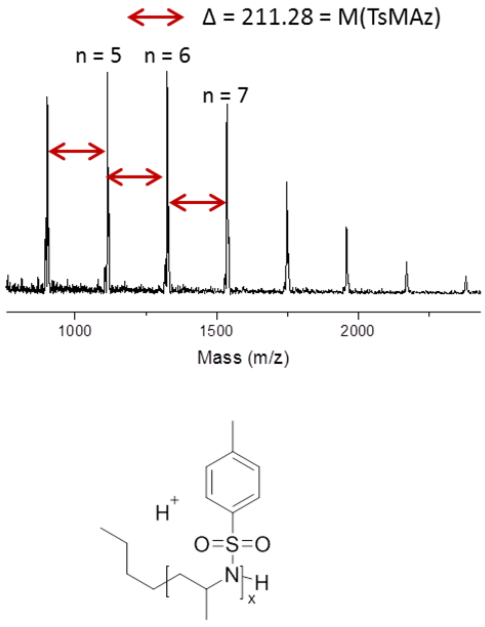

Figure S2.12. Zoom into the MALDI ToF mass spectrum of Bu-P(TsMAz).

2.7.6 SEC kinetics.

All polymerizations were carried out in analogy to the conventional procedure in a Schlenk-flask. 100 µL-samples were taken in specific time intervals and analyzed by SEC and ^{1}H NMR.

LiMDS

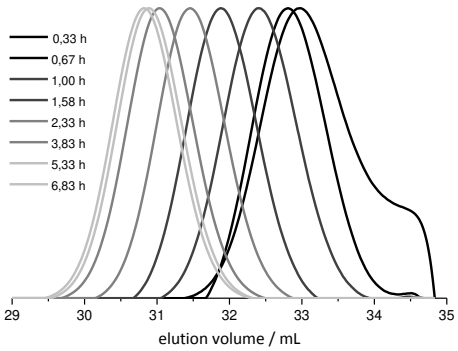

Figure S2.13. SEC-kinetics of MsMAz (**1**) (monomer), BnN**Li**Ms (**3**) (initiator) at 50 °C in DMF (RI-signal, PEO-standard).

NaMDS

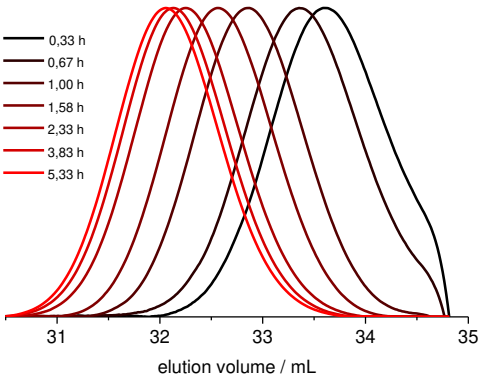

Figure S2.14. SEC-kinetics of MsMAz (**1**) (monomer), BnN**Na**Ms (**3**) (initiator) at 50 °C in DMF (RI-signal, PEO-standard).

2.7.7 Chain extension experiments.

All polymerizations were carried out in analogy to the conventional procedure in a Schlenk-flask. The first monomer and the initiator were dissolved in 2 mL anhydrous *N,N*-dimethylformamide (DMF) each. A stock solution of the initiator system was prepared and only the appropriate volume extracted and added to the monomer solution. After stirring the mixture for 10 h at the respective temperature, the second monomer, in 1 mL DMF, was added and stirred for further 24 h at the same temperature. To terminate the polymerization, 0.5 mL degassed methanol were added and the reaction mixture was precipitated in ca. 30 mL methanol.

P(TsMAz-block-MsMAz) at 50 °C

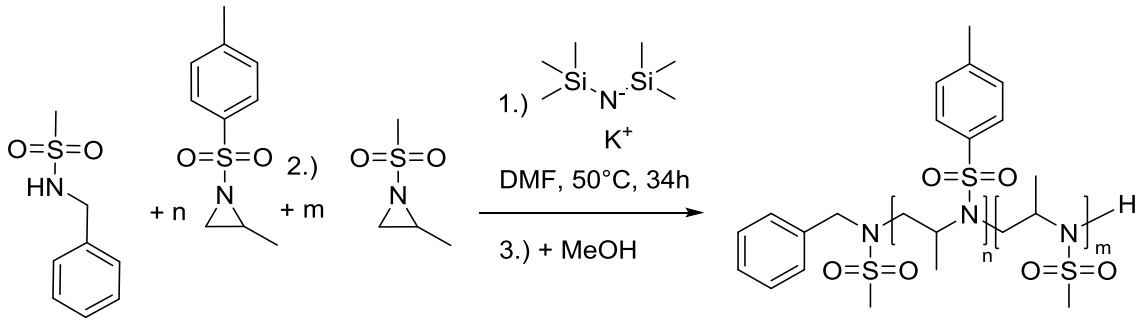

P(TsMAz$_{50(theo)}$-*block*-MsMAz$_{50(theo)}$): [1.) TsMAz (**2**) (100.0 mg, 0.47 mmol), 2.) MsMAz (**1**) (63.9 mg, 0.47 mmol), BnNHMs (**3**) (1.8 mg, 9.5 µmol), KMDS (1.9 mg, 9.5 µmol)].

1. block: SEC (RID, DMF, PEO): M_n = 3200; $Đ$ = 1.13

2. block: SEC (RID, DMF, PEO): M_n = 4800; $Đ$ = 1.11

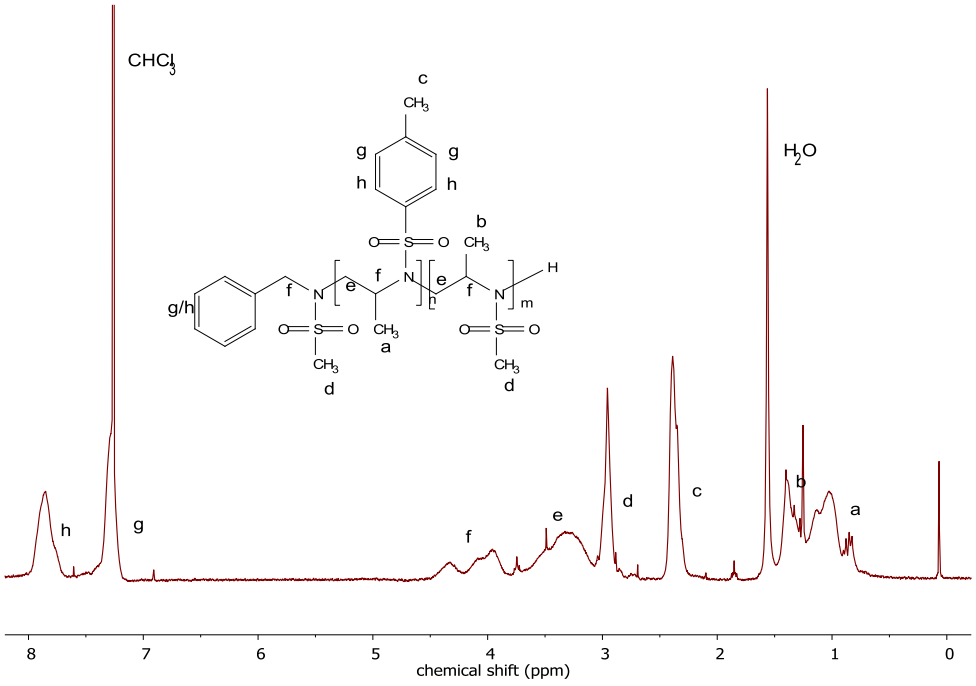

Figure S2.15. ^{1}H NMR (300 MHz, 298 K, $CDCl_3$) of P(TsMAz-*block*-MsMAz).

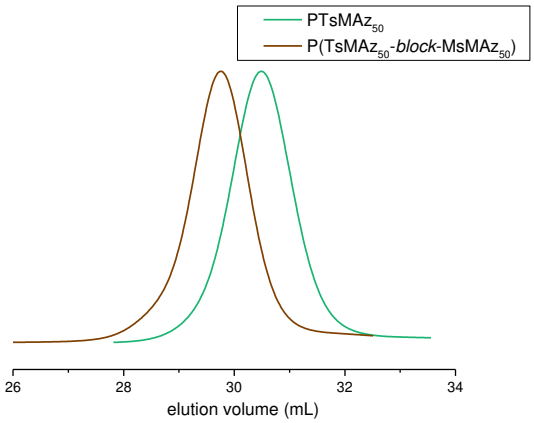

Figure S2.16. SEC traces of P(TsMAz-*block*-MsMAz) in DMF (RI signal).

P(MsMAz-block-MsMAz) at 100 °C

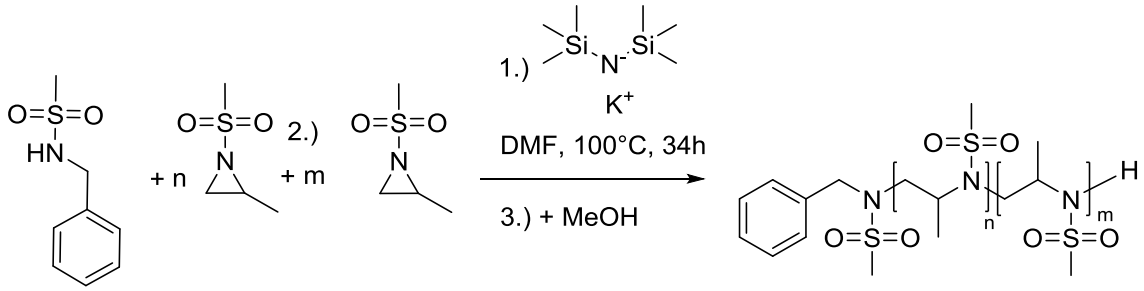

P(MsMAz$_{30(theo)}$-*block*-MsMAz$_{30(theo)}$): [1.) MsMAz (**1**) (100.0 mg, 0.74 mmol), 2.) MsMAz (**1**) (100.0 mg, 0.74 mmol), BnNHMs (**3**) (4.6 mg, 24.7 µmol), KMDS (4.9 mg, 24.7 µmol)].

1. block: SEC (RID, DMF, PEO): M_n = 700; $Đ$ = 1.14

2. block: SEC (RID, DMF, PEO): M_n = 1200; $Đ$ = 1.13

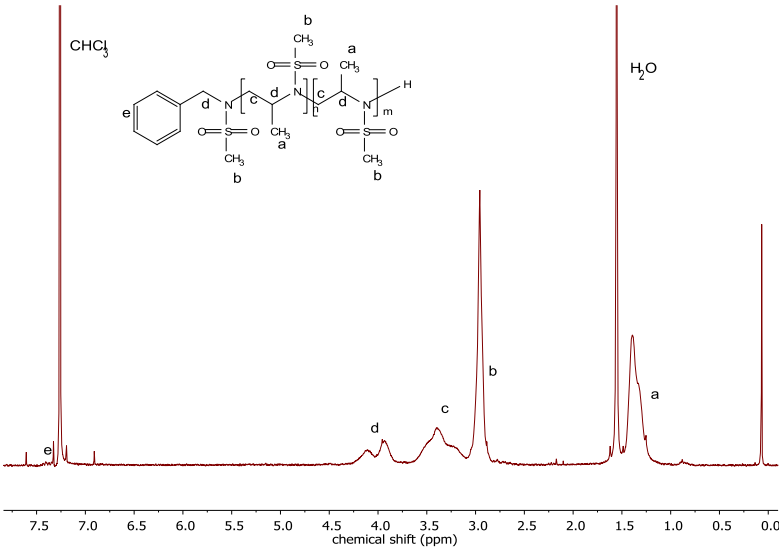

Figure S2.17. ^{1}H NMR (300 MHz, 298 K, $CDCl_3$) of P(MsMAz-*block*-MsMAz).

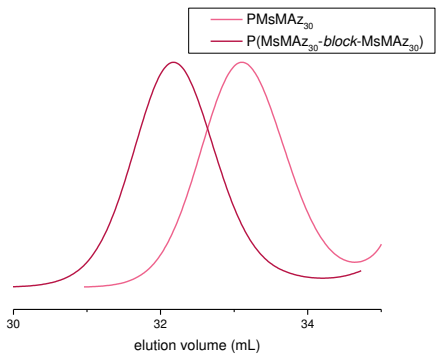

Figure S2.18. SEC traces of P(MsMAz-*block*-MsMAz) in DMF (RI signal).

2.8 References

1. Szwarc, M.; Levy, M.; Milkovich, R., *J. Am. Chem. Soc.* **1956,** *78* (11), 2656-2657.
2. Odian, G., *Principles of Polymerization*. 4. ed.; John Wiley & Sons, Inc. : Hoboken, New Jersey, USA, **2004**.
3. Hadjichristidis, N.; Hirao, A., *Anionic Polymerization: Principles, Practice, Strength, Consequences and Applications*. Springer Japan: **2015**.
4. Stewart, I. C.; Lee, C. C.; Bergman, R. G.; Toste, F. D., *Journal of the American Chemical Society* **2005,** *127* (50), 17616-17617.
5. Thomi, L.; Wurm, F. R., *Macromol. Rapid Commun.* **2014,** *35* (5), 585-589.
6. Thomi, L.; Wurm, F. R., *Macromolecular Symposia* **2015,** *349* (1), 51-56.
7. Rieger, E.; Alkan, A.; Manhart, A.; Wagner, M.; Wurm, F. R., *Macromol. Rapid Commun.* **2016,** *37* (10), 833-839.
8. Rieger, E.; Manhart, A.; Wurm, F. R., *ACS Macro Letters* **2016,** *5* (2), 195-198.
9. Reisman, L.; Mbarushimana, C. P.; Cassidy, S. J.; Rupar, P. A., *ACS Macro Letters* **2016,** *5* (10), 1137-1140.
10. Kobayashi, M.; Uchino, K.; Ishizone, T., *Journal of Polymer Science Part A: Polymer Chemistry* **2005,** *43* (18), 4126-4135.
11. Spork, A. P.; Donohoe, T. J., *Org Biomol Chem* **2015,** *13* (31), 8545-8549.
12. Jang, H.-J.; Lee, J. T.; Yoon, H. J., *Polymer Chemistry* **2015,** *6* (18), 3387-3391.
13. McLeod, D. C.; Tsarevsky, N. V., *Macromol Rapid Commun* **2016,** *37* (20), 1694-1700.
14. Moon, H. K.; Kang, S.; Yoon, H. J., *Polym. Chem.* **2017,** *8* (15), 2287-2291.
15. Homann-Müller, T.; Rieger, E.; Alkan, A.; Wurm, F. R., *Polym. Chem.* **2016,** *7* (35), 5501-5506.
16. Bakkali-Hassani, C.; Rieger, E.; Vignolle, J.; Wurm, F. R.; Carlotti, S.; Taton, D., *Chem. Commun.* **2016,** *52* (62), 9719-9722.
17. Sweeney, J. B., *Chemical Society Reviews* **2002,** *31* (5), 247-258.
18. Bednarek, M.; Kubisa, P.; Penczek, S., *Macromolecules* **1999,** *32*, 5257-5263.
19. Monnery, B. D.; Hoogenboom, R., Synthesis and Properties of Polyalkylenimines. In *Cationic Polymers in Regenerative Medicine*, Royal Society of Chemistry: London, **2015**; 30-61
20. Freeman, R.; Hill, H. D. W.; Kaptein, R., *J. Magn. Reson.* **1972,** *7*, 327-329.
21. Alkan, A.; Natalello, A.; Wagner, M.; Frey, H.; Wurm, F. R., *Macromolecules* **2014,** *47* (7), 2242-2249.
22. Natalello, A.; Alkan, A.; von Tiedemann, P.; Wurm, F. R.; Frey, H., *ACS Macro Letters* **2014,** *3* (6), 560-564.
23. Beylen, M. v.; Bhattacharyya, D.; Smid, J.; Szwarc, M., *The Journal of Physical Chemistry* **1966,** *70* (1), 157-161.

24. Kazanskii, K. S.; Solovyanov, A. A.; Entelis, S. G., *European Polymer Journal* **1971,** *7*, 1421-1433.
25. Szwarc, M., Living polymers and mechanisms of anionic polymerization. In *Living Polymers and Mechanisms of Anionic Polymerization*, Springer: **1983**; 1-177.
26. Matyjaszewski, K.; Müller, A. H. E., *Controlled and Living Polymerizations: From Mechanisms to Applications*. John Wiley & Sons: Weinheim, Germany, **2009**; p 634.
27. Herzberger, J.; Niederer, K.; Pohlit, H.; Seiwert, J.; Worm, M.; Wurm, F. R.; Frey, H., *Chemical Reviews* **2016,** *116* (4), 2170-2243.
28. Van Beylen, M.; Bywater, S.; Smets, G.; Szwarc, M.; Worsfold, D. J., Developments in anionic polymerization—a critical review. In *Polysiloxane Copolymers/Anionic Polymerization*, Springer: **1988**; 87-143.
29. Jeuck, H.; Müller, A. H., *Macromolecular Rapid Communications* **1982,** *3* (2), 121-125.
30. Dainton, F.; East, G.; Harpell, G.; Hurworth, N.; Ivin, K.; LaFlair, R.; Pallen, R.; Hui, K., *Macromolecular Chemistry and Physics* **1965,** *89* (1), 257-262.
31. Roovers, J.; Bywater, S., *Transactions of the Faraday Society* **1966,** *62*, 701-706.
32. Neander, S.; Behrens, U., *Z. Anorg. Allg. Chem.* **1999,** *625*, 1429-1434.
33. Holleman, A. F. W., E., *Lehrbuch der Anorganischen Chemie*. 34. ed. ed.; Walter de Gruyter Co.: Berlin, Germany, **1995**; Vol. 101.
34. Johnson, D. C.; Widlanski, T. S., *J. Org. Chem.* **2003,** *68*, 5300-5309.

3. Sequence-Controlled Polymers *via* Simultaneous Living Anionic Copolymerization of Competing Monomers

Elisabeth Rieger, Arda Alkan, Angelika Manhart, Manfred Wagner, Frederik R. Wurm

Max Planck Institute for Polymer Research, Ackermannweg 10, 55128 Mainz, Germany

Reproduced with permission from "*Macromolecular Rapid Communications,* **2016**, *37*, 833-839".

The evaluation of kinetic measurements was done by Elisabeth Rieger and partially together with Arda Alkan. Parts of the monomers were synthesized by Angelika Manhart. NMR kinetic measurements were performed in collaboration with Manfred Wagner.

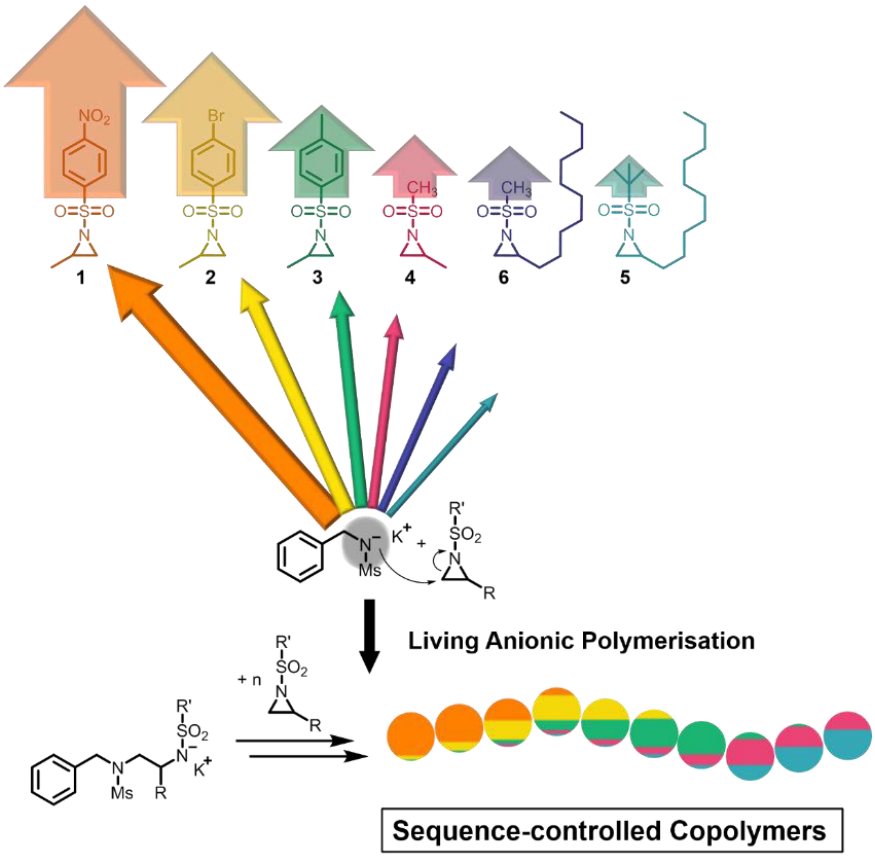

Keywords: Anionic Polymerization, Sequence-controlled polymers, Aziridine, Ring-Opening Polymerization, Copolymerization.

3.1 Abstract

Natural macromolecules, i.e. sequence-controlled polymers, build the basis for life. In synthetic macromolecular chemistry, reliable tools for the formation of sequence-controlled macromolecules are rare. We present a robust and efficient chain-growth approach based on the simultaneous living anionic polymerization of sulfonamide-activated aziridines for sequence control of up to five competing monomers resulting in gradient copolymers. The simultaneous azaanionic copolymerization is monitored by real-time ^{1}H NMR spectroscopy for each monomer at any time during the reaction. The monomer sequence can be adjusted by the monomer reactivity, depending on the electron-withdrawing effect by the sulfonamide (nosyl-, brosyl-, tosyl-, mesyl-, busyl-) groups. This method offers unique opportunities for sequence control by competing copolymerization: a step forward to well-engineered synthetic polymers with defined microstructures.

3.2 Introduction

Complex macromolecules are the basis for life: the genetic information is stored in exactly coded polyesters, i.e. DNA and RNA. In polymer science, synthetic macromolecules - far from their perfectly structured natural counterparts - have been created by men to fulfill certain scientific and industrial properties. All these synthetic macromolecules, however, rely on rather simple sequences, i.e. mainly homopolymers, statistical or diblock copolymers. The design of sequence-controlled macromolecules is a current challenge to achieve a new breakthrough for synthetic polymers. Meaningful applications in information storage, nanotechnology, biomaterials and catalysis are envisaged.[1-2]

Current strategies to generate sequence-controlled macromolecules rely on the sequential addition of monomers or solid-phase syntheses.[3-6] These strategies are perfect for the generation of well-defined model compounds on small scale (typically several hundred milligrams); however, they are not suitable for large-scale production and cannot be combined with established techniques. Achieving control over monomer sequence with classical monomers and/or polymerization techniques would be very attractive, as it allows transfer to industrial application and the use of a plethora of available monomers.[7] After all, macroscopic properties, such as crystallinity or glass transition can be tuned by the monomer sequence.[8]

Only living anionic polymerization (LAP) brings polymer chemistry close to natures' precision of generating macromolecules with a single molecular weight and complex architecture.[9-10] Handling of different building blocks is well-established, e.g. basic vinyl monomers (styrenes and acrylates) or epoxides, with high control in the university-lab as well as industrially on a ton scale to generate block copolymers and other structures, which are

commodities today.[10] The competing, sequence-controlled (ionic) copolymerization of several monomers to high molecular (multi)block copolymers is rarely reported. Simultaneous copolymerization of different monomers by anionic polymerization is difficult, as in most cases control over monomer incorporation is lost, mainly due to the different nucleophilicities of the propagating species[11] and had only limited success;[7, 12-17] the terpolymerization of styrene with diphenylethylene (DPE) derivatives was reported to exhibit sequence-cotnrolled behavior by tuning of the DPE reactivity.[18]

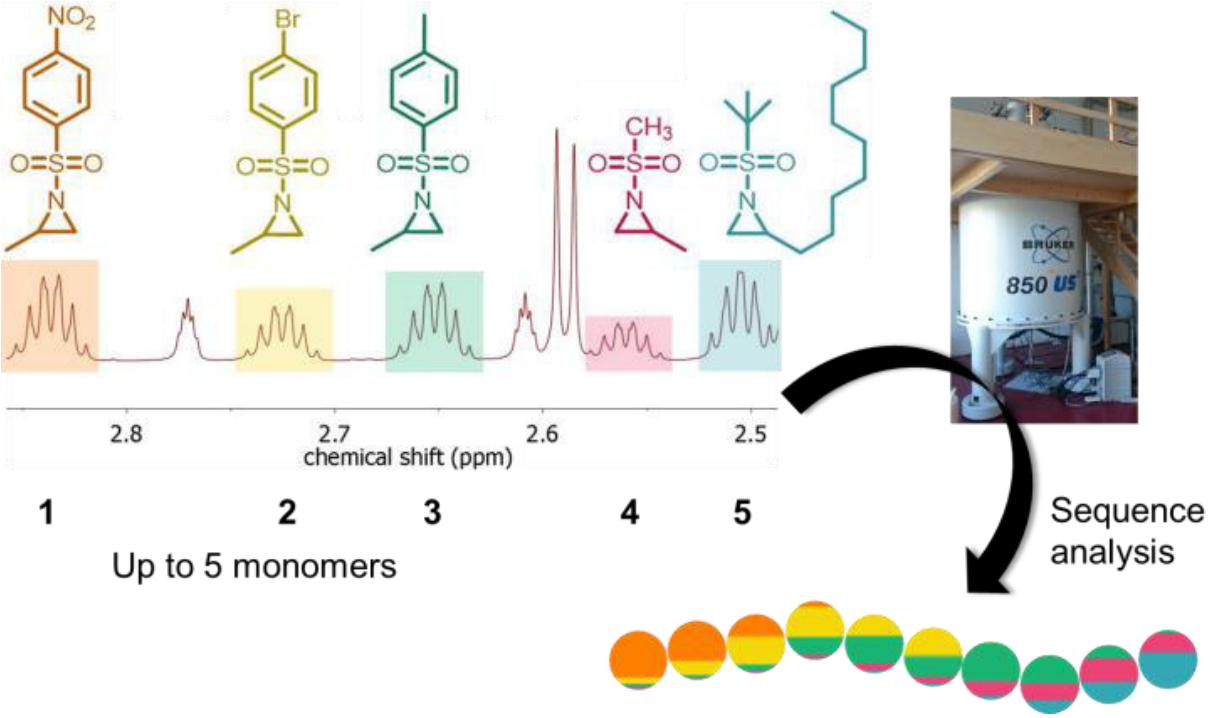

Figure 3.1. Real-time NMR allows following the sequence distribution. Monomer chemistry determines the monomer reactivity and the sequential incorporation which is monitored by ^{1}H NMR spectroscopy.

Herein, the simultaneous, sequence-controlled copolymerization of up to five different *N*-sulfonyl-aziridines, **1**-**5** (Figure 3.1) in a one-step, one-pot reaction is presented, i.e. omitting sequential monomer addition.

Activated aziridines differing in their side-chains (methyl or decyl) and their activating groups (mesyl-, busyl-, tosyl-, brosyl-, or nosyl-) have been developed. In contrast to styrene or acrylate-derivatives, the different sulfonamide derivatives allow – due to the different electron-withdrawing strength – adjusting the reactivities of the growing chain end and the monomer. Ter-, quater-, and quinto- copolymers have been prepared by simultaneous anionic ring-opening polymerization (AROP) for the first time with M_w/M_n = 1.1-1.2 and control over monomer sequence along the polymer backbone.

N-sulfonyl aziridines represent a rather new monomer class for the AROP,[19-21] with a direct access to poly(ethylene imine)-derivatives. With a comparable ring strain of ca. 111 kJ/mol[22] (for ethylene imine) and 114 kJ/mol[23] for ethylene oxide, aziridines can undergo ring-opening reactions and are typically polymerized by an uncontrolled cationic mechanism.[22, 24] Since nitrogen is trivalent, branched polymers with broad molecular weight distributions are obtained. The acidic proton needs to be altered to allow the anionic ring-opening of an aziridine.[22] This is an ideal handle to control the monomer reactivity by the nature of the activating group and to generate sequence-controlled polymers. We have chosen different sulfonamides as activating groups to control the kinetics of the nucleophilic ring-opening. The amide resonance contributes to the stability of the aziridine itself and the resulting amide anion after ring-opening. These monomers are prepared in high yield reactions, are convenient to handle, often crystalline, and can be combined with the current setup for anionic polymerization.

To date only very few report use *in situ* techniques to follow the individual monomer incorporation rates during co-polymerizations. Infrared or UV spectroscopy was applied to monitor cationic polymerizations at low temperatures[16-17] and the copolymerization of styrene and isoprene.[25-26] Real-time ^{1}H and/or ^{13}C NMR spectroscopy was used for the anionic copolymerization of oxiranes[12, 27] and styrenes.[14-15]

3.3 Results and Discussion

All aziridine monomers prepared herein can be distinguished in their ^{1}H (either the ring methylenes or methines) and ^{15}N NMR resonances (compare Supporting Information 3.6.3), which indicates their different electron densities in the rings, similar to the *β*-^{13}C NMR shift for styrenes.[11] Thus, we expected different polymerization rate constants for all monomers. As the AROP of tosyl- and mesyl-substituted aziridines has been reported to follow a living polymerization mechanism,[19, 21] real-time ^{1}H NMR spectroscopy is the ideal tool to monitor monomer incorporation. For all monomers, their homopolymerization rate constants have been determined and chain extension experiments have proven a living polymerization mechanism (cf. Supp. Info). In homopolymerizations the reaction rates followed directly the electron withdrawing effects of the sulfonamides with nosyl- substituted monomers being the most reactive, followed by brosyl > tosyl > mesyl. Thus, when two aziridines with different activating groups are simultaneously copolymerized, copolymers with a gradient depending on the difference in reaction kinetics are expected. In the case of brosyl- and mesyl-activated aziridines (2-**m**ethyl-*N*-**b**ro**s**yl**az**iridine (BsMAz, **2**) and 2-**m**ethyl-*N*-**m**e**s**yl**az**iridine (MsMAz,**4**)) copolymers with two separate glass transition temperatures (T_g) were obtained (poly(BsMAz-*co*-MsMAz) ($T_g(1)$ = 142 °C and $T_g(2)$ = 175 °C, Figure 3.2) indicating a block-like structure. Copolymers of

two monomers with the same activating groups show a single T_g (Figure 3.2). Motivated by these initial findings, the simultaneous copolymerization of up to five different aziridines has been studied. By simple electronic consideration we expected the propagation rates to decrease in the following order regarding the activation groups nosyl > brosyl > tosyl > mesyl ≥ busyl due to electronic effects. In addition, the effect of the pendant side chain (methyl or decyl) was analyzed.

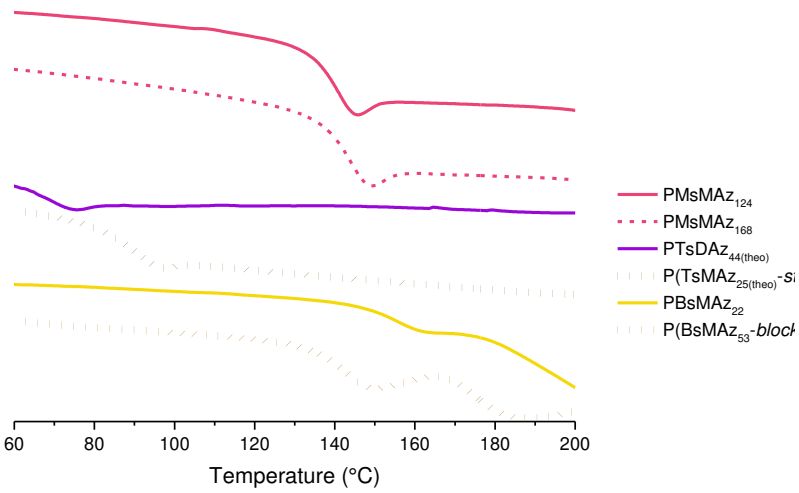

Figure 3.2. DSC curves (3rd run (heating)) of representative poly(aziridine)s – homopolymers, random copolymers, diblock copolymers.

Terpolymerization. The simultaneous copolymerization BsMAz, 2-**m**ethyl-*N*-**t**o**s**yl**az**iridine (TsMAz), and MsMAz was studied after initiation at 50 °C by the addition of the potassium salt of *N*-benzyl-sulfonamide (BnNKMs). From the recorded real-time ^{1}H NMR spectra, the fast incorporation of the brosylated aziridine (BsMAz) is obvious from the fast disappearance of the doublet of the ring methylenes of BsMAz at 2.25 ppm (Figure 3.3A, yellow). The distinct doublets at 2.18 and 2.15 ppm for the ring methylenes of the two other monomers, i.e. TsMAz and MsMAz respectively, disappear subsequently regarding their propagation rate constants (Ts > Ms), while simultaneously the broad resonance of the polymer backbone emerges at ca. 4.64-3.01 ppm. By integration of the well-separated monomer resonances over time (Figure 3.3A: signals **a**, **b** and **c**) and normalization to the amount of unreacted monomer, plotting of the assembly of each monomer in the growing polymer chain *vs.* the reaction time or total conversion is possible (Figure 3.3). By fitting these values, the probability of comonomer incorporation, which is mathematically the mole fraction of the incorporated comonomer, the monomer sequence distribution over the final polymer was calculated and is shown schematically with every sphere

summarizing 10% of monomer conversion (the color code and proportions display the incorporation probability of each comonomer in the respective polymer segment Figure 3.3D).

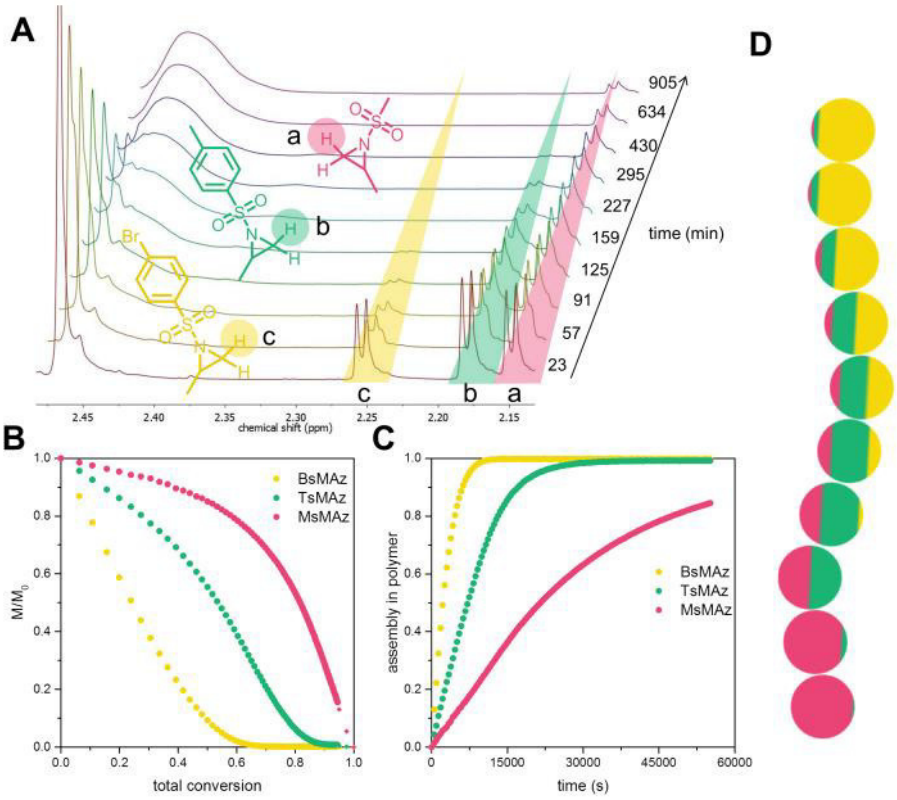

Figure 3.3. Simultaneous copolymerization of BsMAz, TsMAz, and MsMAz. (A) Zoom into the real-time ^{1}H NMR spectra of the terpolymerization, showing the consumption of the monomers. (BsMAz (yellow), TsMAz (green), MsMAz (red)). (B) Normalized monomer concentrations in the reaction *vs*. total conversion. (C) Assembly of each monomer in the polymer *vs*. reaction time. (D) Visualization of a single chain for poly(BsMAz-*co*-TsMAz-*co*-MsMAz) - each sphere stands for 10% conversion.

Figure 3.3C reveals that BsMAz is fully consumed within the first three hours, while at that time only 50% of TsMAz have reacted. For full consumption of TsMAz, additional five hours are required, whereas MsMAz needs more than 17 h to reach full conversion, i.e. the monomer incorporation follows the trend of the homopolymerization rate constants (cf. Table S3.1, i.e. BsMAz> TsMAz > MsMAz). These plots clearly show the formation of copolymers with very sharp gradients between the three segments; however, overlapping areas cannot be prevented, as expected for a chain-growth copolymerization compared to sequential monomer addition. This simultaneous terpolymerization allows the generation of sequence-controlled terpolymers by AROP. There is a single report on the simultaneous AROP of three lactones for the synthesis of terpolymers, but monomer incorporation rates were not investigated.[28]

Quaterpolymerization. When 2-**m**ethyl-*N*-**n**o**s**yl**az**iridine (NsMAz), carrying a nosyl activating group was additionally added to the polymerization mixture, a copolymer with four segments was expected. Figure 3.4 shows the copolymerization behavior of the copolymerization of NsMAz (orange), BsMAz (yellow), TsMAz (green), and MsMAz (red). The influence of the four different sulfonamides on the incorporation rate of the monomers in the polymer chain follows their individual rate constants. NsMAz with the highest polymerization rate constant was incorporated into the polymer chain as twice the rate as BsMAz. From the real-time ^{1}H NMR spectra, the resonances of the methylene group of NsMAz at 2.35 ppm (Figure 3.4A) are consumed quickly followed by the other three monomers sequentially and according to their relative homopolymerization rate constants. Thus, the incorporation rate follows the same general trends, i.e. the more electron-withdrawing the *N*-sulfonyl-group, the faster its incorporation rate; this results in a segmented copolymer with gradient structure nosyl > brosyl > tosyl > mesyl (poly(NsMAz-*co*-BsMAz-*co*-TsMAz-*co*-MsMAz), Figure 3.4). The SEC trace after the reaction under conventional conditions proves full conversion of all monomers and M_w/M_n of 1.16 (Figure S30: SEC, Figure S22: ^{1}H NMR of the final copolymer).

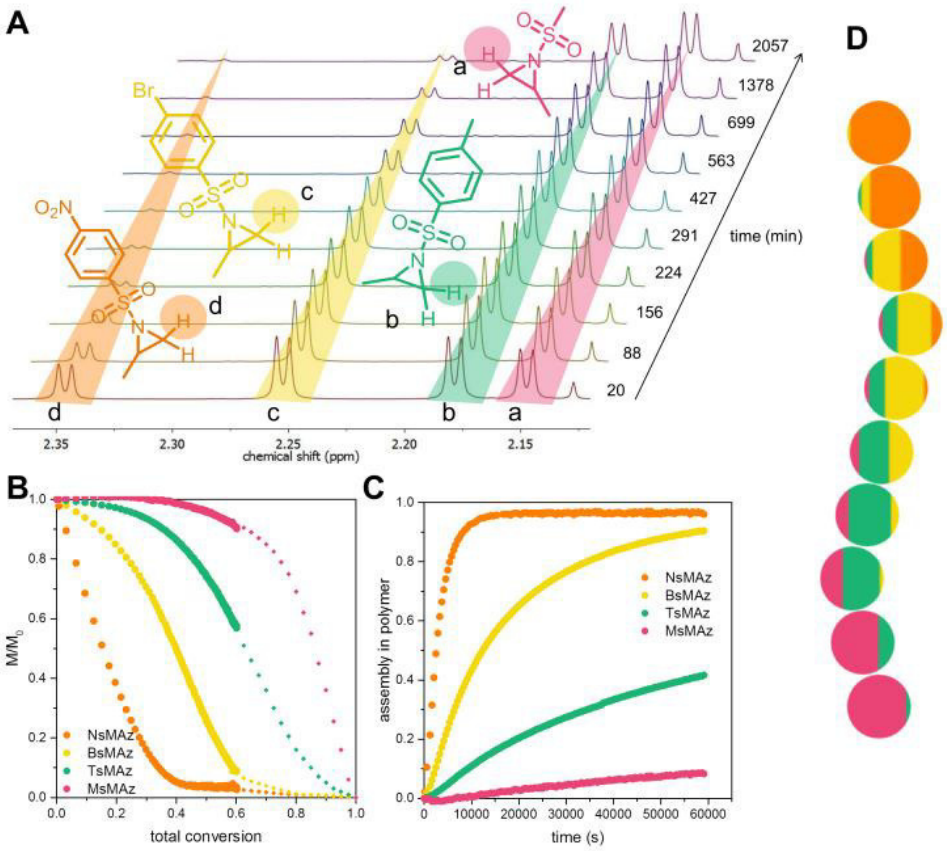

Figure 3.4. Simultaneous copolymerization of NsMAz, BsMAz, TsMAz and MsMAz. (A) Zoom into the real-time ^{1}H NMR measurement (NsMAz (orange), BsMAz (yellow), TsMAz (green), MsMAz (red)). (B) Normalized monomer concentrations in the reaction *vs.* total conversion (diamonds: extrapolated). (C) Assembly of each monomer in the polymer *vs.* reaction time. (D) Visualization of a single chain for poly(NsMAz-*co*-BsMAz-*co*-TsMAz-*co*-MsMAz).

In the following, the steric effect of the side chains with the same activating groups was investigated. Following the above mentioned trends, a copolymer from NsMAz, BsMAz, MsMAz, and 2-**d**ecyl-*N*-**m**e**s**yl**az**iridine (MsDAz) was synthesized (compare Figure 3.5). In this mixture two monomers carry the same sulfonamide chain, i.e. mesyl, but the side chain differs (methyl *vs.* decyl). Figure 3.5 summarizes the results: both mesyl-monomers show lower polymerization rates compared to the nosylated and brosylated monomers in the mixture and are not fully consumed during the real-time NMR measurement. Interestingly, the sterically demanding decyl-side chain has only a slight impact on the polymerization rates, thus resulting in a copolymer with three segments, while the third segment has almost random distribution of MsMAz and MsDAz (poly(NsMAz-*co*-BsMAz-*co*-(MsMAz-*co*-MsDAz)).

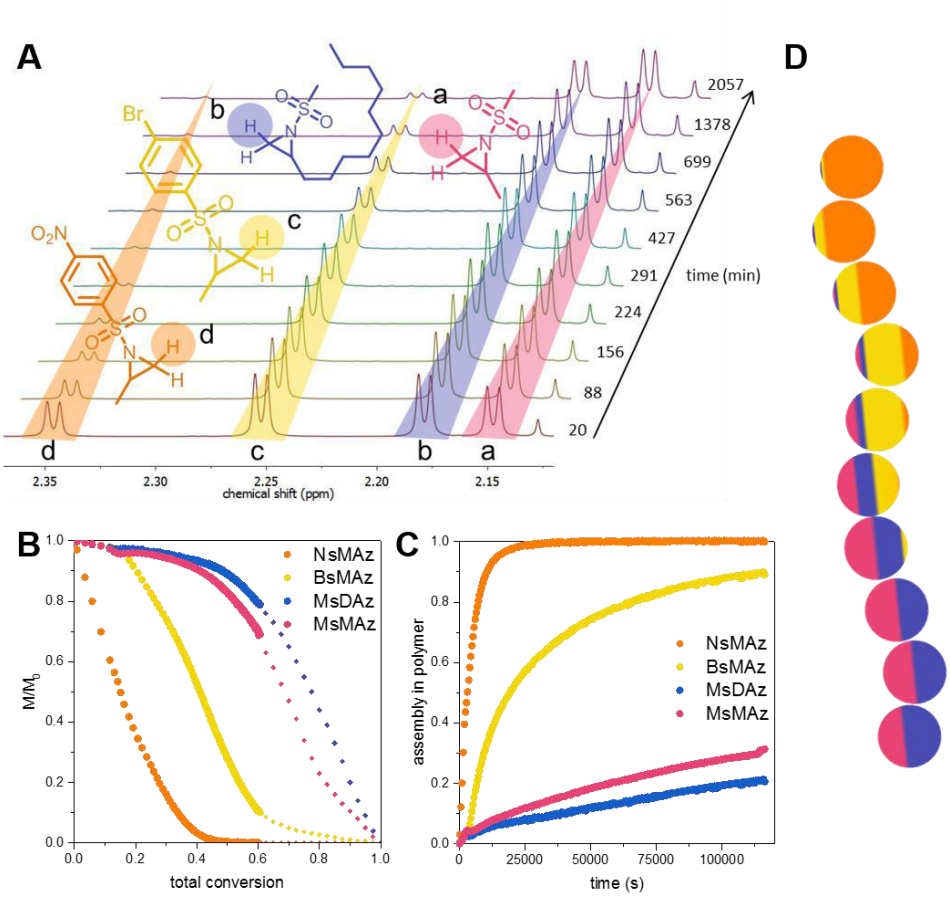

Figure 3.5. Simultaneous copolymerization of NsMAz, BsMAz, MsMAz and MsDAz. (A) Zoom into the real-time ^{1}H NMR measurement (NsMAz (orange), BsMAz (yellow), MsMAz (red), MsDAz (blue)). (B) Normalized monomer concentrations in the reaction *vs.* total conversion (diamonds: extrapolated). (C) Assembly of each monomer in the polymer *vs.* reaction time. (D) Visualization of a single chain for poly(NsMAz-*co*-BsMAz-*co*-MsMAz-*co*-MsDAz).

Quintopolymerization. To the best of our knowledge, a simultaneous polymerization of five different monomers has not been conducted to date by any ionic polymerization strategy; only sequential monomer addition has been used to prepare pentablock quintopolymers.[29-30] The simultaneous copolymerization of five different activated aziridines can be monitored via ^{1}H NMR spectroscopy. As an additional handle, a new monomer was synthesized, i.e. 2-**d**ecyl-*N*-*tert*-**bu**tyl**s**ulfonyl**az**iridine (BusDAz) carrying a busyl activating group. All monomers can be distinguished by their ^{1}H NMR resonances of their ring methines in this case (Figure 3.6: multiplets at 3.01-2.97 ppm (NsMAz - orange), 2.90-2.86 ppm (BsMAz - yellow), 2.83-2.79 ppm (TsMAz - green), 2.73-2.70 ppm (MsMAz - red), and 2.68-2.64 ppm (BusDAz - cyan)). Also for the competing copolymerization of five comonomers the trends of monomer incorporation follows the trends of the homopolymerization rate constants of the individual monomers. NsMAz is incorporated as fastest monomer into the living polymer (note: the slight decreasing in Figure 3.6C is due to partial overlapping to the polymer backbone, as in this case the methine resonances of the monomers had to be used). The incorporation of NsMAz is followed by BsMAz > TsMAz > MsMAz. The additional BusDAz shows the slowest incorporation, probably caused by the less negative inductive effect of the *tert*-butyl-group of the busyl group *vs*. the methyl-group in the mesylate due to the additional methyl-groups and additional steric hindrance (separate polymerization however, proves their living nature and full conversion). Thus the different polymerization rate constants of these five monomers allow the synthesis of copolymer with a sequenced gradient poly(NsMAz-*co*-BsMAz-*co*-TsMAz-*co*-MsMAz-*co*-BusDAz).

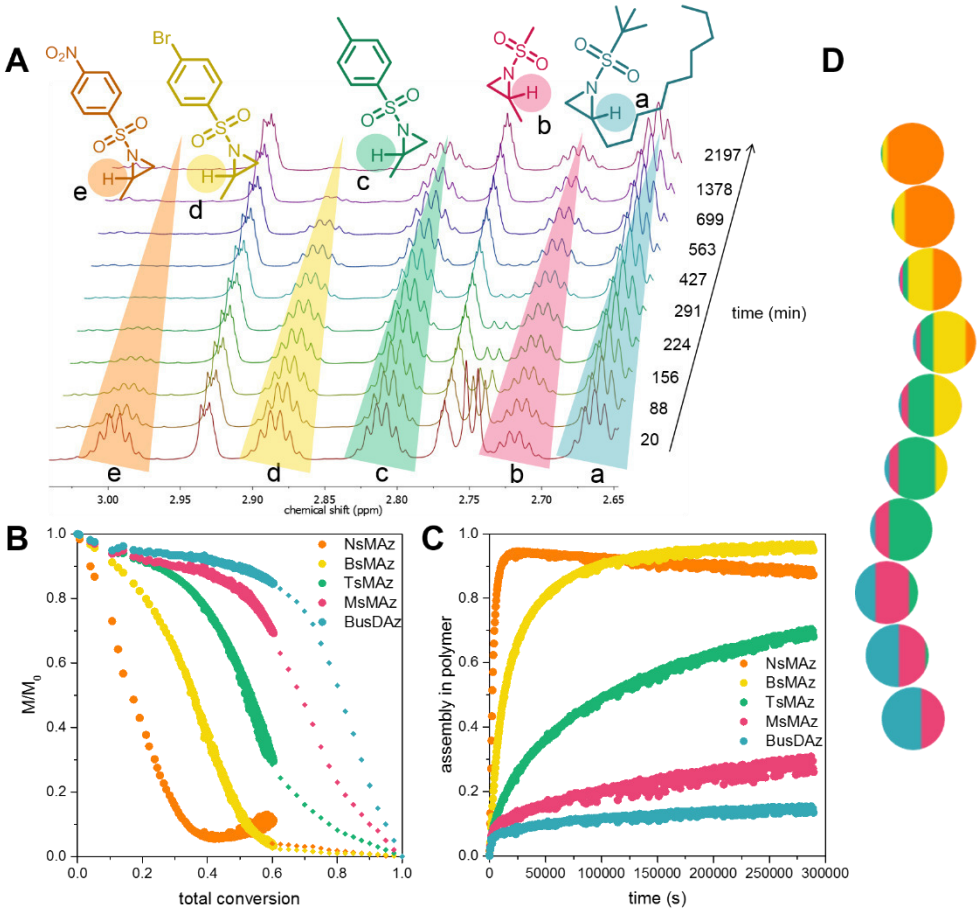

Figure 3.6. Simultaneous copolymerization of NsMAz, BsMAz, TsMAz, MsMAz, and BusDAz. (A) Zoom into the real-time ^{1}H NMR measurement (NsMAz, (orange), BsMAz (yellow), TsMAz (green), MsMAz (red), BusDAz (cyan)). (B) Normalized monomer concentrations in the solution *vs*. total conversion (diamonds: extrapolated). (C) Assembly of monomer in the polymer *vs*. time. (D) Visualization of a single chain for poly(NsMAz-*co*-BsMAz-*co*-TsMAz-*co*-MsMAz-*co*-BusDAz).

3.4 Summary

In summary, the anionic copolymerization of a series of competing *N*-sulfonyl aziridines allowed for the first time to synthesize gradient copolymers with up to five different monomers. Control over monomer incorporation brings classical polymerization methods closer to natures' perfection and allows the production of advanced polymers for various applications in materials science. As the polymerization follows a living polymerization mechanism (without termination/ transfer), simultaneous copolymerization of aziridines is possible and due to excellent signal separation, the polymerization can be monitored by real-time ^{1}H NMR spectroscopy. The monomers were designed to exhibit distinctively different polymerization rate constants due to the electronic nature of the activating group (NsMAz > BsMAz > TsMAz > MsMAz ≥ MsDAz ≥ BusDAz). This allows the synthesis of copolymers with sharp gradients in a competing copolymerization affording polymers typically with $M_w/M_n < 1.2$. We believe that this platform is new efficient way to design polyamides with a controlled gradient structure and well-defined polyamines (after removal of the activating groups). Furthermore, the combination with other anionic polymerization techniques such as epoxides or vinyl monomers is worth to be investigated. This allows for the first time the combination of aziridine-based polymers with commodity monomers. The toolbox of monomers presented in this study will open the way for the establishment of aziridines as new monomer class for anionic polymerization.

3.5 Acknowledgments

The authors thank Prof. Dr. Katharina Landfester for continuous support. E.R. thanks the BMBF/MPG network MaxSynBio. The authors thank the Deutsche Forschungsgemeinschaft (DFG WU/750 7-1) for support.

3.6 Supporting Information

The Supporting Information contains additional synthetic procedures, characterization data for monomers, polymers and kinetic measurements.

Content

3.6.1 Synthetic Protocols – Monomers and Initiator.

Materials.

All solvents and reagents were purchased from Sigma-Aldrich, Acros Organics or Fluka and used as received unless otherwise mentioned. Deuterated *N,N*-dimethylformamide (DMF-d_7) was purchased from Deutero GmbH and was distilled from CaH_2 and stored in a glovebox prior to use. All monomers and the initiator were dried extensively by azeotropic distillation with benzene prior to polymerization.

Instrumentation and Characterization Techniques.

NMR. ^{1}H NMR, ^{13}C NMR and ^{15}N NMR spectra were recorded using a Bruker Avance III 250, a Bruker Avance 300, a Bruker Avance III 500, a Bruker Avance III 700 and a Bruker Avance III 850. All spectra were referenced internally to residual proton signals of the deuterated solvent.

SEC. For size exclusion chromatography measurements in DMF (containing 0.25 g/L of lithium bromide as an additive) an Agilent 1100 Series was used as an integrated instrument, including a PSS HEMA column (106/105/104 g/mol), a UV detector (275 nm), and a RI detector at a flow rate of 1 mL/min at 50 °C. Calibration was carried out using PEO standards provided by Polymer Standards Service.

DSC. Differential scanning calorimetry measurements were performed using a Mettler Toledo DSC 823 calorimeter. Three scanning cycles of heating-cooling were performed in the temperature range from −140 to 250 °C. Heating rates of 10 °C/min were employed under nitrogen (30 mL/min).

IR. The monomers were pressed with KBr to form a pellet and the absorption between 4,000 and 400 cm^{-1} was recorded in a Spectrum BX spectrometer from PerkinElmer.

Elemental analyses were determined with a Elementar Vario EL.

HRMS. High resolution mass spectroscopy spectra were recorded on a Q-ToF-Ultima 3 instrument (Waters, Milford, Massachusetts) with LockSprayTM interface and a suitable external calibrant.

Monomers derived from methylaziridine.

2-Methyl-N-mesylaziridine (MsMAz).

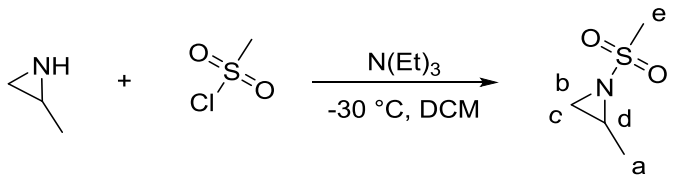

The compound was synthesized according to literature procedure.[19] Briefly, ca. 15 mL 2-methylaziridine were cryo transferred for purification. 2-Methylaziridine (10.7 g, 187 mmol) and triethylamine (37.4 mL, 281 mmol) were dissolved in anhydrous dichloromethane (DCM) (200 mL). The solution was cooled to -30 °C and mesylchloride (16.7 mL, 215 mmol) was added dropwise over a period of 20 minutes. Afterwards, the reaction mixture was stirred at -30 °C for one hour. Saturated aqueous sodium bicarbonate (200 mL) was added and the mixture was allowed to reach room temperature. After washing with brine, the organic phases were combined, dried over magnesium sulfate and concentrated at reduced pressure. The product was purified via chromatography over silica gel (petroleum ether/ethyl acetate 1:1) and sublimation at 35 °C at 0.05 mbar. The yield of the colorless needles was 11.68 g, 86 mmol, 46%. ^{1}H NMR (300 MHz, 295 K, Chloroform-*d*): δ 3.05 (s, 3H, e), 2.85–2.76 (m, 1H, d), 2.60 (d, *J* = 7.0 Hz, 1H, c), 2.07 (d, *J* = 4.6 Hz, 1H, b), 1.34 (d, *J* = 5.6 Hz, 3H, a). ^{13}C NMR (176 MHz, 298 K, Chloroform-*d*): δ 39.67, 35.25, 34.32, 16.90. ^{15}N NMR (71 MHz, 298 K, Chloroform-*d*): δ 78.27. HRMS (*m/z*): $[M]^+$ calcd. for $C_4H_{10}NO_2S$, 136.0432; found, 136.0442. Analysis (calcd., found for $C_4H_{10}NO_2S$): C (33.58, 33.67), H (7.15, 7.02), N (10.06, 9.90), S (12.15, 12.29). IR: $\tilde{\nu}$: 3090 (w), 3022 (w), 2989 (w), 2936 (w), 1454 (s), 1399 (w), 1302 (b), 1236 (m), 1187 (m), 1141 (s), 794 (s), 665 (s) cm^{-1}.

2-Methyl-N-tosylaziridine (TsMAz).

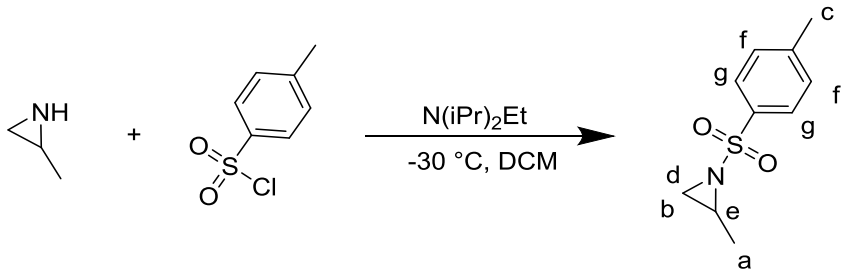

5 mL 2-methylaziridine were cryo transferred for purification. 2-Methylaziridine (4.36 g, 76 mmol) and *N,N*-diisopropylethylamine (19.4 mL, 115 mmol) were dissolved in anhydrous DCM (100 mL). The solution was cooled to -30 °C and tosylchloride (17.96 g, 94 mmol) in anhydrous DCM (50 mL) was added over a period of 25 minutes. Afterwards the reaction mixture was stirred at -30 °C for 1.5 hour. Saturated aqueous sodium bicarbonate (150 mL) was added and the mixture

was allowed to reach room temperature and stirred overnight. After washing with saturated aqueous sodium bicarbonate and brine, the organic phases were combined, dried over magnesium sulfate and concentrated at reduced pressure. Chromatography over silica gel (petroleum ether/ethyl acetate 5:1) yielded the product as a colorless solid (12.04 g, 57 mmol, 75%). ^{1}H NMR (300 MHz, 295 K, Chloroform-*d*): δ 7.89-7.71 (m, 2H, g), 7.37–7.28 (m, 2H, f), 2.92–2.74 (m, 1H, e), 2.59 (d, *J* = 7.0 Hz, 1H, d), 2.42 (s, 3H, c), 2.00 (d, *J* = 4.6 Hz, 1H, b), 1.23 (d, *J* = 5.6 Hz, 3H, a). ^{13}C NMR (176 MHz, 298 K, Chloroform-*d*): δ 144.47, 135.41, 129.75, 127.85, 35.92, 34.79, 21.68, 16.84. ^{15}N NMR (71 MHz, 298 K, Chloroform-*d*): δ 80.45. HRMS (*m/z*): $[M]^+$ calcd. for $C_{10}H_{14}NO_2S$, 212.0745; found, 212.0749. Analysis (calcd., found for $C_{10}H_{14}NO_2S$): C (55.96, 56.12), H (5.95, 5.83), N (6.99, 7.19), S (15.19, 15.39). IR: $\tilde{\nu}$: 3066 (w), 2976 (w), 2929 (w), 1597 (s), 1447 (s), 1402 (m), 1320 (b), 1238 (s), 1154 (s), 1098 (m), 1034 (m), 848 (s), 769 (s), 714 (s), 687 (s), 659 (s) cm^{-1}.

2-Methyl-N-brosylaziridine (BsMAz).

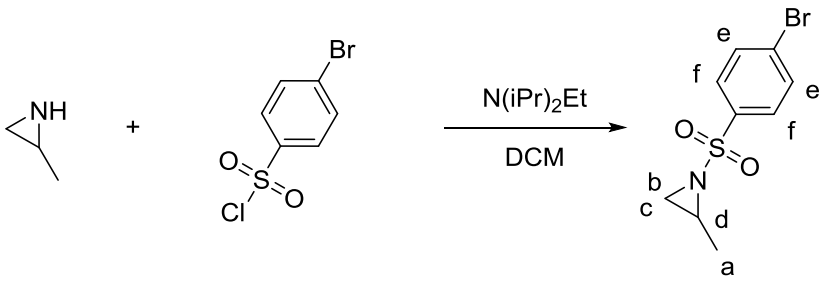

Prior to the reaction 2 mL 2-methylaziridine were cryo transferred for purification. 2-Methylaziridine (1.60 g, 28 mmol) and *N,N*-diisopropylethylamine (7.2 mL, 42 mmol) were dissolved in anhydrous DCM (60 mL). The solution was cooled to -30 °C and brosylchloride (8.18 g, 32 mmol) in anhydrous DCM (10 mL) was added over a period of 30 minutes. Afterwards the reaction mixture was stirred at -30 °C for half an hour and then allowed to reach room temperature. The mixture was washed with deionized water, hydrochloric acid (2%), saturated aqueous sodium bicarbonate and brine, the organic phases were combined, dried over magnesium sulfate and concentrated at reduced pressure. Chromatography over silica gel (hexanes/ethyl acetate 10:1) yielded the product as a colorless solid (1.55 g, 5.6 mmol, 20%, yield not optimized). ^{1}H NMR (300 MHz, 295 K, Chloroform-*d*): δ 7.80–7.69 (m, 2H, f), 7.68–7.56 (m, 2H, e), 2.86-2.78 (m, 1H, d), 2.57 (d, *J* = 7.0 Hz, 1H, c), 1.99 (d, *J* = 4.7 Hz, 1H, b), 1.20 (d, *J* = 5.6 Hz, 3H, a). ^{13}C NMR (176 MHz, 298 K, Chloro- form-*d*): δ 137.69, 132.55, 129.41, 128.70, 50.27, 49.47, 36.39, 35.17, 19.21, 16.90. ^{15}N NMR (71 MHz, 298 K, Chloroform-*d*): δ 80.13. HRMS (*m/z*): $[M]^+$ calcd. for $C_9H_{11}NO_2SBr$, 275.9694; found, 275.9697. Analysis (calcd., found for $C_9H_{11}NO_2SBr$): C (38.18), H (4.88), N (4.85), S (10.42). IR: $\tilde{\nu}$: 3301 (w), 3088 (w), 2970 (w), 1573 (s), 1429 (s), 1391 (s), 1330 (ss), 1275 (m), 1238 (m), 1162 (ss), 1069 (s), 1038 (s), 848 (s), 825 (s), 772 (s), 742 (s), 708 (s), 676 (s), 610 (s), 559 (s) cm^{-1}.

2-Methyl-N-nosylaziridine (NsMAz).

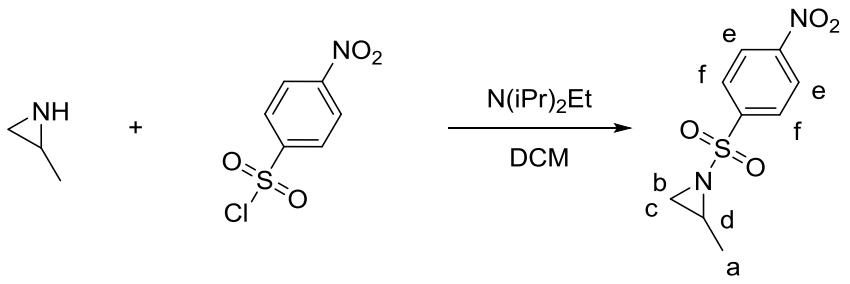

Prior to the reaction 2 mL 2-methylaziridine were cryo transferred for purification. 2-Methylaziridine (2.50 g, 44 mmol) and *N,N*-diisopropylethylamine (7.5 mL, 44 mmol) were dissolved in anhydrous DCM (90 mL). The solution was cooled to -30 °C and nosylchloride (11.16 g, 50 mmol) in anhydrous DCM (20 mL) was added over a period of 30 minutes. Afterwards the reaction mixture was stirred at -30 °C for half an hour and then allowed to reach room temperature. The mixture was washed with deionized water, hydrochloric acid (2%) and brine, the organic phases were combined, dried over magnesium sulfate and concentrated at reduced pressure. Recristallisation from Methyl *tert*-butyl ether (TBME) yielded the product as a slightly yellow solid (4.00 g, 46.5 mmol, 38%). ^{1}H NMR (250 MHz, 297 K, Chloroform-*d*): δ 8.48–8.31 (m, 2H, f), 8.24–8.03 (m, 2H, e), 3.05–2.81 (m, 1H, d), 2.70 (d, *J* = 7.1 Hz, 1H, c), 2.13 (d, *J* = 4.7 Hz, 1H, b), 1.26 (d, *J* = 5.6 Hz, 3H, a). ^{13}C NMR (176 MHz, 298 K, Chloro-form-*d*): δ 150.70, 144.41, 129.22, 124.42, 36.96, 35.64, 16.91. ^{15}N NMR (71 MHz, 298 K, Chloroform-*d*): δ 80.03. HRMS (*m/z*): $[M]^+$ calcd. for $C_9H_{11}N_2O_4S$, 243.0440; found, 243.0439. Analysis (calcd., found for $C_9H_{11}N_2O_4S$): C (43.93, 43.75), H (4.42, 4.30), N (10.17, 10.17), S (13.16, 12.91). IR: $\tilde{\nu}$: 3107 (w), 3068 (w), 2977 (w), 2936 (w), 1607 (s), 1529 (ss), 1449 (s), 1401 (s), 1351 (s), 1328 (s), 1240 (s), 1161 (ss), 1099 (s), 1033 (s), 849 (s), 768 (s), 692 (s), 615 (s) cm^{-1}.

Monomers derived from olefins.

2-Decyl-N-tosylaziridine (TsDAz).

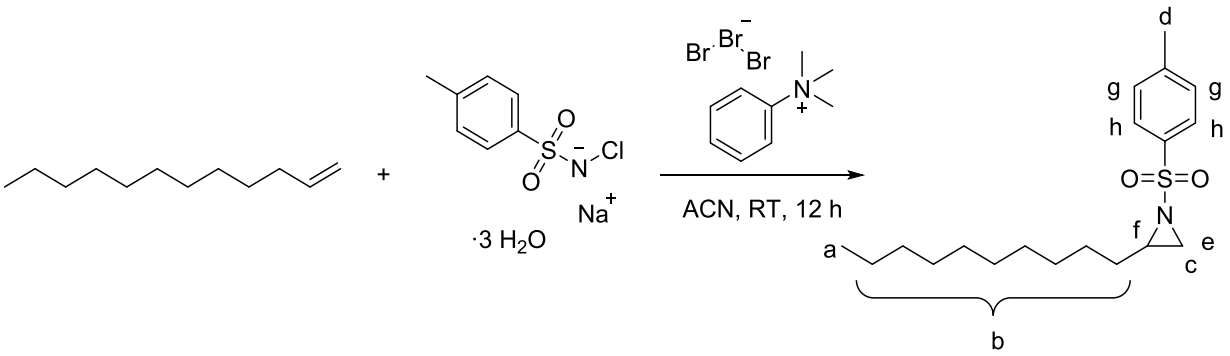

The compound was synthesized according to literature procedures.[31] Chloramine-T (13.99 g, 50 mmol) was dried azeotropically with benzene *in vacuo* for 6 h and at 90 °C for additional 8 h to remove the water. The anhydrous chloramine-T and 1-dodecene (10 mL, 45 mmol) were dissolved in anhydrous acetonitrile (ACN) (200 mL). Phenyltrimethylammonium tribromide (PTAB) (1.70 g, 4.5 mmol), dissolved in ACN (100 mL) was added and the mixture was stirred at room temperature for 16 hours. Ethyl acetate (40 mL) and deionized water (40 mL) were added. After washing with brine, the organic phases were combined, dried over magnesium sulfate and concentrated at reduced pressure. Chromatography over silica gel (hexanes/ethyl acetate 10:1 to 9:1) yielded the product as a yellowish oily liquid (7.12 g, 21 mmol, 47%). ^{1}H NMR (300 MHz, 295 K, Chloroform-*d*): δ 7.83 (d, *J* = 8.1 Hz, 2H, h), 7.33 (d, *J* = 8.1 Hz, 2H, g), 2.74–2.67 (m, 1H, f), 2.63 (d, *J* = 7.0 Hz, 1H, e), 2.44 (s, 3H, d), 2.05 (d, *J* = 4.5 Hz, 1H, c), 1.37–1.07 (m, 18H, b), 0.94–0.82 (m, 3H, a). ^{13}C NMR (176 MHz, 298 K, Chloroform-*d*): δ 144.44, 135.30, 129.66, 128.05, 40.55, 33.82, 31.96, 31.37, 29.50, 29.08, 26.82, 22.74, 21.66, 14.17. ^{15}N NMR (71 MHz, 298 K, Chloroform-*d*): δ 79.82. HRMS (*m/z*): $[M]^+$ calcd. for $C_{19}H_{32}NO_2S$, 338.2154; found, 338.2151. Analysis (calcd., found for $C_{19}H_{32}NO_2S$): C (67.16), H (6.66), N (6.00), S (10.78). IR: $\tilde{\nu}$: 3446 (w), 2926 (ss), 2855 (s), 1598 (s), 1461 (s), 1327 (ss), 1333 (s), 1162 (ss), 1193 (s), 816 (s), 715 (s), 694 (s), 662 (w) cm^{-1}.

2-Decyl-N-mesylaziridine (MsDAz).

Tert-butyl hypochlorite (tBuOCl).

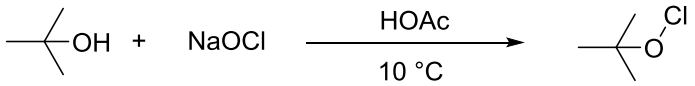

The complete procedure was carried out in the absence of light. In an Erlenmeyer-flask a solution (372.26 g, 500 mmol) of sodium hypochlorite (14%) was cooled down to 10 °C and stirred rigorously. *Tert*-butanol (66 mL, 500 mmol) and acetic acid (40 mL, 500 mmol) were added in small portions. The mixture was stirred for another 5 minutes. The aqueous phase was separated. The organic phase was washed with aqueous sodium bicarbonate (10%) and deionized water and yielded the product as a yellow liquid with a pungent odor, which was used without further purification (39.48 g, 364 mmol, 73%).

Sodium chloro(methylsulfonyl)amide (Chloramine-M).

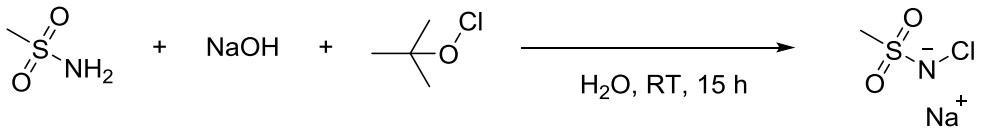

Methanesulfonamide (13.32 g, 140 mmol) was solved in 120 mL deionized water and sodium hydroxide (5.60 g, 140 mmol) was added. 16 mL of the freshly prepared *tert*-butyl hypochlorite were added and the mixture instantly turned colorless and heated up slightly. The solution was stirred at room temperature for three days. The solvent was removed at reduced pressure and the crude was washed with acetone. The solid was dried *in vacuo* for several days and yielded the product as a colorless solid (18.87 g, 135 mmol, 89%) and was used without further purification.

2-Decyl-N-mesylaziridine (MsDAz).

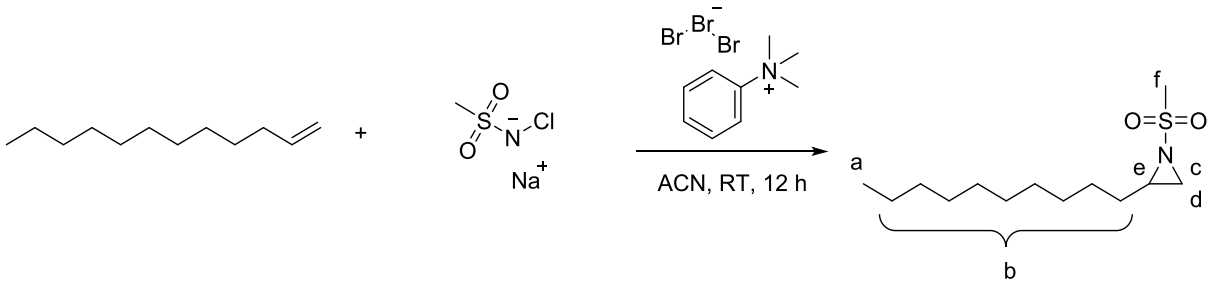

Chloramine-M (6.77 g, 44.70 mmol) was dried from benzene three times *in vacuo* for eight hours. Chloramine-M and 1-dodecene (9 mL, 40.64 mmol) were dissolved in anhydrous acetonitrile (ACN) (200 mL), phenyltrimethylammonium tribromide (PTAB) (1.53 g, 4.06 mmol) was added and the mixture was stirred at room temperature for 26 h. Ethyl acetate (40 mL) and deionized water (40 mL) were added and the phases were separated. After washing with brine, the organic phases were combined, dried over magnesium sulfate and concentrated at reduced pressure. Chromatography over silica gel by gradient (starting with 100% petroleum ether to petroleum ether/ethyl acetate 15:1 stepwise to 8:1) yielded the product as a yellowish oily liquid (5.28 g, 20 mmol, 49%). ^{1}H NMR (300 MHz, 295 K, Chloroform-*d*): δ 3.05 (s, 3H, f), 2.77-2.68 (m, 1H, e), 2.59 (d, J = 7.0 Hz, 1H, d), 2.10 (d, J = 4.6 Hz, 1H, c), 1.50–1.23 (m, 18H, b), 0.91–0.87 (m, 3H, a). ^{13}C NMR (176 MHz, 298 K, Chloroform-*d*): δ 40.02–39.37, 33.45, 31.94, 31.41, 29.97–28.90, 26.92, 22.73, 14.16. ^{15}N NMR (71 MHz, 298 K, Chloroform-*d*): δ 78.81. HRMS (*m/z*): $[M]^+$ calcd. for $C_{13}H_{28}NO_2S$, 262.1841; found, 262.1841. Analysis (calcd., found for $C_{13}H_{28}NO_2S$): C (59.67, 59.76), H (10.10, 10.31), N (6.07, 6.21), S (12.15, 12.29). IR: $\tilde{\nu}$: 3437 (w), 2926 (ss), 2856 (s), 1462 (s), 1372 (w), 1319 (ss), 1235 (w), 1153 (ss), 792 (m), 672 (w) cm^{-1}.

2-Decyl-N-busylaziridine (BusDAz).

Sodium chloro(tert-butylsulfonyl)amide (Chloramine-Bus).

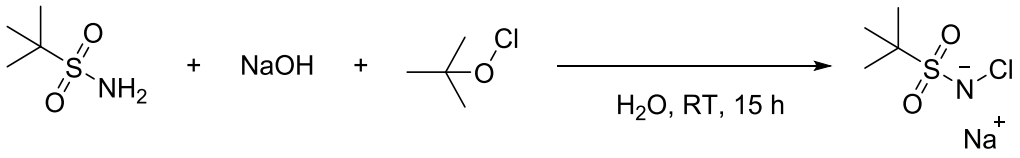

Tert-butylsulfonyl-amide (5 g, 35 mmol) was solved in 30 mL deionized water and sodium hydroxide (1.39 g, 35 mmol) was added. 3.3 mL of the freshly prepared *tert*-butyl hypochlorite were added and the mixture instantly turned colorless and heated up slightly. The solution was stirred at room temperature for three days. The solvent was removed at reduced pressure and the crude was washed with acetone. The solid was dried *in vacuo* from benzene for several days and yielded the product as a colorless solid (6.6 g, 35 mmol, 99%) and was used without further purification.

2-Decyl-N-busylaziridine (BusDAz).

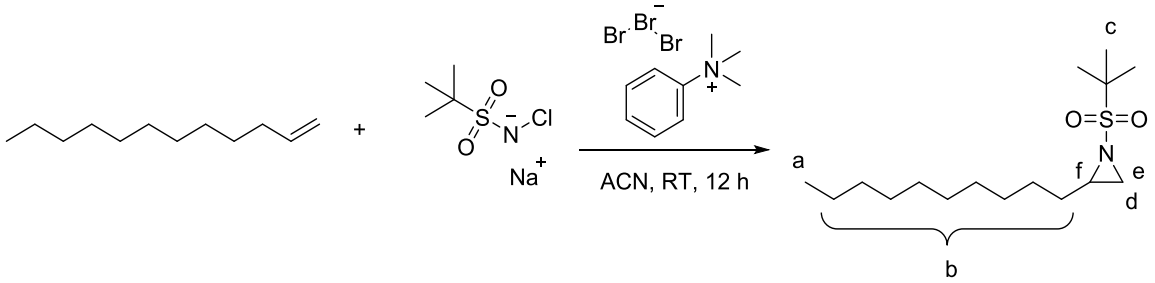

Chloramine-Bus (2.58 g, 12.4 mmol) was dried from benzene three times *in vacuo* for eight hours. Chloramine-Bus and 1-dodecene (1.9 g, 11.3 mmol) were dissolved in anhydrous acetonitrile (ACN) (55 mL), phenyltrimethylammonium tribromide (PTAB) (420 mg, 1.13 mmol) was added and the mixture was stirred at room temperature for 48 h. Ethyl acetate (40 mL) and deionized water (40 mL) were added and the phases were separated. After washing with brine, the organic phases were combined, dried over magnesium sulfate and concentrated at reduced pressure. Chromatography over silica gel (petroleum ether/ethyl acetate 20:3) yielded the product as a colorless oily liquid (1.4 g, 6 mmol, 50%). ^{1}H NMR (250 MHz, 297 K, Chloroform-*d*): δ 2.76-2.65 (m, 1H, f), 2.57 (d, *J* = 6.9 Hz, 1H, e), 2.05 (d, *J* = 4.6 Hz, 1H, d), 1.48 (s, 9H, c), 1.45-1.11 (m, 18H, b), 0.95–0.80 (m, 3H, a). ^{13}C NMR (176 MHz, 298 K, Chloroform-*d*): δ 59.34, 38.89, 34.04, 32.03, 31.46, 29.95–28.95, 26.44, 24.36, 22.81, 14.25. ^{15}N NMR (71 MHz, 298 K, Chloroform-*d*): δ 66.39. HRMS (*m/z*): $[M + Na]^+$ calcd. for $C_{16}H_{33}NO_2SNa$, 326.2130; found, 326.2124. Analysis (calcd., found for $C_{16}H_{33}NO_2S$): C (63.34, 63.15), H (11.97, 12.15), N (5.44, 5.64), S (10.99, 11.19). IR: $\tilde{\nu}$: 2926 (ss), 2855 (s), 1462 (s), 1398 (w), 1368 (w), 1310 (ss), 1132 (s), 711 (m), 658 (w) cm^{-1}.

Initiators.

N-benzyl-sulfonamide (BnNHMs).

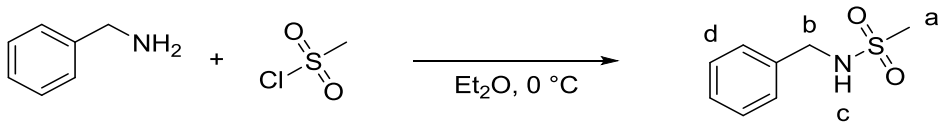

The compound was synthesized according to literature procedures.[32] A solution of benzylamine (15.3 mL, 139 mmol) in dry diethylether (360 mL) was cooled to 0 °C. Mesylchloride (5.2 mL, 66 mmol) was added dropwise. The reaction mixture was stirred overnight at room temperature. The precipitate was filtered and washed with diethylether. The organic phase was washed with 2 M hydrochloric acid and brine, dried over sodium sulfate and concentrated at reduced pressure. The resulting crude product was dissolved in THF (80 mL) and stirred for three hours at room temperature with a solution of 10% MeOH/ $NaHCO_3$ (40 mL). The mixture was concentrated at reduced pressure, the obtained syrup was dissolved in DCM. The organic phase was washed with water, dried over magnesium sulfate and concentrated at reduced pressure. The product was obtained as a colorless solid (7.83 g, 42 mmol, 30%). ^{1}H NMR (300 MHz, 295 K, Chloroform-*d*): δ 7.37–7.26 (m, 5H, d), 4.93 (s, 1H, c), 4.30 (d, 2H, J = 5.6 Hz, b), 2.84 (s, 3H, a).

3.6.2 Synthetic Protocols – Polymers.

All glassware was dried by *in vacuo* for at least three times. All reactants (except potassium bis(trimethylsilyl)amide (KHMDS)) were dried from benzene *in vacuo* for at least 6 h. The monomers and the BnNHMs-initiator were dissolved in 2 and 1 mL respectively anhydrous *N,N*-dimethylformamide (DMF). KHMDS was added very fast as a solid in argon-counter flow to the BnNHMs-solution and the sample boat was rinsed with another 1 mL DMF. The initiator-solution was transferred via syringe to the monomer-solution. For kinetic studies and syntheses of longer polymer chains due to the smaller amount, a stock solution of the initiator system was prepared and only the appropriate volume extracted and added to the monomer solution. The mixture was stirred at 55 °C for at least 18 h. To terminate the polymers, 0.5 mL degassed methanol were added and the reaction mixture was precipitated in ca. 30 mL methanol. The colorless solids were collected by centrifugation and dried at 70 °C *in vacuo.*

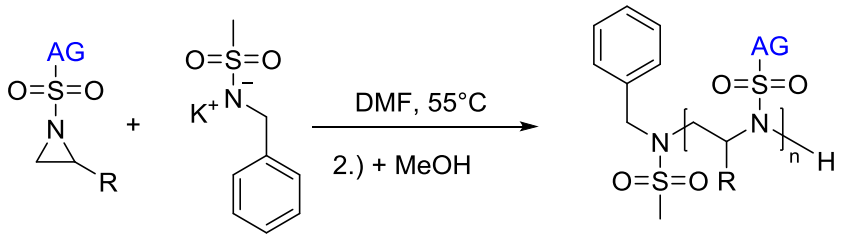

AG = Ns, Bs, Ts, Ms, Bus

Scheme S3.1. Azanionic polymerization of activated aziridines.

Monitoring (co)polymerizations by real-time ^{1}H NMR. All (co)polymerizations were carried out in analogy to the conventional procedure in a Schlenk-flask (compare Supp. Info.). Inside of a glove box under nitrogen the respective monomers were dissolved as a ca. 10 wt% solution in a total volume of 1 mL DMF-d_7. The initiator solution in 1 mL DMF-d_7 was prepared separately (exemplarily for the terpolymerization that is TsMAz (30.0 mg), MsMAz (19.2 mg), BsMAz (39.2 mg) and the initiator-system: BnNHMs (1.3 mg), Potassium bis(trimethylsilyl)-amide (KHMDS) (1.4 mg)). A conventional NMR-tube was filled with the reaction mixture and sealed with a rubber-septum. Prior to initiation, the pure monomer-solvent mixture was measured at 50 °C. From the stock solution of the initiator 100 µL were added to the monomer mixture, mixed quickly and inserted into the spectrometer. ^{1}H NMR kinetics were recorded using a Bruker Avance III 700 and a Bruker Avance III 850. All spectra were referenced internally to residual proton signals of the deuterated solvent dimethylformamide at 8.03 ppm. The π/2-pulse for the proton measurements varied between 9.3 and 11 µs for the different frequency. The spectra of the polymerizations and terpolymerization were recorded at 700 MHz with 32 number of scans (equal to 404 s), a relaxation time of 2 s after every pulse over a period of at least 15 h. Quaterpolymerizations and the quinterpolymerization were recorded at 850 MHz with 64 number of scans (equal to 413 s) and a relaxation time of 2 s over a period of at least 17 h. No B-field optimizing routine was used over the kinetic measurement time. The relaxation rate (T1) of the protons was measured before the kinetic run with the inversion recovery method.[33]

Homo- and Copolymers.

Poly(2-methyl-N-mesylaziridine) - P(MsMAz).

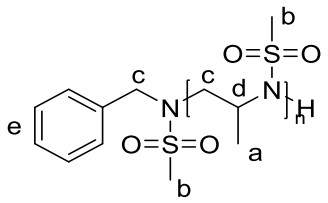

PMsMAz$_{124}$: [MsMAz (300.0 mg, 2.22 mmol), BnNHMs (9.3 mg, 50 µmol), KHMDS (10.1 mg, 50 µmol)]. ^{1}H NMR (300 MHz, 295 K, Methylene Chloride-d_2): δ 7.50–7.28 (m, e), 4.21–3.76 (m, d), 3.60–3.10 (m, c), 3.08–2.84 (m, b), 1.45–1.24 (m, a). M_n (SEC) = 4900 g/mol, $Đ$ = 1.08, M_n (NMR) = 16000 g/mol.

PMsMAz$_{168}$: [MsMAz (507.0 mg, 3.75 mmol), BnNHMs (2.8 mg, 15 µmol), KHMDS (3.0 mg, 15 µmol)]. ^{1}H NMR (300 MHz, 295 K, Methylene Chloride-d_2): δ 7.48–7.28 (m, e), 4.25–3.72 (m, d), 3.66–3.07 (m, c), 3.07–2.83 (m, b), 1.48–1.12 (m, 511H, a). M_n (SEC) = 11900 g/mol, $Đ$ = 1.15, M_n (NMR) = 22700 g/mol.

Poly(2-decyl-N-tosylaziridine) - (PTsDAz).

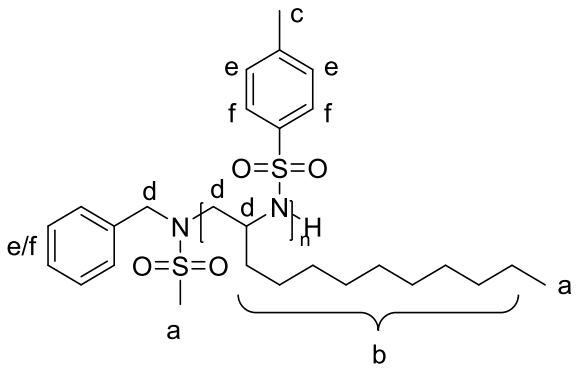

PTsDAz$_{26(theo)}$: [TsDAz (450.0 mg, 1.33 mmol), BnNHMs (9.3 mg, 50 µmol), KHMDS (10.1 mg, 50 µmol)]. ^{1}H NMR (300 MHz, 295 K, Methylene Chloride-d_2): δ 8.17–7.66 (m, f), 7.50–7.13 (m, e), 4.42–2.91 (m, d), 2.52–2.24 (m, c), 1.43–0.89 (m, b), 0.90–0.80 (m, a). M_n (SEC) = 4400 g/mol, $Đ$ = 1.10.

Poly(2-methyl-N-brosylaziridine) (PBsMAz)

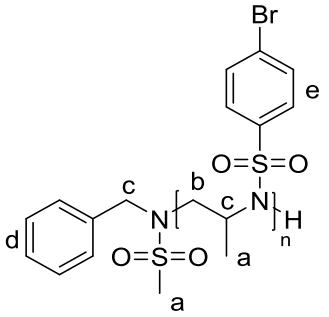

PBsMAz$_{22}$: [BsMAz (200.0 mg, 724 µmol), BnNHMs (6.7 mg, 36 µmol), KHMDS (7.2 mg, 36 µmol)]. ^{1}H NMR (300 MHz, 295 K, Methylene Chloride-d_2): δ 8.01–7.52 (m, e), 7.52-7.35 (m, d), 4.43–3.75 (m, c), 3.75–2.96 (m, b), 1.23–0.82 (m, a). M_n (SEC) = 3100 g/mol, $Đ$ = 1.10, M_n (NMR) = 6100 g/mol.

Poly(TsMAz-co-TsDAz).

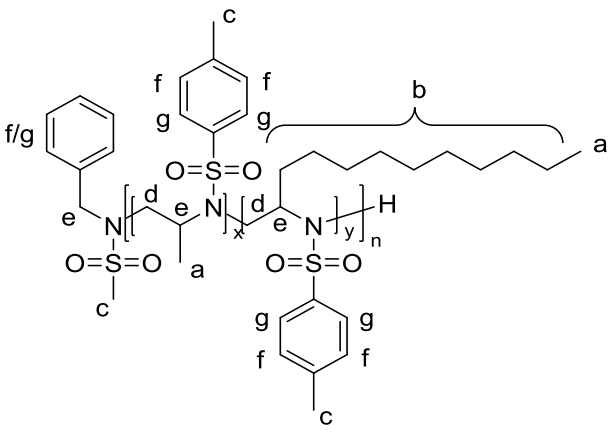

Poly(TsMAz$_{25(theo)}$-*co*-TsDAz$_{25(theo)}$): [TsMAz (211.3 mg, 1.0 mmol), TsDAz (337.5 mg, 1.0 mmol), BnNHMs (7.4 mg, 40 µmol), KHMDS (8.0 mg, 40 µmol)]. ^{1}H NMR (300 MHz, 295 K, Methylene Chloride-d_2): δ 8.01–7.52 (m, g), 7.41–6.99 (m, f), 4.42–3.63 (m, e), 3.61–2.55 (m, d), 2.49–2.13 (m, c), 1.31–0.86 (m, b), 0.84–0.69 (m, a). M_n (SEC) = 5200 g/mol, $Đ$ = 1.09.

Poly(BsMAz-co-MsMAz)

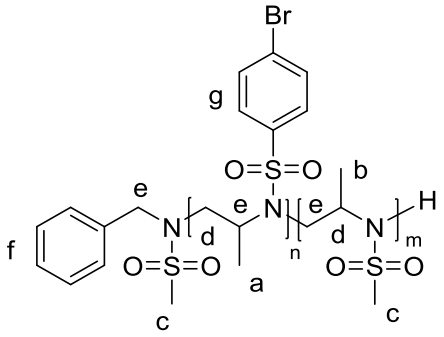

Poly(BsMAz$_{53}$-*co*-MsMAz$_{24}$): [BsMAz (306 mg, 1.1 mmol), MsMAz (150 mg, 1.1 mmol), BnNHMs (4.1 mg, 22 µmol), KHMDS (4.4 mg, 22 µmol)]. ^{1}H NMR (500 MHz, 298 K, Methylene Chloride-d_2): δ 7.97–7.55 (m, g), 7.52–7.36 (m, f), 4.48–3.76 (m, e), 3.76–3.07 (m, d), 3.07-2.81 (m, c), 1.56–1.27 (m, b), 1.20–0.69 (m, a). M_n (SEC) = 3900 g/mol, $Đ$ = 1.14, M_n (NMR) = 17800 g/mol.

Poly(NsMAz-co-BsMAz-co-TsMAz-co-MsMAz).

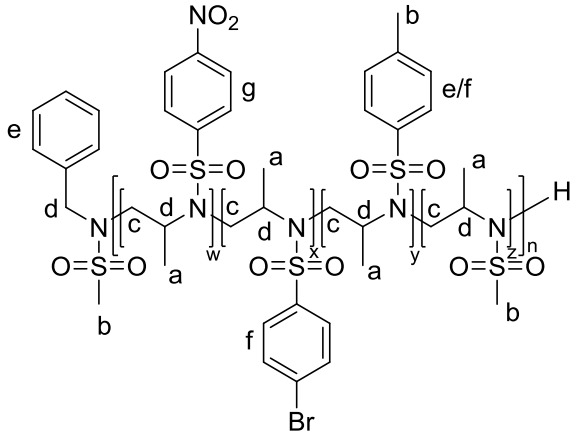

Poly(NsMAz$_{20(theo)}$-*co*-BsMAz$_{20(theo)}$-*co*-TsMAz$_{20(theo)}$-*co*-MsMAz$_{20(theo)}$): [MsMAz (75.0 mg, 555 µmol), TsMAz (117.2 mg, 555 µmol), BsMAz (153.2 mg, 555 µmol), NsMAz (134.4 mg, 555 µmol), BnNHMs (5.1 mg, 27.7 µmol), KHMDS (5.5 mg, 27.7 µmol)]. ^{1}H NMR (250 MHz, 297 K, Chloroform-*d*): δ 8.53–7.99 (m, g), 7.99–7.53 (m, f), 7.41–7.20 (m, e), 4.63–3.78 (m, d), 3.78–2.87 (m, c), 2.51–2.26 (m, b), 1.44–0.64 (m, a). M_n (SEC) = 4600 g/mol, $Đ$ = 1.16.

Copolymers for living polymerizations.

All copolymerizations were carried out in analogy to the conventional procedure. The first monomer and the BnNHMs-initiator were dissolved in 1 mL anhydrous *N,N*-dimethylformamide (DMF). KHMDS was added very fast as a solid in argon-counter flow to the BnNHMs-solution and the sample boat was rinsed with another 1 mL DMF. The initiator-solution was transferred via syringe to the monomer-solution. After stirring the mixture for 18 h at 55 °C, the second monomer was added and stirred for further 24 h at 55 °C.

Poly(NsMAz-block-TsMAz)

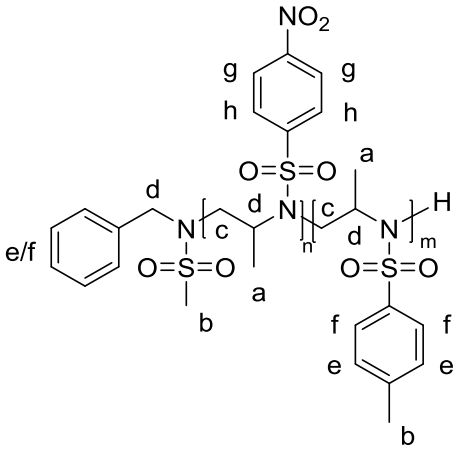

Poly(NsMAz$_{30(theo)}$-*block*-TsMAz$_{30(theo)}$): [1. NsMAz (115 mg, 473 µmol), 2. TsMAz (100 mg, 473 µmol), BnNHMs (2.9 mg, 16 µmol), KHMDS (3.2 mg, 16 µmol)]. ^{1}H NMR (250 MHz, 297 K, DMSO-d_6): δ 8.56–8.22 (m, h), 8.21–7.91 (m, g), 7.91–7.53 (m, f), 7.53–7.21 (m, e), 4.34–3.65 (m, d), 3.65–2.94 (m, c), 2.52–2.17 (m, b), 1.43–0.58 (m, a). M_n (SEC) = 7000 g/mol, $Đ$ = 1.20.

Poly(BsMAz-co-TsMAz)

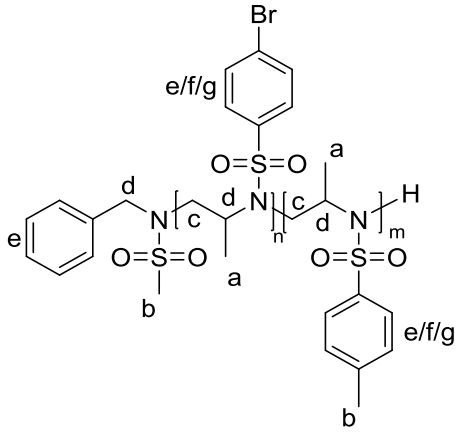

Poly(BsMAz$_{30(theo)}$-*block*-TsMAz$_{30(theo)}$): [1. BsMAz (131 mg, 473 µmol), 2. TsMAz (100 mg, 473 µmol), BnNHMs (2.9 mg, 16 µmol), KHMDS (3.2 mg, 16 µmol)]. ^{1}H NMR (250 MHz, 297 K, Chloroform-*d*): δ 7.97–7.74 (m, g), 7.74–7.49 (m, f), 7.39–7.17 (m, e), 4.54–3.82 (m, d), 3.82–2.99 (m, c), 2.49–2.22 (m, b), 1.22–0.70 (m, a). M_n (SEC) = 6100 g/mol, $Đ$ = 1.15.

Copolymers for kinetic measurements.

Poly(BsMAz-co-TsMAz-co-MsMAz).

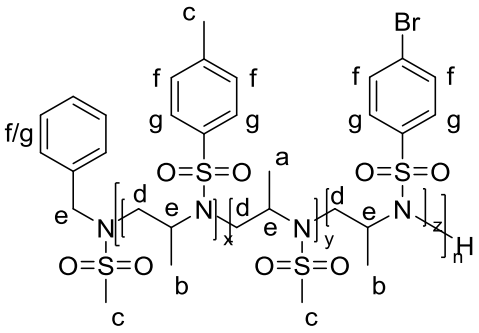

Poly(BsMAz$_{20(theo)}$-*co*-TsMAz$_{20(theo)}$-*co*-MsMAz$_{20(theo)}$): [TsMAz (30.0 mg, 142 µmol), MsMAz (19.2 mg, 142 µmol), BsMAz (39.2 mg, 142 µmol), BnNHMs (1.3 mg, 7.1 µmol), KHMDS (1.4 mg, 7.1 µmol)]. ^{1}H NMR (700 MHz, 323 K, *N,N*-dimethylformamide-d_7): δ 8.01–7.69 (m, g), 7.54-7.34 (m, f), 4.64–3.91 (m, e), 3.90–3.01 (m, d), 2.52–2.30 (m, c), 1.58–1.47 (m, b), 1.24–0.94 (m, a).

Poly(NsMAz-co-BsMAz-co-MsMAz-co-MsDAz).

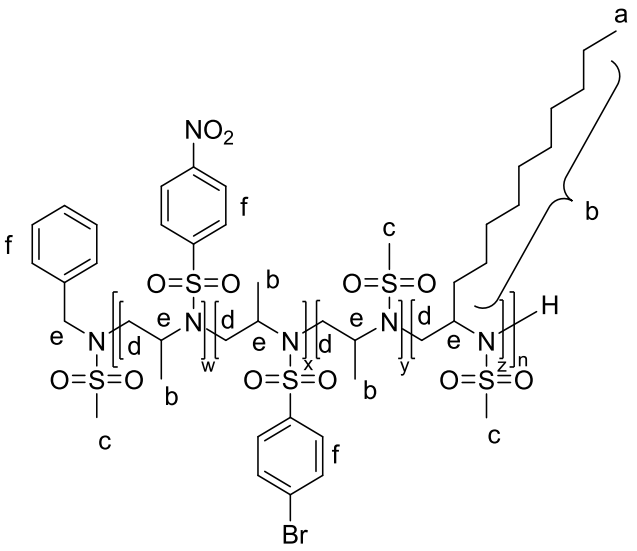

Poly(NsMAz$_{20(theo)}$-*co*-BsMAz$_{20(theo)}$-*co*-MsMAz$_{20(theo)}$-*co*-MsDAz$_{20(theo)}$): [MsMAz (15.0 mg, 111 µmol), MsDAz (29.0 mg, 111 µmol), BsMAz (30.6 mg, 111 µmol), NsMAz (26.9 mg, 111 µmol), BnNHMs (1.0 mg, 5.6 µmol), KHMDS (1.1 mg, 5.6 µmol)]. ^{1}H NMR (850 MHz, 323 K, *N,N*-dimethylformamide-d_7): δ 8.57–7.66 (m, f), 4.57–3.98 (m, e), 3.98–3.25 (m, d), 3.18–3.12 (m, c), 1.65–1.26 (m, b), 0.94–0.85 (m, a).

Poly(NsMAz-co-BsMAz-co-TsMAz-co-MsMAz).

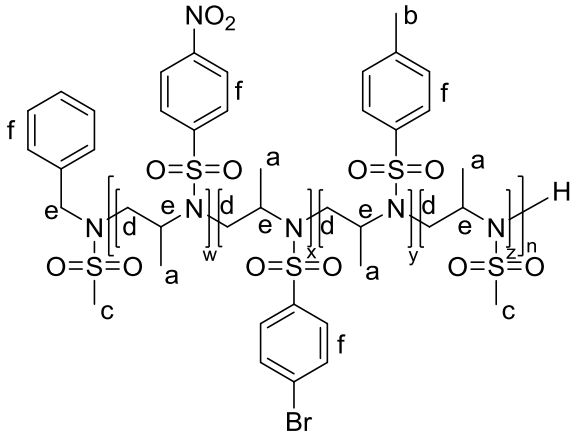

Poly(NsMAz$_{20(theo)}$-*co*-BsMAz$_{20(theo)}$-*co*-TsMAz$_{20(theo)}$-*co*-MsMAz$_{20(theo)}$): [MsMAz (15.0 mg, 111 µmol), TsMAz (23.4 mg, 111 µmol), BsMAz (30.6 mg, 111 µmol), NsMAz (26.9 mg, 111 µmol), BnNHMs (1.0 mg, 5.6 µmol), KHMDS (1.1 mg, 5.6 µmol)]. ^{1}H NMR (850 MHz, 323 K, *N,N*-dimethylformamide-d_7): δ 8.57–7.65 (m, f), 4.55–3.94 (m, e), 3.94–3.18 (m, d), 3.16–3.12 (m, c), 2.49–2.40 (m, b), 1.39–0.94 (m, a).

Poly(NsMAz-co-BsMAz-co-TsMAz-co-MsMAz-co-BusDAz).

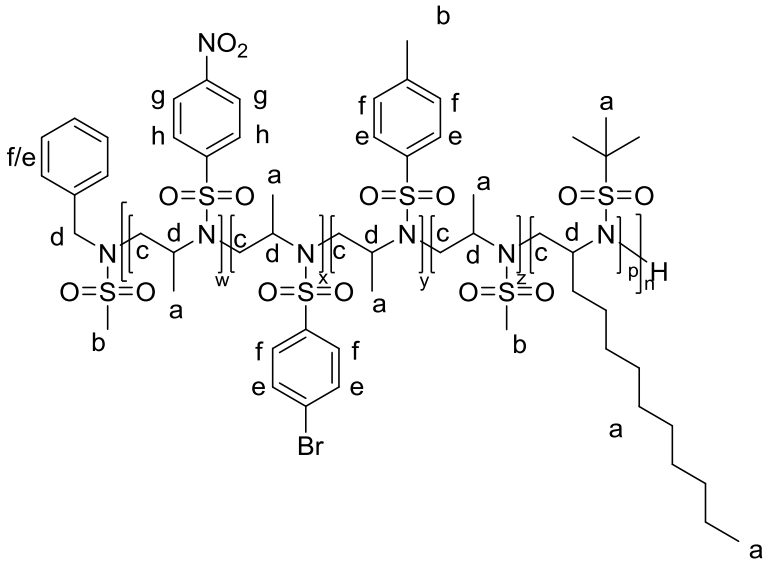

Poly(NsMAz$_{20(theo)}$-*co*-BsMAz$_{20(theo)}$-*co*-TsMAz$_{20(theo)}$-*co*-MsMAz$_{20(theo)}$-*co*-BusDAz$_{20(theo)}$): [MsMAz (13.0 mg, 96 µmol), BusDAz (29.2 mg, 96 mmol), TsMAz (20.3 mg, 96 µmol), BsMAz (26.6 mg, 96 µmol), NsMAz (23.3 mg, 96 µmol), BnNHMs (0.9 mg, 4.8 µmol), KHMDS (1.0 mg, 4.8 µmol)]. ^{1}H NMR (850 MHz, 323 K, *N,N*-dimethylformamide-d_7): δ 8.64–8.38 (m, h), 8.38–8.18 (m, g), 8.02–7.74 (m, f), 7.62–7.33 (m, e), 4.56–3.86 (m, d), 3.86–3.19 (m, c), 2.54–2.37 (m, b), 1.68–0.93 (m, a).

3.6.3 Spectroscopic Characterization.

Small molecules.

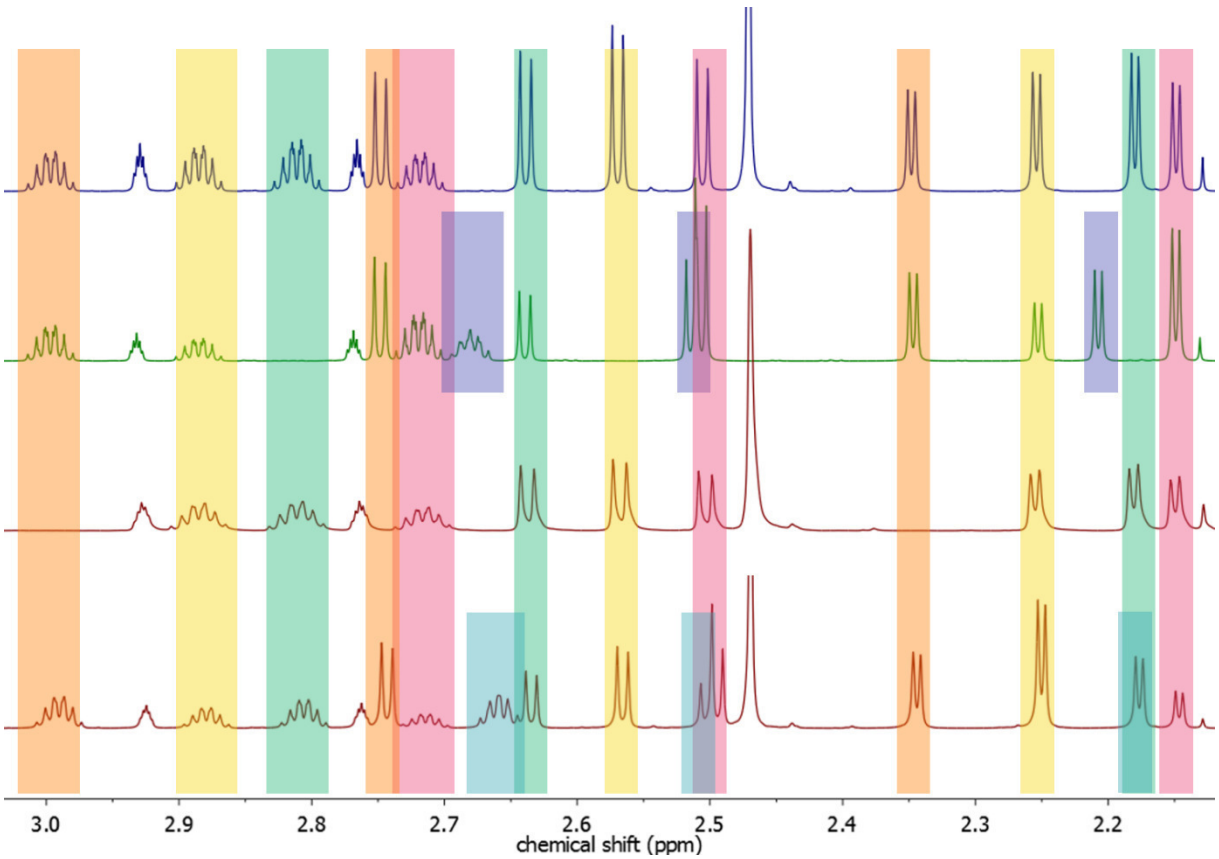

Figure S3.1. Overlay of the ^{1}H NMR spectra of monomer mixtures showing no signal overlap for all monomer combinations. Color codes of the monomers: NsMAz (orange), BsMAz (yellow), TsMAz (green), MsMAz (red), MsDAz (blue) and BusDAz (cyan).

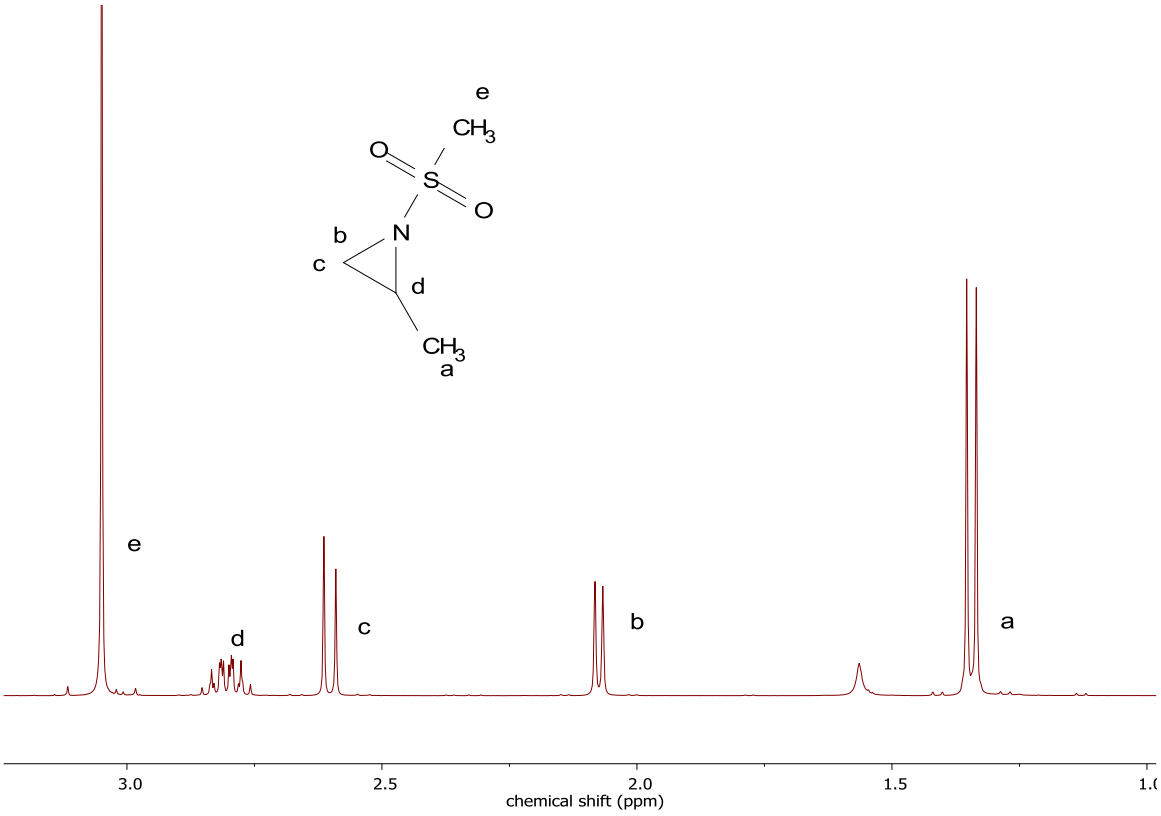

Figure S3.2. ^{1}H NMR (300 MHz, 295 K, Chloroform-*d*) of 2-Methyl-*N*-mesylaziridine (MsMAz).

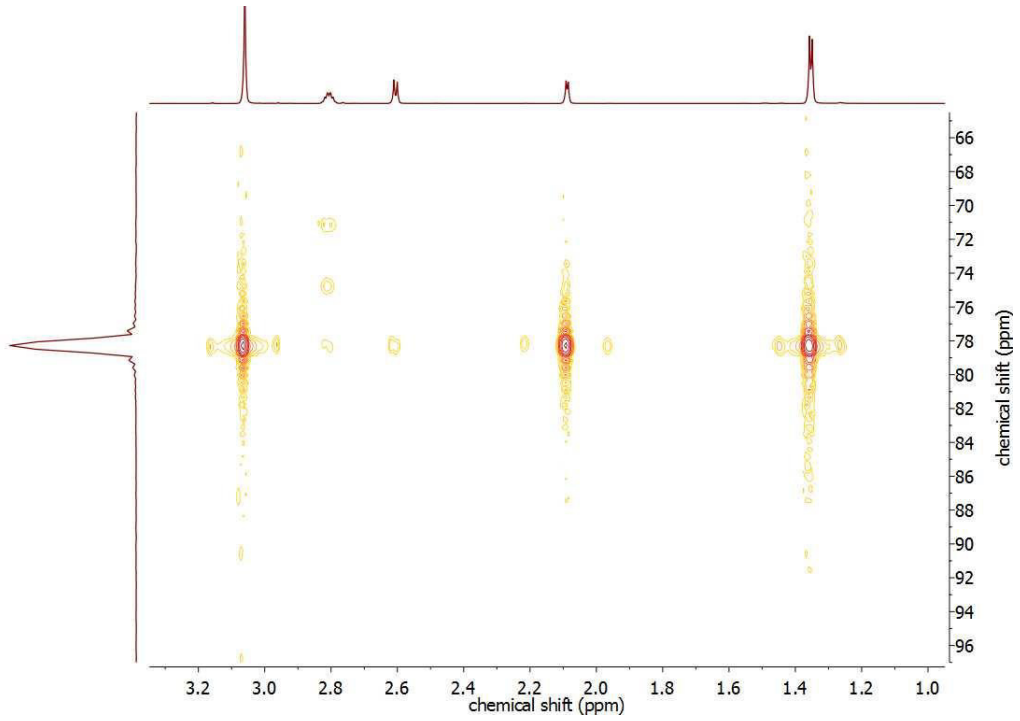

Figure S3.3. $^{1}H^{15}N$, HMBC-^{15}N-spectrum (71 MHz, 298 K, Chloroform-*d*) of 2-Methyl-*N*-mesylaziridine (MsMAz).

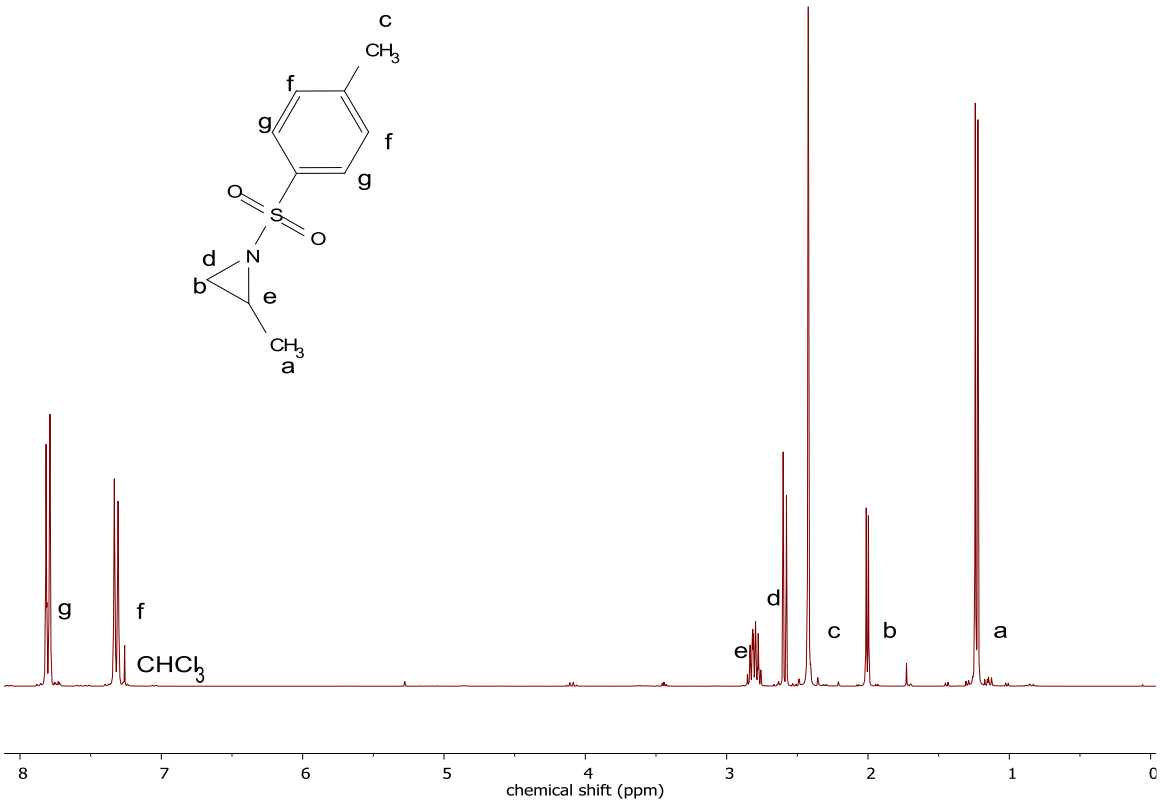

Figure S3.4. ^{1}H NMR (300 MHz, 295 K, Chloroform-*d*) of 2-Methyl-*N*-tosylaziridine (TsMAz).

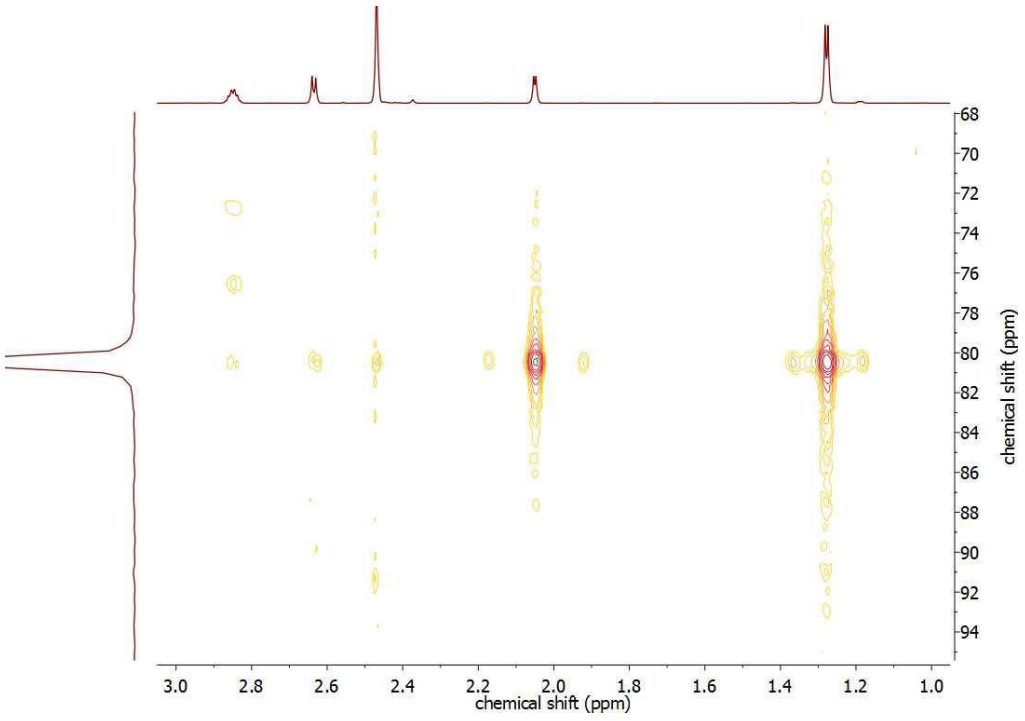

Figure S3.5. ^{1}H^{15}N, HMBC-^{15}N-spectrum (71 MHz, 298 K, Chloroform-*d*) of 2-Methyl-*N*-tosylaziridine (TsMAz).

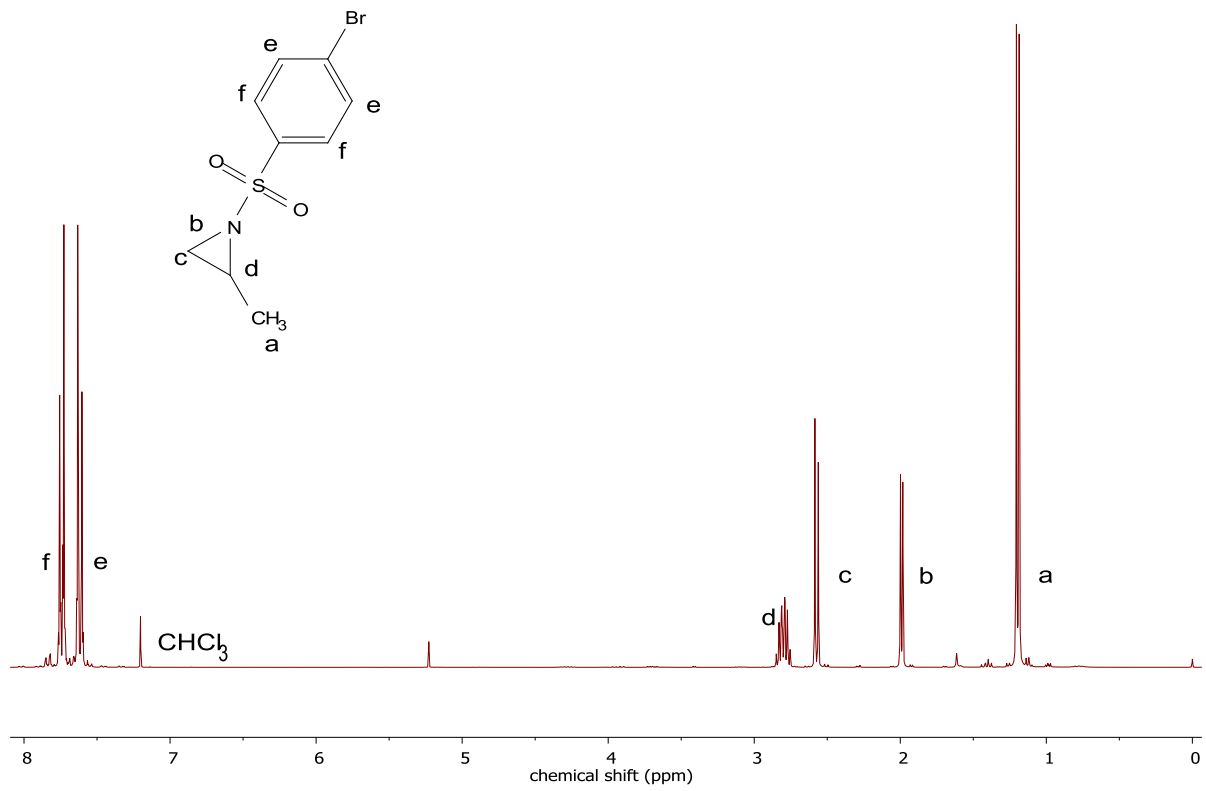

Figure S3.6. ^{1}H NMR (300 MHz, 295 K, Chloroform-*d*) of 2-Methyl-*N*-brosylaziridine (BsMAz).

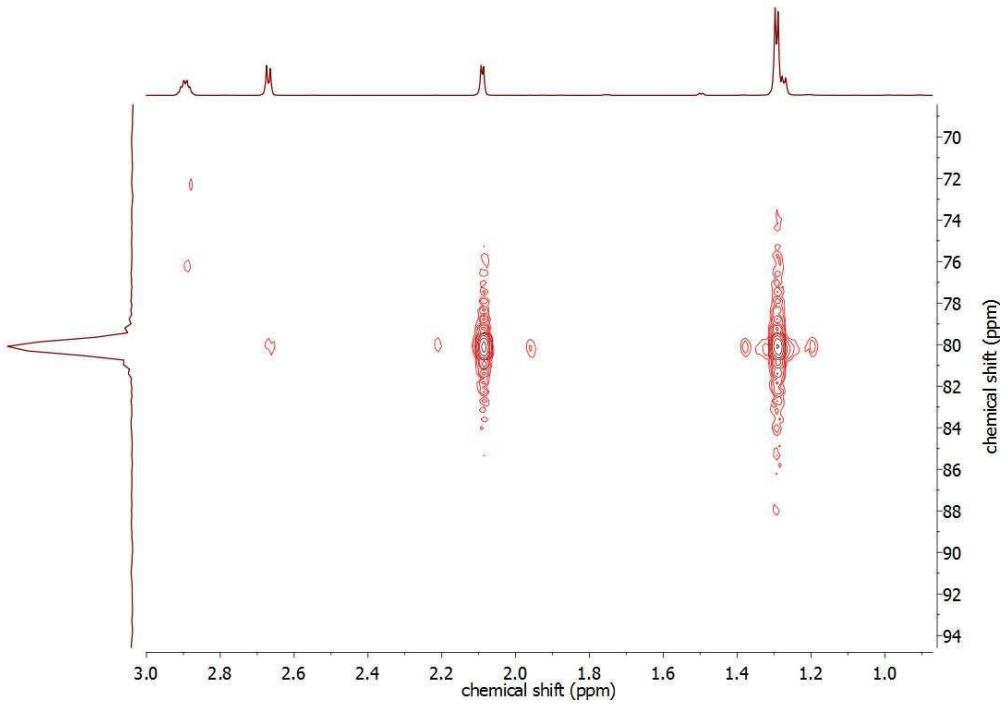

Figure S3.7. ^{1}H^{15}N, HMBC-^{15}N-spectrum (71 MHz, 298 K, Chloroform-*d*) of 2-Methyl-*N*-brosylaziridine (BsMAz).

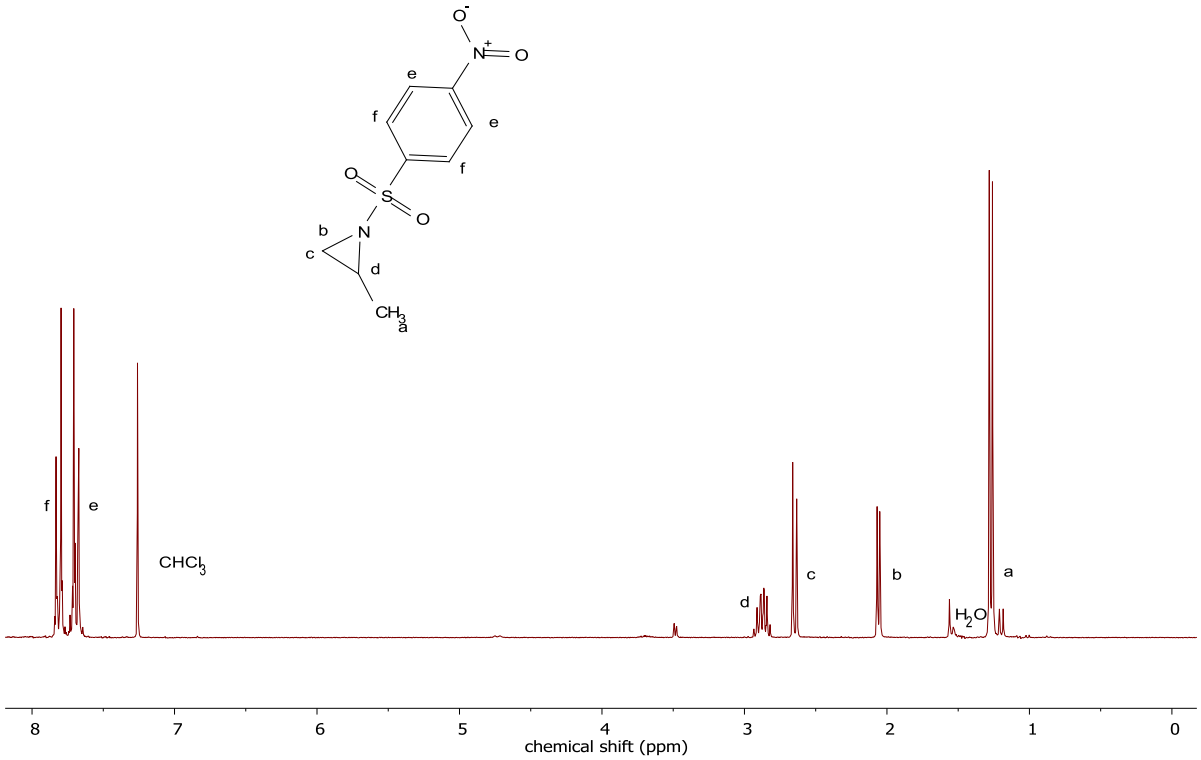

Figure S3.8. ^{1}H NMR (250 MHz, 297 K, Chloroform-*d*) of 2-Methyl-*N*-nosylaziridine (NsMAz).

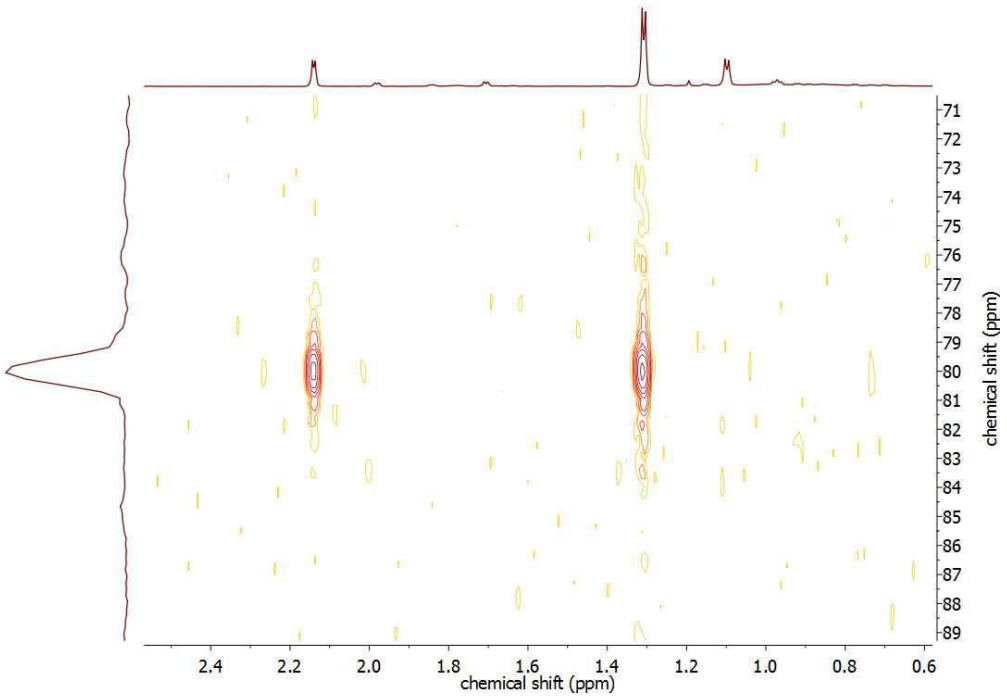

Figure S3.9. ^{1}H^{15}N, HMBC-^{15}N-spectrum (71 MHz, 298 K, Chloroform-*d*) of 2-Methyl-*N*-nosylaziridine (NsMAz).

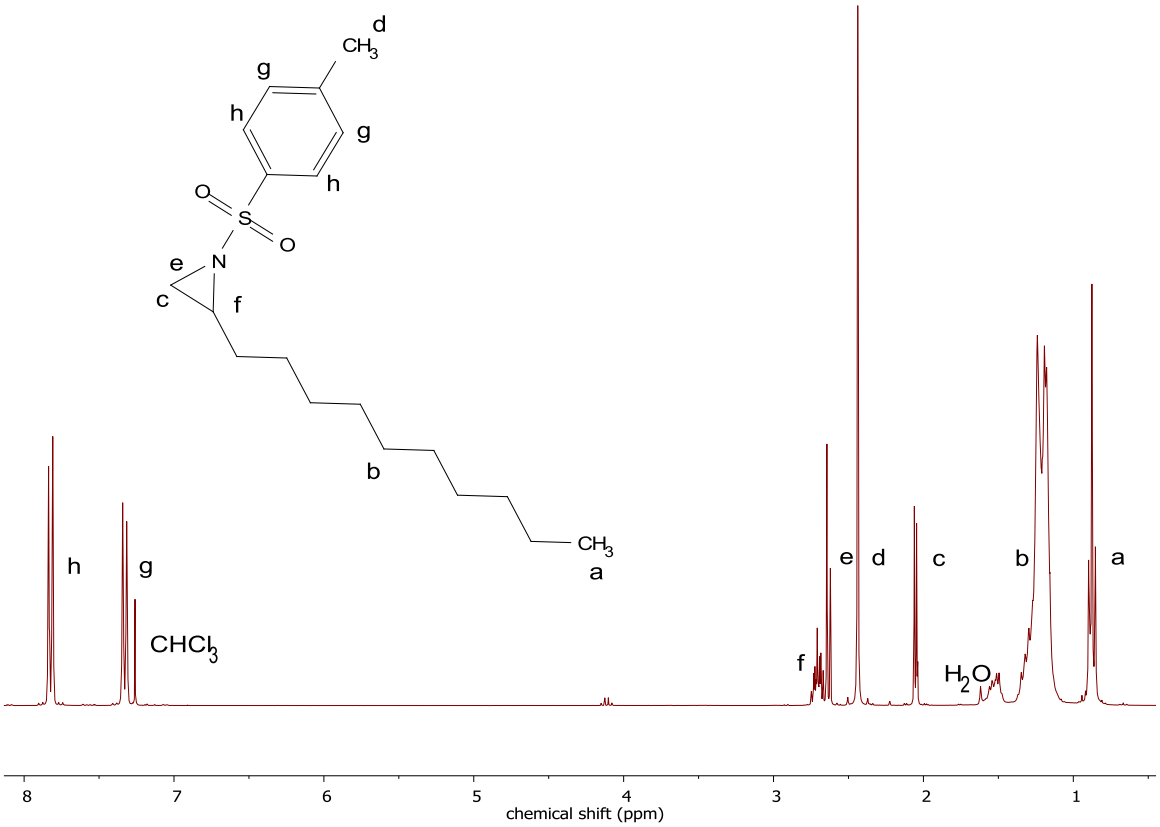

Figure S3.10. ^{1}H NMR (300 MHz, 295 K, Chloroform-*d*) of 2-Decyl-*N*-tosylaziridine (TsDAz).

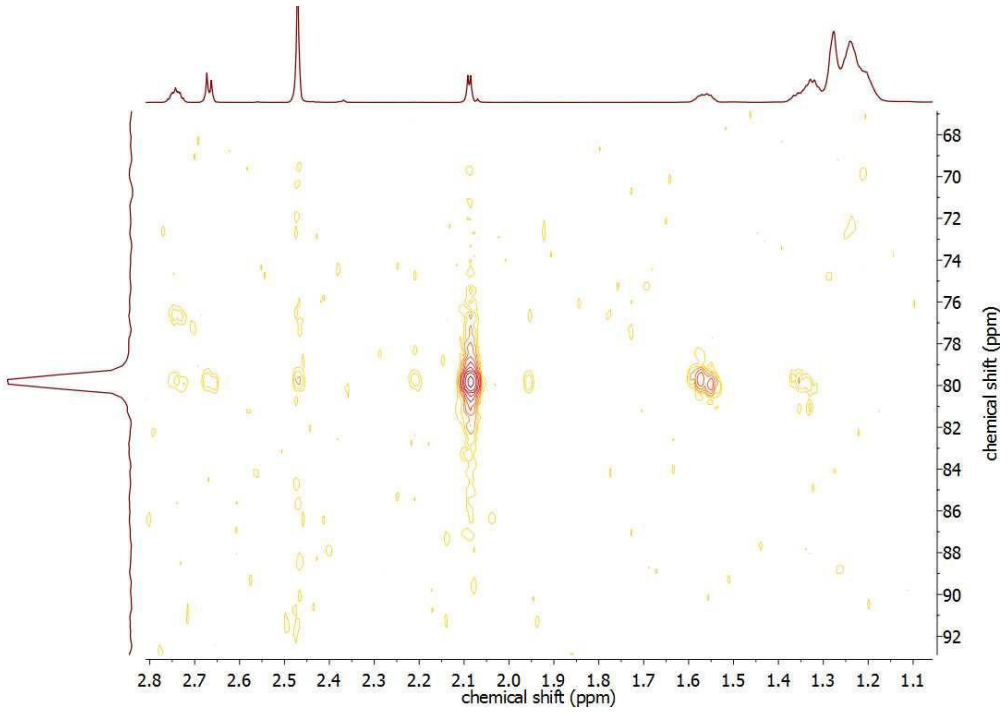

Figure S3.11. ^{1}H^{15}N, HMBC-^{15}N-spectrum (71 MHz, 298 K, Chloroform-*d*) of 2-Decyl-*N*-tosylaziridine (TsDAz).

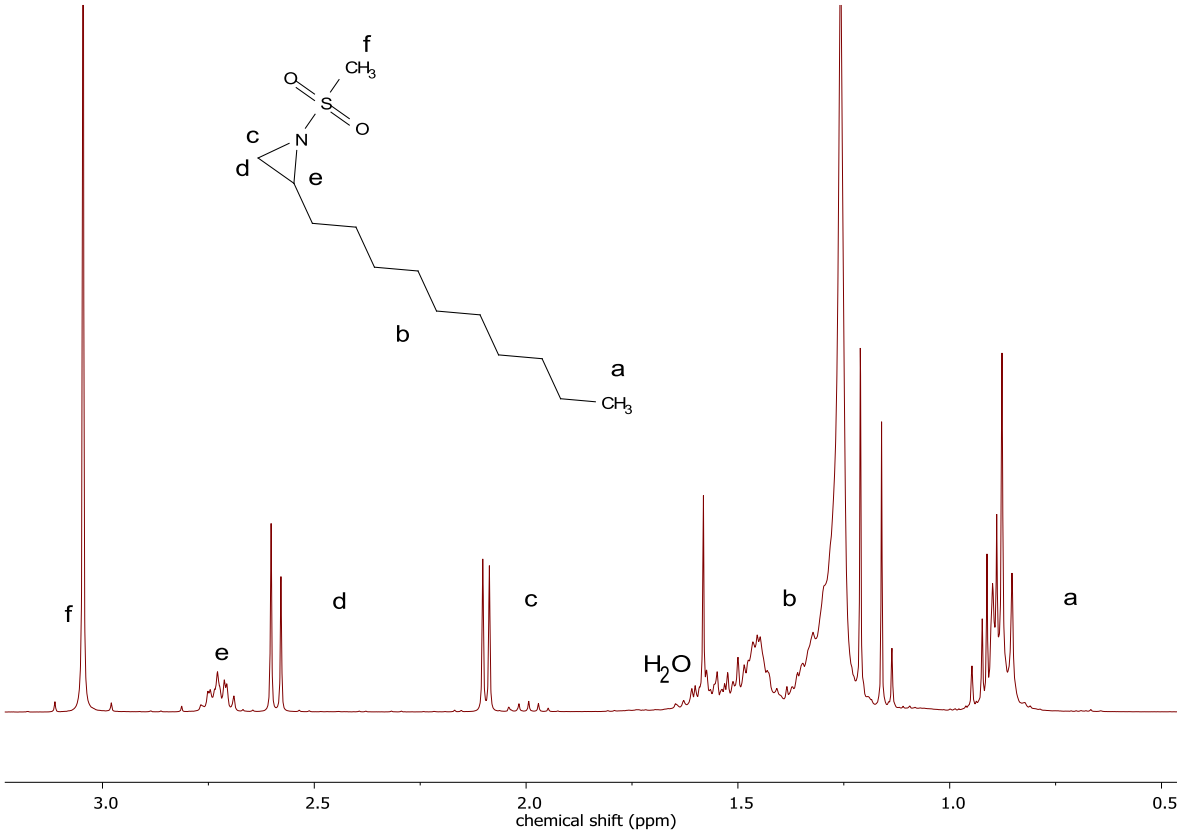

Figure S3.12. ^{1}H NMR (300 MHz, 295 K, Chloroform-*d*) of 2-Decyl-*N*-mesylaziridine (MsDAz).

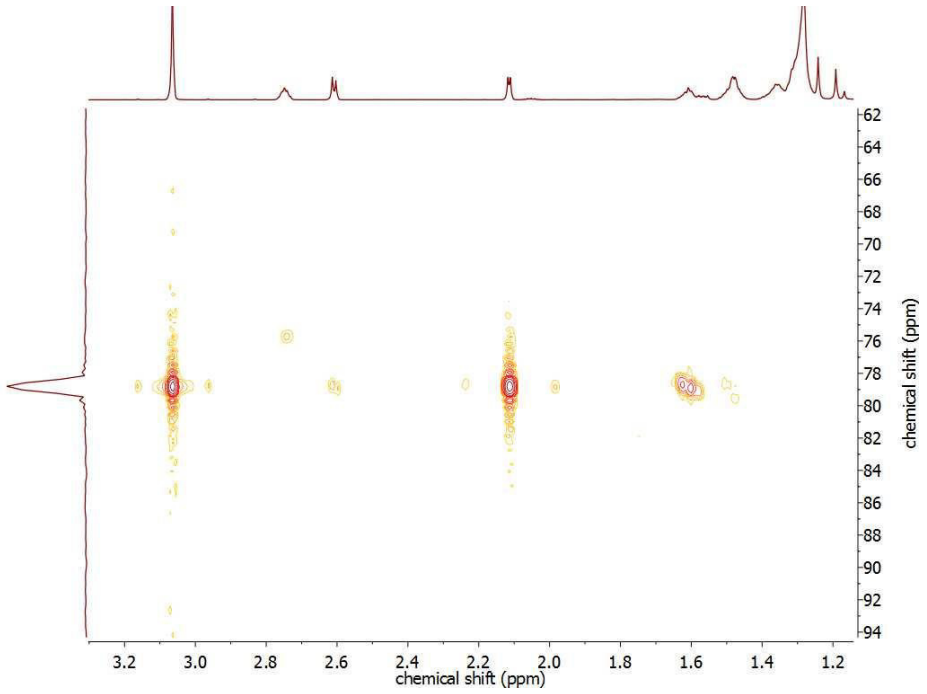

Figure S3.13. ^{1}H^{15}N, HMBC-^{15}N-spectrum (71 MHz, 298 K, Chloroform-*d*) of 2-Decyl-*N*-mesylaziridine (MsDAz).

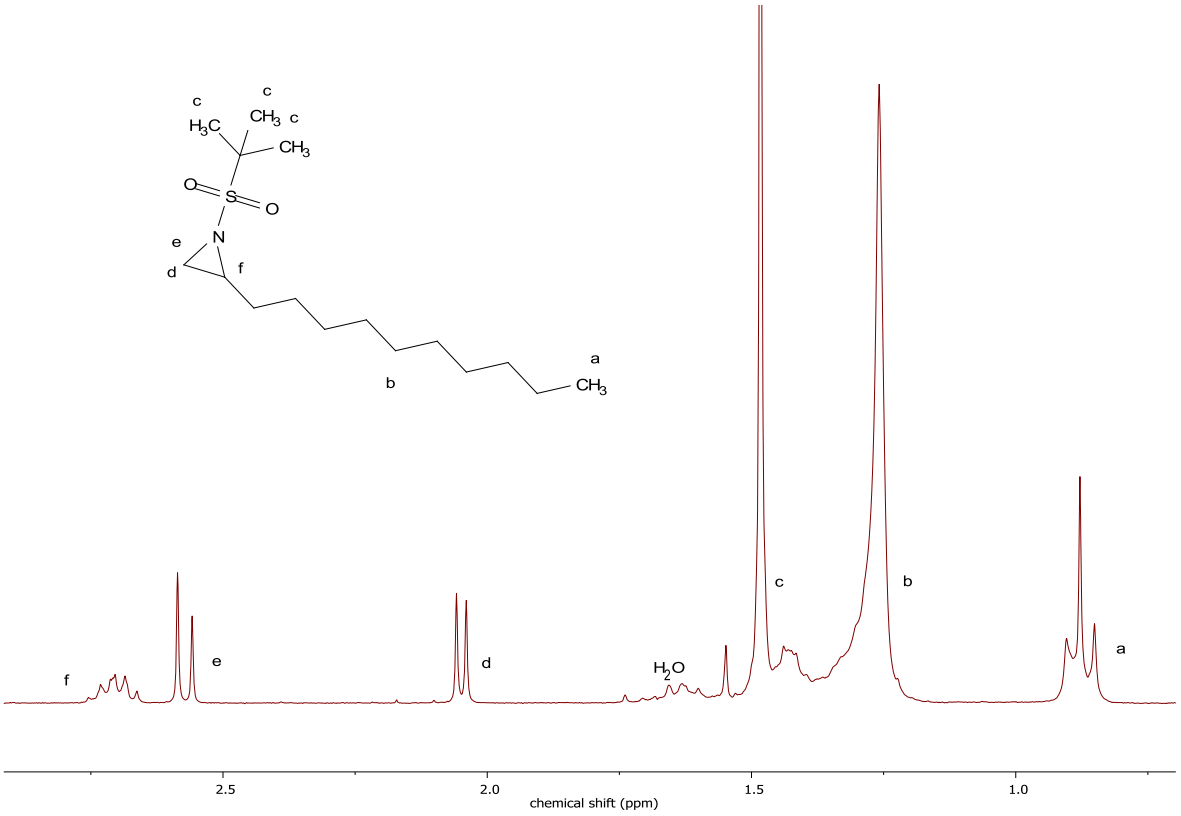

Figure S3.14. ^{1}H NMR (250 MHz, 297 K, Chloroform-*d*) of 2-Decyl-*N*-busylaziridine (BusDAz).

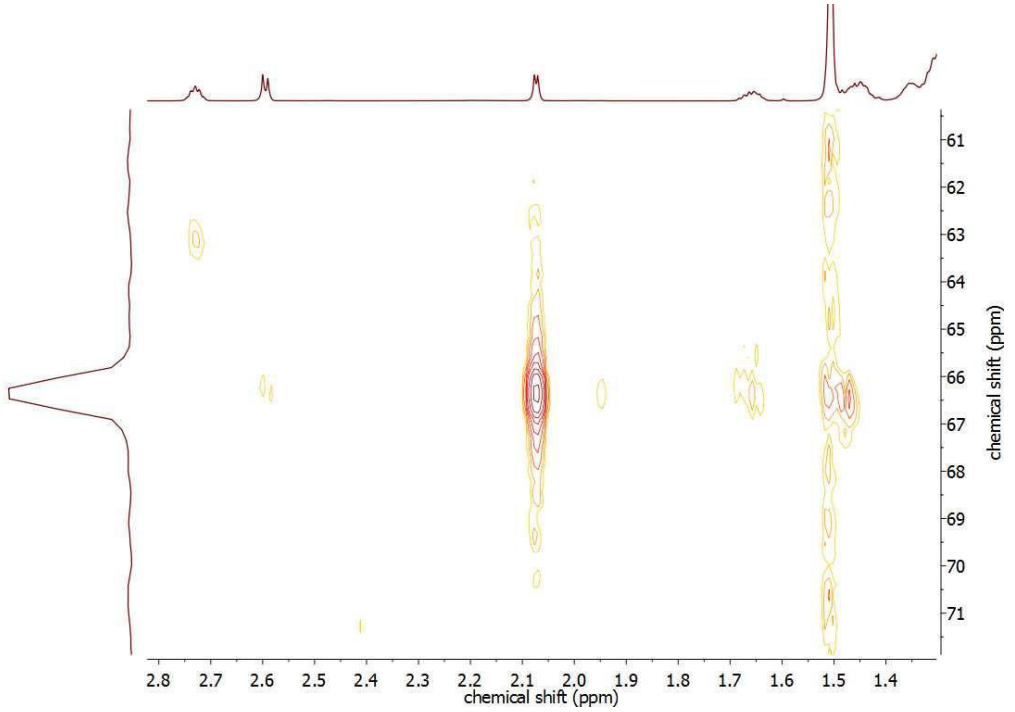

Figure S3.15. ^{1}H^{15}N, HMBC-^{15}N-spectrum (71 MHz, 298 K, Chloroform-*d*) of 2-Decyl-*N*-busylaziridine (BusDAz).

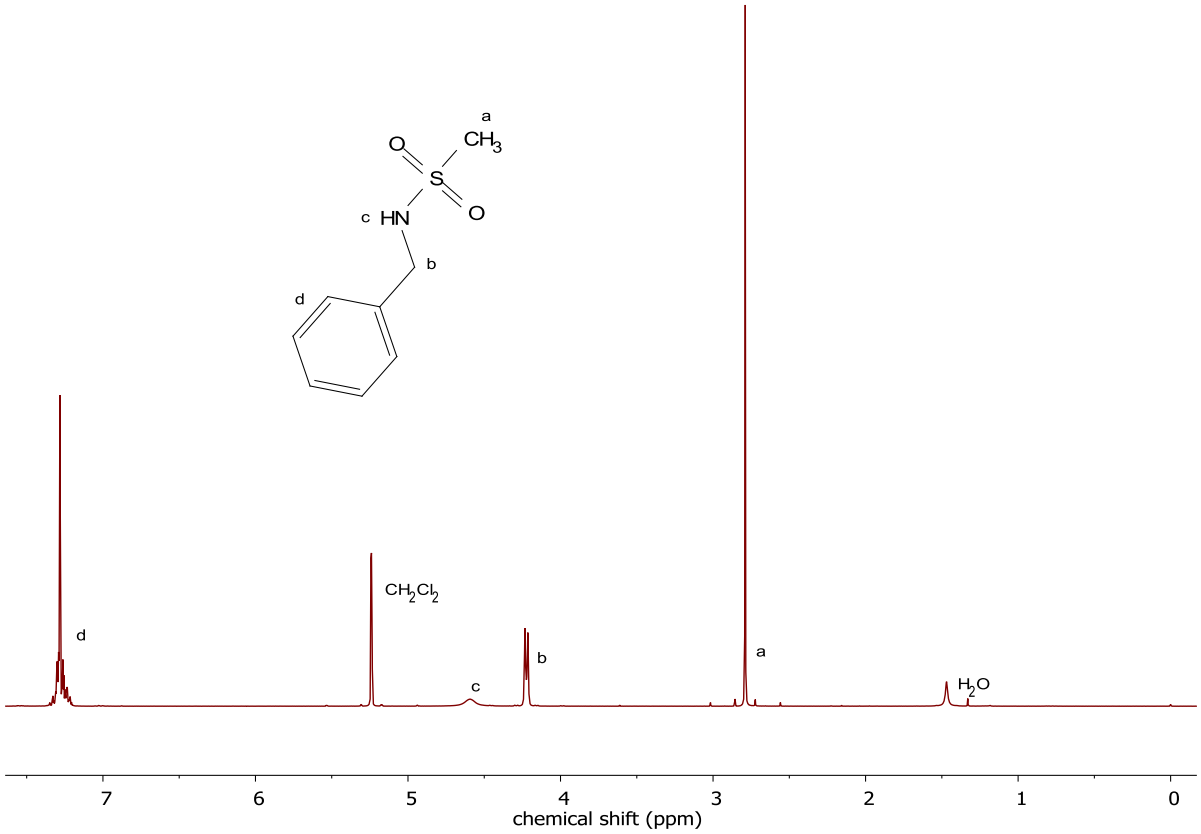

Figure S3.16. ^{1}H NMR (300 MHz, 295 K, Chloroform-*d*) of *N*-benzyl-mesylamide (BnNHMs).

Polymers.

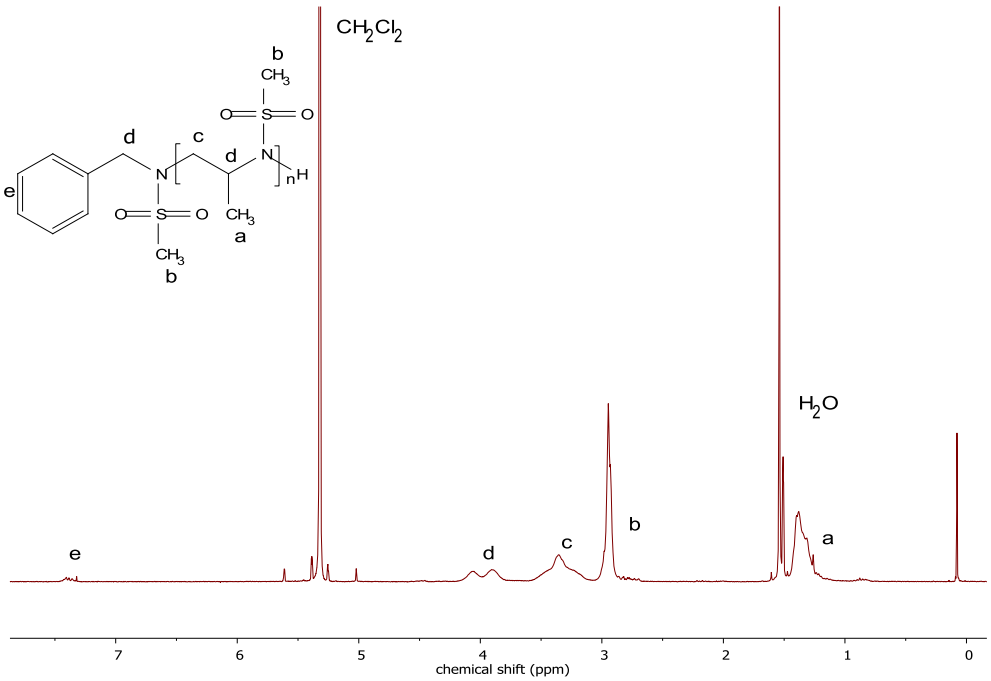

Figure S3.17. ^{1}H NMR (300 MHz, 295 K, Methylene Chloride-d_2) of Poly(2-methyl-*N*-mesylaziridine) - P(MsMAz).

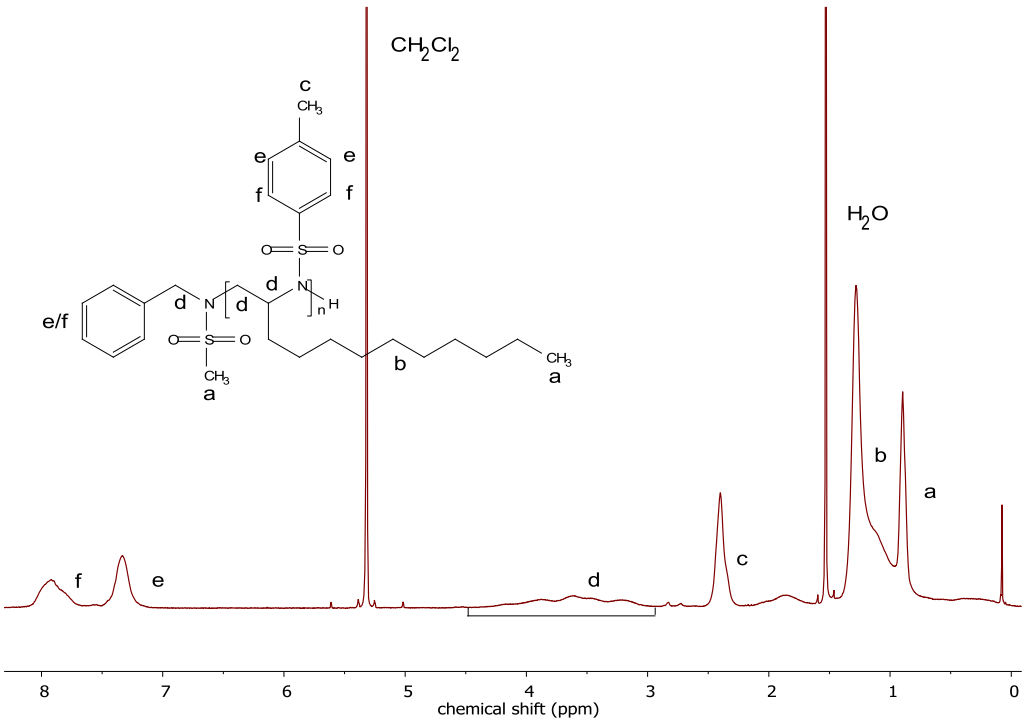

Figure S3.18. ^{1}H NMR (300 MHz, 295 K, Methylene Chloride-d_2) of Poly(2-decyl-*N*-tosylaziridine) - P(TsDAz).

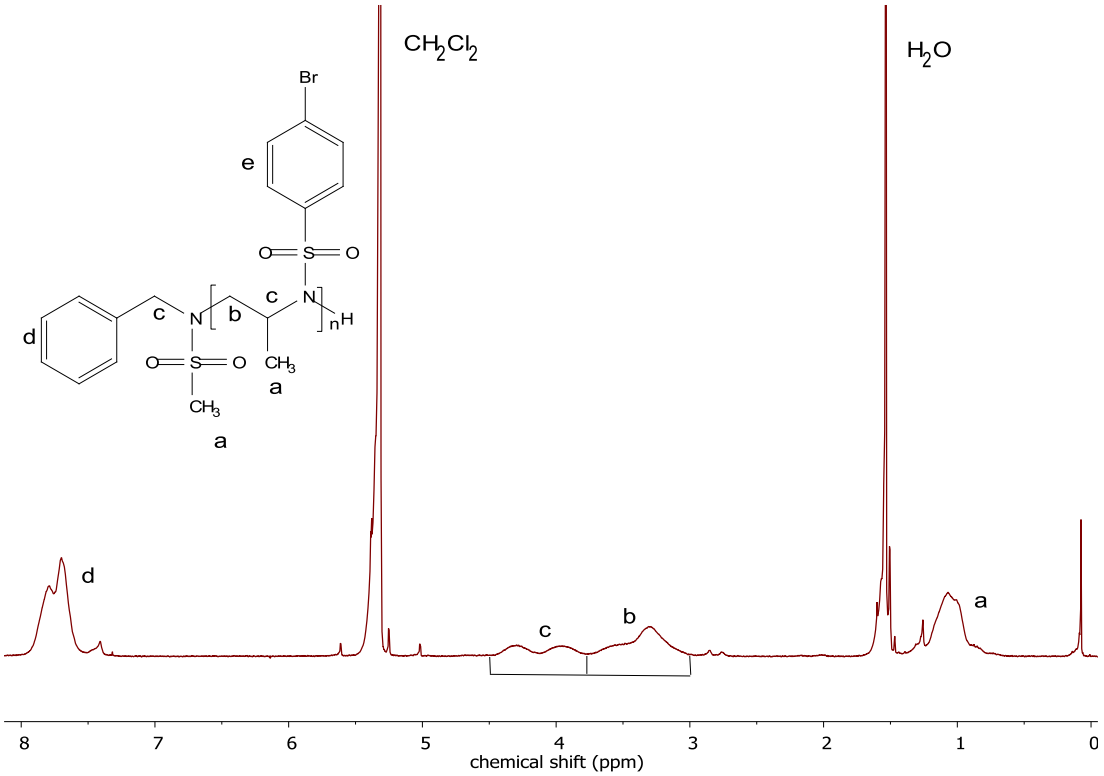

Figure S3.19. ^{1}H NMR (300 MHz, 295 K, Methylene Chloride-d_2) of Poly(2-methyl-*N*-brosylaziridine) - P(BsMAz).

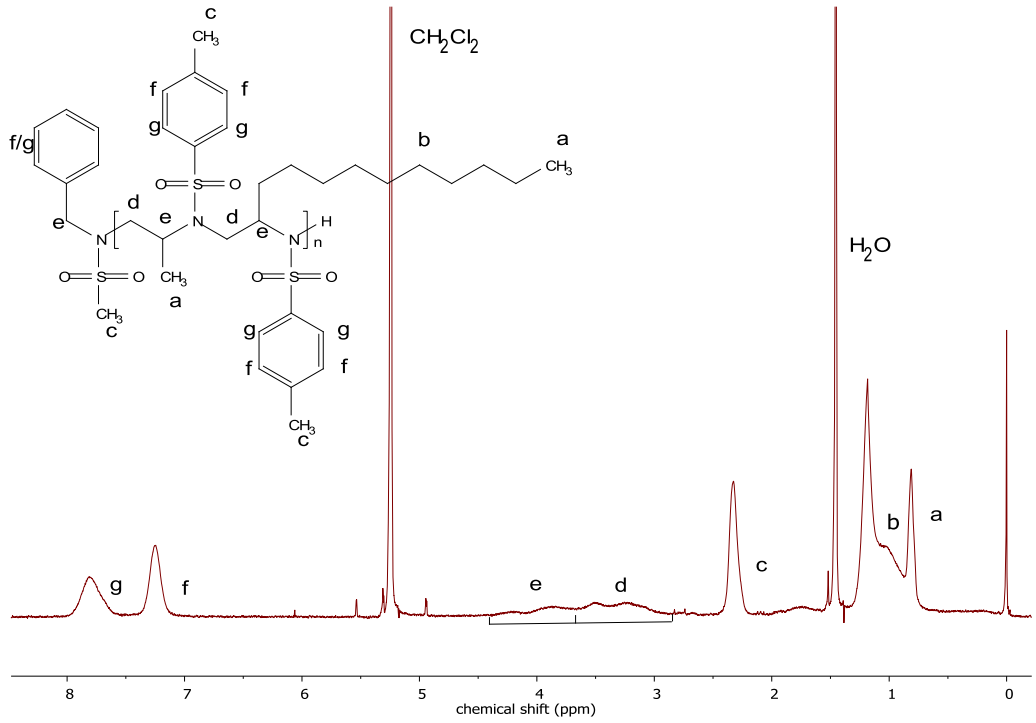

Figure S3.20. ^{1}H NMR (300 MHz, 295 K, Methylene Chloride-d_2) of Poly(2-methyl-*N*-tosylaziridine)-*co*-(2-decyl-*N*-tosylaziridine) - P(TsMAz-*co*-TsDAz).

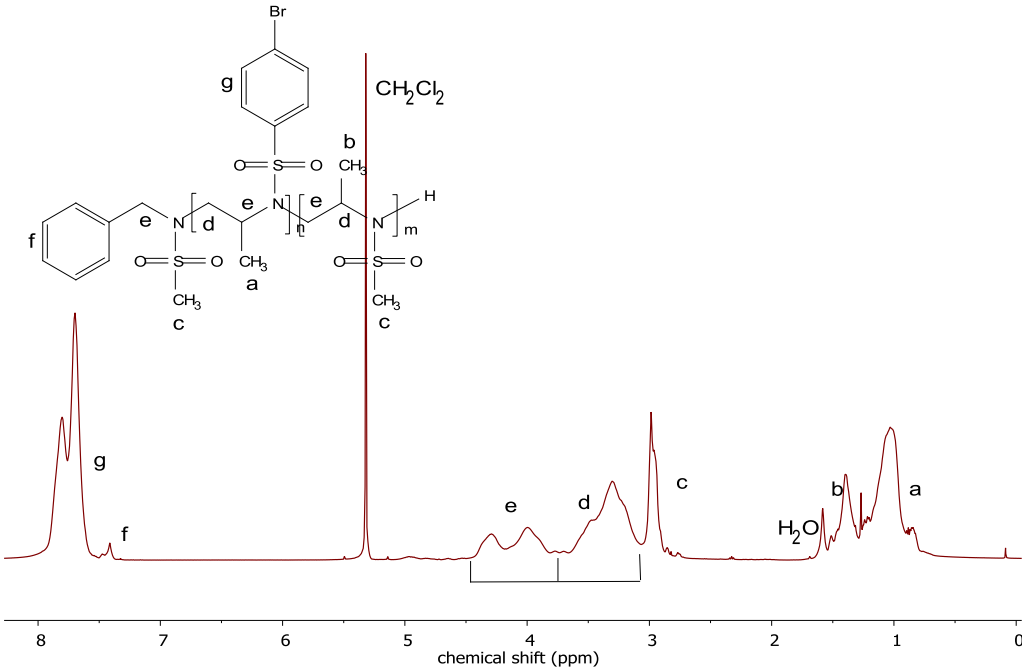

Figure S3.21. ^{1}H NMR (500 MHz, 298 K, Methylene Chloride-d_2) of Poly(2-methyl-*N*-brosylaziridine)-*co*-(2-methyl-*N*-mesylaziridine) - P(BsMAz-*co*-MsMAz).

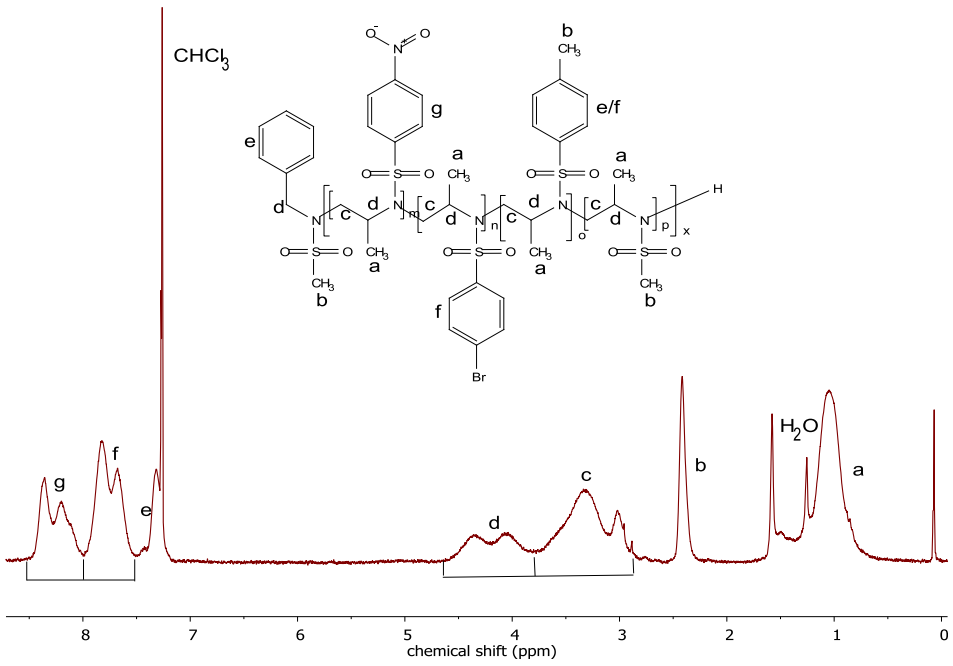

Figure S3.22. ^{1}H NMR (250 MHz, 297 K, Chloroform-*d*) of Poly(2-methyl-*N*-nosylaziridine-*co*-2-methyl-*N*-brosylaziridine-*co*-2-methyl-*N*-tosylaziridine-*co*-2-methyl-*N*-mesylaziridine) - P(NsMAz-*co*-BsMAz-*co*-TsMAz-*co*-MsMAz).

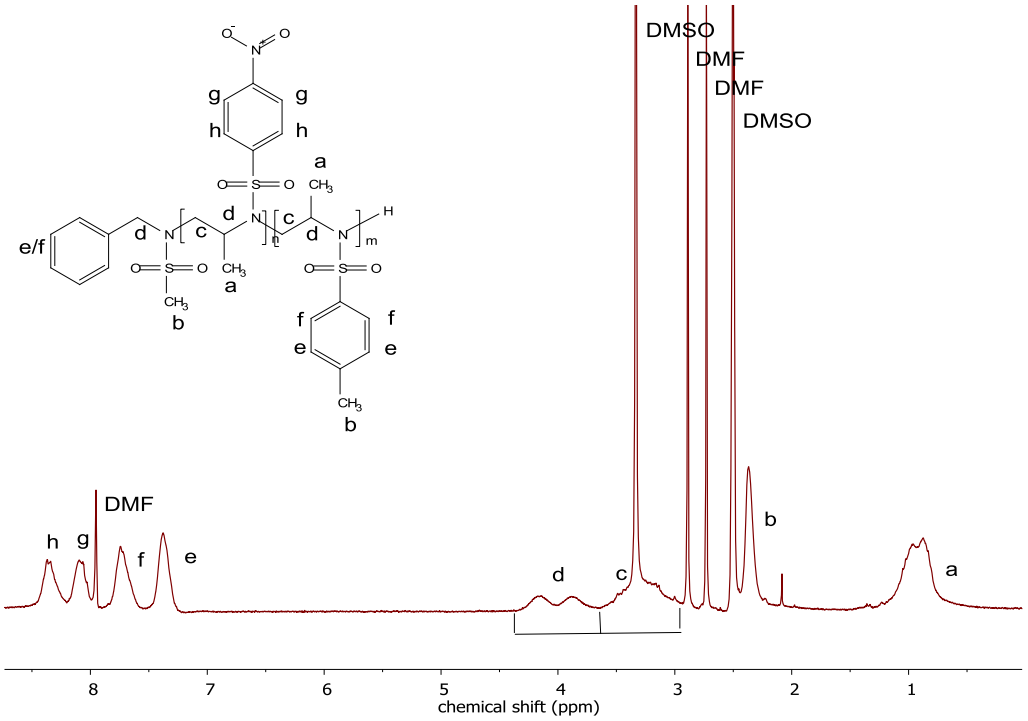

Figure S3.23. ^{1}H NMR (250 MHz, 297 K, Dimethyl sulfoxide-d_6) of Poly(2-methyl-*N*-nosylaziridine)-*block*-(2-methyl-*N*-tosylaziridine) - P(NsMAz-*block*-TsMAz).

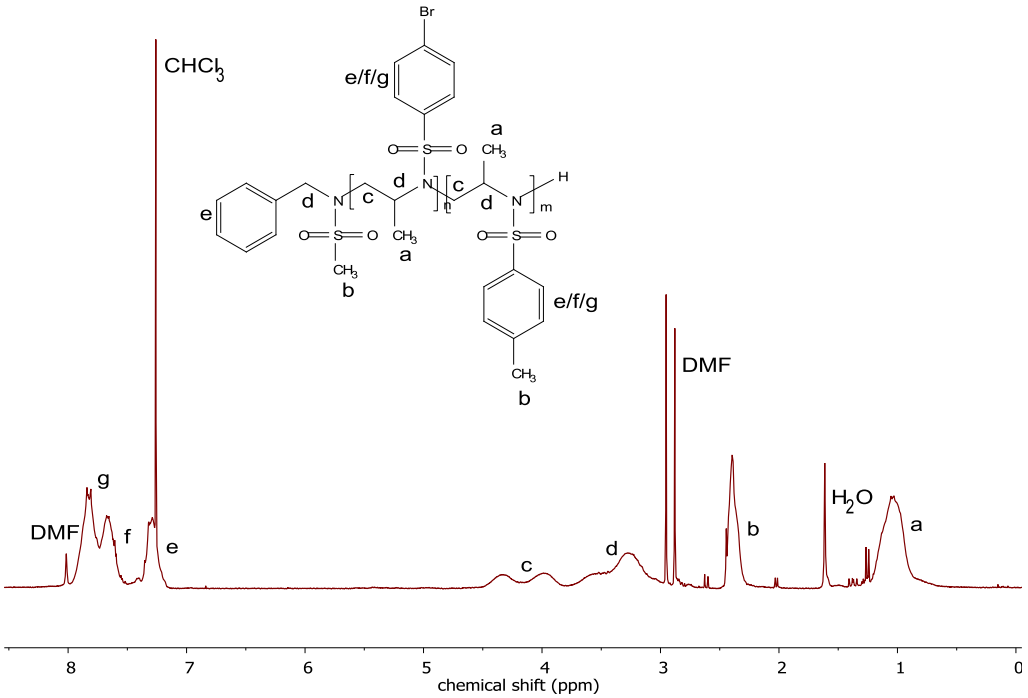

Figure S3.24. ^{1}H NMR (250 MHz, 297 K, Chloroform-*d*) of Poly(2-methyl-*N*-brosylaziridine)-*block*-(2-methyl-*N*-tosylaziridine) - P(BsMAz-*block*-TsMAz).

3.6.4 Representative SECs of several homo- and copolymers.

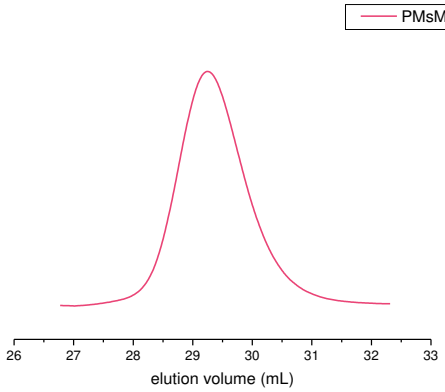

Figure S3.25. SEC traces of Poly(2-methyl-*N*-mesylaziridine) - P(MsMAz) in DMF (RI signal).

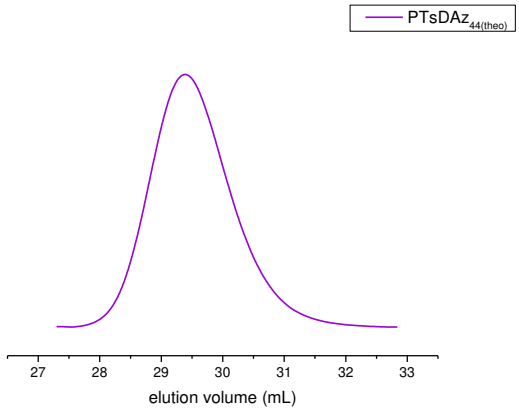

Figure S3.26. SEC traces of Poly(2-decyl-*N*-tosylaziridine) - P(TsDAz) in DMF (RI signal).

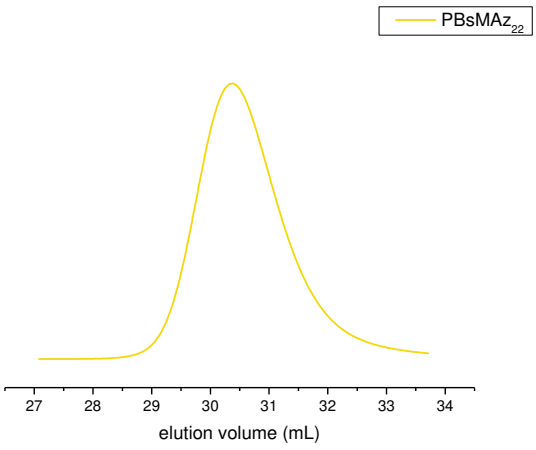

Figure S3.27. SEC traces of Poly(2-methyl-*N*-brosylaziridine) - P(BsMAz) in DMF (RI signal).

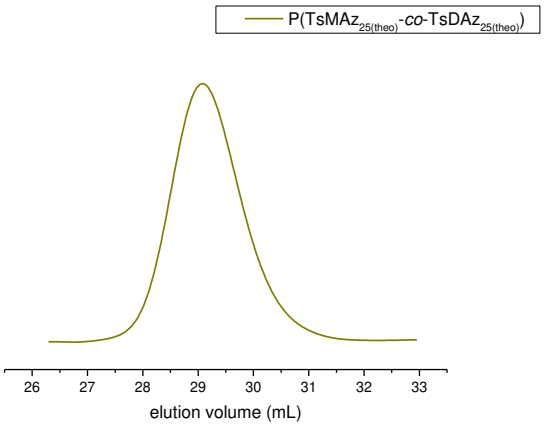

Figure S3.28. SEC traces of Poly(2-methyl-*N*-tosylaziridine)-*co*-(2-decyl-*N*-tosylaziridine) - P(TsMAz-*co*-TsDAz) in DMF (RI signal).

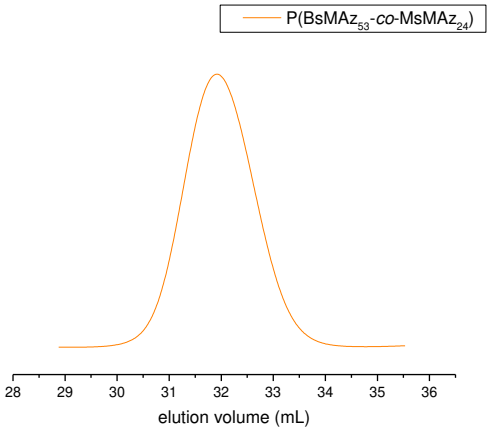

Figure S3.29. SEC traces of Poly(2-methyl-*N*-brosylaziridine)-*co*-(2-methyl-*N*-mesylaziridine) - P(BsMAz-*co*-MsMAz) in DMF (RI signal).

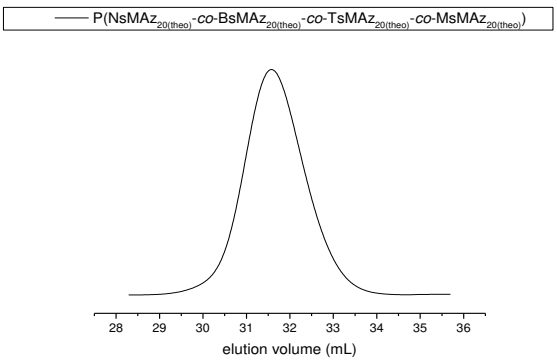

Figure S3.30. SEC traces of Poly(2-methyl-*N*-nosylaziridine-*co*-2-methyl-*N*-brosylaziridine-*co*-2-methyl-*N*-tosylaziridine-*co*-2-methyl-*N*-mesylaziridine) - P(NsMAz-*co*-BsMAz-*co*-TsMAz-*co*-MsMAz) in DMF (RI signal).

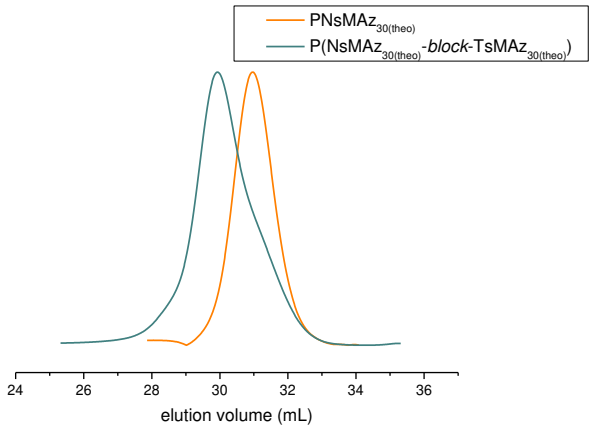

Figure S3.31. SEC traces of Poly(2-methyl-*N*-nosylaziridine) and Poly(2-methyl-*N*-nosylaziridine)-*block*-(2-methyl-*N*-tosylaziridine) after sequential addition of TsMAz - P(NsMAz-*block*-TsMAz) in DMF (RI signal).

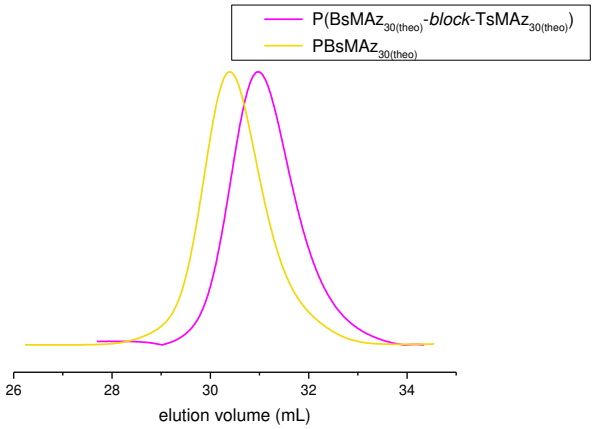

Figure S3.32. SEC traces of Poly(2-methyl-*N*-brosylaziridine) and Poly(2-methyl-*N*-brosylaziridine)-*block*-(2-methyl-*N*-tosylaziridine) after sequential addition of TsMAz - P(BsMAz-*block*-TsMAz) in DMF (RI signal).

3.6.5 *k*-values.

Table S3.1. Propagation rate constants (*k*-values) calculated from kinetic ^{1}H NMR measurements from homopolymerizations, using $\ln(M_0/M_t) = k_{app}t$.

	NsMAz	BsMAz	TsMAz	MsMAz	BusDAz
k / 10^{-3} L mol^{-1} s^{-1}	97	71	41	15	5

3.7 References

1. Lutz, J.-F.; Ouchi, M.; Liu, D. R.; Sawamoto, M., *Science* **2013,** *341* (6146).
2. Mutlu, H.; Lutz, J.-F., *Angew. Chem. Int. Ed.* **2014,** *53* (48), 13010-13019.
3. Alsubaie, F.; Anastasaki, A.; Wilson, P.; Haddleton, D. M., *Polym. Chem.* **2015,** *6* (3), 406-417.
4. ten Brummelhuis, N., *Polymer Chemistry* **2015,** *6* (5), 654-667.
5. Porel, M.; Alabi, C. A., *J. Am. Chem. Soc.* **2014,** *136* (38), 13162-13165.
6. Gody, G.; Maschmeyer, T.; Zetterlund, P. B.; Perrier, S., *Nat Commun* **2013,** *4*, 2505.
7. Hutchings, L. R.; Brooks, P. P.; Parker, D.; Mosely, J. A.; Sevinc, S., *Macromolecules* **2015,** *48* (3), 610-628.
8. Srichan, S.; Kayunkid, N.; Oswald, L.; Lotz, B.; Lutz, J.-F., *Macromolecules* **2014,** *47* (5), 1570-1577.
9. Hadjichristidis, N.; Pitsikalis, M.; Pispas, S.; Iatrou, H., *Chem. Rev.* **2001,** *101* (12), 3747-3792.
10. Baskaran, D.; Müller, A. H. E., Anionic Vinyl Polymerization. In *Controlled and Living Polymerizations*, Wiley-VCH Verlag GmbH & Co. KGaA: **2010**; 1-56.
11. Hirao, A.; Takenaka, K., Nonpolar Monomers: Styrene and 1,3-Butadiene Derivatives. In *Anionic Polymerization*, Hadjichristidis, N.; Hirao, A., Eds. Springer Japan: **2015**; 61-126.
12. Alkan, A.; Natalello, A.; Wagner, M.; Frey, H.; Wurm, F. R., *Macromolecules* **2014,** *47* (7), 2242-2249.
13. Brooks, P. P.; Natalello, A.; Hall, J. N.; Eccles, E. A. L.; Kimani, S. M.; Bley, K.; Hutchings, L. R., *Macromolecular Symposia* **2013,** *323* (1), 42-50.
14. Natalello, A.; Alkan, A.; von Tiedemann, P.; Wurm, F. R.; Frey, H., *ACS Macro Letters* **2014,** *3* (6), 560-564.
15. Natalello, A.; Werre, M.; Alkan, A.; Frey, H., *Macromolecules* **2013,** *46* (21), 8467-8471.
16. Puskas, J. E.; McAuley, K. B.; Chan, S. W. P., *Macromolecular Symposia* **2006,** *243* (1), 46-52.
17. Shaikh, S.; Puskas, J. E.; Kaszas, G., *Journal of Polymer Science Part A: Polymer Chemistry* **2004,** *42* (16), 4084-4100.
18. Natalello, A.; Hall, J. N.; Eccles, E. A. L.; Kimani, S. M.; Hutchings, L. R., *Macromol. Rapid Commun.* **2011,** *32* (2), 233-237.
19. Stewart, I. C.; Lee, C. C.; Bergman, R. G.; Toste, F. D., *Journal of the American Chemical Society* **2005,** *127* (50), 17616-17617.
20. Thomi, L.; Wurm, F. R., *Macromol. Rapid Commun.* **2014,** *35* (5), 585-589.
21. Thomi, L.; Wurm, F. R., *Macromolecular Symposia* **2015,** *349* (1), 51-56.
22. Sweeney, J. B., *Chem. Soc. Rev.* **2002,** *31* (5), 247-258.
23. Bednarek, M.; Kubisa, P.; Penczek, S., *Macromolecules* **1999,** *32*, 5257-5263.

24. Tanaka, R.; Ueoka, I.; Takaki, Y.; Kataoka, K.; Saito, S., *Macromolecules* **1983,** *16* (6), 849-853.
25. Quinebèche, S.; Navarro, C.; Gnanou, Y.; Fontanille, M., *Polymer* **2009,** *50* (6), 1351-1357.
26. Long, T. E.; Liu, H. Y.; Schell, B. A.; Teegarden, D. M.; Uerz, D. S., *Macromolecules* **1993,** *26* (23), 6237-6242.
27. Tonhauser, C.; Alkan, A.; Schömer, M.; Dingels, C.; Ritz, S.; Mailänder, V.; Frey, H.; Wurm, F. R., *Macromolecules* **2013,** *46* (3), 647-655.
28. Barbaud, C.; Faÿ, F.; Abdillah, F.; Randriamahefa, S.; Guérin, P., *Macromol. Chem. Phys.* **2004,** *205* (2), 199-207.
29. Fragouli, P.; Iatrou, H.; Lohse, D. J.; Hadjichristidis, N., *J. Polym. Sci., Part A: Polym. Chem.* **2008,** *46* (12), 3938-3946.
30. Ekizoglou, N.; Hadjichristidis, N., *J. Polym. Sci., Part A: Polym. Chem.* **2002,** *40* (13), 2166-2170.
31. Jeong, J. U.; Tao, B.; Sagasser, I.; Henniges, H.; Sharpless, K. B., *Journal of the American Chemical Society* **1998,** *120*, 6844-6845.
32. Johnson, D. C.; Widlanski, T. S., *J. Org. Chem.* **2003,** *68*, 5300-5309.
33. Freeman, R.; Hill, H. D. W.; Kaptein, R., *J. Magn. Reson.* **1972,** *7*, 327-329.

4. Controlling the Polymer Microstructure in Anionic Polymerization by Compartmentalization

Elisabeth Rieger,[1] Jan Blankenburg,[2,3] Eduard Grune,[2,3] Manfred Wagner,[1] Katharina Landfester,[1] Frederik R. Wurm[1]

[1]*Max Planck Institute for Polymer Research, Ackermannweg 10, 55128 Mainz, Germany*
[2]*Institute for Organic Chemistry, Johannes Gutenberg-University Mainz, 55128 Mainz, Germany*
[3]*Graduate School Materials Science in Mainz, 55128 Mainz, Germany*

Jan Blankenburg determined and simulated the microstructures. Eduard Grune determined the reactivity ratios. NMR kinetic measurements were performed in collaboration with Manfred Wagner.

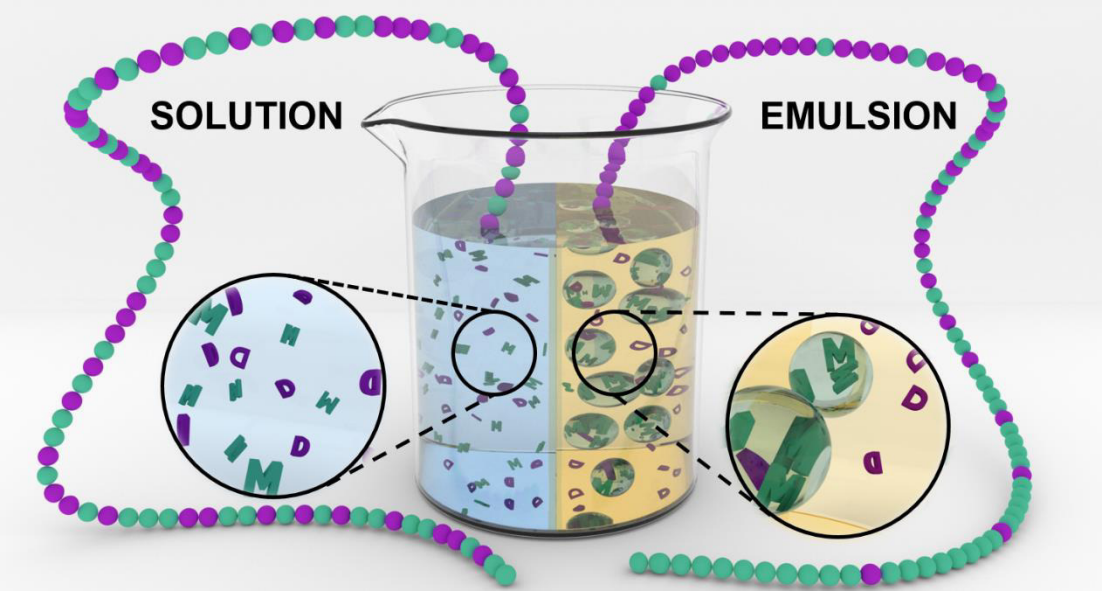

Keywords: Anionic Polymerization, Aziridines, Compartmentalization, Copolymerization, Emulsions.

4.1 Abstract

An ideal random anionic copolymerization is forced to gradient structures by physical separation of two monomers in emulsion compartments. One monomer (M) is preferably soluble in the droplets, while the other one (D) prefers the continuous phase of a DMSO-in-cyclohexane emulsion. The living anionic copolymerization of two activated aziridines is thus confined to the DMSO compartments as polymerization occurs selectively in the droplets. Dilution of the continuous phase adjusts the local concentration of monomer D in the droplets and thus the gradient of the resulting copolymer. The copolymerizations in emulsion are monitored by real-time ^{1}H NMR kinetics, proving a change of the reactivity ratios of both monomers upon dilution of the continuous phase from ideal random to adjustable gradients by simple dilution. This model system will allow the preparation of copolymer libraries in the future in a one-pot, one-shot reaction, without any sequential monomer addition

4.2 Introduction

Compartmentalization is the spatial separation of reagents within organisms, which allows nature to prepare complex molecules. Proteins with their perfect amino acid sequence, leading to complex 3D structures are only one example that was developed by evolution and relies on the compartmentalization of reagents.[1-2]

Controlling the sequence in synthetic peptides (or other polymers) is typically achieved by sequential addition of reagents – either by manual injection or complex setups with automated addition (e.g. peptide synthesizer).[3] In contrast, nature separates several reagents by cell membranes or in different organelles within cells. The easiest mimic of such compartmentalization in the synthesis lab is the formation of an emulsion with reagents separated in the dispersed and the continuous phase.

Through this strategy we could force a competing anionic copolymerization of two monomers to produce, instead of the random copolymer, gradient copolymers with adjustable gradient structure, depending on the ratio of dispersed to continuous phase; we did not resort to opening of the reactor or adding the monomer sequentially.

Such gradient materials, exhibiting a gradual, continuous change in the chemical composition, provide access to unique materials with interesting properties.[4] A recent review summarizes conventional methods for the preparation of gradient polymers (*e.g.* microfluidics, copolymerization, controlled monomer addition, etc.).[5]

Emulsion polymerizations are already well-established and widely used in industry for large-scale productions of numerous products for daily life. The controlled environment in suspension or (mini- and micro-) emulsions offer many advantages, in particular for radical polymerizations, which are not producible in solution.[6-10]

Despite the development of living and controlled polymerization techniques in the last decades,[11] the use of competitive copolymerization to control monomer sequences was not well established; however, many complex macromolecular architectures are currently available by sequential or iterative protocols.[12] Simultaneous copolymerization of two comonomers was used recently to prepare block copolymers[13] or sequence-controlled polymers[14] in radical emulsion polymerization, as emulsion templating reduces the number of radical side reactions.[6, 15-18] Other strategies that rely on spatial separation to control polymer sequence are based on freezing out of one phase[19] or overlaying of two immiscible solvents.[20]

We present a straightforward approach to force a comonomer pair, which undergoes random anionic copolymerization in solution, to form gradient structures only through physical separation. The different solubilities of the monomers in each of the phases are exploited by reaction in a (mini)emulsion with nanometer-sized droplets as the compartments.

4.3 Results and Discussion

We have chosen the living anionic ring-opening polymerization (AROP) of sulfonyl aziridines to achieve selective copolymerization by such emulsified compartments (Figure 4.1).[21] The monomer reactivity of sulfonyl aziridines depends strongly on the nature of the sulfonyl group: more electron withdrawing groups increase the polymerization rate, in the order of nosyl > brosyl > tosyl > mesyl.[22-24] In contrast, *n*-alkyl substituents on the aziridine ring only slightly influence the kinetics of the ROP. Thus we can manipulate the monomers at this position and fine-tune, for example their solubility profile, without altering the comonomer reactivity. This makes the aziridines an ideal model system for competing polymerization in emulsion.

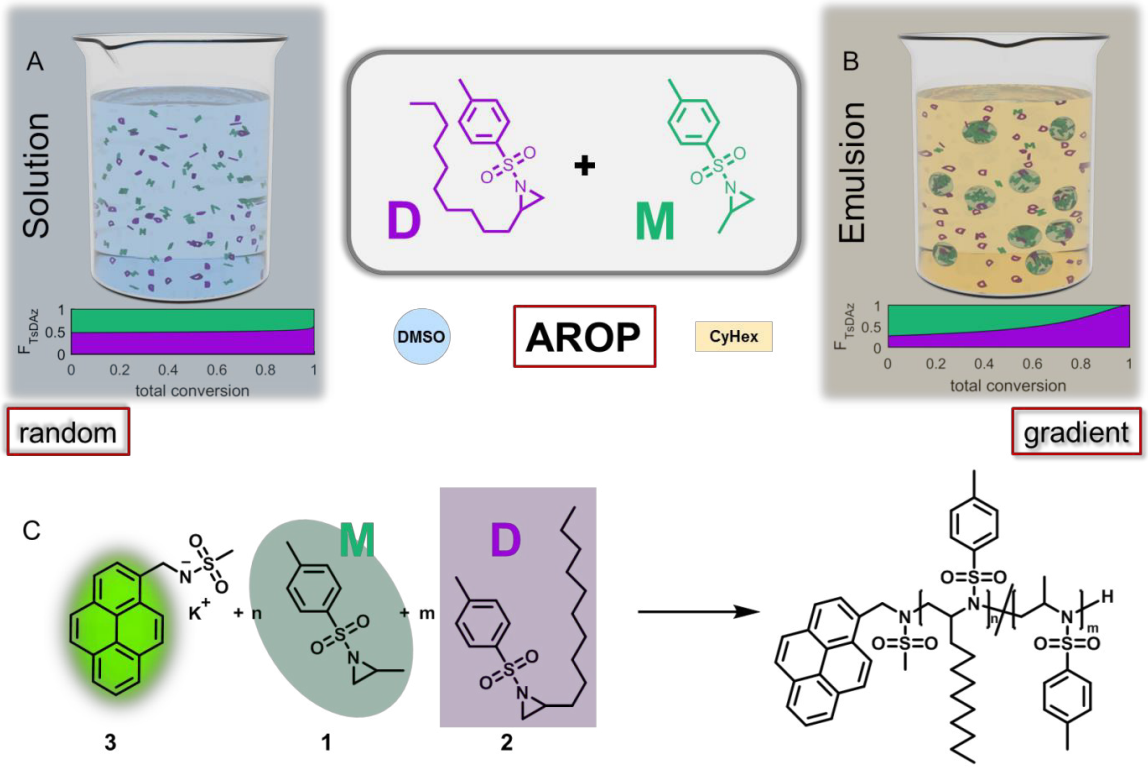

Figure 4.1. Azaanionic polymerization in solution (A) of a molar fraction of 1:50:50, leading to a random copolymer or in a 1:4 DMSO:CyHex-emulsion (B), leading to a gradient microstructure (C) Reaction scheme for the copolymerization of **1** and **2**.

With this tool-box, the random copolymerization of 2-methyl-*N*-tosylaziridine (**1**, M, TsMAz) and 2-decyl-*N*-tosylaziridine (**2**, D, TsDAz) in homogeneous solution is the obvious result (Figure 4.1A). However, if these two monomers are spatially separated in an emulsion due to their selective solubility, the preferred random copolymerization is forced to produce gradient up to almost block-like structures. Monomer **1** is preferably soluble in the dispersed phased, in our case dimethyl sulfoxide (DMSO), while monomer **2** dissolves (due to the long alkyl tail) preferably in the continuous cyclohexane (CyHex) phase (Figure 4.1B). The copolymers are soluble in DMSO and insoluble in cyclohexane. In addition, we have proven that no propagation occurs in the continuous phase (CyHex) for the azaanionic polymerization of aziridines: thus the propagation is located selectively within the DMSO droplets.[25] The location of the polymerization was further visualized by the use of a pyrene derivative as the initiator of the polymerization (Figure 4.2B shows a fluorescent microscopy image, proving fluorescence only inside of the dispersed phase). This implies that the copolymer composition depends only on the local monomer concentration within the DMSO-droplets, which re-equilibrates as the monomer is consumed. The anionic polymerization proceeds in the emulsion either with or without the addition of a surfactant, making the polymers interesting for further applications, where surfactant might

be beneficial or not necessary. This monomer sequence control confers potential for molecular targeting, recognition and biocatalysis.

To determine the reactivity ratios in homogeneous solution, the simultaneous copolymerization of the two monomers was investigated by real-time ^{1}H NMR spectroscopy. Due to their similar reactivity, the shift in the composition of the monomer mixture is small and multiple ^{1}H NMR kinetic measurements with different monomer ratios were combined. The data were evaluated by the methods of Fineman-Ross[26] and Kelen Tüdos[11, 27] and proved that the two monomers have almost equal reactivity: r_1(**1**) = 1.08, r_2(**2**) = 0.98, $r_1 \cdot r_2$ = 1.05 (Kelen-Tüdos) (cf. Supplementary Information Table S4.1-S4.2), revealing an almost ideal copolymerization in DMSO (ideal is defined with r_1 = 1 and r_2 = 1 or $r_1 \cdot r_2$ = 1). The microstructure of the 1:1 eq. polymer was predicted by numerical integration of the Mayo-Lewis equation,[28] showing a slightly favored incorporation of TsMAz (**1**, M, green) at the beginning of the copolymer and a slightly favored incorporation of TsDAz (**2**, D, purple) at the end of the polymer (Figure 4.1A).[29]

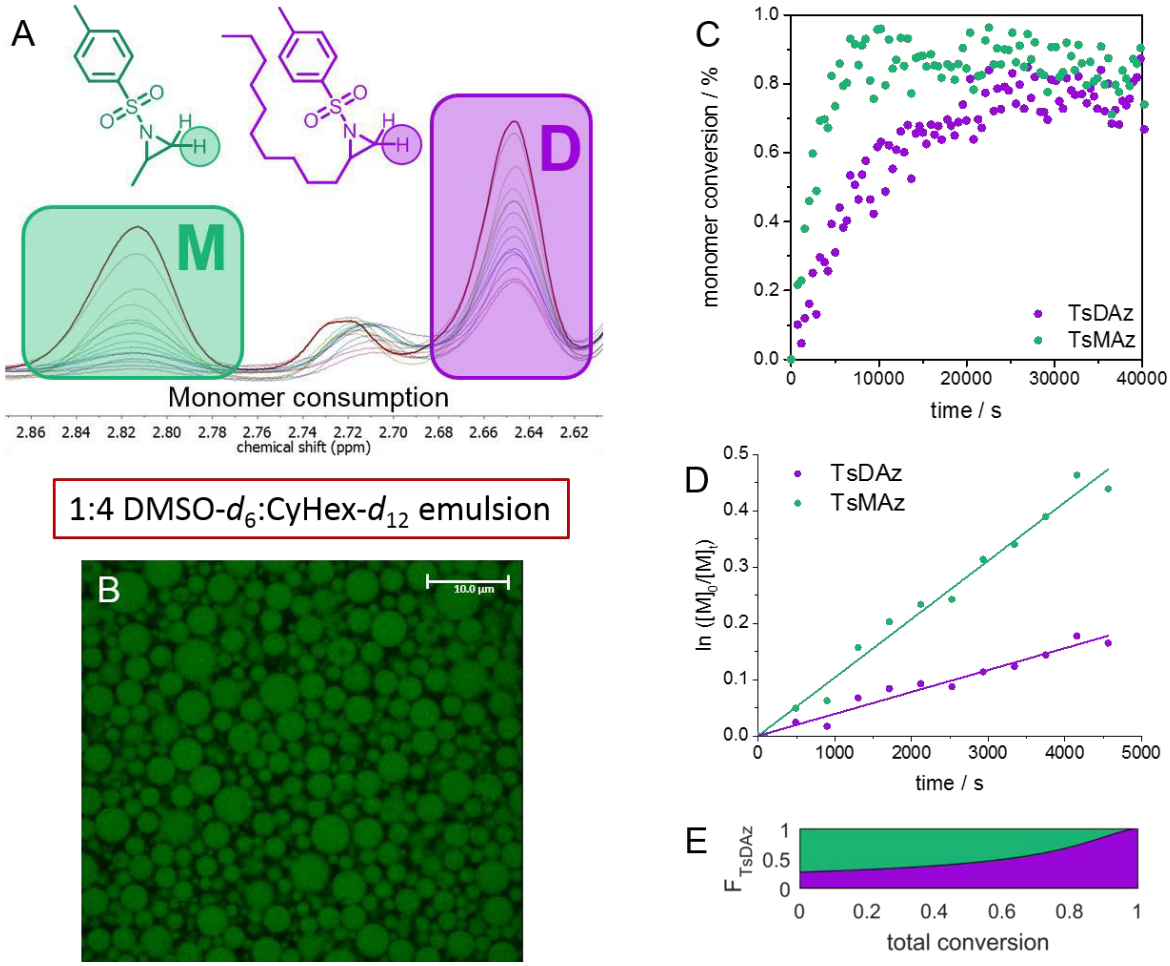

Figure 4.2. Azaanionic copolymerization of TsMAz (**1**, M) and TsDAz (**2**, D) in emulsion at 50 °C: (A) Real-time ^{1}H NMR kinetics of copolymerization in emulsion. (B) cLSM image of the emulsion showing the fluorescent initiator inside of the droplets. (C) Monomer conversion *vs*. time. (D) Kinetic plots of $\ln([M]_0/[M]_t)$ *vs*. time. (E) Incorporation probability of TsDAz (F_{TsDAz}) *vs* total conversion.

As the two monomers exhibit distinctively different solubilities, we physically separated them in a DMSO-in-cyclohexane (mini)emulsion. Monomer **1** prefers DMSO, while **2** with its long alkyl tail has a higher solubility in cyclohexane. Physical separation of the monomers was either achieved by surfactant-free emulsification with continuous, vigorous stirring or by the addition of surfactant and ultrasound mixing to form a stable miniemulsion (Figures S4.1 and S4.4). The copolymerization behavior was studied by real-time ^{1}H NMR spectroscopy of the miniemulsions as phase separation in the non-stirred NMR tube is efficiently prevented by the surfactant. From these spectra (Figure 4.2A and Figure S4.13) both monomer consumptions and propagation rates (k_p) were calculated.[25] The miniemulsions were stable for at least several days under this conditions with droplet diameters between 200 and 800 nm. ^{1}H NMR and size-exclusion chromatography (SEC) data demonstrated that the azaanionic polymerization remained living in the (mini)emulsion process and provided polymers with monomodal and rather narrow molecular weight distributions ($Đ$ < 1.2, a slightly higher dispersity than that in a normal glass reactor might be rationalized, as contents of the NMR tube is not stirred during the polymerization, but shaken by hand after every fourth spectra). The living character of the AROP was proven by chain extension experiments and the linear slope of the plots $\ln([M]_0/[M]_t)$ *vs.* time (cf. Figures 4.2, 4.3, and S4.3). Polymerizations reached almost complete monomer conversion (approx. 90%). More importantly, HPLC-measurements indicate that the surfactant was not involved in the polymerization (Figure S4.5). Interfacial tension (γ) between water and toluene was measured in the presence of the different copolymers by the spinning drop method: the random P(**1**-*co*-**2**), prepared from solution, reduces γ only slightly from 32 mN·m^{-1} to 29.1 mN·m^{-1}, while the amphiphilic block copolymer prepared by sequential monomer addition P**1**-*b*-P**2** reduces γ to 22 mN·m^{-1}. The gradient P(**1**-*gr*-**2**) prepared from the 1:10 mixture reduces γ to 27 mN·m^{-1}, an intermediate value, proving the effect of gradient formation during the confined copolymerization in emulsion.

Separation of the monomers by an emulsion clearly forces them to produce gradient copolymers (Figure 4.2), as the local concentration in the DMSO droplets of both monomers is controlled by their solubility profiles. Since the kinetics of an anionic polymerization strongly depend on the solvent polarity, it is important that the copolymerization is restricted to one solvent (here, the DMSO compartments). Thus, we assume that the reactivity ratios do not change during the polymerization in emulsion and that only the dilution of the continuous phase affects the monomer feed of **2** into the DMSO compartments. This changes the comonomer incorporation, which results in apparent reactivity ratios (r_{app}) that are only dependent on the solvent ratios and are necessary for the comparison of the two-phase systems with homogeneous polymerization. As r_1(**1**) · r_2(**2**) ≈ 1 in solution, the copolymerization can be assumed as ideal, which simplifies the Mayo-Lewis equation and enables the determination of the apparent reactivity ratios directly from the propagation ratios, as $r_1 = k_p$(**1**) / k_p(**2**) and *vice versa* $r_2 = k_p$(**2**) / k_p(**1**).[30-32]

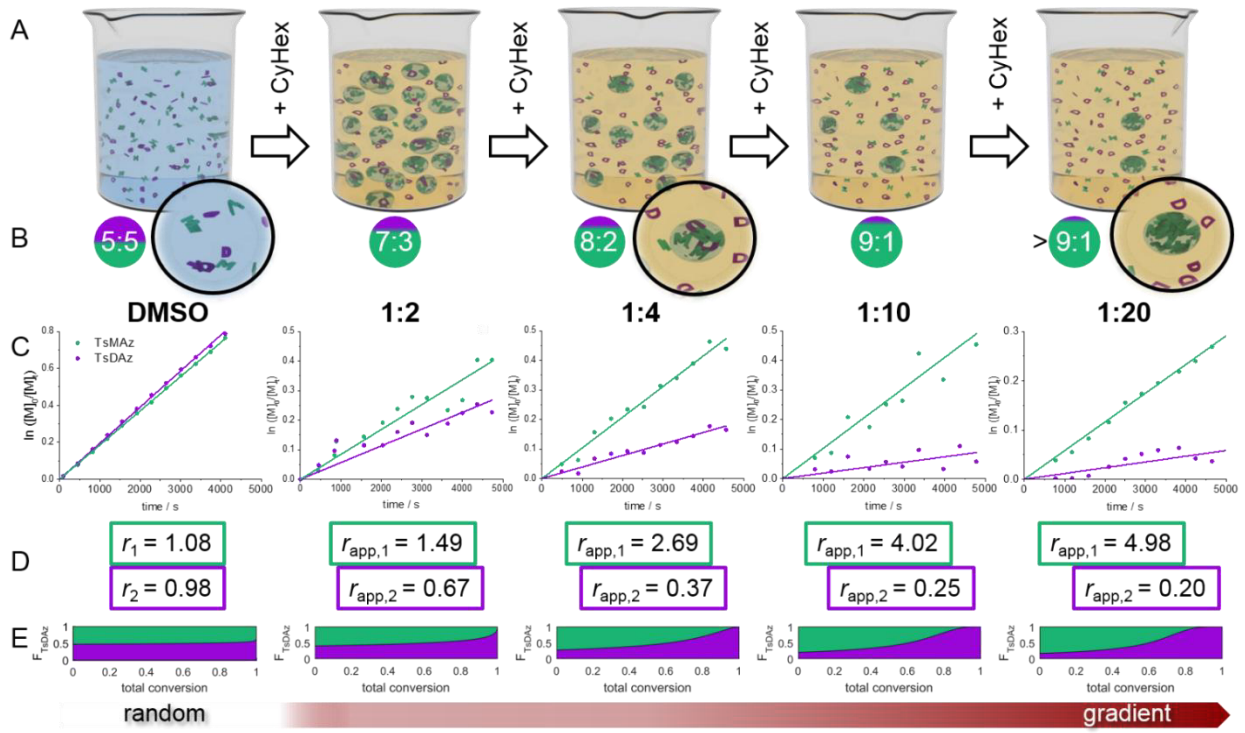

Figure 4.3. Controlling the monomer separation by dilution of the emulsion: (A) Adjustment of the DMSO (blue) : cyclohexane (yellow) ratio. (B) Monomer ratio inside of the DMSO-droplets, determined by HPLC, and zoom-in: with increasing cyclohexane-dilution M is enriched inside of the DMSO-droplets. (C) Kinetic plots of $\ln([M]_0/[M]_t)$ *vs.* time of TsMAz (**1**, M), TsDAz (**2**, D) in different emulsions. (D) Reactivity ratios of the different solvent-mixtures. (E) Incorporation probability of TsDAz (F_{TsDAz}) *vs.* total conversion proves increased gradients upon dilution.

By variation of the dilution of the continuous phase, the local monomer concentration of **2**, that is, the partitioning of the two monomers between the phases, can be further adjusted, which will directly influence the gradient in the product (cf. Figure 4.3B). From HPLC measurements, partition coefficients (log *P*-values, ($\log P_{CyHex/DMSO} = \log([M]_{CyHex}/[M]_{DMSO})$) of the monomer-pair in DMSO and cyclohexane were calculated, proving the preference of TsMAz for DMSO. Monomer partitioning can be also tuned by other solvent pairs: DMF was used as dispersed phase, resulting in a slightly lower monomer separation (cf. Supp. Info. Table S4.4-S4.6). Different ratios of the dispersed to the continuous phase (1:2, 1:4, 1:10, 1:20) were explored, with increasing amount of cyclohexane. For the 1:2 DMSO/CyHex solvent ratio, the initial monomer ratio in the DMSO droplets is ca. 7:3 (TsMAz/TsDAz) and the ratio increases to 8:2 (for DMSO/CyHex = 1:4) to 9:1 (1:10) up to more than > 9:1 (for 1:20). The differential Mayo-Lewis equation was solved numerically to reveal the microstructure of a copolymerization ratio pair and a given initial monomer ratio (Figure 4.3E).[29, 32] With increasing dilution, the apparent reactivity ratios (Figure 4.3D, Table S4.3) changed from an ideal random copolymerization into more pronounced gradient copolymers.

4.4 Summary

In conclusion, by compartmentalization and spatial separation of two monomers in an emulsion, we were able to force a random copolymerization to produce gradient copolymers with adjustable gradient strength. This is the first example of forcing copolymerization behavior by spatial separation of the reaction mixture in an emulsion for an anionic copolymerization, resulting in gradient copolymers with surface-active properties. Real-time ^{1}H NMR spectroscopy was used to monitor the reactions and calculate the final copolymer microstructure. As the propagation of the living anions occurs selectively within the DMSO compartments, dilution of the continuous phase made it possible to adjust the gradient strength of the copolymers. Apparent reactivity ratios *(r_{app})* were calculated, which depend only on the local concentration in the compartments. For the first time, this allowed us to control the comonomer sequence distribution along a polymer chain by simple dilution of the emulsion with the continuous solvent.

The emulsion platform for the anionic polymerization might be used for several applications, as it is free of heavy metals and can be performed with or without surfactants. We believe that this strategy can be extended to other monomers and will give access to libraries of copolymers with adjustable gradient strength in a closed one-pot reaction, just by changing the ratio of dispersed to continuous phase in a (mini)emulsion.

4.5 Acknowledgments

The authors thank the Deutsche Forschungsgemeinschaft (DFG WU750/ 7-1) and the BMBF/MPG network MaxSynBio for funding. The authors thank Stefan Spang for the NMR measurements, Dr. Anke Kaltbeitzel for cLSM-measurements and Beate Müller for HPLC-measurements.

4.6 Supporting Information

The Supporting Information contains additional synthetic procedures, characterization data and kinetic measurements for polymers, data plots and overview tables for the evaluation of copolymerization parameters and the determination of partition coefficients.

Content

4.6.1 Materials and Methods.

Chemicals.

All solvents and reagents were purchased from Sigma-Aldrich, Acros Organics or Fluka and used as received unless otherwise mentioned. All deuterated solvents were purchased from Deutero GmbH, cyclohexane-d_{12} was distilled from sodium, DMSO-d_6 from CaH_2 and stored in a glovebox prior to use. All monomers and the initiator were dried extensively by azeotropic distillation with benzene prior to polymerization. 2-methyl-*N*-tosylaziridine (**1**, M, TsMAz) and 2-decyl-*N*-tosylaziridine (**2**, D, TsDAz) were synthesized to our previously published protocol,[24] 1-pyrenemethylmethanesulfonamide (**3**, PyNHMs) was synthesized according to literature.[33] The block copolymer surfactant P(B/E-*b*-EO), consisting of a poly(butylene-*co*-ethylene) block (M_n = 3700 g mol^{-1}) and a poly(ethylene oxide) block (M_n = 3000 g mol^{-1}), was synthesized by conventional anionic polymerization.[34]

Methods.

NMR. ^{1}H NMR spectra were recorded using a Bruker Avance 300 or a Bruker Avance III 700. All spectra were referenced internally to residual proton signals of the deuterated solvent.

SEC. Size exclusion chromatography (SEC) measurements of standard polymers were performed in DMF (1 g L^{-1} LiBr added) at 60°C and a flow rate of 1 mL min^{-1} with a PSS SECcurity as an integrated instrument, including a PSS GRAM 100-1000 column and a refractive index (RI) detector. Calibration was carried out using poly(ethylene glycol) standards provided by Polymer Standards Service.

DLS. (Dynamic Light Scattering) was used to measure the droplet size, using a Nicomp 380 Submicron Particle Sizer (PSS-Nicomp, Particle Sizing Systems, Santa Barbara, CA, USA) at a fixed scattering angle of 90 °.

CLSM (Confocal laser scanning microscopy). Green fluorescence of the pyrene after several seconds of UV photoactivation was used to image the dispersed phase of the emulsion. The emulsion was spread between 2 coverslips using a distance holder of 50 µm. Images were taken on a confocal microscope (Leica TCS SP5, Wetzlar, Germany). Excitation was provided by the 458 nm and 488 nm line of an Argon laser, the fluorescence was detected with a photomultiplier using a detection range of 511-625 nm.

HPLC (high performance liquid chromatography)

HPLC measurements for determining the partition coefficient (log *P*). Agilent Series 1200; Column: Macherey-Nagel (MN) HD8; Eluent: Start THF/Water + 0.1% TFA 40/60, Gradient over 10 min to 100% THF, 1 mL min^{-1} at 20 °C) at 260 nm.

HPLC measurements to identify the surfactant. Agilent Series 1200; Column: Macherey-Nagel (MN) HTEC C18; Eluent: Start THF/Water + 0.1% TFA 50/50, Gradient over 10 min to 100% THF, 1 mL min^{-1} at 20 °C) at 240 nm.

4.6.2 Synthetic Protocols.

General procedure for the azaanionic polymerization. All glassware (Schlenk flasks) was flame-dried by *in vacuo* for at least three times. All reactants (except potassium bis(trimethylsilyl)amide (KHMDS)) were dried from benzene *in vacuo* for at least 4 h. The monomers and the PyNHMs-initiator were dissolved in 2 and 1 mL respectively anhydrous *N,N*-dimethylformamide (DMF). KHMDS was added quickly in argon-counter flow to the PyNHMs-solution and the sample boat was rinsed with another 1 mL DMF. From the initiator-solution the appropriate volume was added to the monomer solution. The mixture was stirred at 50 °C for at least 18 h. To terminate the polymers, 0.5 mL acidic methanol were added and the reaction mixture was precipitated in ca. 30 mL methanol. The colorless solids were collected by centrifugation and dried at 70 °C *in vacuo.*

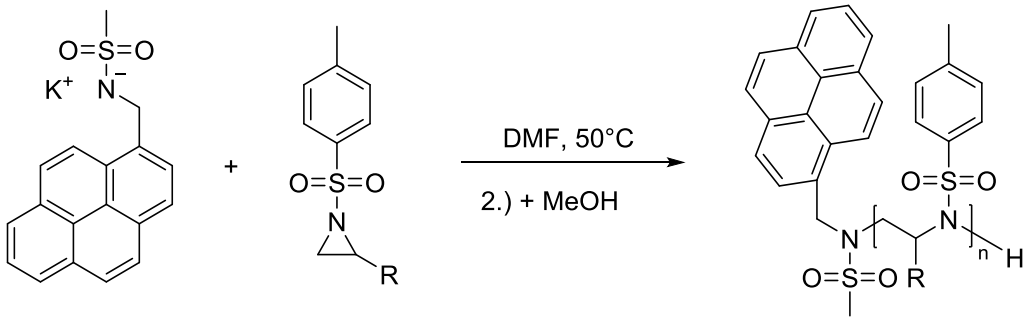

R = -Methyl, -Decyl

Copolymerization in emulsion (1:4), without surfactant.

Poly(TsMAz-co-TsDAz)-1.

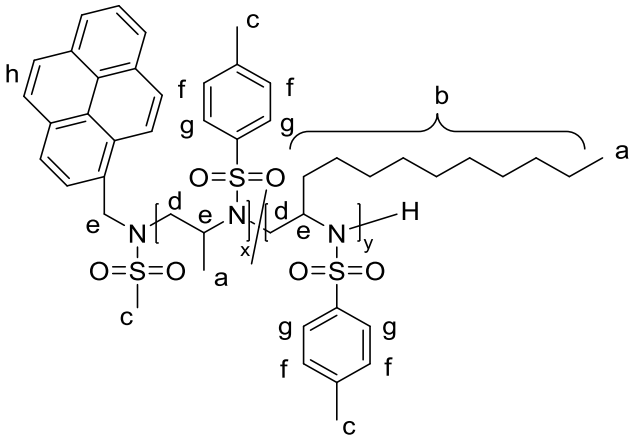

Poly(TsMAz$_{50(theo)}$-*co*-TsDAz$_{50(theo)}$)-1: [TsMAz (106.4 mg, 504 µmol), TsDAz (168.4 mg, 499 µmol), PyNHMs (3.0 mg, 9.7 µmol), KHMDS (1.9 mg, 9.7 µmol)], 3.3 mL DMSO, 12.5 mL cyclohexane.

Final copolymer Poly(TsMAz-*co*-TsDAz)-1: ^{1}H NMR (700 MHz, 298 K, DMSO-d_6): δ 8.41 – 8.02 (m, h), 7.91 – 7.48 (m, g), 7.48–7.08 (m, f), 4.38 – 3.60 (m, e), 3.60–2.83 (m, d), 2.48–2.15 (m, c), 1.28 – 0.96 (m, b), 0.90 – 0.50 (m, a).

M_n (SEC) = 2300 g mol^{-1}, $Đ$ = 1.19.

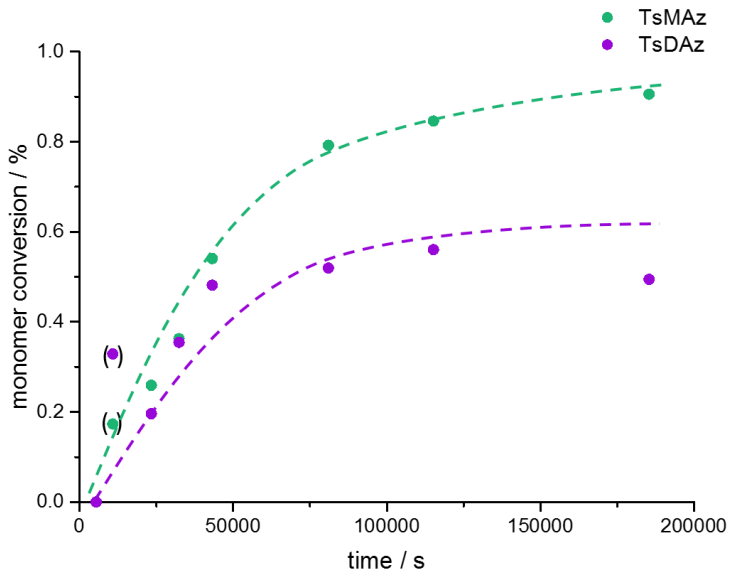

Figure S4.1. Batch-copolymerization in emulsion, without surfactant: Kinetics by taking samples at certain times, analyzed by ^{1}H NMR: monomer conversion of (Poly(TsMAz$_{50(theo)}$-*co*-TsDAz$_{50(theo)}$)-1) *versus* reaction time. Values in brackets unrealistic, due to measurement inaccuracy.

Copolymerization in emulsion (1:4), without surfactant – chain extension.

Poly(TsMAz-co-TsDAz)-3 – chain extension.

The polymerization was carried out in analogy to the conventional procedure in a Schlenk-flask. The first 50 equivalents of both monomers were dissolved in 1.4 mL anhydrous *N,N* dimethylformamide (DMF) and respective in 8 mL anhydrous cyclohexane. The initiator was dissolved in 1 mL *N,N*-dimethylformamide (DMF) each. A stock solution of the initiator system was prepared and only the appropriate volume (100 µL) extracted and added to the DMF-solution. Both monomer-solutions were combined (1:4 emulsion). After stirring (1000 rpm) the mixture for 48 h at 50 °C, additional 100 mg (another 50 equivalents) of TsMAz, dissolved in 0.3 µL dry DMF, were added and stirred for further 48 h at the same temperature. To terminate the polymerization, 0.5 mL degassed methanol were added and the reaction mixture was precipitated in ca. 30 mL methanol and dried for further analyses.

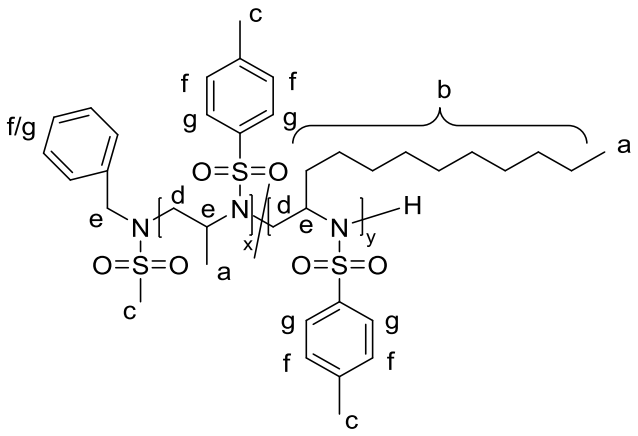

Poly(TsMAz$_{50(theo)}$-*co*-TsDAz$_{50(theo)}$)-3-I: [TsMAz-I (100.1 mg, 473 µmol), TsDAz (159.7 mg, 473 µmol), BnNHMs (1.17 mg, 6.3 µmol), KHMDS (1.3 mg, 6.3 µmol)]. TsMAz-II (100.1 mg, 473 µmol)

I. block: SEC (RID, DMF, PEO): M_n = 8300 g mol^{-1}; $Đ$ = 1.14

II. block: SEC (RID, DMF, PEO): M_n = 11200 g mol^{-1}; $Đ$ = 1.27

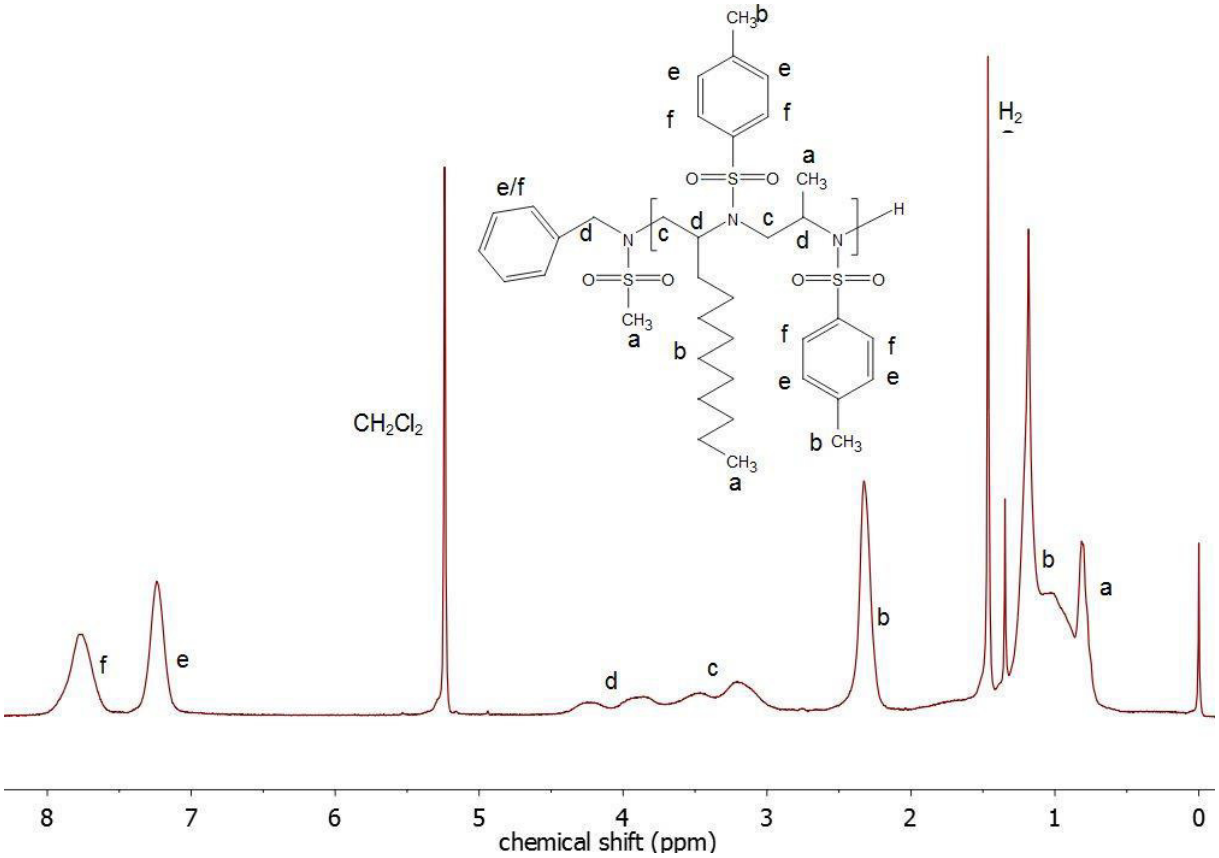

Figure S4.2. ^{1}H NMR (300 MHz, 298 K, $CDCl_3$) of P((TsMAz-*co*-TsDAz)-*block*-TsMAz).

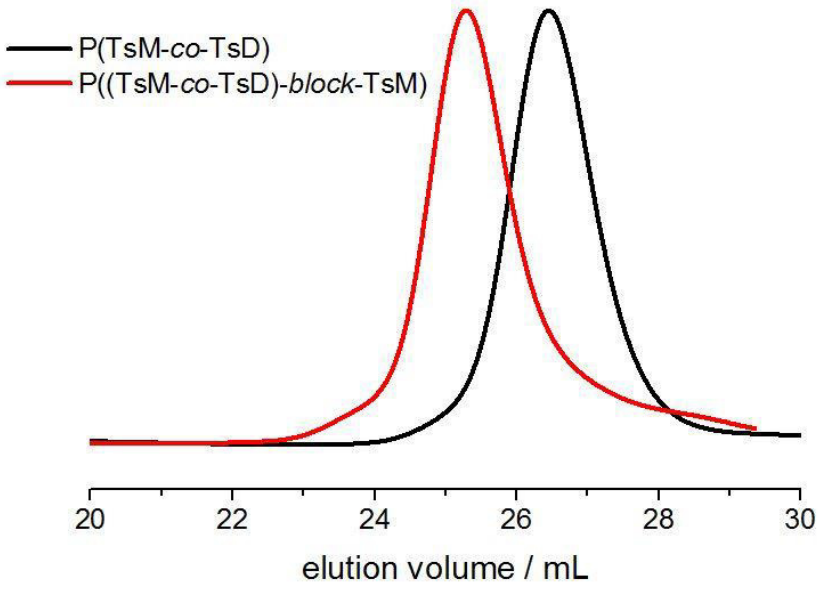

Figure S4.3. SEC traces of P(TsMAz-*co*-TsDAz) and P((TsMAz-*gradient*-TsDAz)-*block*-TsMAz) in DMF (RI signal).

Copolymerization in miniemulsion (1:4), with surfactant.

Poly(TsMAz-co-TsDAz)-2.

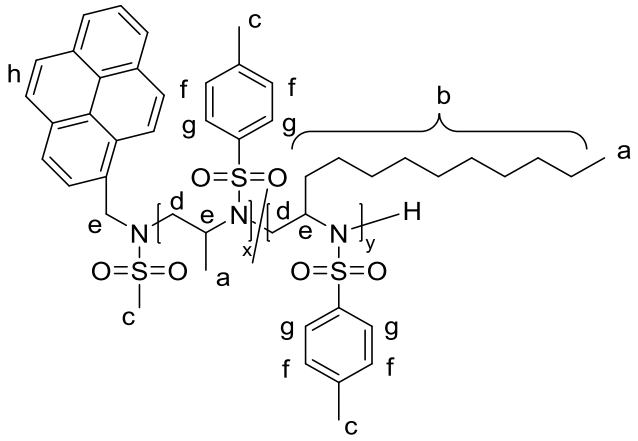

Poly(TsMAz$_{50(theo)}$-*co*-TsDAz$_{50(theo)}$)-2: [TsMAz (18.3 mg, 87 µmol), TsDAz (29.4 mg, 87 µmol), PyNHMs (0.55 mg, 1.8 µmol), KHMDS (0.29 mg, 1.5 µmol)], 0.32 mL DMSO, 1.8 mL Cyclohexane, 8.4 mg surfactant (0.6 weight% of cyclohexane). All samples were homogenized using a Branson 450 W sonifier with an inverse cup tip (60 s, 20 s sonication, 10 s pause, 70% amplitude) at 4 °C. The reaction-mixture was divided into small screw-cap vials inside of a glovebox and terminated with acidic methanol after certain time intervals and analyzed via ^{1}H NMR.

Final copolymer Poly(TsMAz-*co*-TsDAz)-2: ^{1}H NMR (300 MHz, 295 K, Chloroform-*d*): δ 8.34 – 8.07 (m, h), 8.06 – 7.61 (m, g), 7.38–7.12 (m, f), 4.56 – 3.77 (m, e), 3.77–2.95 (m, d), 2.43–2.23 (m, c), 1.26 – 0.94 (m, b), 0.90 – 0.74 (m, a).

M_n (SEC) = 2300 g mol^{-1}, $Đ$ = 1.21.

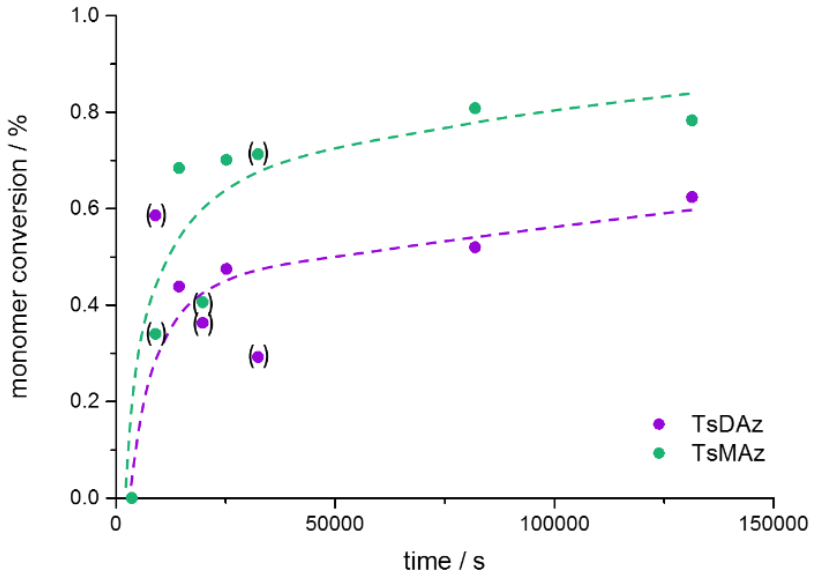

Figure S4.4. Batch-copolymerization in miniemulsion. Kinetics by termination of the same reaction mixtures, divided in different vials, at certain times, analyzed by ^{1}H NMR: monomer conversion of (Poly(TsMAz$_{50(theo)}$-*co*-TsDAz$_{50(theo)}$)-2) *versus* reaction time. Values in brackets unrealistic, due to measurement inaccuracy.

To further ensure, that the surfactant was not involved in the polymerization process, HPLC-analyses were carried out. For comparison, the surfactant (P(B/E-*b*-EO)) (black), homopolymers of both monomers (P(TsMAz), green and P(TsDAz), purple), a random copolymer of both monomers (brown) and the gradient copolymer (blue) produced in miniemulsion, including the surfactant, were analyzed. By change in their elution times, the surfactant was identified to elute at its maximum at 20.4 mL, whereas all polymers show different maxima of elution volumes. The gradient polymer (blue), including the surfactant, shows an additional peak at the same volume, which is almost completely separated from the polyaziridine (marked in red), belonging to the surfactant.

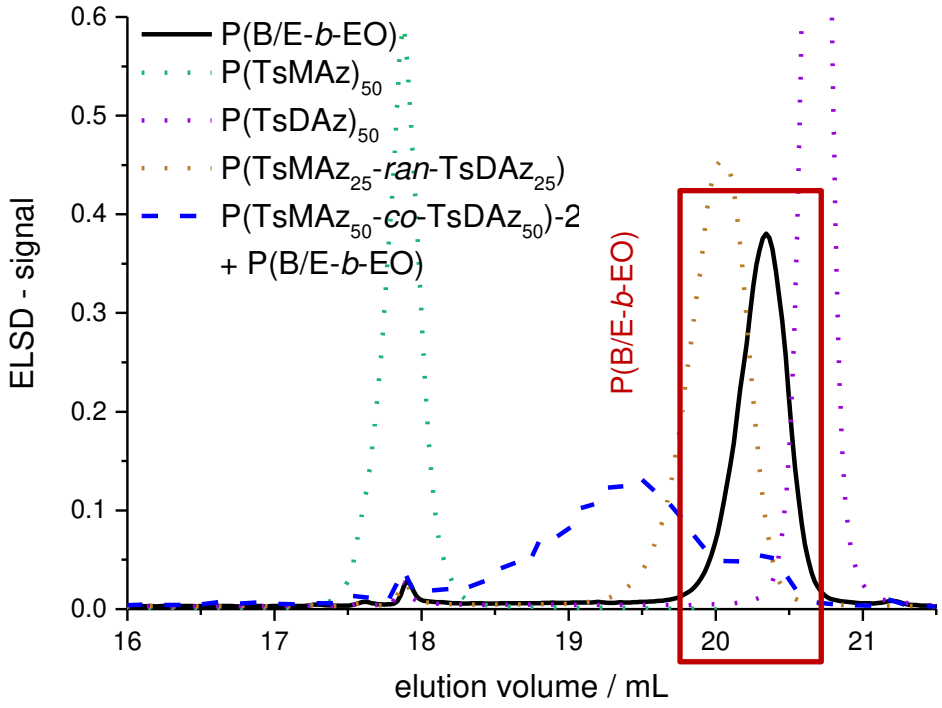

Figure S4.5. HPLC-elugrams of the surfactant (P(B/E-*b*-EO)-black), the homopolymers prepared withouot the use of surfactant of TsMAz (green) and TsDAz (purple), the random copolymer of TsMAz and TsDAz (brown), and the copolymer from miniemulsion, including surfactant, in blue – revealing that the surfactant is not involved in the polymerization (ELSD (Evaporated Light Scattering Detector) signal).

4.6.3 NMR kinetics in solution for determining r-parameters.

Monitoring polymerizations by real-time ^{1}H NMR spectroscopy. All polymerizations were carried out in analogy to the conventional procedure: Inside of a glovebox in a nitrogen-atmosphere both monomers in the respective ratio (compare Table S4.1) were dissolved in a total volume of 1 mL of deuterated DMSO. The initiator-solution in 1 mL DMSO-d_6 was prepared separately (5.5 mg, 17.8 µmol). A conventional NMR-tube was filled with the monomer mixture and sealed with a rubber-septum. Prior to initiation, the pure monomer-solvent mixture was measured at 50 °C. From the stock solution of the initiator 100 µL were added to the monomer mixture, mixed quickly and inserted into the spectrometer. All spectra were referenced internally to residual proton signals of DMSO-d_6 at 2.50 ppm. The π/2-pulse for the proton measurements was 13.1 µs. The spectra of the polymerizations were recorded at 700 MHz with 32 scans (equal to 404 s (acquisition time of 2.595 s and a relaxation time of 10 s after every pulse)) over a period of at least 3 h. No B-field optimizing routine was used over the kinetic measurement time. The spin-lattice relaxation rate (T1) of the ring-protons, which are used afterwards for integration, was measured before the kinetic run with the inversion recovery method.[24-25, 35]

Due to the small composition shift during the copolymerization multiple NMR kinetic experiment were carried out to determine the copolymerization parameters. Each data point in the graphs corresponds to one NMR kinetic experiment. All data can be found in Table S4.1. From those data, r-parameters were calculated, considering different methods (Fineman-Ross, Kelen-Tüdos and Mayo Lewis and ideal case considered by Wall), all graphs are listed below, including Table S4.2 with the different r-parameters.[26-29, 32]

Table S4.1. Overview over the performed NMR-kinetics in DMSO-d_6-solution to determine the r-parameters.

Monomer ratio (M:D) (theo.)	60:40	80:20	50:50	20:80
m(PyNHMs) / mg	1.1	1.1	1.1	1.0
n(PyNHMs) / µmol	3.5	3.5	3.5	3.4
m(TsM) / mg	43.7	58.8	36.1	17.8
n(TsM) / µmol	208.9	278.3	170.9	84.2
m(TsD) / mg	43.3	20.0	57.0	93.3
n(TsD) / µmol	129.6	59.3	168.9	276.4
k_p(TsM) / 10^{-3} L mol^{-1} s^{-1}	33.2	44.1	51.6	101.3
k_p(TsD) / 10^{-3} L mol^{-1} s^{-1}	34.5	40.9	54.4	102.7
$Đ^a$ (SEC)	1.25	1.23	1.32	1.37
$M_n{}^a$(SEC)	2700	1300	2800	2200
Conversion / %	100	100	100	100
Reaction time / h	10	10	10	10

[a] number-average molecular weight and molecular weight dispersity determined via SEC in DMF (vs. PEO standards)

Definitions Mayo-Lewis equation.

$$\frac{d[M_1]}{d[M_2]} = \frac{[M_1]}{[M_2]} \frac{r_1[M_1]+[M_2]}{r_2[M_2]+[M_1]}$$

$$y = x\frac{r_1 x + 1}{r_2 + x}$$

$$x = \frac{[M_1]}{[M_2]};\ y = \frac{d[M_1]}{d[M_2]}$$

Fineman-Ross

$$\frac{x(y-1)}{y} = r_1 \frac{x^2}{y} - r_2$$

Fineman-Ross inverted

$$\frac{(y-1)}{x} = -r_2 \frac{y}{x^2} + r_1$$

Kelen-Tüdos

$$\frac{x(y-1)}{ay + x^2} = \left(r_1 + \frac{r_2}{a}\right)\frac{x^2}{ay + x^2} - \frac{r_2}{a}$$

$$a = \sqrt{\left(\frac{x^2}{y}\right)_{min} \cdot \left(\frac{x^2}{y}\right)_{max}}$$

Mayo Lewis:

$$r_1 = \frac{y}{x^2} r_2 + \frac{y-1}{x}$$

Ideal case Wall

$$\frac{d[M_1]}{d[M_2]} = r_1 \frac{[M_1]}{[M_2]}$$

$$r_2 = {}^{1}\!/_{r_1}$$

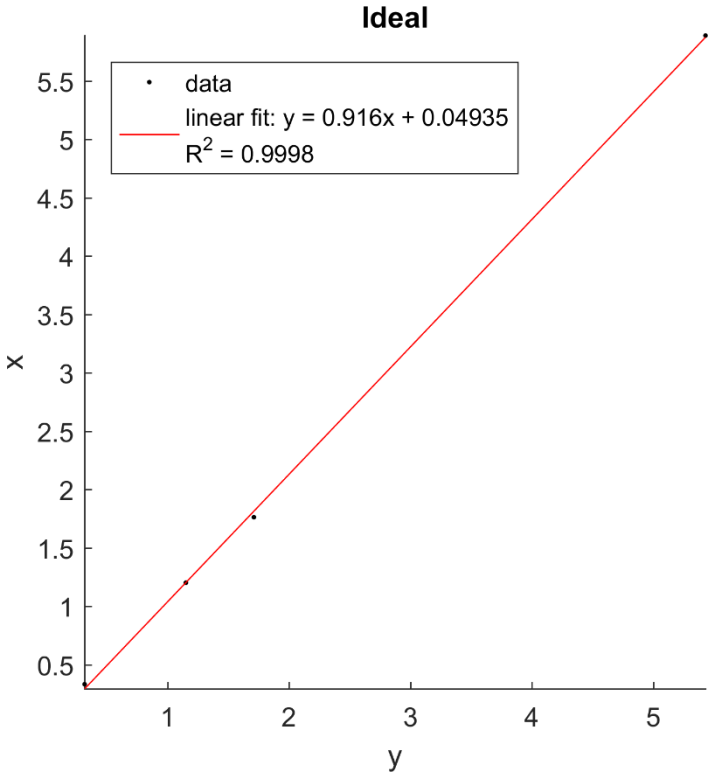

Figure S4.6. Evaluation of copolymerization parameters with a model of an ideal copolymerization.

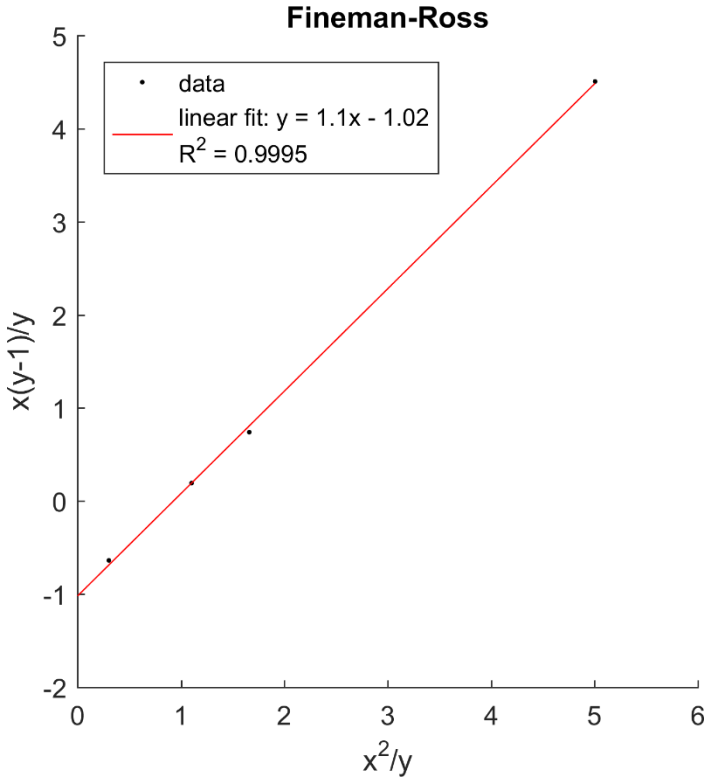

Figure S4.7. Fineman-Ross evaluation of the copolymerization parameters.

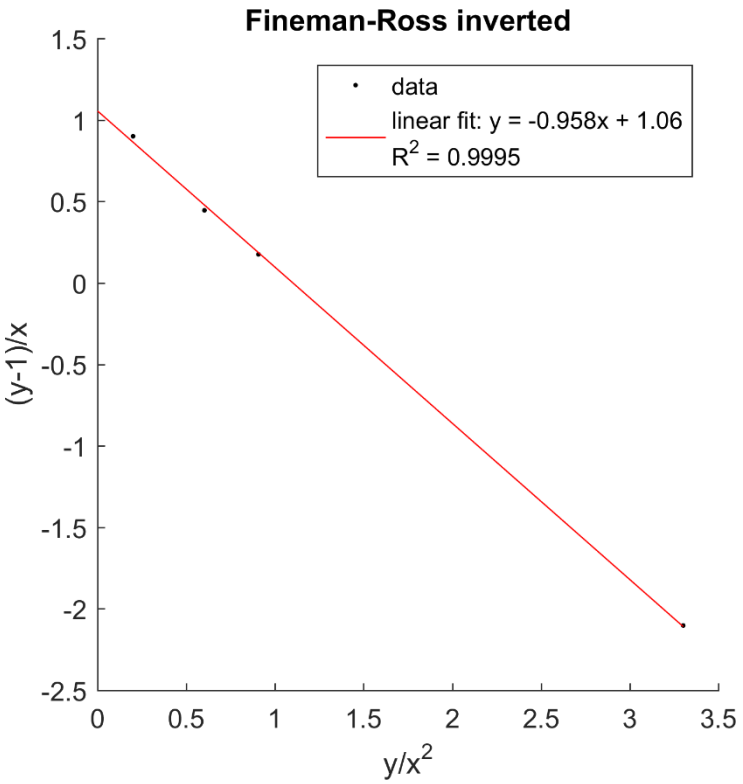

Figure S4.8. Inverted Fineman-Ross evaluation of the copolymerization parameters.

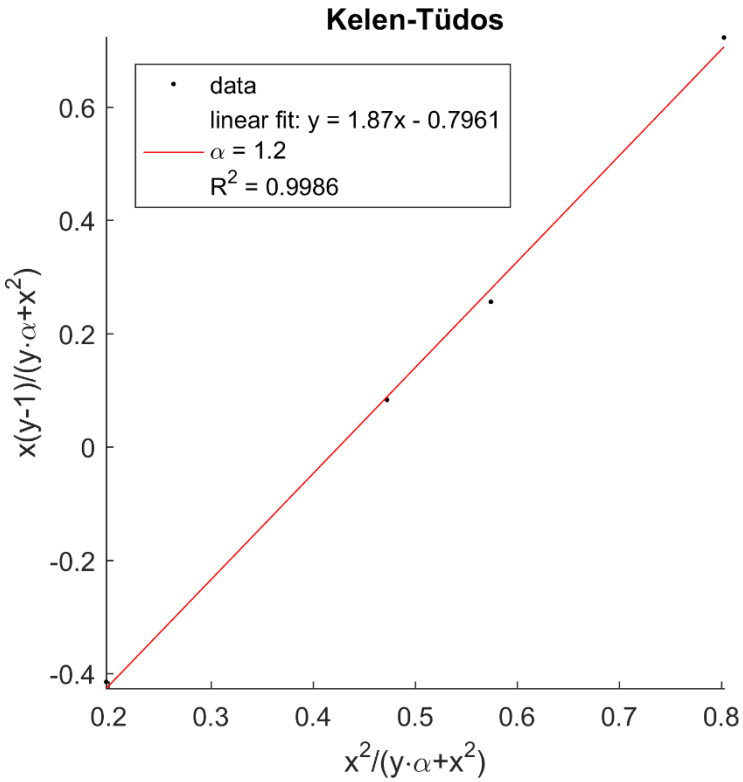

Figure S4.9. Kelen-Tüdos evaluation of the copolymerization parameters.

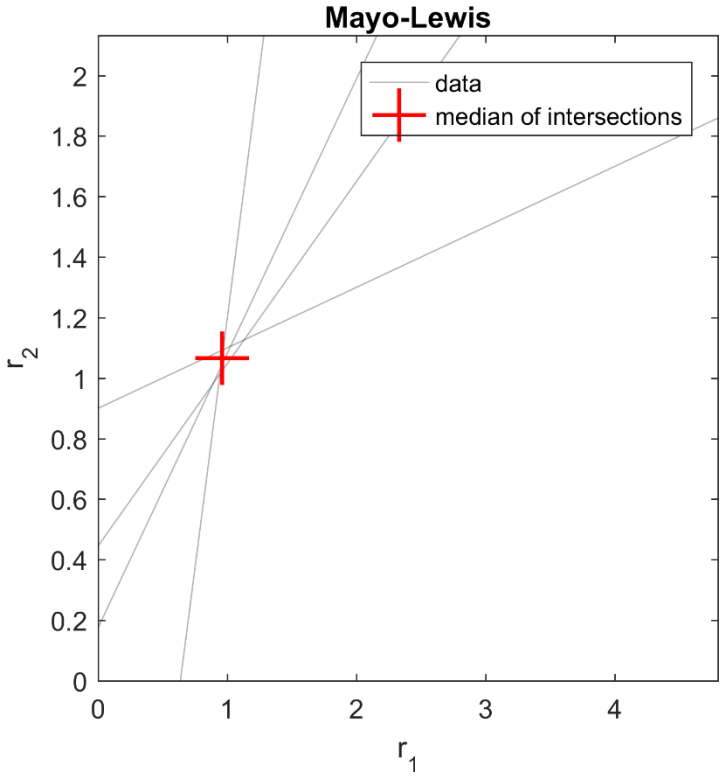

Figure S4.10. Mayo-Lewis evaluation of the copolymerization parameters.

Monomer fraction in solution and corresponding incorporation into the polymer:

$$F_1 = \frac{d[M_1]}{d[M_1] + d[M_2]}$$

$$F_1 = 1 - F_2 = \frac{r_1 f_1^2 + f_1 f_2}{r_1 f_1^2 + 2 f_1 f_2 + r_2 f_2^2}$$

$$f_1 = 1 - f_2 = \frac{[M_1]}{[M_1] + [M_2]}$$

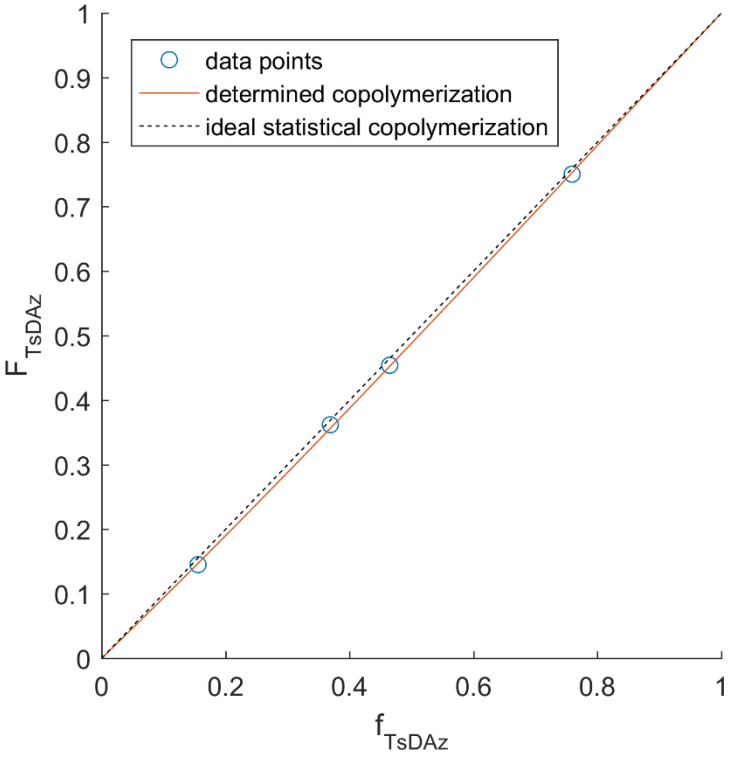

Figure S4.11. The copolymerization shows an almost ideal statistical behavior (parameters from Kelen-Tüdos).

Table S4.2. Overview of all r-parameters in solution, calculated from different methods.

Method	r_1 (TsMAz)	r_2 (TsDAz)	$r_1 * r_2$
Fineman-Ross	1.10	1.02	1.12
Fineman Ross inverted	1.06	0.96	1.01
Kelen-Tüdos	1.08	0.98	1.05
Mayo-Lewis	1.07	0.96	1.02
Ideal (Wall)	1.09	0.92	1.00

All methods give a very similar result with a product of both copolymerization parameters close to one. This indicates an ideal copolymerization, and the result of the evaluation with the ideal model gives almost the same results.[30]

4.6.4 NMR miniemulsion kinetics.

To assign the resonances in the miniemulsion, separate miniemulsions of the surfactant (Fig. S4.12-1), both monomers (Fig. S4.12-2, S4.12-3) and their combination, including the initiator (Fig. S4.12-4), were prepared in DMSO-d_6 (not dried before) and cyclohexane-d_{12} and analyzed *via* ^{1}H NMR at a Bruker Avance III 700.

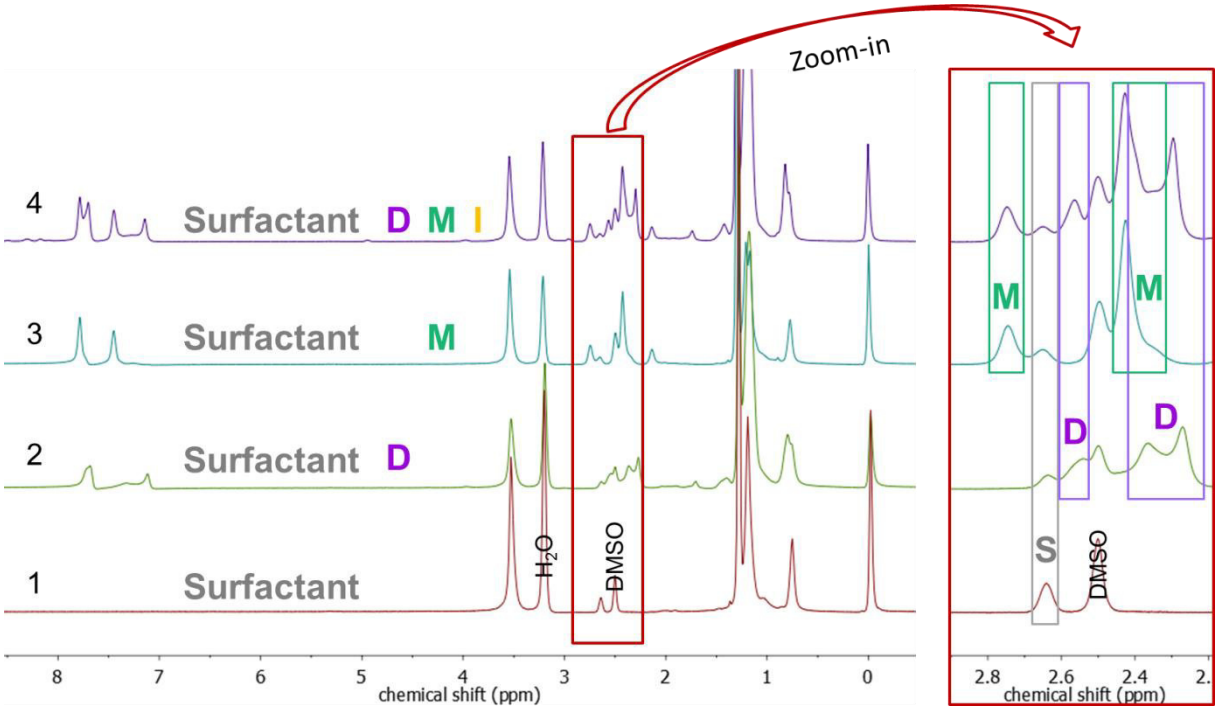

Figure S4.12. ^{1}H NMR (700 MHz, 323 K, DMSO-d_6) of miniemulsions. Identification of different peaks in the miniemulsions: Separate NMR-spectra with only surfactant (1, grey), both monomers separately (2, purple and 3, green) and a combination of the surfactant, both monomers and the initiator (4), including the zoom-in to the relevant monomer-signals.

Preparation of the miniemulsions for real-time NMR kinetics. All polymerizations were carried out in analogy to the conventional procedure in a Schlenk flask, here exemplarily for the polymerization of TsMAz (**1**) and TsDAz (**2**) and the initiator-system: PyNHMs (**3**), Potassium bis(trimethylsilyl)-amide (KHMDS) in a 1:4 DMSO-d_6:CyHexd_{12}-emulsion (wt.%), with P(B/E-*b*-EO) as a surfactant. Inside of a glovebox in a nitrogen-atmosphere 18.8 mg (89 µmol) of TsMAz (**1**) were dissolved in 220 µL DMSO-d_6, whereas the second monomer TsDAz (**2**) (30 mg, 89 µmol) and 8.4 mg surfactant (0.6 wt.% of cyclohexane) was dissolved in 1800 µL cyclohexane-d_{12}. The initiator-solution of 5.5 mg (0.5 µmol) PyNHMs (**3**) and 3.5 mg (0.5 µmol) KHMDS, in 1 mL DMSO-d_6 was prepared separately calculated for a monomer to initiator of $[M_1]_0$: $[M_2]_0$: $[I]_0$ = 50:50:1. From that stock solution 100 µL were added to the TsMAz-DMSO-d_6-solution, and directly added to the cyclohexane-mixture. After mixing both phases with the syringe several times, the solution were divided equally in two glass-vials, equipped with screw caps and directly homogenized using a Branson 450 W sonifier with an inverse cup tip (60 s, 20 s sonication, 10 s pause, 70% amplitude) at 4 °C. In case of higher dilutions, the respected amount of cyclohexane-d_{12} was added. Afterwards 1 mL of the sample was transferred inside of the glovebox into a conventional NMR-tube and sealed with a rubber-septum and quickly and inserted into the spectrometer. All ^{1}H NMR kinetics were recorded using a Bruker Avance III 700. All spectra were referenced internally to residual proton signals of the deuterated solvent dimethylsulfoxide-d_6 at 2.50 ppm. The π/2-pulse for the proton measurements was 13.1 µs. The spectra of the polymerizations were recorded at 700 MHz with 32 scans (equal to 404 s (acquisition time of 2.595 s and a relaxation time of 10 s after every pulse)) over a period of at least 3 h. No B-field optimizing routine was used over the kinetic measurement time. The spin-lattice relaxation rate (T1) of the ring-protons, which are used afterwards for integration, was measured before the kinetic run with the inversion recovery method.[35] Compared to NMR-kinetics in solution, all resonances of the emulsion lack a well-resolved microstructure, since the chemical environment is changed in the miniemulsion. At the interfaces of the droplets, the molecular mobility of stabilizing surfactant molecules is restricted, leading to residual dipolar couplings between nuclear spins. Moreover, local differences in the magnetic susceptibility between the surrounding solvent and the interior of the droplet lead to gradual changes of the outer magnetic field at the surface of the droplet. Both phenomena are observed in NMR spectroscopy as a broadening of the NMR signals. Nevertheless, as overlapping with solvents or surfactants was prevented, monitoring the monomer consumptions is possible.

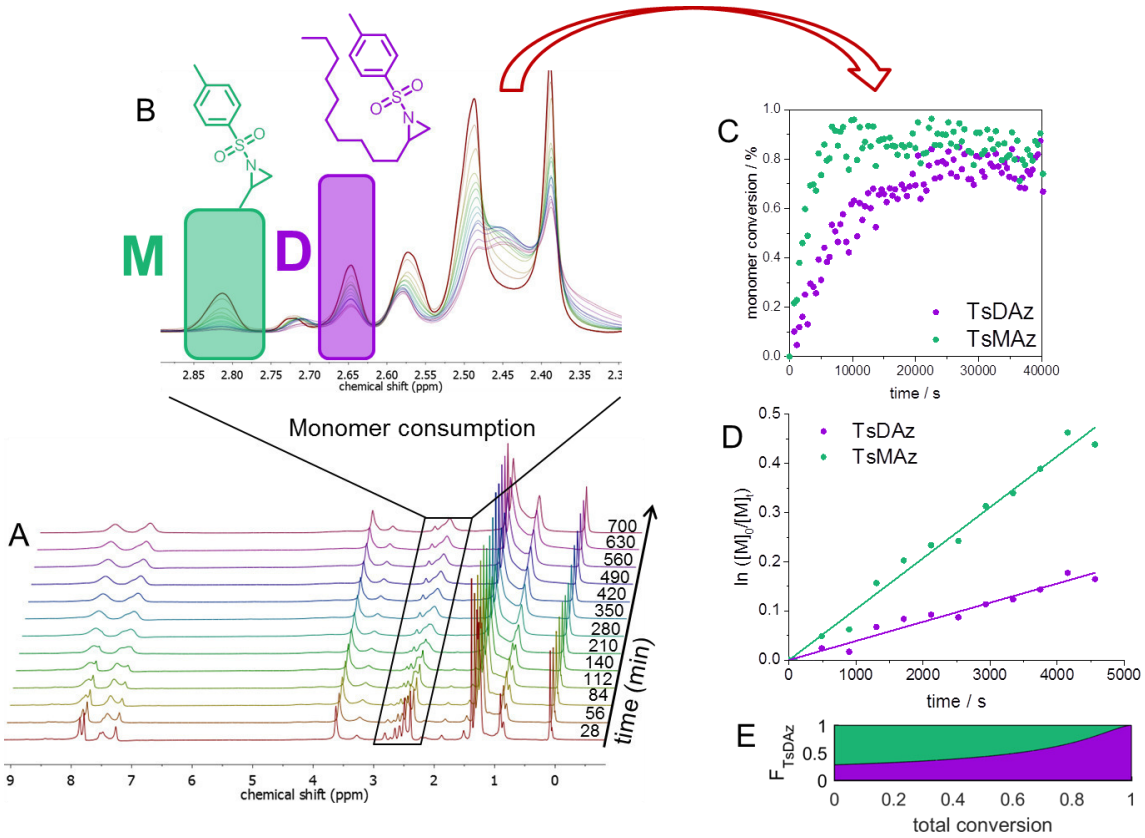

Figure S4.13. Anionic Copolymerization in emulsion: (A) Selection of ^{1}H NMR spectra of the azaanionic polymerization of TsMAz (1, M, green) and TsDAz (2, D, purple) in a 1:4 DMSO-d_6:CyHex-d_{12}-emulsion, at 50 °C. (B) Zoom-in of the relevant signals of the monomer ring-protons, showing the consumption of the monomer. (C) Monomer conversion *versus* reaction time. (D) Kinetic Plots of $\ln([M]_0/[M]_t)$ *vs.* time of TsMAz (1, M, green), TsDAz (2, D, purple). (E) Incorporation probability of TsDAz (F_{TsDAz}) *vs* total conversion.

Exemplary on the 1:4-miniemulsion, the NMR-kinetics are demonstrated: A spectrum was measured every 7 minutes, after every fourth spectrum, the NMR-tube was taken out of the device and shaken vigorously to ensure the homogenous distribution of the miniemulsion. As the monomer is consumed during the polymerization, the monomer signals disappear over time and simultaneously the growing polymer-backbone emerges between 3.5 to 4.5 ppm (Figure S4.13 A). From the separated monomer peaks (Figure S4.13 B) the monomer depletion was integrated over time, normalized to the unreacted monomer. Those data can be converted to assembly of the monomer in the polymer chain and it can be plotted against time (Figure S4.13 C). With those data at hand, propagation rates (k_p) can be evaluated, when plotting $\ln([M]_0/[M]_t)$ *versus* time of the first 11 spectra (Figure S4.13 D). This slope is equivalent to the apparent propagation rate (k_{app}), which, divided by the initiator-concentration, reveals the propagation rate (k_p). As shown below, also the final microstructure and the apparent r-parameters (r_{app}) can be calculated (for more detailed instructions of analyzing and calculating NMR-kinetics, compare previous published literature.[24-25, 29-31])

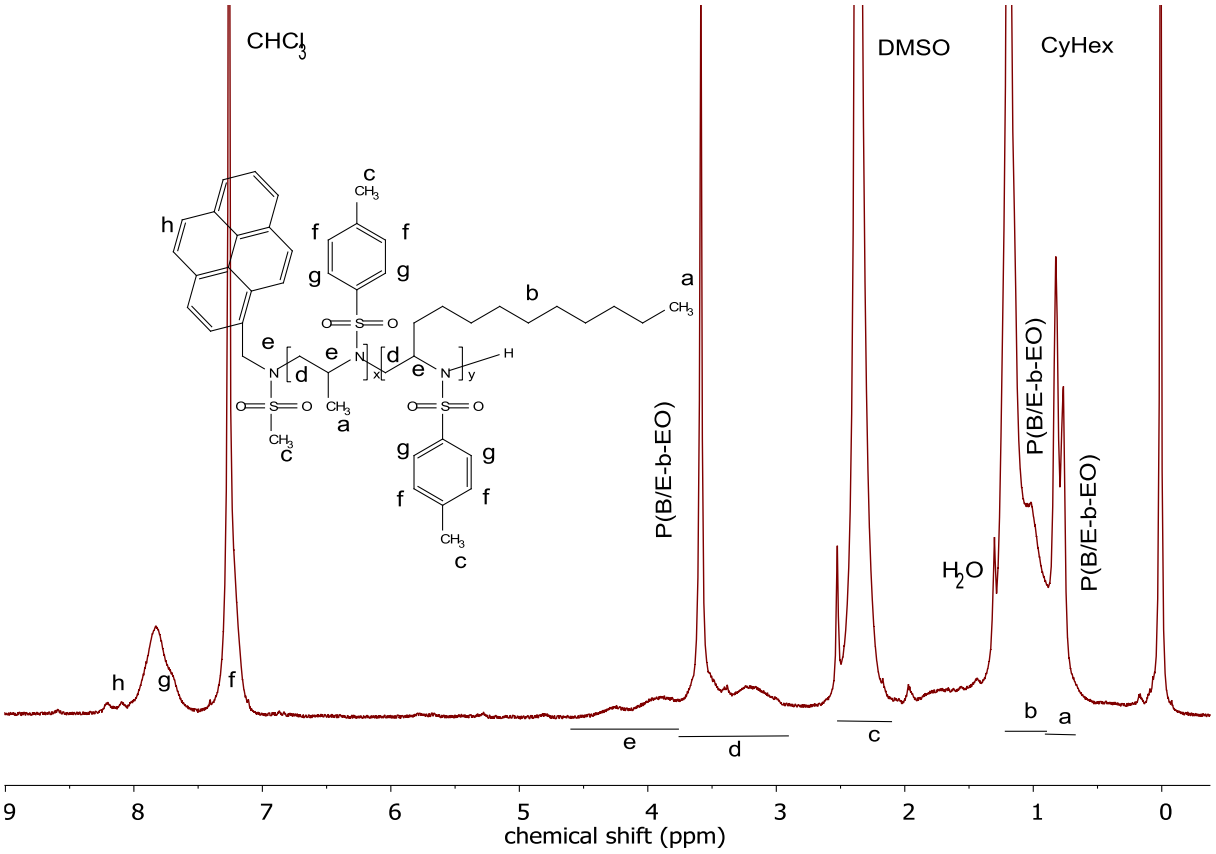

Figure S4.14. Final ^{1}H NMR (700 MHz, 298 K, chloroform-*d*) of Poly(TsMAz-*co*-TsDAz)-3 and surfactant from miniemulsion-kinetics.

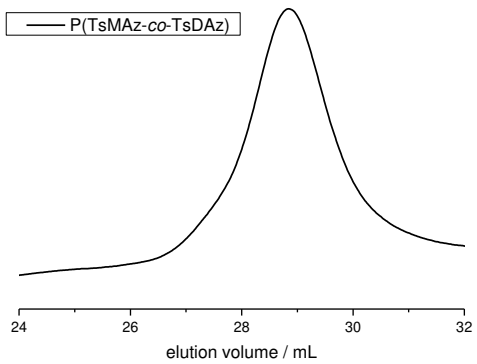

Figure S4.15. SEC traces of of Poly(TsMAz-*co*-TsDAz)-3 from NMR-kinetics in a 1:4 miniemulsion in DMF (RI signal).

Table S4.3. NMR kinetic data overview of the observation volume inside of the NMR-tube.

Solvent wt.% ratio (DMSO-d_6 : CyHex-d_{12})	**1:2**	**1:4**	**1:10**	**1:20**
c(Py) / µmol/µL	0.0058	0.0056	0.0058	0.0059
m(TsM) / mg	19.5	9.5	4.0	2.0
n(TsM) / µmol	92.3	45.0	19.0	10.0
c(TsM) in DMSO / mol/L	0.28	0.28	0.28	0.28
m(TsD) / mg	24.0	15.0	6.3	3.2
n(TsD) / µmol	71.1	45.0	18.0	10.0
c(TsD) in CyHex / mol/L	0.08	0.05	0.02	0.01
m(surfactant) / mg	6.4	4.4	1.9	0.9
V(DMSO) / µL	320	160	67	34
V(CH) / µL	900	900	945	968
k_p(TsM) / 10^{-3} L mol^{-1} s^{-1}	**49.5**	**507.5**	**380.2**	**330.3**
$r_{app,1}$(TsMAz)	**1.49**	**2.69**	**4.02**	**4.98**
k_p(TsD) / 10^{-3} L mol^{-1} s^{-1}	**33.3**	**188.5**	**94.6**	**66.3**
$r_{app,2}$(TsDAz)	**0.67**	**0.37**	**0.25**	**0.20**
$Đ^a$ (SEC)	1.20	1.16	1.12	1.18
$M_n{}^a$(SEC)	1500	3400	2800	2400

[a] number-average molecular weight and molecular weight dispersity determined via SEC in DMF (vs. PEO standards)

4.6.5 Partition coefficient.

From HPLC measurements, partition coefficients (log *P*-values, (log $P_{CyHex/DMSO}$ = log ($[M]_{CyHex}/[M]_{DMSO}$)) of the monomer-pair in DMSO and cyclohexane were calculated. The smaller the log *P* for the respective monomer, the more of this monomer is present in the DMSO phase and *vice versa*. In a 1:2-mixture of DMSO:CyHex the log *P* = -1.12, proving the preference of TsMAz for DMSO. When the dispersed phase is reduced to 1:20 (DMSO:CyHex), TsMAz still prefers the DMSO droplets (log *P* = -0.21), but almost 50% locates in the continuous phase due to the high dilution. Importantly, for TsDAz the opposite effect is expected with a positive log *P*, i.e. it prefers cyclohexane over DMSO, starting with a log *P* of 0.25 at a solvent-ratio of 1:2 up to a log *P*(TsDAz) = 1.23 at a solvent-ratio of 1:20, and thus TsDAz remains almost completely in the continuous phase – by such alterations the gradient structure of the copolymer can be controlled.

To determine the partition coefficient, TsMAz was dissolved in DMSO or DMF, TsDAz in cyclohexane in the same ratios as used for further emulsion-experiments (see Experimental Part). Those stock solutions were mixed in the respective weight-ratio of the solvents and diluted with more cyclohexane to examine different solvent ratios. The mixtures were stirred in closed vials for one hour at 50 °C (temperature of reaction). After about four hours of standing to get separated phases, the same amount (200 µL) were carefully taken of both phases and analyzed via HPLC. As the areas below the HPLC-graphs have a linear relationship to the amount of substance in the samples, the ratio of those areas can be related to each other (after multiplication with the concentration factor), to reveal the amount of monomer in both solvents and therefore to calculate the partition coefficient.

Table S4.4. Calculation of log *P* data to compare DMF and DMSO with cyclohexane.

Sample	Integral[1] (TsM)	Corrected area[2]	**log *P* (TsM)**	Area (TsD) [2]	Corrected area[2]	**log *P* (TsD)**
TsM+TsD **1:1** in **DMF**	5347	5347		3903	3903	
TsM+TsD **1:1** in CyHex	1171	1171	**-0.66**	1506	1506	**-0.41**
TsM+TsD **1:4** in **DMF**	13338	13338		6930	6930	
TsM+TsD **1:4** in CyHex	1509	6037	**-0.34**	2017	8067	**0.07**
TsM+TsD **1:1** in **DMSO**	5927	5927		3345	3345	
TsM+TsD **1:1** in CyHex	152	152	**-1.59**	2576	2576	**-0.11**
TsM+TsD **1:4** in **DMSO**	13531	13531		3740	3740	
TsM+TsD **1:4** in CyHex	340	1359	**-1.00**	2952	11806	**0.50**

[1] Integral value determined from the elugram. [2] Integral value corrected with the respective dilution factor.

Table S4.5. Calculation of log *P* data to compare different solvent ratios of DMSO and cyclohexane.

Sample	Integral[1] (TsM)	Corrected area[2]	**log *P* (TsM)**	Area (TsD) [2]	Corrected area[2]	**log *P* (TsD)**
TsM+TsD **1:2** in DMSO	4204	4204		1174	1174	
TsM+TsD **1:2** in CyHex	161	322	**-1.12**	1055	2110	**0.25**
TsM+TsD **1:4** in DMSO	4078	4078		896	896	
TsM+TsD **1:4** in CyHex	119	476	**-0.93**	732	2929	**0.51**
TsM+TsD **1:10** in DMSO	3681	3681		355	355	
TsM+TsD **1:10** in CyHex	119	1189	**-0.49**	285	2849	**0.91**
TsM+TsD **1:20** in DMSO	3049	3049		181	181	
TsM+TsD **1:20** in CyHex	95	1899	**-0.21**	153	3060	**1.23**

[1] Integral value determined from the elugram. [2] Integral value corrected with the respective dilution factor.

From those data also the amount of both monomers in the DMSO-phase and the dispersed phase in the beginning of the polymerization were calculated, which is identical to the initial composition of the final copolymer.

Table S4.6. Amount of monomer in the different solvents at different ratios.

Ratio solvents (DMSO/CyHex)	**1:2**	**1:4**	**1:10**	**1:20**
n(M) DMSO / µmol	83	80	67	55
n(M) CyHex / µmol	6	9	22	34
n(D) DMSO / µmol	32	21	10	5
n(D) CyHex / µmol	57	68	79	84

4.7 References

1. Eigen, M.; Winkler, R., *Steps towards life: a perspective on evolution*. Oxford University Press, Incorporated: **1992**.
2. Berg, J. M.; Tymoczko, J. L.; Stryer, L., *Biochemistry*. 8th ed.; WH Freeman: New York, **2015**.
3. Merrifield, R. B., *J. Am. Chem. Soc.* **1963,** *85* (14), 2149-2154.
4. Jasinski, F.; Teo, V. L.; Kuchel, R. P.; Mballa Mballa, M.; Thickett, S. C.; Brinkhuis, R. H. G.; Weaver, W.; Zetterlund, P. B., *Polym. Chem.* **2017,** *8* (3), 495-499.
5. Claussen, K. U.; Scheibel, T.; Schmidt, H. W.; Giesa, R., *Macromolecular Materials and Engineering* **2012,** *297* (10), 938-957.
6. Zetterlund, P. B.; Thickett, S. C.; Perrier, S.; Bourgeat-Lami, E.; Lansalot, M., *Chem. Rev.* **2015,** *115* (18), 9745-9800.
7. Truong, N. P.; Whittaker, M. R.; Anastasaki, A.; Haddleton, D. M.; Quinn, J. F.; Davis, T. P., *Polym. Chem.* **2016,** *7* (2), 430-440.
8. Gilbert, R. G., *Emulsion polymerization: a mechanistic approach*. Academic Pr: **1995**.
9. Thickett, S. C.; Gilbert, R. G., *Polymer* **2007,** *48* (24), 6965-6991.
10. Piradashvili, K.; Alexandrino, E. M.; Wurm, F. R.; Landfester, K., *Chem. Rev.* **2016,** *116* (4), 2141-2169.
11. Odian, G., *Principles of Polymerization*. 4. ed.; John Wiley & Sons, Inc. : Hoboken, New Jersey, USA, **2004**.
12. Ouchi, M.; Badi, N.; Lutz, J.-F.; Sawamoto, M., *Nature chemistry* **2011,** *3* (12), 917-924.
13. Lu, C.; Urban, M. W., *ACS Macro Letters* **2015,** *4* (12), 1317-1320.
14. Engelis, N. G.; Anastasaki, A.; Nurumbetov, G.; Truong, N. P.; Nikolaou, V.; Shegiwal, A.; Whittaker, M. R.; Davis, T. P.; Haddleton, D. M., *Nature chemistry* **2017,** *9* (2), 171-178.
15. Zetterlund, P. B.; Kagawa, Y.; Okubo, M., *Chem. Rev.* **2008,** *108* (9), 3747-3794.
16. Zetterlund, P. B.; Gody, G.; Perrier, S., *Macromolecular Theory and Simulations* **2014,** *23* (5), 331-339.
17. Tardy, A.; Bhullar, K. A.; Lim, D. Q.; Thickett, S. C.; Zetterlund, P. B., *J. Polym. Sci., Part A: Polym. Chem.* **2017**, *55* (9), 1590-1600.
18. Zetterlund, P. B., *Polymer Chemistry* **2011,** *2* (3), 534-549.
19. Carmean, R. N.; Figg, C. A.; Becker, T. E.; Sumerlin, B. S., *Angew. Chem. Int. Ed. Engl.* **2016,** *55* (30), 8624-8629.
20. Yamada, M.; Nishikawa, T.; Kanazawa, A.; Kanaoka, S.; Aoshima, S., *Journal of Polymer Science Part A: Polymer Chemistry* **2016,** *54* (17), 2656-2661.
21. Rieger, E.; Manhart, A.; Wurm, F. R., *ACS Macro Letters* **2016,** *5* (2), 195-198.
22. Homann-Müller, T.; Rieger, E.; Alkan, A.; Wurm, F. R., *Polym. Chem.* **2016,** *7* (35), 5501-5506.

23. Reisman, L.; Mbarushimana, C. P.; Cassidy, S. J.; Rupar, P. A., *ACS Macro Letters* **2016,** *5* (10), 1137-1140.
24. Rieger, E.; Alkan, A.; Manhart, A.; Wagner, M.; Wurm, F. R., *Macromol. Rapid Commun.* **2016,** *37* (10), 833-839.
25. Rieger, E.; Gleede, T.; Weber, K.; Manhart, A.; Wagner, M.; Wurm, F. R., *Polym. Chem.* **2017,** *8* (18), 2824-2832.
26. Fineman, M.; Ross, S. D., *Journal of Polymer Science* **1950,** *5* (2), 259-265.
27. Kelen, T.; Tüdös, F., *Journal of Macromolecular Science: Part A - Chemistry* **1975,** *9* (1), 1-27.
28. Mayo, F. R.; Lewis, F. M., *Journal of the American Chemical Society* **1944,** *66* (9), 1594-1601.
29. Skeist, I., *J. Am. Chem. Soc.* **1946,** *68*, 1781-1784.
30. Wall, F. T., *J. Am. Chem. Soc.* **1946,** *63*, 1862-1866.
31. Jaacks, V. V., *Die Makromolekulare Chemie* **1967,** *105* (1), 289-291.
32. Blankenburg, J.; Wagner, M.; Frey, H., *Macromolecules* **2017,** *50* (22), 8885-8893.
33. Stewart, I. C.; Lee, C. C.; Bergman, R. G.; Toste, F. D., *Journal of the American Chemical Society* **2005,** *127* (50), 17616-17617.
34. Schlaad, H.; Kukula, H.; Rudloff, J.; Below, I., *Macromolecules* **2001,** *34* (13), 4302-4304.
35. Freeman, R.; Hill, H. D. W.; Kaptein, R., *J. Magn. Reson.* **1972,** *7*, 327-329.

5. Multihydroxy-Polyamines by Living Anionic Polymerization of Aziridines

Elisabeth Rieger, Angelika Manhart, Frederik R. Wurm

Max Planck Institute for Polymer Research, Ackermannweg 10, 55128 Mainz, Germany

Reproduced with permission from "*ACS Macro Lett.* **2016**, *5 (2)*, 195-198". Copyright 2016, published by American Chemical Society.

The monomer syntheses and parts of the polymerizations and postmodifications were performed by Angelika Manhart.

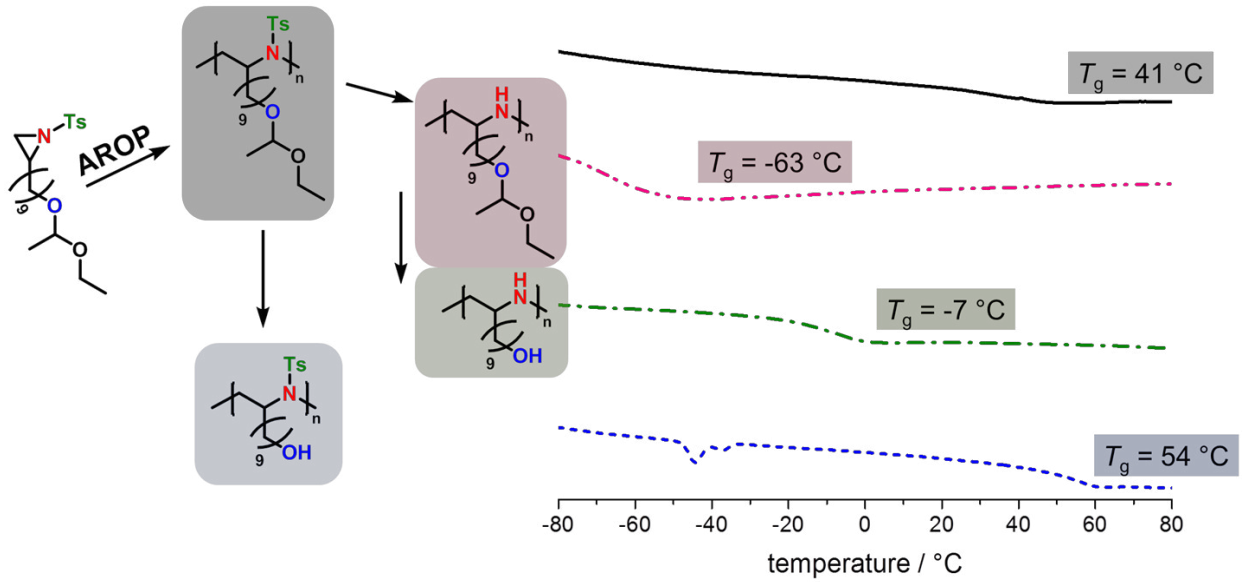

Keywords: Anionic Polymerization, Aziridine, Sulfonamide, Ring-Opening Polymerization, Azaanionic Polymerization.

5.1 Abstract

Acetal-protected and sulfonamide-activated aziridines (Az) have been prepared and polymerized by living anionic polymerization with molecular weight dispersities in most cases below $Đ < 1.2$ and controlled molecular weights. Three new monomers have been prepared varying in the length of the pendant chain. The resulting double protected polymers can be selectively deprotected in order to release the polyamine or the polyol structures. Detailed structural characterization was performed for all polymers, chain extension proves their living polymerization behavior and the formation of block copolymers. Thermal analysis can be used in order to follow the deprotection steps. These new protected monomers broaden the scope of the azaanionic polymerization of aziridines and may find useful applications as well-defined functional poly(ethylene imine) derivatives.

5.2 Introduction

After 60 years of its discovery, living anionic polymerization (LAP) is still the polymerization technique with the highest control over molecular weight and distribution, highest precision for the synthesis of block copolymers, end-functionalized polymers and other well-defined architectures.[1-4] Besides the classic vinyl- and acrylate-monomers, also anionic ring-opening (AROP) strategies for epoxides are standard procedures today.[4-6] Due to the high reactivity of the living anion towards most functional (electrophilic) groups, protective groups are common in LAP to generate (poly)functional materials.[7] In the last years linear polyglycerol (linPG) as a multifunctional analogue of poly(ethylene glycol) (PEG) gathered a lot of attention in the biomedical field. It is accessible by AROP of several protected glycidyl ethers.[8] Especially the acetal-protected ethoxy ethyl glycidyl ether (EEGE), which was developed already in 1987,[9] became a standard monomer for oxyanionic polymerization today (cf. Figure 5.1).[6, 8, 10-11]

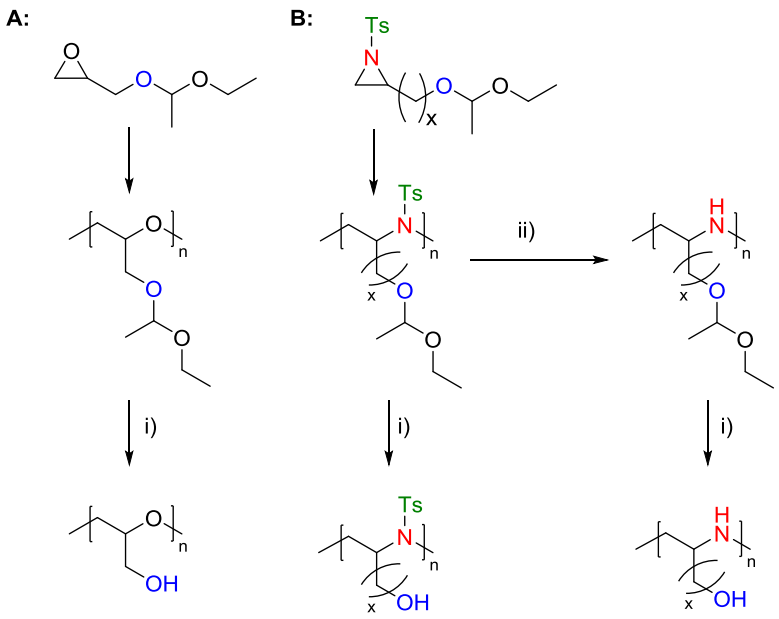

Figure 5.1. Synthesis of A: linear poly(glycerol) by anionic polymerization of ethoxy ethyl glycidyl ether with subsequent acidic hydrolysis. B: Acetal-protected poly(sulfonamide)s and selective deprotection (i) diluted HCl, ii) Red-Al, x = 1,2,9, Ts = *p*-toluenesulfonyl).

Poly(ethylene imine)-derivatives are an important gene transfection agent today, which are only available by uncontrolled cationic polymerization of aziridine or living cationic polymerization of oxazolines with subsequent hydrolysis.[12-14] The ring-opening of aziridine derivatives is attractive as it allows direct access to branched polymers or materials functionalized at the nitrogen.[15-17] The synthesis of well-defined poly(ethylene imine)-derivatives by anionic polymerization carrying additional functional groups has not been accomplished to date.

Herein, we present the first acetal-protected and sulfonamide-activated aziridines for the living azaanionic polymerization. These monomers can be regarded as aziridine-analogues of EEGE and double-protected precursors to polyhydroxyl-PEI-derivatives. *N*-sulfonyl aziridines represent a rather new monomer class for the AROP. To date, mainly the uncontrolled cationic polymerization of various aziridines is used for synthesis of polyamines and -imines. The anionic polymerization of aziridines, however, is not found in textbooks. It was a single report by the group of Toste,[18] showing the feasibility of the AROP of sulfonamide-activated aziridines. Our group has recently expanded the family of sulfonyl aziridines for the termination of carbanionic polymerization or the synthesis of polyvinyl poly(aziridine) (PAz).[19-20] The general “trick” for enabling anionic ROP is to activate the aziridine ring for other nucleophiles. This can be achieved by amidation at the ring-nitrogen with electron withdrawing substituents, such as tosyl- or mesyl-groups. These electron deficient aziridines can be ring-opened by strong nucleophiles and allow the polymerization of a variety of substituted aziridines mostly in a living manner to produce

poly(aziridine)s (PAz – the abbreviation PAz is used herein to differentiate their origin from the typically polyamines made by cationic polymerization, such as poly(ethylene imine) (PEI)).[19-20]

5.3 Results and Discussion

In this paper a family of double-protected aziridines (**1**, **2**, **3**, Scheme 1) is synthesized and polymerized by LAP. The resulting acetal- and sulfonamide-protected polymers can be selectively and/or consecutively treated to release either hydroxyl- or amine-groups (Figure 5.1).

A new class of bifunctional aziridines has been designed that can be synthesized by a convenient two-step protocol: the first step is the aziridination of the double bond in an α-hydroxy-ω-alkene via the bromine-catalyzed addition of chloramine-T (Scheme 5.1a).[21] The alcohol is then protected by the reaction with ethyl vinyl ether to introduce the ethoxy ethyl group (Scheme 5.1b).[9]

Three novel monomers with varying side chain lengths have been synthesized: 2-((1-**e**thoxy**e**thoxy)**m**ethyl)-*N*-**t**o**s**yl**az**iridine (MEETsAz, **1**), 2-((1-**e**thoxy**e**thoxy)**e**thyl)-*N*-**t**o**s**yl**az**iridine (EEETsAz, **2**) and 2-((1-**e**thoxy**e**thoxy)**n**onyl)-*N*-**t**o**s**yl**az**iridine (NEETsAz, **3**), (Scheme 5.1).

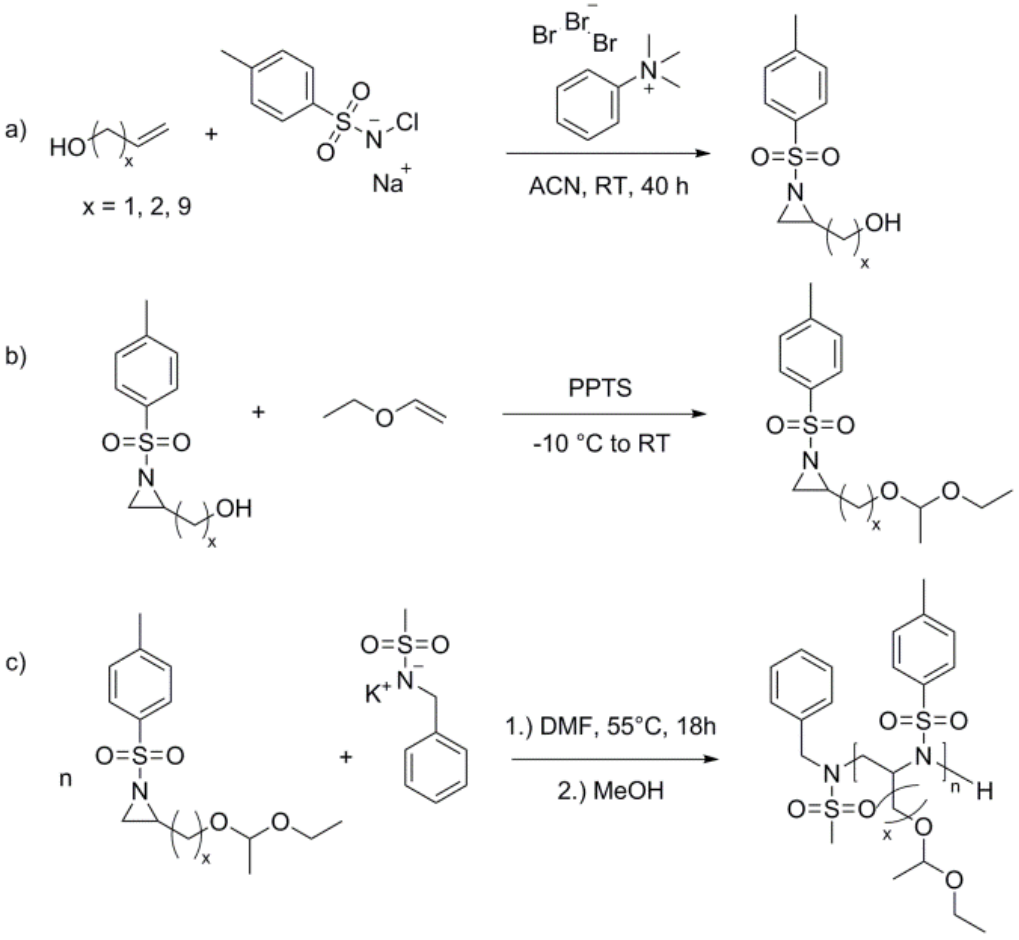

Scheme 5.1. Synthesis of the acetal-protected, sulfonamide-activated aziridines: (a) aziridination of α-hydroxy-ω-alkenes; (b) acetalization; (ACN = acetonitrile, PPTS = Pyridinium *p*-toluene-sulfonate) (c) Anionic polymerization of acetal-protected, sulfonamide-activated aziridines.

High purity of the monomers was achieved after thorough chromatographic purification, which was verified by ^{1}H and ^{13}C NMR spectroscopy. In Figure 5.2 the ^{1}H NMR spectrum of **3** is shown exemplarily (the spectra for **1** and **2** are to be seen in the Supporting Information). The characteristic resonances of the three protons at the substituted aziridine-ring are detectable as a multiplet (f) at 2.78-2.65 ppm for the methine and two doublets at 2.63 ppm (e) and 2.05 ppm (c) for the methylene protons. Furthermore the resonances (g) with a multiplet at ca. 3.76-3.33 ppm and (h) with a quartet at 4.68 ppm can be assigned to the methylene-groups next to the oxygen center in the ethoxy ethyl protection groups. All other resonances can be assigned as indicated in Figure 5.2.

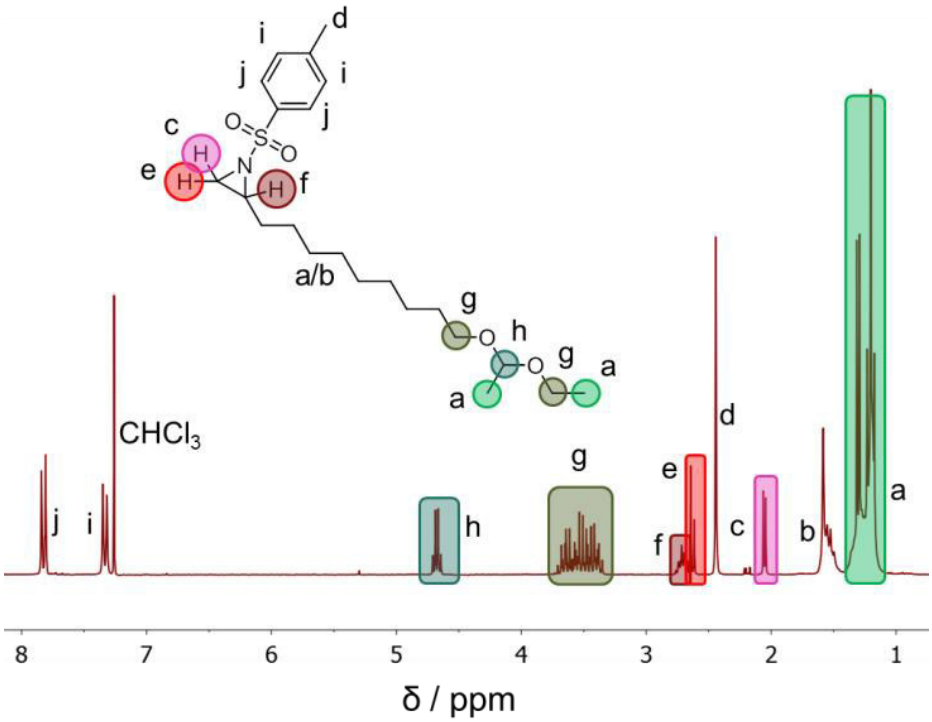

Figure 5.2. ^{1}H NMR ($CDCl_3$, 250 MHz, 298K) of 2-((1-ethoxyethoxy)nonyl)-*N*-tosylaziridine (**3**).

All monomers were successfully polymerized at 55 °C in dry DMF over a period of 18 h with full conversion. The initiator was generated by deprotonation of *N*-benzyl methanesulfonamide (BnNHMs) with bis(trimethyl-silyl)amide (KHMDS) prior to the addition of the monomer (Scheme 5.1). KHMDS can also be used as initiator itself, however, initiation kinetics are not optimal (data not shown). The living polymerizations – with the typical yellow/orange color of the azaanion – were terminated by the addition of degassed methanol and then precipitated into methanol.

Table 5.1. Characterization data for all polymers and all deprotected polymers.

	M_n[a]	M_n[b]	M_w/M_n[b]	T_g / °C[c]
P1-1	9200	2200	1.23	+61
P1-2	15100	3700	1.18	n.d.
P1-3	10200	2800	1.19	n.d.
P1-4	12300	5000	1.25	n.d.
P1-1-OH	7000	2300	1.25	+132
P2-1	9600	2900	1.09	+79
P2-2	15900	6400	1.10	+78
P2-3	15900	4600	1.12	n.d.
P2-4	15900	3700	1.12	n.d.
P2-3-OH	12300	5100	1.15	+92
P3-1	6400	1700	1.18	+41
P3-2	6400	1400	1.14	n.d.
P3-2-OH	13600	2000	1.20	+54
P3-3	6400	2300	1.15	n.d.
P3-4	6400	2600	1.17	n.d.
P3-4-NH	4100	700	1.53	-63
P3-4-NH-OH	3000	900	2.01	-7

[a]Theoretical number-average molecular weight (in g/mol).
[b]Number-average molecular weight and molecular weight dispersity determined via SEC in DMF (*vs.* PEO standards).
[c]Glass transition temperature determined via DSC.

All polymers were characterized by ^{1}H NMR spectroscopy, size exclusion chromatography (SEC) and differential scanning calorimetry (DSC) (see Table 5.1, all details are listed in the Supporting Information). The SEC elugrams of all polymers exhibit a monomodal and narrow molecular weight distribution with $M_w/M_n < 1.25$ in all cases, indicating a living mechanism under the applied conditions as reported for other sulfonyl-aziridines.[19-20] To prove the living character, chain extension experiments were performed, using the monomers **1** and **3** as first block. After 13 h, monomer **1** was added to both reactions. ^{1}H NMR and SEC-data demonstrate the increasing molecular weight of P1-4(**1**+**1**) and P4(**3**+**1**), including the successful formation of the blockcopolymer P4 (cf. Figures S5.33-S5.36). In addition, the polymerization kinetics of **1** with two different initiators (BnNHMs and 1-pyrenemethylmethane-sulfonamide (PyNHMs)) were studied to prove the high control over the molecular weight distribution (see Supporting

information for all data). Figure S5.28 and S5.31 show the plots of $\ln([M]_0/[M])$ *versus* time, both (P1-2 and P1-3) reveal a linear behavior for a living polymerization. In Figure S5.27 and S5.30 the plots of the number average molecular weight (M_n) *versus* conversion are shown, also increasing linearly. Both data-sets indicate a constant concentration of the growing chains, thus a living character of the polymerizations.

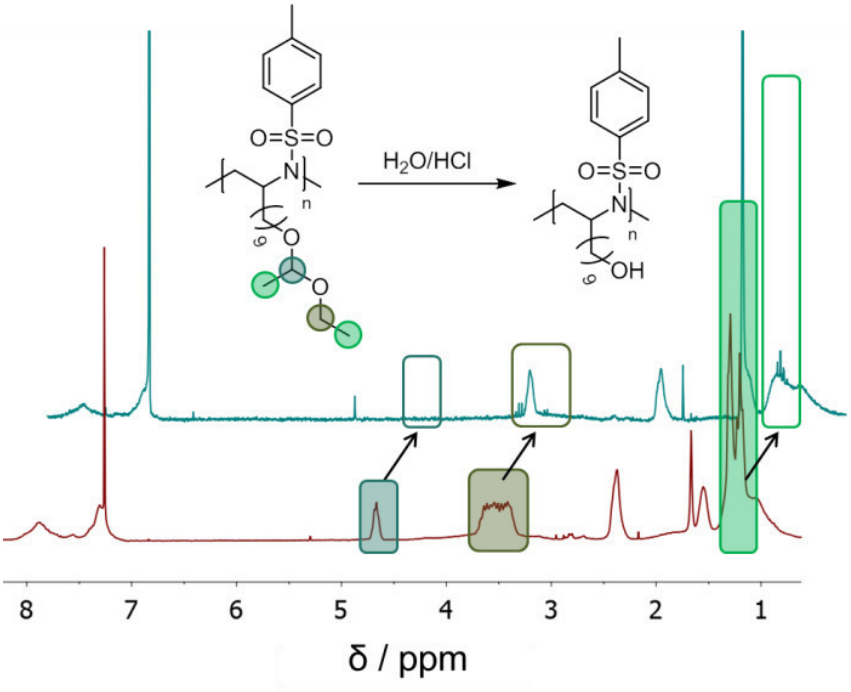

Figure 5.3. ^{1}H NMR ($CDCl_3$, 250 MHz, 298K) of poly(2-((1-ethoxyethoxy)nonyl)-*N*-tosylaziridine) (P3-2) and poly(*N*-tosyl-2-aziridinenonanol) (P3-2-OH).

In Figure 5.3 the ^{1}H NMR spectrum of **P3-2** is depicted as a representative example. All signals are detected as broad polymer resonances, the aziridines-ring resonances disappear and turned into the backbone of the polymer (4.38-2.72 ppm). The two methylene-groups of the acetal-protected side chain overlap with these signals and cannot be differentiated exactly (3.74-3.29 ppm). The broad signal between 1.45-0.61 ppm can be attributed to the two methyl-groups of the acetal-substituent and to the alkyl side-chain, whereas the methyl-group of the tosyl-substituent evolves at signal (2.53-2.23 ppm).

To release the pendant hydroxyl-groups, the polymer was dissolved in ethanol and stirred with concentrated hydrochloric acid at 70 °C overnight. As an example for this reaction, both ^{1}H NMR spectra of the polymer protected P3-2 and the P3-2-OH are shown in Figure 5.3. After the acidic hydrolysis, no acetal-protons are detectable in the characteristic regions (highlighted in green) proving quantitative hydrolysis and release of the hydroxyl groups (equal to the degree of polymerization).

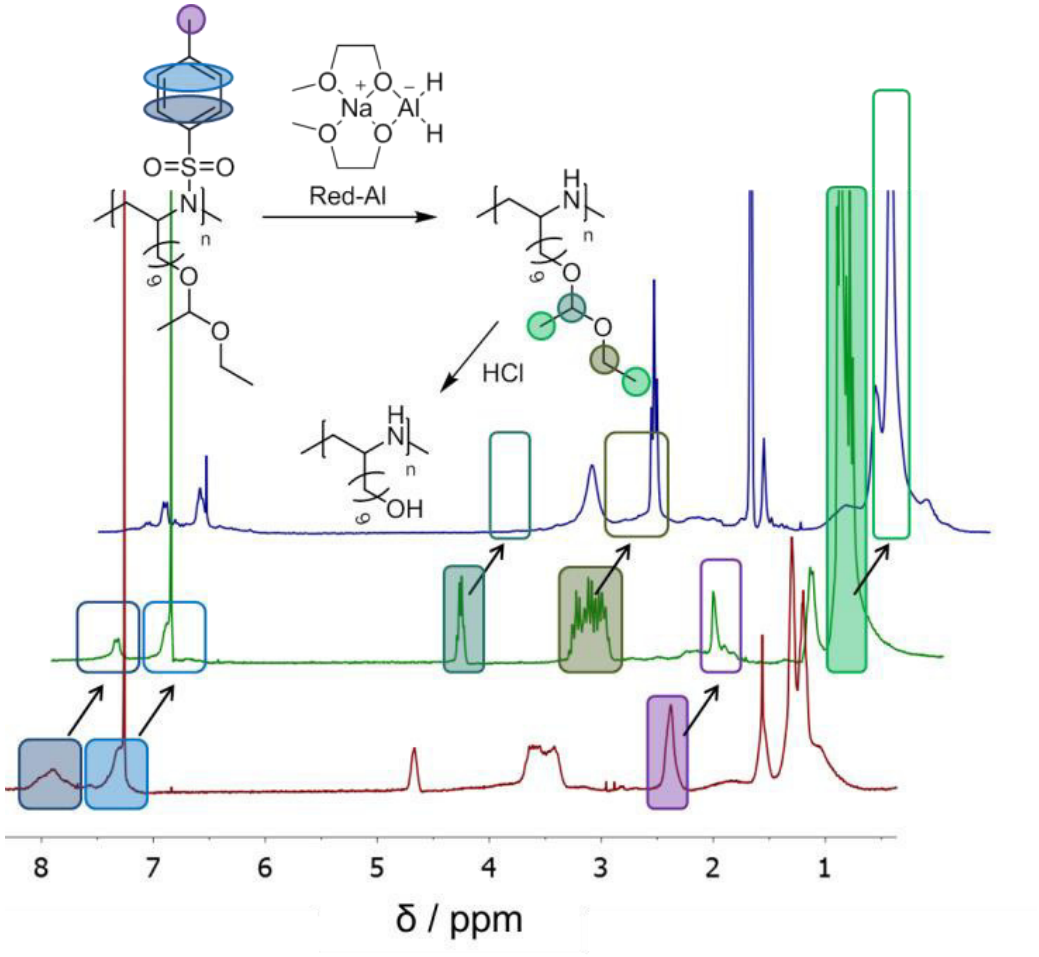

Figure 5.4. ^{1}H NMR ($CDCl_3$, 250 MHz, 298 K) of poly(2-((1-ethoxyethoxy)nonyl)-*N*-tosylaziridine) (P3-4), poly(2-((1-ethoxy-ethoxy)nonyl)-aziridine) (P3-4-NH) and poly(2-aziridinenonanol) (P3-4-NH-OH).

After the hydrolysis of the acetals, all polymers retained their narrow molecular weight distributions, however, the apparent molecular weights of most polyhydroxy-sulfonamides from SEC shifted to higher values, i.e. to lower elution times (Figures S5.12, S5.18 and S5.20). This is attributed to the change in polarity of the polyols. No change in the molecular weight dispersity excludes possible side reactions in analogy to PEEGE.[22]

As SEC is a relative method, no absolute molecular weights were determined and all molecular weights are apparent *vs.* PEG standards. Presumably, the hydrodynamic radius of PAz is smaller than PEG in DMF due to the higher hydrophobicity. Compared to the theoretical molecular weight (compare Table 5.1), a living polymerization mechanism and full monomer conversion, the absolute molecular weight should be higher than measured in SEC under these conditions.[20] For the chain extension experiments PyNHMs was employed as the initiator allowing NMR end group analysis for molecular weight determination. These polymers exhibit molecular weights two to three times higher compared to the apparent SEC values. The molecular weight

of P1-4 was about 14400 g/mol, compared to 5000 g/mol (SEC-analysis) (more data is shown in the Supporting Information). Herein, polymers with molecular weights (SEC-data) between 1700 and 6400 g/mol were synthesized, but this should not be regarded as an upper limit.

The sulfonamide groups along the polymer backbone were removed by treatment of the acetal-protected polymers with sodium bis(2-methoxyethoxy)aluminum hydride. Under these conditions ca. 76% of the amino groups can be released (compare Figures 5.4 and S5.23, S5.24) Subsequent treatment of these polymers with hydrochloric acid releases also the pendant hydroxyl groups. For both deprotection steps the NMR spectra prove successful reaction, however, SEC traces reveal a broadening in the molecular weight dispersity. This is, however, probably attributed to interactions of the polyamine with the column material under the applied conditions, which was reported earlier for amine-containing polyethers.[23] We do not claim, that no chain scission occurs during the relatively harsh deprotection step. Nevertheless, diffusion-ordered (DOSY) ^{1}H NMR-data of P3-4-NH and P3-4-NH-OH (see Fig S5.23b and S5.25b) show that all ^{1}H NMR resonances can be assigned to the same diffusion signal, proving the existence of an intact polymer-chain.

All polymers are amorphous materials, showing glass transition temperatures (T_g) between ca. 40 and 80 °C in the protected form (determined by DSC-measurements: T_g(P1) = 61 °C, T_g(P2-1) = 79 °C, T_g(P3-1) = 41 °C) independent of the molecular weights synthesized herein. After deprotection of the acetals, all hydroxyl-functional polymers showed higher T_g than the starting compounds (T_g(P1-OH) = 132 °C, T_g(P2-3-OH) = 92 °C, T_g(P3-2-OH) = 54 °C). When the sulfonamide was removed first, the polyamine (with acetals) showed a glass transition temperature of T_g(P3-4-NH) = -63 °C, which increased after the acetal deprotection to T_g(P3-4-NH-OH) = -7 °C.

5.4 Summary

In summary, the first azaanionic polymerization of acetal-protected, sulfonamide-activated aziridines is presented. A convenient protocol for the two-step synthesis of three novel monomers was established. All monomers were polymerized to well-defined homopolymers and exhibited full conversions with narrow molecular weight distributions ($Đ \leq 1.25$). The ethoxy ethyl protecting group can be conveniently removed, yielding linear polysulfonamides with free hydroxyl groups in every repeating unit. Also, subsequent deprotection of the sulfonamides and the acetal-groups proved to be possible rendering these materials as highly interesting for novel polyelectrolytes, which are compatible with conventional anionic polymerization setups, for example.

5.5 Acknowledgments

F.R.W. thanks the Deutsche Forschungsgemeinschaft (DFG WU 750/7-1) for funding. The authors thank Prof. Dr. Katharina Landfester for continuous support and BMBF/MPG network MaxSynBio.

5.6 Supporting Information

The Supporting Information contains additional synthetic procedures, characterization data for monomers, polymers and kinetic measurements.

Content

5.6.1 Materials and Methods.

Materials.

All chemicals were purchased from common suppliers (Acros, Fisher Scientific, Fluka, Roth, Sigma-Aldrich, TCI Europe) and used without further purification unless stated otherwise. Deuterated solvents were purchased from Deutero GmbH (Kastellaun, Germany) and stored over molecular sieves. *N*-benzyl-mesylamide (BnNHMs) and 1-pyrenemethylmethanesulfonamide (PyNHMs) were synthesized according to literature.[18,24]

Instrumentation and Characterization Techniques.

NMR. ^{1}H NMR and ^{13}C NMR spectra were recorded using a Bruker Avance III 250, a Bruker Avance 300, a Bruker Avance III 500, a Bruker Avance III 700. All spectra were referenced internally to residual proton signals of the deuterated solvent.

SEC. For SEC measurements in DMF (containing 0.25 g/L of lithium bromide as an additive) an Agilent 1100 Series was used as an integrated instrument, including a PSS HEMA column (106/105/104 g/mol), a UV detector (275 nm), and a RI detector at a flow rate of 1 mL/min at 50 °C. Calibration was carried out using PEO standards provided by Polymer Standards Service.

DSC. DSC measurements were performed using a Mettler Toledo DSC 823 calorimeter. Three scanning cycles of heating-cooling were performed in the temperature range from −140 to 250 °C. Heating rates of 10 °C/min were employed under nitrogen (30 mL/min).

5.6.2 Monomer Syntheses.

N-tosyl-2-aziridinemethanol (MOTsAz)

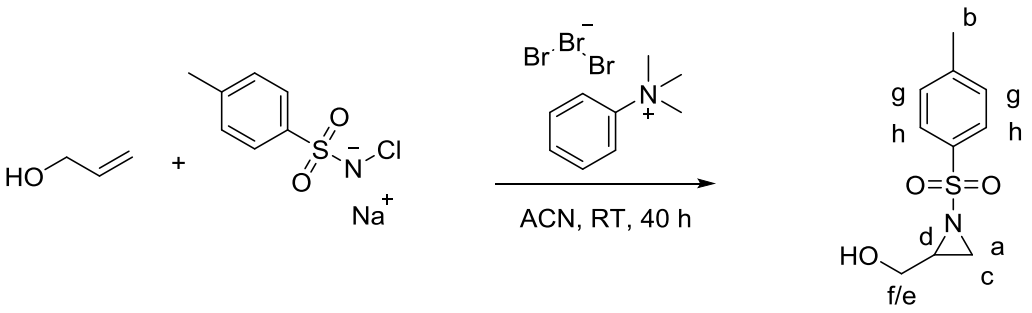

The compound was synthesized according to literature procedures.[21] Chloramine-T (9.0 g, 39.5 mmol) was dried by azeotropic distillation with benzene *in vacuo* for 6 h and at 90 °C for additional 8 h. The anhydrous chloramine-T and 3-propenol (6.65 mL, 119 mmol) were dissolved in anhydrous acetonitrile (ACN) (100 mL). Phenyltrimethylammonium tribromide (PTAB) (3.6 g, 11.8 mmol), dissolved in ACN (100 mL) was added and the mixture was stirred at room temperature for 40 hours. Ethyl acetate (40 mL) and deionized water (40 mL) were added. After washing with brine, the organic phases were combined, dried over magnesium sulfate and concentrated at reduced pressure. Chromatography over silica gel (dichloromethane/diethyl ether 2:1) yielded the product as a colorless oily liquid (4.5 g, 19.6 mmol, 19%).

^{1}H NMR (250 MHz, 298 K, chloroform-*d*): δ 7.91 – 7.78 (m, 2H, h), 7.44 – 7.31 (m, 2H, g), 3.87 (dd, *J* = 12.5, 3.2 Hz, 1H,f), 3.64 – 3.42 (m, 1H, e), 3.12 – 2.95 (m, 1H, d), 2.64 (d, *J* = 7.1 Hz, 1H, c), 2.46 (s, 3H, b), 2.33 (d, *J* = 4.6 Hz, 1H, a).

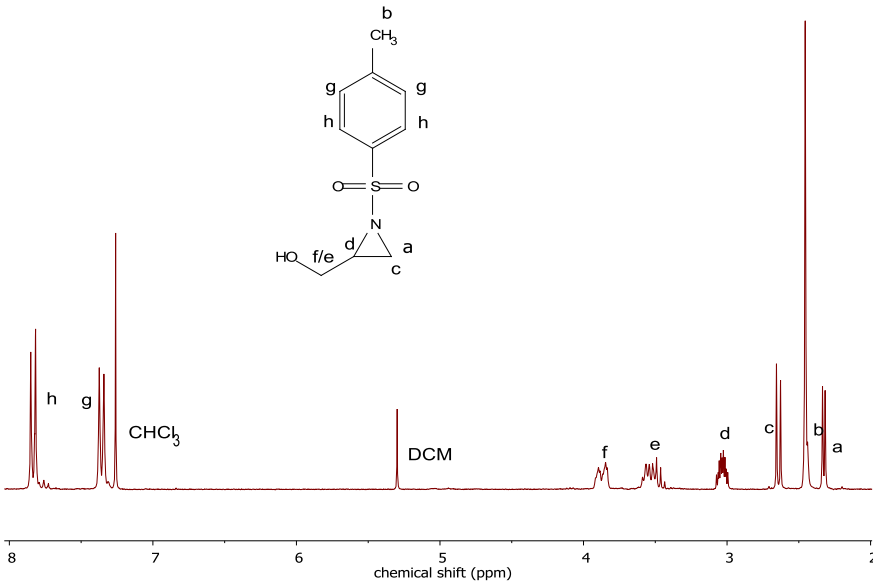

Figure S5.1. ^{1}H NMR (250 MHz, 298 K, $CDCl_3$) of *N*-tosyl-2-aziridinemethanol (MOTsAz).

2-((1-Ethoxyethoxy)methyl)-N-tosylaziridine (MEETsAz)

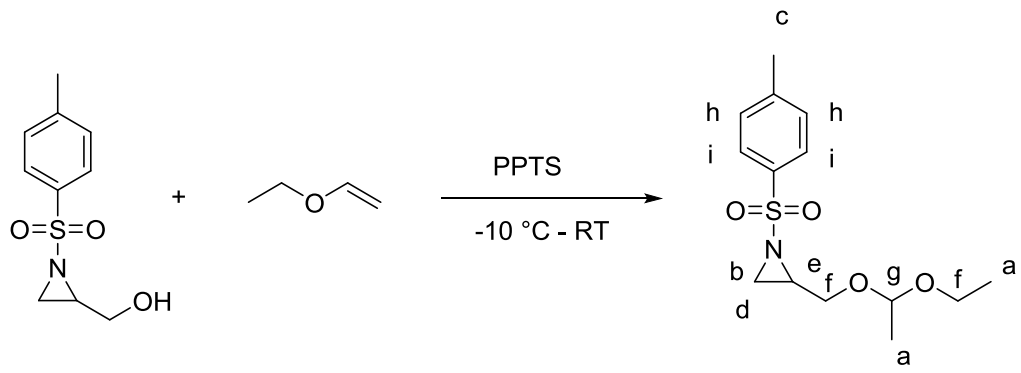

N-tosyl-2-aziridinemethanol (MOTsAz) (1.75 g, 7.7 mmol) was dissolved in 10 mL freshly distilled ethyl vinyl ether. The solution was cooled to -10 °C and 39 mg (0.15 mmol) of pyridinium *p*-toluenesulfonate were added. The mixture was stirred overnight and allowed to reach room temperature. After adding a small amount of potassium carbonate, the excess of ethyl vinyl ether was removed at reduced pressure. Chromatography over silica gel (ethyl acetate/petroleum ether 1:3) yielded the product as a colorless oily liquid (1.4 g, 4.68 mmol, 61%).

^{1}H NMR (250 MHz, 298 K, chloroform-*d*): δ 7.91 – 7.75 (m, 2H, i), 7.42 – 7.29 (m, 2H, h), 4.63 (dq, *J* = 7.2, 5.4 Hz, 1H, g), 3.68 – 3.25 (m, 4H, f), 3.06 – 2.89 (m, 1H, e), 2.66 (dd, *J* = 7.1, 2.1 Hz, 1H, d), 2.44 (s, 3H, c), 2.21 (dd, *J* = 10.5, 4.5 Hz, 1H, b), 1.31 – 1.04 (m, 6H, a).

^{13}C NMR (176 MHz, 298 K, chloroform-*d*): δ 144.56, 144.53, 134.96, 134.93, 129.62, 128.07, 128.02, 99.35, 99.28, 63.73, 63.29, 60.81, 60.70, 39.13, 38.83, 31.12, 30.86, 21.62, 19.53, 19.46, 15.21.

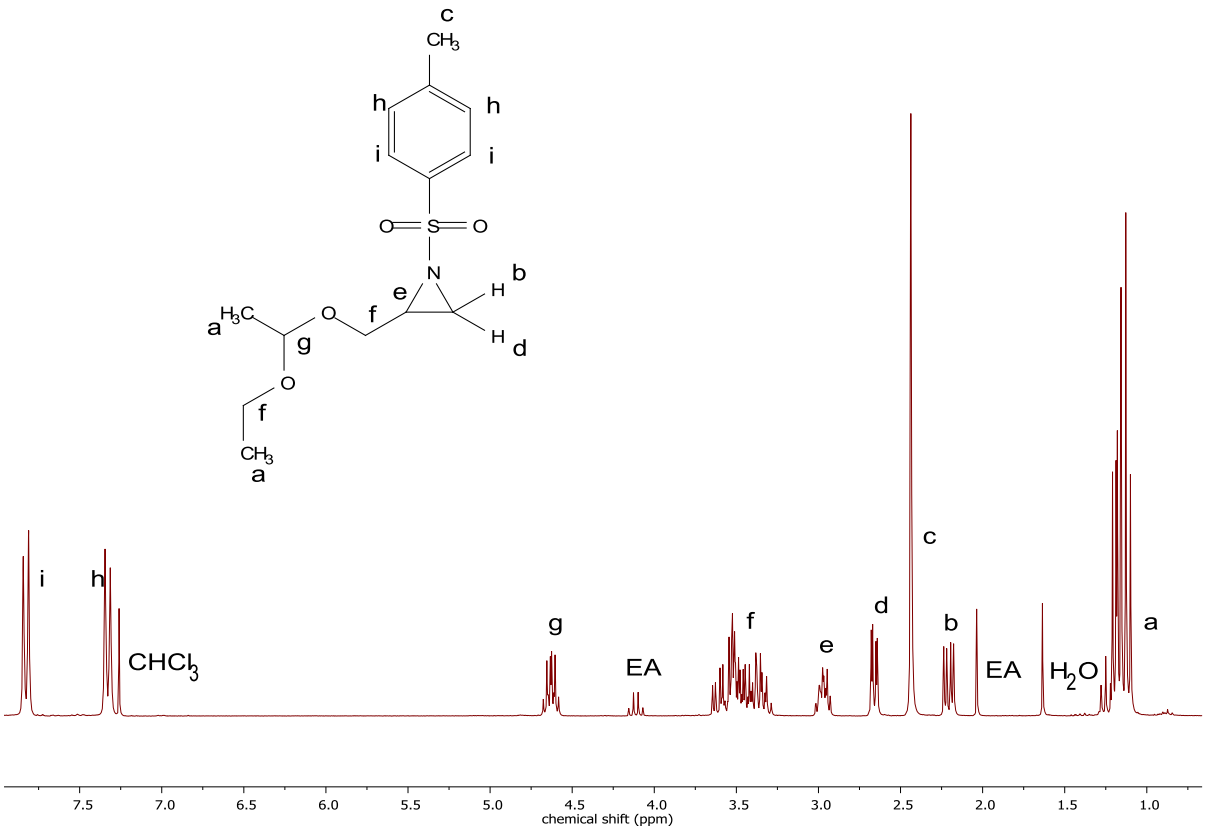

Figure S5.2. ^{1}H NMR (250 MHz, 298 K, $CDCl_3$) of 2-((1-ethoxyethoxy)methyl)-*N*-tosylaziridine (MEETsAz).

N-tosyl-2-aziridineethanol (EOTsAz)

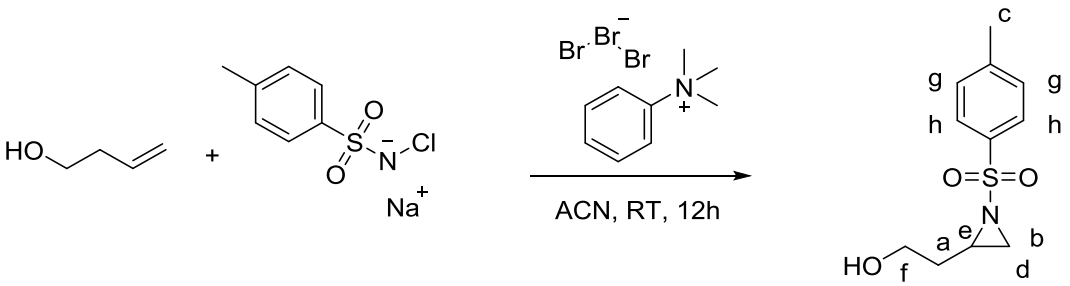

Chloramine-T (3.8 g, 16.6 mmol) was dried by azeotropic distillation with benzene *in vacuo* for 6 h and at 90 °C for additional 8 h. The anhydrous chloramine-T and but-3-en-1-ol (3.34 mL, 39.5 mmol) were dissolved in anhydrous acetonitrile (ACN) (50 mL). Phenyltrimethylammonium tribromide (PTAB) (1.48 g, 3.9 mmol), dissolved in ACN (50 mL) was added and the mixture was stirred at room temperature overnight. Ethyl acetate (40 mL) and deionized water (40 mL) were added. After washing with brine, the organic phases were combined, dried over magnesium sulfate and concentrated at reduced pressure. Chromatography over silica gel (dichloromethane/diethyl ether 2:1) yielded the product as a colorless oily liquid (1.65 g, 6.8 mmol, 17%).

^{1}H NMR (250 MHz, 298 K, chloroform-*d*): δ 7.90 – 7.76 (m, 2H, h), 7.43 – 7.29 (m, 2H, g), 3.81 – 3.54 (m, 2H, f), 3.00 - 2.85 (m, 1H, e), 2.65 (d, *J* = 7.1 Hz, 1H, d), 2.45 (s, 3H, c), 2.15 (d, *J* = 4.6 Hz, 1H, b), 2.09 - 1.90 (m, 1H, a).

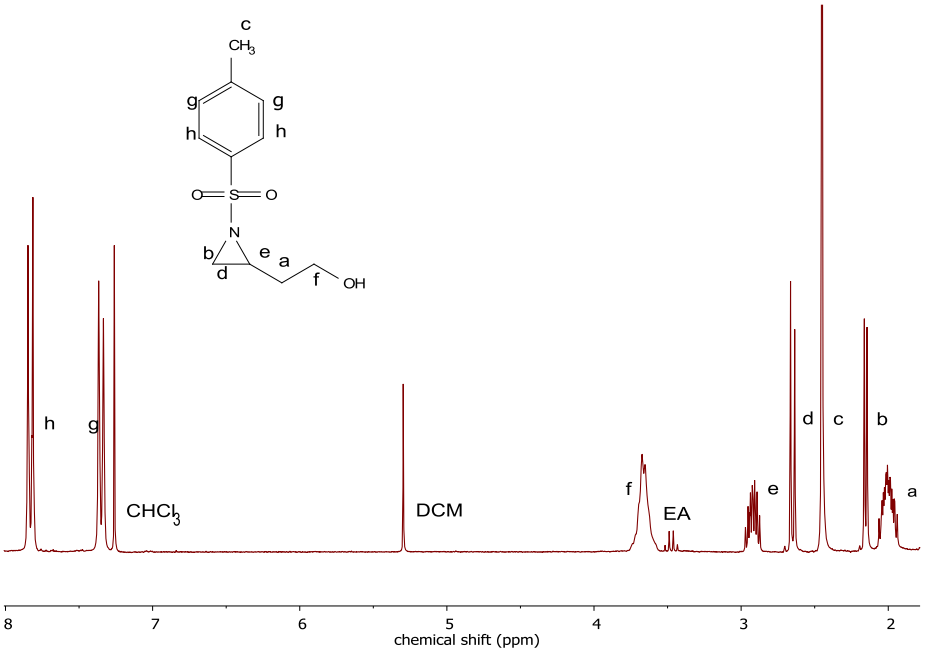

Figure S5.3. ^{1}H NMR (250 MHz, 298 K, $CDCl_3$) of *N*-tosyl-2-aziridineethanol (EOTsAz).

2-((1-Ethoxyethoxy)ethyl)-N-tosylaziridine (EEETsAz)

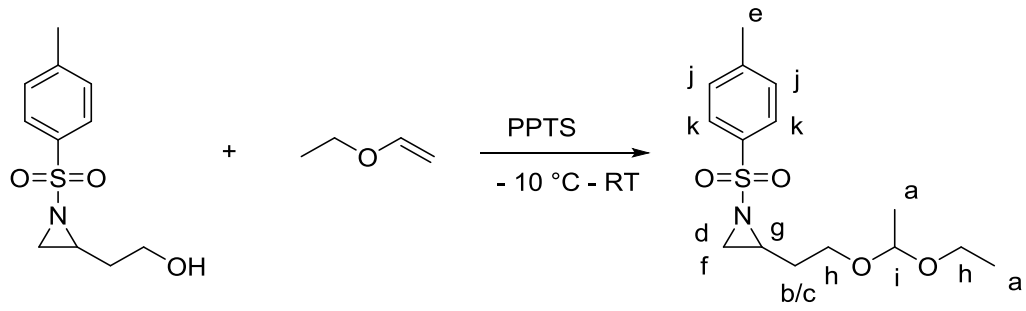

N-tosyl-2-aziridineethanol (EOTsAz) (1.6 g, 6.6 mmol) was dissolved in 10 mL freshly destilled ethyl vinyl ether. The solution was cooled down to -10 °C and 41 mg (0.16 mmol) of pyridinium *p*-toluenesulfonate were added. The mixture was stirred overnight and slowly heated to room temperature. After adding a small amount of potassium carbonate, the excess of ethyl vinyl ether was removed at reduced pressure. Chromatography over silica gel (ethyl acetate/petroleum ether 1:3) yielded the product as a colorless oily liquid (1.7 g, 5.4 mmol, 82 %).

^{1}H NMR (250 MHz, 298 K, chloroform-*d*): δ 7.87 – 7.74 (m, 2H, k), 7.38 – 7.27 (m, 2H, j), 4.54 (dd, *J* = 25.4, 5.3 Hz, 1H, i), 3.69 – 3.19 (m, 4H, h), 2.96 – 2.78 (m, 1H, g), 2.62 (dd, *J* = 7.0, 4.7 Hz, 1H, f), 2.42 (s, 3H, e), 2.10 (dd, *J* = 4.6, 3.6 Hz, 1H, d), 1.96 – 1.70 (m, 1H, c), 1.70 – 1.41 (m, 1H, b), 1.31 – 1.07 (m, 6H, a).

^{13}C NMR (176 MHz, 298 K, Chloroform-*d*): δ 144.48, 135.08, 129.66, 129.63, 128.02, 127.98, 99.92, 99.62, 62.80, 61.87, 61.18, 60.81, 37.90, 33.68, 31.84, 21.63, 19.71, 15.30.

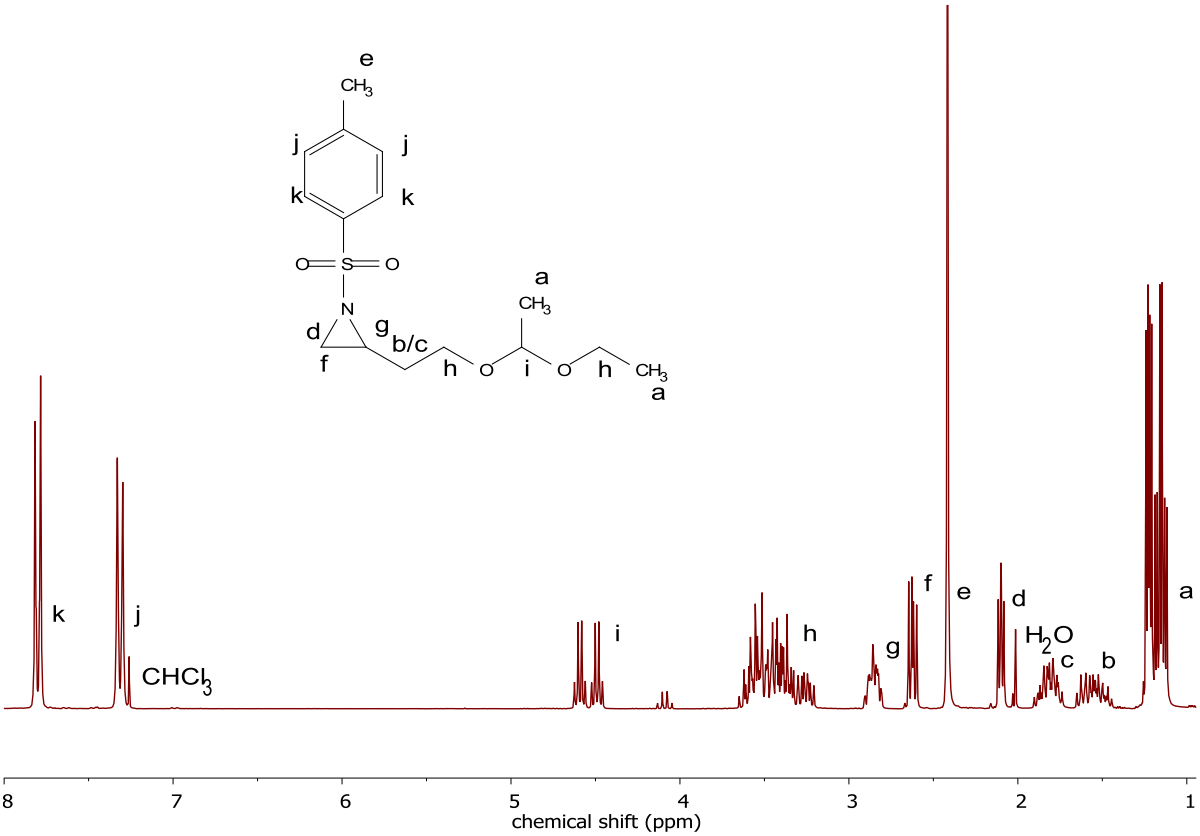

Figure S5.4. ^{1}H NMR (250 MHz, 298 K, $CDCl_3$) of 2-((1-ethoxyethoxy)ethyl)-*N*-tosylaziridine (EEETsAz).

N-tosyl-9-aziridinenonanol (NOTsAz)

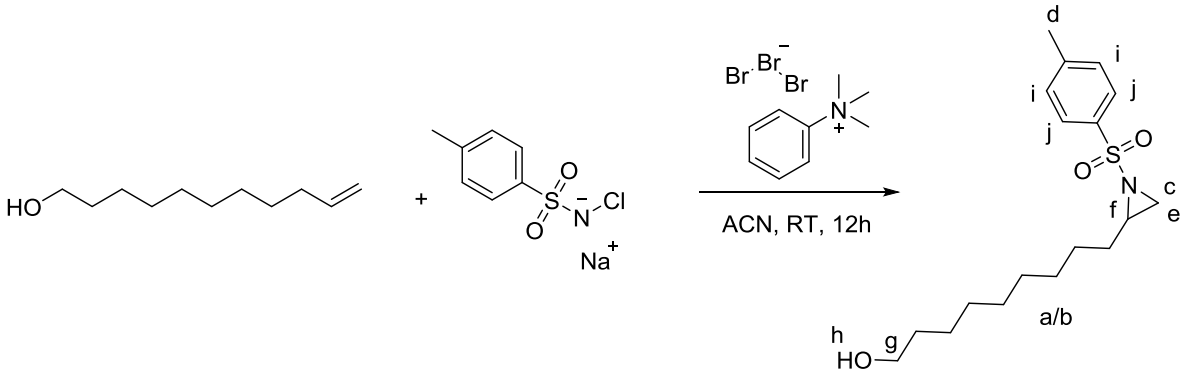

Chloramine-T (5.0 g, 21.9 mmol) was dried by azeotropic distillation with benzene *in vacuo* for 6 h and at 90 °C for additional 8 h. The anhydrous chloramine-T and undec-10-en-1-ol (8.8 mL, 43.9 mmol) were dissolved in anhydrous acetonitrile (ACN) (60 mL). Phenyltrimethylammonium tribromide (PTAB) (1.65 g, 4.4 mmol), dissolved in ACN (60 mL) was added and the mixture was stirred at room temperature for 40 hours. Ethyl acetate (40 mL) and deionized water (40 mL) were added. After washing with brine, the organic phases were combined, dried over magnesium sulfate and concentrated at reduced pressure. Chromatography over silica gel (dichloromethane/diethyl ether 2:1) yielded the product as a colorless oily liquid (4.40 g, 13.0 mmol, 30%).

^{1}H NMR (250 MHz, 298 K, chloroform-*d*): δ 7.91 – 7.77 (m, 2H, j), 7.42 – 7.29 (m, 2H, i), 4.75 (s, 1H, h), 3.64 (t, *J* = 6.6 Hz, 2H, g), 2.85 – 2.66 (m, 1H, f), 2.63 (d, *J* = 7.0 Hz, 1H, e), 2.44 (d, *J* = 3.0 Hz, 3H, d), 2.05 (d, *J* = 4.6 Hz, 1H, c), 1.69 – 1.43 (m, 4H, b), 1.42 – 1.08 (m, 12H, a).

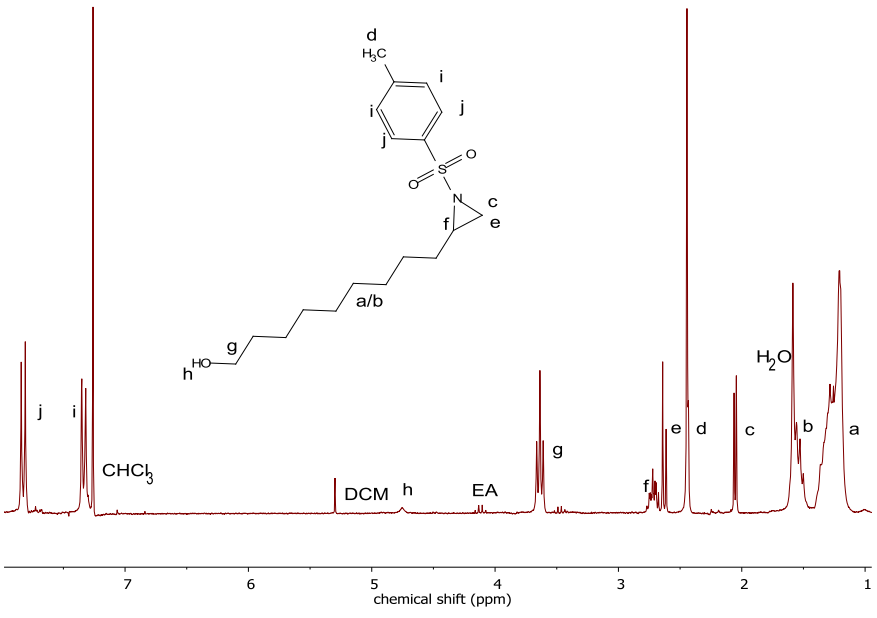

Figure S5.5. ^{1}H NMR (250 MHz, 298 K, $CDCl_3$) of *N*-tosyl-9-aziridinenonanol (NOTsAz).

2-((1-Ethoxyethoxy)nonyl)-N-tosylaziridine (NEETsAz)

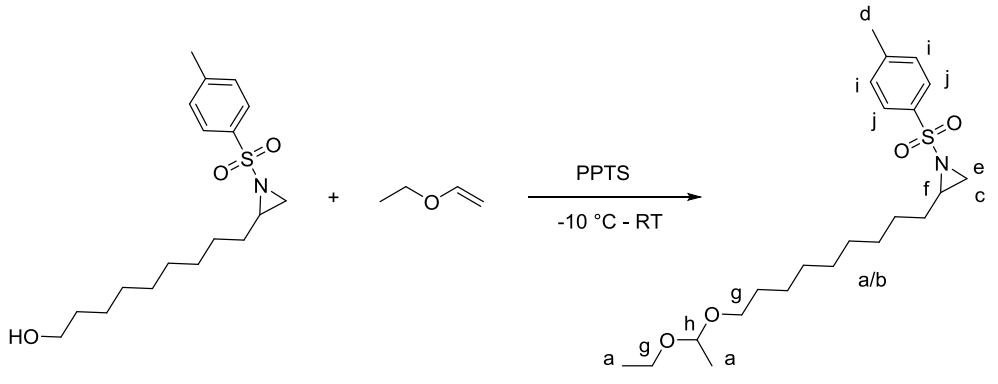

N-tosyl-9-aziridinenonanol (NOTsAz) (1.0 g, 2.9 mmol) was dissolved in 10 mL freshly distilled ethyl vinyl ether. The solution was cooled to -10 °C and 43 mg (0.17 mmol) of pyridinium *p*-toluenesulfonate were added. The mixture was stirred overnight and allowed to reach room temperature. After adding a small amount of potassium carbonate, the excess of ethyl vinyl ether was removed at reduced pressure. Chromatography over silica gel (ethyl acetate/petroleum ether 3:7) yielded the product as a colorless oily liquid (0.85 g, 2.1 mmol, 70%).

^{1}H NMR (700 MHz, 298 K, chloroform-*d*): δ 7.88 – 7.77 (m, 2H, j), 7.33 (d, *J* = 8.2 Hz, 2H, i), 4.67 (p, *J* = 5.3 Hz, 1H, h), 3.75 – 3.33 (m, 4H, g), 2.71 (q, *J* = 5.6 Hz, 1H, f), 2.63 (t, *J* = 4.9 Hz, 1H, e), 2.44 (d, *J* = 3.4 Hz, 3H, d), 2.05 (d, *J* = 4.6 Hz, 1H, c), 1.59 – 1.48 (m, 4H, b), 1.37 – 1.09 (m, 18H, a).

^{13}C NMR (176 MHz, 298 K, chloroform-*d*): δ 144.39, 135.23, 129.61, 127.99, 99.53, 65.28, 60.67, 40.46, 33.80, 31.31, 29.90, 29.43, 29.39, 29.35, 29.01, 26.75, 26.24, 21.63, 19.90, 15.34.

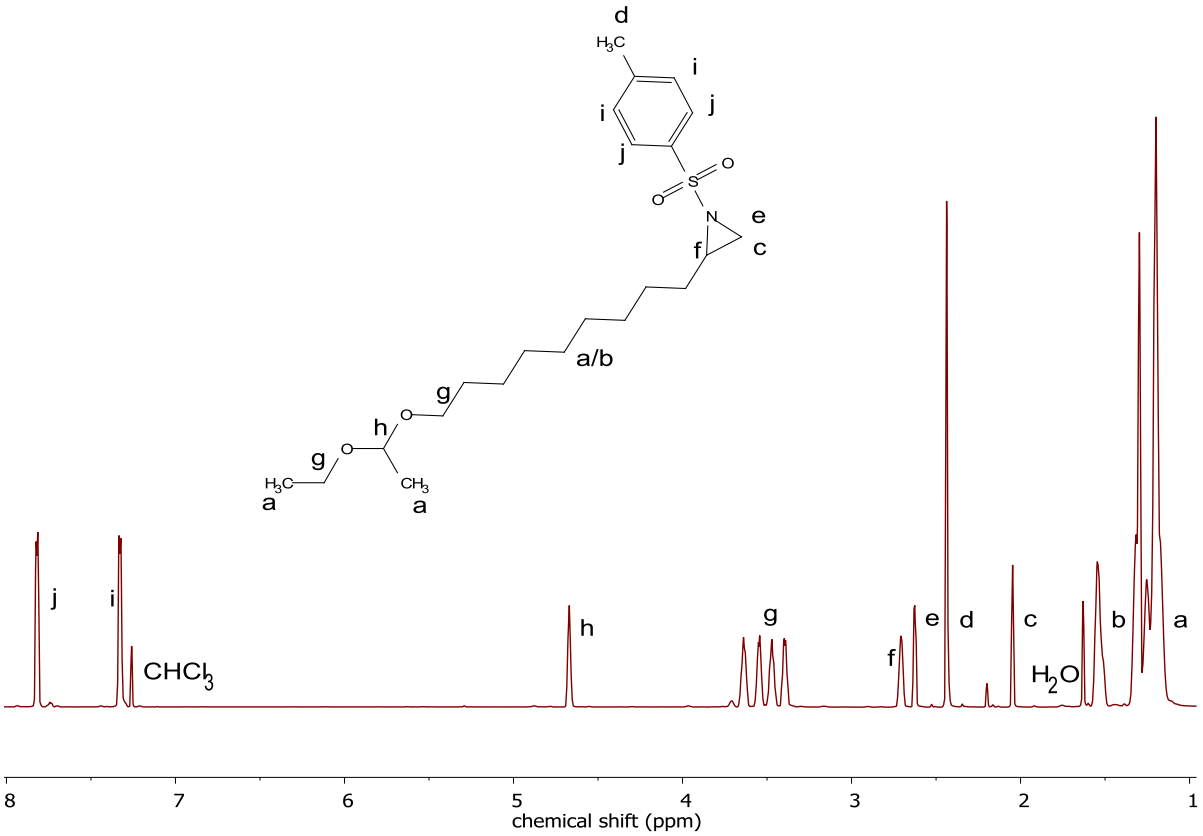

Figure S5.6. ^{1}H NMR (700 MHz, 298 K, $CDCl_3$) of 2-((1-ethoxyethoxy)nonyl)-*N*-tosylaziridine (NEETsAz).

5.6.3 Polymerization and Postmodification.

The glassware was dried by heating *in vacuo* for at least three times. All reactants (except potassium bis(trimethylsilyl)amide (KHMDS)) were dried from benzene *in vacuo* for at least 6 h. The monomers and the BnNHMs-initiator were dissolved in 2 and 1 mL respectively anhydrous *N,N*-dimethylformamide (DMF). KHMDS was added quickly as a solid in argon-counter flow to the BnNHMs-solution and the sample boat was rinsed with another 1 mL DMF. The calculated amount of the initiator-solution was transferred via syringe to the monomer-solution. The mixture was stirred at 55 °C for 18 h. To terminate the polymerization, 0.5 mL degassed methanol were added and the reaction mixture was precipitated in ca. 30 mL methanol. The colorless solids were collected by centrifugation and dried at 70 °C *in vacuo.*

In the following, a representative example is given of every polymerization and deprotection, with characterization data. For all data, please refer to Table 5.1 in the manuscript.

P(MEETsAz): Poly(2-((1-ethoxyethoxy)methyl)-N-tosylaziridine) (P1-1)

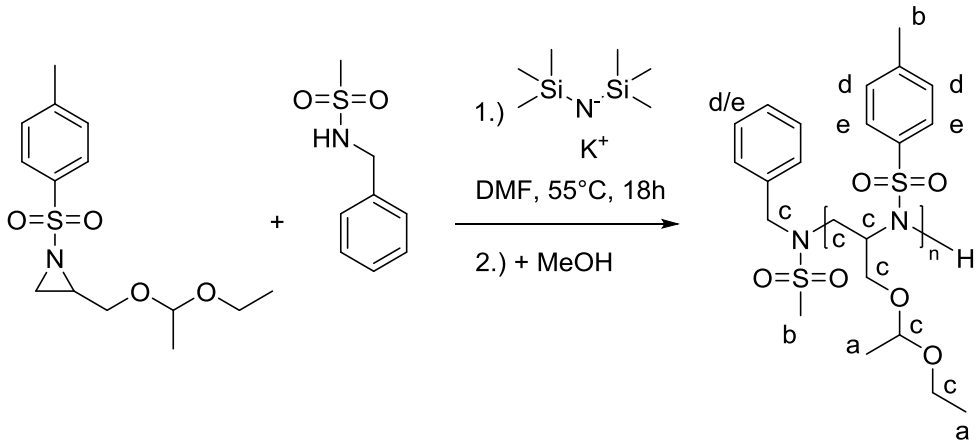

PMEETsAz$_{30(theo)}$: [MEETsAz (200.0 mg, 0.67 mmol), BnNHMs (4.12 mg, 22 µmol), KHMDS (4.44 mg, 22 µmol)].

^{1}H NMR (700 MHz, 298 K, DMF-d_7): δ 8.20 – 7.67 (m, e), 7.67 – 7.21 (m, d), 4.95 – 3.06 (m, c), 2.64 – 2.25 (m, b), 1.36 – 0.70 (m, a).

SEC (RID, DMF, PEO): M_n = 2200; $Đ$ = 1.23

DSC: T_g = 61 °C

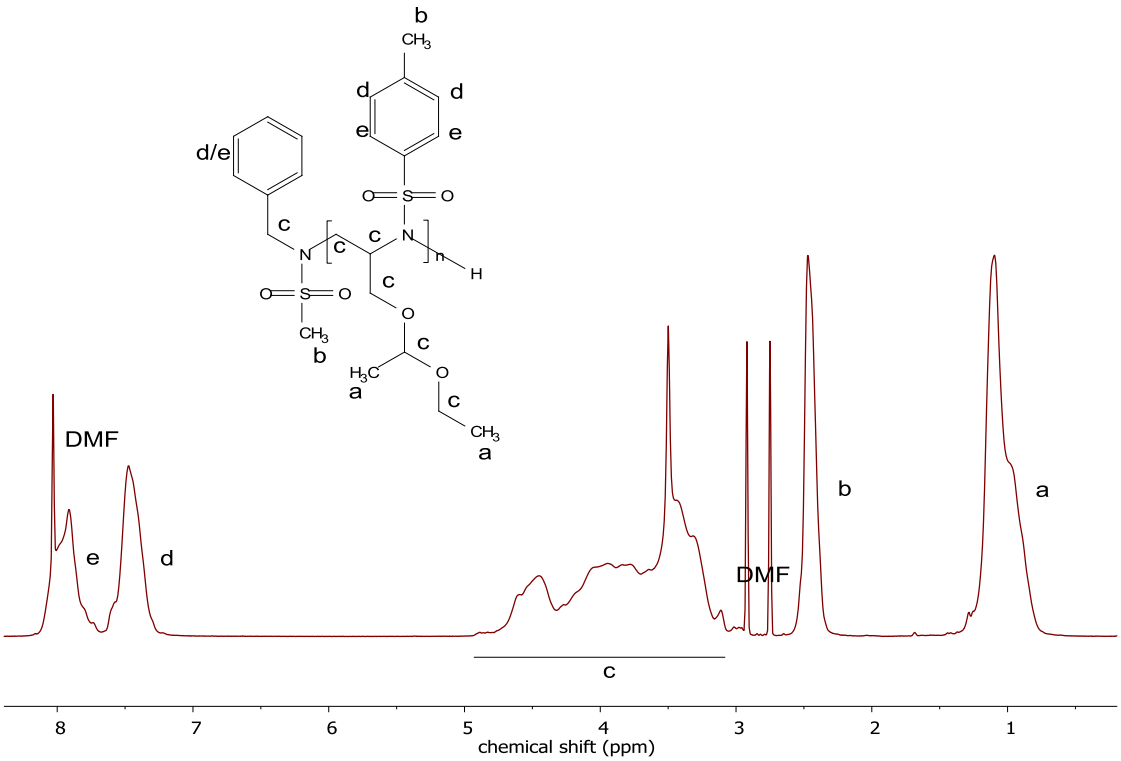

Figure S5.7. ^{1}H NMR (700 MHz, 298 K, DMF-d_7) of poly(2-((1-ethoxyethoxy)methyl)-*N*-tosylaziridine) (PMEETsAz).

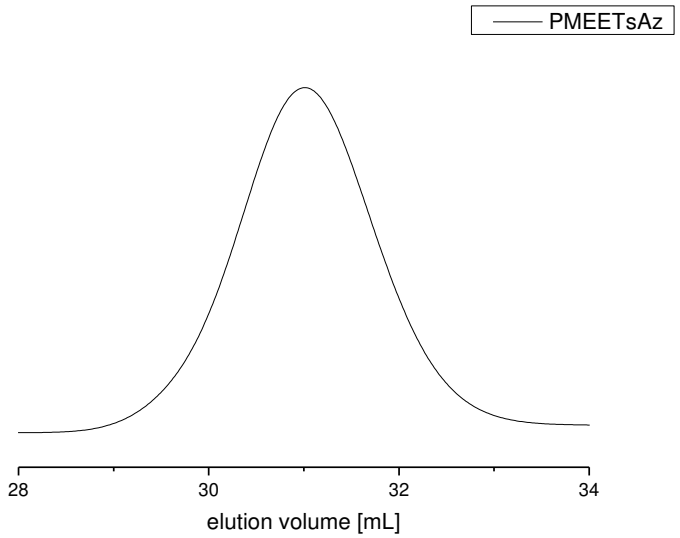

Figure S5.8. SEC traces of poly(2-((1-ethoxyethoxy)methyl)-*N*-tosylaziridine) (PMEETsAz) in DMF (RI signal).

P(MOTsAz): Poly(N-tosyl-2-aziridinemethanol) (P1-1-OH)

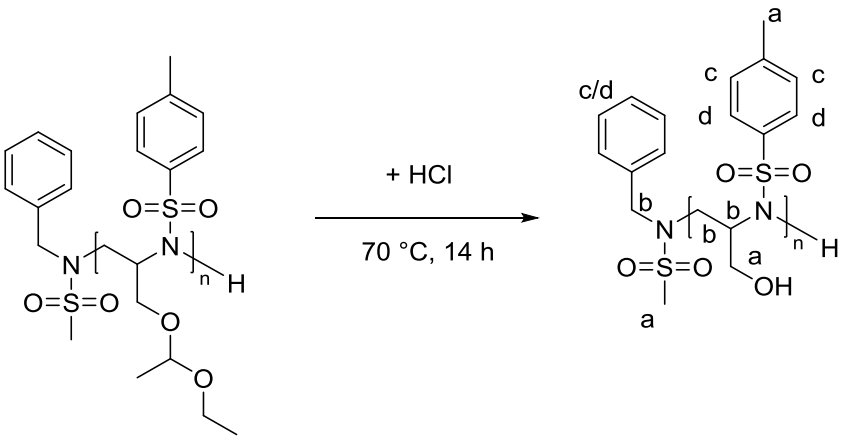

100 mg of the polymer were dissolved in 2 mL ethanol. One drop of water and 1 mL concentrated hydrochlorid acid were added and stirred at 70 °C overnight. The solvents were removed at reduced pressure. The resulting brown solid was analyzed without further purification.

^{1}H NMR (500 MHz, 298 K, DMF-d_7): δ 7.91 – 7.64 (m, d), 7.51 – 7.15 (m, c), 4.72 - 3.25 (m, b), 2.49 – 2.25 (m, a).

SEC (RID, DMF, PEO): M_n = 2300; $Đ$ = 1.36

DSC: T_g = 132 °C

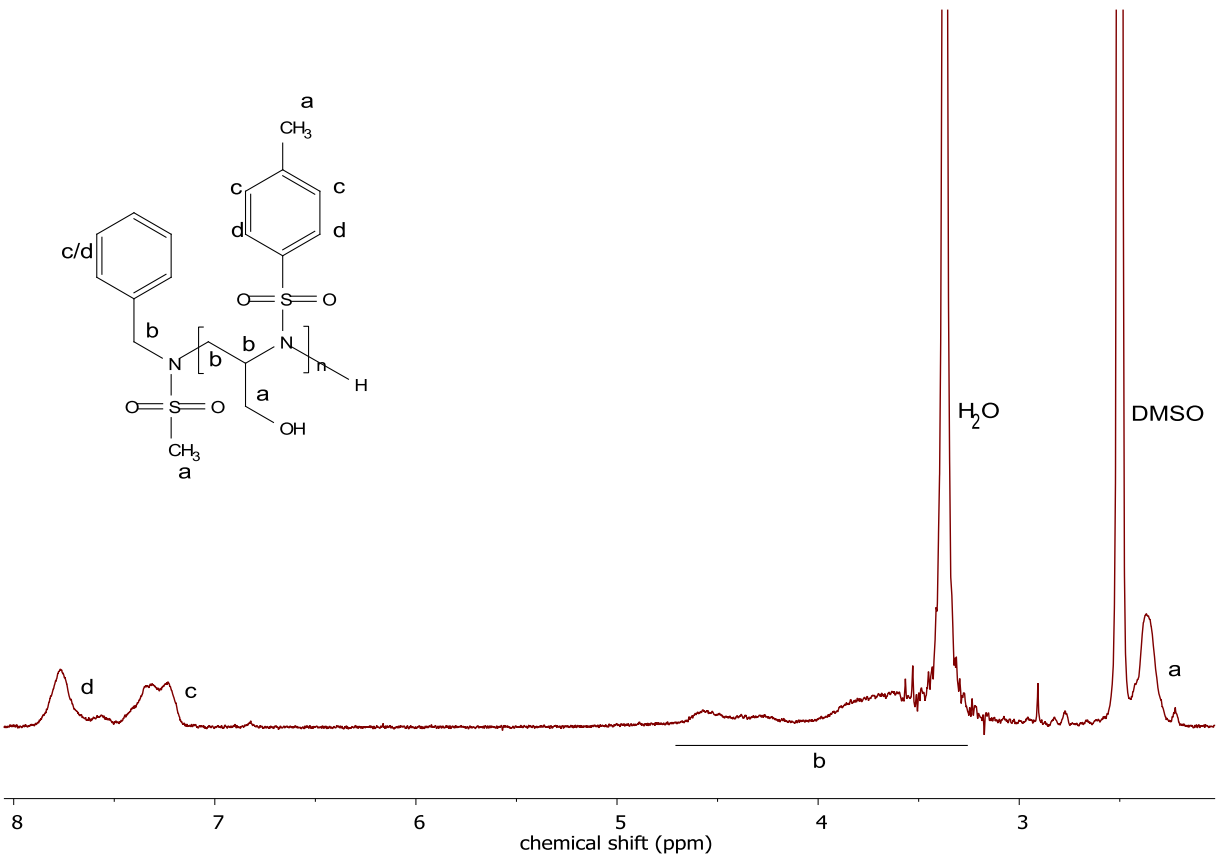

Figure S5.9. ^{1}H NMR (250 MHz, 298 K, DMSO-d_6) of poly(*N*-tosyl-2-aziridinemethanol) (PMOTsAz).

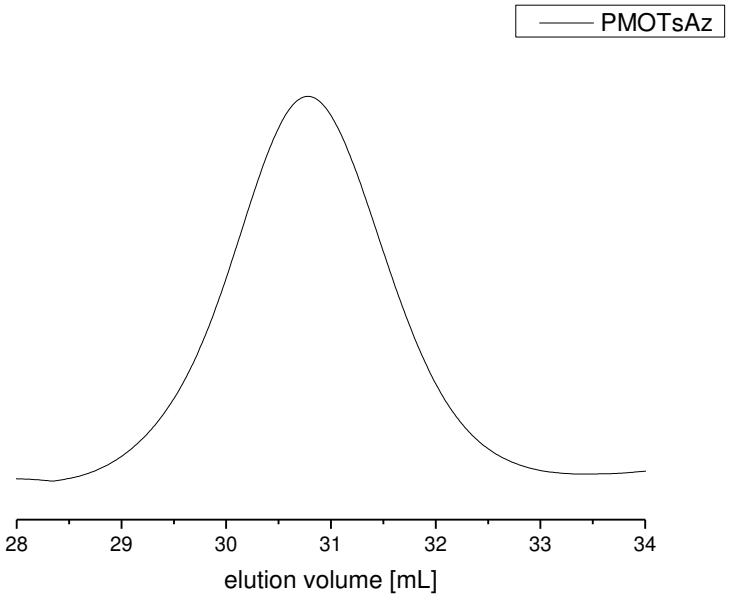

Figure S5.10. SEC traces of poly(*N*-tosyl-2-aziridinemethanol) (PMOTsAz) in DMF (RI signal).

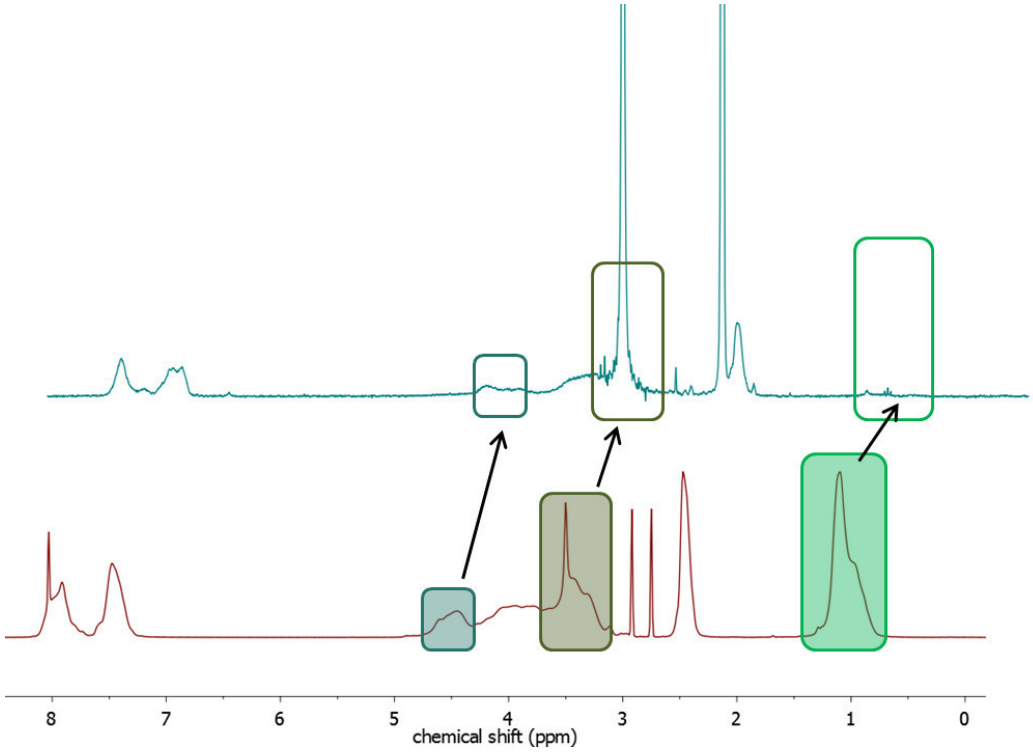

Figure S5.11. Comparison of: ^{1}H NMR (250 MHz, 298 K, DMSO-d_6) of poly(*N*-tosyl-2-aziridinemethanol) (PMOTsAz) and ^{1}H NMR (250 MHz, 298 K, DMF-d_7) of poly(2-((1-ethoxyethoxy)methyl)-*N*-tosylaziridine) (PMEETsAz).

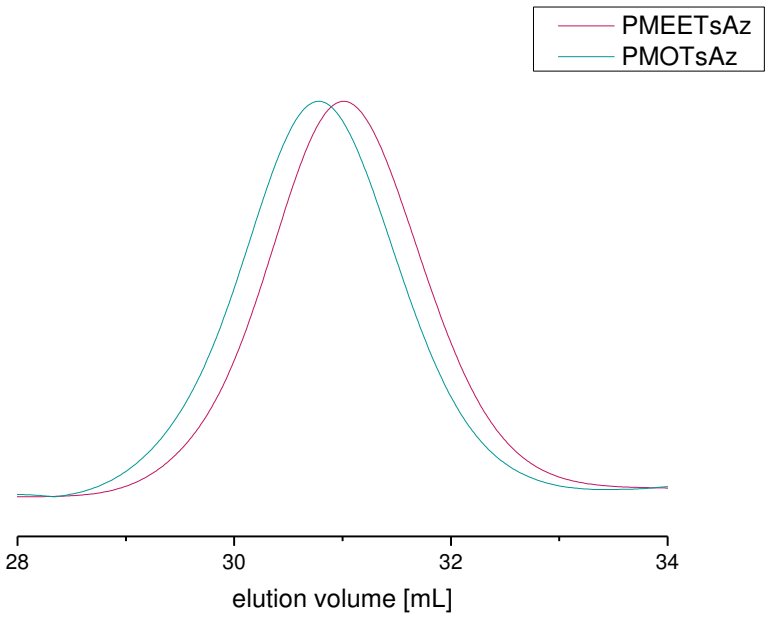

Figure S5.12. SEC traces of poly(*N*-tosyl-2-aziridinemethanol) (PMOTsAz) and poly(2-((1-ethoxyethoxy)methyl)-*N*-tosylaziridine) (PMEETsAz) in DMF (RI signal).

P(EEETsAz): Poly(2-((1-ethoxyethoxy)ethyl)-N-tosylaziridine) (P2-4)

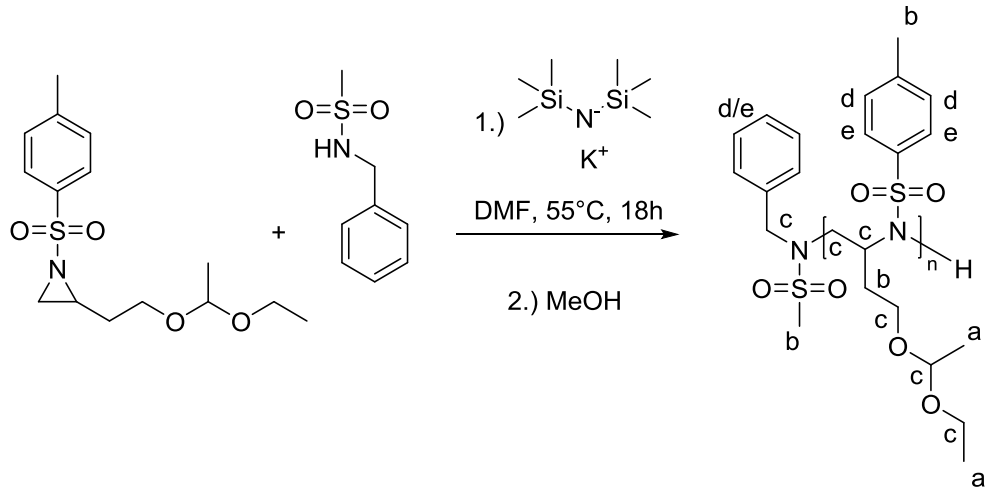

PEEETsAz$_{50(theo)}$: [EEETsAz (450.0 mg, 1.4 mmol), BnNHMs (5.32 mg, 29 µmol), KHMDS (5.73 mg, 29 µmol)].

^{1}H NMR (700 MHz, 298 K, DMF-d_7): δ 8.28 – 7.77 (m, e), 7.75 – 7.27 (m, d), 4.83 – 3.17 (m, c), 2.60 – 1.53 (m, b), 1.44 – 0.87 (m, a).

SEC (RID, DMF, PEO): M_n = 3700; $Đ$ = 1.12

DSC: T_g = 78 °C (P2-2)

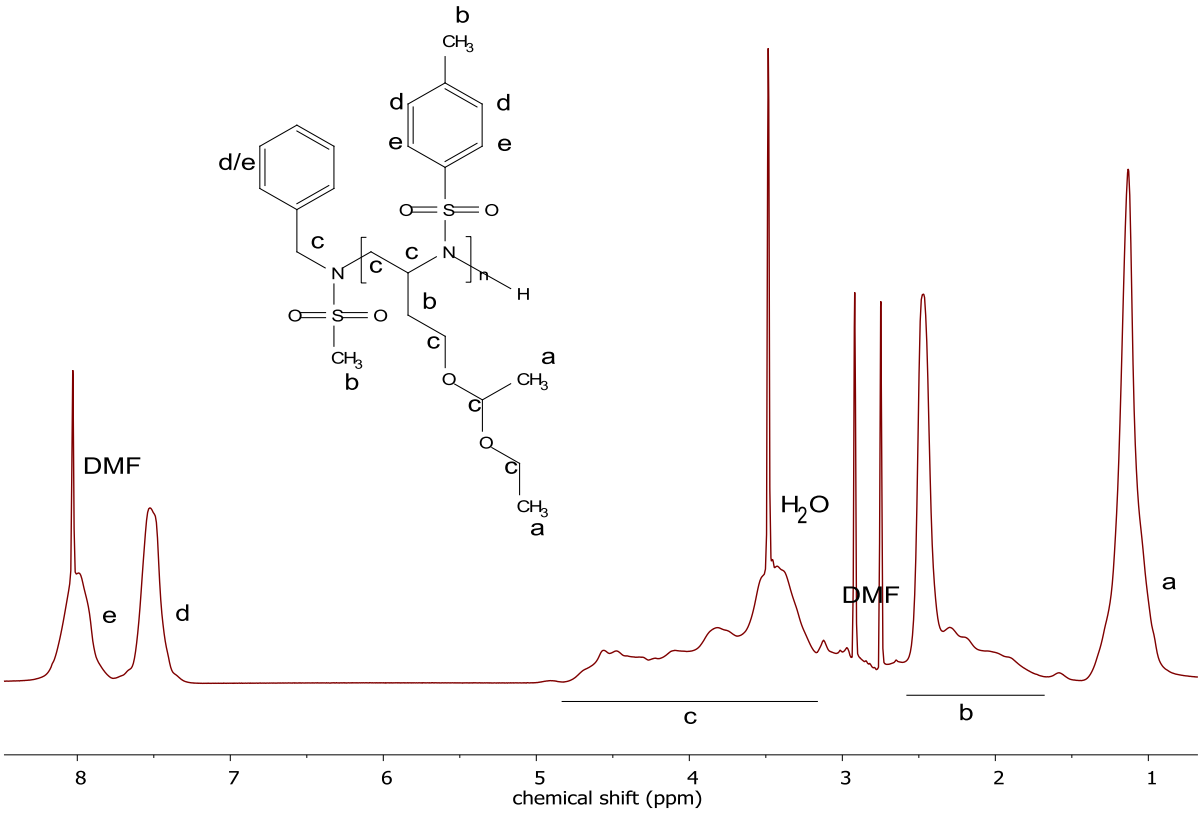

Figure S5.13. ^{1}H NMR (700 MHz, 298 K, DMF-d_7) of poly(2-((1-ethoxyethoxy)ethyl)-*N*-tosylaziridine) (PEEETsAz).

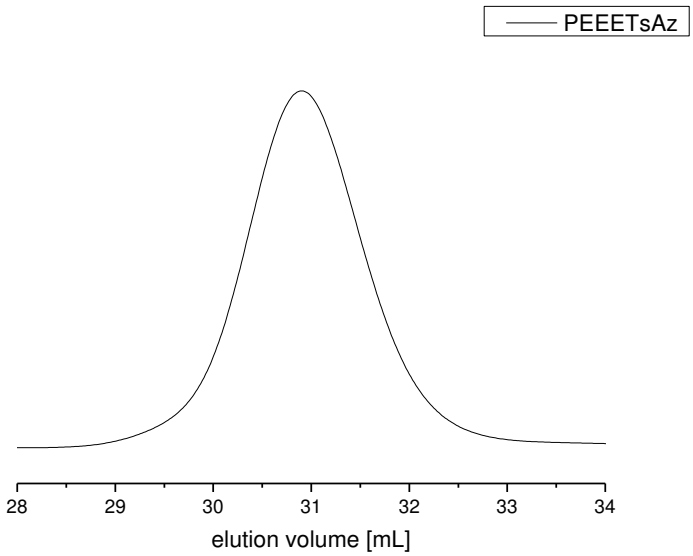

Figure S5.14. SEC traces of poly(2-((1-ethoxyethoxy)ethyl)-*N*-tosylaziridine) (PMEETsAz) in DMF (RI signal).

P(EOTsAz): Poly(N-tosyl-2-aziridineethanol) (P2-3-OH)

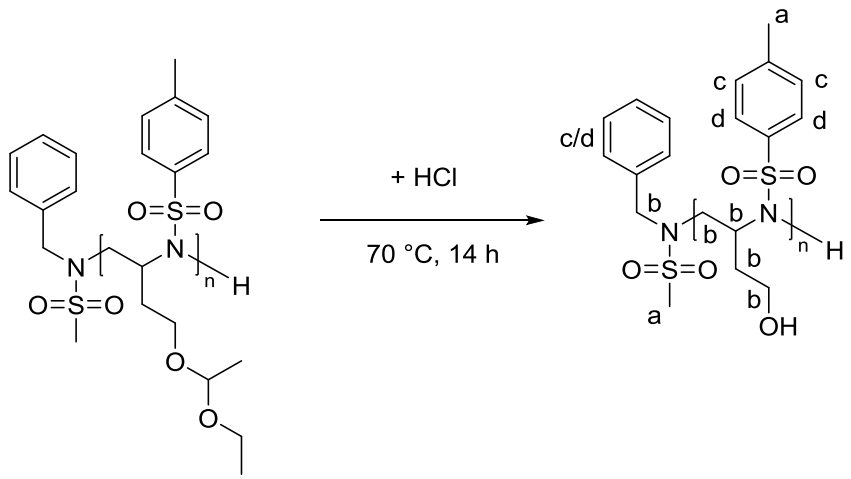

100 mg of the polymer were dissolved in 2 mL ethanol. One drop of water and 1 mL concentrated hydrochlorid acid were added and stirred at 70 °C overnight. The solvents were removed at reduced pressure. The resulting brown solid was analyzed without further purification.

^{1}H NMR (500 MHz, 298 K, DMF-d_7): δ 8.32 – 7.87 (m, d), 7.71 – 7.26 (m, c), 4.73 - 3.16 (m, b), 2.65 – 1.70 (m, a).

SEC (RID, DMF, PEO): M_n = 5100; $Đ$ = 1.15

DSC: T_g = 92 °C

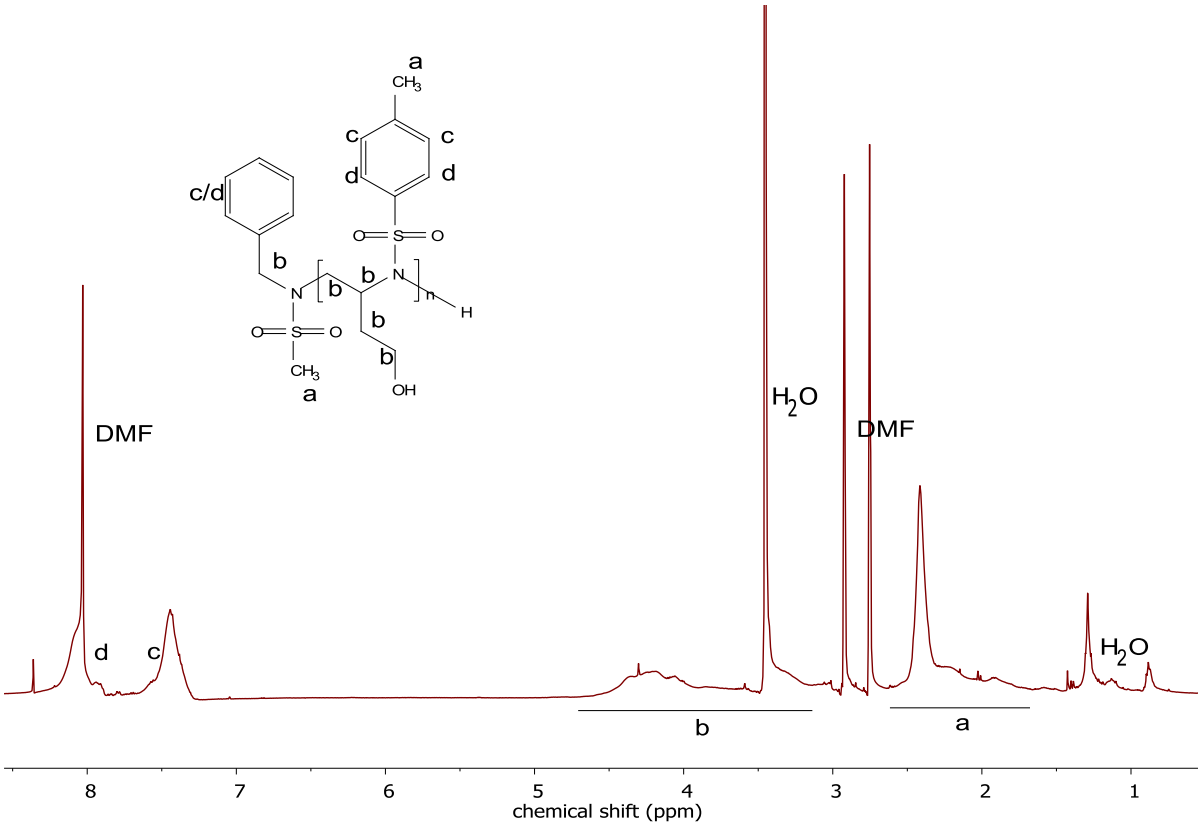

Figure S5.15. ^{1}H NMR (500 MHz, 298 K, DMSO-d_6) of poly(*N*-tosyl-2-aziridineethanol) (PEOTsAz).

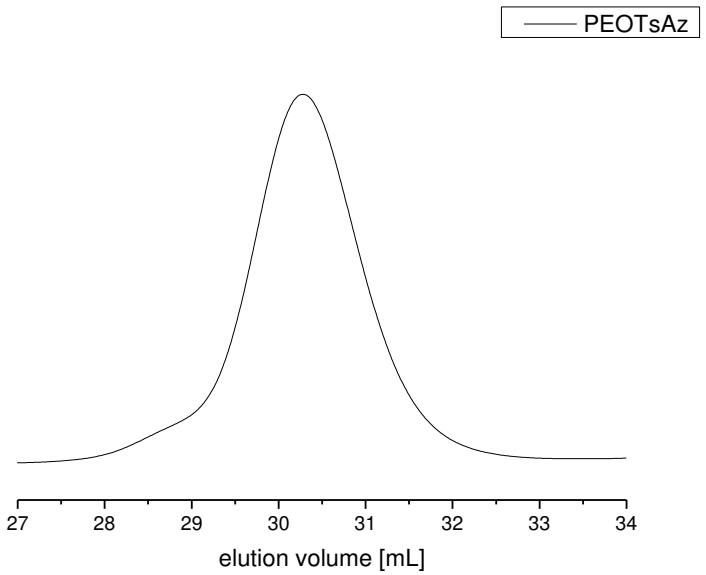

Figure S5.16. SEC traces of poly(*N*-tosyl-2-aziridineethanol) (PEOTsAz) in DMF (RI signal).

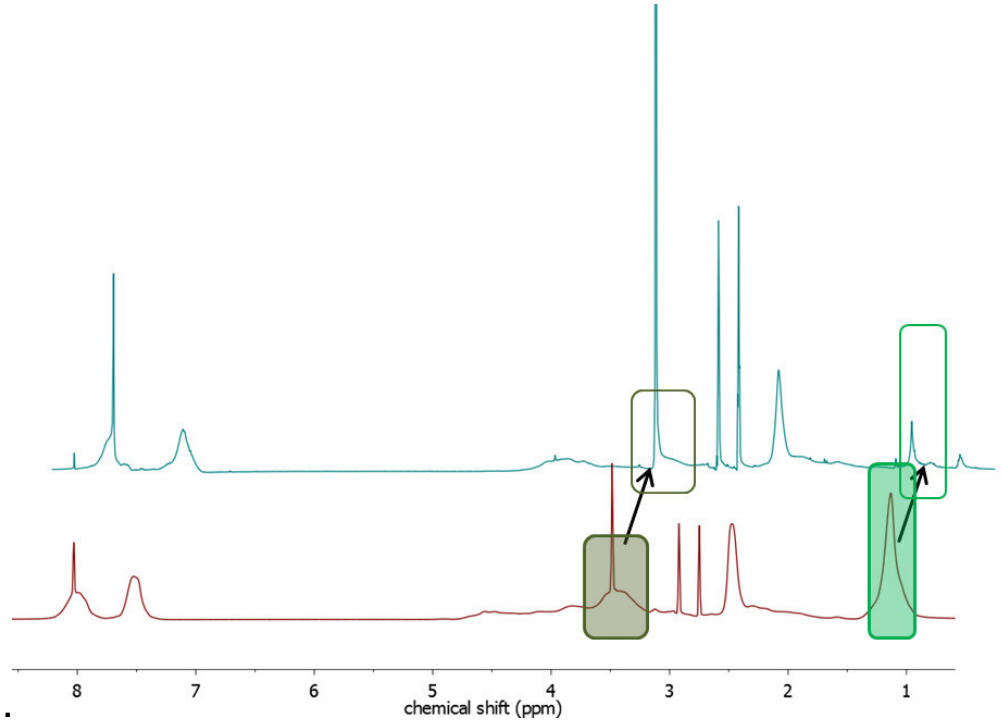

Figure S5.17. Comparison of: ^{1}H NMR (500 MHz, 298 K, DMF-d_7) of poly(*N*-tosyl-2-aziridineethanol) (PEOTsAz) and ^{1}H NMR (700 MHz, 298 K, DMF-d_7) of poly(2-((1-ethoxyethoxy)ethyl)-*N*-tosylaziridine) (PEEETsAz).

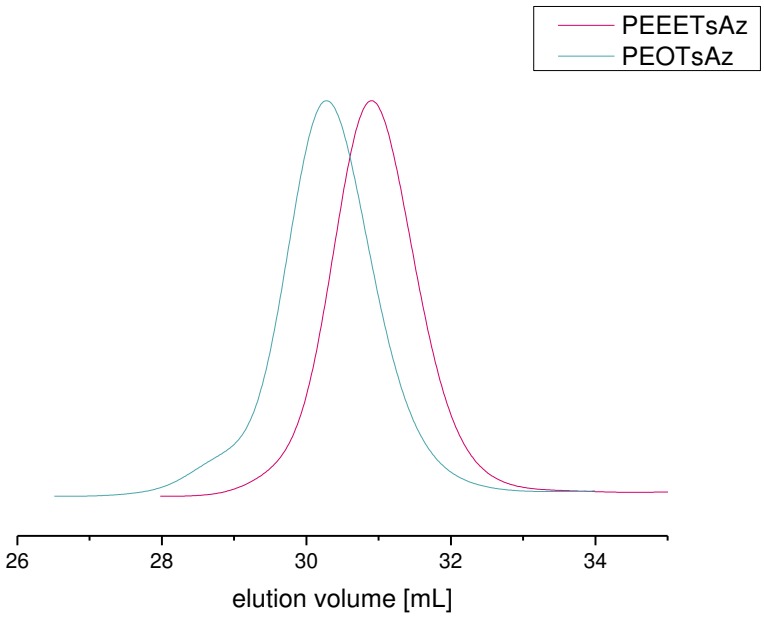

Figure S5.18. SEC traces of poly(*N*-tosyl-2-aziridineethanol) (PEOTsAz) and poly(2-((1-ethoxyethoxy)ethyl)-*N*-tosylaziridine) (PEEETsAz) in DMF (RI signal).

P(NEETsAz): Poly(2-((1-ethoxyethoxy)nonyl)-N-tosylaziridine) (P3-1)

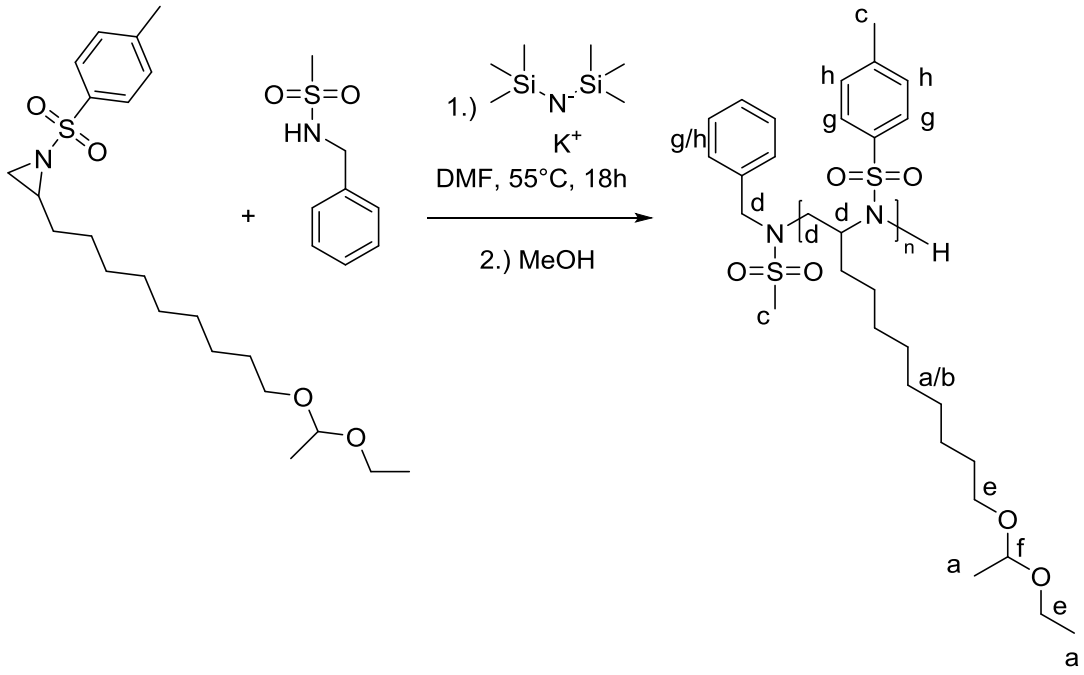

PNEETsAz$_{15(theo)}$: [NEETsAz (200.0 mg, 0.49 mmol), BnNHMs (6.00 mg, 33 µmol), KHMDS (6.46 mg, 33 µmol)].

^{1}H NMR (250 MHz, 298 K, chloroform-*d*): δ 8.13 - 7.66 (m, h), 7.48 – 7.05 (m, g), 4.76 – 4.58 (m, f), 3.74 – 3.29 (m, e), 4.38 – 2.72 (m, d), 2.53 – 2.23 (m, c), 1.63 – 1.41 (m, b), 1.45 – 0.61 (m, a).

SEC (RID, DMF, PEO): M_n = 1700; $Đ$ = 1.18

DSC: T_g = 41 °C

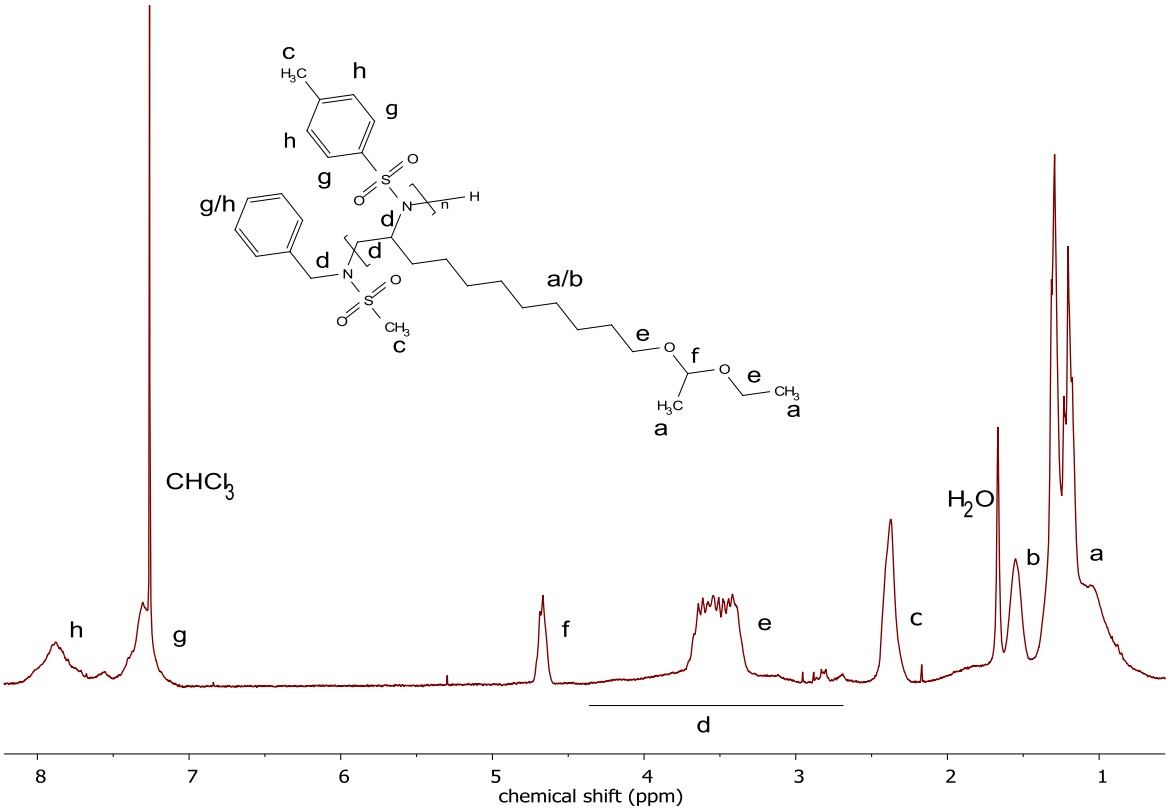

Figure S5.19a. ^{1}H NMR (250 MHz, 298 K, $CDCl_3$) of poly(2-((1-ethoxyethoxy)nonyl)-*N*-tosylaziridine) (PNEETsAz).

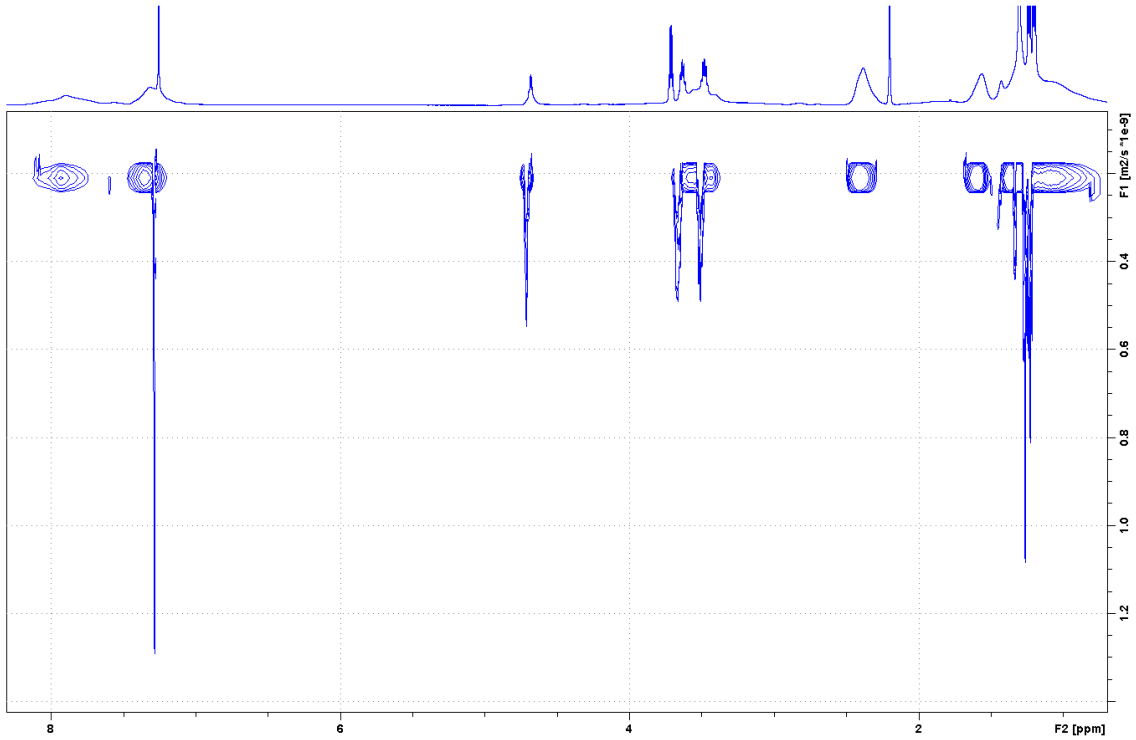

Figure S5.19b. DOSY ^{1}H NMR (700 MHz, 298 K, $CDCl_3$) of poly(2-((1-ethoxyethoxy)nonyl)-*N*-tosylaziridine) (PNEETsAz).

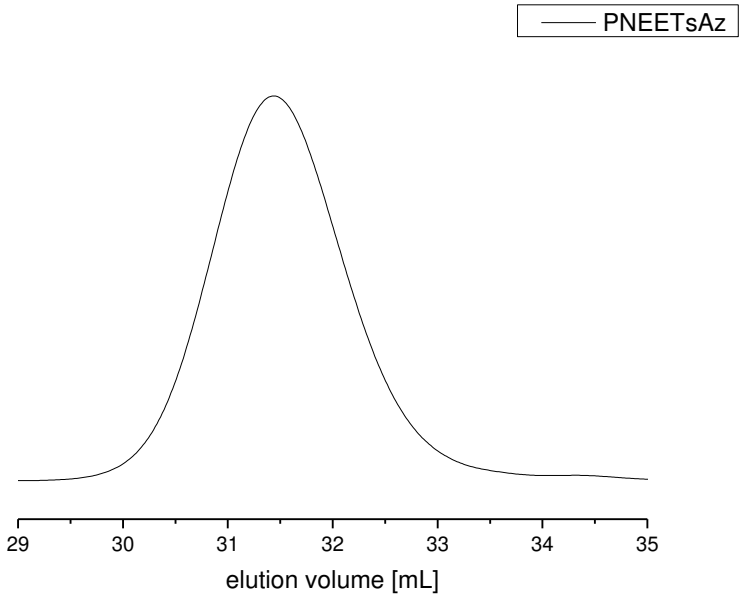

Figure S5.20. SEC traces of poly(2-((1-ethoxyethoxy)nonyl)-*N*-tosylaziridine) (PNEETsAz) in DMF (RI signal).

P(NOTsAz): Poly(N-tosyl-2-aziridinenonanol) (P3-2-OH)

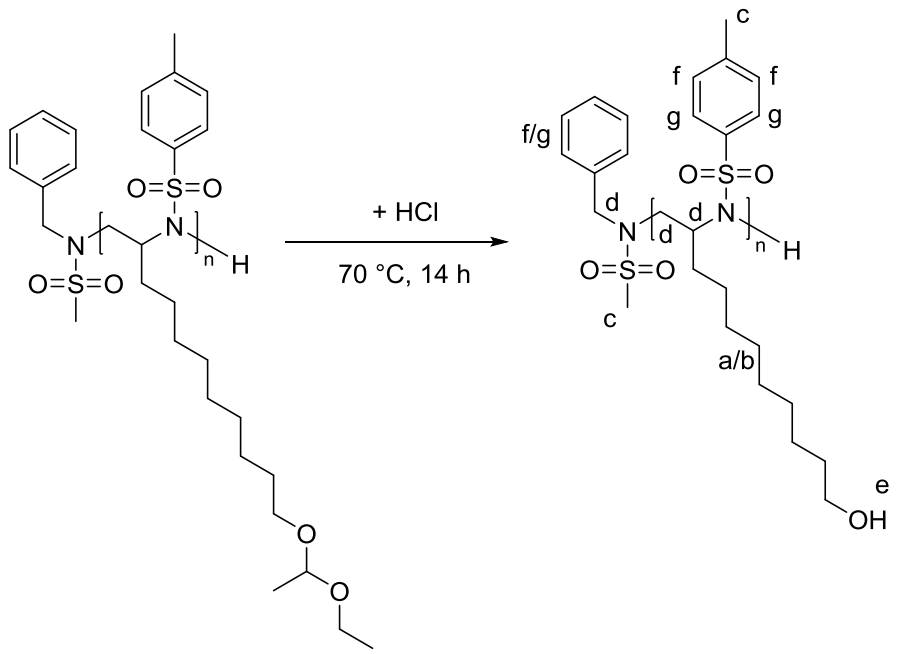

100 mg of the polymer were dissolved in 2 mL ethanol. One drop of water and 1 mL concentrated hydrochloride acid were added and stirred at 70 °C overnight. The solvents were removed at reduced pressure. The resulting brown solid was analyzed without further purification.

^{1}H NMR (250 MHz, 298 K, chloroform-*d*): δ 8.13 - 7.68 (m, g), 7.62 - 7.11 (m, f), 3.69 – 3.56 (m, e), 4.03 – 2.73 (m, d), 2.55 - 2.21 (m, c), 1.76 – 1.41 (m, b), 1.40 – 0.77 (m, a).

SEC (RID, DMF, PEO): M_n = 2000; $Đ$ = 1.20

DSC: T_g = 54 °C

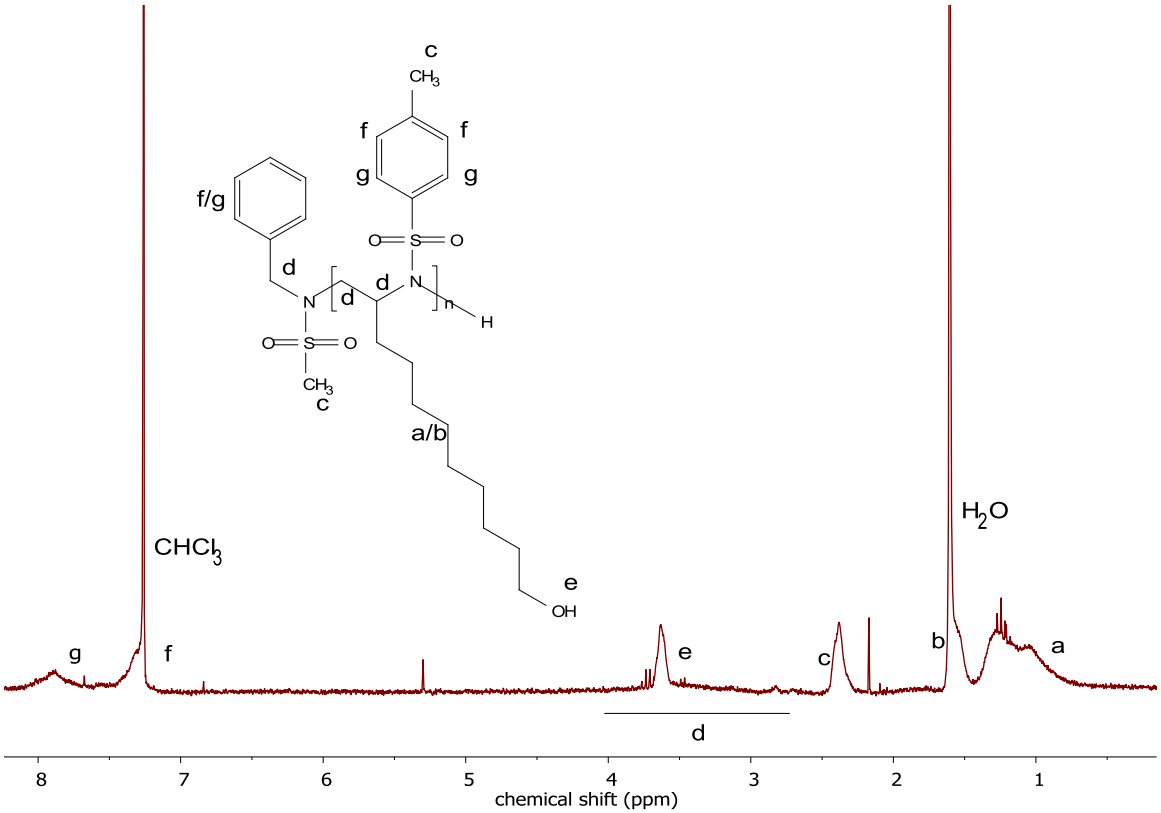

Figure S5.21. ^{1}H NMR (250 MHz, 298 K, $CDCl_3$) of poly(*N*-tosyl-2-aziridinenonanol) (PNOTsAz).

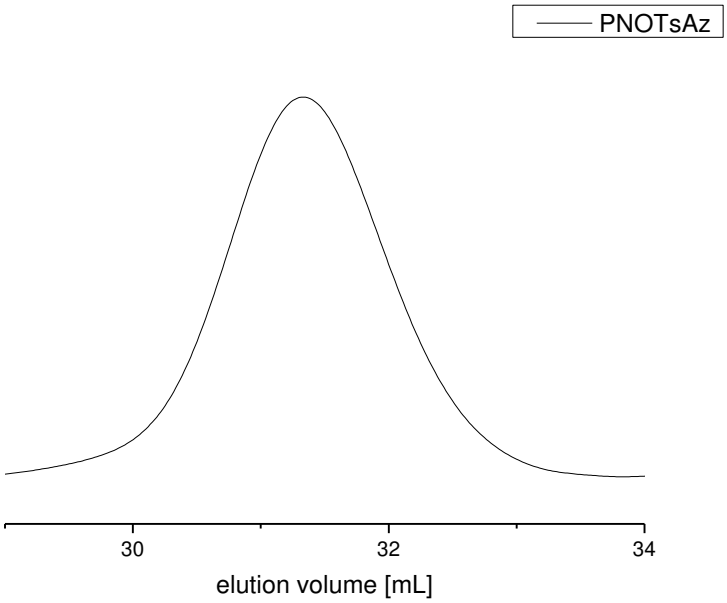

Figure S5.22. SEC traces of poly(*N*-tosyl-2-aziridinenonanol) (PNOTsAz) in DMF (RI signal).

P(NEEAz): Poly(2-((1-ethoxyethoxy)nonyl)-aziridine) (P3-4-NH)

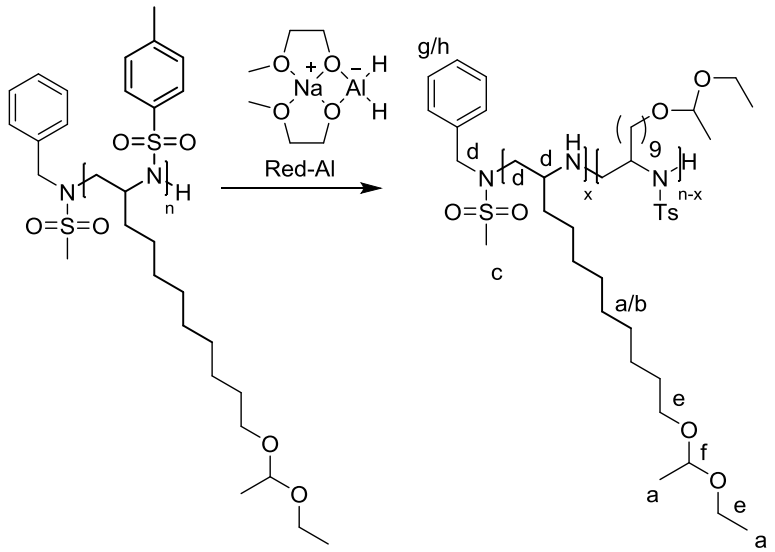

100 mg of the polymer were dissolved in 10 mL toluene, 2.11 mL (7.37 mmol) sodium bis(2-methoxyethoxy)aluminiumhydride (Red-Al) were added and the mixture was stirred at 110 °C overnight. The toluene was removed at reduced pressure. The yellow residue was dissolved in 30 mL water and dialyzed in a 0.1 molar sodium hydroxide-solution for two days and subsequent in water/tetrahydrofuran. The residue was extracted in dichloromethane and concentrated at reduced pressure to recover the product as slightly yellow oil with a degree of deprotection of ca. 76%.

^{1}H NMR (250 MHz, 298 K, chloroform-*d*): δ 7.78 – 7.54 (m, h), 7.33 – 7.12 (m, g), 4.68 – 4.53 (m, f), 3.67 – 3.22 (m, e), 3.84 – 1.93 (m, d), 2.39 - 2.29 (m, c), 1.58 – 1.36 (m, b), 1.34 – 0.82 (m, a).

SEC (RID, DMF, PEO): M_n = 700; $Đ$ = 1.53

DSC: T_g = -63 °C

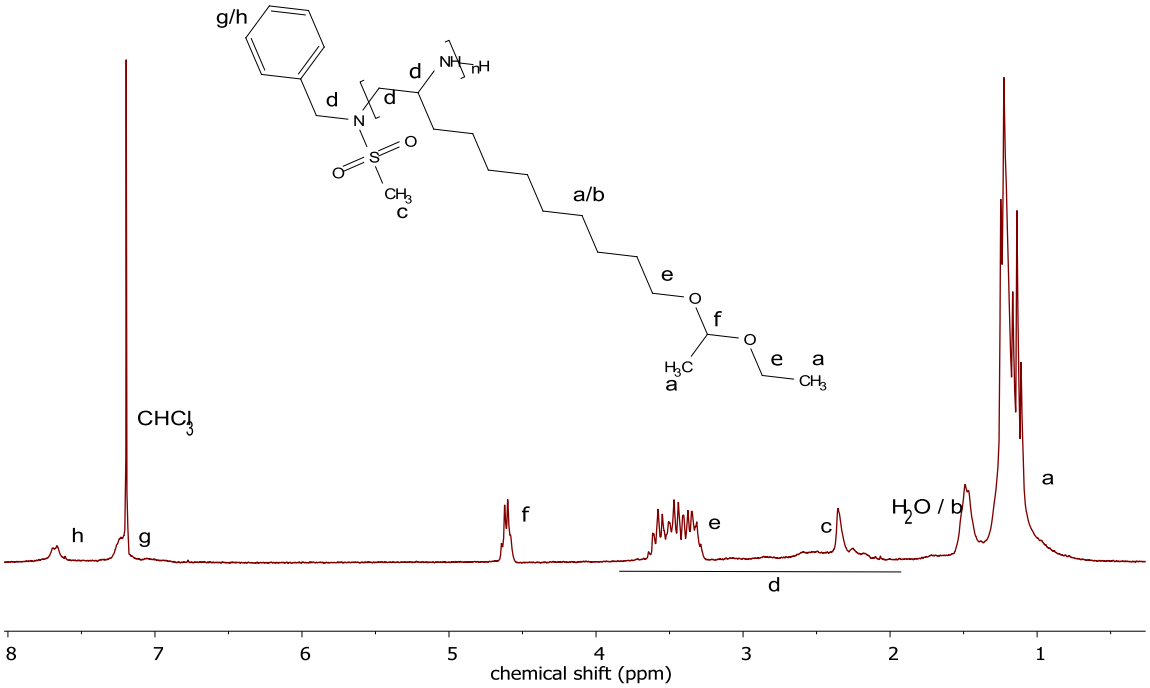

Figure S5.23a. ^{1}H NMR (250 MHz, 298 K, $CDCl_3$) of poly(2-((1-ethoxyethoxy)nonyl)-aziridine) (PNEEAz).

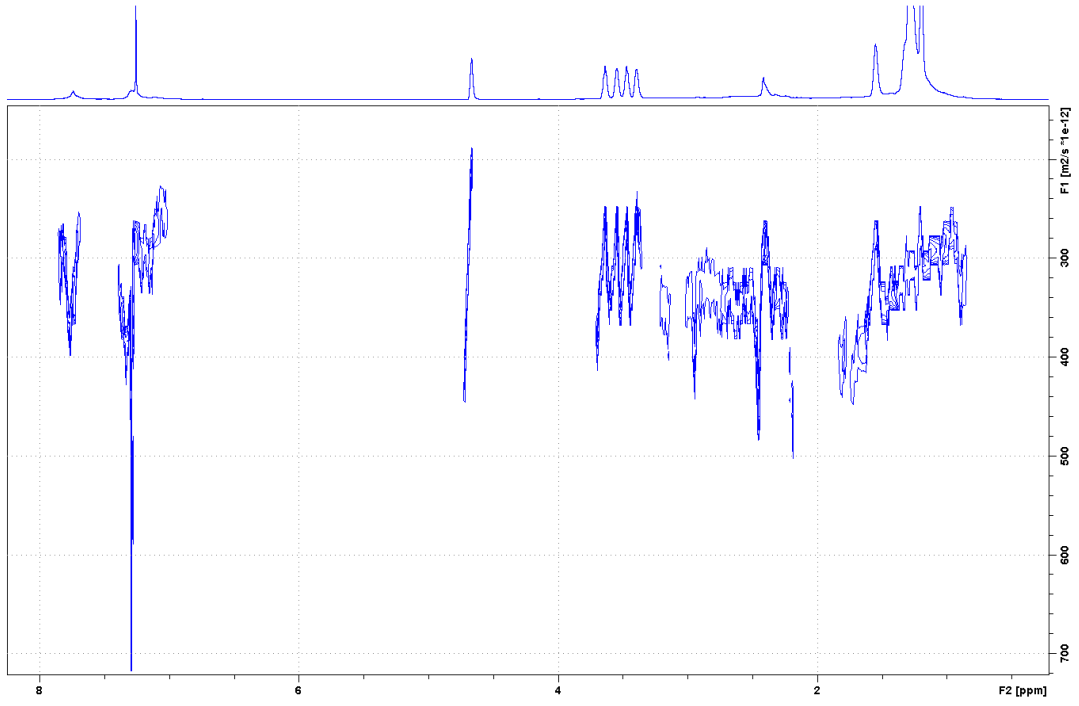

Figure S5.23b. DOSY ^{1}H NMR (700 MHz, 298 K, $CDCl_{3,}$) of poly(2-((1-ethoxyethoxy)nonyl)-aziridine) (PNEEAz).

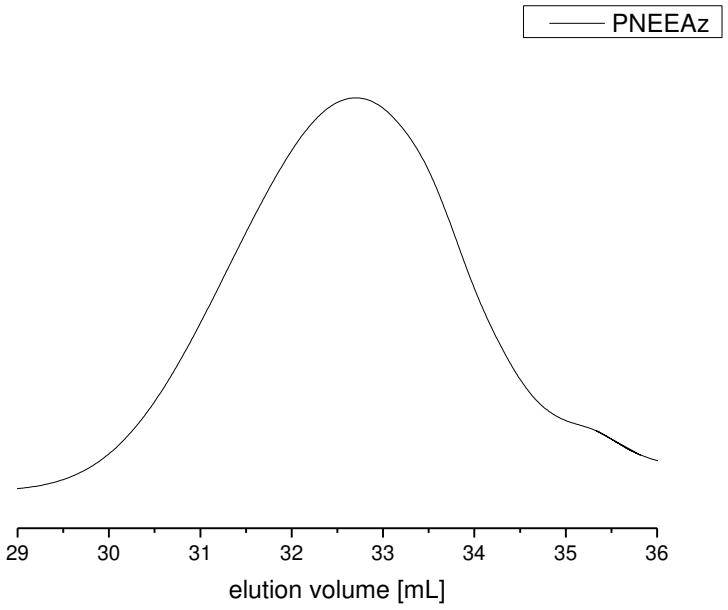

Figure S5.24. SEC traces of poly(2-((1-ethoxyethoxy)nonyl)-aziridine) (PNEEAz) in DMF (RI signal).

P(NOAz): Poly(2-aziridinenonanol) (P3-4-NH-OH)

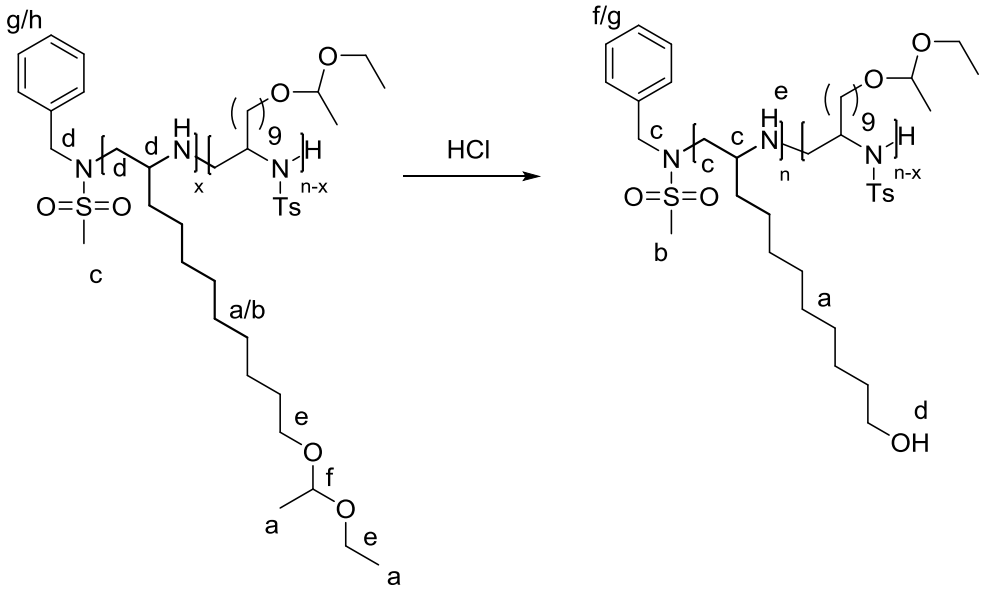

100 mg of the polymer were dissolved in 2 mL ethanol. One drop of water and 1 mL concentrated hydrochloride acid were added and stirred at 70 °C overnight. The solvents were removed at reduced pressure. The resulting brown solid was analyzed without further purification.

^{1}H NMR (250 MHz, 298 K, chloroform-*d*): δ 7.65 – 7.51 (m, g), 7.34 – 7.15 (m, f), 3.90 – 3.57 (m, e), 3.28 – 3.10 (m, d), 4.40 – 2.53 (m, c), 2.26 - 2.15 (m, b), 1.37 – 0.56 (m, a).

SEC (RID, DMF, PEO): M_n = 900; $Đ$ = 2.01

DSC: T_g = -7 °C

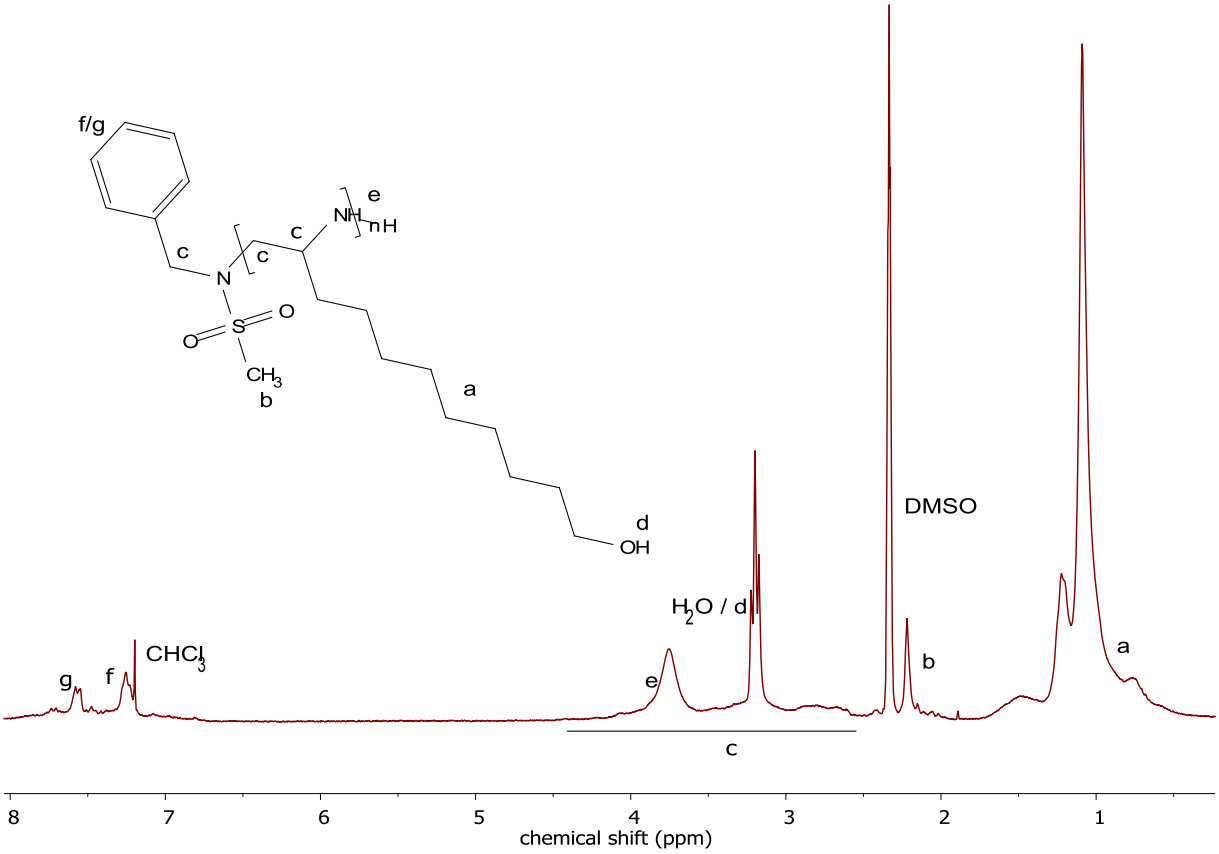

Figure S5.25a. ^{1}H NMR (250 MHz, 298 K, $CDCl_3$) of poly(2-aziridinenonanol) (PNOAz).

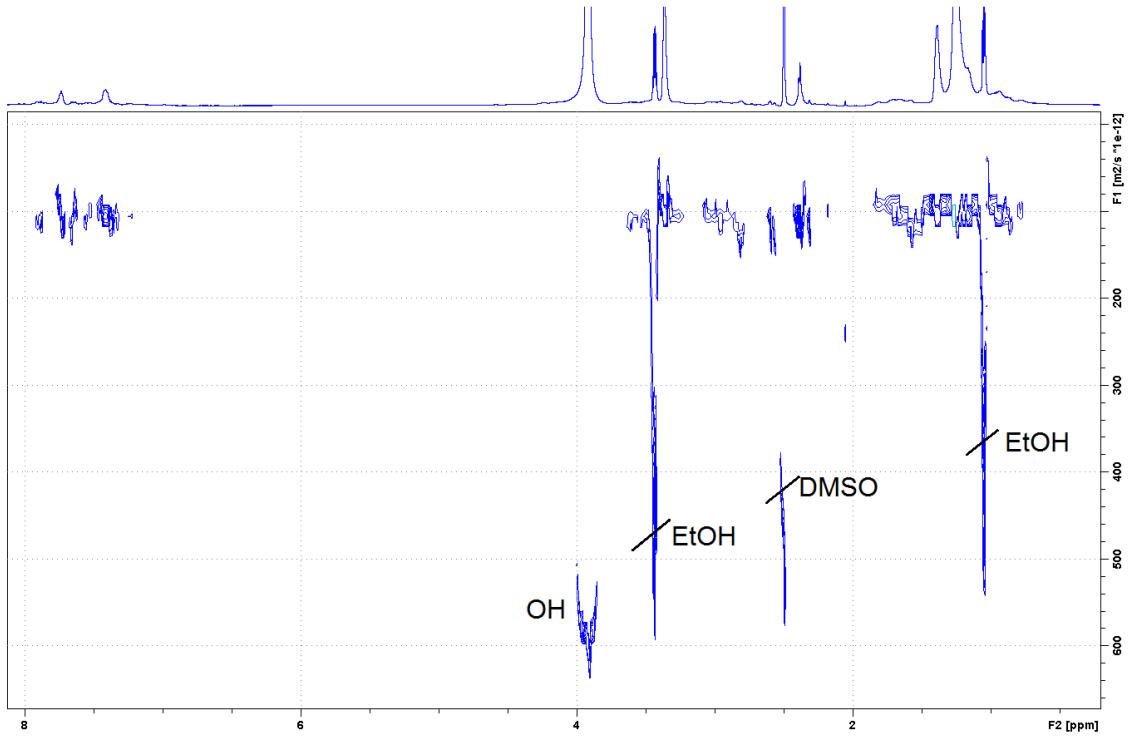

Figure S5.25b. DOSY ^{1}H NMR (700 MHz, 298 K, $CDCl_3$) of poly(2-aziridinenonanol) (PNOAz).

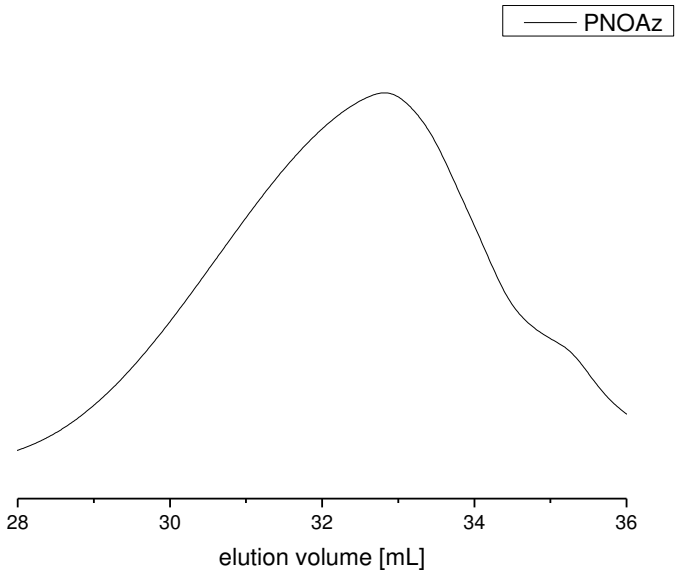

Figure S5.26. SEC traces of poly(2-aziridinenonanol) (PNOAz) in DMF (RI signal).

5.6.4 Polymerization kinetics.

All polymerizations were carried out in analogy to the conventional procedure in a Schlenk-flask. The monomers and the initiator were dissolved in 4 and 1.5 mL respectively anhydrous *N,N*-dimethylformamide (DMF). The mixture was stirred at 55 °C for 23 h. 100 µL-samples were taken in specific intervals and terminated with 50 µL degassed methanol and analyzed by GPC and ^{1}H NMR.

P(MEETsAz): Poly(2-((1-ethoxyethoxy)methyl)-N-tosylaziridine) (P1-2)

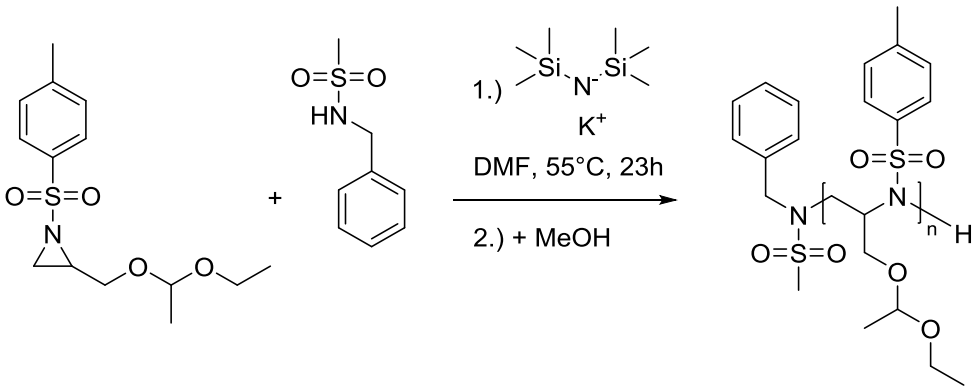

PMEETsAz$_{50(theo)}$: [MEETsAz (200.0 mg, 0.67 mmol), BnNHMs (2.47 mg, 13 µmol), KHMDS (2.67 mg, 13 µmol)].

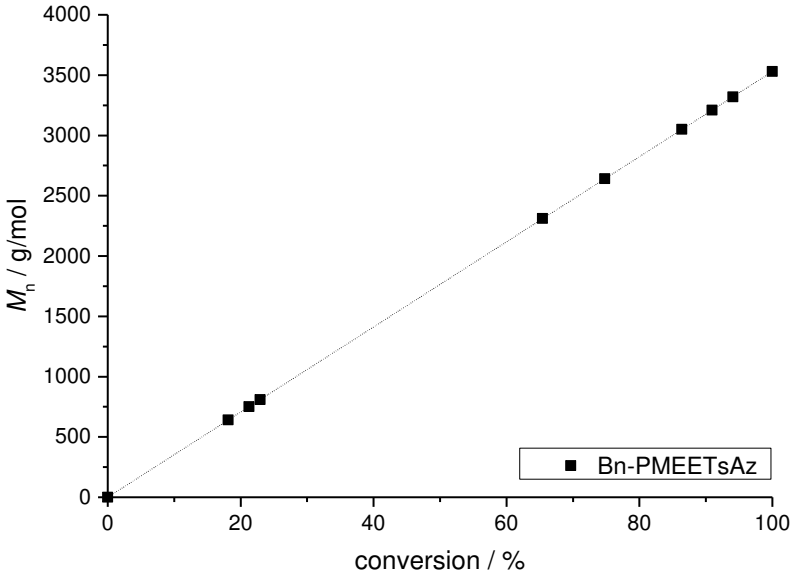

Figure S5.27. Kinetic studies; Plots of M_n *vs.* conversion of poly(2-((1-ethoxyethoxy)methyl)-N-tosylaziridine) (PMEETsAz) using BnNHMs as initiator.

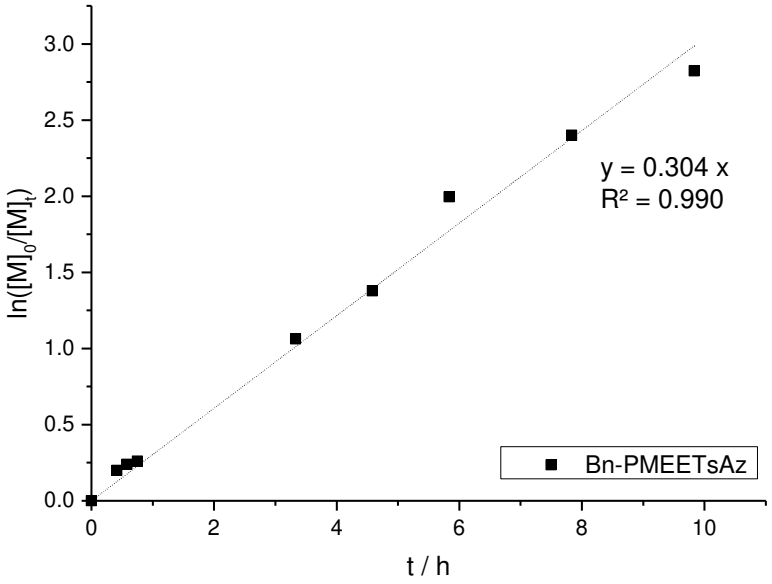

Figure S5.28. Kinetic studies; Plots of $\ln([M]_0/[M])$ *vs.* time of poly(2-((1-ethoxyethoxy)methyl)-*N*-tosylaziridine) (PMEETsAz) using BnNHMs as initiator.

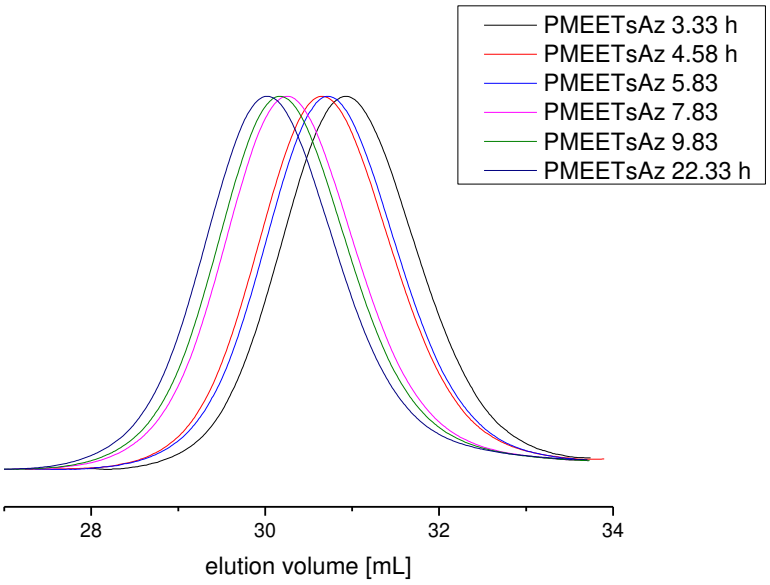

Figure S5.29. SEC traces of poly(2-((1-ethoxyethoxy)methyl)-*N*-tosylaziridine) (PMEETsAz) in DMF (RI signal) using BnNHMs as initiator.

P(MEETsAz): Poly(2-((1-ethoxyethoxy)methyl)-N-tosylaziridine) (P1-3)

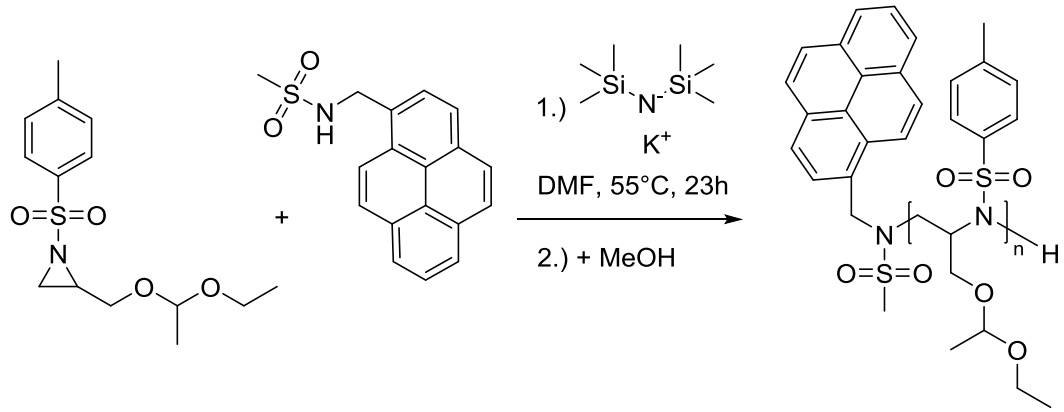

$PMEETsAz_{50(theo)}$: [MEETsAz (200.0 mg, 0.67 mmol), PyNHMs (4.13 mg, 13 µmol), KHMDS (2.67 mg, 13 µmol)].

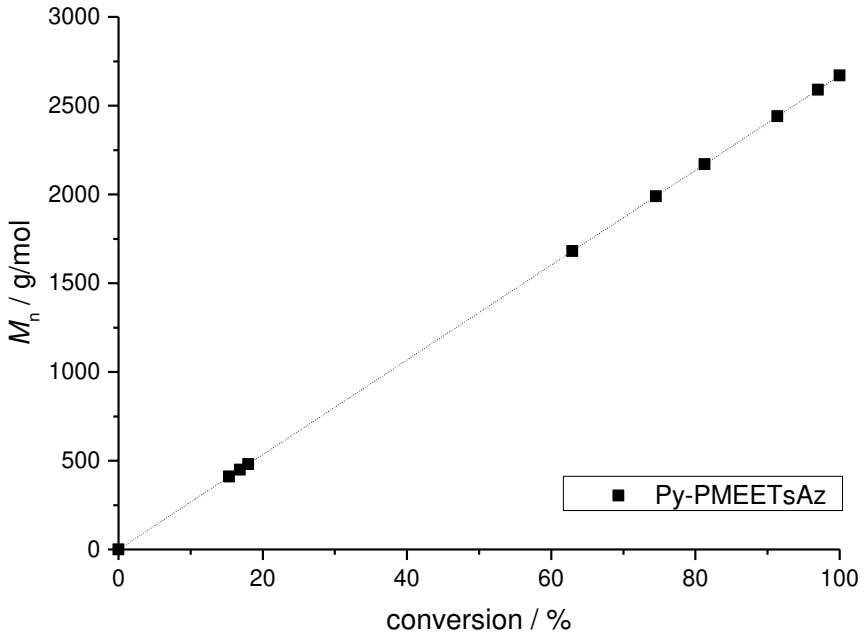

Figure S5.30. Kinetic studies; Plots of M_n *vs*. conversion of poly(2-((1-ethoxyethoxy)methyl)-*N*-tosylaziridine) (PMEETsAz) using PyNHMs as initiator.

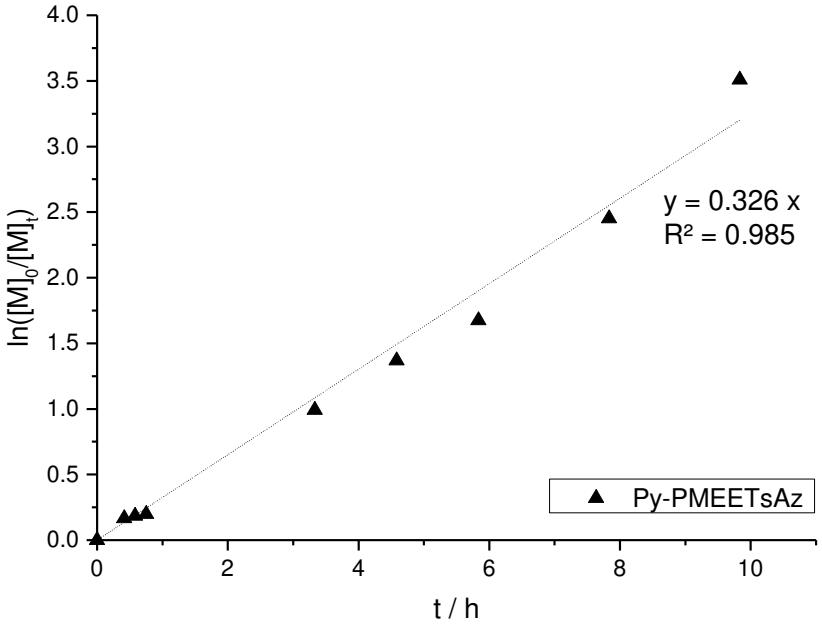

Figure S5.31. Kinetic studies; Plots of $\ln([M]_0/[M])$ *vs.* time of poly(2-((1-ethoxyethoxy)methyl)-*N*-tosylaziridine) (PMEETsAz) using PyNHMs as initiator.

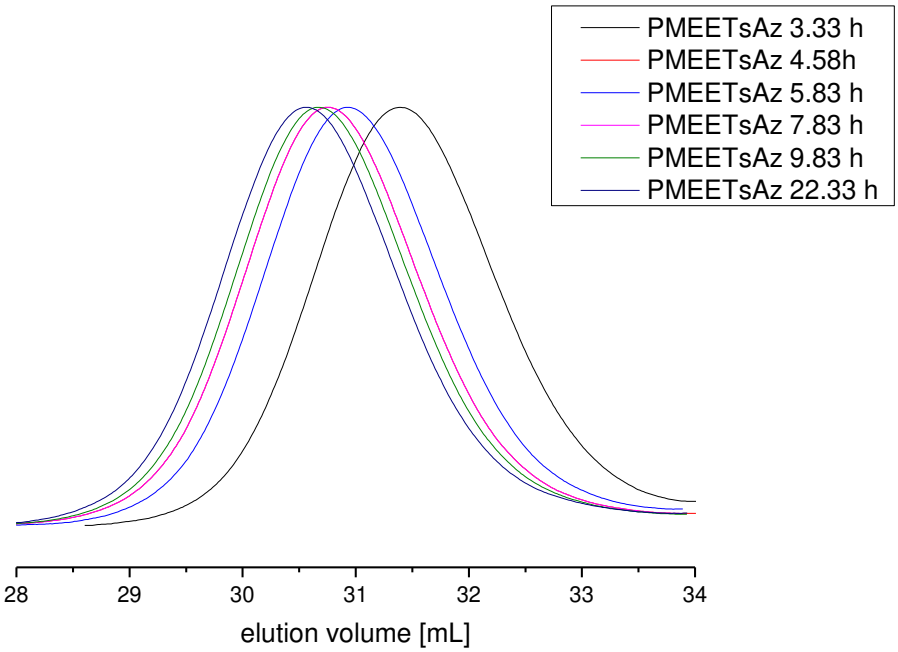

Figure S5.32. SEC traces of poly(2-((1-ethoxyethoxy)methyl)-*N*-tosylaziridine) (PMEETsAz) in DMF (RI signal) using PyNHMs as initiator.

5.6.5 Chain extension experiments.

All polymerizations were carried out in analogy to the conventional procedure in a Schlenk-flask. The first monomer and the initiator were dissolved in 2 mL anhydrous *N,N*-dimethylformamide (DMF) each. After stirring the mixture for 13 h at 55 °C, the second monomer, in 1 mL DMF, was added and stirred for further 24 h at 55 °C. To terminate the polymerization, 0.5 mL degassed methanol were added and the reaction mixture was precipitated in ca. 30 mL methanol.

P(MEETsAz-block-MEETsAz): Poly(2-((1-ethoxyethoxy)methyl)-N-tosylaziridine) (P1-4)

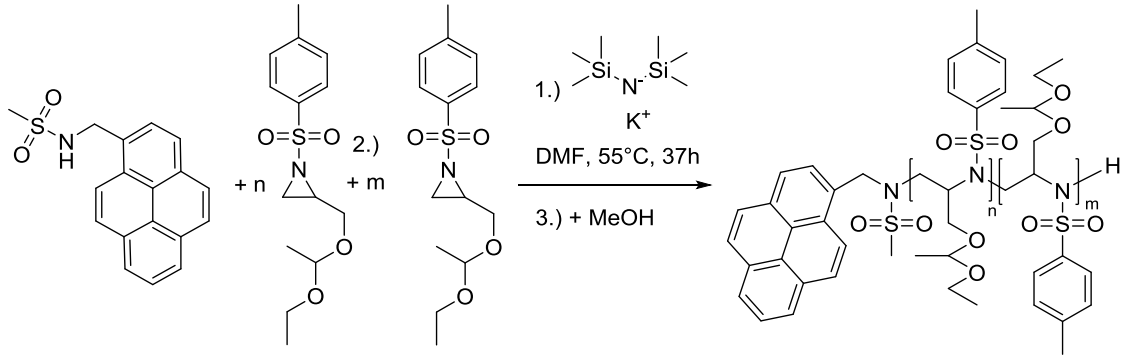

P(MEETsAz$_{30(theo)}$-*block*-MEETsAz$_{30(theo)}$): [1.) MEETsAz (200.0 mg, 0.67 mmol), 2.) MEETsAz (200.0 mg, 0.67 mmol), PyNHMs (6.89 mg, 22 µmol), KHMDS (4.44 mg, 22 µmol)].

1.) SEC (RID, DMF, PEO): M_n = 3200; $Đ$ = 1.19

1.) ^{1}H NMR: M_n = 6300 g/mol

2.) SEC (RID, DMF, PEO): M_n = 5000; $Đ$ = 1.25

2.) ^{1}H NMR: M_n = 14400 g/mol

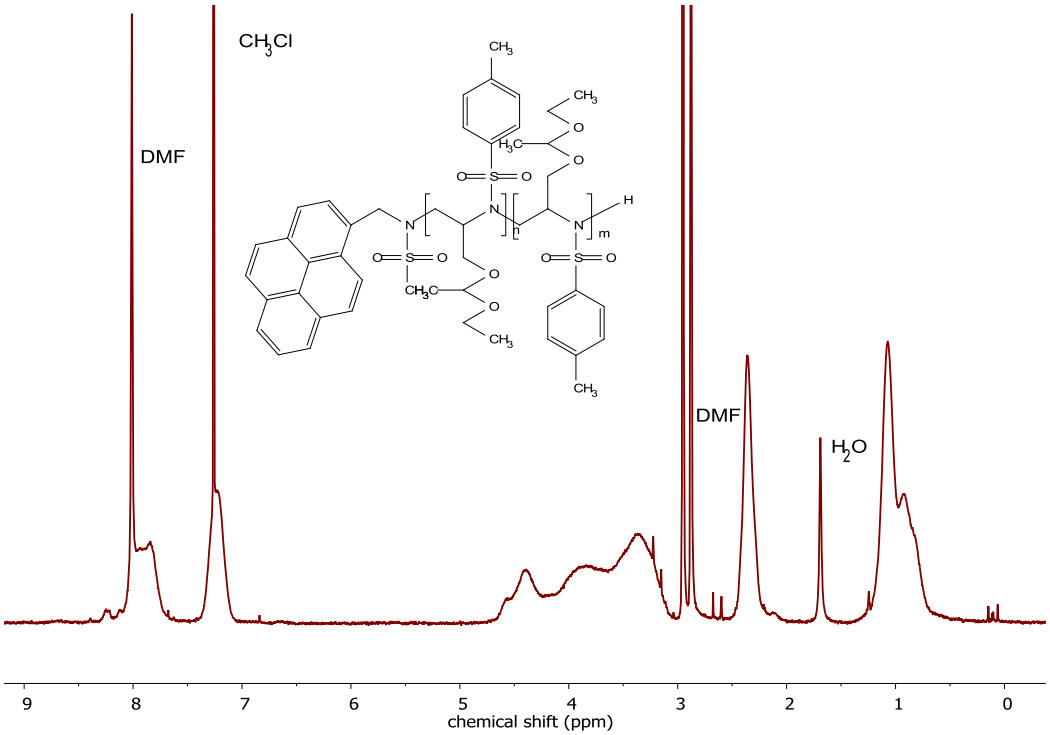

Figure S5.33. ^{1}H NMR (250 MHz, 298 K, $CDCl_3$) of poly(2-((1-ethoxyethoxy)methyl)-*N*-tosylaziridine)-*block*-(2-((1-ethoxyethoxy)methyl)-*N*-tosylaziridine))).

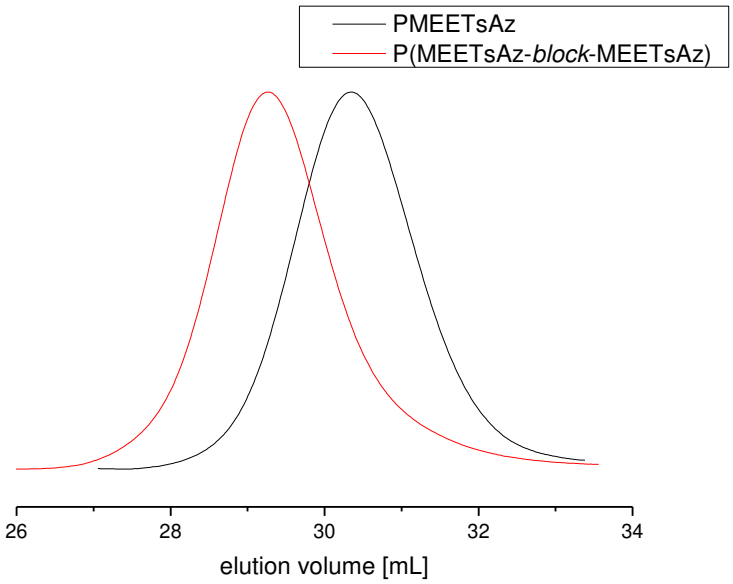

Figure S5.34. SEC traces of poly(2-((1-ethoxyethoxy)methyl)-*N*-tosylaziridine))) (PMEETsAz) in DMF (RI signal).

P(NEETsAz-block-MEETsAz): Poly(2-((1-ethoxyethoxy)nonyl)-N-tosylaziridine)-block-(2-((1-ethoxyethoxy)methyl)-N-tosylaziridine)) (P4)

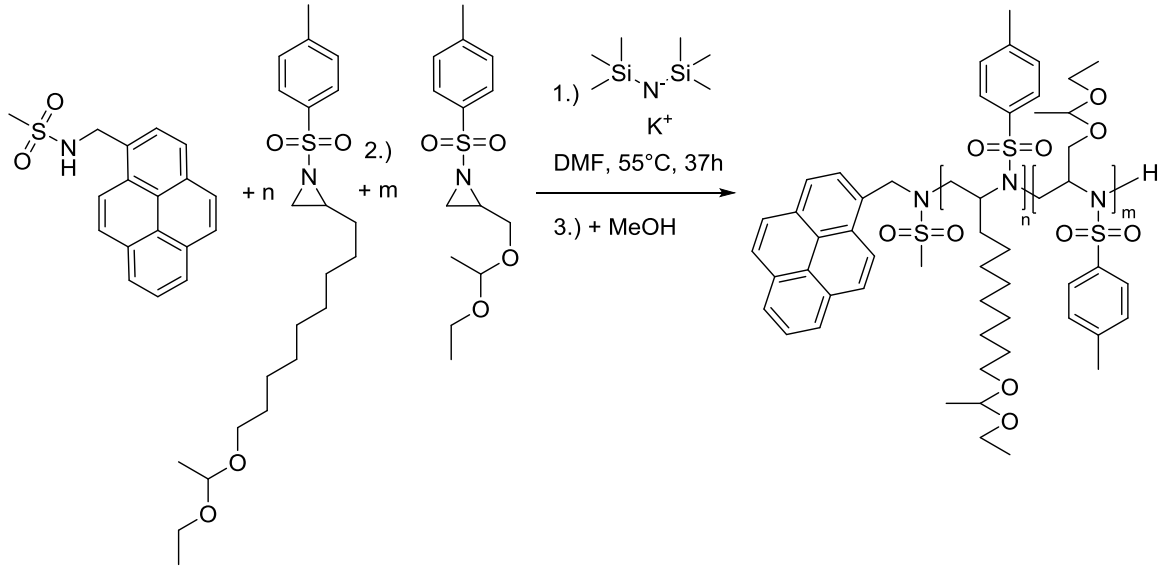

P(NEETsAz$_{20(theo)}$-*block*-MEETsAz$_{30(theo)}$): [1.) NEETsAz (200.0 mg, 0.49 mmol), 2.) MEETsAz (200.0 mg, 0.67 mmol), PyNHMs (6.89 mg, 22 µmol), KHMDS (4.44 mg, 22 µmol)].

1.) SEC (RID, DMF, PEO): M_n = 2400; $Đ$ = 1.15

1.) ^{1}H NMR: M_n = 5200 g/mol

2.) SEC (RID, DMF, PEO): M_n = 3600; $Đ$ = 1.20

2.) ^{1}H NMR: M_n = 9700 g/mol

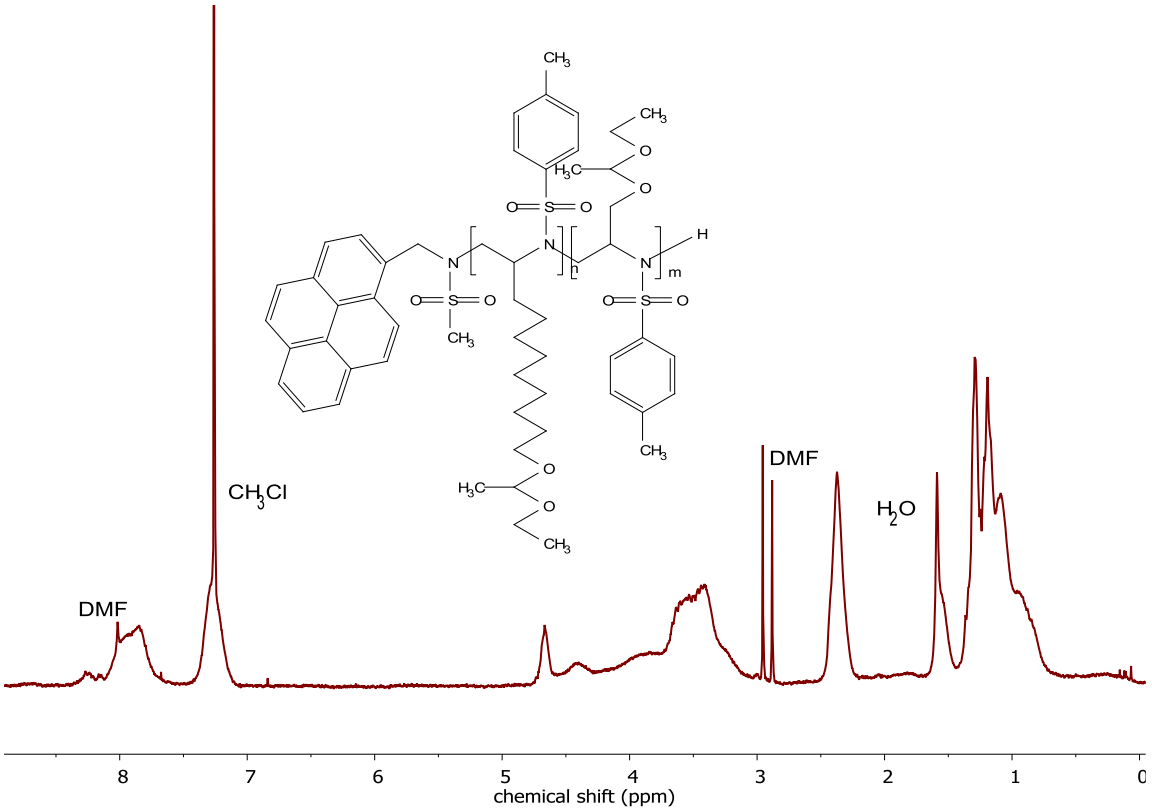

Figure S5.3. ^{1}H NMR (250 MHz, 298 K, $CDCl_3$) of poly(2-((1-ethoxyethoxy)nonyl)-*N*-tosylaziridine)-*block*-(2-((1-ethoxyethoxy)methyl)-*N*-tosylaziridine))).

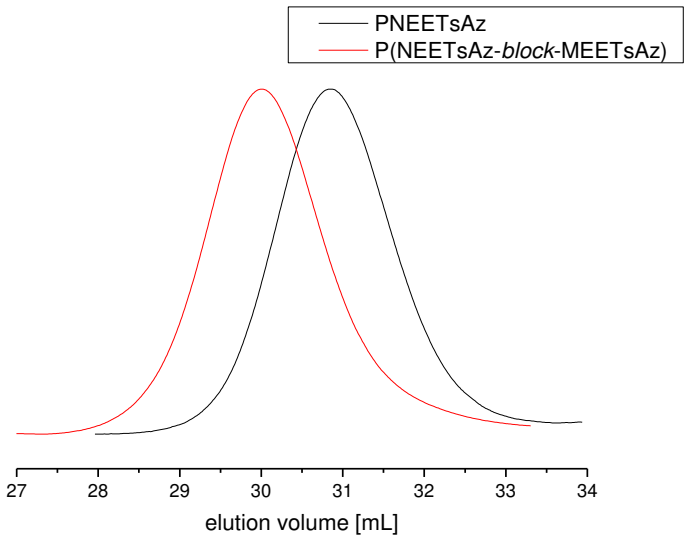

Figure S5.36. SEC traces of poly(2-((1-ethoxyethoxy)nonyl)-*N*-tosylaziridine) (PNEETsAz) and poly(2-((1-ethoxyethoxy)nonyl)-*N*-tosylaziridine)-*block*-(2-((1-ethoxyethoxy)methyl)-*N*-tosylaziridine)) in DMF (RI signal).

5.7 References

1. Szwarc, M.; Levy, M.; Milkovich, R., *J. Am. Chem. Soc.* **1956,** *78* (11), 2656-2657.
2. Tonhauser, C.; Frey, H., *Macromol Rapid Commun* **2010,** *31* (22), 1938-1947.
3. Baskaran, D.; Müller, A. H. E., *Anionic Vinyl Polymerization*. WILEY-VCH Verlag GmbH & Co. KGaA, Weinheim: **2009**.
4. Hirao, A.; Goseki, R.; Ishizone, T., *Macromolecules* **2014,** *47* (6), 1883-1905.
5. Higashihara, T.; Hayashi, M.; Hirao, A., *Progress in Polymer Science* **2011,** *36* (3), 323-375.
6. Obermeier, B.; Wurm, F.; Mangold, C.; Frey, H., *Angewandte Chemie Int. Ed. Engl.* **2011,** *50* (35), 7988-7997.
7. Natalello, A.; Alkan, A.; von Tiedemann, P.; Wurm, F. R.; Frey, H., *ACS Macro Letters* **2014,** *3* (6), 560-564.
8. Thomas, A.; Müller, S. S.; Frey, H., *Biomacromolecules* **2014,** *15* (6), 1935-54.
9. Fitton, A. O.; Hill, J.; Jane, D. E.; Millar, R., *Synthesis communications* **1987**, 1140-1142.
10. Mangold, C.; Wurm, F.; Frey, H., *Polymer Chemistry* **2012,** *3* (7), 1714-1721.
11. Taton, D.; Le Borgne, A.; Sepulchre, M.; Spassky, N., *Macromol. Chem. Phys.* **1994,** *195*, 139-148.
12. Tauhardt, L.; Kempe, K.; Knop, K.; Altuntaş, E.; Jäger, M.; Schubert, S.; Fischer, D.; Schubert, U. S., *Macromolecular Chemistry and Physics* **2011**, *212* (17), 1918-1924.
13. Jaeger, M.; Schubert, S.; Ochrimenko, S.; Fischer, D.; Schubert, U. S., *Chem. Soc. Rev.* **2012,** *41* (13), 4755-4767.
14. Monnery, B. D.; Hoogenboom, R., Synthesis and Properties of Polyalkylenimines. In *Cationic Polymers in Regenerative Medicine*, Royal Society of Chemistry: London, **2015**; 30-61.
15. Jang, H.-J.; Lee, J. T.; Yoon, H. J., *Polymer Chemistry* **2015,** *6* (18), 3387-3391.
16. Suzuki, T.; Kusakabe, J.-i.; Ishizone, T., *Macromolecules* **2008,** *41*, 1929-1936.
17. Lava, K.; Verbraeken, B.; Hoogenboom, R., *European Polymer Journal* **2015,** *65*, 98-111.
18. Stewart, I. C.; Lee, C. C.; Bergman, R. G.; Toste, F. D., *Journal of the American Chemical Society* **2005,** *127* (50), 17616-17617.
19. Thomi, L.; Wurm, F. R., *Macromolecular Rapid Communications* **2014,** *35* (5), 585-589.
20. Thomi, L.; Wurm, F. R., *Macromolecular Symposia* **2015,** *349* (1), 51-56.
21. Jeong, J. U.; Tao, B.; Sagasser, I.; Henniges, H.; Sharpless, K. B., *Journal of the American Chemical Society* **1998,** *120*, 6844-6845.
22. Wurm, F.; Nieberle, J.; Frey, H., *Macromolecules* **2008,** *41*, 1184-1188.
23. Dingels, C.; Wurm, F.; Wagner, M.; Klok, H. A.; Frey, H., *Chemistry* **2012,** *18* (52), 16828-16235.

6. Living Anionic Polymerization of Aziridines Tolerates the Presence of Water and Alcohols

Elisabeth Rieger,[1] Tassilo Gleede,[1] Lei Liu,[1] Camille Bakkali-Hassani,[2] Manfred Wagner,[1] Stéphane Carlotti,[2] Daniel Taton,[2] Denis Andrienko,[1] Frederik R. Wurm[1]

[1]*Max Planck Institute for Polymer Research, Ackermannweg 10, 55128 Mainz, Germany*
[2]*Laboratoire de Chimie des Polymères Organiques (LCPO), Université de Bordeaux, IPB-ENSCBP, 16 av. Pey Berland, 33607 PESSAC cedex, France*

Unpublished results

Elisabeth Rieger and Tassilo Gleede are first authors. Lei Liu made the DFT-calculations. MALDI-TOF spectra were measured by Camille Bakkali-Hassani. NMR kinetic measurements were performed in collaboration with Manfred Wagner.

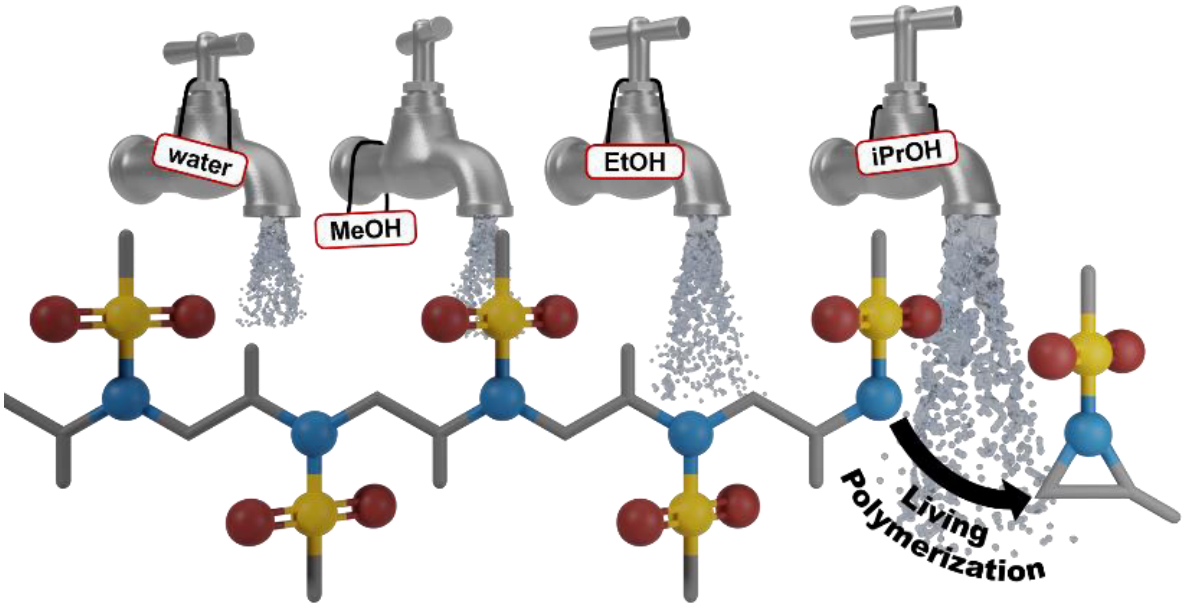

Keywords: Sulfonamides, Azaanionic, Nucleophilicity, Kinetics, Controlled Polymerization Anionic Polymerization.

6.1 Abstract

Living anionic polymerization gives access to well-defined polymers, but demands strict purification of reagents and solvents. This work presents the azaanionic polymerization of aziridines as a robust living polymerization technique, with the ease of controlled radical polymerizations. Anionic polymerization of activated aziridines retains its living character in the presence of large excess of protic contaminations (water, methanol, ethanol, isopropanol) and does not require inert atmosphere. The polymerization of mesyl-, tosyl-, and brosyl-activated aziridines was studied in the presence of up to 1000 eq. of the respective additives. The living nature of the polymerization was retained with up to 100 fold excess of a protic impurity with, in most cases, negligible amount of secondary initiation. This allows the preparation of polyols by anionic polymerization without protective groups, as only minor initiation occurs from the alcohols. The reason of the tolerance against protic additives lies in the electron withdrawing effect of the activating groups, decreasing the basicity of the propagating species, while maintaining a strong nucleophilic character. In this way, competing alcohols and water are only slightly involved in the polymerization.

6.2 Introduction

Living anionic polymerization (LAP) is still the polymerization technique with the highest control of molecular weights, chain-end fidelity, and narrow molecular weight distributions.[1-2] However, the strict avoidance of protic impurities (and oxygen in many cases) makes the preparation of well-defined (co)polymers by anionic techniques tedious and time-consuming.[3-4] Thorough drying of reagents and solvents, high-vacuum techniques and inert gas purifications made anionic polymerization unattractive compared to the much easier to conduct controlled radical polymerizations, which cannot compete in terms of precision or the introduction of heteroatoms in the polymer backbone with the LAP.[5-6]

We present the first living anionic polymerization that proceeds in open air and in the presence of large amounts of protic impurities (water and alcohols). The azaanionic ring-opening polymerization (A-AROP) was chosen as a unique technique to access well-defined polysulfonamide- or polyamine-structures (Scheme 6.1). The great tolerance towards water and alcohols during the polymerization further allows the preparation of polyols by living anionic polymerization avoiding any protective groups for the first time.

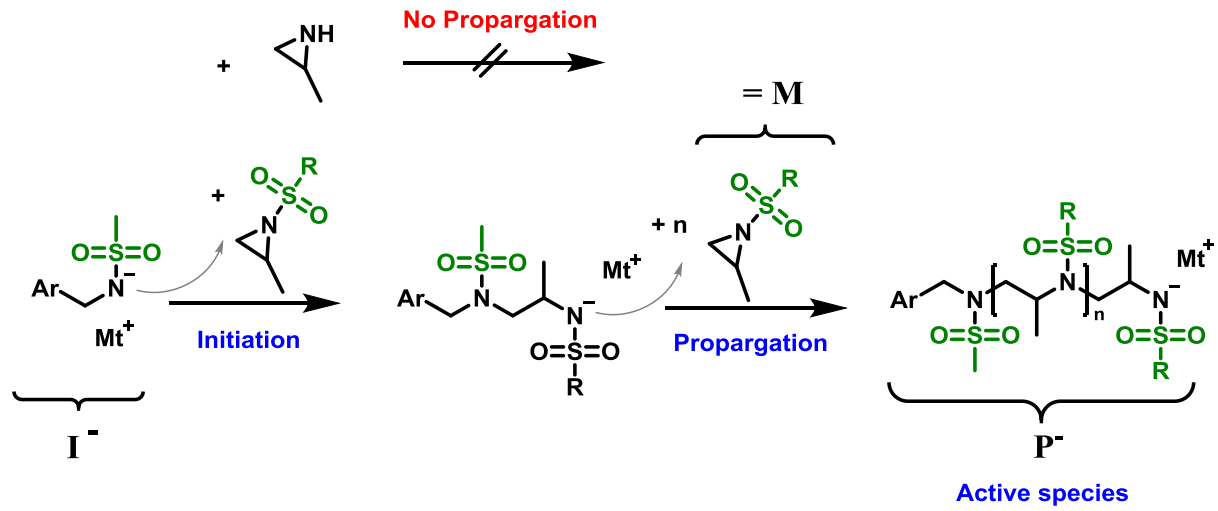

I⁻ = Initiator
→ Ar (Aromat) = -Pyrene (PyNHMs) (4), -Ph (BnNHMs) (5)
Mt^+ = Counter ion (Li^+, K^+)
M = Monomer
→ -SO_2R = -Mesyl (Ms) (1), -Tosyl (Ts) (2), -Brosyl (Bs) (3)

Scheme 6.1. Mechanism of azaanionic polymerization of sulfonamide-activated aziridines.

Polysulfonamides, prepared from the A-AROP of sulfonyl-activated aziridines, have continuously gained importance since they had been first polymerized *via* living polymerization in 2005 (Scheme 6.1).[7] In the last decade, the monomer family was growing constantly[8-9] and several methods were developed to polymerize sulfonamides, namely organocatalyticaly,[10-12] *via* anionic polymerization in solution[13-15] or in emulsion;[16] all techniques require inert gas atmosphere and dry conditions. After cleavage of the sulfonyl groups this polymer family offers an alternative pathway to linear polyethylene imine (LPEI),[14, 17] which is together with (*hb*PEI) (hyperbranched PEI) the standard for synthetic cationic transfection agents.[18-21] The cationic ROP of aziridine only leads to statistically *hb*PEI with broad molecular weight distributions.[22] In contrast, LPEI is prepared by cationic ring-opening polymerization (CROP) of oxazolines, but suffers from termination and side reactions, leading to less controlled polymers. Lower molecular weight polymers usually contaminate LPEI.[23]

Compared to CROP, the AROP of sulfonyl aziridines with multiple functional- and activating groups is a powerful alternative to classical literature protocols to polyamines. The activating groups allowed us to influence the microstructure of co-polymers,[15] but they also regulate the nucleophilicity and basicity of the active chain end, which is a direct handle towards tolerating additives, protic solvents or nucleophilic functionalities in the monomers.

In contrast, carbanionic polymerizations are terminated by minor amounts of moisture, protic solvents or CO_2.[24] As the living chain end in oxyanionic polymerization is less basic than a carbanion, protonation of the active chain end leads to a reversible termination with very fast

proton exchange.[25-26] Full monomer conversion is still obtained, but nucleophilic impurities can act as initiator and thus produce side-products of typically lower molecular weight.[27] Importantly, protic impurities at concentrations above the initiator concentration would inhibit the propagation, which makes protecting groups, e.g. for alcohols, essential.

A robust anionic polymerization which tolerates protic solvents, especially water, while maintaining the living character is not known. To elegantly circumvent the demanding conditions of anionic polymerization, emulsion polymerization is the only technique allowing the performance of ionic polymerizations in protic solvents, as they exploit the hydrophobic nature of monomers and polymers to separate the active chain end from the protic aqueous phase. The polymerization takes place at the interface or inside of the hydrophobic dispersed phase. However, anionic emulsion polymerization typically cannot suppress termination or transfer reactions which was reported for the aqueous emulsion polymerization of cyclic siloxanes[28-29] or phenyl glycidyl ether (PGE), leading to low molecular weight products with low control over dispersity.[30] Similar approaches of anionic polymerizations like *α*-carbonyl acids[31] in basic water or the preparation of polyglycidol in the presence of water[32] bypass the typical anionic polymerization mechanism e.g. by monomer-activation.

Herein, we systematically investigate the influence of protic additives, that are water and different alcohols (methanol (MeOH), ethanol (EtOH), isopropanol (iPrOH)) on the azaanionic polymerization of different sulfonyl aziridines. Even at large excess of the protic impurity (more than 100 eq. compared to the initiator), the AROP of sulfonyl aziridines leads to quantitative monomer conversion and retains excellent control over molecular weight and size distribution. We chose three different monomers, in order of their increasing propagation rates and different nucleophilicity of the chain end: 2-methyl-*N*-mesyl-aziridine (MsMAz, 1) 2-methyl-*N*-tosylaziridine (TsMAz, 2), 2-methyl-*N*-brosylaziridine (BsMAz, 3) (Scheme 6.1 and 6.2).[15]

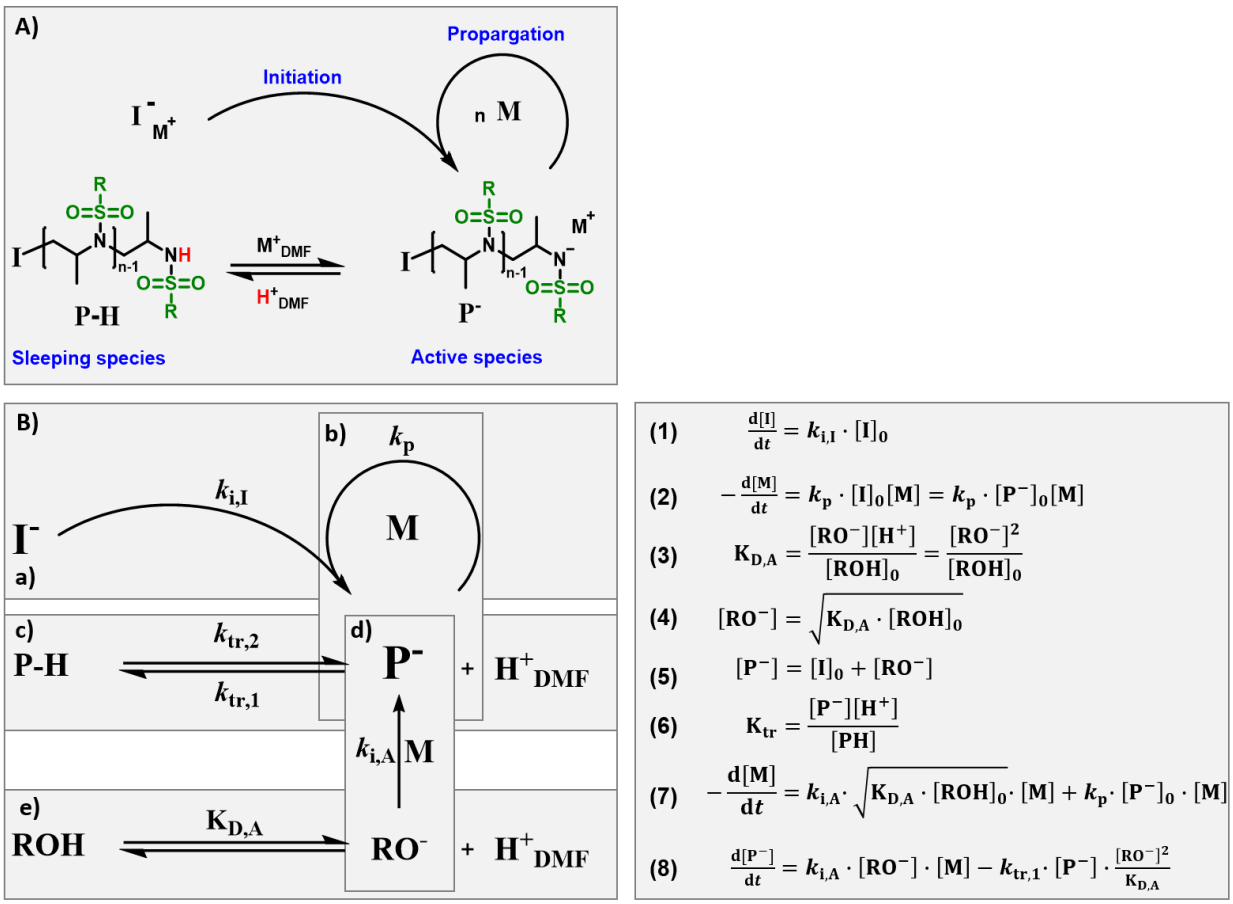

Scheme 6.2. Schematic overview of the A-AROP with additives and corresponding equations. A) Mechanism of A-AROP, including the proposed sleeping polymer species (P-H). B) Simplified scheme including the involved protic species (ROH), followed by their equations.

Scheme 6.2B shows a proposed, schematic mechanism for the azaanionic polymerization with protic additives, including a dormant species: boxes a) and b) illustrate the initiation ($k_{i,I}$) and propagation (k_p) of the polymerization. For a living polymerization,[27] the initiation needs to be faster than the propagation ($k_{i,I} \gg k_p$), resulting in first-order kinetics, therefore, equation (1) can be neglected. Additionally, every initiator (I) starts a growing chain (P^-), the starting initiator-concentration $[I]_0$ is equal to $[P^-]_0$, resulting in the overall equation (2) for the reaction kinetics.[13] This set of equations is expanded, when protic additives (ROH) are introduced that take part in deprotonation equilibria, depending on their respective pK_a-value ((Scheme 6.2 (e), equation 3). The concentration of the competing nucleophiles (RO^-), which act as secondary initiator, is given in equation (4) and illustrated in Scheme 6.2 (d). Due to the strong nucleophilic character of deprotonated additives, very fast initiation is expected ($k_{i,A} \gg k_p$). The concentration of propagating chain ends would than increase to $[P^-]$, (equation 5). Consequently, protons (H^+) from the additives will form a dormant species of the original living chain end (PH) (Scheme 6.2 (c)). Equation (6) illustrates, the equilibrium between active and dormant species

highly depends on the amount of protons, which are only released by additives. To fully describe the system, the monomer consumption and the chain concentration of the active chain ends are expressed in equation (7 and 8).

6.3 Results and discussion

To control the polymerization of sulfonyl aziridines, all previously published articles highlighted the necessity to strictly avoid moisture, impurities and the protection of nucleophilic groups. Preparation of the experiment and the polymerization were thus conducted in a glovebox or with Schlenk techniques under inert gas.[10-11, 13-14] Concerning their water content, an *in situ* distillation from elemental sodium or calcium hydride is established for anionic polymerization, but it is known that some solvents are difficult to dry efficiently.[4, 26] A method that sustains the presence of protic compounds is necessary. In 1988, Boileau and coworkers were able to show that the LAP of *α*-Methyl-*α*-*n*-propyl-*β*-propiolactone can sustain the presence of water.[33] Also cyanoacrylates are known to polymerize in the presence of moisture[34] or in emulsion,[35-37] due to their fast propagation rates. This, however, uncontrolled polymerization can be explained by the strong electron withdrawing effect of the CN-group, which increases the monomer electrophilicity and reduces the chain-end nucleophilicity significantly. The tolerance of the active chain end in an anionic polymerization towards nucleophilic impurities (such as water or alcohols) strongly depends on the pK_b-value of the growing chain end and the propagation rate constants. For sulfonyl-aziridines, both factors can be tuned precisely by the choice of the activating group that influences the basicity of the azaanionic chain end, but at the same time also the propagation rates and thus controls the chance of initiation of protic impurities in the reaction mixture.

We found that polymerizations can also be carried out in open vials. The polymerization of MsMAz (1) and TsMAz (2) conducted in an open glass vial in DMF (without any purification or drying), resulting in narrowly distributed PAz ($Đ \leq 1.11$), which remained living and allowed further chain extension, proving the living nature under such wet conditions, without recognizable initiation of water (Figure S6.36 and SI, 6.6.6). Additionally, the AROP of 2 followed living characteristics in reactive solvents, which would inhibit other anionic polymerizations (P(TsMAz)$_{50}$, in acetone ($Đ$ =1.16), ethyl acetate ($Đ$ = 1.18) and iPrOH ($Đ$ = 1.23)). The narrow molecular weight distributions from the polymers prepared in open air or such solvents prove that the A-AROP is unaffected by CO_2 and O_2 remains living in “exotic” solvents for anionic polymerization (Figure S6.25, S6.30, S6.31).

In order to understand the influence of chain-end and monomer reactivity on the control of the A-AROP, (1) and (2) were polymerized in the presence of protic additives. Different amounts (1 eq. – 1000 eq. compared to the initiator) of water (H_2O), methanol (MeOH), ethanol (EtOH)

and isopropanol (iPrOH), which usually act as transfer agents or inhibitors for other anionic polymerizations, were added to the polymerization. The maximum amount of each additive was limited due to the solubility of the polymers in polar solvent mixtures (see Experimental for details). However, if the amounts of water were increased to 1170 eq. for (2) and 740 eq. for (1) a significant reduction in the molecular weight of the final polymer was detected, indicating a non-negligible amount of initiation by the additive (Figure S6.22, S6.27). In all cases, chain extension experiments with additives were performed (90 – 360 equivalents depending on the solvent), proving that the chain ends remained reactive for further monomer addition with reasonable final dispersities ($Đ \leq 1.25$). (see SI, 6.6.6, Figure S6.38 - S6.41).

Taking a closer look at the two monomers 1 and 2, TsMAz (2) with its stronger electron withdrawing group, demonstrated a higher tolerance to the presence of the additives, as propagation rates are fivefold faster compared to MsMAz (compare Figure S 6.22 – S 6.25 for (1) and Figure S 6.26 – S 36.0 for (2)).

The influence of counter ions (K^+, Li^+) was also studied with all additives tested, showing no significant difference, both show full monomer conversion and low molecular weight distributions ($Đ < 1.25$, compare Figure S6.26 – S6.30, S6.32, S6.33).

In order to assess the polymerization kinetics and to quantify the PAz, initiated by the additive, we conducted real-time ^{1}H NMR spectroscopy of the polymerizations of 1, 2, and BsMAz (3) in the presence of ^{13}C-labeled alcohols. In Figure 6.1, the polymerization kinetics of 2 are summarized, proving a slight influence of the protic additives on the overall reaction rates. Within the presence of 100 eq. of isopropanol (green) almost the same k_p-value was determined as for the polymerization in dry DMF (black) without any additive. However, propagation rates decreased in the presence of ethanol (orange), water (blue) and methanol (red), probably due to an increased concentration of initiating species from the additives. Nevertheless, in all cases, PAz with molecular weights close to the theoretical value and narrow molecular weight distributions were obtained (Table 6.1), (Figure 6.1b).

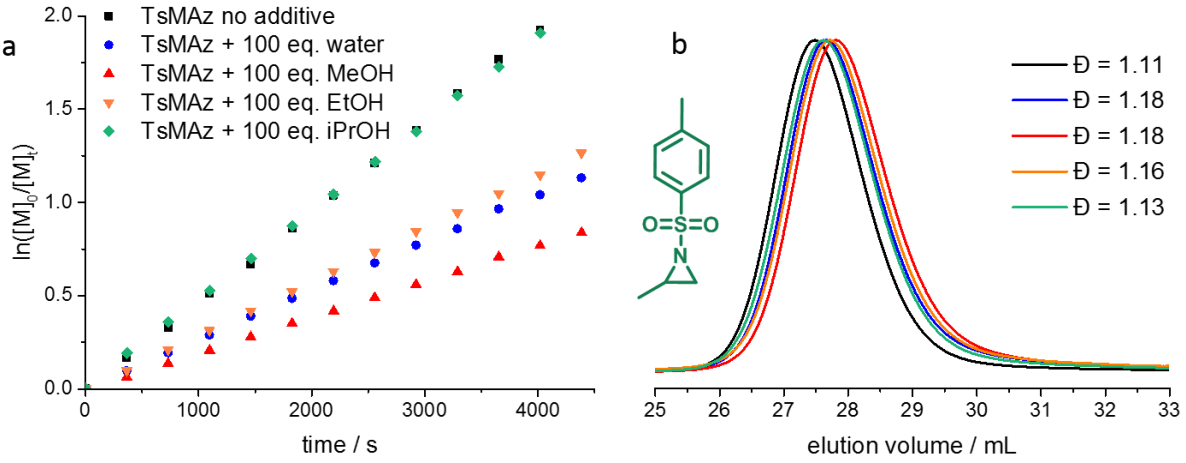

Figure 6.1. a) Kinetic plots of $\ln([M]_0/[M]_t)$ *vs.* time of TsMAz (2) and different additives in DMF-d_7 at 50 °C. b) SEC traces in DMF (RI signal) (data listed in Table **6.1**).

Table 6.1. Overview of the polymerization kinetics of TsMAz (2) in DMF-d_7 with the respective additive, including SEC-analyses and calculated propagation rates (k_p).

Monomer	TsMAz (2)	TsMAz (2)	TsMAz (2)	TsMAz (2)	TsMAz (2)
Additive	Pure	H_2O	MeOH	EtOH	iPrOH
k_p / 10^{-3} L mol^{-1} s^{-1}	**49.9±3.6**	**28.1±2.0**	**22.9±1.4**	**29.6±2.1**	**48.6±3.5**
M_n[a] / g mol^{-1}	5500	4700	4400	4800	5100
$Đ$[a]	1.11	1.18	1.18	1.16	1.13
Reaction time / h	2.6	5.5	9.4	4.7	2.8
Conversion / %	>99	>99	>99	>99	>99

[a] Number-average molecular weight and molecular weight dispersities determined via SEC in DMF (*vs.* PEO standards).

Table 6.1 summarizes the data from the real-time NMR measurements of TsMAz. The trend observed from the kinetic plots in Figure 6.1a is reflected in the propagation rates (k_p), that range between 22.9±1.4 · 10^{-3} L mol^{-1} s^{-1} for methanol to 49.9±3.6 · 10^{-3} L mol^{-1} s^{-1} for the pure reaction mixture. Also reaction times from 2.6 h (pure) to 9.4 h (MeOH) for full conversion, indicate the presence of the dormant species, as the protonation of the chain end is reversible (Scheme 6.2). This trend is also confirmed by a slight decrease of M_n -values and an increase of the molecular weight dispersities, indicating a second initiation process. Notably, iPrOH as a secondary alcohol does not influence the k_p-value, with only a minor influence on M_n or $Đ$.

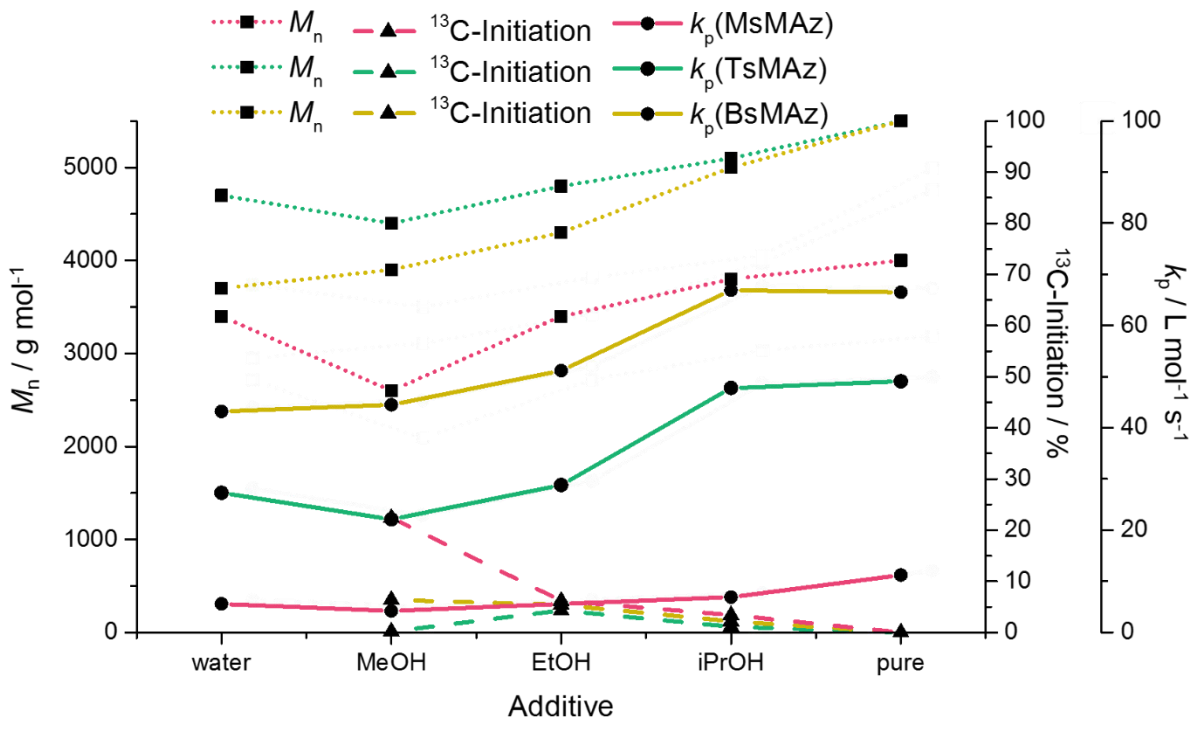

Figure 6.2. Comparison of the molecular weights (M_n) (dotted line, squares, left y-axis), amount of ^{13}C-initiation (dashed line, triangles, first right y-axis) and propagation rates (k_p) (solid line, points, right y-axis) of all online NMR-kinetics of the three monomers MsMAz (1, red), TsMAz (2, green) and BsMAz (3, yellow) with the respective additives (pure, water, MeOH, EtOH, iPrOH).

For the other two monomers (1 and 3), similar trends were observed (cf. SI, 6.6.2). A comparison of their propagation rates (k_p) in Figure 6.2 (solid line, points) depicts, that the general reactivity of the monomers to one another increases from MsMAz (1, red) to TsMAz (2, green) to BsMAz (3, yellow), as reported earlier.[15]

The trend of decreasing molecular weights (M_n) (Figure 6.2, dotted line, squares) is in strong accordance to the decreasing propagation rates, which is contributed to the second initiation of the additives. MALDI-TOF-spectra of P(TsMAz), polymerized in the presence of 100 equivalents of additives (H_2O, MeOH, EtOH, iPrOH) (compare Supporting Information, 6.6.5), show a narrowly distributed main fraction of the PAz, initiated with the sulfonamide initiator. In all cases a smaller second fraction can be identified as TsMAz, initiated by the additives. As MALDI is not quantitative, we used ^{13}C NMR to quantify the ether signal of ^{13}C-labeled alcohols, used as additives. HSQC-spectra proved the existence of ^{13}C-labeled ether (see SI, 6.6.3). Distinctive ^{13}C-ether resonances below 10% (except for MsMAz with MeOH as additive) were detected, as depicted in Figure 6.2 (dashed line, triangles) and summarized in Table S6.3. TsMAz (2) is the most tolerant monomer, as all ^{13}C-ether signals are below the quantification limit of NMR-spectroscopy (≤1%), determined by a high signal / noise ratio (S/N). For all three monomers, the

signals of ^{13}C-isopropyl ether are also below the quantification limit of NMR-spectroscopy, showing a negligible amount of initiation for this secondary alcohol. The more acidic and nucleophilic the additive, the higher the amount of secondary initiation.

Such amounts of “undesired” initiation can be circumvented by working under absolute inert conditions as typical for anionic polymerizations, however compared to controlled radical polymerizations were sometimes also up to 10% of all chain ends are undesirably initiated, not including “dead” polymers by termination,[38-40] we believe the ease of reaction conditions makes the AROP of aziridines an attractive alternative. In most cases quantified, the secondary initiation was also below 10%, (MsMAz with MeOH around 22%), but without “dead” polymers for this LAP. The highest percentage of secondary initiation is demonstrated for MsMAz (1), as its slow reaction kinetics allows also the slow initiation of alkoxides occurs simultaneously. Whereas, BsMAz (3) (the most reactive monomer), reveals a higher percentage of ^{13}C-signals than TsMAz (2), most likely due to its stronger electrophilic character, which makes the monomer susceptible for nucleophilic attacks. Concluding, that TsMAz (2) is well balanced between fast reaction kinetic and susceptibility for nucleophilic attacks, (2) is the most robust monomer of the three tested ones (Figure 6.3).

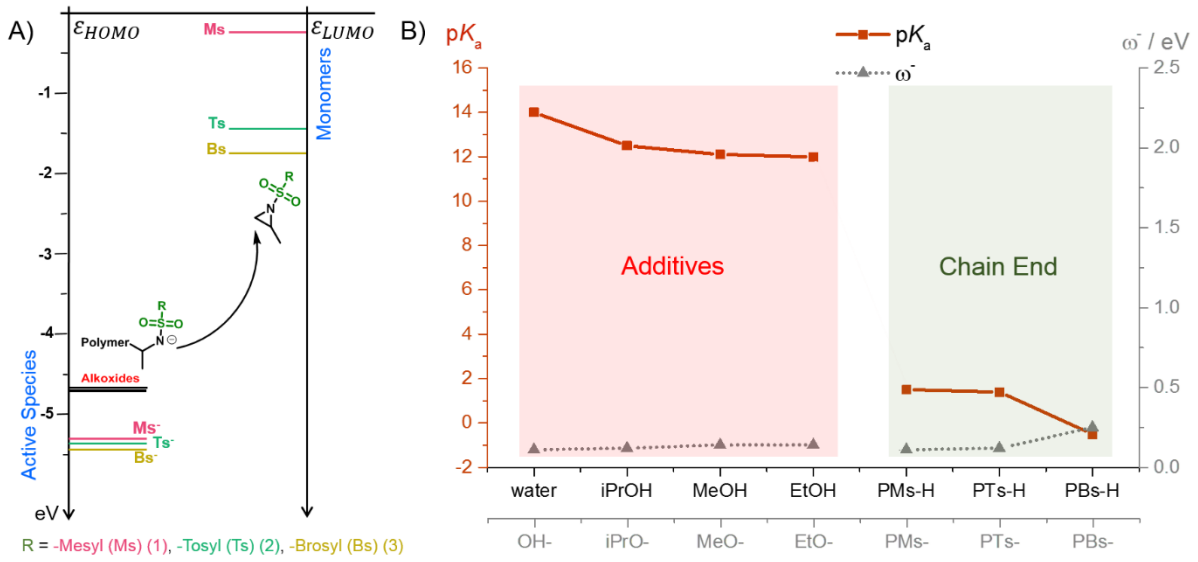

Figure 6.3. A) HOMO levels of the active species: chain ends and alkoxides (left), and LUMO levels of the monomers (right). B) pK_a-values (dark red solid line, squares, left y-axis) and the nucleophilicity index (ω^-) (grey dotted line, triangles, right y-axis and grey x-axis on the bottom) for the additives – highlighted in red (left) - and the chain ends – highlighted in green (right).

To rationalize the effect of initiation of the different additives, we performed density functional theory (DFT) calculations for the propagation steps. The results are summarized in Table S6.19-S6.21 and Figure 6.3A (for computational details see SI, 6.6.7). The chain end and monomer

reactivity can be elaborated from the comparison of the energies of the frontier orbitals. The highest occupied molecular orbitals (HOMO) of the active chain ends were calculated from corresponding model compounds of deprotonated *sec*-butyl(-*R*-)amides ((Table S6.20), *R* = brosyl (Bs), tosyl (Ts) or mesyl (Ms)). The activating groups proved to have a stronger effect on the monomer reactivity compared to the active chain ends, as the difference (-0.24 - -1.75 eV) in LUMO levels are larger than the HOMO levels (-5.30 - -5.44 eV). In addition, calculations proved that the alkoxides (from deprotonation of the added alcohols) exhibit more reactive HOMO levels of ca. -4.7 eV, which are around 0.7 eV higher in energy than the HOMO levels of the chain ends. These findings go along with the expectations that lower LUMO levels are easier to be occupied by nucleophiles with higher HOMO levels, *i.e.* the alkoxides should preferably act as an initiator for the azaanionic polymerization, as soon as they are formed in solution. Moreover, we have computed the electrophilicity index ω^+ and the nucleophilicity index ω^- regarding the homopolymerization of each monomer (Figure 6.3B and Table S6.19, S6.20). The nucleophilicity of additives and sulfonamides only differs in the range of 0.13 - 0.27 eV which show that alkoxides should be considered as strong competitors to the active chain ends, especially if the concentration of alcohol exceeds the initiator concentration. However, due to the enormous difference in the pK_a-values of a sulfonamide (pK_a = -0.5 - 1.5) and the additives (pK_a = 12.0 - 14.0) propagation *via* the azaanion is clearly favored over the deprotonation and initiation by additives (Figure 6.3B and Table S6.21). DFT calculations support the reported experimental data in strong accordance, that additives such as alcohols or even water can be tolerated by this type of azaanionic ring-opening polymerization.

As a consequence, protic functionalities need not to be protected, e.g. as acetals, allowing a direct access to polyols via living AROP.[17] The unprotected 2-ω-propanol-*N*-tosylaziridine (Ts-*ω*PrOH-Az, 6) could be polymerized with full monomer conversion and reasonable molecular weight distributions of ($Đ$ = 1.26-1.37) were obtained under standard conditions of A-AROP (compare SI, 6.6.8). A small amount of branching cannot be ruled out, but neither ^{1}H, ^{13}C NMR spectra (Figure S6.43, S6.44) nor SEC-data (Figure 6.4, Table S6.22) can provide this information, since the monomer is not ^{13}C-labeled and from the experiments in the presence of alcohols only a small amount of branching can be assumed.

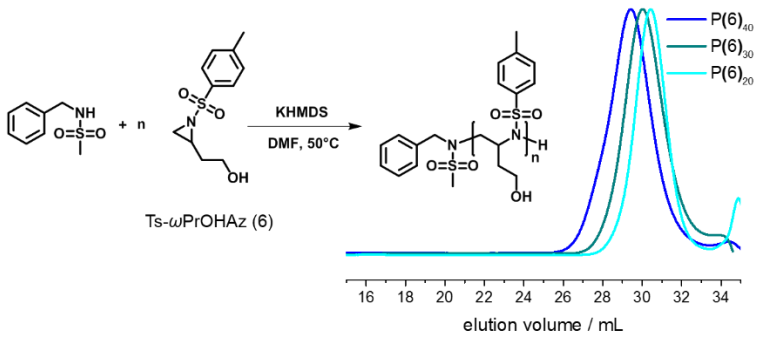

Figure 6.4. Anionic polymerization of Ts-ωPrOHAz (6), including SEC traces of three different polymers of 6 with theoretical repeating units (20, 30, 40) in DMF (RI signal) (data listed in Table S6.22).

6.4 Summary

To conclude, the A-AROP of aziridines overcomes the tedious purification steps and high-vacuum techniques, which make an anionic polymerization often unattractive compared to controlled radical polymerizations. The A-AROP can be conducted in open air and in the presence of large excess of protic solvents or unprotected alcohol functions. The combination of different analyses (*in situ* ^{1}H NMR spectroscopy, MALDI-TOF, SEC and ^{13}C NMR) and additional DFT-calculations confirmed a second slow initiation of protic solvents, of up to 10% with 100 eq. of additives (except for MsMAz with MeOH as additive). Attributed to the high nucleophilicity of additives and high pK_a-values, the propagation remains almost unaffected by the presence of additives (especially for TsMAz) and the polymerization keeps its living character. As a high control over molecular weight, chain fidelity, size distribution and quantitative monomer conversion remains, the access to well-defined polyamides (and polyamines after hydrolysis) is still guaranteed. With this robust A-AROP polyols are accessible without the need of protection groups. Therefore, the comfort of easier handling is in the same range as controlled radical polymerization, where less than 10% of “wrongly” initiated polymers are accepted, while any termination is avoided.

6.5 Acknowledgments

The authors thank Prof. Dr. Katharina Landfester for continuous support. The authors thank the Deutsche Forschungsgemeinschaft (DFG WU750/ 7-1) for funding. The authors thank Stefan Spang for the NMR measurements, Angelika Manhart for synthetic support, Stefan Schuhmacher for the TOC-design and Prof. Dr. Axel H. E. Müller (Johannes Gutenberg-University, Mainz, Germany) for enlightening discussions.

6.6 Supporting Information

The Supporting Information contains additional synthetic procedures, characterization data for monomers, polymers and kinetic measurements and tables.

Content

6.6.1 Materials and Methods.

Materials.

All solvents and reagents were purchased from Sigma-Aldrich, Acros Organics or Fluka and used as received unless otherwise mentioned. All deuterated solvents were purchased from Deutero GmbH and were distilled from CaH_2 or sodium and stored over molecular sieve prior to use. The ^{13}C-labeled solvents were purchased from Sigma-Aldrich and dried with molecular sieves. All monomers and initiators were dried extensively by azeotropic freeze drying with benzene prior to polymerization unless otherwise mentioned. 2-methyl-*N*-mesyl-aziridine (MsMAz, 1) 2-methyl-*N*-tosylaziridine (TsMAz, 2), 2-methyl-*N*-brosylaziridine (BsMAz, 3), *N*-pyrene-methanesulfonamide (PyNHMs, 4) and *N*-benzylsulfonamide (BnNHMs, 5) were synthesized according to our previously published protocol.[15, 17]All solvents

Instrumentation and Characterization Techniques.

NMR. ^1H NMR spectra were recorded using a Bruker Avance 300, a Bruker Avance III 500 or a Bruker Avance III 700 spectrometer. All spectra were referenced internally to residual proton signals of the deuterated solvent.

SEC. Size exclusion chromatography (SEC) measurements of standard polymers were performed in DMF (1 g L^{-1} LiBr added) at 60°C and a flow rate of 1 mL min^{-1} with an PSS SECcurity as an integrated instrument, including a PSS GRAM 100-1000 column and a refractive index (RI) detector. Calibration was carried out using poly(ethylene glycol) standards provided by Polymer Standards Service.

MALDI-TOF. MALDI-TOF spectra were performed by the CESAMO (Bordeaux, France) on a Voyager mass spectrometer (Applieds Biosystems). Spectra were recorded in the positive-ion mode using the reflectron and with an accelerating voltage of 20 kV. Samples were dissolved in THF at 10 mL min^{-1}. The matrix solution (trans-3-indoleacrylic acid, IAA) was prepared by dissolving 10 mg in 1 mL of THF. A MeOH-solution of cationization agent (NaI, 10 mL min^{-1}) was also prepared. Solutions were combined in a 10:1:1 volume ratio of matrix to sample to cationization agent.

General procedure for the azaanionic polymerization.

All polymerizations were run in screw cap vials if not otherwise noted. Vials were taken directly from the box, not flame dried neither treated *in vacuo* or using standard Schlenk technique. Neither monomers nor the initiators and the bases (bis(trimethylsilyl)amide salts) were pretreated for purification. The monomers and the initiator were dissolved in dry *N,N*-dimethylformamide (DMF). The initiator solution was added to the bis(trimethylsilyl)amide salt under normal atmosphere, the initiator-solution was transferred to the reaction flask, containing the monomer. The resulting concentration was kept constant by 10 wt.% monomer in DMF. The mixture was stirred at the desired temperature and over the desired time (to ensure complete reaction: 18 h Reaction time at 50 °C). The polymers were obtained as slightly yellow powder after evaporation of the solvent. Colorless dry powders can be obtained if the polymers are precipitation of the reaction mixture into 30 mL methanol and after drying at reduced pressure.[13, 15, 17]

For experiments with different amount of protic solvents the above mentioned general procedure for the azaanionic polymerization was followed. After initiation (5 to 10 seconds) the protic solvent was added by an Eppendorf Pipette.

6.6.2 Kinetics.

Monitoring polymerizations by real-time ^{1}H NMR spectroscopy.

All polymerizations were carried out in analogy to the conventional procedure in a Schlenk flask and already described in previous publications.[13, 15] All glassware was dried by *in vacuo* for at least three times. All reactants (except the bis(trimethylsilyl)amide salts) were dried from benzene *in vacuo* for at least 4 h. Inside of a glovebox in a nitrogen-atmosphere the respective monomer was dissolved DMF-d_7 as a total volume of 5.0 mL of DMF-d_7, calculated for a monomer to initiator of $[M]_0$:$[I]_0$ = 50:1. The initiator-solution in 1 mL DMF-d_7 was prepared separately. Therefore 1 eq. of PyNHMs was solved in 1 mL DMF-d_7 and transferred to Lithium bis(trimethylsilyl)-amide (LiHMDS) 0.95 eq. The active initiator was then transferred to the monomer-solution to yield a 10 wt.% solution. Previously dried (drying oven at 50 °C under vacuum) conventional NMR-tubes were equipped with 100 eq. of the protic additives (none, H_2O, ^{13}C-MeOH, ^{13}C-EtOH, ^{13}C-iPrOH). The NMR-tubes were filled with the reaction mixture and sealed by melting the top of the NMR-tube with a hot flame. To prevent polymerization of the samples, which were monitored the following days, the NMR-tubes were shock frosted in liquid nitrogen and stored at -80 °C (below the melting point of DMF).

The NMR-tubes were one after another warmed up to room temperature and all ^{1}H NMR kinetics were recorded using a Bruker Avance III 700. All spectra were referenced internally to residual proton signals of the deuterated solvent dimethylformamide-d_7 at 8.03 ppm. The π/2-pulse for the proton measurements was 13.1 µs. The spectra of the polymerizations were recorded at 700 MHz with 16 scans (equal to 404 s (acquisition time of 2.595 s and a relaxation time of 20 s after every pulse)) over a period of time, until the polymerization had full conversion. No B-field optimizing routine was used over the kinetic measurement time. The spin-lattice relaxation rate (T_1) of the ring-protons, which are used afterwards for integration, was measured before the kinetic run with the inversion recovery method.[41]

The method for the evaluation of the NMR-data to calculate the respective k_p-values is followed as described in previous publications.[13].

Stock solution kinetics of MsMAz (1)

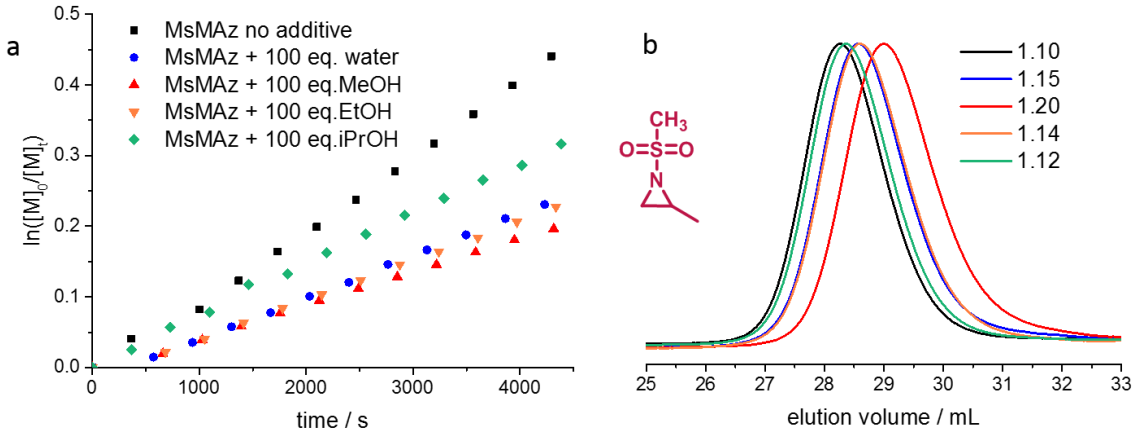

Figure S6.1. a) Kinetic plots of $\ln([M]_0/[M]_t)$ *vs.* time of MsMAz (1) and different additives in DMF-d_7 at 50 °C. b) SEC traces in DMF (RI signal) (data listed in Table S6.1).

Table S6.1. Overview of the polymerization kinetics of MsMAz (1) in DMF-d_7 with the respective additive, including SEC-analyses and calculated propagation rates (k_p).

Monomer	MsMAz (1)	MsMAz (1)	MsMAz (1)	MsMAz (1)	MsMAz (1)
Additive	Pure	H_2O	MeOH	EtOH	iPrOH
k_p / 10^{-3} L mol^{-1} s^{-1}	**12.0±0.8**	**6.4±0.5**	**5.0±0.4**	**6.4±0.4**	**7.7±0.5**
M_n[a] / g mol^{-1}	4000	3400	2600	3400	3800
$Đ$[a]	1.10	1.15	1.20	1.14	1.12
Reaction time / h	10.3	23	>23.9	22.2	17.5
Conversion / %	>99	>99	98	>99	>99

[a] Number-average molecular weight and molecular weight dispersity determined via SEC in DMF (*vs.* PEO standards).

Stock solution kinetics of BsMAz (3)

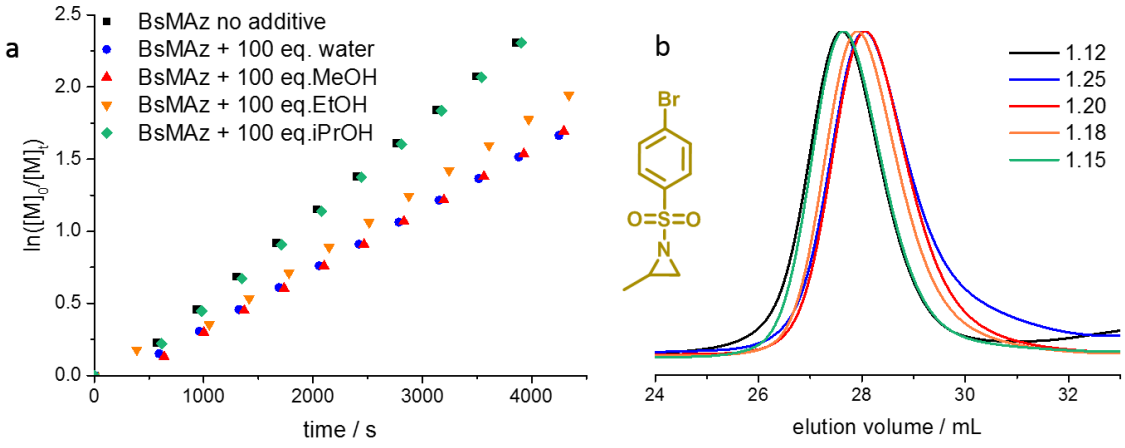

Figure S6.2. a) Kinetic plots of $\ln([M]_0/[M]_t)$ *vs.* time of BsMAz (3) and different additives in DMF-d_7 at 50 °C. b) SEC traces in DMF (RI signal) (data listed in Table S6.2).

Table S6.2. Overview of the polymerization kinetics of BsMAz (3) in DMF-d_7 with the respective additive, including SEC-analyses and calculated propagation rates (k_p).

Monomer	BsMAz (3)	BsMAz (3)	BsMAz (3)	BsMAz (3)	BsMAz (3)
Additive	Pure	H_2O	MeOH	EtOH	iPrOH
k_p / 10^{-3} L mol^{-1} s^{-1}	**67.3±4.6**	**44.0±3.0**	**45.3±3.1**	**52.0±3.6**	**67.7±4.6**
M_n[a] / g mol^{-1}	5500	3700	3900	4300	5000
$Đ$[a]	1.12	1.25	1.20	1.18	1.15
Reaction time / h	2.1	3.3	3.0	2.8	2.1
Conversion / %	>99	>99	>99	>99	>99

[a] Number-average molecular weight and molecular weight dispersity determined via SEC in DMF (*vs.* PEO standards).

^{13}C ether signals from kinetics

Table S6.3. Overview of the performed polymerization kinetics regarding initiation via alkoxides:

Sample	eq (monomer)[a]	Integral ^{13}C ether[b]	S/N (rms) ^{13}C ether[c]	S/N (rms) reference signal [c]	^{13}C ether / %[d]	Relative standard deviation / %[e]
P(MsMAz)-MeOH	50	0.57	83.6	18.2	**22.4**	**4.5**
P(MsMAz)-EtOH	50	0.13	22.1	18.0	**6.2**	**4.5**
P(MsMAz)-iPrOH	50	0.07	1.8	19.6	**3.4***	**≥20.0**
P(TsMAz)-MeOH	56	0.003	3.6	82.4	**0.2***	**≥20.0**
P(TsMAz)-EtOH	56	0.08	4.0	106.0	**4.3***	**≥20.0**
P(TsMAz)-iPrOH	56	0.02	3.9	78.0	**1.1***	**≥20.0**
P(BsMAz)-MeOH	56	0.12	15.8	80.8	**6.4**	**≥4.5**
P(BsMAz)-EtOH	56	0.10	14.4	147.7	**5.4**	**≥4.5**
P(BsMAz)-iPrOH	56	0.04	7.5	170.0	**2.2***	**≥20.0**

[a] Determined by ^{1}H NMR from stock solution without additives. [b] Determined by ^{13}C NMR normalized to repeating unit (reference signal, integral = 1).[c] Determined with Top Spin software. [d] Calculated by the equation below. [e] Estimation refers to literature.[42-43] * Value of ^{13}C ether is overestimated due to high signal to noise ratios (S/N).

$$= \frac{\frac{\int {}^{13}C\ ether}{99} \cdot eq(monomer)}{1 + \frac{\int {}^{13}C\ ether}{99} \cdot eq(monomer)} \cdot 100\%$$

Example P(MsMAz)-MeOH:

$$\frac{\frac{0.57}{99} \cdot 50}{1 + \frac{0.57}{99} \cdot 50} \cdot 100\% = 22.4\%$$

6.6.3 ^{13}C NMRs and 2D NMRs of the kinetics.

To quantify the amount of alcohol acted as initiator, ^{13}C-labeled additives were used to follow this process by NMR. After evaporating the solvent and residual ^{13}C-labeled alcohols in ultra-low vacuum, quantification of polymers with ^{13}C-labeled ethers, which are formed after initiation, is possible by ^{13}C NMR- and HSQC NMR-spectroscopy.

P(TsMAz)

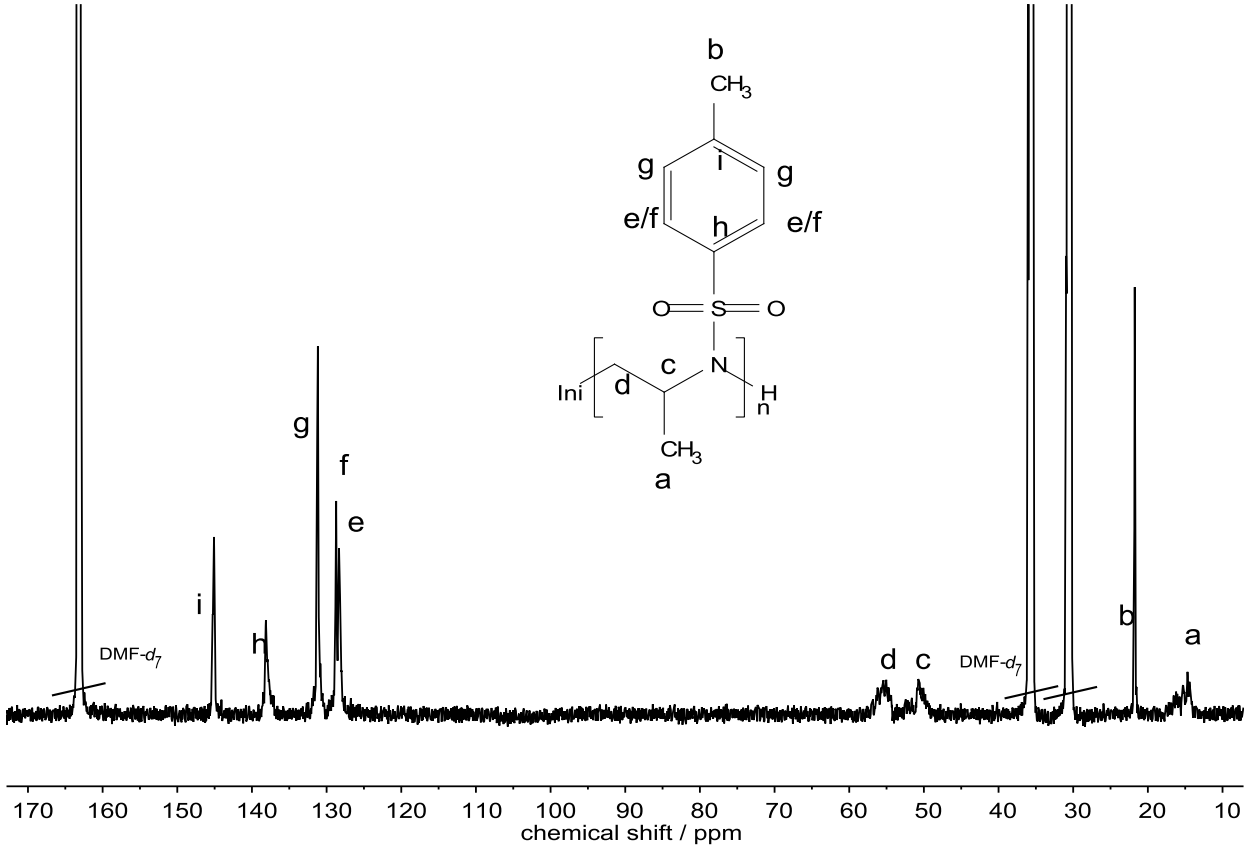

Figure S6.3. ^{13}C NMR, quantitative (176 MHz, 323 K, DMF-d_7) of P(TsMAz), H_2O as additive. δ [ppm] = 145.07 (s, 1C, arom., i), 138.04 (s, 1C, arom., h), 131.16 (s, 2C, arom., g), 128.70 (s, 1C, arom., f), 128.31 (s, 1C, arom., e), 56.32-54.19 (m, 1C, backbone, d), 49.06 – 52.62 (m, 1C, backbone, c) 21,75 (s, 1C, aromat-CH_3, b), 13.76-17.58 (m, 1C, backbone-CH_3, a).

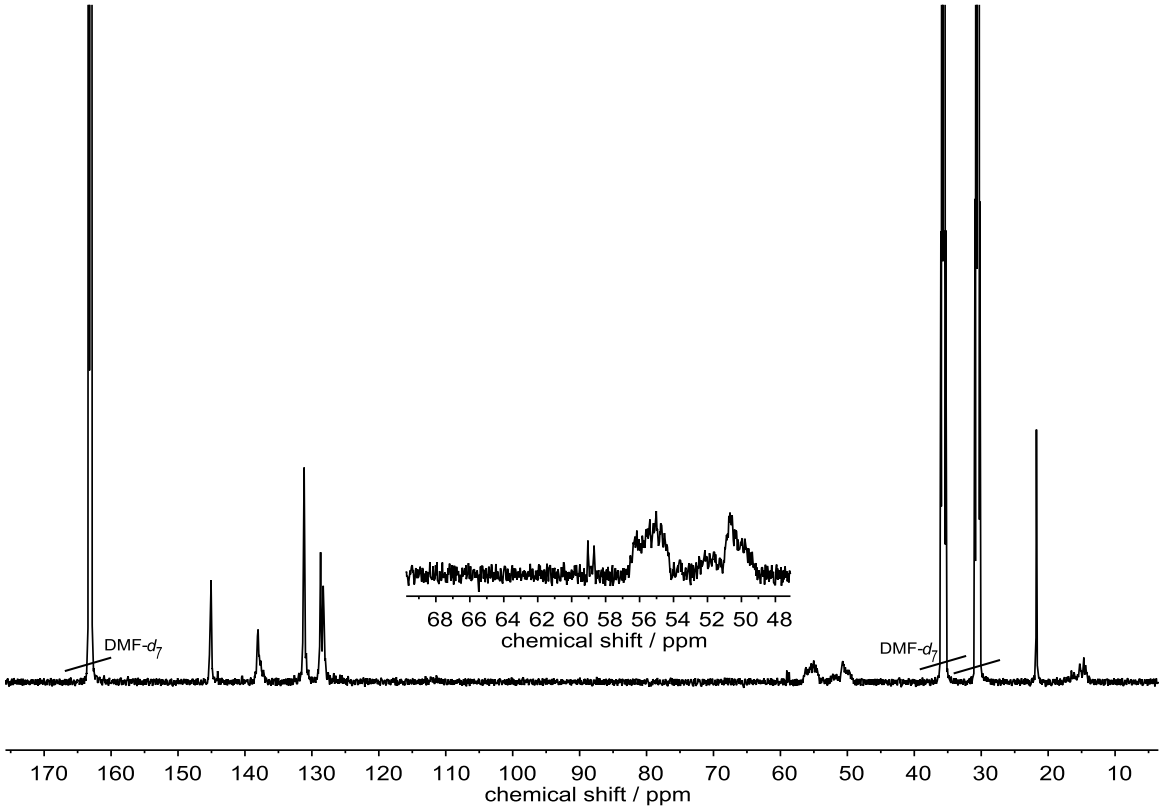

Figure S6.4. ^{13}C NMR, quantitative (176 MHz, 323 K, DMF-d_7) of P(TsMAz), methanol-^{13}C as additive. δ [ppm] = 145.07 (s, 1C, arom.), 138.04 (s, 1C, arom.), 131.16 (s, 2C, arom.), 128.70 (s, 1C, arom.), 128.31 (s, 1C, arom.), 58.68-59.04 (m, 0.03, methyl-^{13}C-ether) 56.32-54.19 (m, 1C, backbone), 49.06 – 52.62 (m, 1C, backbone) 21,75 (s, 1C, aromat-CH_3), 13.76-17.58 (m, 1C, backbone-CH_3).

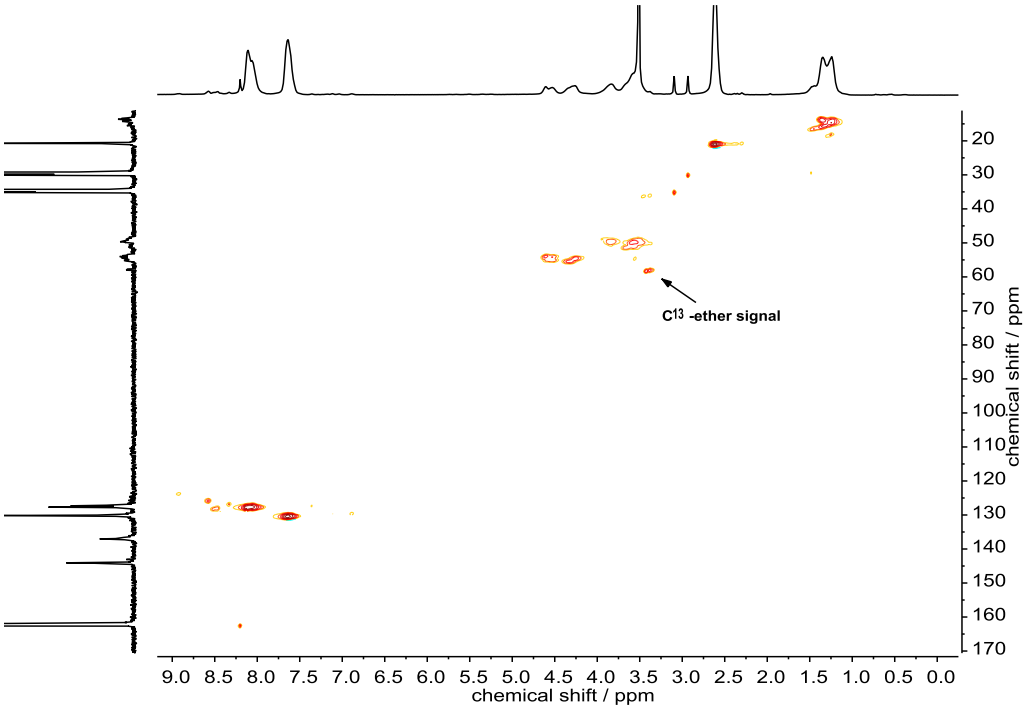

Figure S6.5. HSQC NMR (700, 176 MHz, DMF-d_7) of P(TsMAz), methanol-^{13}C as additive.

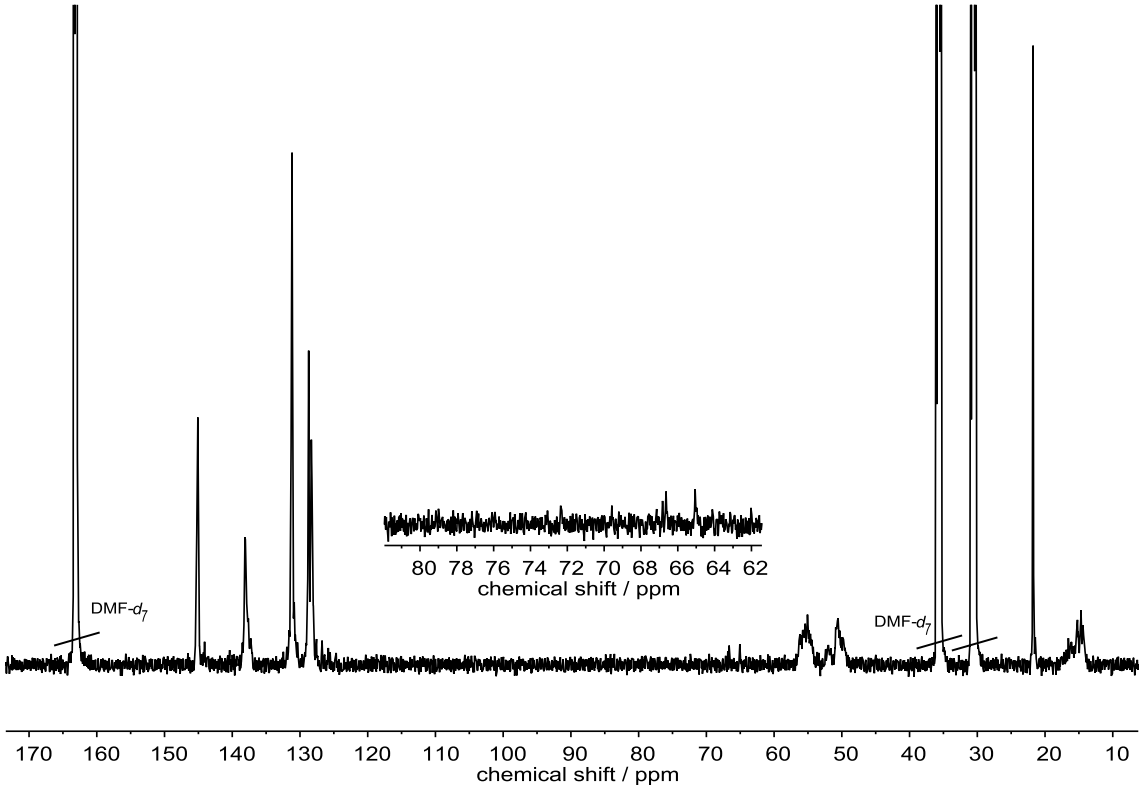

Figure S6.6. ^{13}C NMR, quantitative (176 MHz, 323 K, DMF-d_7) of P(TsMAz), ethanol-1-$^{13}C_1$ as additive. δ [ppm] = 145.07 (s, 1C, arom.), 138.04 (s, 1C, arom.), 131.16 (s, 2C, arom.), 128.70 (s, 1C, arom.), 128.31 (s, 1C, arom.), 66.10 (m, 0.05, ethyl-1-$^{13}C_1$-ether) 56.32-54.19 (m, 1C, backbone), 49.06 – 52.62 (m, 1C, backbone) 21,75 (s, 1C, aromat-CH_3), 13.76-17.58 (m, 1C, backbone-CH_3).

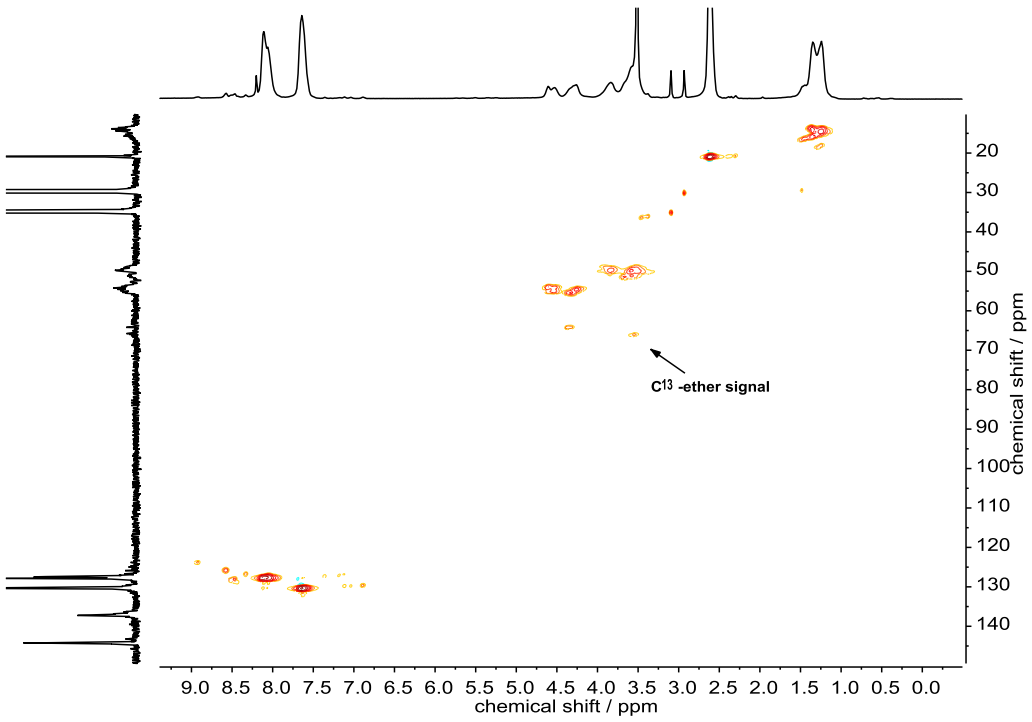

Figure S6.7. HSQC NMR (700, 176 MHz, DMF-d_7) of P(TsMAz), ethanol-1-$^{13}C_1$ as additive.

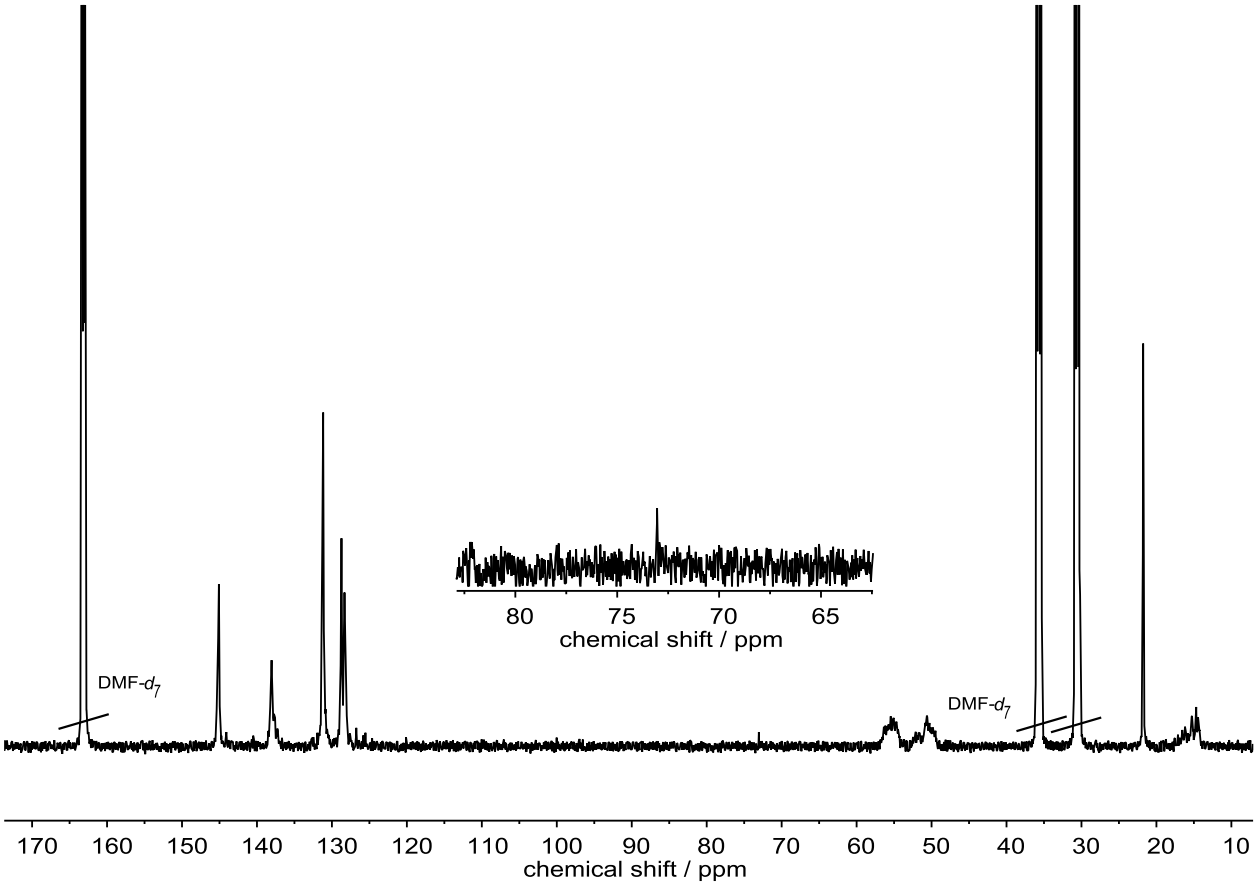

Figure S6.8. ^{13}C NMR, quantitative (176 MHz, 323 K, DMF-d_7) of P(TsMAz), isopropanol-2-$^{13}C_1$ as additive. δ [ppm] = 145.07 (s, 1C, arom.), 138.04 (s, 1C, arom.), 131.16 (s, 2C, arom.), 128.70 (s, 1C, arom.), 128.31 (s, 1C, arom.), 73.04 (s, 0.03, isopropyl-2-$^{13}C_1$-ether) 56.32-54.19 (m, 1C, backbone), 49.06 – 52.62 (m, 1C, backbone) 21,75 (s, 1C, aromat-CH_3), 13.76-17.58 (m, 1C, backbone-CH_3).

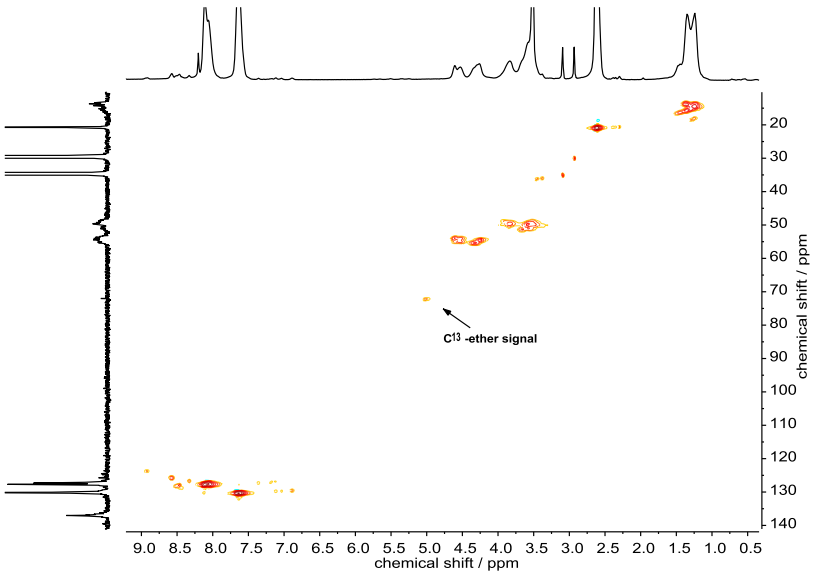

Figure S6.9. HSQC NMR (700, 176 MHz, DMF-d_7) of P(TsMAz), isopropanol-2-$^{13}C_1$ as additive.

P(BsMAz)

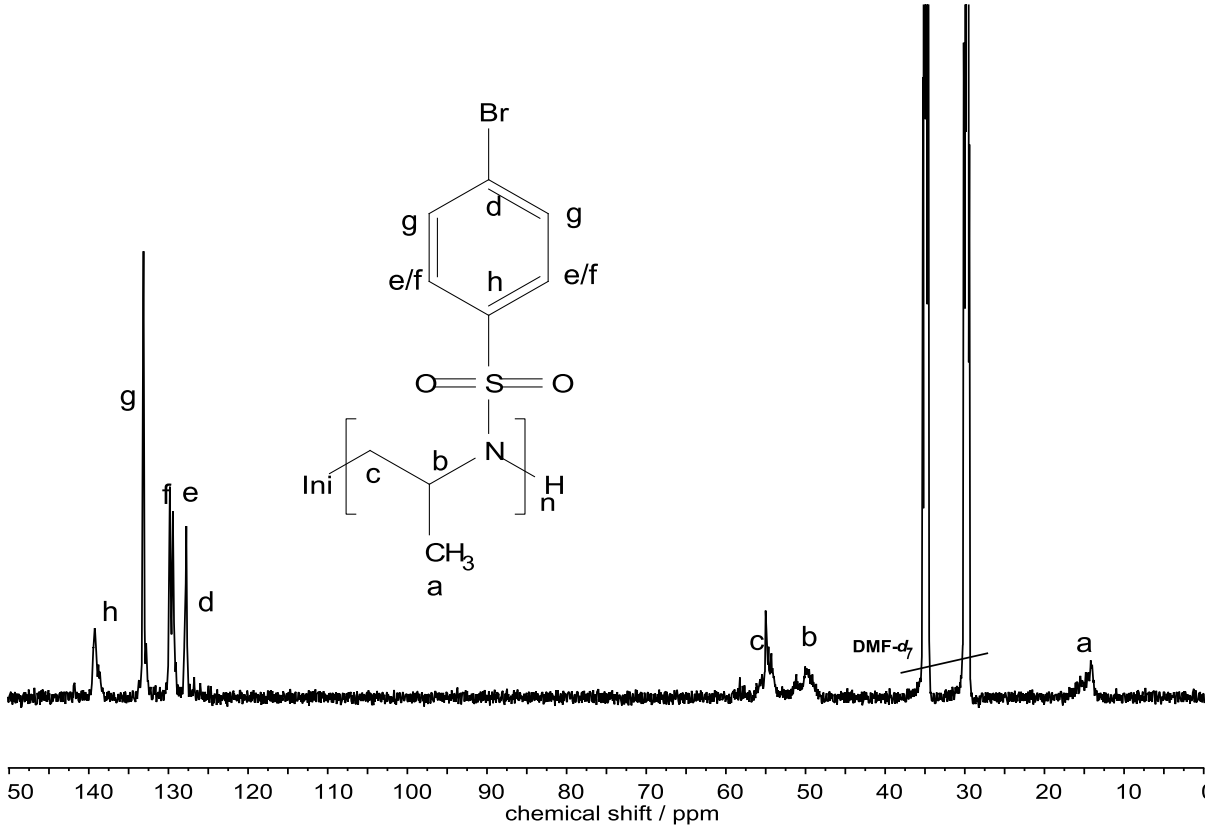

Figure S6.10. ^{13}C NMR, quantitative (176 MHz, 323 K, DMF-d_7) of P(BsMAz), methanol-^{13}C as additive. δ [ppm] = 139.26 (s, 1C, arom., h), 133.08 (s, 2C, arom., g), 129.81 (s, 1C, arom., f), 129.41 (s, 1C, arom., e), 127.82 (s, 1C, arom., d), 58.24, 55.10 (m, 0.29, methyl-^{13}C-ether) 56.83-53.51 (m, 1C, backbone, c), 52.19 – 47.99 (m, 1C, backbone, b), 17.55-13.35 (m, 1C, backbone-CH_3, a).

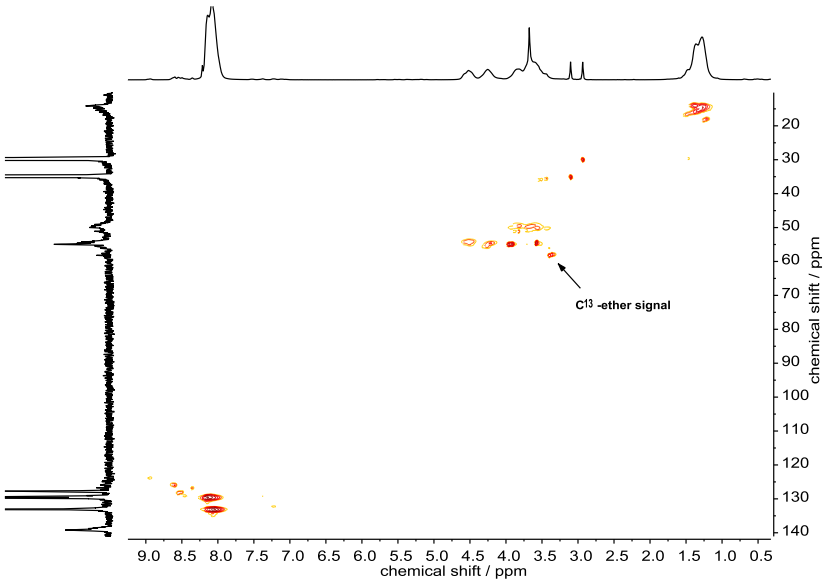

Figure S6.11. HSQC NMR (700, 176 MHz, DMF-d_7) of P(BsMAz), methanol-^{13}C as additive.

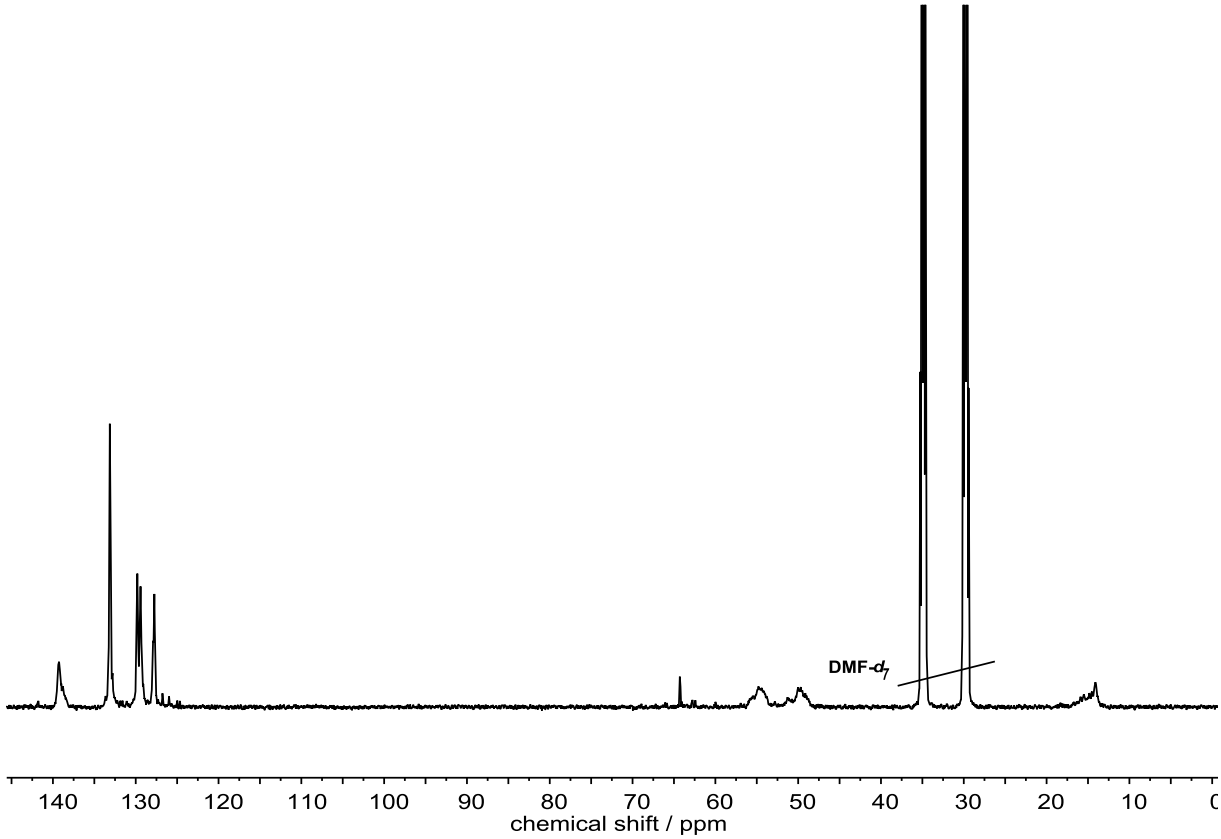

Figure S6.12. ^{13}C NMR, quantitative (176 MHz, 323 K, DMF-d_7) of P(BsMAz), ethanol-1-$^{13}C_1$ as additive. δ [ppm] = 139.26 (s, 1C, arom.), 133.08 (s, 2C, arom.), 129.81 (s, 1C, arom.), 129.41 (s, 1C, arom.), 127.82 (s, 1C, arom.), 58.24, 64.17 (s, 0.14, methyl-^{13}C-ether) 56.83-53.51 (m, 1C, backbone), 52.19 – 47.99 (m, 1C, backbone), 17.55-13.35 (m, 1C, backbone-CH_3).

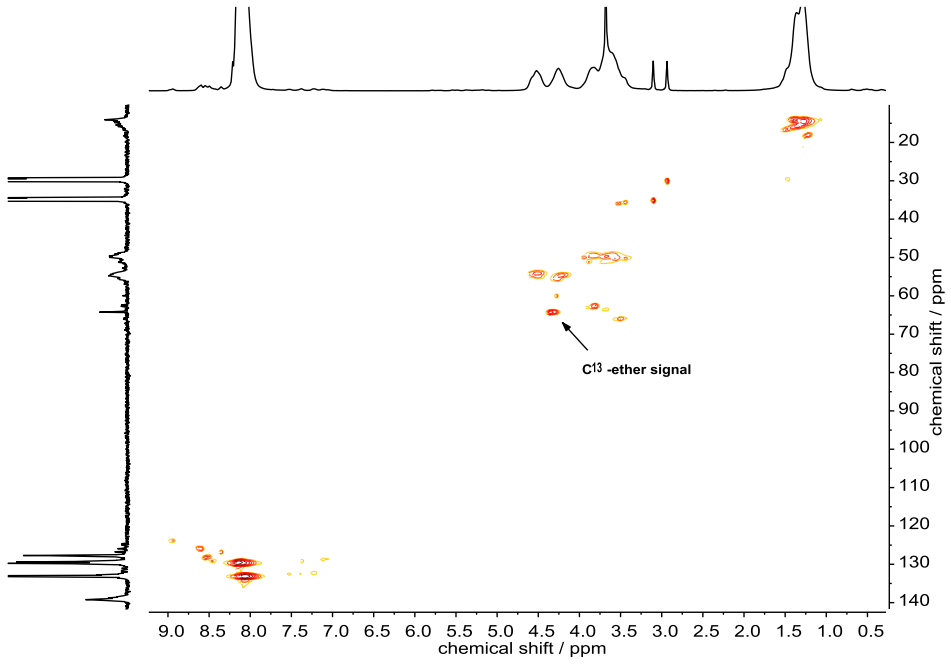

Figure S6.13. HSQC NMR (700, 176 MHz, DMF-d_7) of P(BsMAz), ethanol-1-$^{13}C_1$ as additive.

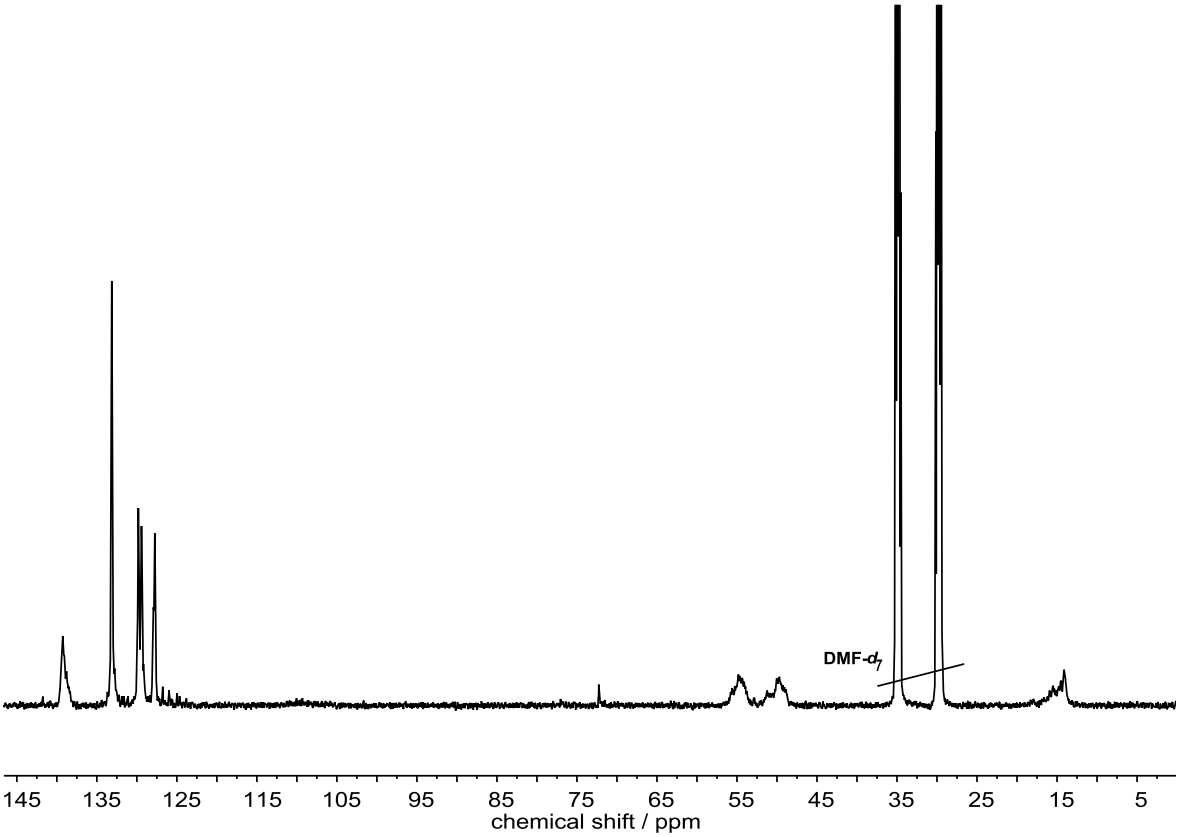

Figure S6.14. ^{13}C NMR, quantitative (176 MHz, 323 K, DMF-d_7) of P(BsMAz), isopropanol-2-$^{13}C_1$ as additive. δ [ppm] = 139.26 (s, 1C, arom.), 133.08 (s, 2C, arom.), 129.81 (s, 1C, arom.), 129.41 (s, 1C, arom.), 127.82 (s, 1C, arom.), 58.24, 72.27 (s, 0.07, methyl-^{13}C-ether) 56.83-53.51 (m, 1C, backbone), 52.19 – 47.99 (m, 1C, backbone), 17.55-13.35 (m, 1C, backbone-CH_3).

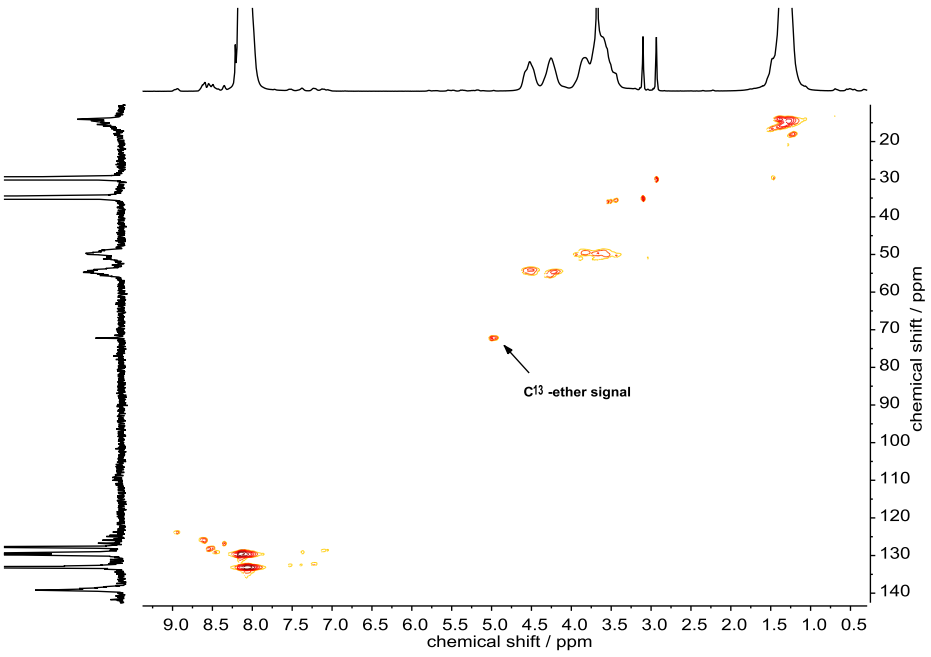

Figure S6.15. HSQC NMR (700, 176 MHz, DMF-d_7) of P(BsMAz), isopropanol-2-$^{13}C_1$ as additive.

P(MsMAz)

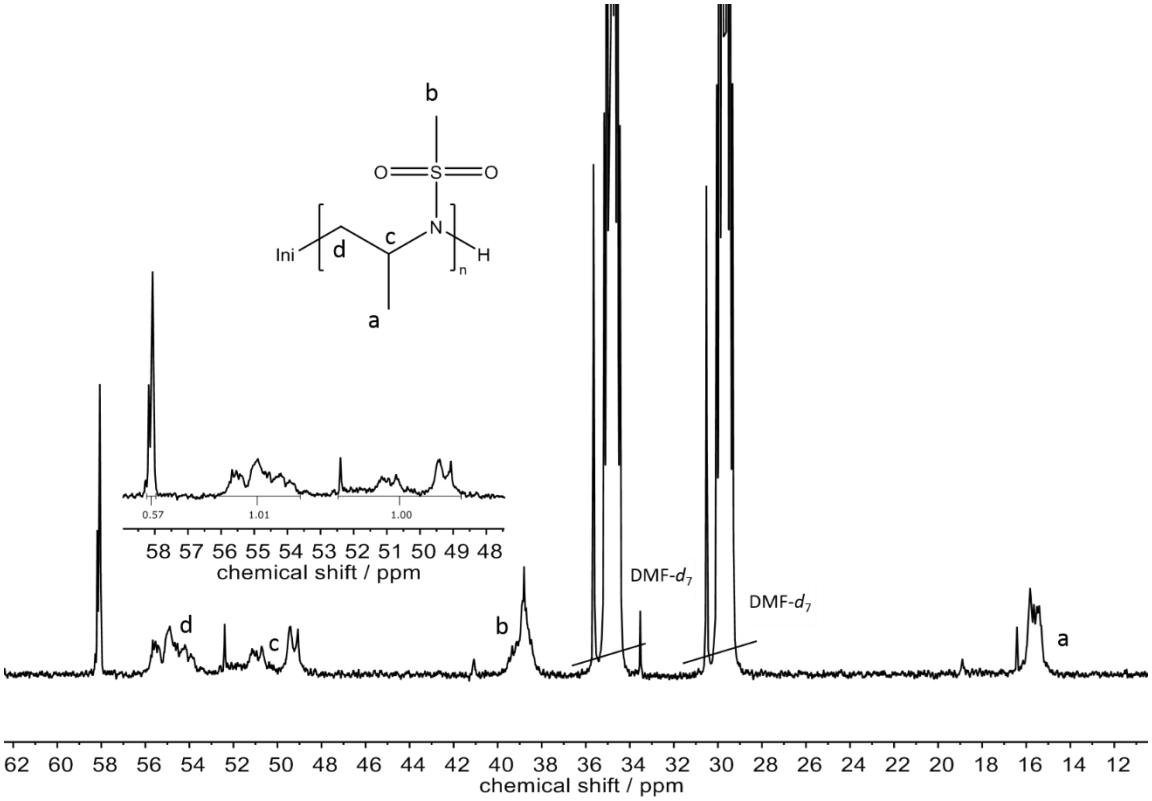

Figure S6.16. ^{13}C NMR, quantitative (176 MHz, 323 K, DMF-d_7) of P(MsMAz), methanol ^{13}C as additive. δ [ppm] = 58.14 (m 0.57, methyl-^{13}C-ether), 56.06-53.20 (m, 1C, backbone, d), 51.87 – 48.62 (m, 1C, backbone, c) 40.13-37.96 (m, 1C, mesyl-CH_3, b), 16.86-14.81 (m, 1C, backbone-CH_3, a).

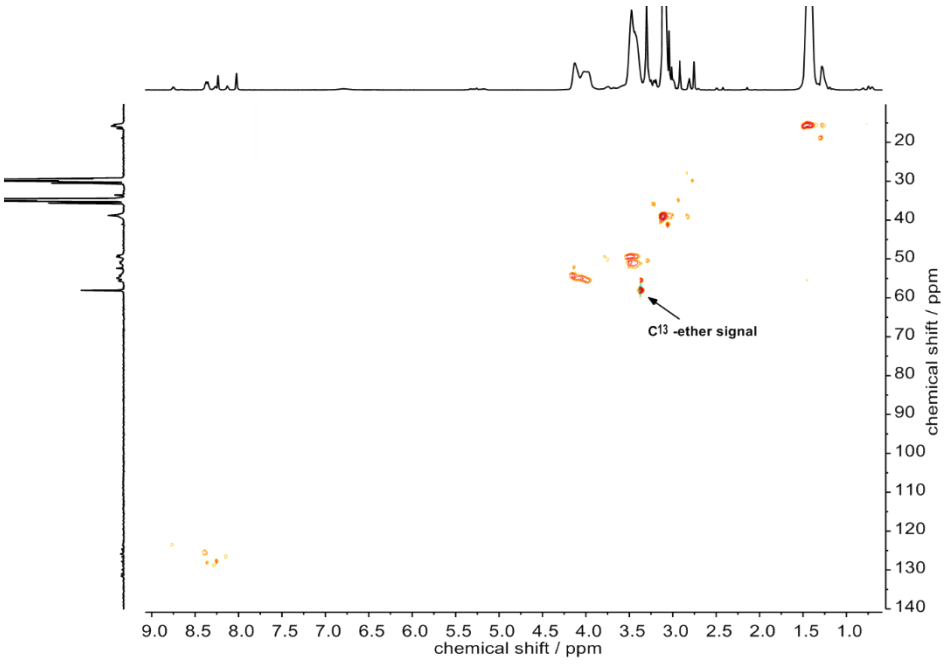

Figure S6.17. HSQC NMR (700, 176 MHz, DMF-d_7) of P(MsMAz), methanol ^{13}C as additive.

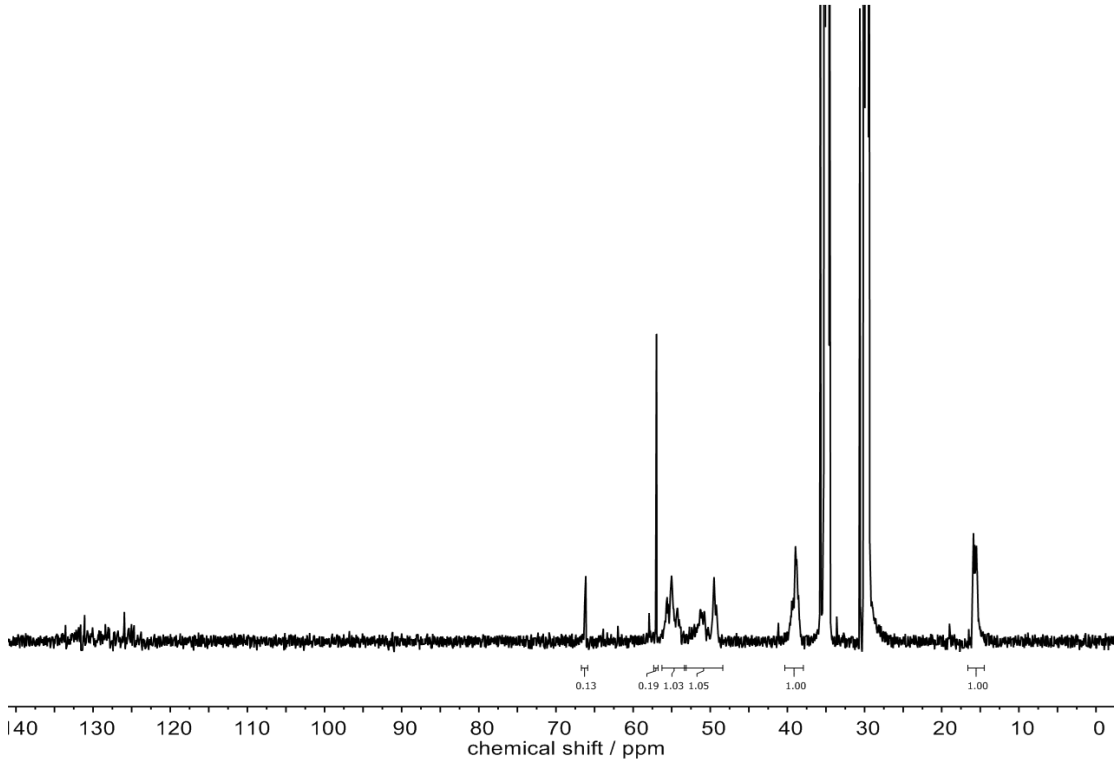

Figure S6.18. ^{13}C NMR, quantitative (176 MHz, 323 K, DMF-d_7) of P(MsMAz), ethanol-1-$^{13}C_1$ as additive. δ [ppm] = 66.06 (s 0.20, ethyl-1-$^{13}C_1$-ether), 56.06-53.20 (m, 1C, backbone), 51.87 – 48.62 (m, 1C, backbone) 40.13-37.96 (m, 1C, mesyl-CH_3), 16.86-14.81 (m, 1C, backbone-CH_3). The signal at 57.4 ppm belongs to residual ethanol-1-$^{13}C_1$.

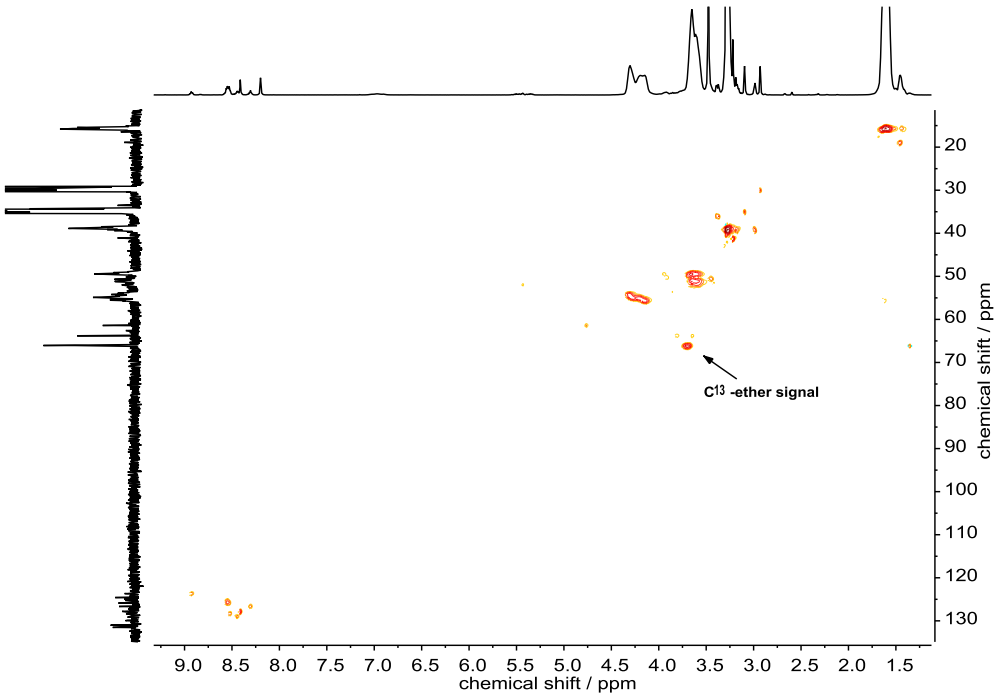

Figure S6.19. HSQC NMR (700, 176 MHz, DMF-d_7) of P(MsMAz), ethanol-1-$^{13}C_1$ as additive.

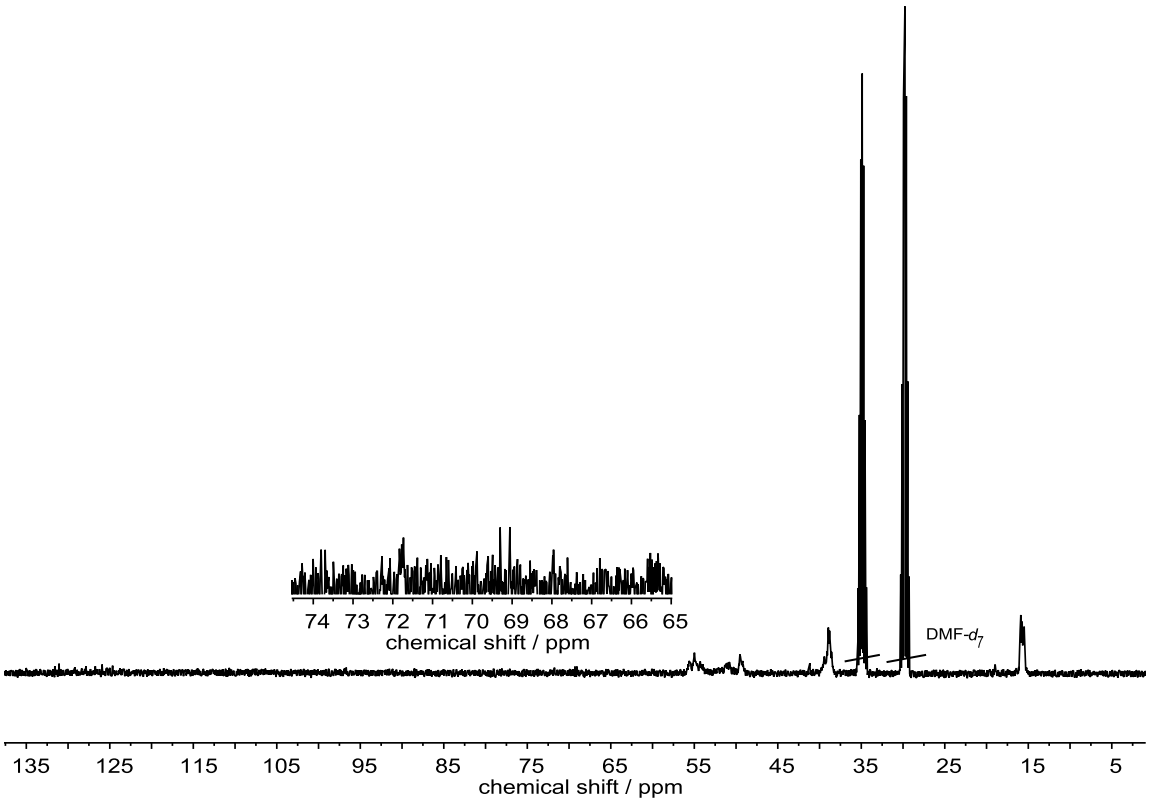

Figure S6.20. ^{13}C NMR, quantitative (176 MHz, 323 K, DMF-d_7) of P(MsMAz), isopropanol-2-$^{13}C_1$ as additive. δ [ppm] = 71.8 (m, 0.01, isopropyl-1-$^{13}C_1$-ether), 56.06-53.20 (m, 1C, backbone), 51.87 – 48.62 (m, 1C, backbone) 40.13-37.96 (m, 1C, mesyl-CH_3), 16.86-14.81 (m, 1C, backbone-CH_3).

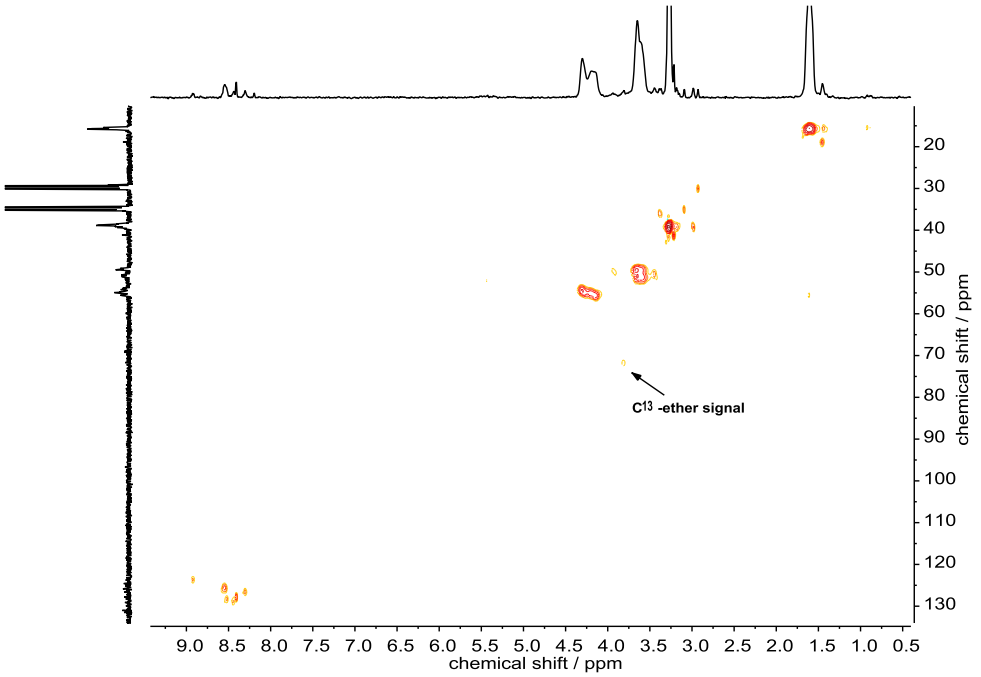

Figure S6.21. HSQC NMR (700, 176 MHz, DMF-d_7) of P(MsMAz), isopropanol-2-$^{13}C_1$ as additive.

6.6.4 Reaction in vials.

P(MsMAz)

MsMAz (1) (100 mg, 0.739 mmol) in 1 mL DMF, BnNHMs (5) (2.8 mg, 0.015 mmol) and KHMDS (3.0 mg, 0.015 mmol) in 0.1 mL DMF at 50 °C. Samples taken after 24, 48 and 120 hours

Table S6.4. Overview of the performed polymerizations of MsMAz (1) from stock solutions in DMF with different amounts of water as additive, including SEC-analyses.

Monomer	MsMAz (1)	MsMAz (1)	MsMAz (1)
Additive	H_2O	H_2O	H_2O
V / µL	50	100	200
Equivalents (to initiator)	185	370	740
M_n[a] / g mol^{-1}	1400	900	500
$Đ$[a]	1.48	1.37	> 2
Reaction time / h	<120	<120	>120
Conversion / %	~95	~95	~60
Name	P(Ms)-H_2O-50-µL	P(Ms)-H_2O-100-µL	P(Ms)-H_2O-200-µL

[a] Number-average molecular weight and molecular weight dispersity determined via SEC in DMF (*vs.* PEO standards).

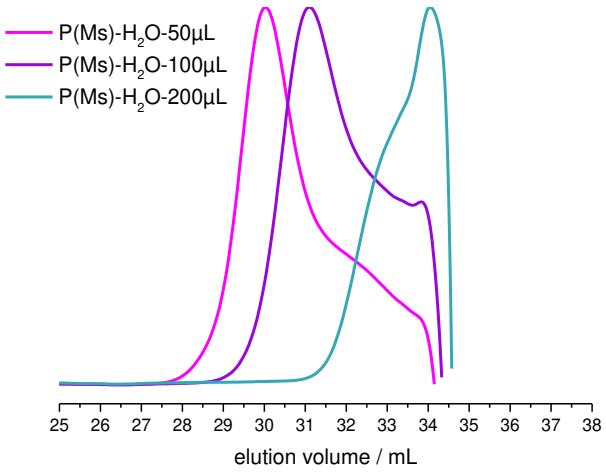

Figure S6.22. SEC traces of P(MsMAz) with water (50, 100, 200 µL) as additive in DMF (RI signal).

Table S6.5. Overview of the performed polymerizations of MsMAz (1) from stock solutions in DMF with different amounts of methanol as additive, including SEC-analyses.

Monomer	MsMAz (1)	MsMAz (1)	MsMAz (1)
Additive	MeOH	MeOH	MeOH
V / µL	50	100	200
Equivalents (to initiator)	115	229	458
M_n[a] / g mol^{-1}	2800	1700	800
$Đ$[a]	1.23	1.27	1.29
Reaction time / h	<24	<48	<120
Conversion / %	>99	~95	~95
Name	P(Ms)-MeOH-50-µL	P(Ms)-MeOH-100-µL	P(Ms)-MeOH-200-µL

[a] Number-average molecular weight and molecular weight dispersity determined via SEC in DMF (*vs.* PEO standards).

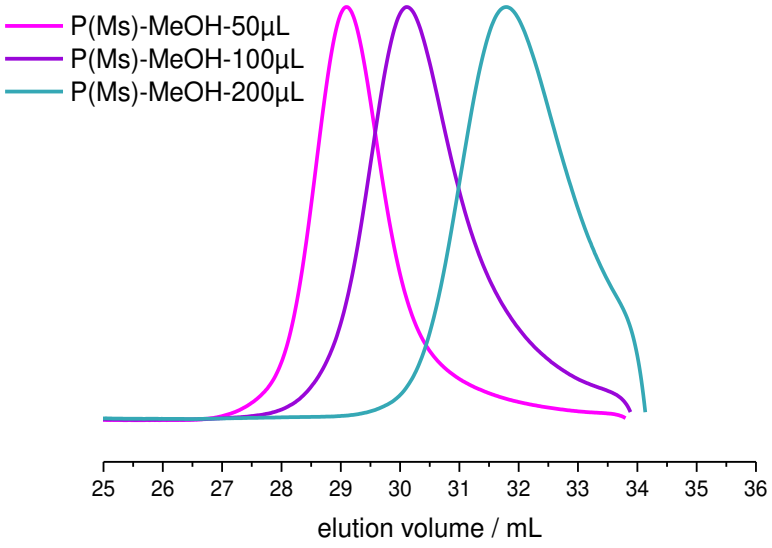

Figure S6.23. SEC traces of P(MsMAz) with methanol (50, 100, 200 µL) as additive in DMF (RI signal).

Table S6.6. Overview of the performed polymerizations of MsMAz (1) from stock solutions in DMF with different amounts of ethanol as additive, including SEC-analyses.

Monomer	MsMAz (1)	MsMAz (1)	MsMAz (1)	MsMAz (1)
Additive	EtOH	EtOH	EtOH	EtOH
V / µL	50	100	200	400
Equivalents (to initiator)	57	114	228	457
M_n[a] / g mol^{-1}	3500	2100	2900	1900
$Đ$[a]	1.15	1.24	1.19	1.22
Reaction time / h	<24	<24	<48	<24
Conversion / %	>99	>99	~95	~95
Name	P(Ms)-EtOH-50-µL	P(Ms)-EtOH-100-µL	P(Ms)-EtOH-200-µL	P(Ms)-EtOH-400-µL

[a] Number-average molecular weight and molecular weight dispersity determined via SEC in DMF (*vs.* PEO standards).

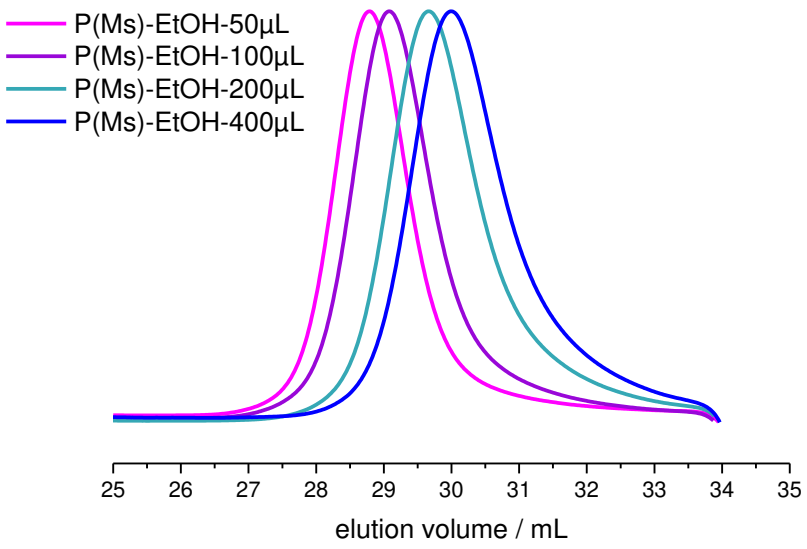

Figure S6.24. SEC traces of P(MsMAz) with ethanol (50, 100, 200, 400 µL) as additive in DMF (RI signal).

Table S6.7. Overview of the performed polymerizations of MsMAz (1) from stock solutions in DMF in an open vial and with isopropanol as additive, including SEC-analyses.

Monomer	MsMAz (1)	MsMAz (1)
Additive	Open	iPrOH
V / µL	---	400
Equivalents (to initiator)	---	349
M_n[a] / g mol^{-1}	3400	2900
$Đ$[a]	1.09	1.15
Reaction time / h	<24	<24
Conversion / %	>99	~95
Name	P(Ms)-open vial	P(Ms)-iPrOH-400-µL

[a] Number-average molecular weight and molecular weight dispersity determined via SEC in DMF (*vs.* PEO standards).

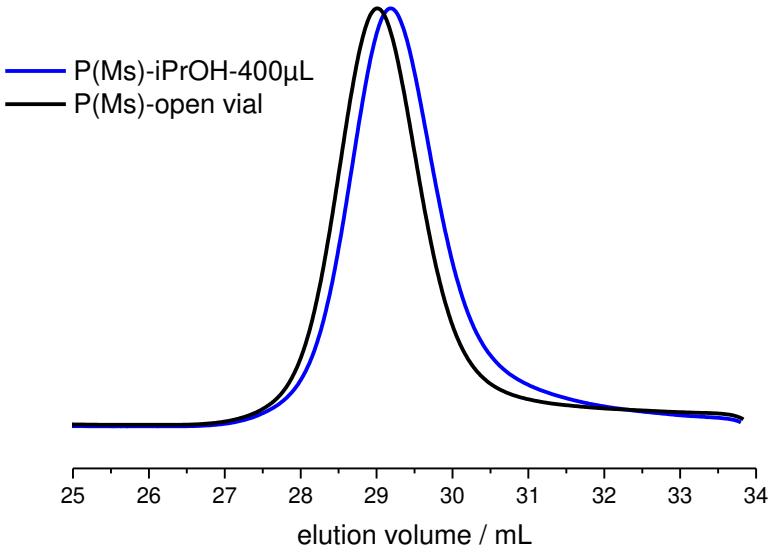

Figure S6.25. SEC traces of P(MsMAz) in an open vial and with isopropanol (400 µL) as additive in DMF (RI signal).

P(TsMAz)

TsMAz (2) (100 mg, 0.473 mmol) in 1 mL DMF, BnNHMs (5) (1.75 mg, 0.0095 mmol) and KHMDS (1.89 mg, 0.0095 mmol) in 0.1 mL DMF at 50 °C. Samples taken after 24, 44 and 48 hours.

Table S6.8. Overview of the performed polymerizations of TsMAz (2) from stock solutions in DMF with different amounts of water as additive, including SEC-analyses.

Monomer	TsMAz (2)	TsMAz (2)	TsMAz (2)	TsMAz (2)	TsMAz (2)	TsMAz (2)
Additive	H_2O	H_2O	H_2O	H_2O	H_2O	H_2O
V / µL	0.17	1.7	17	50	100	200
Equivalents (to initiator)	1	10	100	292	584	1169
M_n[a] / g mol^{-1}	4400	4000	3600	2700	2000	1200
$Đ$[a]	1.15	1.16	1.27	1.25	1.41	1.31
Reaction time / h	<40	<40	<40	<24	<24	>48
Conversion / %	>99	>99	>99	>99	~95	~60
Name	P(Ts)-H_2O-1eq	P(Ts)-H_2O-10eq	P(Ts)-H_2O-100eq	P(Ts)-H_2O-50-µL	P(Ts)-H_2O-100-µL	P(Ts)-H_2O-200-µL

[a] Number-average molecular weight and molecular weight dispersity determined via SEC in DMF (*vs.* PEO standards).

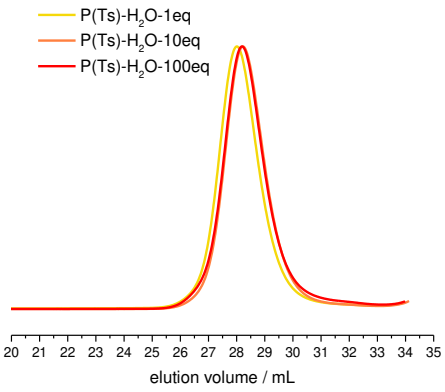

Figure S6.26. SEC traces of P(TsMAz) with water (1, 10, 100 eq.) as additive in DMF (RI signal).

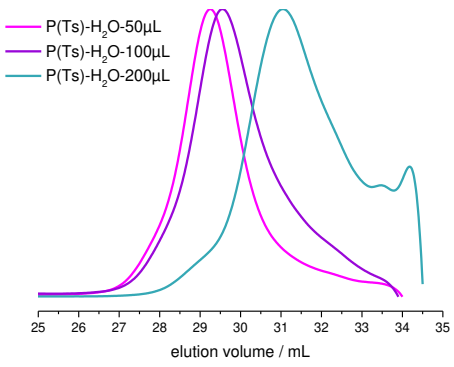

Figure S6.27. SEC traces of P(TsMAz) with water (50, 100, 200 µL) as additive in DMF (RI signal).

Table S6.9. Overview of the performed polymerizations of TsMAz (2) from stock solutions in DMF with different amounts of dry methanol as additive, including SEC-analyses.

Monomer	TsMAz (2)	TsMAz (2)	TsMAz (2)	TsMAz (2)
Additive	MeOH	MeOH	MeOH	MeOH
V / µL	38	50	100	200
Equivalents (to initiator)	100	181	362	724
M_n[a] / g mol^{-1}	4000	3400	2600	1500
$Đ$[a]	1.21	1.25	1.25	1.28
Reaction time / h	<40	<24	<24	>48
Conversion / %	>99	>99	>99	>99
Name	P(Ts)-MeOH-100eq	P(Ts)-MeOH-50-µL	P(Ts)-MeOH-100-µL	P(Ts)-MeOH-200-µL

[a] Number-average molecular weight and molecular weight dispersity determined via SEC in DMF (*vs.* PEO standards).

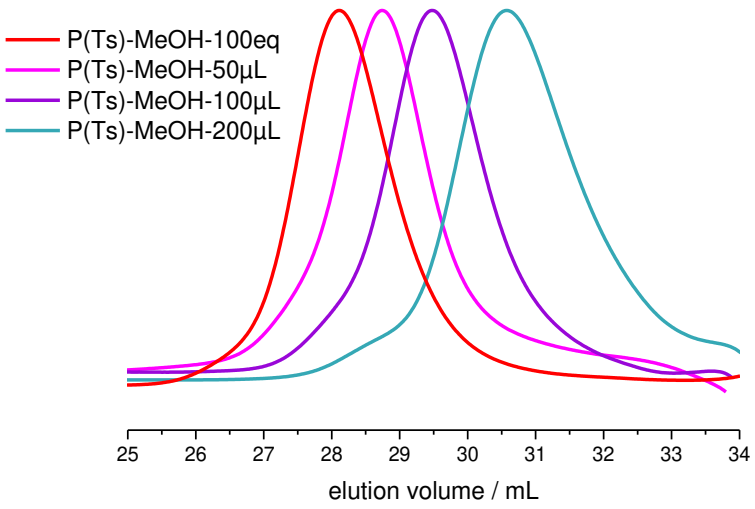

Figure S6.28. SEC traces of P(TsMAz) with methanol (100 eq., 50, 100, 200 µL) as additive in DMF (RI signal).

Table S6.10. Overview of the performed polymerizations of TsMAz (2) from stock solutions in DMF with different amounts of dry ethanol as additive, including SEC-analyses.

Monomer	TsMAz (2)	TsMAz (2)	TsMAz (2)	TsMAz (2)
Additive	EtOH	EtOH	EtOH	EtOH
V / µL	50	55	100	200
Equivalents (to initiator)	90	100	180	361
M_n[a] / g mol^{-1}	3800	3700	3600	3100
$Đ$[a]	1.16	1.18	1.20	1.21
Reaction time / h	<24	<40	<24	>48
Conversion / %	>99	>99	>99	>99
Name	P(Ts)-EtOH-50-µL	P(Ts)-EtOH-100eq	P(Ts)-EtOH-100-µL	P(Ts)-EtOH-200-µL

[a] Number-average molecular weight and molecular weight dispersity determined via SEC in DMF (*vs*. PEO standards).

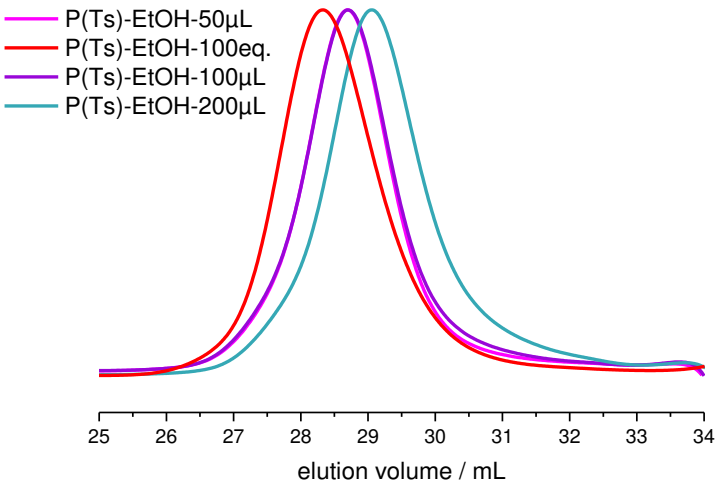

Figure S6.29. SEC traces of P(TsMAz) with ethanol (100 eq., 50, 100, 200 µL) as additive in DMF (RI signal).

Table S6.11. Overview of the performed polymerizations of TsMAz (2) from stock solutions in DMF with different amounts of dry isopropanol as additive, including SEC-analyses. In case of 1000 µL iPrOH, the monomer was only dissolved in iPrOH, only the initiator was added from a stock solution in DMF.

Monomer	TsMAz (2)	TsMAz (2)	TsMAz (2)
Additive	iPrOH	iPrOH	iPrOH
V / µL	73	200	1000
Equivalents (to initiator)	100	275	872
M_n[a] / g mol^{-1}	3900	3800	2500
$Đ$[a]	1.18	1.16	1.23
Reaction time / h	<40	<24	<48
Conversion / %	>99	~60	~95
Name	P(Ts)-iPrOH-100-eq	P(Ts)-iPrOH-200-µL	P(Ts)-iPrOH-1000-µL

[a] Number-average molecular weight and molecular weight dispersity determined via SEC in DMF (*vs*. PEO standards).

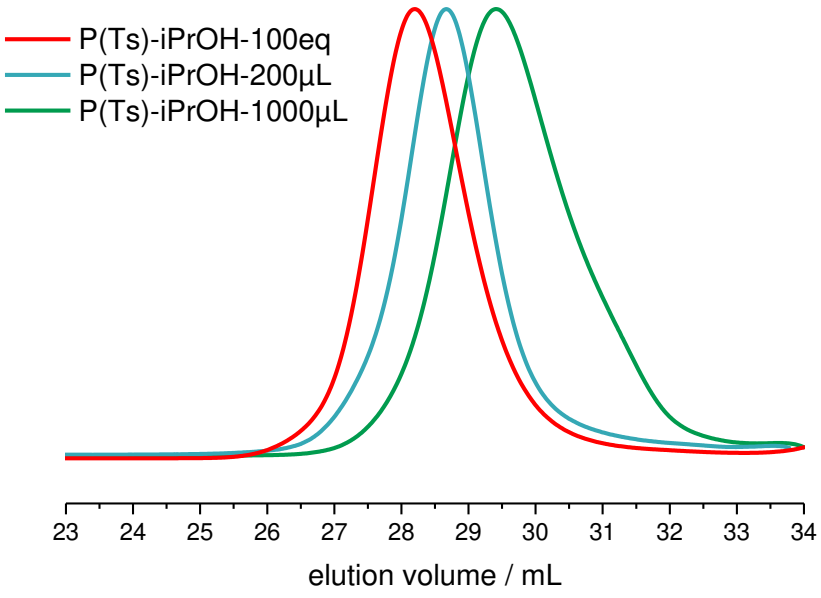

Figure S6.30. SEC traces of P(TsMAz) with isopropanol (100 eq., 200, 1000 µL) as additive in DMF (RI signal).

Table S6.12. Overview of the performed polymerizations of TsMAz (2) from stock solutions in DMF in an open vial and with dry acetone and ethyl acetate (EtOAc) as additive, including SEC-analyses. In case of 1000 µL solvent, the monomer was only dissolved in the respective solvent, only the initiator was added from a stock solution in DMF.

Monomer	TsMAz (2)	TsMAz (2)	TsMAz (2)
Additive	Open	Acetone	Ethyl acetate
V / µL	---	1000	1000
M_n[a] / g mol^{-1}	4400	6400*	3700
$Đ$[a]	1.11	1.16	1.18
Reaction time / h	<40	<24	<24
Conversion / %	>99	>99	>99
Name	P(Ts)-open vial	P(Ts)-acetone-1000-µL	P(Ts)-EtOAc-1000-µL

[a] Number-average molecular weight and molecular weight dispersity determined via SEC in DMF (*vs.* PEO standards). * Higher molecular weight, as less than the usual 100 µL of the initiator-solution was added.

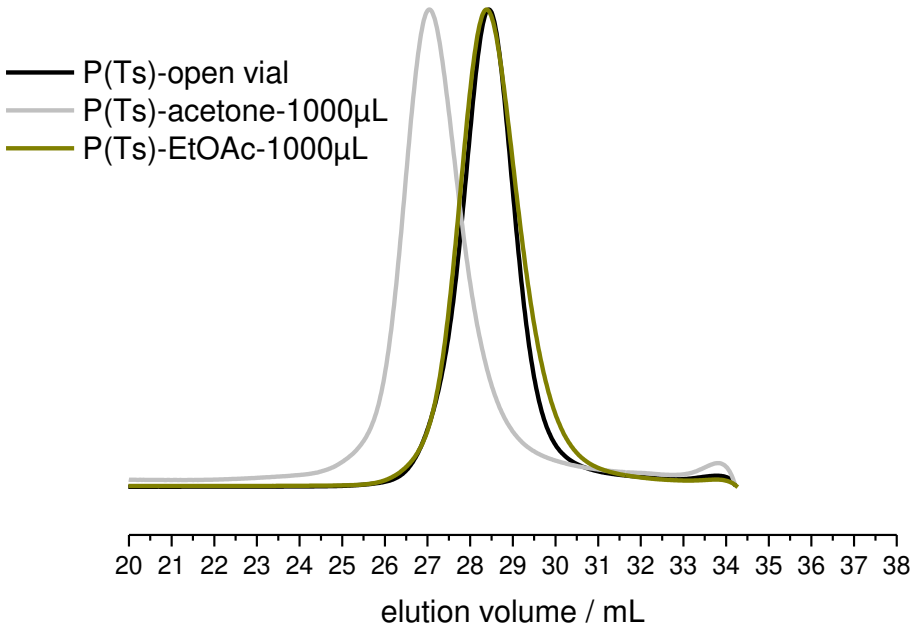

Figure S6.31. SEC traces of P(TsMAz) in an open vial, acetone and ethyl acetate in DMF (RI signal).

P(TsMAz)-Li as counter ion

TsMAz (2) (100 mg, 0.473 mmol) in 1 mL DMF, BnNHMs (1.75 mg, 0.0095 mmol) and LiHMDS (1.58 mg, 0.0095 mmol) in 0.1 mL DMF at 50 °C.

Table S6.13. Overview of the performed polymerizations of TsMAz (2) from stock solutions in DMF, with Lithium as counter ion and different amounts of water as additive, including SEC-analyses.

Monomer	TsMAz (2)	TsMAz (2)	TsMAz (2)
Additive	H_2O	H_2O	H_2O
V / µL	0.17	1.7	17
Equivalents (to initiator)	1	10	100
M_n[a] / g mol^{-1}	5700	7700	4600
Đ[a]	1.14	1.11	1.20
Reaction time / h	<48	<48	<48
Conversion / %	>99	>99	>99
Name	P(Ts)-Li-H_2O-1eq	P(Ts)-Li-H_2O-10eq	P(Ts)-Li-H_2O-100eq

[a] Number-average molecular weight and molecular weight dispersity determined via SEC in DMF (*vs.* PEO standards).

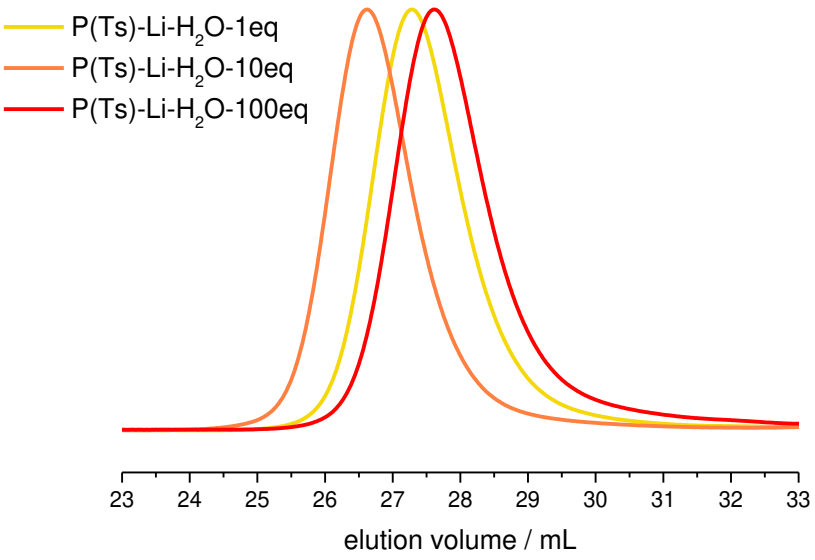

Figure S6.32. SEC traces of P(TsMAz), with Lithium as counter ion with water (1, 10, 100 eq.) as additive in DMF (RI signal).

Table S6.14. Overview of the performed polymerizations of TsMAz (2) from stock solutions in DMF, with Lithium as counter ion and different additives, including SEC-analyses.

Monomer	TsMAz (2)	TsMAz (2)	TsMAz (2)	TsMAz (2)
Additive	H_2O	MeOH	EtOH	iPrOH
V / µL	17	38	55	73
Equivalents (to initiator)	100	100	100	100
M_n[a] / g mol^{-1}	4600	5400	5400	5000
$Đ$[a]	1.20	1.19	1.16	1.16
Reaction time / h	<48	<48	<48	<48
Conversion / %	>99	>99	>99	>99
Name	P(Ts)-Li-H_2O-100eq	P(Ts)-Li-MeOH-100eq	P(Ts)-Li-EtOH-100eq	P(Ts)-Li-iPrOH-100eq

[a] Number-average molecular weight and molecular weight dispersity determined via SEC in DMF (*vs.* PEO standards).

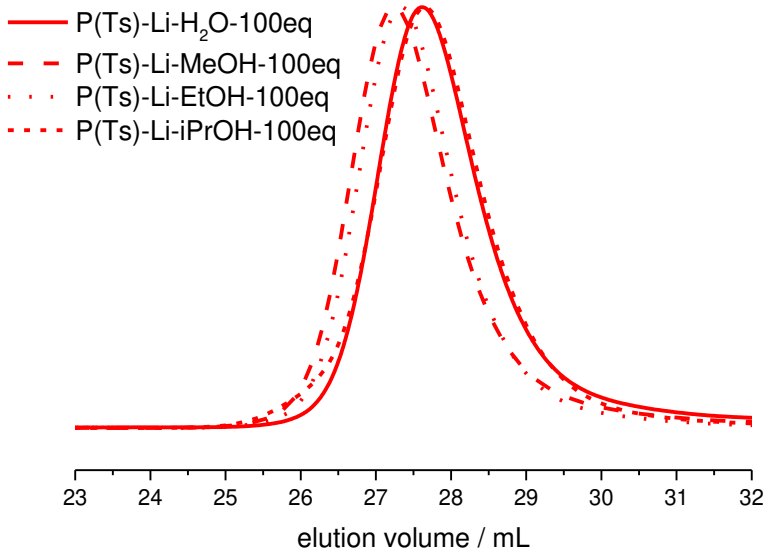

Figure S6.33. SEC traces of P(TsMAz), with Lithium as counter ion and different additives (100 eq.) in DMF (RI signal).

6.6.5 MALDI-TOF spectra.

In each frame masses of initiator, potassium-ion and the repeating monomer mass of (2) was determined (highlighted in black). The second fraction exhibits smaller molecular weights, which is based on a slow and continuous initiation of the additives. Well-known for MALDI-TOF spectroscopy, intensities of frames do not correlate quantitatively. Due to a more efficient desorption and ionization process, smaller polymers have a higher intensity than heavier ones.

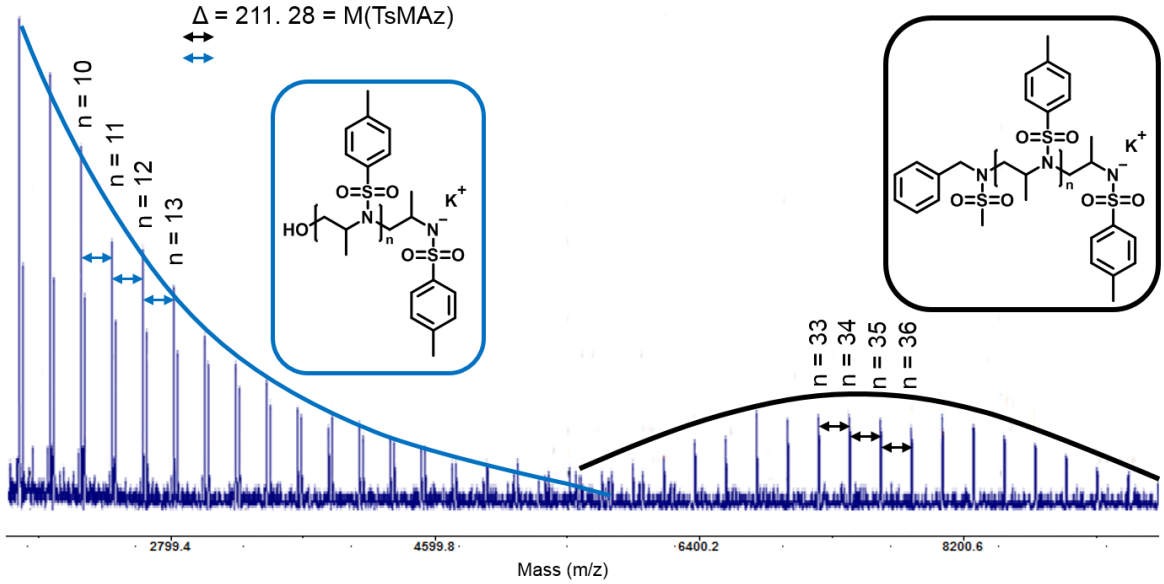

Figure S6.34. MALDI-TOF-spectrum of P(Ts)-H_2O-100eq (Table S6.7).

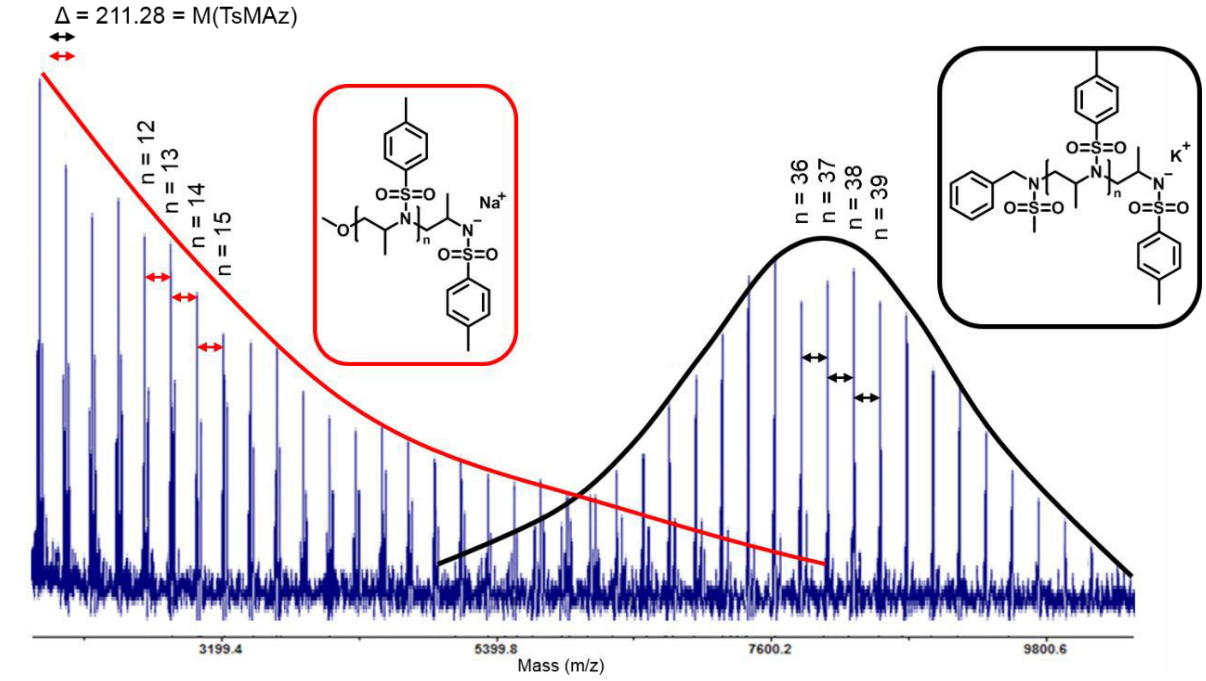

Figure S6.35. MALDI-TOF-spectrum of P(Ts)-MeOH-100eq (Table S6.8).

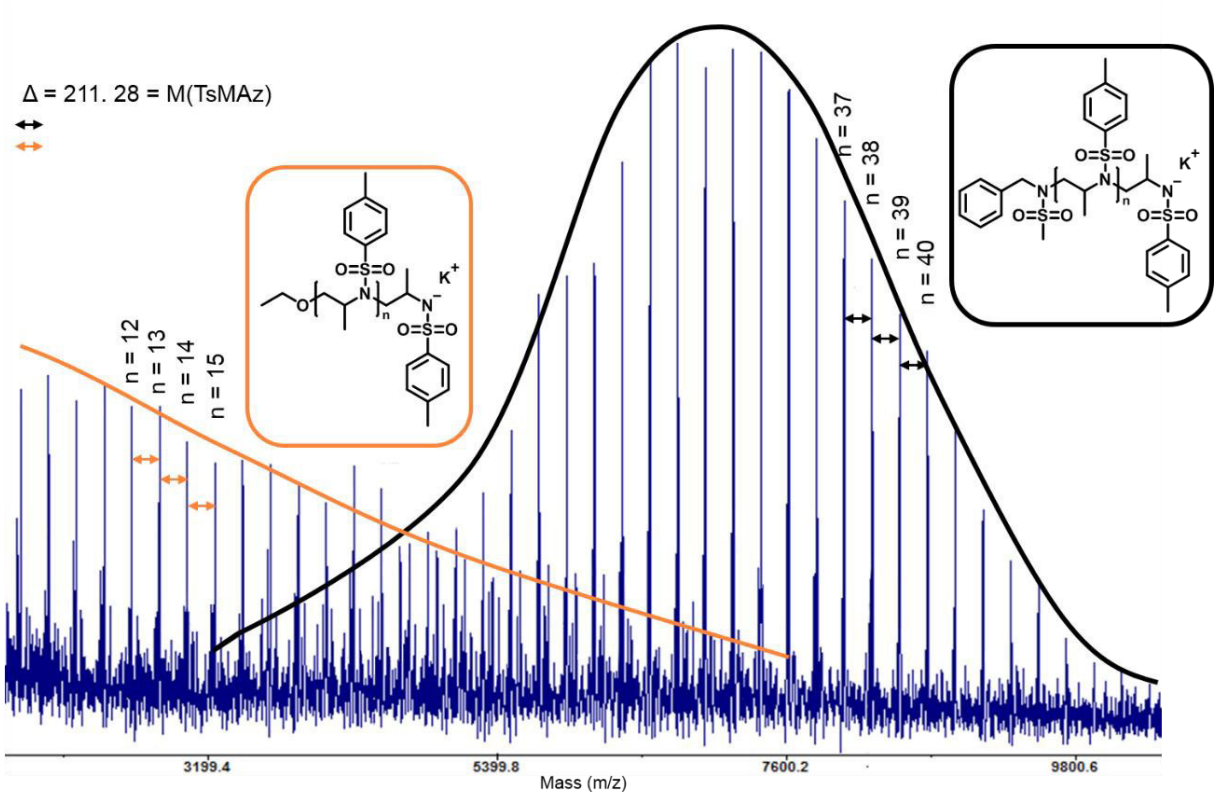

Figure S6.36. MALDI-TOF-spectrum of P(Ts)-EtOH-100eq (Table S6.9).

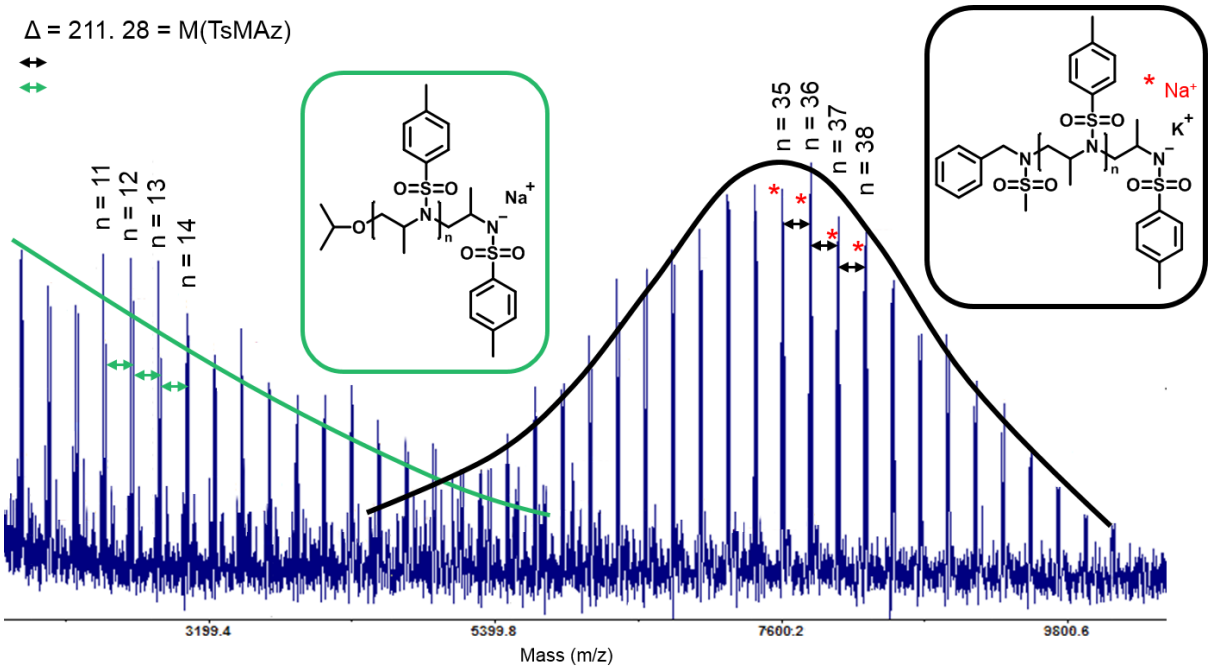

Figure S6.37. MALDI-TOF-spectrum of P(Ts)-iPrOH-100eq (Table S6.10).

6.6.6 Chain extension experiments.

For chain extension experiments the polymerizations were carried out in analogy to the procedure above. After stirring the mixtures for at least 18 h, a 100 µL-sample was taken out for further analyses and the second monomer, in 1 mL DMF, was added to the screw cap vial and stirred for further 24 h at the same temperature.

Table S6.15. Overview of the performed chain extension polymerizations of TsMAz (2) from stock solutions in DMF with 100 equivalents water as additive, including SEC-analyses.

Monomer	TsMAz (2)	TsMAz (2)
Additive	H_2O	
V / µL	17	
Equivalents (to initiator)	100	
M_n[a] / g mol^{-1}	3700	5800
$Đ$[a]	1.16	1.18
Reaction time / h	<24	<24
Conversion / %	>99	>99
Name	P(Ts)-H_2O-100eq	P(Ts-*b*-Ts)-H_2O-100eq

[a] Number-average molecular weight and molecular weight dispersity determined via SEC in DMF (*vs*. PEO standards).

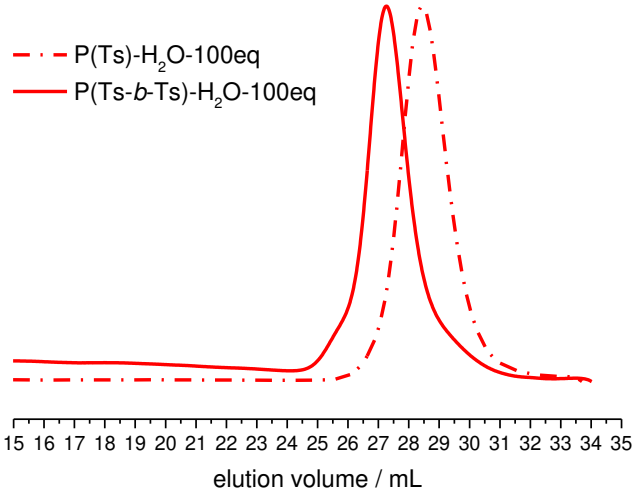

Figure S6.38. SEC traces of the chain extension of P(TsMAz) and P(TsMAz-*b*-TsMAz) with water (100 eq.) as additive in DMF (RI signal).

Table S6.16. Overview of the performed chain extension polymerizations of TsMAz (2) from stock solutions in DMF with 100 µL methanol as additive, including SEC-analyses.

Monomer	TsMAz (2)	TsMAz (2)
Additive	MeOH	
V / µL	100	
Equivalents (to initiator)	362	
M_n[a] / g mol^{-1}	2600	5400
$Đ$[a]	1.25	1.21
Reaction time / h	<24	<24
Conversion / %	>99	>99
Name	P(Ts)-MeOH-100µL	P(Ts-*b*-Ts)-MeOH-100µL

[a] Number-average molecular weight and molecular weight dispersity determined via SEC in DMF (*vs*. PEO standards).

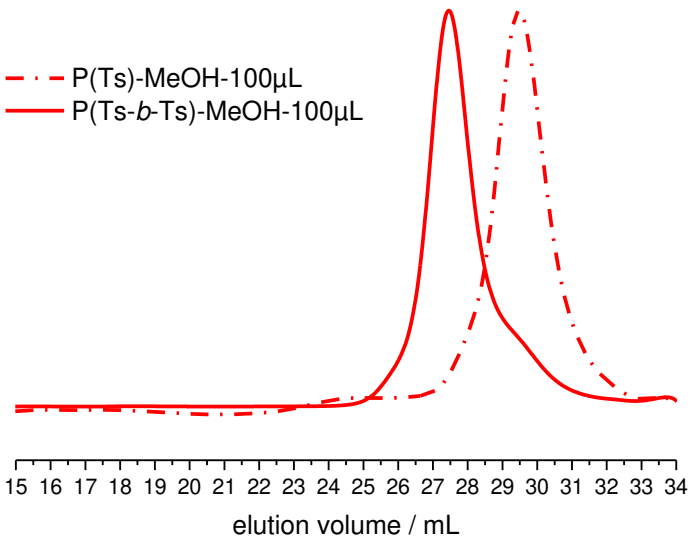

Figure S6.39. SEC traces of the chain extension of P(TsMAz) and P(TsMAz-*b*-TsMAz) with methanol (100 eq.) as additive in DMF (RI signal).

Table S6.17. Overview of the performed chain extension polymerizations of TsMAz (2) from stock solutions in DMF with 50 µL ethanol as additive, including SEC-analyses.

Monomer	TsMAz (2)	TsMAz (2)
Additive	EtOH	
V / µL	50	
Equivalents (to initiator)	90	
M_n[a] / g mol^{-1}	3800	6200
$Đ$[a]	1.16	1.17
Reaction time / h	<24	<24
Conversion / %	>99	>99
Name	P(Ts)-EtOH-50µL	P(Ts-*b*-Ts)-EtOH-50µL

[a] Number-average molecular weight and molecular weight dispersity determined via SEC in DMF (*vs.* PEO standards).

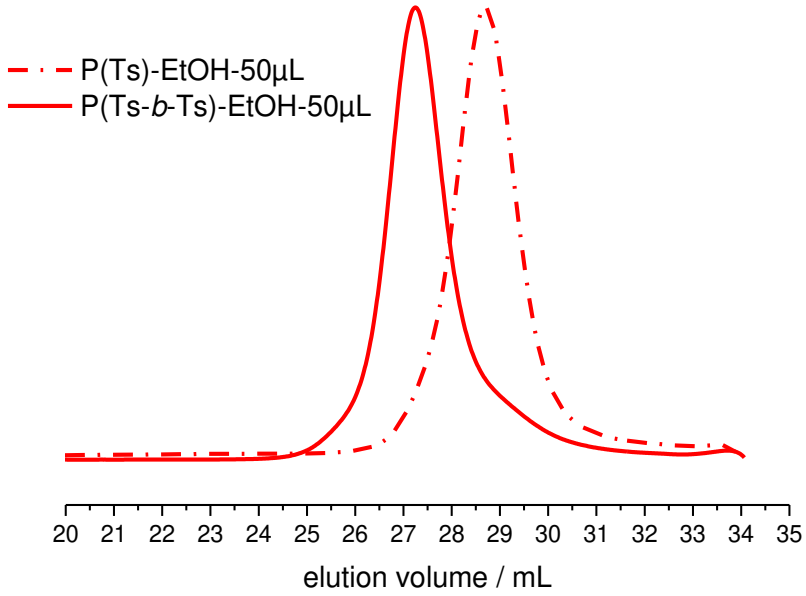

Figure S6.40. SEC traces of the chain extension of P(TsMAz) and P(TsMAz-*b*-TsMAz) with ethanol (50 µL) as additive in DMF (RI signal).

Table S6.18. Overview of the performed chain extension polymerizations of TsMAz (2) from stock solutions in DMF with 100 µL isopropanol as additive, including SEC-analyses.

Monomer	TsMAz (2)	TsMAz (2)
Additive	iPrOH	
V / µL	200	
Equivalents (to initiator)	275	
M_n[a] / g mol^{-1}	3800	6200
$Đ$[a]	1.16	1.20
Reaction time / h	<24	<24
Conversion / %	~60	>99
Name	P(Ts)-iPrOH-200µL	P(Ts-*b*-Ts)-iPrOH-200µL

[a] Number-average molecular weight and molecular weight dispersity determined via SEC in DMF (*vs.* PEO standards).

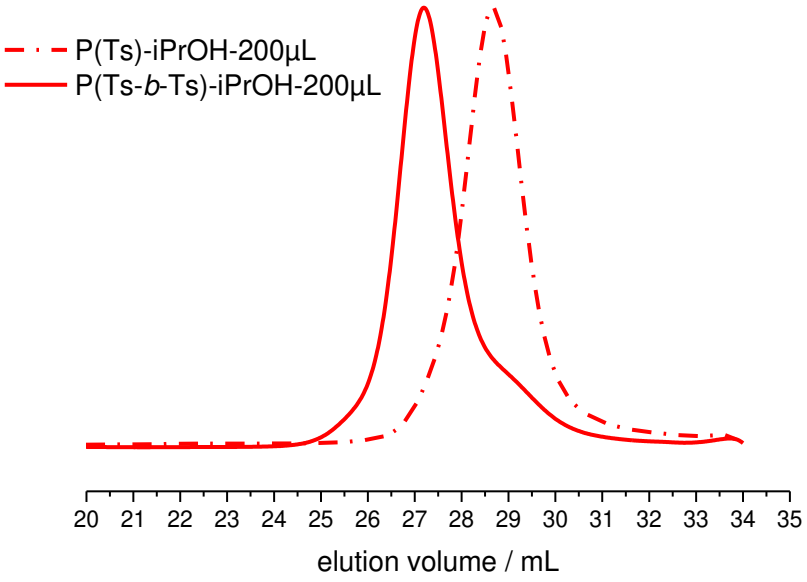

Figure S6.41. SEC traces of the chain extension of P(TsMAz) and P(TsMAz-*b*-TsMAz) with isopropanol (200 µL) as additive in DMF (RI signal).

6.6.7 Computational Detail.

All DFT calculations were carried out with the Gaussian 09 package.[44] All structures were fully optimized at the B3LYP level of theory,[45] with the basis set of 6-31+G*.[46-47] The harmonic frequency calculations were performed at the same level of theory to characterize the nature of stationary points, i.e. no imaginary frequencies were found for all optimized structures. The thermostatistical contributions to the free energy were obtained from a harmonic oscillator approximation at temperatures of 323.15 K and for 1 atm pressure. Accurate electronic energies were obtained from single point calculations at the B3LYP level upon the optimized structures, in conjunction with the 6-311++G** basis set.[46, 48] The single point calculations were performed together with PCM (Polarizable Continuum Model) model[49-51] by employing DMF as the solvent. To calculate the pK_a values, the SMD solvation model[52] was used to compute the solvation Gibbs free energies by employing the gas-phase optimized structures, and with DMF as the solvent. The final Gibbs free energies in solution were calculated from the gas-phase single point electronic energies plus the gas-phase thermostatistical contributions, and the SMD solvation Gibbs free energies.

The following equations have been used to calculate interested properties:

$$\mu = -\frac{1}{2}(\mathrm{IP} + \mathrm{EA}) \tag{1}$$

$$\eta = \mathrm{IP} - \mathrm{EA} \tag{2}$$

where IP is ionization potential, EA is electron affinity, η is chemical potential and μ is chemical hardness.

$$\omega^{+} = \frac{\mu^2}{2\eta} \tag{3}$$

$$\omega^{-} = \frac{1}{2}\frac{(\mu_A - \mu_B)^2}{(\eta_A + \eta_B)^2}\eta_A \tag{4}$$

where ω^{+} is electrophilicity index,[53] and ω^{-} is nucleophilicity index.[54] Details of these two indexes can be found in ref.[55].

Table S6.19. Calculated ionization potential (IP), electron affinity (EA), chemical potential (μ), chemical hardness (η), energies of LUMO (ε_{LUMO}) and HOMO (ε_{HOMO}), electrophilicity index ($\boldsymbol{\omega^+}$) all values are in eV. NBO charges on N, C and O atoms.

Monomer	IP	EA	μ	η	ε_{LUMO}	$\boldsymbol{\omega^+}$	q_C
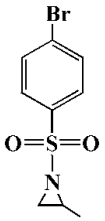	7.06	2.22	-4.64	4.84	-1.75	2.22	-0.1937
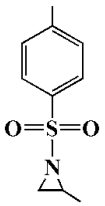	6.96	1.95	-4.45	5.01	-1.44	1.98	-0.1952
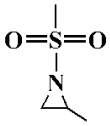	7.19	0.80	-3.99	6.39	-0.24	1.25	-0.1945

Table S6.20. Calculated ionization potential (IP), electron affinity (EA), chemical potential (μ), chemical hardness (η), energies of LUMO (ε_{LUMO}) and HOMO (ε_{HOMO}), nucleophilicity index (ω^-), all values are in eV. NBO charges on N and O atoms.

Nucleophile	IP	EA	μ	η	ε_{HOMO}	ω^-	N/O
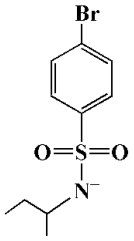	4.91	-2.76	-1.07	7.67	-5.44	0.27	-1.0303
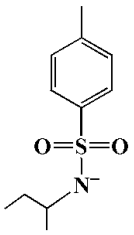	4.82	-0.74	-2.04	5.56	-5.36	0.14	-1.0328
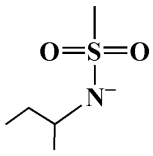	4.81	-0.57	-2.12	5.38	-5.30	0.13	-1.0405
isoPrO$^-$	4.55	-0.42	-2.07	4.97	-4.72	0.14	-1.0525
EtO$^-$	4.37	-0.48	-1.94	4.85	-4.70	0.16	-1.0484
MeO$^-$	4.38	-0.53	-1.93	4.91	-4.67	0.16	-1.0569
HO$^-$	5.16	-0.63	-2.27	5.79	-5.40	0.13	-1.4002

Table S6.21. Calculated Δ*G* (in kcal mol^{-1}) and pK_a values with DMF as solvent and at 323.15 K.

Protonated species	Δ*G*	pK_a
H_2O	20.7	14.0
MeOH	17.9	12.1
EtOH	17.8	12.0
isoPrOH	18.5	12.5
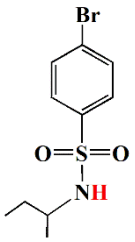	-0.8	-0.5
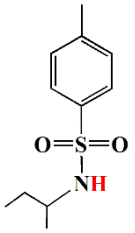	2.0	1.4
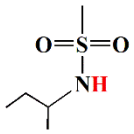	2.3	1.5

6.6.8 Ts-ω-PrOHAz.

Monomer synthesis of 2-*ω*-propanol-*N*-tosylaziridine (Ts-ωPrOHAz) (6)

Chloramine-T (7.01 g, 46 mmol, 1 eq.) was dried by freeze-drying with benzene in vacuum overnight. But-3-en-1-ol (12 mL, 138 mmol, 3 eq.) was added together with Chloramine-T and Phenyltrimethylammonium tribromide (PTAB) (1.74 g, 4.6 mmol, 0.1 eq.) to the reaction flask, the mixture was dissolved in anhydrous acetonitrile (ACN) (100 mL). The mixture was stirred at room temperature for 3 days. 100 mL of Ethyl acetate and water were added to the reaction flask, the organic phase was washed with brine and dried with Mg_2SO_4. The organic phase was concentrated at 30 °C and reduced pressure. The product was purified by column chromatography over silica gel (Et_2O 100%; Rf: 0.2). The pure product crystalized as withe crystals from a colorless oil.

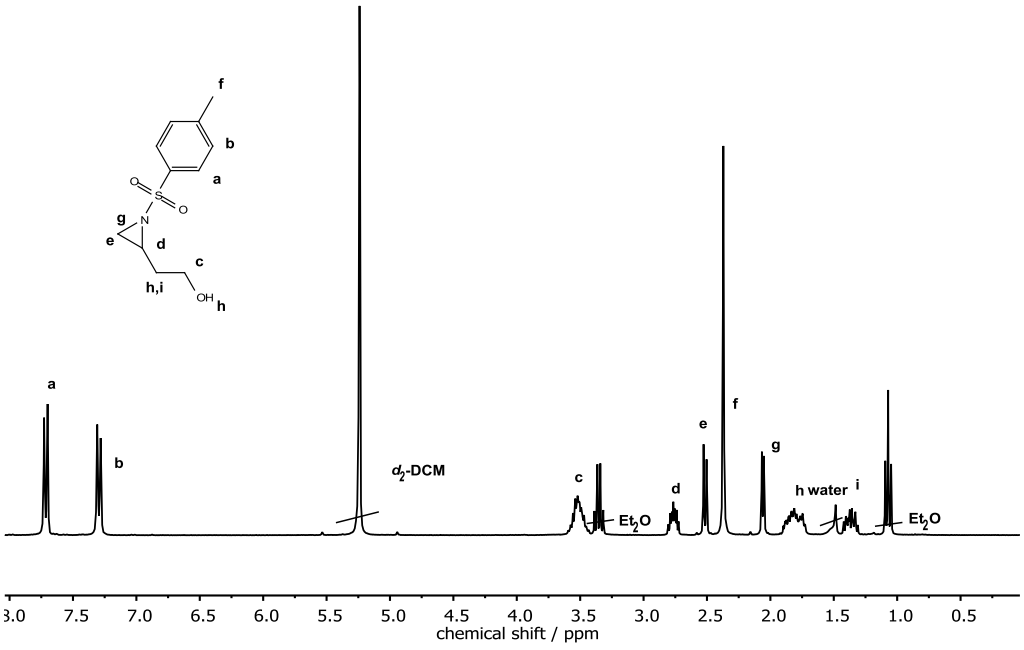

Figure S6.42. ^{1}H NMR (300 MHz, 298K, DCM-d_2) of Ts-ωPrOHAz (6).

δ [ppm] = 7.70 (d, 2H, a), 7.30 (d, 2H, b), 3.61 – 3.46 (m, 2H, c), 2.76 (m, 1H, d), 2.51 (d, 1H, d), 2.37 (s, 3H, f), 2.06 (d, 1H, g), 1.92 – 1.69 (m, 2H, h), 1.37 (m, 1H, i).

Polymerizations: Example for P(Ts-*ω*PrOHAz)$_{20}$

All glassware was flame dried in vacuum for three times. All reactants were freeze dried with benzene, KHMDS was dried in vacuum without benzene. (6) (0.38 mmol, 20 eq.) was dissolved in 1 mL *N,N*-dimethylformamid (DMF). The Initiator (BnNHMs) was dissolved in 1 mL DMF and added to KHMDS (1/1), 1 eq. of the deprotonated initiator was then transferred with a syringe to the reaction flask, containing the monomer. The mixture was stirred at 55 °C for 20 h. Pure polymer was obtained by removing DMF in vacuum.

Table S6.22. Overview of performed polymerizations with Ts-*ω*PrOH (6).

Sample	*Đ*	M_n (SEC)	M_p(SEC)	M_n(Theory)
Bn-(6)$_{20}$	1.26	1600	2000	3300
Bn-(6)$_{30}$	1.30	1700	2100	5000
Bn-(6)$_{40}$	1.34	2300	2800	6600

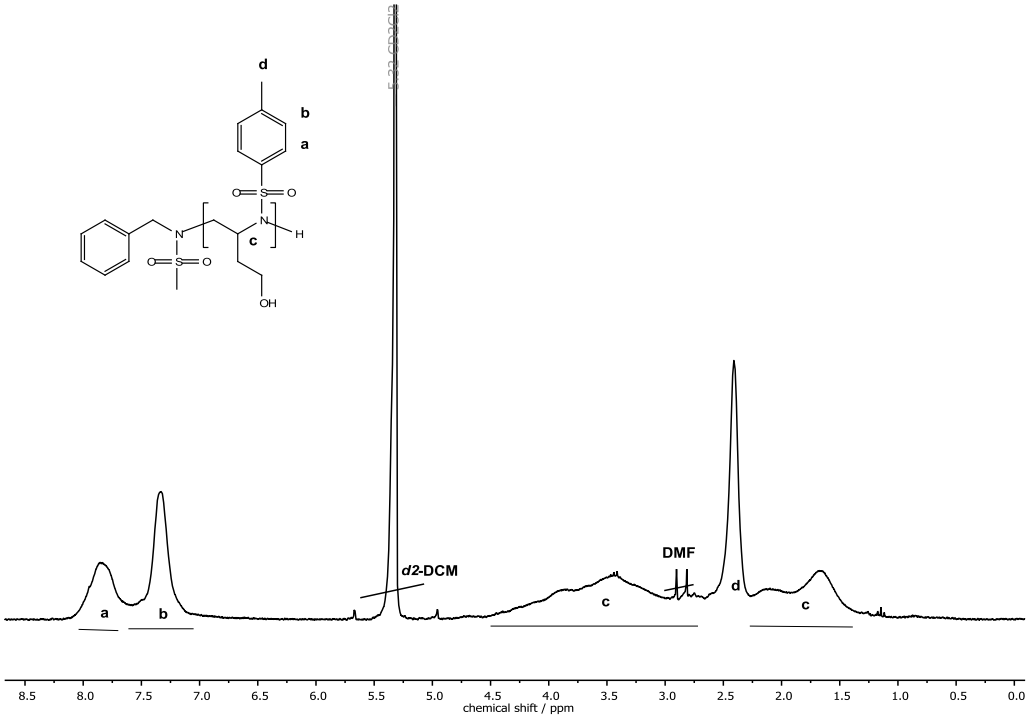

Figure S6.43. ^{1}H NMR (300 MHz, 298 K, DCM-d_2) of P(6)$_{20}$: δ 7.84 (s, 2H, a), 7.33 (s, 2H, b), 4.50 – 2.67, 1.30-2.12 (m, 7H, c).

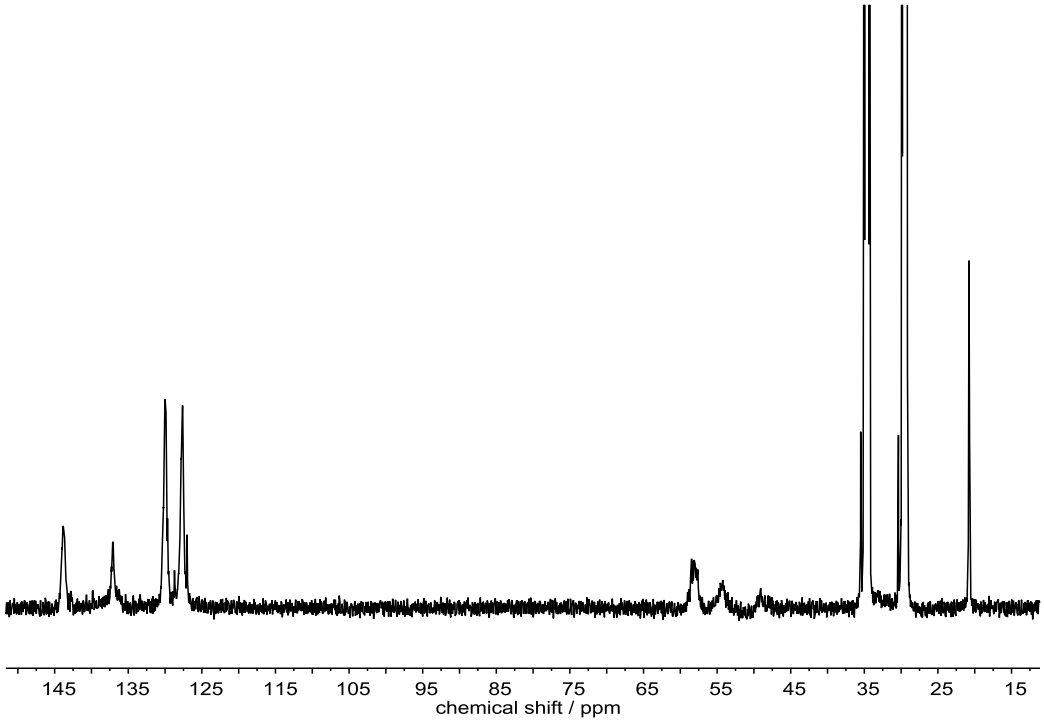

Figure S6.44. ^{13}C NMR, quantitative (176 MHz, 323 K, DMF-d_7) of P(6)$_{20}$, δ [ppm] =144.02 (s, 1C, arom.), 137.21 (s, 1C, arom.), 130.40 (s, 2C, arom.), 127.41 (s, 2C, arom.), 59.49-45.72 (m, 4C, backbone), 21.10 (s, 1C, aromat-CH_3).

6.7 References

1. Frey, H.; Ishizone, T., *Macromolecular Chemistry and Physics* **2017,** *218* (12), 1700217.
2. Hirao, A.; Goseki, R.; Ishizone, T., *Macromolecules* **2014,** *47* (6), 1883-1905.
3. Hadjichristidis, N.; Hirao, A., *Anionic Polymerization*. Springer Japan: Japan, **2015**; p 1082.
4. Hadjichristidis, N.; Iatrou, H.; Pispas, S.; Pitsikalis, M., *Journal of Polymer Science Part A: Polymer Chemistry* **2000,** *38* (18), 3211-3234.
5. Matyjaszewski, K.; Müller, A. H. E., *Controlled and Living Polymerizations: From Mechanisms to Applications*. John Wiley & Sons: Weinheim, Germany, **2009**; p 634.
6. Braunecker, W. A.; Matyjaszewski, K., *Progress in Polymer Science* **2007,** *32* (1), 93-146.
7. Stewart, I. C.; Lee, C. C.; Bergman, R. G.; Toste, F. D., *Journal of the American Chemical Society* **2005,** *127* (50), 17616-17617.
8. Gleede, T.; Rieger, E.; Homann-Müller, T.; Wurm, F. R., *Macromolecular Chemistry and Physics* **2017**, 1700145.
9. Homann-Müller, T.; Rieger, E.; Alkan, A.; Wurm, F. R., *Polym. Chem.* **2016,** *7* (35), 5501-5506.
10. Wang, X.; Liu, Y.; Li, Z.; Wang, H.; Gebru, H.; Chen, S.; Zhu, H.; Wei, F.; Guo, K., *ACS Macro Letters* **2017,** *6* (12), 1331-1336.
11. Bakkali-Hassani, C.; Rieger, E.; Vignolle, J.; Wurm, F. R.; Carlotti, S.; Taton, D., *Chem. Commun. (Camb)* **2016,** *52* (62), 9719-9722.
12. Bakkali-Hassani, C.; Rieger, E.; Vignolle, J.; Wurm, F. R.; Carlotti, S.; Taton, D., *European Polymer Journal* **2017,** *95*, 746-755.
13. Rieger, E.; Gleede, T.; Weber, K.; Manhart, A.; Wagner, M.; Wurm, F. R., *Polym. Chem.* **2017,** *8* (18), 2824-2832.
14. Reisman, L.; Mbarushimana, C. P.; Cassidy, S. J.; Rupar, P. A., *ACS Macro Letters* **2016,** *5* (10), 1137-1140.
15. Rieger, E.; Alkan, A.; Manhart, A.; Wagner, M.; Wurm, F. R., *Macromolecular Rapid Communications* **2016,** *37* (10), 833-839.
16. Rieger, E.; Blankenburg, J.; Grune, E.; Wagner, M.; Landfester, K.; Wurm, F. R., *Angewandte Chemie International Edition* **2018,** *57*, DOI:10.1002/anie.201710417.
17. Rieger, E.; Manhart, A.; Wurm, F. R., *ACS Macro Letters* **2016,** *5* (2), 195-198.
18. Lungwitz, U.; Breunig, M.; Blunk, T.; Gopferich, A., *Eur. J. Pharm. Biopharm.* **2005,** *60* (2), 247-66.
19. Boussif, O.; Lezoualc'h, F.; Zanta, M. A.; Mergny, M. D.; Scherman, D.; Demeneix, B.; Behr, J.-P., *Proceedings of the National Academy of Sciences* **1995,** *92* (16), 7297-7301.
20. Perevyazko, I. Y.; Bauer, M.; Pavlov, G. M.; Hoeppener, S.; Schubert, S.; Fischer, D.; Schubert, U. S., *Langmuir* **2012,** *28* (46), 16167-16176.

21. Islam, M. A.; Park, T. E.; Singh, B.; Maharjan, S.; Firdous, J.; Cho, M.-H.; Kang, S.-K.; Yun, C.-H.; Choi, Y. J.; Cho, C.-S., *Journal of Controlled Release* **2014,** *193*, 74-89.
22. Jones, G. D.; Langsjoen, A.; NEUMANN, S. M. M. C.; Zomlefer, J., *The Journal of Organic Chemistry* **1944,** *9* (2), 125-147.
23. Perevyazko, I.; Gubarev, A. S.; Tauhardt, L.; Dobrodumov, A.; Pavlov, G. M.; Schubert, U. S., *Polymer Chemistry* **2017,** *8* (46), 7169-7179.
24. Szwarc, M., Living polymers and mechanisms of anionic polymerization. In *Living Polymers and Mechanisms of Anionic Polymerization*, Springer: **1983**; pp 1-177.
25. Asami, R.; Khanna, S.; Levy, M.; Szwarc, M., *Transactions of the Faraday Society* **1962,** *58*, 1821-1826.
26. Herzberger, J.; Niederer, K.; Pohlit, H.; Seiwert, J.; Worm, M.; Wurm, F. R.; Frey, H., *Chemical Reviews* **2016,** *116* (4), 2170-2243.
27. Odian, G., *Principles of Polymerization*. 4. ed.; John Wiley & Sons, Inc. : Hoboken, New Jersey, USA, **2004**.
28. Barrere, M.; Ganachaud, F.; Bendejacq, D.; Dourges, M.-A.; Maitre, C.; Hémery, P., *Polymer* **2001,** *42* (17), 7239-7246.
29. Barrère, M.; Maitre, C.; Dourges, M.; Hémery, P., *Macromolecules* **2001,** *34* (21), 7276-7280.
30. Maitre, C.; Ganachaud, F.; Ferreira, O.; Lutz, J. F.; Paintoux, Y.; Hémery, P., *Macromolecules* **2000,** *33* (21), 7730-7736.
31. Kimura, H., *Journal of Polymer Science Part A: Polymer Chemistry* **1998,** *36* (1), 189-193.
32. Spears, B. R.; Marin, M. A.; Montenegro-Burke, J. R.; Evans, B. C.; McLean, J.; Harth, E., *Macromolecules* **2016,** *49* (6), 2022-2027.
33. Camps, M.; Ait-Hamouda, R.; Boileau, S.; Hemery, P.; Lenz, R., *Macromolecules* **1988,** *21* (4), 891-894.
34. Eromosele, I. C.; Pepper, D. C.; Ryan, B., *Macromolecular Chemistry and Physics* **1989,** *190* (7), 1613-1622.
35. Nicolas, J.; Couvreur, P., *Wiley Interdisciplinary Reviews: Nanomedicine and Nanobiotechnology* **2009,** *1* (1), 111-127.
36. Weiss, C. K.; Ziener, U.; Landfester, K., *Macromolecules* **2007,** *40* (4), 928-938.
37. Behan, N.; Birkinshaw, C., *Macromolecular rapid communications* **2000,** *21* (13), 884-886.
38. Li, Y.; Schadler, L.; Benicewicz, B.; Barner-Kowollik, C., *Handbook of RAFT Polymerization*. Wiley-VCH: Weinheim: **2008**.
39. Perrier, S. b., *Macromolecules* **2017,** *50* (19), 7433-7447.
40. Matyjaszewski, K., *Macromolecules* **2012,** *45* (10), 4015-4039.
41. Freeman, R.; Hill, H.; Kaptein, R., *Journal of Magnetic Resonance (1969)* **1972,** *7* (3), 327-329.

42. Popov, M., *Modern NMR techniques and their application in chemistry*. CRC Press: **1990**.
43. Sotak, C.; Dumoulin, C., *Wiley, New York* **1984,** *4*, 91.
44. Frisch, M.; Trucks, G.; Schlegel, H.; Scuseria, G.; Robb, M.; Cheeseman, J.; Scalmani, G.; Barone, V.; Mennucci, B.; Petersson, G., Gaussian 09, revision D. 01. Gaussian, Inc., Wallingford CT: **2009**.
45. Becke, A. D., *The Journal of chemical physics* **1993,** *98* (7), 5648-5652.
46. Clark, T.; Chandrasekhar, J.; Spitznagel, G. W.; Schleyer, P. V. R., *Journal of Computational Chemistry* **1983,** *4* (3), 294-301.
47. Ditchfield, R.; Hehre, W. J.; Pople, J. A., *The Journal of Chemical Physics* **1971,** *54* (2), 724-728.
48. McLean, A.; Chandler, G., *The Journal of Chemical Physics* **1980,** *72* (10), 5639-5648.
49. Miertuš, S.; Scrocco, E.; Tomasi, J., *Chemical Physics* **1981,** *55* (1), 117-129.
50. Miertus, S.; Tomasi, J., *Chemical physics* **1982,** *65* (2), 239-245.
51. Pascual-ahuir, J.-L.; Silla, E.; Tunon, I., *Journal of Computational Chemistry* **1994,** *15* (10), 1127-1138.
52. Marenich, A. V.; Cramer, C. J.; Truhlar, D. G., *The Journal of Physical Chemistry B* **2009,** *113* (18), 6378-6396.
53. Parr, R. G.; Szentpaly, L. v.; Liu, S., *Journal of the American Chemical Society* **1999,** *121* (9), 1922-1924.
54. Jaramillo, P.; Pérez, P.; Contreras, R.; Tiznado, W.; Fuentealba, P., *The Journal of Physical Chemistry A* **2006,** *110* (26), 8181-8187.
55. Jhon, Y. H.; Shim, J.-G.; Kim, J.-H.; Lee, J. H.; Jang, K.-R.; Kim, J., *The Journal of Physical Chemistry A* **2010,** *114* (49), 12907-12913.

7. Microwave-assisted Desulfonylation of Polysulfonamides towards linear Polypropylenimine

Elisabeth Rieger,[1] Angelika Manhart,[1] Tassilo Gleede,[1] Markus Lamla,[2] Frederik R. Wurm[1]

[1]Max Planck Institute for Polymer Research, Ackermannweg 10, 55128 Mainz, Germany
[2]Institute for Organic Chemistry III/Macromolecular Chemistry, University of Ulm, Albert-Einstein-Allee 11, 89081 Ulm, Germany

Unpublished results

Parts of the deprotection experiments were performed by Angelika Manhart and Tassilo Gleede. The monomers were synthesized by Angelika Manhart. MALDI-TOF were performed by Markus Lamla.

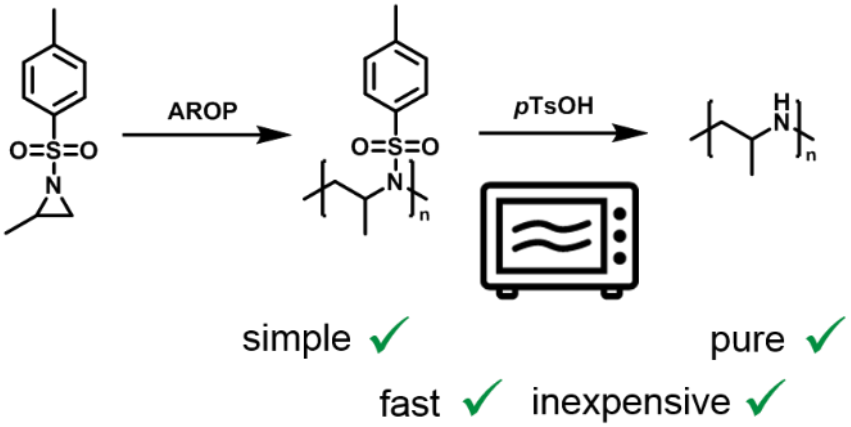

Keywords: Living Anionic Polymerization, Polyaziridine, linear PEI, Hydrolysis, Deprotection.

7.1 Abstract

Linear poly(ethyleneimine) (LPEI) has been the gold standard for gene delivery, but drawbacks like toxicity issues require optimization of this system. In this work, we investigate the desulfonylation of poly(aziridine)s (PAz) – a new polymer class for controlled anionic polymerization with a great variety of functionalities – to afford linear poly(propylenimine) (LPPI) as a more hydrophobic alternative to LPEI. We studied and compared different deprotection methods for tosyl- (Ts) and mesyl- (Ms) PAz-derivatives. The reductive cleavage, using Red-Al yielded 80% deprotection of P(TsMAz) and P(TsMAz-*co*-MsMAz). Quantitative conversion to LPPI was obtained when P(TsMAz) was hydrolyzed by *p*TsOH under microwave (MW) irradiation. The same treatment removed 90% of the mesyl groups from P(MsMAz). The MW-assisted acidic hydrolysis represents a fast, inexpensive and easy approach in comparison to other methods, where complex reaction conditions and tedious purifications are major drawbacks. The high purity of the obtained products, as well as the control achieved by living anionic polymerization, demonstrate many advantages of our strategy, especially for future biomedical implementations.

7.2 Introduction

The living anionic polymerization (LAP) of activated aziridines, i.e. sulfonyl aziridines, gives access to poly(sulfonamide)s with various structures. This azaanionic polymerization, first reported in 2005, and revived by our group in 2013, allows the synthesis of polymers with nitrogen atoms in the polymer backbone, which were not accessible before.[1-5] Recent publications studied the mechanism in detail [6-8] or the control of polymer microstructure by copolymerization of various activated aziridines,[9-10] thriving the understanding of azaanionic polymerization, next to the well-known oxy- and carbanionic polymerizations.[11-12] The interest in polyaziridines (PAz), i.e. the poly(sulfonamide)s which are obtained after the polymerization of sulfonyl-aziridines, is mainly motivated by the possibility to prepare various polyamines after desulfonylation. Well-defined polyamines are interesting materials as polyelectrolytes or transfection agents. Today, linear poly(ethyleneimine) (LPEI) is extensively used for non-viral gene transfection, due to its high efficiency.[13-14] However, its synthesis *via* the cationic polymerization of oxazolines,[15] also requires a hydrolysis step, which is often not complete and molecular characterization of commercial PEI batches (linear and branched from the cationic polymerization of aziridine) is challenging.[16] Concerns about the high toxicity of PEI make research for less toxic alternatives necessary. The anionic polymerization of activated aziridines might be a powerful strategy to meet the needs, as it can be combined with other anionic polymerization techniques and the broad monomer scope might result in efficient but less toxic alternatives to PEI. Further, various strategies for desulfonylation of low molecular weight sulfonamides are known (see below).

Surprisingly, the focus of research on non-viral transfection agents was almost exclusively on LPEI, while linear poly(propylenimine) (LPPI), with one more methyl-group, has not been considered to date, even though a reasonable synthesis had been reported already decades ago.[17] Compared to living anionic polymerization, cationic polymerizations are often limited, especially for high molecular weights.[12] However, also PAz need a reasonable desulfonylation in order to prepare the polyamine. Many different strategies on deprotection of low-molecular weight sulfonamides, especially for toluene-sulfonamides, have been reported.[18-19] Classic routes employ sodium or lithium naphthalenide,[18-23] sodium or lithium in liquid ammonia,[18-19, 24] strong acids[18-19, 24-25] and sodium amalgam.[19, 26-27] Several other methods, such as the mild samarium(II)-iodide (SmI_2),[18-19, 28-31] electrochemistry,[19, 24, 31-35] microwave (MW) irradiation,[19, 36-37] tributyltin hydride / azoisobutyronitrile (Bu_3SnH/AIBN),[19, 30] trimethylsilyl iodide (TMSI),[19, 38] different titanium-compounds,[19, 30, 39-40] magnesium in methanol,[18-19, 41] other metal complexes,[19, 42] photolysis,[19, 43-44] tetra-*n*-butylammonium fluoride (TBAF)[19, 45-46] have been reported. Some of those methodologies only cleave very "active" sulfonamides, i.e. with additional electron withdrawing groups (e.g. nosyl)[47-48] or secondary sulfonamides.[19]

However, for PAz additional issues for the desulfonylation step need to be addressed. Especially, the change in solubility from the polysulfonamide to the polyamine, accompanied with difficult purification procedures are more complex than for low molecular weight compounds. Therefore, many desulfonylation strategies are not applicable for polymeric structures. Only in four publications, the deprotection of PAz has been reported. Acidic hydrolysis of tosyl groups was achieved on a poly(styrene$_{37}$-*b*-TsAz$_2$) with hydrobromic acid and phenol in refluxing THF.[49] Bergman and Toste reported the desulfonylation with lithium naphthalenide (LiNp), but did not show details on the obtained products, e.g. molecular weight distribution or NMR spectra of the product.[8] The group of Rupar was able to fully remove the sulfonyl groups, using elemental lithium and *tert*-butanol (*t*-BuOH) in hexamethylphosphoramide (HMPA) and tetrahydrofuran (THF), to obtain LPEI.[3] This is a reasonable method with good yields, but with lithium metal and the toxicity of HMPA and the low temperatures (-20 – 5 °C), this strategy is not attractive for larger scales. We recently reported the desulfonylation of polyaziridines under reductive conditions using sodium bis(2-methoxyethoxy)aluminiumhydride (Red-Al) in toluene. Under these conditions, ca. 80% of desulfonylation was achieved and further acetal-protected alcohols remained intact.[4]

Herein, we investigated different methods for the desulfonylation of poly(aziridine)s, namely P(TsMAz)$_{60}$, P(MsMAz)$_{47}$ and copolymers of P((TsMAz)$_{25}$-*co*-(MsMAz)$_{25}$). The goal was to find a facile methodology, which is at best non-toxic and metal-free. Especially for biomedical applications, removal of heavy metals might be challenging and their use should be avoided. The simple acidic hydrolysis with toluene sulfonic acid under microwave irradiation was found to meet most of those requirements and is highlighted herein.

7.3 Results and Discussion

The polyaziridines were synthesized *via* the living anionic ring-opening polymerization of sulfonyl aziridines (2-methyl-*N*-mesyl-aziridine (MsMAz, 1) and 2-methyl-*N*-tosylaziridine (TsMAz, 2)), initiated by *N*-pyrene-methanesulfonamide (PyNHMs), according to literature (Scheme 7.1).[4, 6, 9-10]

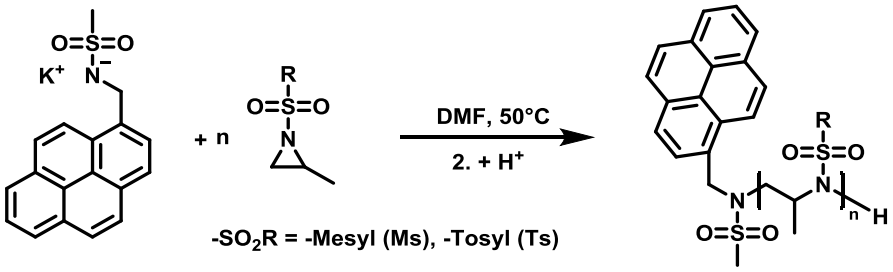

Scheme 7.1. Azaanionic ring-opening polymerization of activated aziridines.

Experimental details and analytical data of the obtained polymers P(MsMAz)$_{47}$ (P1), P(TsMAz)$_{60}$ (P2) and P((TsMAz)$_{25}$-*co*-(MsMAz)$_{25}$) (P(2-*co*-1)) are summarized in Table 7.1 and the Supporting Information (7.6.2). The repeating units, given as a subscript number, were determined *via* endgroup analysis from the ^{1}H NMR-spectra. All polymers have monomodal molecular weight distributions with $Đ \leq 1.15$ and showed full monomer conversion and quantitative yield.

Table 7.1. Characterization data of polyaziridines.

Polymer	#	M_n(th)[a]	M_n[b]	M_n[c]	M_w/M_n[c]
P(MsMAz)$_{47}$	P1	7100	6700	8000	1.10
P(TsMAz)$_{60}$	P2	10900	13000	20500	1.10
P((TsMAz)$_{25}$-*co*-(MsMAz)$_{25}$)	P(2-*co*-1)	9000	9000	12600	1.11

[a] Theoretical number average molecular weight (g/mol). [b] Number average molecular weight determined by endgroup analysis from ^{1}H NMR. [c] Number average molecular weight and molecular weight dispersity determined *via* SEC in HFIP (*vs.* PMMA standards).

The desulfonylation was investigated *via* electrochemistry, arene radicals (NaNp), reduction with mild samarium(II) iodide (SmI_2), Red-Al, and *via* the acidic hydrolysis under microwave irradiation. Electrochemical reduction of low molecular weight sulfonamides was reported in literature.[19] This rather mild and easy to conduct procedure was attempted (in analogy to literature reports) in DMF, which is both a good solvent for the polysulfonamide and the polyamine. Different

conditions were investigated (cf. Supp Info for details), but under these conditions, neither P1 nor P2 could be desulfonylated. After 3-5 h of reaction, a dark unidentified material was deposited on the platin-electrodes, indicating that insolubility issues might have inhibited the reaction (potentially, amide anions could be formed which might also be insoluble in DMF). Conversely, when sodium naphathalenide (NaNp)[8, 18-20] or SmI_2[18-19, 28-31] were employed, NMR spectroscopy indicated a successful removal of the sulfonamides from P2 (indicated by sharp resonances of a tosyl derivative). However, in both cases purification of the polyamine was challenging and not further attempted. Both methods might be reinvestigated, however, as our aim was to establish a fast and convenient pathway to polyamines, we continued with other procedures.

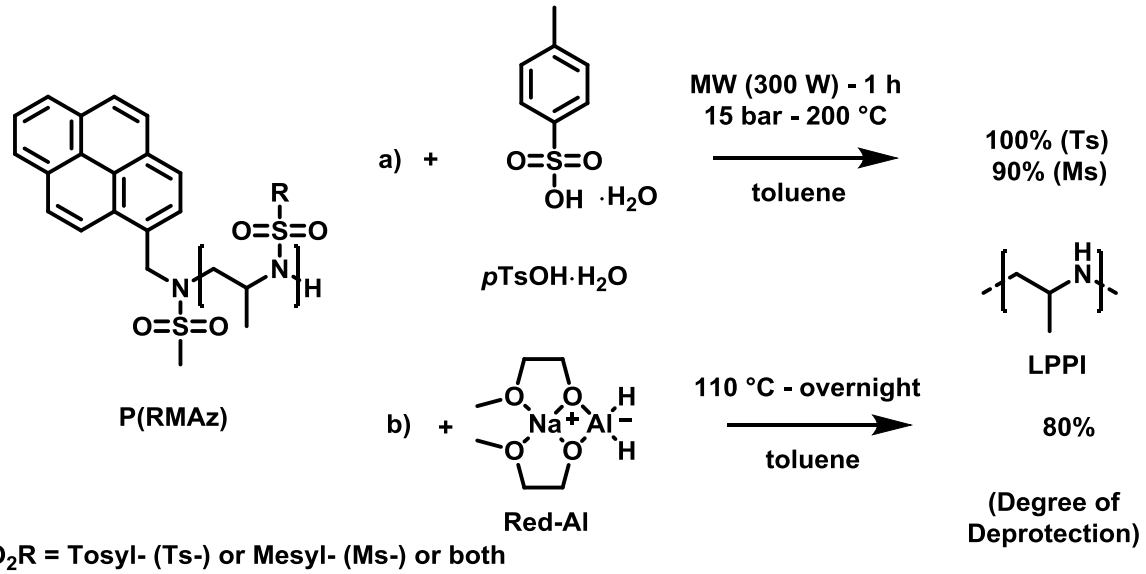

Scheme 7.2. Deprotection of polyaziridines *via* a) hydrolytic cleavage under microwave irradiation, 100% linear poly(propylenimine) (LPPI) and b) reductive removal with Red-Al, about 80% LPPI.

The reduction with Red-Al was reported as a mild method for acetal-protected poly(tosylaziridine)s with ca. 80% of desulfonylation.[4] We conducted experiments with the mesylated, the tosylated, and the copolymer to assess the applicability of Red-Al for general desulfonylation of polysulfonamides (Scheme 7.2b & the supporting information for experimental details). P(TsMAz) (P2) was treated with Red-Al in refluxing toluene and ca. 80% of the tosyl groups were removed (cf. SI, Figure S7.7-7.8 for P2-1). Removal of aluminum side products from the crude mixture was difficult and probably some inorganic residues remained in the products (cf. the ^{1}H NMR spectra in Figure S7.7 and S7.9). In contrast, P(MsMAz) (P1) was insoluble in toluene and THF and no reaction with Red-Al after refluxing the suspension at 110 °C overnight was observed, probably due to its low solubility. When the copolymer (P(2-*co*-1)) was treated with

Red-Al, the NMR spectra of the reaction mixture indicated again the removal of most of the tosyl groups, while the mesyl groups were also partly removed. However, purification of the materials from the inorganic side products was challenging and NMR spectra showed broad resonances, from which the degree of deprotection can only be estimated (the resonances belonging to the remaining mesyl groups are labeled with a star (*), compare Figure S7.9). Overall, the reductive deprotection *via* Red-Al was able to remove the sulfonamides partly under the investigated conditions, but probably solubility and aggregation hamper a complete desulfonylation.

Table 7.2. Overview over the performed desulfonylations, starting from polyaziridines.

Removed Activating group	**Solv.**	**Add.**	**Cond.**	**Purification**	**Result**	**Depro. / %**	**Lit.**	**Comment**
unspec.[1]	n.d.	LiNp	RT, over-night	filtration	LPPI	n.d.	[8]	no data shown
Ms-^{s}Bus[2]	HMPA, THF	Li, *t*-BuOH	-20 – 5 °C, 6.5 h	precipitation and washing	LPEI	100	[3]	laborious, toxic solvent
Ms-^{s}Bus-*b*-Ms[3]	HMPA, THF	Li, *t*-BuOH	-20 – 5 °C, 6.5 h	precipitation and washing	LPEI-*b*-PPI	100	[3]	laborious, toxic solvent
Ts	toluene	Red-Al	110 °C, over-night	Filtration, Dialyses	Polyhy-droxy amine	~ 80	[4]	complex purification, intact acetal groups
Ts (P2)	toluene	Red-Al	110 °C, over-night	Filtration, Dialyses	LPPI (P2-1)	~ 80	this work	complex purification
Ts-Ms[4] (P(2-*co*-1))	toluene	Red-Al	110 °C, over-night	Filtration, Dialyses	LPPI (P(2-*co*-1)-1)	~ 80	this work	complex purification
Ts (P2)	toluene	*p*TsOH	200 °C, 1 h, 300 W, 15 bar	Extraction, Ion Exchange Resin	LPPI (P2-2)	100	this work	fast, pure, chain scission?
Ms (P1)	toluene	*p*TsOH	200 °C, 1.5 h, 300 W, 15 bar	Extraction, Ion Exchange Resin	LPPI (P1-2)	~ 90	this work	fast, pure, chain scission?

[1] activating groups not specified, tosyl- (Ts) or mesyl- (Ms) group. [2] Poly(mesyl-*co*-(*sec*-butylsulfonyl)aziridine).
[3] Poly((mesyl-*co*-(*sec*-butylsulfonyl))-*block*-mesyl)aziridine. [4] Poly(tosyl-*co*-(mesyl)aziridine).

Acidic hydrolysis of sulfonamides is an attractive method to release the polyamines. In order to overcome solubility issues, we used a suspension of the starting materials in combination with the microwave-assisted acidic hydrolysis in the presence of *p*-toluenesulfonic acid. Similar strategies have been successfully employed for the deprotection of poly(oxazoline)s to obtain LPEI.[50] When hydrochloric acid (HCl) or sulfuric acid (H_2SO_4) were used and the PAz suspended in the respective acid, only a very low degree of desulfonylation was achieved. With *p*TsOH·H_2O as the acidic catalyst, the polymer was suspended in toluene and the reaction was performed under MW irradiation of 300 W, at 200 °C, with a maximum pressure of 15 bar. After one hour reaction time, the crude solid inside the microwave reactor was dissolved in water and washed with chloroform. The polymer was further purified by an anionic exchange resin, yielding quantitatively deprotected LPPI (P2-2) in case of P(TsMAz) (P2) (see Figure 7.1). The ratio of the integrals of the doublet at 1.04 ppm, belonging to the methyl side chain and the multiplet at 3.04 – 2.36 ppm from the backbone is 1:1, which is in agreement to expectations.[17] Furthermore, no aromatic signals were detected, proving full deprotection and also indicating the partial removal of the initiator, which might occur under these conditions. SEC-data (Figure 7.1) shows a clear shift of the elution volume for the deprotected polymer P2-2 to higher elution volumes, indicating the decrease in molecular weight, due to desulfonylation. The monomodal molecular weight distribution remained intact, but the dispersity increased to 1.39, which might be due to chain scission during the acid treatment or also interactions with the column material during the SEC experiment. The MALDI-ToF-spectrum confirms the presence of the repeating unit of propyleneimine (PI, 57 g/mol) in the product (see Figure S7.15). Calculating the absolute composition of the different distributions further indicate fragmentation of the polymer and the presence of the initiator in some subdistributions. However, as fragmentation of LPEI during mass spectrometry was reported, MALDI-ToF cannot fully confirm the presence of chain scission in the product (e.g. no olefin signals were detected in the NMR spectra).[51]

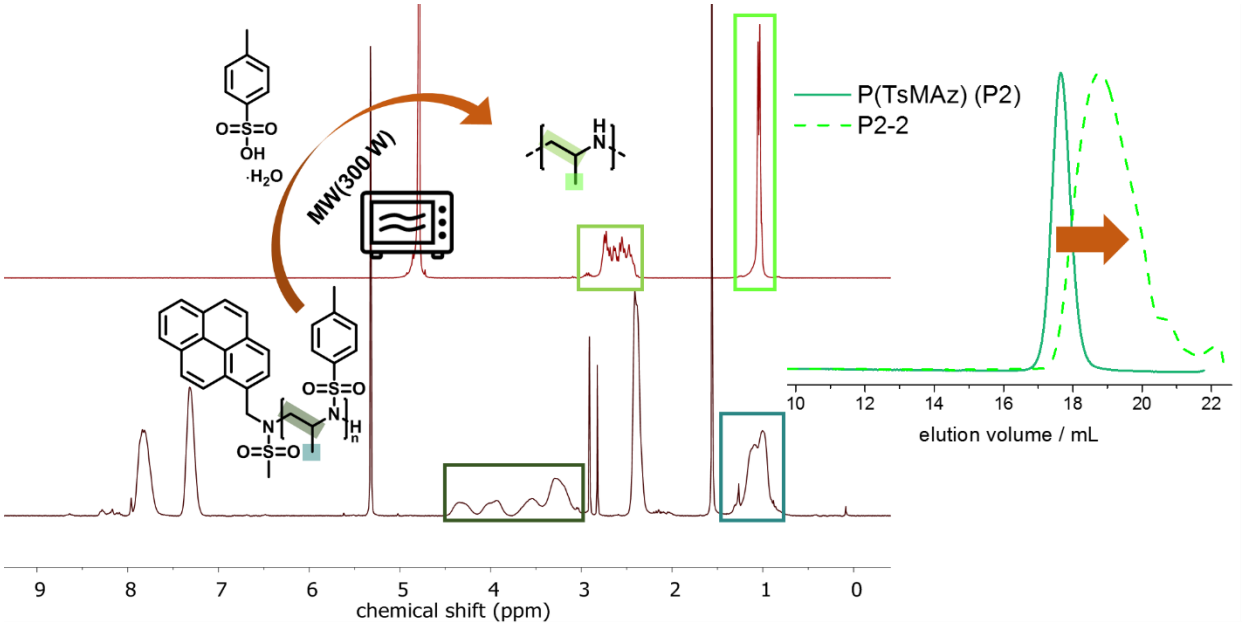

Figure 7.1. ^{1}H NMR-spectra and SEC-traces of P(TsMAz) (P2) and LPPI (P2-2) derived from P2 from acidic hydrolysis under microwave irradiation

When P(MsMAz) (P1) was suspended in toluene together with *p*-toluenesulfonic acid and reacted under the same conditions for 1.5 h, ^{1}H NMR shows that ca. 10% mesyl units remained intact (cf. SI Figure S7.17); a slightly lower degree of desulfonylation was obtained, when repeated under the same conditions, but only one hour of reaction time. SEC-data shows a monomodal distribution with $Đ = 1.36$, also shifted to higher elution times, indicating the desulfonylation. However, the MALDI-TOF-spectrum of P1-2 showed exclusively the repeating unit of PI, no mesyl unit can be assigned, potentially due to a partially desorption during the measurement (Figure S7.19). For both polymers, lower temperatures during the desulfonylation in the microwave were investigated, but did not result in any optimization. All tested conditions and the results are summarized in Table S7.1. The acidic hydrolysis under microwave irradiation is a nonselective method for desulfonylation and the experimental handling is very simple (no inert atmosphere, no extra steps or low temperature conditions are necessary) and additionally inexpensive. Furthermore, the purification is straightforward and no metal compound is involved. However, due to the harsh reaction conditions chain-scission cannot ruled out, which might limit the process.

7.4 Summary

In summary, we present the deprotection of polyaziridines *via* a reductive mechanism using Red-Al, which leads to a desulfonylation of ca 80% for the tosyl groups. The MW-assisted acidic hydrolysis resulted in fully deprotected LPPI for P(TsMAz) and 90% of P(MsMAz). The acidic hydrolysis *via* microwave irradiation is a cost-efficient, simple and non-toxic method in terms of reaction conditions and purification, as all by-products are easily removed. However, as chain scission cannot be excluded, optimization is still advisable, towards reaction conditions, copolymers as well as other activating groups, which are cleavable, following a different mechanism, as nosyl groups, which we are currently exploiting.

7.5 Acknowledgments

The authors thank Prof. Dr. Katharina Landfester for continuous support. The authors thank the Deutsche Forschungsgemeinschaft (DFG WU750/ 7-1). E. R. thanks Regina Holm (Johannes Gutenberg-University, Mainz, Germany) for the HFIP-SEC-measurements, Barbara Riehl (Johannes Gutenberg-University, Mainz, Germany) and Prof. Dr. Siegfried R. Waldvogel (Johannes Gutenberg-University, Mainz, Germany) for providing the equipment and conducting the electrochemical reactions.

7.6 Supporting Information

The Supporting Information contains additional synthetic procedures and characterization data for polymers.

Content

7.6.1 Materials and Methods.

Materials.

All solvents and reagents were purchased from Sigma-Aldrich, Acros Organics, Alfa Aesar, TCI Europe or Fluka and used as received unless otherwise mentioned. All monomers and initiators were dried extensively by azeotropic freeze drying with benzene prior to polymerization unless otherwise mentioned. 2-methyl-*N*-mesyl-aziridine (MsMAz, 1) 2-methyl-*N*-tosylaziridine (TsMAz, 2), *N*-pyrene-methanesulfonamide (PyNHMs, 3) were synthesized by our previously published protocol.[4, 8-9] Dialyses were performed, using pre-wetted Spectra/Por membranes (Roth) from regenerated cellulose with a nominal molecular weight cutoff of 1000 g/mol. The ion exchange resin: Amberlite IRA-402(OH) was obtained from Alfa Aesar and washed with milliQ-water before usage.

Instrumentation and Characterization Techniques.

Microwave. The hydrolysis experiments were performed, using a Discover® SP Microwave Synthesizer, from CEM Corporation, equipped with an Explorer 12 SP Hybrid Upgrade auto sampler.

NMR. ^{1}H NMR spectra were recorded using a Bruker Avance 250 and a Bruker Avance 300. All spectra were referenced internally to residual proton signals of the deuterated solvent.

SEC. Size exclusion chromatography (SEC) measurements of were performed in hexafluoroisopropanol (HFIP) (3 g L^{-1} potassium trifluoroacetate (KTFA) added) at 40°C and a flow rate of 0.8 mL min^{-1}. The columns were packed with modified silica (PFG columns particle size: 7 µm, porosity: 100 Å and 1000 Å). Calibration was carried out using PMMA standards (provided by Polymer Standards Service) with toluene as internal standard. A refractive index (RI) detector (G1362A RID) and an UV/VIS detector (at 230 nm; Jasco UV-2075 Plus) were used for polymer detection.

MALDI-TOF. The polymers were characterized by MALDI-FTICR-MS using a solariX mass spectrometer (Bruker). The samples were prepared using a dried droplet method with dithranol (40 mg mL^{-1} in THF) as matrix.

7.6.2 Polyaziridines (PAz).

General procedure for the azaanionic polymerization. All glassware (Schlenk flasks) was flame-dried by *in vacuo* for at least three times. All reactants (except potassium bis(trimethylsilyl)amide (KHMDS)) were dried from benzene *in vacuo* for at least 4 h. The monomers and the PyNHMs-initiator were dissolved in 5 and 1 mL respectively anhydrous *N,N*-dimethylformamide (DMF). KHMDS was added quickly in argon-counter flow to the PyNHMs-solution. From the initiator-solution the appropriate volume was added to the monomer solution. The mixture was stirred at 50 °C for at least 18 h. To terminate the polymers, 0.5 mL acidic methanol were added and the reaction mixture was precipitated in ca. 30 mL methanol. The colorless solids were collected by centrifugation and dried at 70 °C *in vacuo,* yields: 95-98% [4, 6, 9]

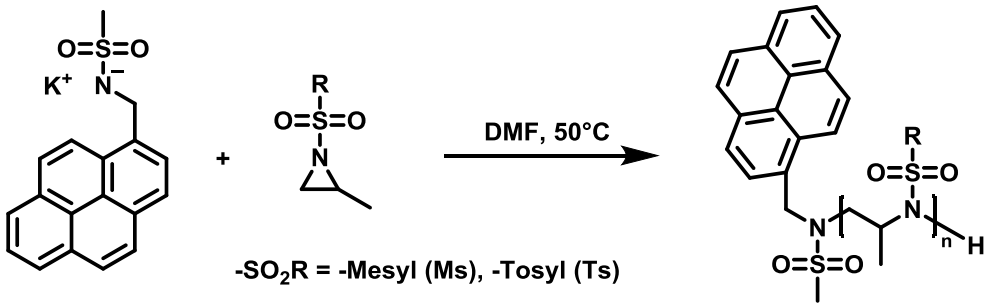

Scheme S7.1. Azaanionic ring-opening polymerization of activated aziridines.

Poly(MsMAz) (P1)

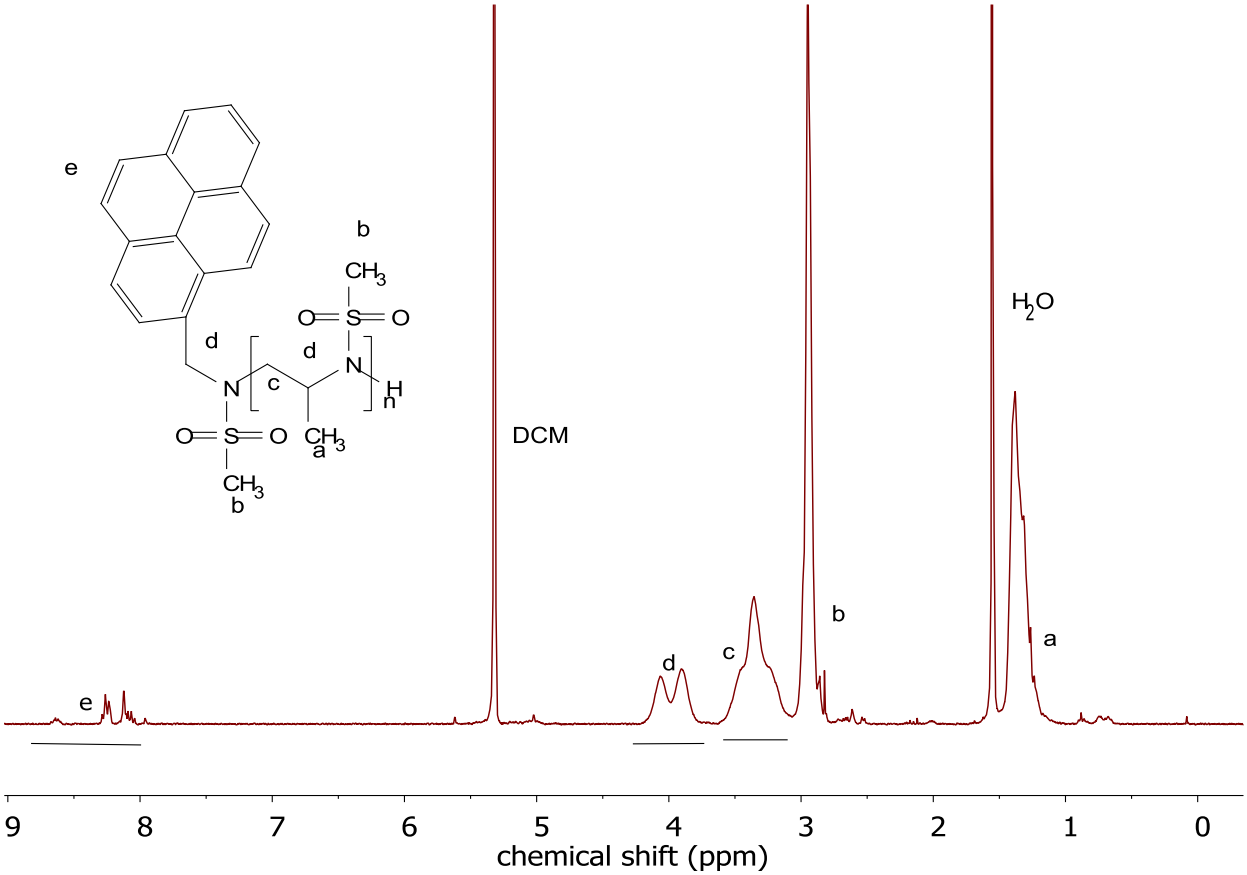

Figure S7.1. ^{1}H NMR (DCM-d_2, 300 MHz, 298 K) of poly(MsMAz) (P1).

Poly(MsMAz)$_{47}$: [MsMAz (3.20 g, 23.8 mmol), PyNHMs (146.4 mg, 473 µmol), KHMDS (94.4 mg, 473 µmol)] in 30 mL DMF. m(P1) = 3.06 g

^{1}H NMR (300 MHz, 298 K, DCM-d_2): δ 8.71 – 8.00 (m, **e**), 4.21 – 3.76 (m, **d**), 3.95 – 3.11 (m, **c**),3.05 – 2.79 (m, **b**), 1.49 – 1.05 (m, **a**). M_n (NMR) = 6400

^{13}C NMR (176 MHz, 298 K, $CDCl_3$): δ 57.23 - 51.83 (m, backbone-CH_2, d), 51.83 – 48.33 (m, backbone-CH, c) 40.61 - 36.02 (m, mesyl-CH_3, b), 16.19 - 14.54 (m, methyl-CH_3, a)

SEC (RID, HFIP, PMMA): M_n = 8000; $Đ$ = 1.10

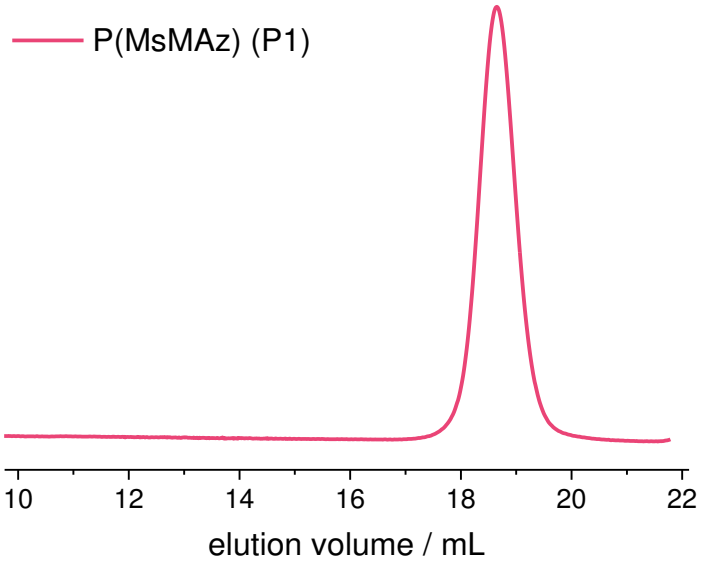

Figure S7.2. SEC traces of poly(MsMAz) (P1) in HFIP (RI signal).

Poly(TsMAz) (P2)

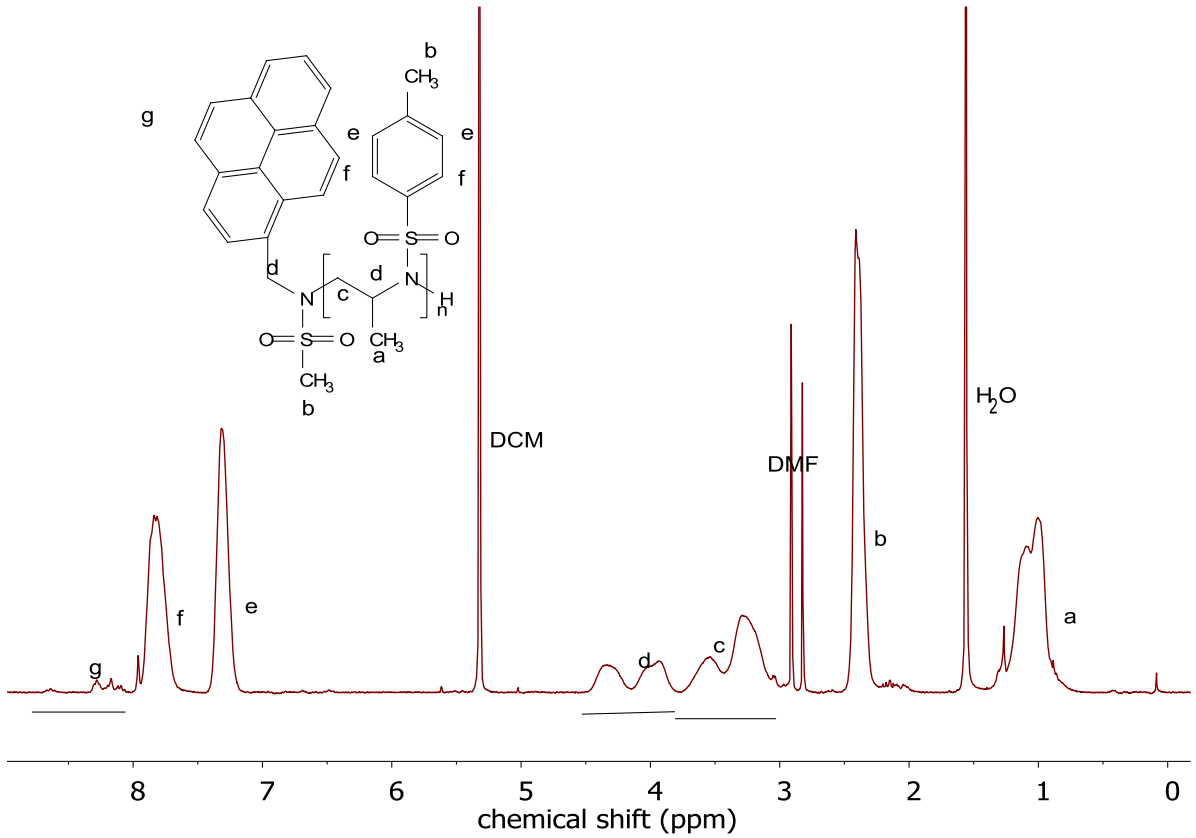

Figure S7.3. ^{1}H NMR (DCM-d_2, 300 MHz, 298 K) of poly(TsMAz) (P2).

Poly(TsMAz)$_{60}$: [TsMAz (5.02 g, 23.8 mmol), PyNHMs (146.4 mg, 473 µmol), KHMDS (94.4 mg, 473 µmol)] in 50 mL DMF. m(P2) = 4.77 g

^{1}H NMR (300 MHz, 298 K, DCM-d_2): δ 8.71 – 8.03 (m, **g**), 7.97 – 7.61 (m, **f**), 7.43 – 7.13 (m, **e**), 4.52 – 3.78 (m, **d**), 3.76 – 2.98 (m, **c**), 2.53 – 2.25 (m, **b**), 1.36 – 0.70 (m, **a**). M_n (NMR) = 12700

^{13}C NMR (176 MHz, 298 K, $CDCl_3$): δ 144.28 (s, arom-C, i), 137.07 (s, arom.-C, h), 129.97 (s, 2C, arom.-CH, g), 128.33 (s, arom.-CH, f), 127.27 (s, arom.-CH, e), 55.14 - 52.63 (m, backbone CH_2, d), 52.52 – 47.41 (m, backbone-CH, c) 21.07 (s, tosyl-CH_3, b), 16.21 - 12.58 (m, methyl-CH_3, a)

SEC (RID, HFIP, PMMA): M_n = 20500; $Đ$ = 1.10

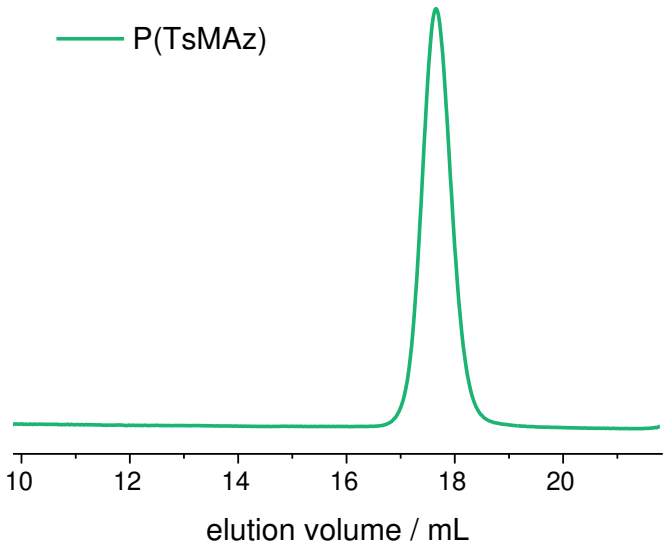

Figure S7.4. SEC traces of poly(TsMAz) (P2) in HFIP (RI signal).

Poly(TsMAz-co-MsMAz) (P(2-co-1))

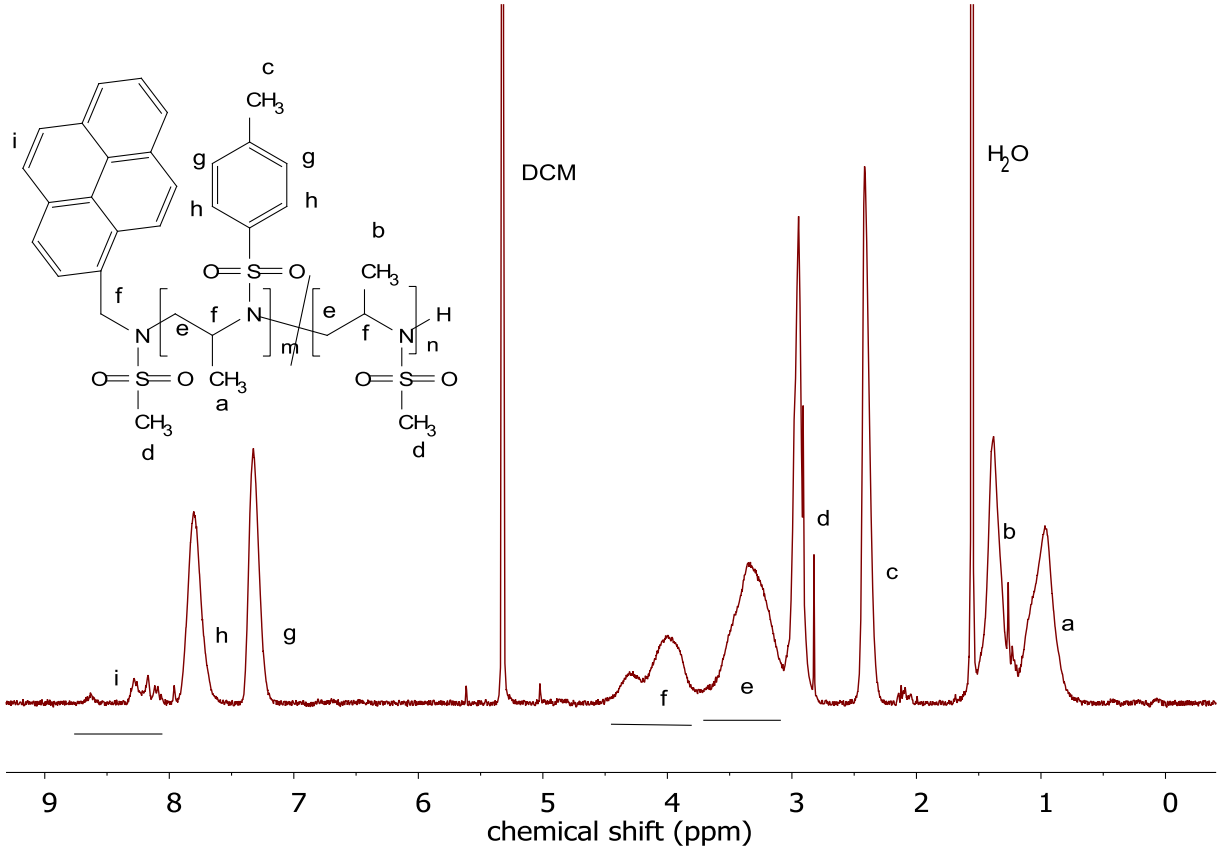

Figure S7.5. ^{1}H NMR (DCM-d_2, 300 MHz, 298 K) of poly(TsMAz-*co*-MsMAz) P(2-*co*-1).

Poly((TsMAz)$_{27}$-*co*-(MsMAz)$_{27}$): [TsMAz (5.02 g, 23.8 mmol), MsMAz (3.20 g, 23.8 mmol), PyNHMs (146.4 mg, 473 µmol), KHMDS (94.4 mg, 473 µmol)] in 50 mL DMF. m(P2-*co*-1) = 2.18 g

^{1}H NMR (300 MHz, 298 K, DCM-d_2): δ 8.74 – 8.03 (m, **i**), 7.95 – 7.59 (m, **h**), 7.42 – 7.15 (m, **g**), 4.48 – 3.77 (m, **f**), 3.75 – 3.06 (m, **e**), 3.06 – 2.71 (m, **d**), 2.49 – 2.25 (m, **c**), 1.64 – 1.16 (m, **b**), 1.20 – 0.71 (m, **a**). M_n (NMR) = 9400

SEC (RID, HFIP, PMMA): M_n = 12600; $Đ$ = 1.11

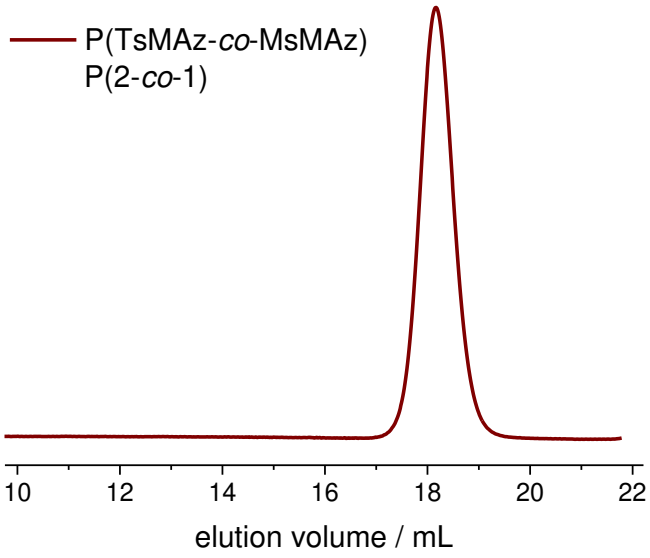

Figure S7.6. SEC traces of poly(TsMAz-*co*-MsMAz) P(2-*co*-1) in HFIP (RI signal).

7.6.3 Overview over the different conditions of the presented, successful desulfonylations.

Table S7.1. Overview over the different conditions for the presented desulfonylation. Shown on bold are the most successful reactions, which experimental handling and their analyses are described below.

Original Polymer	Type	Additive	Solvent	Conditions	Depro. / %	Result
P(MsMAz) (P1)	Reduction	Red-Al	toluene, THF	110 °C, overnight	0%	PAz
P(TsMAz) (P2)-I	Reduction	Red-Al	toluene	110 °C, overnight	80%	LPPI
P(TsMAz) (P2)-II	**Reduction**	**Red-Al**	**toluene**	**110 °C, overnight**	**80%**	**LPPI (P2-1)**
P(TsMAz-*co*-MsMAz) (P(2-*co*-1))	**Reduction**	**Red-Al**	**toluene**	**110 °C, overnight**	**80%**	**LPPI (P(2-*co*-1)-1)**
P(MsMAz) (P1)	Hydrolysis	*p*TsOH	toluene	150 °C, 2 h, 300 W, 15 bar	> 10%	PAz
P(MsMAz) (P1)	Hydrolysis	*p*TsOH	toluene	100 °C, 2 h, 300 W, 15 bar	0%	PAz
P(MsMAz) (P1)-I	Hydrolysis	*p*TsOH	toluene	200 °C, 1 h, 300 W, 15 bar	85%	LPPI
P(MsMAz) (P1)-II	**Hydrolysis**	***p*TsOH**	**toluene**	**200 °C, 1.5 h, 300 W, 15 bar**	**90%**	**LPPI (P1-2)**
P(TsMAz) (P2)	Hydrolysis	25% H_2SO_4	water	200 °C, 1 h, 300 W, 15 bar	0%	PAz
P(TsMAz) (P2)	Hydrolysis	1M HCl	water	200 °C, 1 h, 300 W, 15 bar	0%	PAz
P(TsMAz) (P2)	Hydrolysis	*p*TsOH	toluene	150 °C, 45 min, 300 W, 15 bar	> 10%	PAz
P(TsMAz) (P2)	Hydrolysis	*p*TsOH	toluene	100 °C, 1 h, 300 W, 15 bar	0%	PAz
P(TsMAz) (P2)-I	Hydrolysis	*p*TsOH	toluene	200 °C, 1 h, 300 W, 15 bar	100%	LPPI
P(TsMAz) (P2)-II	**Hydrolysis**	***p*TsOH**	**toluene**	**200 °C, 1 h, 300 W, 15 bar**	**100%**	**LPPI (P2-2)**

7.6.4 Poly(propylenimine) (P2-1) from P2 *via* reductive cleavage with Red-Al.

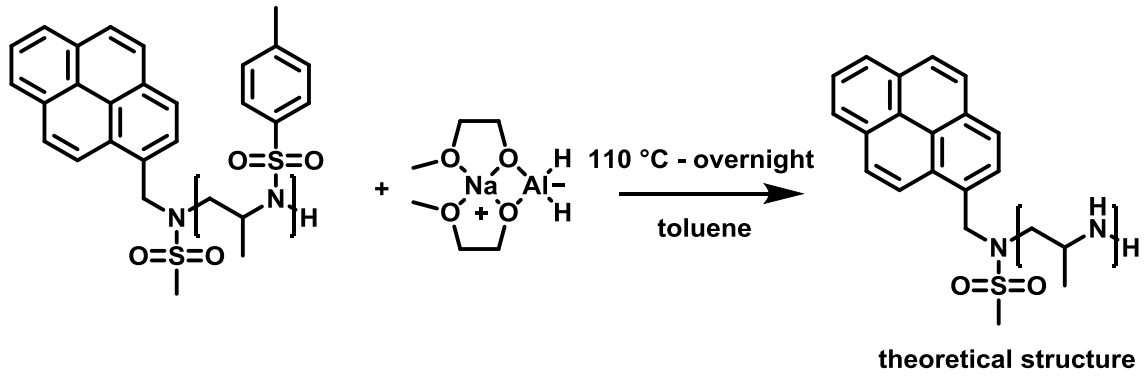

Scheme S7.2. Reductive cleavage of poly(TsMAz) (P2) with RedAl to P2-1.

The reductive cleavage was performed according to literature.[4, 52] 250 mg of the polymer (P2) were dissolved in dry toluene, the solution was heated to 110 °C. 1.31 mL (4.73 mmol) Sodium bis(2-methoxyethoxy)aluminiumhydride (Red-Al) was added and the mixture was stirred overnight at 110 °C. The toluene was removed at reduced pressure from the brown reaction mixture. The residue was suspended in water, the insoluble residues were filtered. The aqueous solution was dialyzed in a 0.1 molar sodium hydroxide solution for one day, subsequent in water/tetrahydrofuran for one day. The resulting suspension was centrifuged at 4000 rpm for 50 minutes and the solubilized material separated from the residue. After removal of the solvent, the product was recovered as a brownish solid, with a degree of deprotection of ca. 80%.

^{1}H NMR (300 MHz, 298 K, D_2O-d_2): δ 3.33 – 2.04 (m, **b**), 1.37 – 0.71 (m, **a**). Residual Ts-group-signals labeled with **.

SEC (RID, HFIP, PMMA): M_n = 3400; $Đ$ = 1.60

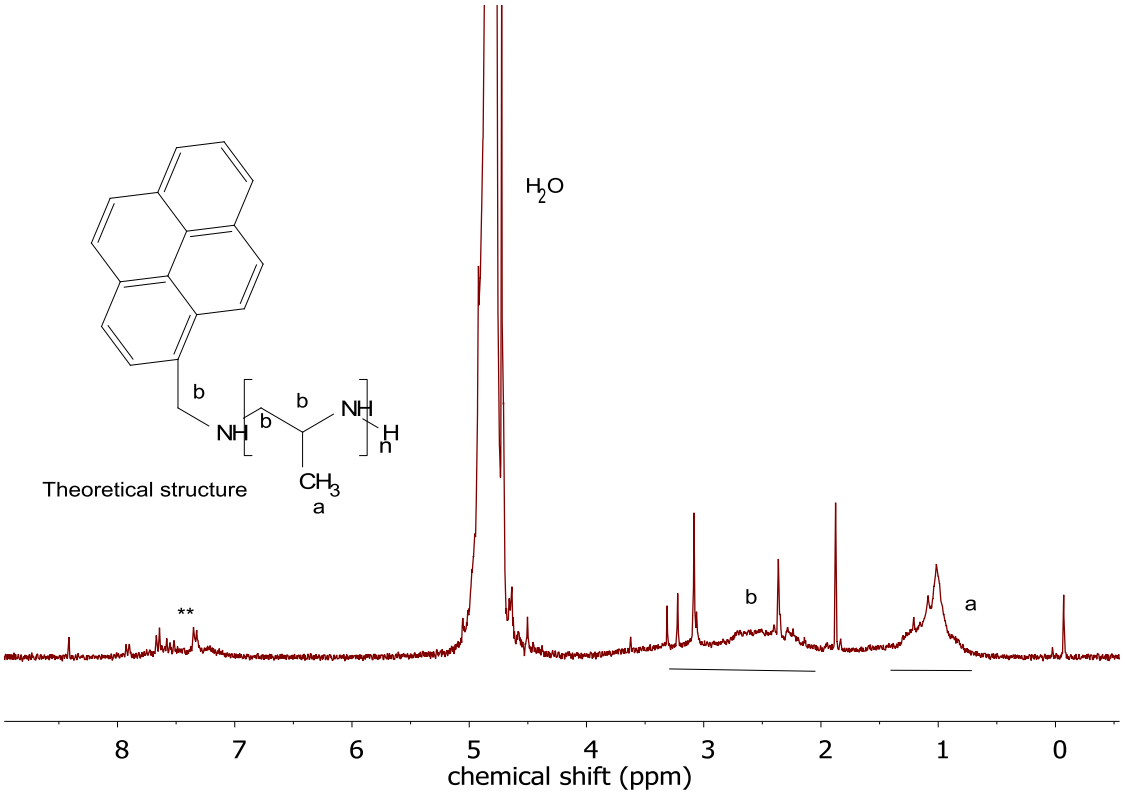

Figure S7.7. ^{1}H NMR (D_2O, 300 MHz, 298 K) of P2-1 derived from poly(TsMAz) *via* reductive cleavage with RedAl. Residual Ts-group-signals labeled with **. Not assigned signals from impurities.

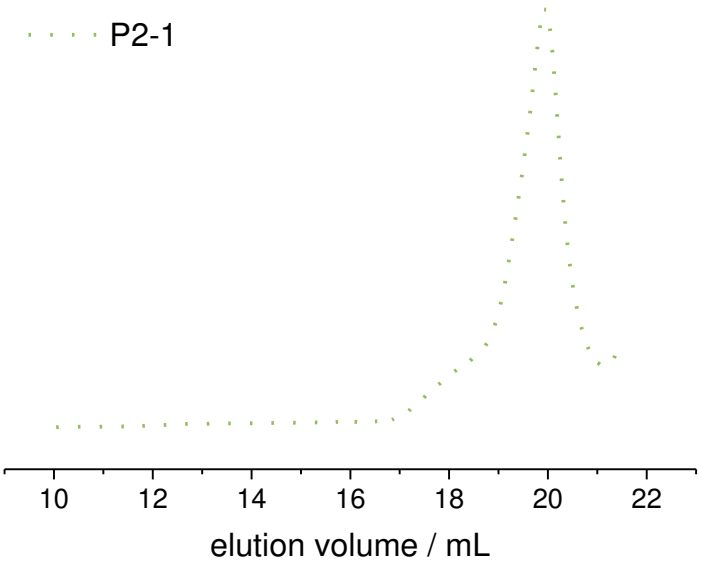

Figure S7.8. SEC traces of P2-1 derived from poly(TsMAz) (P2) *via* reductive cleavage with RedAl in HFIP (RI signal).

7.6.5 Poly(propylenimine) (P(2-co1)-1) from P(2-*co*-1) *via* reductive cleavage with Red-Al.

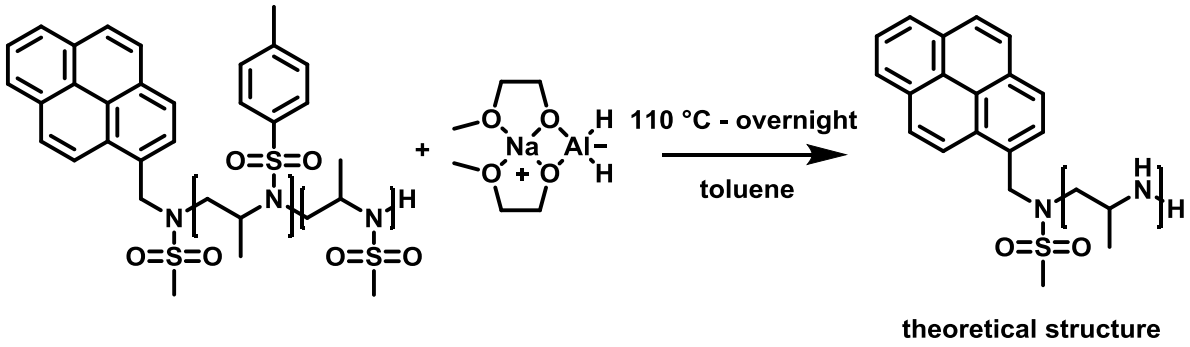

Scheme S7.1. Reductive cleavage of poly(TsMAz-*co*-MsMAz) (P(2-*co*-1)) with RedAl to P(2-*co*-1)-1.

The reductive cleavage was performed as described in 7.6.4. Herein 250 mg of the copolymer (P(2-*co*-1)) and 1.58 mL (5.68 mmol) sodium bis(2-methoxyethoxy)aluminiumhydride (Red-Al) were used. The final product was recovered as a brownish solid, with a degree of deprotection of ca. 80% overall.

^{1}H NMR (300 MHz, 298 K, D_2O-d_2): δ 4.12 – 2.71 (m, **b**), 1.57 – 1.03 (m, **a**). Residual Ms-group-signals labeled with *, Ts-group-signals labeled with **.

SEC (RID, HFIP, PMMA): M_n = 2000; $Đ$ = 1.72

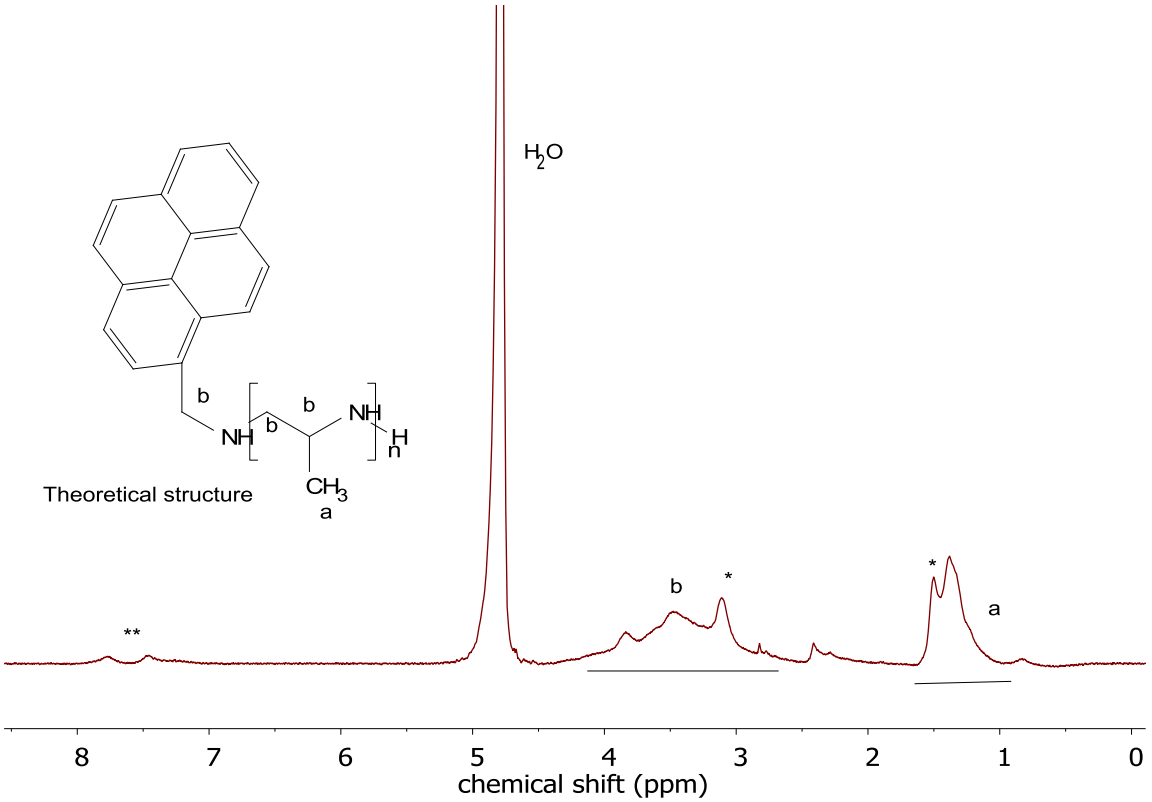

Figure S7.9. ^{1}H NMR (D_2O, 300 MHz, 298 K) of P(2-*co*-1)-1 derived from poly(TsMAz-*co*-MsMAz) (P(2-*co*-1)) *via* reductive cleavage with RedAl. Residual Ms-group labeled with * and Ts-group labeled with **.

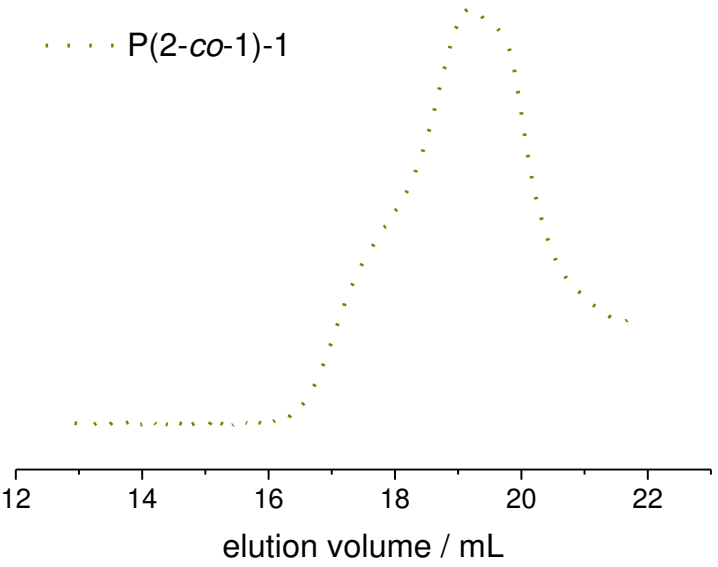

Figure S7.10. SEC traces of P(2-*co*-1)-1 derived from poly(TsMAz-*co*-MsMAz) (P(2-*co*-1)) *via* reductive cleavage with RedAl in HFIP (RI signal).

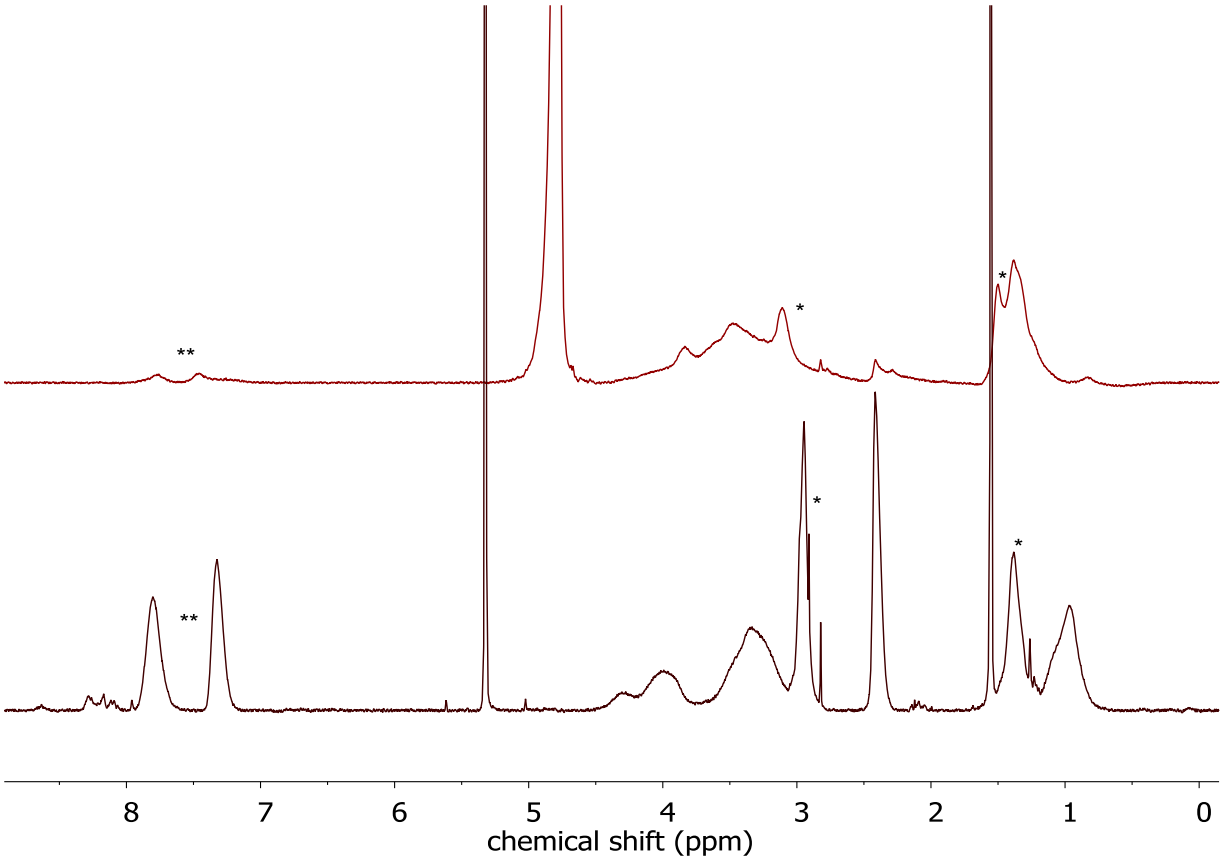

Figure S7.11. Comparison of: ^{1}H NMR (D_2O, 300 MHz, 298 K, upper spectrum) of P(2-*co*-1)-1 derived from (P(2-*co*-1)) *via* reductive cleavage with RedAl. Residual Ms-group labeled with * and Ts-group labeled with ** and ^{1}H NMR (DCM-d_2, 300 MHz, 298 K, lower spectrum) of poly(TsMAz-*co*-MsMAz) (P(2-*co*-1)).

7.6.6 Poly(propylenimine) (P2-2) from P2 *via* acidic hydrolysis.

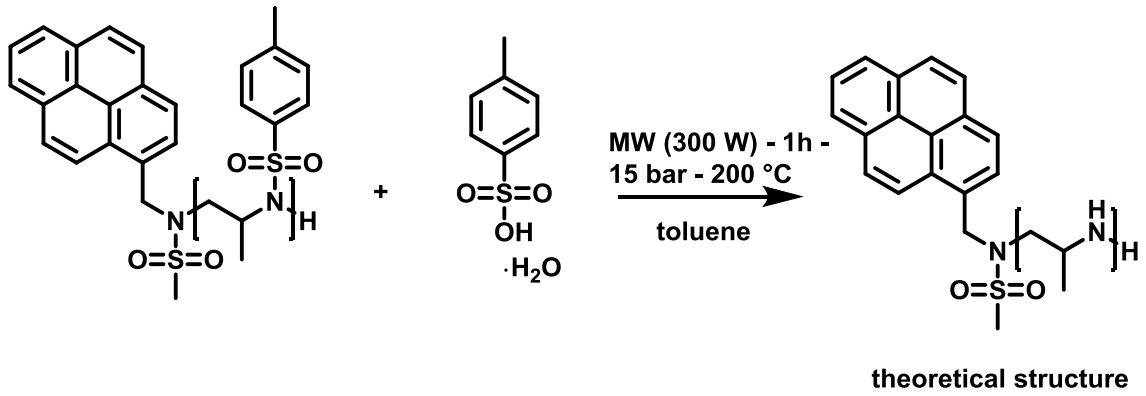

Scheme S7.2. Acidic hydrolysis of poly(TsMAz) (P2) to (P2-2).

250 mg P(TsMAz) (P2) and (1 g, 5.26 mmol) *p*-toluenesulfonic acid monohydrate (*p*TsOH·H_2O) were suspended in 5 mL toluene in a microwave tube. The sealed vial was heated to 200 °C, with the maximum of 15 bar and 300 W for 1 h.[36, 50] The solid at the bottom of the reaction vessel was dissolved in deionized water and washed three times with chloroform, to obtain a colorless solution. This aqueous solution was shaken for 20 minutes together with ca. 20 g ion exchange resin: Amberlite IRA-402(OH), which was rinsed with MilliQ-water beforehand. The resin was washed with MilliQ-water for three times. All fractions were collected and lyophilized. This procedure was repeated until the water was neutral and lyophilized again to isolate the product.

^{1}H NMR (300 MHz, 298 K, D_2O-d_2): δ 3.04 – 2.36 (m, **b**), 1.04 (d, 6.1Hz, **a**).

^{13}C NMR (176 MHz, 298 K, $CDCl_3$): δ 54.74 – 53.29 (m, backbone-CH_2, c), 53.28 – 52.65 (m, backbone-CH, b), 18.46 - 16.25 (m, methyl-CH_3, a)

SEC (RID, HFIP, PMMA): M_n = 5900; $Đ$ = 1.39

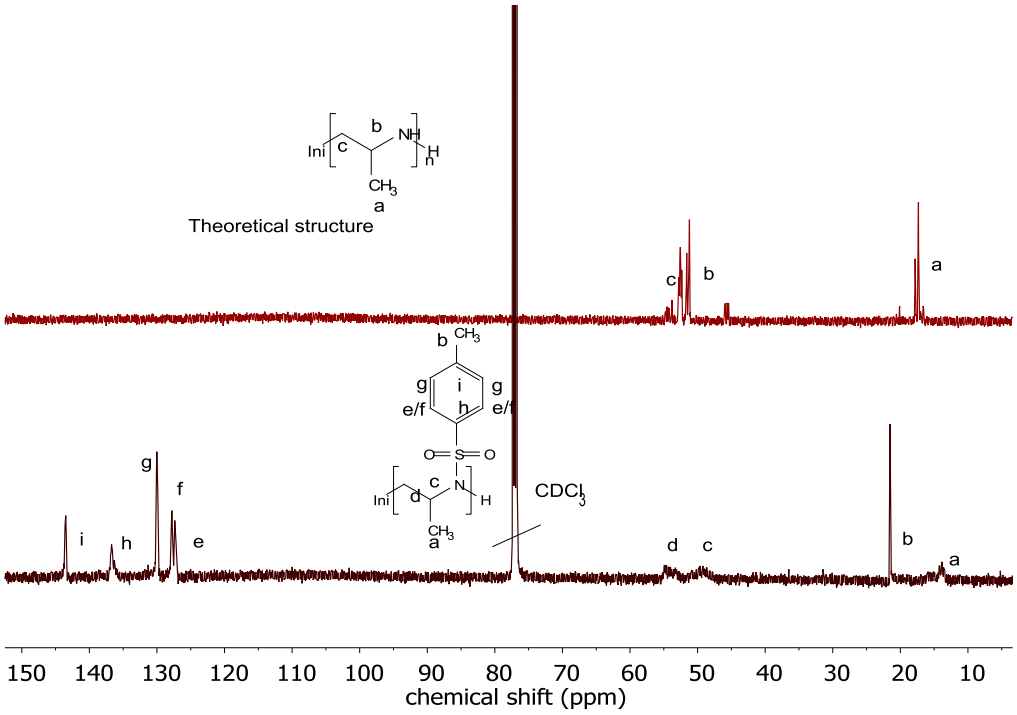

Figure S7.12. Comparison of: ^{13}C NMR (D_2O, 176 MHz, 298 K, upper spectrum) of P2-2 derived from poly(TsMAz) (P2) *via* acidic hydrolysis and ^{13}C NMR ($CDCl_3$, 176 MHz, 298 K, lower spectrum) of poly(TsMAz) (P2).

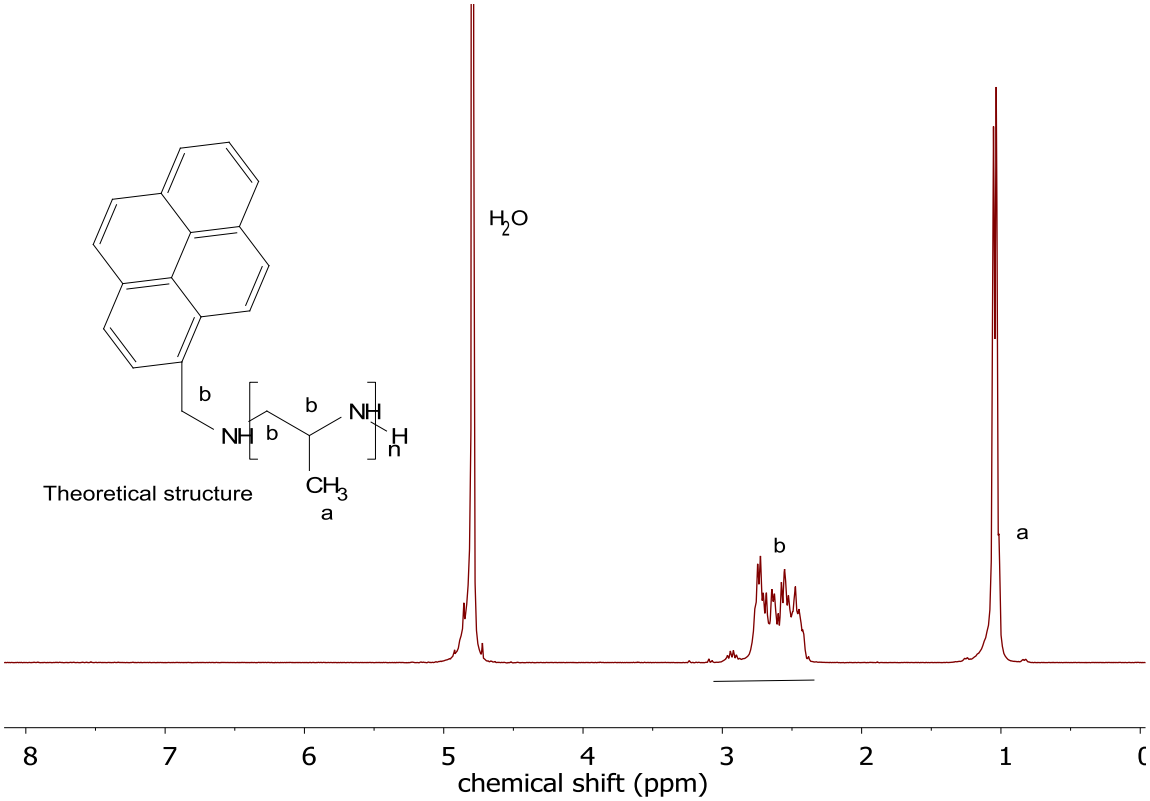

Figure S7.13. ^1H NMR (D_2O, 300 MHz, 298 K) of (P2-2) derived from poly(TsMAz) (P2) *via* acidic hydrolysis.

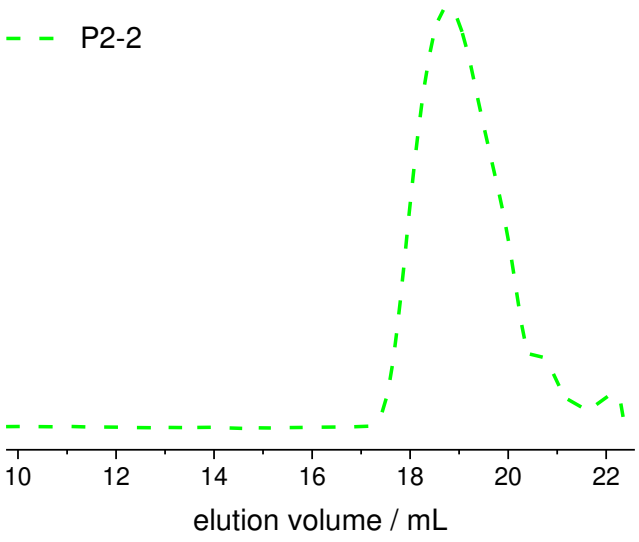

Figure S7.14. SEC traces of (P2-2) derived from poly(TsMAz) (P2) *via* acidic hydrolysis in HFIP (RI signal).

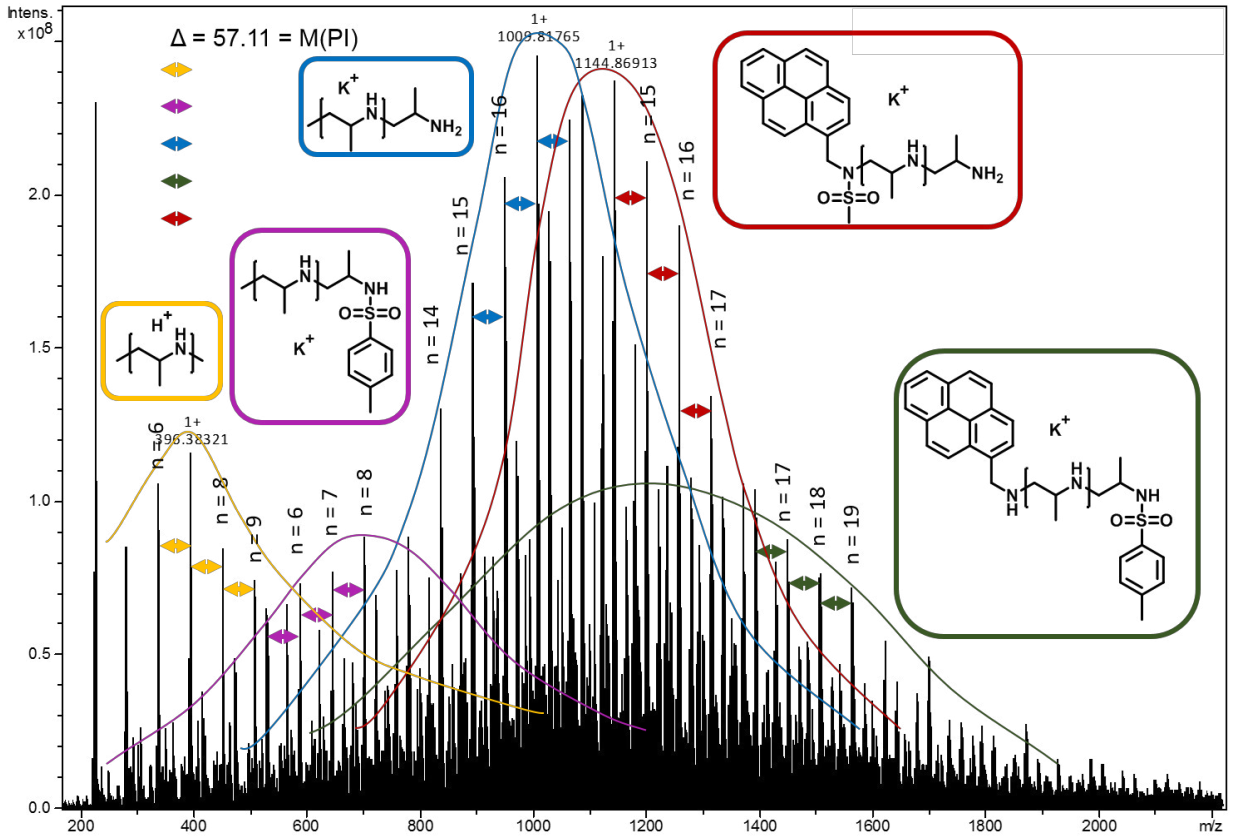

Figure S15. MALDI-ToF-spectrum of (P2-2) derived from poly(TsMAz) (P2) *via* acidic hydrolysis with potential peak assignments. The two major series (blue and red) and the small yellow distribution are potentially attributed to the fully deprotected polymer, with (red) and without the PyNHMs-initiator. In case of the green and purple fraction, the distributions might be assigned to fully deprotected polymers, with one *p*-TsOH attached.[51]

7.6.7 Poly(propylenimine) (P1-2) from P1 *via* acidic hydrolysis.

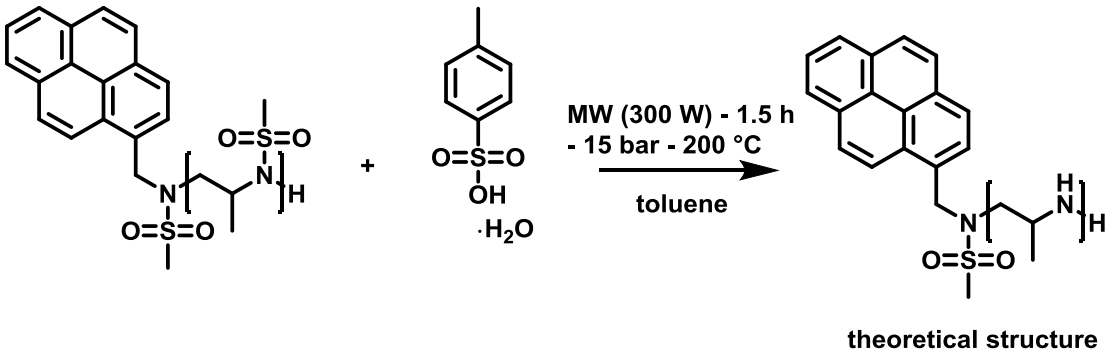

Scheme S7.3. Acidic hydrolysis of poly(MsMAz) (P1) to P1-2.

The acidic hydrolsyis was performed as described in 7.6.6. Herein 200 mg P(MsMAz) (P1) and (1 g, 5.26 mmol) *p*-toluenesulfonic acid monohydrate (*p*TsOH·H_2O) were used and the reaction was carried out for 1.5 hours.

^{1}H NMR (300 MHz, 298 K, D_2O-d_2): δ 3.01 – 2.30 (m, **b**), 1.04 (d, 5.9 Hz, **a**). Residual Ms-groups-signals labeled with *.

^{13}C NMR (176 MHz, 298 K, $CDCl_3$): δ 55.37 – 52.14 (m, backbone-CH_2, c), 52.14 – 50.26 (m, backbone-CH, b), 17.89 (s, methyl-CH_3, a). Residual Ms-groups-signals labeled with *.

SEC (RID, HFIP, PMMA): M_n = 3800; $Đ$ = 1.36

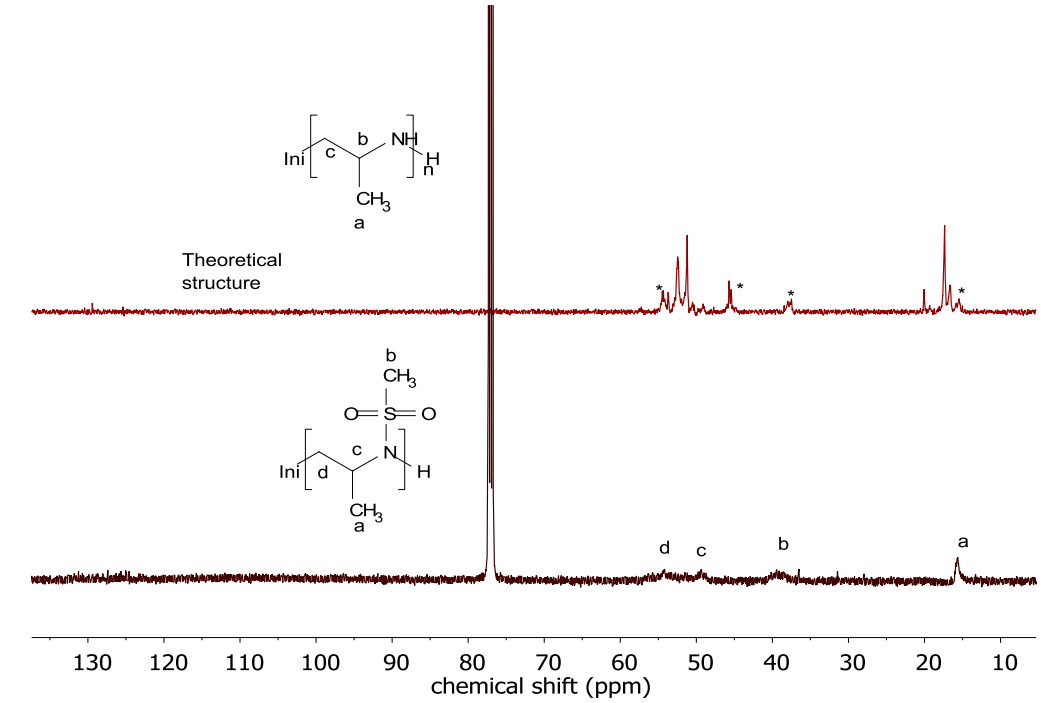

Figure S7.16. Comparison of: ^{13}C NMR (D_2O, 176 MHz, 298 K, upper spectrum) of P1-2 derived from poly(MsMAz) (P1) *via* acidic hydrolysis and ^{13}C NMR ($CDCl_3$, 176 MHz, 298 K, lower spectrum) of poly(MsMAz) (P1).

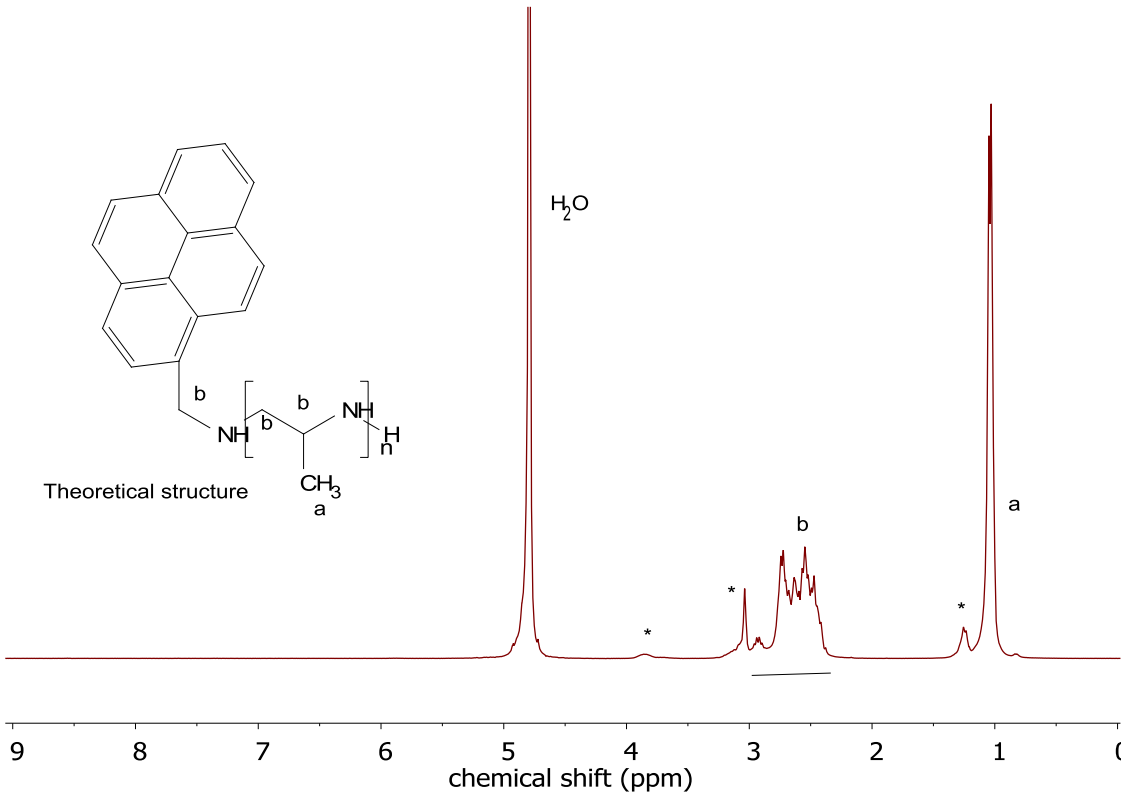

Figure S7.17. ^1H NMR (D_2O, 300 MHz, 298 K) of P1-2 derived from poly(MsMAz) (P1) *via* acidic hydrolysis. Residual Ms-group-signals labeled with *.

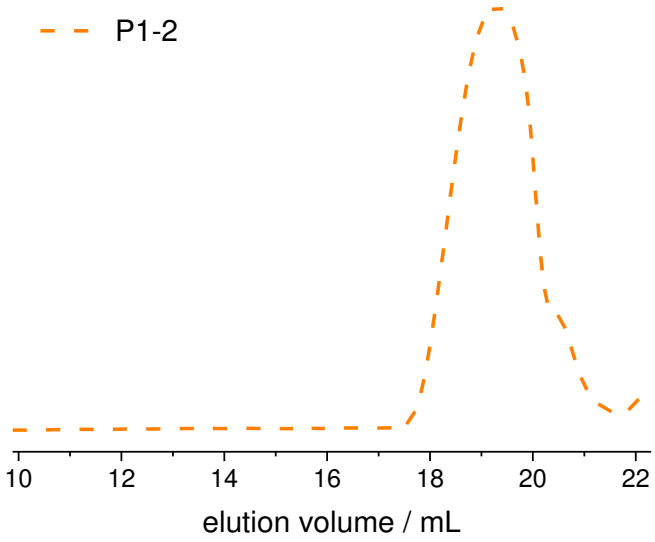

Figure S7.18. SEC traces of P1-2 derived from poly(MsMAz) (P1) *via* acidic hydrolysis in HFIP (RI signal).

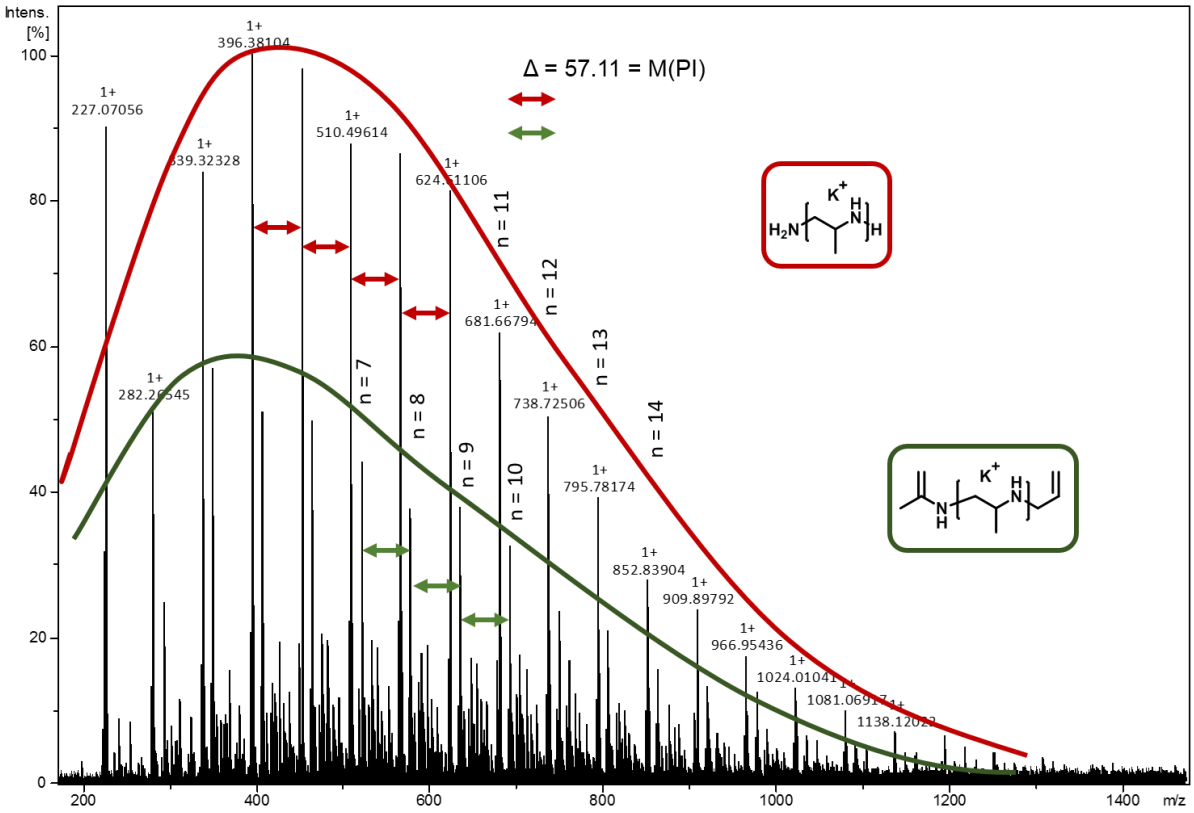

Figure S7.19. MALDI-ToF-spectrum of P1-2 derived from poly(MsMAz) (P1) *via* acidic hydrolysis with possible peak assignments. (different potential fragmentations might take place during the measurement).[51]

7.6.8 Electrochemical Approach.

General protocol.

Beaker-type teflon cells and beaker-type glas cells were home-made by the local mechanical shop at the university. The undivided beaker-type cell is briefly described here, whereas more details are reported in literature.[53-54] It is used with platinum, zinc and magnesium electrodes. The electrolysis was performed with constant current.

Screening cell (beaker-type)

A solution of the polymer (0.47 mmol, 1.0 eq) , naphthalene (0.24 mmol, 0.5 eq) and *N*,*N*,*N*,*N*-tretraethylammonium bromide (0.10 g, 0.10 mmol) in 5 mL *N*,*N*-dimethylformamide (DMF) was transferred into a screening cell equipped with a platinum cathode and zinc or magnesium anode. A constant current electrolysis with a current density of 5.0 mA cm^{-2} was performed at r.t.. After application of 91 C [136 C] (2.0 F [3.0 F] per polymer) the electrolysis was stopped and the crude solvent mixture was condensend and analyzed by ^{1}H NMR spectroscopy.

A detailed description of this set up was published recently.[53] Dimensions of electrodes are 7.0 x 1.0 x 0.3 cm. Using a 5 mL reaction mixture, electrodes immersed 1.5 cm into solution.

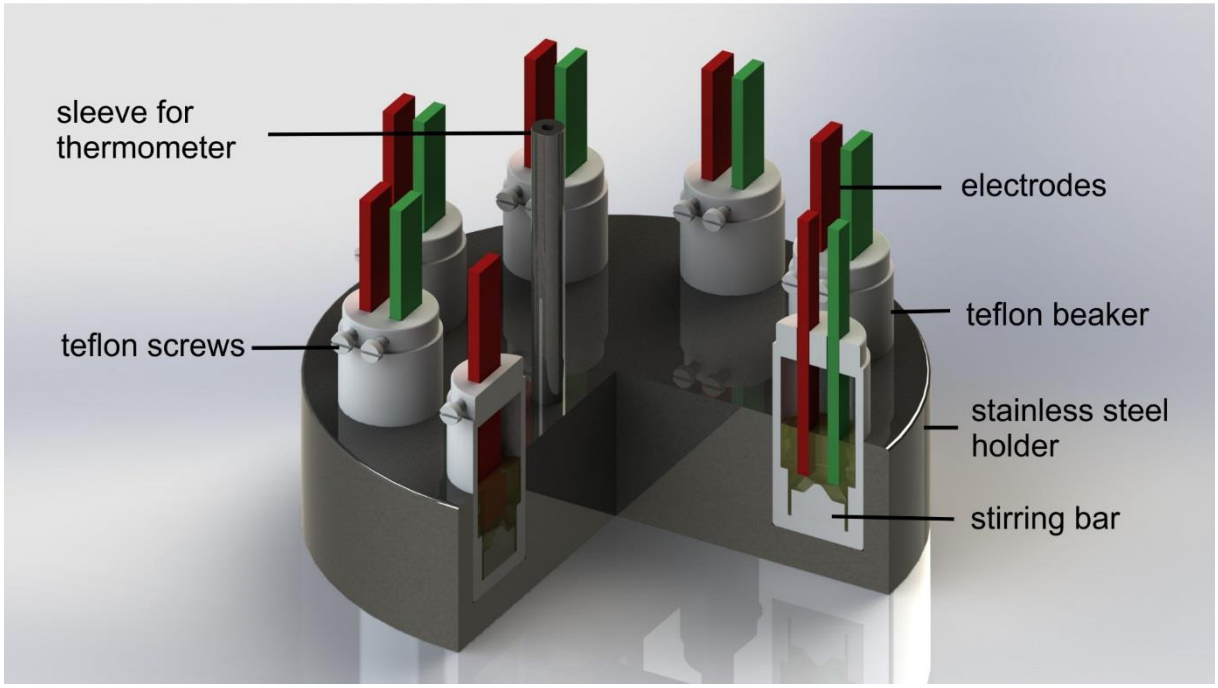

Figure S7.20. Schematic view of undivided screening cells in a screening arrangement.[53]

Table S7.1. Electrolysis in the screening cell.

Entry	***polymer***	***cathode***	***anode***	***Q / F/mol***	***I / mA***	***J / mA/cm²***
1	*P(TsMAz) (P2)*	Pt	Mg	2.0	7.5	5.0
2	*P(TsMAz) (P2)*	Pt	Mg	3.0	7.5	5.0
3	*P(TsMAz) (P2)*	Pt	Zn	2.0	7.5	5.0
4	*P(TsMAz) (P2)*	Pt	Zn	3.0	7.5	5.0
5	*P(MsMAz) (P1)*	Pt	Mg	2.0	7.5	5.0
6	*P(MsMAz) (P1)*	Pt	Mg	3.0	7.5	5.0
7	*P(MsMAz) (P1)*	Pt	Zn	2.0	7.5	5.0
8	*P(MsMAz) (P1)*	Pt	Zn	3.0	7.5	5.0

Beaker-type cell (25 mL)

A solution of P(TsMAz) (P2) (250 mg, 1.18 mmol), naphthalene (77 mg, 0.60 mmol) and *N*,*N*,*N*,*N*-tretrabutylammonium tetrafluoroborate (271 mg, 1.25 mmol) in 12.5 mL *N*,*N*-dimethylformamide (DMF) was transferred into a undivided beaker-type electrolysis cell equipped with a platinum cathode and zinc or magnesium anode. A constant current electrolysis with a current density of 5 mA cm^{-2} was performed at 100 °C. After application of 228 C (2 F per mol PTsMAz) the electrolysis was stopped and the solvent mixture was recovered *in vacuo* (50 °C, 200 – 70 mbar). The crude solvent mixture was condensend and analyzed by ^{1}H NMR spectroscopy.

The beaker-type cell (25 mL) consists of a simple glass beaker with or without cooling jacket and covered with a teflon plug. This cap allows precise location of the electrodes. A single electrode has upon immersion into the electrolyte an active surface of 3.6 cm^2 (2 x 1.8 cm).[55]

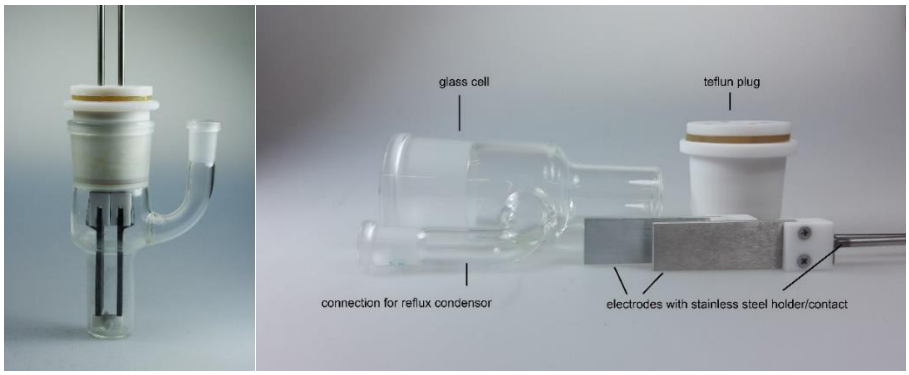

Figure S7.21. Picture of an undivided beaker-type electrolysis cell. Essential parts are labeled.

7.7 References

1. Gleede, T.; Rieger, E.; Homann-Müller, T.; Wurm, F. R., *Macromolecular Chemistry and Physics* **2017**, 1700145.
2. Homann-Müller, T.; Rieger, E.; Alkan, A.; Wurm, F. R., *Polym. Chem.* **2016,** *7* (35), 5501-5506.
3. Reisman, L.; Mbarushimana, C. P.; Cassidy, S. J.; Rupar, P. A., *ACS Macro Letters* **2016,** *5* (10), 1137-1140.
4. Rieger, E.; Manhart, A.; Wurm, F. R., *ACS Macro Letters* **2016,** *5* (2), 195-198.
5. Thomi, L.; Wurm, F. R., *Macromolecular Symposia* **2015,** *349* (1), 51-56.
6. Rieger, E.; Gleede, T.; Weber, K.; Manhart, A.; Wagner, M.; Wurm, F. R., *Polym. Chem.* **2017,** *8* (18), 2824-2832.
7. Wang, X.; Liu, Y.; Li, Z.; Wang, H.; Gebru, H.; Chen, S.; Zhu, H.; Wei, F.; Guo, K., *ACS Macro Letters* **2017,** *6* (12), 1331-1336.
8. Stewart, I. C.; Lee, C. C.; Bergman, R. G.; Toste, F. D., *Journal of the American Chemical Society* **2005,** *127* (50), 17616-17617.
9. Rieger, E.; Alkan, A.; Manhart, A.; Wagner, M.; Wurm, F. R., *Macromol. Rapid Commun.* **2016,** *37* (10), 833-839.
10. Rieger, E.; Blankenburg, J.; Grune, E.; Wagner, M.; Landfester, K.; Wurm, F. R., *Angewandte Chemie International Edition* **2018,** *57,* DOI:10.1002/anie.201710417.
11. Hadjichristidis, N.; Hirao, A., *Anionic Polymerization*. Springer Japan: Japan, 2015; p 1082.
12. Odian, G., *Principles of Polymerization*. 4. ed.; John Wiley & Sons, Inc. : Hoboken, New Jersey, USA, 2004.
13. Boussif, O.; Lezoualc'h, F.; Zanta, M. A.; Mergny, M. D.; Scherman, D.; Demeneix, B.; Behr, J.-P., *Proceedings of the National Academy of Sciences* **1995,** *92* (16), 7297-7301.
14. Islam, M. A.; Park, T. E.; Singh, B.; Maharjan, S.; Firdous, J.; Cho, M.-H.; Kang, S.-K.; Yun, C.-H.; Choi, Y. J.; Cho, C.-S., *Journal of Controlled Release* **2014,** *193*, 74-89.
15. Jaeger, M.; Schubert, S.; Ochrimenko, S.; Fischer, D.; Schubert, U. S., *Chemical Society Reviews* **2012,** *41* (13), 4755-4767.
16. Perevyazko, I.; Gubarev, A. S.; Tauhardt, L.; Dobrodumov, A.; Pavlov, G. M.; Schubert, U. S., *Polymer Chemistry* **2017,** *8* (46), 7169-7179.
17. Saegusa, T.; Kobayashi, S.; Ishiguro, M., *Macromolecules* **1974,** *7* (6), 958-959.
18. Alonso, D. A.; Andersson, P. G., *The Journal of Organic Chemistry* **1998,** *63* (25), 9455-9461.
19. Senboku, H.; Nakahara, K.; Fukuhara, T.; Hara, S., *Tetrahedron Letters* **2010,** *51* (2), 435-438.

20. Ji, S.; Gortler, L. B.; Waring, A.; Battisti, A. J.; Bank, S.; Closson, W. D.; Wriede, P. A., *Journal of the American Chemical Society* **1967,** *89* (20), 5311-5312.
21. Bergmeier, S. C.; Seth, P. P., *Tetrahedron Letters* **1999,** *40* (34), 6181-6184.
22. Henry, J. R.; Marcin, L. R.; McIntosh, M. C.; Scola, P. M.; Davis Harris, G.; Weinreb, S. M., *Tetrahedron Letters* **1989,** *30* (42), 5709-5712.
23. Alonso, E.; Ramón, D. J.; Yus, M., *Tetrahedron* **1997,** *53* (42), 14355-14368.
24. Roemmele, R. C.; Rapoport, H., *The Journal of Organic Chemistry* **1988,** *53* (10), 2367-2371.
25. Kudav, D. P.; Samant, S. P.; Hosangadi, B. D., *Synthetic Communications* **1987,** *17* (10), 1185-1187.
26. Chavez, F.; Sherry, A., *The Journal of Organic Chemistry* **1989,** *54* (12), 2990-2992.
27. Forshee, P. B.; Sibert, J. W., *Synthesis* **2006,** *2006* (05), 756-758.
28. Szostak, M.; Spain, M.; Procter, D. J., *Chemical Society Reviews* **2013,** *42* (23), 9155-9183.
29. Vedejs, E.; Lin, S., *The Journal of Organic Chemistry* **1994,** *59* (7), 1602-1603.
30. Knowles, H. S.; Parsons, A. F.; Pettifer, R. M.; Rickling, S., *Tetrahedron* **2000,** *56* (7), 979-988.
31. Goulaouic-Dubois, C.; Guggisberg, A.; Hesse, M., *The Journal of Organic Chemistry* **1995,** *60* (18), 5969-5972.
32. Mairanovsky, V. G., *Angewandte Chemie International Edition in English* **1976,** *15* (5), 281-292.
33. Coeffard, V.; Thobie-Gautier, C.; Beaudet, I.; Le Grognec, E.; Quintard, J.-P., *European Journal of Organic Chemistry* **2008,** *2008* (2), 383-391.
34. Scialdone, O.; Belfiore, C.; Filardo, G.; Galia, A.; Sabatino, M. A.; Silvestri, G., *Electrochimica Acta* **2005,** *51* (4), 598-604.
35. Kossai, R.; Emir, B.; Simonet, J.; Mousset, G., *Journal of Electroanalytical Chemistry and Interfacial Electrochemistry* **1989,** *270* (1), 253-260.
36. Kubrakova, I. V.; Formanovsky, A. A.; Mikhura, I. V., *Mendeleev Communications* **1999,** *9* (2), 65-66.
37. Wellner, E.; Sandin, H.; Pääkkönen, L., *Synthesis* **2003,** *2003* (02), 0223-0226.
38. Sabitha, G.; Reddy, B. V. S.; Abraham, S.; Yadav, J. S., *Tetrahedron Letters* **1999,** *40* (8), 1569-1570.
39. Vellemäe, E.; Lebedev, O.; Mäeorg, U., *Tetrahedron Letters* **2008,** *49* (8), 1373-1375.
40. Nayak, S. K., *Synthesis* **2000,** *2000* (11), 1575-1578.
41. Nyasse, B.; Grehn, L.; Ragnarsson, U., *Chemical Communications* **1997,** (11), 1017-1018.

42. Uchiyama, M.; Matsumoto, Y.; Nakamura, S.; Ohwada, T.; Kobayashi, N.; Yamashita, N.; Matsumiya, A.; Sakamoto, T., *Journal of the American Chemical Society* **2004,** *126* (28), 8755-8759.
43. Hamada, T.; Nishida, A.; Yonemitsu, O., *Journal of the American Chemical Society* **1986,** *108* (1), 140-145.
44. Urjasz, W.; Celewicz, L., *Journal of Physical Organic Chemistry* **1998,** *11* (8-9), 618-621.
45. Yasuhara, A.; Sakamoto, T., *Tetrahedron Letters* **1998,** *39* (7), 595-596.
46. Yasuhara, A.; Kameda, M.; Sakamoto, T., *CHEMICAL & PHARMACEUTICAL BULLETIN* **1999,** *47* (6), 809-812.
47. Fukuyama, T.; Cheung, M.; Jow, C.-K.; Hidai, Y.; Kan, T., *Tetrahedron letters* **1997,** *38* (33), 5831-5834.
48. Fukuyama, T.; Jow, C.-K.; Cheung, M., *Tetrahedron Letters* **1995,** *36* (36), 6373-6374.
49. Thomi, L.; Wurm, F. R., *Macromol Rapid Commun* **2014,** *35* (5), 585-589.
50. Victor, R.; Bauwens, E.; Monnery, B. D.; De Geest, B. G.; Hoogenboom, R., *Polymer Chemistry* **2014,** *5* (17), 4957-4964.
51. Altuntaş, E.; Knop, K.; Tauhardt, L.; Kempe, K.; Crecelius, A. C.; Jäger, M.; Hager, M. D.; Schubert, U. S., *Journal of Mass Spectrometry* **2012,** *47* (1), 105-114.
52. Gold, E. H.; Babad, E., *The Journal of Organic Chemistry* **1972,** *37* (13), 2208-2210.
53. Gütz, C.; Klöckner, B.; Waldvogel, S. R., *Organic Process Research & Development* **2015,** *20* (1), 26-32.
54. Kirste, A.; Schnakenburg, G.; Stecker, F.; Fischer, A.; Waldvogel, S. R., *Angewandte Chemie International Edition* **2010,** *49* (5), 971-975.
55. Riehl, B.; Dyballa, K. M.; Franke, R.; Waldvogel, S. R., *Synthesis* **2017,** *49* (02), 252-259.

Outlook

The azaanionic polymerization of activated aziridines recently started and more groups are joining the growing community, the knowledge on this topic is most likely to increase rapidly within the next decade. There is still room for new monomers with various further chemical functionalities, and also materials higher molecular weights than reported to date are envisioned. Initiator systems known from other anionic polymerization methods, like alkoxides and Grignard reagents may become also important for azaanionic polymers, which give access to telechelic polymers in the future. Moreover, initiators with multiple anchor points may act as scaffold for dendritic or star-like macromolecular architectures, which can in turn exhibit interesting properties for further applications. For example, employing the bifunctional initiator presented in this work should make the one-shot synthesis of a thermoplastic elastomer feasible, when using two monomers with very different reactivities.

Besides the possibility to produce functional polymers from functional monomers, also post-modification of the polysulfonamides (e.g. aromatic substitutions at the sulfonamide), or of their deprotected derivatives, is another avenue to obtain various functional materials. The available functional groups along the backbone, such as alcohols or olefins, represent a platform to attach targeting moieties like saccharides, antibodies or peptides, useful conjugates for drug delivery, labeling or sensing in biomedical applications. The potential application as transfection agents of the different deprotected PAz obtained in the current work should be assessed. Additionally, transfection studies of different derivatives, including different copolymers and functionalities are of high interest. Consequently, the deprotection strategies should be further expanded. More selective methods like removal of nosyl-groups *via* thiol chemistry, stand as a promising approach to improve deprotection towards suitable PEI-derivatives. Chemoselective deprotection of one group in the presence of others under very mild conditions would be also desirable.

The unique control of monomer sequence distribution achieved in aziridine copolymerizations may be expanded to synthesize different combinations. Pushing the limits of sequence controlled systems, multi-block copolymers with more than twenty different blocks, including all available monomers, can be envisioned. A major approach will be the combination of different copolymerization techniques, ideally anionic copolymerization in one-pot methodologies. The combination of properties may be also interesting when methacrylates, lactides, thiiranes or other anionic polymerizable monomers are copolymerized simultaneously. Additionally, the change to controlled radical polymerizations via functionalized end groups might offer new block structures with unprecedented properties, not affordable by other means to date. Copolymers with other types of monomers, e.g. ethylene oxide, might be useful for polymerization-induced self-assembly (PISA) studies. The potential manufacture of surfactant-like structures similar to Lubrizol, as PAz-*b*-PEO (amphiphilic) or the desulfonylated version PPI-PEO (hydrophilic) is possible.

Likewise, the generation of brush macromolecules, for instance with short PEGylated side chains grafted to a PAz backbone, is also an interesting pathway to follow.

The concept of physical separation of monomers to change their copolymerization behavior should be further expanded within the aziridines. However, this breakthrough concept can be also exported to other common polymerization techniques, as carbanionic polymerizations and so on, offering new developments in the control of copolymer microstructure. In addition, the combination of different anionic polymerization techniques within compartments might be exploited to yield completely new architectures, even employing more than two monomers simultaneously.

Polymers containing aziridines in their side chains have been already reported. The addressability of those side chains in terms of further azaanionic polymerization might be important in the field of polymer networks. The remarkable degree of control over aziridine polymerization has the potential to be transferred to the mechanical properties of these novel network-based materials. Further ideas already explored in other polymerization techniques, as light driven mechanism to control the monomer incorporation, might been worth to investigate for polyaziridines.

We believe that the research regarding the azaanionic polymerization has just started. We thus anticipate that polyaziridines will become more than a niche product, as soon as more of their potential is discovered. Naturally, the wide range of potential applications of PAz, as they are a recent polymer class, remain to be examined. Nonetheless, a firm underpinning is already provided for the advancement in this novel field of polymer science.

A.1 Cooperation Projects

During my PhD thesis several cooperation projects have been developed successfully. In the following, the published papers on functional poly(aziridine)s are presented. The two publications on OROP of aziridines and ongoing projects are not presented.

A.1.1 Redox-responsive poly(aziridine)s

"*N*-Ferrocenylsulfonyl-2-methylaziridine: the first ferrocene monomer for the anionic (co)polymerization of aziridines." Homann-Müller, T.; Rieger, E.; Alkan, A.; Wurm, F. R. *Polymer Chemistry* **2016**, *7*, 5501-5506.

A.1.2 The first orthogonal aziridine monomer

"4-Styrenesulfonyl-(2-methyl)aziridine: The First Bivalent Aziridine-Monomer for Anionic and Radical Polymerization." Gleede, T.; Rieger, E.; Homann-Müller, T.; Wurm, F. R. *Macromolecular Chemistry and Physics* **2017**, 1700145.

A.1.1 Redox-responsive poly(aziridine)s

Polymer Chemistry

PAPER

Cite this: *Polym. Chem.*, 2016, **7**, 5501

N-Ferrocenylsulfonyl-2-methylaziridine: the first ferrocene monomer for the anionic (co) polymerization of aziridines†

Tatjana Homann-Müller, Elisabeth Rieger, Arda Alkan and Frederik R. Wurm*

Received 13th June 2016,
Accepted 20th July 2016

DOI: 10.1039/c6py01019a

www.rsc.org/polymers

N-Ferrocenylsulfonyl-2-methylaziridine (fcMAz) is synthesized in a convenient three-step protocol from ferrocene. It represents the first aziridine-based monomer suitable for the anionic polymerization, carrying a ferrocenyl-substituent. Sulfonamide-activated aziridines can undergo (mostly living) anionic polymerization and fcMAz is also the first example of a functional sulfonamide-based aziridine monomer. It can be polymerized with different initiators to homo and copolymers (block or statistical) with adjustable molecular weights. The homopolymer is insoluble in common organic solvents, while the copolymers with other aziridines are soluble and exhibit molecular weight dispersities of 1.1–1.5. FcMAz thus broadens the scope of ferrocenyl-containing polymers and may be combined with other anionic polymerization techniques in the future.

Introduction

Ferrocene (fc)-containing polymers have been studied for several decades, due to their reversible redox-properties, self-assembly and related properties.[1–3] To date, the major monomers that are found in the literature, concerning fc-containing materials, are vinyl ferrocene[4] and strained silicon-bridged [1]-ferrocenophanes[5] (mainly ferrocenyldimethyl silane, Fig. 1),

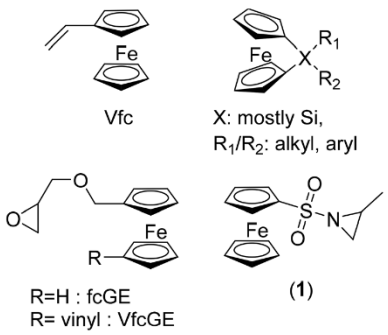

Fig. 1 fc-containing monomers.

Max-Planck-Institut für Polymerforschung, Ackermannweg 10, 55128 Mainz, Germany. E-mail: wurm@mpip-mainz.mpg.de

†Electronic supplementary information (ESI) available. See DOI: 10.1039/c6py01019a

besides several others.[1,3] They can be combined with controlled polymerization techniques, like controlled radical or living anionic polymerization. Our group recently introduced the first fc-containing epoxides, which can undergo oxyanionic polymerization and allow the production of fc-containing polyethers.[6–8]

Herein, we expand the scope of fc-containing monomers to the first fc-aziridine that can undergo anionic polymerization, namely *N*-ferrocenylsulfonyl-2-methylaziridine (fcMAz, **1**). Aziridines have been studied for decades as reactive intermediates[9,10] or as monomers for the mostly uncontrolled cationic ring-opening polymerization to poly(ethylene imine)-derivatives.[11,12] Earlier work on fc-containing aziridines involved attaching the organometallic moiety to the ring-carbons,[13] which were for example used for ring-expansion of the three-membered aziridine to fc-containing oxazolines.[14] Wang *et al.* reported the synthesis of chiral ferrocenyl aziridino alcohols prepared from L-serine and ferrocenecarboxaldehyde; the authors used them as chiral catalysts for the asymmetric addition of diethylzinc to aldehydes.[15,16] In contrast, we attached fc *via* the activating sulfonamide group to the ring-nitrogen of aziridine, allowing subsequent nucleophilic ring-opening[17] to perform anionic homo-[18] and copolymerization with other sulfonylaziridines.[9]

Earlier work on fc-modified poly(ethylene imine) derivatives involved attaching the fc-groups *via* the amines or the carbon atoms in the polymer backbone. These polymers were used as molecular wires to connect the redox centers of enzymes to an electrode surface. Amperometric biosensors for glucose and hydrogen peroxide have been constructed *via* the immobilization of enzymes in crosslinked polymer films.[19–21]

FcMAz was investigated with respect to polymerization control, comonomer incorporation rates in statistical copolymers and thermal and electrochemical properties. Besides the fact that poly(**1**) is insoluble as a homopolymer, it produces soluble and rather well-defined copolymers, allowing the combination with other anionic polymerization techniques for future applications.

Experimental

Materials/methods and additional experimental procedures can be found in the ESI.†

Synthesis of *N*-ferrocenylsulfonyl-2-methylaziridine (fcMAz, 1)

Ammonium ferrocenyl sulfonate.[22] Ferrocene (40 g, 0.22 mol) was suspended in 700 mL acetic anhydride and 15 mL chlorosulfonic acid was added over a period of *ca.* 30 min. After stirring overnight at room temperature the mixture was poured onto 800 mL ice water, concentrated at reduced pressure and extracted overnight with a Soxhlet-setup with methanol. The extract was concentrated to *ca.* 250 mL and *ca.* 100 mL conc. aq. ammonia was added. A brown precipitate was removed by filtration; the filtrate was dried *in vacuo* to yield 26 g (86 mmol, 40%) of ammonium ferrocenyl sulfonate (as monohydrate).

^{1}H NMR (300 MHz, DMSO-d_6): δ [ppm] = 7.15 (br, 4H, NH_4^+), 4.18 (2H, $Cp_{subst.}$), 3.35 (s, 5H, Cp), 2.50 (2H, $Cp_{subst.}$)

Ferrocenyl sulfonic acid chloride.[23] 10.2 g (34 mmol) of ammonium ferrocene sulfonate monohydrate were suspended in 50 mL dry dichloromethane and cooled in an ice-bath. A few drops of dimethylformamide and 5.8 mL oxalyl chloride were added dropwise. The reaction mixture was stirred for 30 min at 0 °C. A gas evolution was noted during this time. The cooling bath was then removed and the solution was allowed to warm up to room-temperature and stirring was continued for additional 12 h. After evaporation of all volatiles, the product was extracted with hexane to yield ferrocenyl sulfonic acid chloride as a red-orange powder (4.3 g, 15 mmol, 45%).

^{1}H NMR (300 MHz, $CDCl_3$): δ [ppm] = 4.87 (m, 2H, cp.), 4.62 (m, 2H, cp), 4.47 (s, 5H, cp).

***N*-Ferrocenylsulfonyl-2-methylaziridine (fcMAz, 1).** *rac*-2-Methylaziridine (0.4 mL, 7 mmol) and 1.8 mL (18.8 mmol) *N*,*N*-diisopropylethylamine were dissolved in 10 mL dry dichloromethane and cooled to −30 °C. Ferrocenyl sulfonic acid chloride (2 g, 7 mmol) was dissolved in 10 mL dry dichloromethane and added dropwise over a period of *ca.* 20 min to the reaction mixture. The mixture was stirred for additional 90 min at −30 °C and allowed to warm up to 23 °C and stirred overnight. Then 20 mL saturated sodium hydrogen carbonate solution was added and stirred for 30 min. The aqueous phase was removed and the organic layer was washed again with brine, dried over magnesium sulfate and evaporated to dryness. Purification of the crude mixture by silica column chromatography (PE/EA 4 : 3, R_f = 0.7) yielded **1** as orange needles (2 g, 6.5 mmol, 94%).

^{1}H NMR (300 MHz, 298 K, $CDCl_3$): δ [ppm] = 4.74–4.68 (m, 2H, g), 4.48–4.44 (t, 2 H, f), 4.43 (s, 5H, e), 2.86–2.75 (m, 1 H, d), 2.50 (d, 1H, c), 2.00 (d, 1H, b), 1.27 (d, 1H, a). ^{13}C NMR (176 MHz, 298 K, $CDCl_3$): δ [ppm] = 149.81; 135.90; 124.04; 35.67; 34.72; 16.88. ^{15}N NMR (71 MHz, 298 K, $CDCl_3$): δ [ppm] = 81.80. ESI MS: theor: 305.173 g mol^{-1}, found (*m*/*z*): 328.00 (M + Na^+), 633.01 (2M + Na^+) (Fig. S12†). Elemental analysis: calc.: $C_{13}H_{15}NO_2SFe$ = C: 51.16%, H: 4.95%, N: 4.59%, O: 10.49%, S: 10.51%, Fe: 18.3%. Found: C: 51.12%, H: 5.04%, N: 4.58%, S: 10.54%. R: $\tilde{\nu}$: 3451 (b), 3105 (s), 2974 (m), 2932 (w), 1730 (b), 1449 (s), 1439 (s), 1411 (w), 1394 (s), 1362 (s), 1330 (ss), 1233 (s), 1196 (s), 1155 (s), 1130 (s), 1031 (s), 987 (s), 906 (s), 845 (ss), 773 (s), 691 (s), 636 (s), 618 (s) cm^{-1}.

Results and discussion

Monomer synthesis

Substitution of the acidic proton at the aziridine is essential to enable its anionic polymerization and typically an electron-withdrawing group, such as a sulfonamide, is attached.[9,18,24–26] For the first time, we demonstrate that a functional and stimuli-responsive group, *i.e.* a ferrocenyl substituent, can be coupled *via* a sulfonamide to the aziridine, allowing us to conduct an anionic polymerization. The synthesis starts with the preparation of ferrocenyl sulfonic acid chloride,[22,23] which is then reacted with *rac*-2-methyl aziridine (Scheme 1), similar to a previously published procedure for tosyl- or mesyl-substituted aziridines.[9] After purification by column chromatography (petroleum ether : ethyl acetate = 4 : 3, R_f = 0.7), *N*-ferrocenylsulfonyl-2-methylaziridine (**1**, fcMAz) is obtained in 94% yield (last step) as orange crystals (a photograph of **1** and poly(**1**) is shown in the ESI†).

The ^{1}H NMR spectrum of **1** (Fig. 2) shows the characteristic resonances of a substituted aziridine: three doublets at 1.27 ppm (a), 2.00 ppm (b), and 2.50 ppm (c) and a multiplet at 2.86–2.75 ppm (d) are indicative of the aziridine derivative. The resonance of the unsubstituted ring-methylenes splits

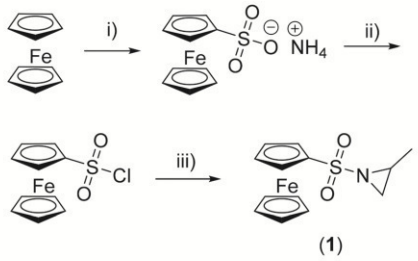

Scheme 1 Synthesis of *N*-ferrocenylsulfonyl-2-methylaziridine (1) (i) acetic anhydride, chlorosulfonic acid, 20 h, room temperature, followed by NH_4OH; (ii) oxalyl chloride, DCM, 0 °C; (iii) *rac*-2-methylaziridine, diisopropyl ethyl amine, DCM, −30 °C.

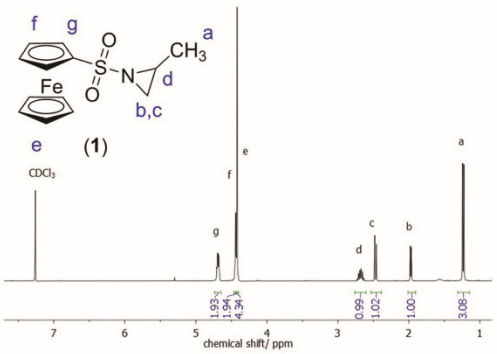

Fig. 2 ^{1}H NMR spectrum of fcMAz (1) ($CDCl_3$, 300 MHz, 298 K).

into two signals due to coupling with the neighboring methine group at a stereo center. The resonances for the ferrocene group are detected at 4.4 ppm (singlet for the unsubstituted cp ring) and between 4.5 and 4.7 ppm (substituted cp ring). ^{15}N NMR spectroscopy reveals a singlet at 81.8 ppm.

Polymerization

The aza-anionic polymerization of aziridines has been previously initiated by sulfonamide anions, such as potassium *N*-benzyl-mesyl amide. The initiator is generated in the reaction flask prior to the polymerization by deprotonation of the respective sulfonamide with potassium hexamethyldisilazide (KHMDS).[18] Alternatively KHMDS can be used as the initiator itself. Also butyl lithium can be used as an initiator, as it was previously shown that aza-anions propagate with lithium counter ions.[25] The polymerization of **1** was conducted under different conditions: polar solvents (DMF, THF, and DMSO) have been used, and the temperature, time (18–72 h) and initiators have been varied (Table 1, Scheme 2a).

In all cases, the polymer precipitated during the reaction from solution. The resulting P(fcMAz) was obtained as an orange powder in quantitative yields, but it was insoluble in all common solvents (DMF, DMSO, acetonitrile, *n*-hexane or THF,

Table 1 Overview of the reaction conditions for the polymerization of 1

#	DP[a]	Solvent	Initiator[b]	*t*/h
1	7	DMF	2	18
2	16	DMF	2	72
3	33	DMSO	2	18
4	37	DMF	2	72
5	7	DMF/DMSO 2 : 1	1	18
6	25	DMSO	1	18
7	22	THF	3	18
8	30	DMF	3	72

[a] Degree of polymerization (DP) theoretical. [b] Initiator system: 1: KHMDS, 2: potassium *N*-benzyl-mesyl amide, 3: *n*-BuLi, temperature 50 °C.

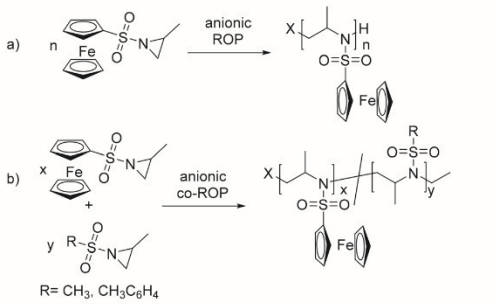

Scheme 2 (a) Anionic ring-opening polymerization of PfcMAz (1) and its copolymerization (b) with MsMAz and TsMAz.

etc.). Also its oxidation with common oxidants, such as silver triflate or hydrogen peroxide, did not produce a soluble polymer. Monomer: initiator ratios of 1 : 7 to 1 : 40 were targeted and in all cases almost full monomer conversion was achieved (as no residual monomer was detectable in the reaction mixture); no higher degrees of polymerization were targeted, due to the formation of an insoluble polymer.

P(**1**) is the first reported insoluble racemic polymer prepared by anionic polymerization from a sulfonamide-substituted aziridine. Characterization of the homopolymers was conducted by solid state NMR spectroscopy (Fig. 2). The spectra indicate the successful formation of PAz. Due to the inherently low resolution of the ^{1}H-SS-NMR spectrum, a clear signal assignment is not possible; however, the signals of the polymer backbone (1–3, in Fig. 2), of the fc moieties (4–13), and of the aromatic initiator (14) can be assumed. The ^{13}C-SS-NMR reveals more details of the polymer structure: the initiator (14) can be detected at *ca.* 130 ppm; the signal of the sulfonamide-bound carbon atom of fc (4) occurs at *ca.* 90 ppm, with the remaining cp signals between 75–65 ppm; in addition, the backbone resonances between 60–45 ppm and the pendant methyl groups at 20–10 ppm are clearly separated (Fig. 3).

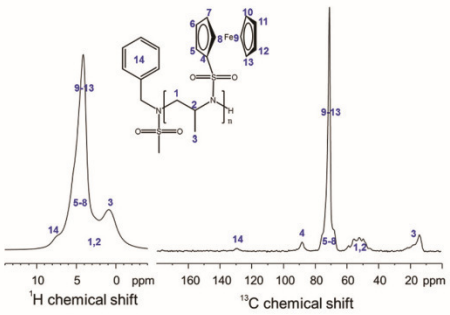

Fig. 3 Solid state NMR of poly(1): ^{1}H (left) and ^{13}C NMR (right) spectra of $PfcMAz_{33}$.

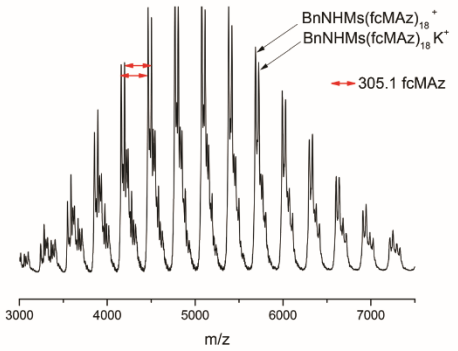

Fig. 4 MALDI-TOF mass spectrum of $PfcMAz_{33}$.

MALDI-TOF mass spectrometry proves the formation of the envisioned PfcMAz. The main distribution can be calculated to contain the mass of the initiator and the monomer mass (*cf.* Fig. 4) with a distance of 305 g mol^{-1}, the molar mass of **1**, up to a detectable molecular weight of *ca.* 7500 g mol^{-1}. The maximum of the distribution corresponds to the molecular weight of 15 repeating units, the initiator and potassium as a counter ion.

Block copolymer synthesis

In addition to the homopolymerization of **1**, copolymers with *N*-mesyl-2-methylaziridine (MsMAz, **2**) and *N*-tosyl-2-methylaziridine (TsMAz, **3**) have been prepared, in order to produce soluble fc-containing PAz structures. Chain extension of living P(**2**) or P(**3**) with fcMAz to block copolymers was achieved; however, only short segments of PfcMAz could be realized, probably due to aggregation of the chain ends, leading to inactivation of the propagation. The ^{1}H NMR spectra reveal the successful formation of a copolymer, with the resonances of both monomers detectable (Fig. 5 and S1†). In Fig. 5 the

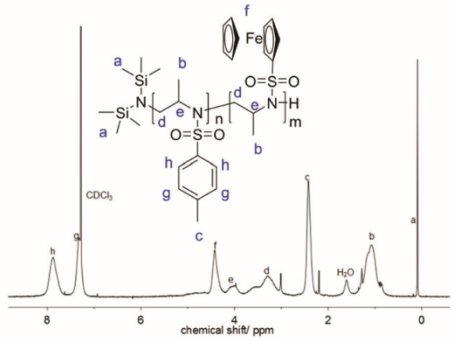

Fig. 5 ^{1}H NMR spectrum of $P(TsMAz)_{22}$-*block*-$P(fcMAz)_5$ ($CDCl_3$, 300 MHz, 298 K).

^{1}H NMR spectrum of $P(TsMAz)_{22}$-*b*-$P(fcMAz)_5$ initiated by KHMDS is shown: the tosyl resonances are detected between 8.31 and 7.16 ppm (h, g) and 2.74–2.1 (c), ferrocene signals (f) appear from 5.25 to 4.22 ppm, the polyaziridine backbone (e, d) at 4.22–2.79 ppm, and the pendant methyl groups (b) from 1.42 to 0.75 ppm. The SEC elugrams for all block copolymers prepared in this study show narrow molecular weight dispersities only for polymers with short fcMAz-segments detected from ^{1}H NMR spectroscopy. For copolymers with several fcMAz units, the dispersity increases to *ca.* 1.4 with a bimodal shape of the elugram; this can be either rationalized by side reactions during the chain extension reaction, or – more probable – due to interactions or micellization during the polymerization and also the SEC measurement (Fig. S3†). MALDI-TOF mass spectrometry further proves the successful incorporation of both monomers into the polymer as the molecular weights of both monomers can be detected with peak distances of 305 g mol^{-1} (for **1**) and 211 g mol^{-1} (for **3**) from the spectrum (Fig. S2†) (Table 2).

Statistical copolymerization

The statistical copolymerization of **1** with **2** or **3** has been conducted, leading to higher fc-fractions (up to 58 wt% fc) in the final polymers (see below). In both cases, successful copolymerization with quantitative monomer incorporation is achieved; the ^{1}H NMR spectra match the ones for the block copolymers. As the initiator signals are overlapping with the polymer signals, only the comonomer incorporation ratio was calculated, which is in agreement with the theoretical values. The molecular weight distributions for the statistical copolymers range between 1.3 and 1.4 with no significant correlation with the fcMAz content (Fig. S4†) (Table 3).

The bimodal shape of the molecular weight distributions could be rationalized due to aggregation phenomena during the polymerization or side reactions with KHMDS as the initiator. ^{1}H NMR spectra do not indicate side reactions, also the monomers are fully consumed at the end of the polymerization.

The Fe-content was also analyzed by UV/Vis spectroscopy monitoring the absorbance band at *ca.* 430 nm (Fig. S5†), matching the values from the NMR spectra.

Real-time ^{1}H NMR kinetic studies of the copolymerization of **1** and **3** in DMSO were conducted. Monomer incorporation

Table 2 Characterization of the chain extension experiments conducted with **1**

#	Polymer	DP[a]	M_n [a]	M_n [b]	D[b]	M_n [c]	DP[c]
1	$P(2)_{37}$-*b*-$P(1)_3$	54/6	9300	2700	1.07	5500	37/1
2	$P(2)_{28}$-*b*-$P(1)_4$	39/5	7000	2300	1.16	4600	28/2
3	$P(3)_{22}$-*b*-$P(1)_5$	22/5	6400	3000	1.25	[d]	[d]
4	$P(3)_{25}$-*b*-$P(1)_6$	25/6	7300	3400	1.36	[d]	[d]

[a] Degree of polymerization (DP) theoretical and theoretical molecular weight (M_n in g mol^{-1}). [b] Determined by SEC in DMF. [c] Degree of polymerization (DP) and molecular weight (M_n in g mol^{-1}) determined from ^{1}H NMR. [d] Not determined.

Table 3 Characterization data for statistical copolymers of 1 with 2 or 3

#	Initiator[a]	DP[b]	M_n [b]	M_n [c]	$Đ$[c]	M_n [d]	DP[d]	Ratio[e]
P(3_{29}-*co*-1_9)	1	29/9	9000	3400	1.3	*f*	*f*	3 : 1
P(3_{32}-*co*-1_{18})	2	32/18	12 500	4500	1.3	*f*	*f*	2 : 1
P(3_{21}-*co*-1_{20})	3	21/20	10 500	2500	1.3	*f*	*f*	5 : 4
P(2_{53}-*co*-1_{18})	3	53/18	12 700	2600	1.3	*f*	*f*	4 : 1
P(2_{21}-*co*-1_{11})	2	21/11	6400	3300	1.4	7200	27/11	5 : 2

[a] Initiator system: 1: KHMDS, 2: KBnMs, 3: *n*-BuLi. [b] Degree of polymerization (DP) theoretical and theoretical molecular weight (M_n in g mol^{-1}). [c] Determined by SEC in DMF. [d] Degree of polymerization (DP) and molecular weight (M_n in g mol^{-1}) determined from ^{1}H NMR. [e] Monomer ratio determined from ^{1}H NMR. [f] Not determined.

over time is measured by integration of the methylene resonances for both monomers (Fig. 6, 2.3 ppm for **1**, and 2.16 ppm for **3**). The integration revealed that the polymerization of **3** is faster than that of **1**, indicating the formation of a gradient copolymer after the copolymerization process. From these spectra the monomer incorporation rates during the copolymerization can be calculated (Fig. 6 and S6–S8†).

Thermal analysis

The thermal properties of the fc-containing PAz were analyzed by DSC and TGA (*cf.* Fig. S9 and S10†). All polymers are amorphous materials with glass transition temperatures in the range of 123 and 144 °C which rises with the increasing content of fc in the copolymers (both for copolymers with **2** and **3**, Table 4). For comparison also homopolymers P(**1**) (T_g = 56 °C), P(**2**) (T_g – 137 °C), and P(**3**) (T_g – 144 °C) have been prepared.

All polymers exhibit a similar thermal stability with a beginning mass loss at *ca.* 350 °C of 53–68 wt%. This weight loss is probably due to the release of the sulfonamide groups. We assume that ferrocene is not eliminated as the polymers with higher iron-content reveal a higher char residue, indicating the formation of iron-containing char. The char residue is 24–36% (36% for the homopolymers poly(**1**)) rather high,

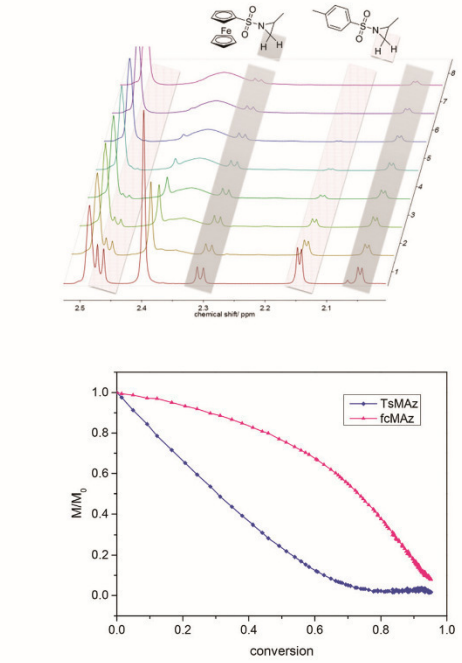

Fig. 6 Top: Real-time ^{1}H-NMR-kinetics for P(TsMAz$_{30}$-*co*-fcMAz$_{12}$) (time interval between the spectra 40 min). Bottom: Monomer conversion determined from NMR for TsMAz and fcMAz in Poly(TsMAz$_{30}$-*co*-fcMAz$_{12}$).

Table 4 Thermal data of fc-containing PAz

#	Wt% fc-monomer[a]	T_g [b]/°C
P(**1**)	100	56
P(2_{44})	0	137
P(2_{53}-*co*-1_{18})	43	123
P(2_{27}-*co*-1_{11})	52	133
P(3_{74})	0	144
P(3_{29}-*co*-1_9)	30	123
P(3_{30}-*co*-1_{13})	37	139
P(3_{32}-*co*-1_{18})	44	143
P(3_{21}-*co*-1_{20})	58	144
P(2_{22}-*b*-P1_5)	19	134

[a] Weight % 1 incorporated. [b] Glass transition temperature, determined from DSC.

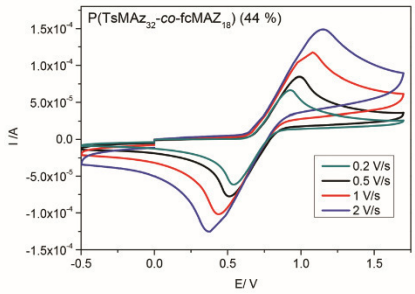

Fig. 7 Cyclic voltammograms of P(TsMAz$_{32}$-*co*-fcMAz$_{18}$) at different scan rates.

making them also interesting candidates for fc-containing performance materials.

Electrochemical behavior

The redox-profiles of all fc-containing PAz were analyzed by cyclic voltammetry (CV) in dichloromethane with tetrabutylammonium hexafluorophosphate as the conducting salt. All polymers exhibit the reversible oxidation of fc, regardless of their microstructure. Fig. 7 exemplarily shows the CV curves at different scan rates of P(TsMAz$_{32}$-*co*-fcMAz$_{18}$) proving the ideal reversibility of the redox profile.

Conclusions

This work presents the synthesis and polymerization of the first *N*-sulfonyl-substituted ferrocene-containing aziridine: *N*-ferrocenylsulfonyl-2-methylaziridine. The monomer is accessible in high yield from ferrocenyl sulfonyl chloride and *rac*-2-methyl aziridine as an orange powder. An insoluble organometallic polymer is prepared *via* the anionic polymerization, which was characterized by solid-state NMR and mass spectrometry, indicating the formation of the desired polysulfonamide. Copolymers with other aziridine monomers were prepared in order to produce soluble materials. For the statistical copolymerization of *N*-ferrocenylsulfonyl-2-methylaziridine with *N*-tosyl-2-methylaziridine real-time ^{1}H NMR kinetics proved the formation of gradient copolymers with the tosylaziridine being incorporated as the first segment. Thermal data reveal the high stability of the polymers (T_{on} *ca.* 350 °C) with a rather high T_g (120–140 °C) depending on the fc-ratio; electrochemical data reveal the reversible redox profile of fc.

These results broaden the scope of fc-containing monomers, which may be combined with other anionic polymerization techniques in the future to prepare redox-responsive materials.

Acknowledgements

The authors thank the Deutsche Forschungsgemeinschaft (DFG-WU 750/7-1) for funding.

References

1 R. D. A. Hudson, *J. Organomet. Chem.*, 2001, **637–639**, 47–69.
2 P. Nguyen, P. Gómez-Elipe and I. Manners, *Chem. Rev.*, 1999, **99**, 1515–1548.
3 J. E. Sheats, C. E. Carraher Jr. and C. U. Pittman, *Metal-containing polymeric systems*, Springer Science & Business Media, 2012.
4 M. G. Baldwin and K. E. Johnson, *J. Polym. Sci., Part A-1: Polym. Chem.*, 1967, **5**, 2091–2098.
5 A. D. Russell, R. A. Musgrave, L. K. Stoll, P. Choi, H. Qiu and I. Manners, *J. Organomet. Chem.*, 2015, **784**, 24–30.
6 A. Alkan, L. Thomi, T. Gleede and F. R. Wurm, *Polym. Chem.*, 2015, **6**, 3617–3624.
7 A. Alkan, C. Steinmetz, K. Landfester and F. R. Wurm, *ACS Appl. Mater. Interfaces*, 2015, 7, 26137–26144.
8 C. Tonhauser, A. Alkan, M. Schoemer, C. Dingels, S. Ritz, V. Mailaender, H. Frey and F. R. Wurm, *Macromolecules*, 2013, **46**, 647–655.
9 E. Rieger, A. Alkan, A. Manhart, M. Wagner and F. R. Wurm, *Macromol. Rapid Commun.*, 2016, **37**, 833–839.
10 A. Padwa and S. S. Murphree, *ARKIVOC*, 2006, **3**, 6–33.
11 M. Jäger, S. Schubert, S. Ochrimenko, D. Fischer and U. S. Schubert, *Chem. Soc. Rev.*, 2012, **41**, 4755–4767.
12 B. D. Monnery and R. Hoogenboom, *Cationic Polym. Regener. Med.*, 2014, 30–61.
13 Ö. Doğan, S. Zeytinci and A. Bulut, *Synth. Commun.*, 2005, **35**, 1067–1076.
14 B. F. Bonini, M. Fochi, M. Comes-Franchini, A. Ricci, L. Thijs and B. Zwanenburg, *Tetrahedron: Asymmetry*, 2003, **14**, 3321–3327.
15 M.-C. Wang, D.-K. Wang, Y. Zhu, L.-T. Liu and Y.-F. Guo, *Tetrahedron: Asymmetry*, 2004, **15**, 1289–1294.
16 M.-C. Wang, L.-T. Liu, J.-S. Zhang, Y.-Y. Shi and D.-K. Wang, *Tetrahedron: Asymmetry*, 2004, **15**, 3853–3859.
17 J. B. Sweeney, *Chem. Soc. Rev.*, 2002, **31**, 247–258.
18 I. C. Stewart, C. C. Lee, R. G. Bergman and F. D. Toste, *J. Am. Chem. Soc.*, 2005, **127**, 17616–17617.
19 S. A. Merchant, D. T. Glatzhofer and D. W. Schmidtke, *Langmuir*, 2007, **23**, 11295–11302.
20 M. T. Meredith, D.-Y. Kao, D. Hickey, D. W. Schmidtke and D. T. Glatzhofer, *J. Electrochem. Soc.*, 2011, **158**, B166–B174.
21 S. A. Merchant, T. O. Tran, M. T. Meredith, T. C. Cline, D. T. Glatzhofer and D. W. Schmidtke, *Langmuir*, 2009, **25**, 7736–7742.
22 M. Herberhold, O. Nuyken and T. P. Öhlmann, *J. Organomet. Chem.*, 1995, **501**, 13–22.
23 M. Jonek, A. Makhloufi, P. Rech, W. Frank and C. Ganter, *J. Organomet. Chem.*, 2014, **750**, 140–149.
24 L. Thomi and F. R. Wurm, *Macromol. Symp.*, 2015, **349**, 51–56.
25 L. Thomi and F. R. Wurm, *Macromol. Rapid Commun.*, 2014, **35**, 585–589.
26 E. Rieger, A. Manhart and F. R. Wurm, *ACS Macro Lett.*, 2016, **5**, 195–198.

Electronic Supplementary Material (ESI) for Polymer Chemistry.

Supporting Information for

N-Ferrocenylsulfonyl-2-methylaziridine: The First Ferrocene Monomer for the Anionic (Co)Polymerization of Aziridines

*Tatjana Homann-Müller, Elisabeth Rieger, Arda Alkan, Frederik R. Wurm**

Max-Planck-Institut für Polymerforschung, Ackermannweg 10, 55128 Mainz, Germany,

wurm@mpip-mainz.mpg.de

Additional protocols and analysis data:

Materials/ Methods

Instrumentation. ^{1}H NMR spectra (300, 400, 500 and 700 MHz) and ^{13}C NMR spectra (75.5 MHz) were recorded using a Bruker AC300, a Bruker AMX400, Bruker Avance 500 and Bruker Avance III. All spectra were referenced internally to residual proton signals of the deuterated solvent. For SEC measurements in DMF (containing 0.25 g·L^{-1} of lithium bromide as an additive) an Agilent 1100 Series was used as an integrated instrument, including a PSS HEMA column (106/105/104 g·mol^{-1}), a UV detector (275 nm), and a RI detector at a flow rate of 1 mL·min^{-1} at 50 °C. Calibration was carried out using PEO standards provided by Polymer Standards Service. DSC measurements were performed using a PerkinElmer 7 series thermal analysis system and a PerkinElmer thermal analysis controller TAC 7/DX. Heating rates of 10 K·min^{-1} were employed under nitrogen. Matrix-assisted laser desorption/ionization time-of-flight (MALDI-ToF) measurements were performed using a Shimadzu Axima CFR MALDI-TOF mass spectrometer, employing dithranol (1,8-dihydroxy-9(10*H*)-anthracenone) as a matrix.

Cyclic voltammetry (CV) was carried out in a conventional three electrode cell using a μ-Autolab Type III potentiostat (Metrohm AG) and dichloromethane as a solvent under argon. The supporting electrolyte was tetrabutylammonium hexafluorophosphate ([0.1 M]). All experiments were performed at 25 °C. A glassy carbon disc served as working electrode and a glassy carbon rod as counter electrode. As reference an Ag/AgCl electrode (silver wire in saturated LiCl/ethanol solution) was employed.

Reagents. Solvents and reagents were purchased from Acros Organics, TCI, Sigma-Aldrich or Fluka and used as received, unless otherwise stated. Deuterated solvents were purchased from Deutero GmbH. TsMAz and MsMAz were synthesized according to the published procedures and dried by azeotropic distillation of benzene to remove traces of water.[1] 2-Methylaziridine was distilled from CaH_2 prior its use.

Polymerization

All glassware was flame-dried prior to the polymerization in vacuo. The monomers were dissolved in ca. 1 mL benzene and dried for ca. 4h *in vacuo* to remove traces of water by azeotropic distillation. The monomers were then dissolved in DMF, DMSO or THF (compare main text, final concentration ca. 10 wt%). If KHMDS was used as initiator, it was used as a DMSO solution and added to the monomer solution at 55°C. BuLi was used as received. If BnNHMs was used as the initiator, the sulfonamide anion was generated in a separate flask by deprotonation with KHMDS and then a calculated amount of this initiator stock solution was added to the monomer solution at 55°C and the reaction was stirred until completion (typically 15h). After the polymerization has reached completion, the living anion was terminated by the addition of methanol and precipitated into a ten-fold excess of methanol. The polymers were recovered by filtration or centrifugation in typically quantitative yield.

Homopolymerisation, example: PFcMAz33: 100 mg (0.327 mmol) fcMAz, 3 mg (0.016 mmol) BnNHMs and 2,6 mg (0,013 mmol; 0,8 eq.) KHMDS were used. Solvent DMF ca. 1 mL.

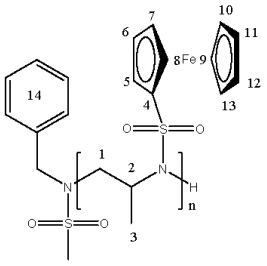

^{1}H MAS NMR (700 MHz): δ [ppm] = 8-7 (br, 5H, 14), 7-2 (br, 5-8, 9-13), 4-2 (br, 1, 2), 2-0 (br, 3). ^{13}C CP MAS NMR (700 MHz): δ [ppm] = 130 (14), 90 (4), 75-65 (br, 5-8, 9-13), 60-45 (br, 1, 2), 20-10 (br, 3). Additional polymers have been synthesized, the data is collected in Table 1. IR: $\tilde{\nu}$: 3444 (b), 3104 (m), 2980 (m), 2930 (w), 1643 (m), 1387 (w), 1325 (ss), 1189 (s), 1134 (ss), 1071 (s), 1021 (s), 825 (s), 707 (s), 613 (s) cm^{-1}.

Copolymers. Copolymerization was conducted analogous to the procedure for homopolymers. For block copolymers, first the polymerization of MsMAz or TsMAz was initiated. To the living polymers, then the calculated amount of fcMAz was added after 2 h and stirring was continued overnight.

P(MsMAz)$_{28}$-b-P(fcMAz)$_{2}$. 19 mg (0.062 mmol) fcMAz, 70 mg (0.518 mmol) MsMAz, 3.4 mg (0.018 mmol) BnNHMs and 2.7 mg (0,014 mmol) KHMDS were used. Solvent DMSO ca 1 mL.

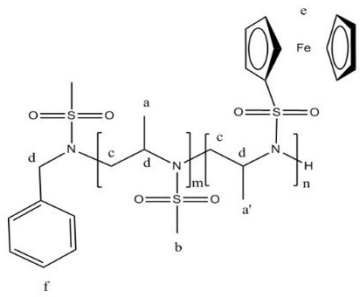

^{1}H NMR (300 MHz, $CDCl_3$): δ [ppm] = 7,41 (m, 5H, f), 5,21- 4,28 (br, 16H, e), 4,30-3,71 (br, 26H, d), 3,72-3,14 (br, 52H, c), 3,15-2,54 (br, 92H, b), 1,55-0,69 (br, 85H, a), 0,98-0,78 (br, 7H, a‘).

$P(TsMAz)_{22}$-b-$P(FcMAz)_5$. 25 mg (0.082 mmol) FcMAz, 70 mg (0.332 mmol) TsMAz und 2.5 mg (0.013 mmol) KHMDS were used. Solvent DMSO ca 2 mL.

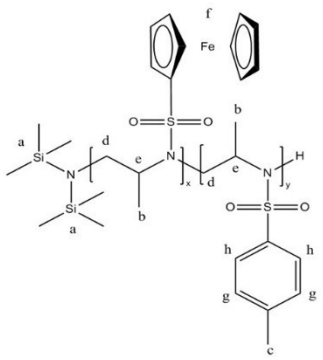

^{1}H NMR (300 MHz, $CDCl_3$): δ [ppm] = 8,31-7,62 (br, h), 7,60-7,16 (br, g), 5,25-4,22 (br, f), 4,22-3,86 (br, e), 3,81-2,79 (br, d), 2,74-2,10 (br, c), 1,42-0,75 (br, b), 0,09 (s, a).

^{1}H NMR Kinetics. The monomers and initiator was prepared as described above. In an Argon-filled glovebox the monomers were dissolved in 0.7 mL dry deuterated DMF and added to an NMR tube, which was sealed with a rubber septum. From this solution a 1H NMR spectrum was measured; then the initiator was added (0.1 mL in deuterated DMF, a respective stock

solution was prepared earlier) and the polymerization was monitored over a period of 15h, continuously taking spectra with each 32 scans (404 s).

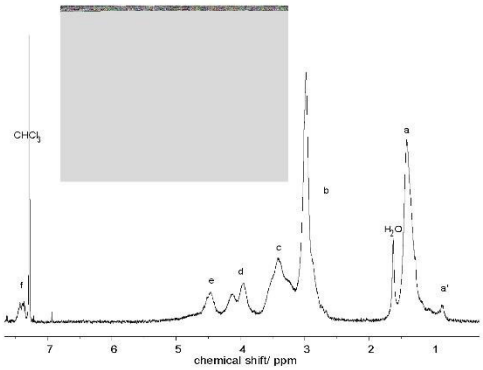

Figure S1: ^{1}H NMR spectrum of P(MsMAz)$_{28}$-*b*-P(FcMAz)$_{4}$ in $CDCl_3$,300 MHz, 298 K.

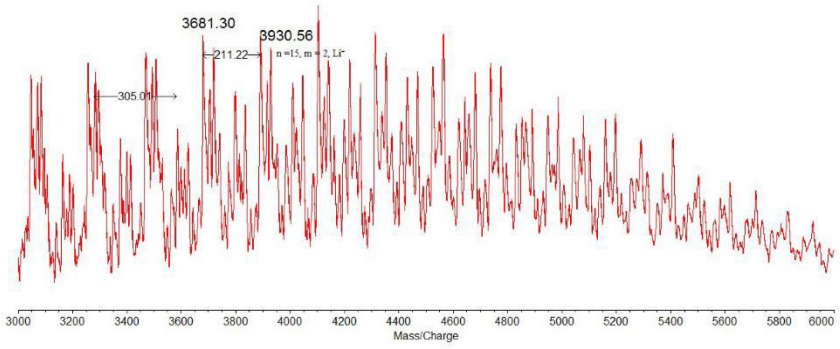

Figures S2: Zoom into the MALDI ToF mass spectrum of P(TsMAz)$_{22}$-*b*-P(fcMAz)$_{5}$.

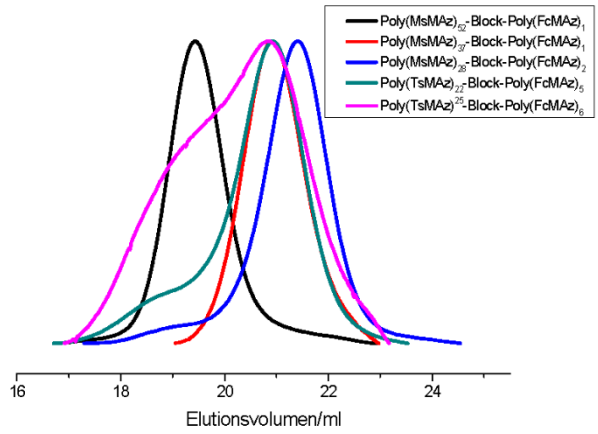

Figure S3: GPC elugrams of block copolymers (DMF, RI detection).

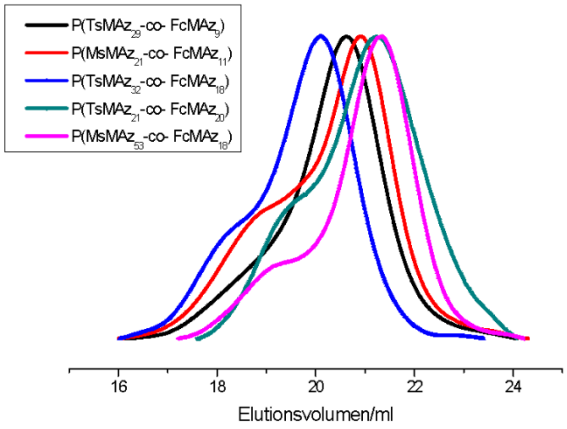

Figure S4: GPC elugrams of statistical copolymers (DMF, RI detection).

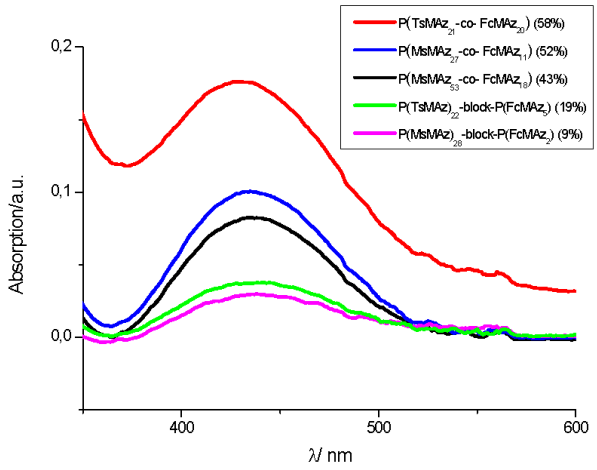

Figure S5: UV/Vis absorption spectra of the fcMAz copolymers with variable fcMAz content in THF.

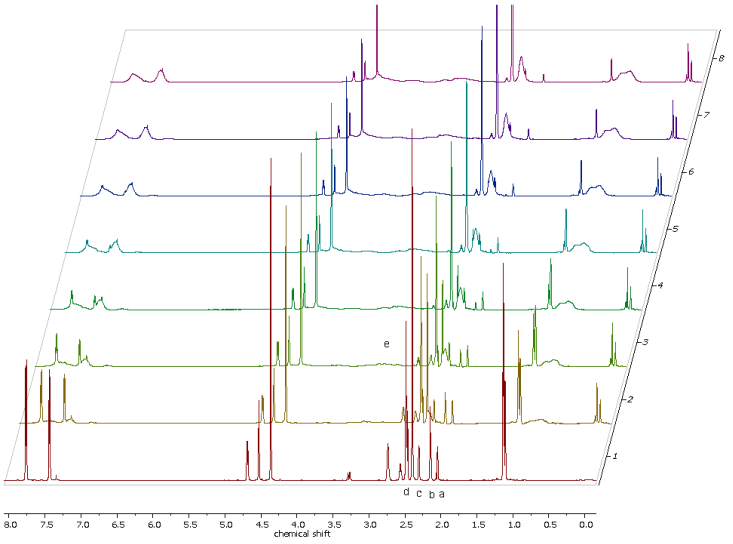

Figure S6 Real-time ^{1}H NMR kinetics of the copolymerization (700 MHz, 303 K) of P(TsMAz$_{30}$-*co*- fcMAz$_{12}$)); time distance between the sprectra 40 min.

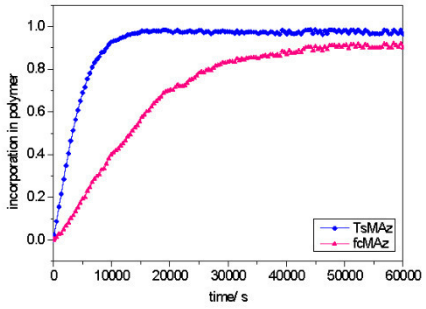

Figure S7: From ^{1}H NMR kinetics: assembly of each monomer in the growing polymer chain *vs.* the reaction time.

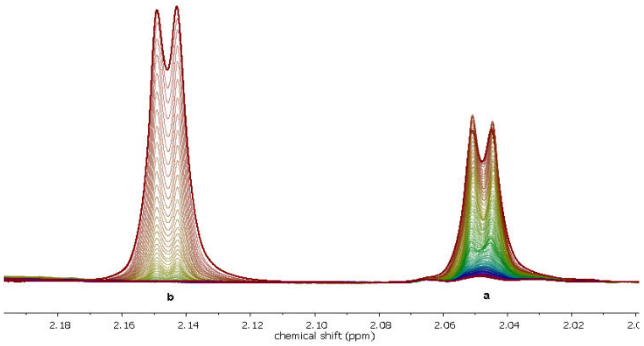

Figure S8: Integrals over the copolymerization of TsMAz (a) and fcMAz (b).

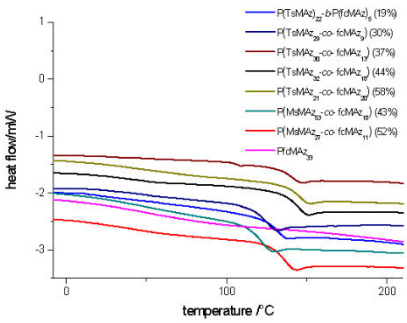

Figure S9: DSC heating curves (2nd heating, 10K/ min) of fcMAz-containing copolymers.

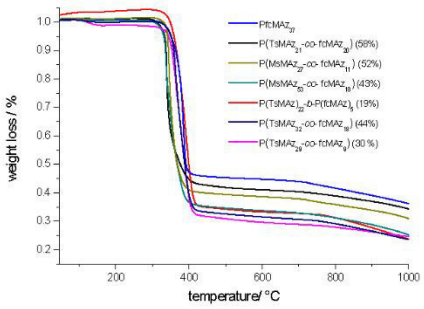

Figure S10: TGA analysis of fcMAz-containing copolymers.

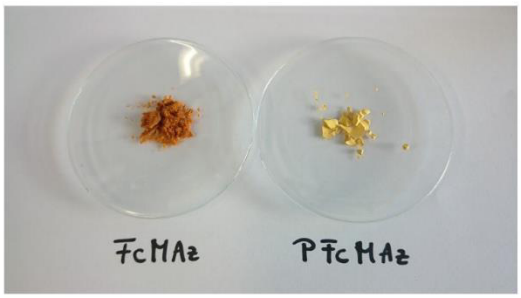

Figure S11: Photograph of **1** and **poly(1).**

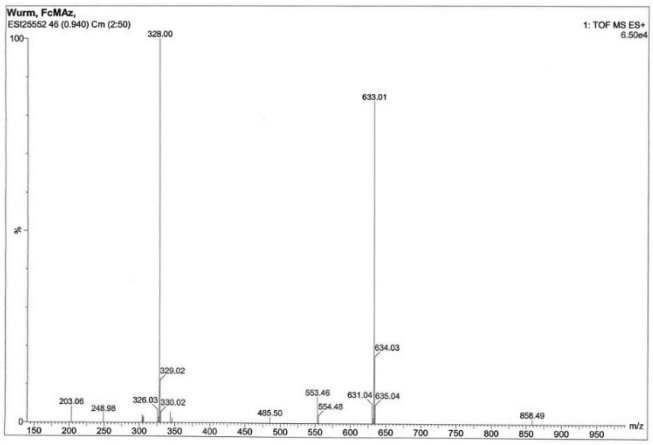

Figure S12: ESI-MS of **1**.

References

1. E. Rieger, A. Alkan, A. Manhart, M. Wagner and F. R. Wurm, *Macromol. Rapid Commun.*, 2016, 37, 833-839.

A.1.2 The first orthogonal aziridine monomer

Full Paper

Macromolecular Journals

Macromolecular Chemistry and Physics

4-Styrenesulfonyl-(2-methyl)aziridine: The First Bivalent Aziridine-Monomer for Anionic and Radical Polymerization

Tassilo Gleede, Elisabeth Rieger, Tatjana Homann-Müller, Frederik R. Wurm*

4-Styrenesulfonyl-(2-methyl)aziridine (StMAz), the first orthogonal aziridine monomer, for both anionic ring-opening and radical polymerization is presented. Both polymerization pathways are accessible without using protective groups. Aza-anionic ring-opening polymerization (A-AROP) of StMAz and other methyl-aziridine derivatives provide multifunctional polyaziridines. Molecular weights between 3000 and 13 000 g mol^{-1} are obtained with low molecular weight dispersities (Đ = 1.1). The amount of vinyl groups in linear polyaziridines from A-AROP depends on the monomer/comonomer ratio. The vinyl groups of P(StMAz)- homo- or copolymers are entirely convertible by thiol-ene addition. This allows modification with multiple functional groups. Free radical polymerization of StMAz leads to polyalkylenes with aziridine side groups, which are known to be efficiently addressable via nucleophiles. Polysulfonamides still belong to a rather new class of polymers accessible by anionic polymerization. Enlarging the scope of postpolymerization modifications on polyaziridines/-sulfonamides is important for further macromolecular architectures. The aziridine and the vinyl group are combined to develop the first orthogonal monomer for aza-anionic polymerization and radical polymerization.

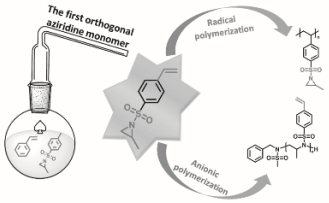

1. Introduction

Nitrogen-containing polymers (N-polymers) are often favored for drug delivery issues regarding cell targeting, like gene delivery studies show.[1,2] Additionally, they are applied in water refinery[3,4] and can serve as direct catalysts by stabilizing transition metals.[5] To fulfill the goals of current scientific challenges, functionalizable groups at N-polymers are essential for fine adjustment of polymer properties. Radical polymerization of vinyl monomers allows fast access to a variety of highly functional polymer materials based on various monomers. On the other side, living ionic polymerization allows the highest control over molecular weights and distributions.[6,7] Ionic polymerizations of epoxides or aziridines can be used to prepare polyethers and polyamines, but most functional groups need to be protected. An outstanding class of monomers, the so-called "bivalent or orthogonal monomers," is polymerized chemoselectively by different mechanisms while maintaining the other group. To date, only few of such monomers have been reported.[8–10]

Aziridinyl ethyl methacrylate (AEMA), for example, can be selectively polymerized by radical or carbanionic polymerization of the acrylate and by cationic polymerization of the aziridine ring, functional polyamines are obtained. AEMA represents to the best of our knowledge the first orthogonal aziridine-containing monomer.[8] However, anionic polymerization of the aziridine cannot

T. Gleede, E. Rieger, T. Homann-Müller, F. R. Wurm
Max-Planck-Institut für Polymerforschung (MPIP)
Ackermannweg 10, 55128 Mainz, Germany
E-mail: wurm@mpip-mainz.mpg.de
The ORCID identification number(s) for the author(s) of this article can be found under https://doi.org/10.1002/macp.201700145.

Macromol. Chem. Phys. **2017**, DOI: 10.1002/macp.201700145

be conducted on such structure as the aziridine ring is not activated. The well-known glycidyl methacrylate is similar to AEMA polymerizable via radical and an ionic mechanism.[9] Vinyl ferrocenyl glycidyl ether represents a monomer which, besides radical polymerization, is suitable for anionic ring-opening polymerization (AROP). The nature of the ferrocene-functionality in the polymer is advantageous for applications where redox response is required.[11,12] Bivalent monomers are applied in industry as additives in several polyacrylates example wise for pigment coating;[13,14] additionally, they are of interest for scientific aspects; with an orthogonal polymerizable or addressable group, those materials can be used for the preparation of graft-polymers, cross-linked gels, or surface modifications.[10,15–17] However, only few bifunctional chemoselective monomers have been reported.

Herein, we report the first bivalent monomer for the aza-anionic ring-opening, carrying an activated aziridine, combined with vinyl functionality for radical polymerization. 4-Styrenesulfonyl-(2-methyl)aziridine (StMAz) is polymerized by two different protocols, free radical and aza-anionic ring-opening polymerization. ^{1}H NMR proved that both protocols allowed a selective reaction with one functional group and maintained the other for post-modifications. Additional to the earlier reported robust way to obtain multihydroxy polyamines from acetals, as protected monomers,[18] we demonstrated, that various functional groups can be added to obtain multihydroxy or carboxy polyamines via an thiol-ene postmodification. The use of different thiols makes the polysulfonamides a platform for various modifications.[19,20]

StMAz showed similar reactivity to previously reported aziridine monomers,[21,22] which allowed us to prepare copolymers with nonfunctional aziridines to further adjust the degree of functionalization. In addition, the free radical polymerization of StMAz leaves the aziridine-group untouched as a potential receptive for nucleophiles. Thermal analyses of the (co)polymers by differential scanning calorimetry (DSC) and thermogravimetric analyses (TGA) proved a remarkably high char yield of ≈50% for both, polyalkylene- and polyethylamine-(StMAz), which indicated a heat induced cross-linking. We believe that StMAz further enriches the toolbox of aziridine monomers, which can be used for the preparation of functional and well-defined architectures by living anionic polymerization.

2. Experimental Section

2.1. Materials

Solvents and reagents were purchased from Acros Organics, TCI, Sigma-Aldrich, or Fluka and used as received, unless otherwise stated. Deuterated solvents were purchased from Deutero GmbH. *N*-benzyl methanesulfonamide (BnNHMs), 2-methyl-*N*-tosylaziridine (TsMAz), and 2-methyl-*N*-mesylaziridine (MsMAz) were synthesized according to already published procedures and dried by azeotropic distillation from benzene to remove traces of water.[23] 2-Methylaziridine was distilled from CaH_2 prior use.

2.2. Methods

2.2.1. Analyses

^{1}H NMR and ^{13}C NMR spectra were recorded using, a Bruker Avance 300, a Bruker Avance III 500, a Bruker Avance III 700. All spectra were referenced internally to residual proton signals of the deuterated solvent.

For SEC measurements in dimethylformamide (DMF) (containing 0.25 g L^{-1} of lithium bromide as an additive), an Agilent 1100 Series was used as an integrated instrument, including a PSS HEMA column (106/105/104 g mol^{-1}), a UV detector (275 nm), and a RI detector at a flow rate of 1 mL min^{-1} at 50 °C. Calibration was carried out using PEO standards provided by Polymer Standards Service.

Matrix-assisted laser desorption/ionization time-of-flight (MALDI-ToF) measurements were performed using a Shimadzu Axima CFR MALDI-TOF mass spectrometer, employing dithranol (1,8-dihydroxy-9(10H)-anthracenone) as a matrix.

Thermogravimetric analysis was performed with the Mettler Toledo ThermoSTAR TGA /SDTA 851-Thermowaage in the temperature range from 25 to 1000 °C with a heating rate of 10 °C min^{-1}.

Differential scanning calorimetry measurements were performed using a Mettler Toledo DSC 823 calorimeter. Three scanning cycles of heating–cooling were performed in the temperature range from −140 to 250 °C. Heating rates of 10 °C min^{-1} were employed under nitrogen (30 mL min^{-1}).

For infrared spectroscopy, the polymers were pressed with KBr to form a pellet and the absorption between 4000 and 400 cm^{-1} was recorded in a Spectrum BX spectrometer from PerkinElmer.

2.2.2. Polymerizations

All glassware was flame-dried at reduced pressure prior use. The monomers were dissolved in ≈1 mL benzene and dried for ≈4 h at reduced pressure to remove traces of water by azeotrope distillation. The monomers were then dissolved in DMF (final concentration 10 wt%). With BnNHMs used as initiator, the sulfonamide anion was generated in a separate flask by deprotonation with potassium bis(trimethylsilyl) amide (KHMDS) in DMF, a calculated amount of this initiator stock solution was added to the monomer solution at 50 °C and the reaction was stirred until completion (typically 15 h). After the polymerization has reached completion, the living anion was terminated by the addition of methanol and precipitated into a tenfold excess of methanol. The polymers were recovered by centrifugation in typically quantitative yield.

Macromol. Chem. Phys. **2017**, DOI: 10.1002/macp.201700145

2.3. Synthesis

2.3.1. Synthesis of StMAz

The 4-vinylbenzene-1-sulfonyl chloride was synthesized according to literature procedure.[24] The product was used without further purification. The 4-vinylbenzene-1-sulfonyl chloride was converted to StMAz with following procedure. *Rac*-2-methylaziridine (2.0 g, 35 mmol) and 6.6 mL (48 mmol) *N,N*-diisopropylethylamine were dissolved in 25 mL dry toluene and cooled to −30 °C. 4-vinylbenzene-1-sulfonyl chloride (6.5 g, 32 mmol) was dissolved in 10 mL dry toluene and added dropwise over a period of 20 min to the reaction. The mixture was stirred for additional 90 min at −30 °C and allowed to warm up to room temperature and stirred overnight. 20 mL saturated sodium hydrogen carbonate solution was added and stirred for 60 min. The aqueous phase was removed and the organic layer was washed again with brine, dried over magnesium sulfate, and evaporated to dryness. 7.1 g (quantitative yield) of off-white oil was obtained. The monomer structure was further confirmed by NMR (Figures SI 1–SI 3, Supporting Information) and MALDI-ToF mass analysis (325.21 g mol^{-1} ($StMAz^*H\text{-}NEt_3^+$), 224.06 g mol^{-1} $StMAz^*H^+$). To inhibit spontaneous polymerization, 2,6-di-*tert*-butyl-4-methylphenol (BHT) could be added. The compound was stored at −20 °C. If necessary, the compound could be purified with column chromatography on silica gel (PE/EA 5:1, R_f = 0.4). For radical and anionic polymerization, the compound was used without further purification.

2.3.2. Synthesis of P(StMAz) via AROP

Example procedure: 100 mg (0.444 mmol, 10 eq) of StMAz and 300 mg (2.2 mmol, 50 eq) of MsMAz were placed in a Schlenk flask and dissolved in 2 mL benzene. The monomers were dried by azeotrope freeze drying in vacuum (≈4 h). In a separated Schlenk flask, the initiator was generated. 8.2 mg (0.044 mmol, 1 eq) BnNHMs was dried by azeotrope freeze drying in vacuum with benzene. 8.8 mg KHMDS (0.044 mmol, 1 eq) dissolved in 3 mL dry DMF was added to BnNHMs. This solution was then added to the monomer mixture. The reaction was performed at 50 °C overnight under argon atmosphere. The polymerization was terminated by addition of acidic methanol. Until termination, standard Schlenk conditions were applied. For purification, the polymer was precipitated in large amount of methanol (see Figures SI 9 and SI 13 in the Supporting Information for analytical data).

2.3.3. Modification via Thiol-ene Reaction

General procedure: 52 mg of the polymer P6 (0,073 mmol, 1 eq regarding the vinyl groups) and 9 mg (0,055 mmol, 0.75 eq) azobis(isobutyronitrile) (AIBN) were placed in a 10 mL Schlenk flask. Then, 114 mg mercaptoethanol (1.5 mmol, 20 eq) was added with 1 mL of DMF. After two freeze–pump–thaw cycles, the mixture was stirred at 75 °C under argon overnight. For purification, the polymer was precipitated in diethylether (Et_2O), dissolved in dichloromethane (DCM), and precipitated again in Et_2O. Drying in vacuum gave pure product (see Figures SI 7–SI 17 in the Supporting Information for analytical data).

2.3.4. Synthesis of Polyalkylene:StMAz via Free Radical Polymerization

StMAz (150 mg, 0.671 mmol) was placed in UV-quartz glass cuvette equipped with a stirring bar. 2,2-Dimethoxy-2-phenylacetophenone (5.75 mg, 22,4 µmol) was dissolved in 2 mL of degassed benzene and transferred into the quartz glass cuvette. The polymerization was performed by irradiation with 6 W UV254 nm light for 5 h. Temperatures did not exceed room temperature during polymerization. Copolymerization with styrene was conducted analogous to the procedure for homopolymers. For purification, the polymer was precipitated in methanol (see Figures SI 4 and SI 18 in the Supporting Information for analytical data).

3. Results and Discussion

3.1. Monomer Synthesis

The activated aziridine monomers have two potential positions, which can be used in order to adjust the polymer properties. First, the variation of the alkyl chain at the 2-position of the aziridine ring allows to attach functional or solubilizing groups. We demonstrated that steric groups such as C-10 chains or bulky phenyl groups do not hamper the polymerization.[22,25] In addition, the electron withdrawing group, which is attached to the aziridine ring by a cleavable sulfonamide, can be used as a handle to control chemical function.[18,26] The electron withdrawing behavior activates the aziridine and thereby influences the polymerization kinetics.[22] StMAz is estimated to have a similar electron withdrawing behavior as the TsMAz. Thereby, the distribution of the reactive vinyl group in polysulfonamides can be adjusted. Polysulfonamides with vinyl groups at the termini, in the middle, or randomly distributed can be obtained by this method.

The synthesis of StMAz starts from commercially available sodium 4-vinylbenzenesulfonate (Scheme 1A). StMAz was produced in a two-step synthesis; the monomer was obtained with an overall yield of 80%. In the first step, 4-styrene sulfonic acid is converted with thionyl chloride to the corresponding sulfonyl chloride. In a second step, the sulfonyl chloride was converted to StMAz by amidation with 2-methylaziridine under basic conditions in dry DCM. Beneficially, StMAz was pure enough for the anionic polymerization after extraction from the reaction mixture (note: to avoid unwanted radical polymerization, BHT can be added as a stabilizer to the monomer).

3.2. Polymerization Kinetics

The anionic copolymerization of StMAz with TsMAz was monitored by real-time ^1H NMR spectroscopy. Figure 1 shows the individual monomer conversion versus total conversion of monomers; Figure SI 21 (Supporting

Macromol. Chem. Phys. **2017**, DOI: 10.1002/macp.201700145

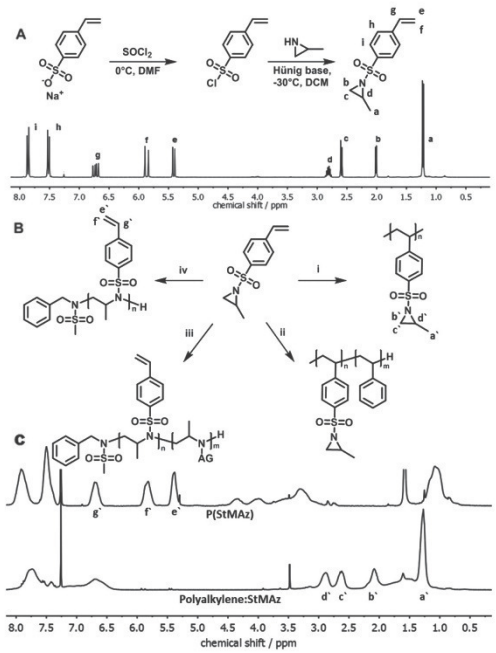

Scheme 1. A) Synthesis route to 4-styrenesulfonyl-(2-methyl) aziridine (StMAz). B) Polymerization of StMAz: (i) free radical polymerization with 2,2-dimethoxy-2-phenylacetophenone in benzene (P7, P9), (ii) free radical copolymerization with styrene, 2,2-dimethoxy-2-phenylacetophenone in benzene (P8), (iii) anionic copolymerization of StMAz with sulfonamide-activated aziridines (P3, P4, P5, P6, P10), (iv) homopolymerization of StMAz with KHMDS, BnNHMs in DMF at 50 °C (P1, P2). C) The ^{1}H NMR spectra of the different homo(StMAz) polymers. P(StMAz) (P1, anionic polymerization), polyalkylene:StMAz (P7, free radical polymerization).

Information) shows the assembly of the monomers in the polymer over time. For the real-time polymerization kinetics, the reaction should proceed in a suitable timescale, usually from minutes to hours. The observed component has to have distinguishable resonances in the ^{1}H NMR spectrum which are consumed during the reaction. The resonances of 1.65–1.62 and 1.61–1.59 ppm (see Figure SI 22 in the Supporting Information) belong to the aziridine ring of the StMAz and TsMAz. A zoom-in to the relevant signals of the monomer is showing the consumption of the monomers. Due to a sufficient chemical shift of the different resonances, the ring protons are predestined to monitor the anionic polymerization. Due to a more pronounced negative mesomeric effect, the electron withdrawing behavior of StMAz is stronger compared to TsMAz. Therefore, we see in Figure 1 a slightly faster monomer consumption of StMAz. Nevertheless, this difference

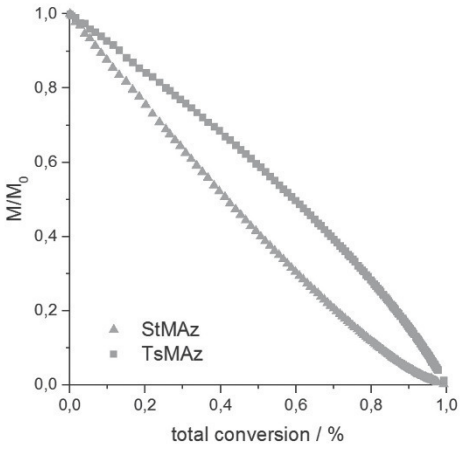

Figure 1. Normalized monomer concentration versus total conversion of the aza-anionic copolymerization of StMAz and TsMAz with BnNKMs as initiator in DMF-d_7 at 50 °C (P10-kinetic).

compared to monomers of previous studies is comparatively weak compared to other activating groups.[22] Concluding the polymerization behavior of StMAz with other monomers is similar to TsMAz.

3.3. Polymerization of StMAz

Aziridines as such were used due to their affinity to nucleophilic ring opening as side groups in polyacrylates and others. For instance, nucleophiles like alcohols can react efficiently.[27] This is known to be a novel method for postmodification of polymers, as it was demonstrated on polyacrylates. Cross-linking and postmodification can be performed. The ring opening reaction of aziridines by nucleophiles was also discussed as a conjugate reaction for clickable polymers.[28,29] As comparison, ring-opening reaction of epoxide groups attached at polymers is known to be problematic due to its high reactivity. Mild conditions have to be found to maintain the epoxide and to functionalize the polymer selectively.[30] Additionally, moisture induced ring-opening makes storage of epoxides difficult.[31] Earlier, Kobayashi and co-workers successfully polymerized a bifunctional monomer (AEMA) consisting of a methacrylate linked to an aziridine by different techniques while leaving the other group intact. They successfully polymerized the MMA-group via free radical and anionic polymerization and the aziridine via cationic polymerization.[8,32] The cationic ring-opening leads to 80% polymer yield and observed molecular weight distributions of $Đ = 2.2$. Nevertheless, the anionic polymerization of the aziridine functionality of AEMA was not possible.

Macromol. Chem. Phys. **2017**, DOI: 10.1002/macp.201700145

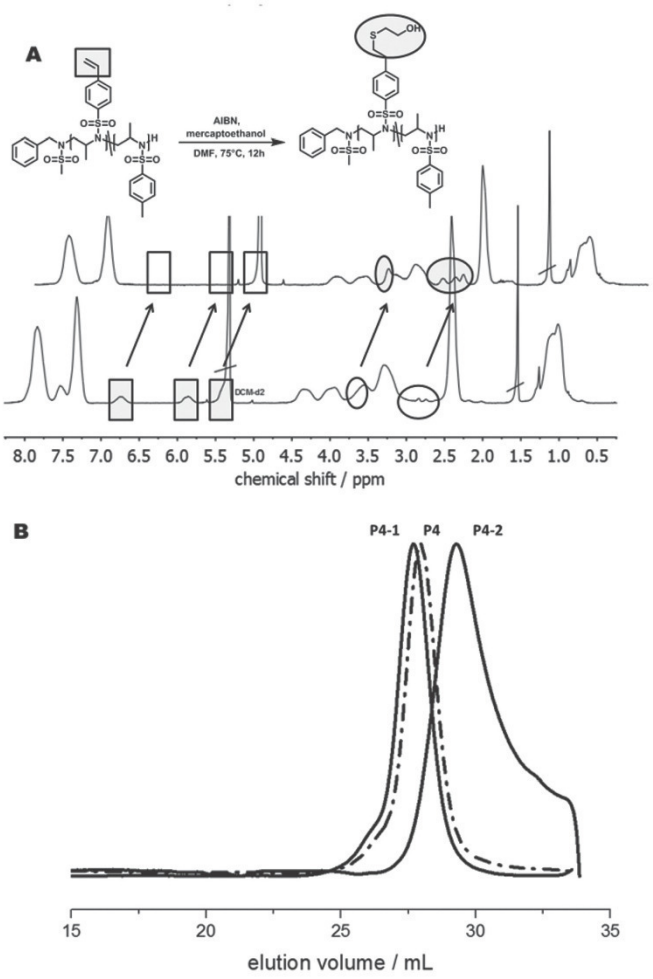

Figure 2. A) 'H NMR of P(TsMAz$_{50}$-*co*-StMAz$_{10}$) before and after thiol-ene addition of mercaptoethanol. Circles highlight the signals of the thioether group. Squares highlight the disappearing vinyl signals. B) SEC traces of P(TsMAz$_{50}$-*co*-StMAz$_{10}$) (P4) and the modified polymer with hydroxyl (P4-1) and carboxy groups (P4-2).

StMAz was successfully polymerized via AROP as homo- and copolymers with TsMAz (P3, P4) and MsMAz (P5, P6) as the respective comonomers. The SEC elugrams confirmed monomodal size and narrow distributions with $M_w/M_n \approx 1.1$ for the copolymers and $M_w/M_n \approx 1.2$ for the homopolymers (Figure 2B and Figure SI 15 (Supporting Information)). Full monomer conversion was confirmed via ^{1}H NMR (Figure 2A). MALDI-ToF mass spectrometry proves the formation of the envisioned StMAz (Figure SI 5, Supporting Information). The main distribution can be calculated to contain the mass of the initiator and the monomer mass with a distance of 223 g mol^{-1} (marked with arrows), the molar mass of StMAz. The incorporation of comonomers (MsMAz) was also confirmed by MALDI-ToF MS (Figure SI 6, Supporting Information): a linear combination of the monomer masses of both repeating units can be detected in the spectrum.

3.4. Thiol-ene-Postpolymerization Modification

The remaining vinyl groups of all synthesized polyaziridines were proven to be intact after polymerization via ^{1}H NMR and postmodification. In an additional step, complete conversion to functionalized thioether was performed with radical thiol-ene addition. To avoid cross-linking of the polymers during the thiol-ene reaction, a 20 equivalent access of thiols regarding one equivalent of vinyl groups was used. As the modified polymers were soluble in DMF and as the molecular weight distributions of the modified polymers are unchanged after modification, cross-linking was not observed. The ^{1}H NMR spectrum of P4 shows the highlighted signals of the vinyl protons in squares (Figure 2). After modification with mercaptoethanol (P4-1) (Figure 2A) or mercaptopropionic acid (P4-2) (Figure SI 10, Supporting Information), those signals vanish and new signals, marked with circles, can be assigned to the thioether groups. Full conversion of the vinyl groups was confirmed for the mesyl analogous copolymer (P6) (see ^{1}H NMR spectra in Figures SI 7 and SI 11 in the Supporting Information). The SEC elugrams of P4 and the modified P4-1 show both monomodal and narrow molecular weight distributions. After the modification with mercaptoethanol, the molecular weight distribution slightly shifts to lower elution times, indicating an increase of the molecular weight. In contrast, the same polymer, modified with mercaptopropionic acid, elutes later (P4-2) under the same chromatographic conditions. This late elution can be assigned to the interactions of the multiple carboxylic acid groups with the column material. This observation was also made for the modified

Macromol. Chem. Phys. **2017**, DOI: 10.1002/macp.201700145

P(MsMAz-*co*-StMAz) derivatives P6-1 and P6-2 (Figures SI 15 and SI 16, Supporting Information). In addition to previous work of our group,[18] this work shows an alternative way to obtain polyhydroxy sulfonamides. Modification of vinyl groups with thiol-ene chemistry has been proven to be a robust and flexible way to introduce various functional groups, such as carboxylic acids, hydroxyl, amines, and many more.[19,20]

3.5. Free Radical Polymerization

Free radical polymerization of StMAz was performed either by thermal or by UV-light induced initiation (AIBN in DMF (P9) or with 2,2-dimethoxy-2-phenylacetophenone and UV irradiation (P7, P8)). Under these conditions, polymers of 3700 and 8000 g mol^{-1} were prepared with molecular weight distributions of ≈1.7–2.4 (Figure SI 17 in the Supporting Information shows the SEC of polyalkylene:StMAz). The ^{1}H NMR spectra of the polyalkylene:StMAz show the characteristic resonances of the aziridine substituents (in Figure 1C: b′, c′, d′ at 2.90, 2.62, and 2.05 ppm), while the vinyl resonances disappeared after the polymerization. The molecular weights determined by SEC in Table 1 are known to be underestimated by the factor of 2 to 3 compared to the theoretical weights. This is due to the PEG standard which was used in our set-up.[18,32]

Table 1. Overview of polymers synthesized from StMAz.

#	Polymer[a)]	M_n[a)] [g mol^{-1}]	M_n[b)] [g mol^{-1}]	M_w/M_n[b)]
P1	$PStMAz_{30}$	6850	4300	1.27
P1-1	P1-mercaptoethanol	9200	7250	1.14
P1-2	P1-mercaptopropionic acid	10 000	n.a.	n.a.
P2	$PStMAz_{50}$	11 300	5000	1.19
P3	P($TsMAz_{50}$-*co*-$StMAz_5$)	8050	9000	1.09
P4	P($TsMAz_{50}$-*co*-$StMAz_{10}$)	9150	10 250	1.11
P4-1	P4-mercaptoethanol	9900	13 150	1.13
P4-2	P4-mercaptopropionic acid	10 200	5250	1.5
P5	P($MsMAz_{50}$-*co*-$StMAz_5$)	11 850	7050	1.16
P6	P($MsMAz_{50}$-*co*-$StMAz_{10}$)	12 950	7050	1.22
P6-1	P6-mercaptoethanol	12 600	10 800	1.15
P6-2	P6-mercaptopropionic acid	14 000	5000	1.64
P7	Polyalkylene:StMAz		3700	1.7
P8	Polyalkylene:StMAz-*co*-St		8000	2.4
P9	Polyalkylene:StMAz		3800	1.7
P10-kinetic	P($TsMAz_{50}$-*co*-$StMAz_{50}$)	21700	5000	1.09

[a)]Theoretical molecular weight; [b)]Molecular weight and molecular weight dispersity determined via SEC in DMF (vs PEO standards). Polymers P1–P6 were polymerized by AROP. Polymers P7–P9 were polymerized by free radical polymerization.

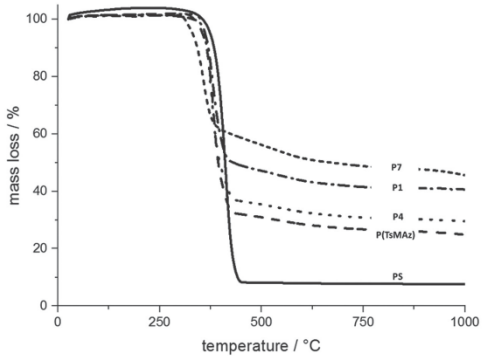

Figure 3. Thermogravimetric analyses, 10 °C min^{-1}, under nitrogen. 48% ash yield at 750 °C (P7), 41% ash yield at 750 °C (P1), 30% ash yield at 750 °C (P4), 26% ash yield at 750 °C (P(TsMAz)), 8% ash yield at 750 °C (polystyrene).

3.6. Thermal Characterization

The thermal properties of the polymers and copolymers have been analyzed by DSC and TGA. TGA of the different P(StMAz)s and copolymers were measured and compared to the homopolymers P(TsMAz) and polystyrene (Figure 3). Decomposition of the polymers, independent of the monomer composition starts at T_{on}(95%) = 340 °C and degradation proceeds in a single step due to degradation of the side groups and of the polymeric backbone. At temperatures above 420 °C, only slightly further degradation takes place and reaches a char yield at 700 °C. Notable is the char yield of the *homo*-P(StMAz) (TGA, P7 and P1) with 48 and 41 wt% remarkably higher compared to polystyrene and also compared to P(TsMAz). This can be explained by thermal cross-linking of the pendant functional groups and thus leads to thermally stable decomposition products, which might be of interest for future applications, e.g., as flame retardant additives.

Cross-linking of the polymers appears to be heat-induced. This was indicated via DSC. A precise T_g of P(StMAz) cannot be detected (Figure SI 18, Supporting Information). A structural difference was observed by infrared spectroscopy. Therefore, a small amount of P(StMAz) was heated to 250 °C under nitrogen atmosphere. A decrease in intensity of the corresponding bands of the double bond (=C–H stretch: ν = 3092, 3045;

Macromol. Chem. Phys. **2017**, DOI: 10.1002/macp.201700145

C=C stretch: ν = 1633; =C–H bend: ν = 920) in the IR-spectrum (see Figure SI 19 in the Supporting Information) was observed. Furthermore, the P(StMAz) is after heating insolubility in all tested solvents ($CDCl_3$, DMSO, DMF).

4. Conclusions

We developed a robust two-step synthesis for StMAz, the first orthogonal monomer for the aza-anionic ring-opening and free radical polymerization. Both polymerization mechanisms lead to highly functional polymers, either carrying reactive vinyl- or aziridine-groups. The living anionic ring-opening polymerization of StMAz leads to polymers with narrow molecular weight distributions and adjustable molecular weights. Also, copolymers with other aziridines were prepared, allowing to control the degree of functionality.

In the presence of thermal or photoinitiators, StMAz undergoes free radical polymerization to form homo- or copolymers, which carry aziridine side groups. They exhibit a cross-linking property during heating, indicated by TGA analysis and ^{1}H NMR. This and the successful copolymerization with other aziridine monomers confirm StMAz to be a novel, suitable member in the family of anionically polymerizing aziridines. The applicability of this monomer is topic of further studies.

Supporting Information

Supporting Information is available from the Wiley Online Library or from the author.

Acknowledgements: The authors thank the Deutsche Forschungsgemeinschaft (DFG WU 750 / 7-1) for funding. The authors thank Maximilian Lorenian (MPIP) for synthetic assistance.

Conflict of Interest: The authors declare no conflict of interest.

Received: March 19, 2017; Revised: April 19, 2017; Published online: ; DOI: 10.1002/macp.201700145

Keywords: anionic polymerization; aziridines; functional monomer; orthogonal monomer; polysulfonamides

[1] S. Taranejoo, J. Liu, P. Verma, K. Hourigan, *J. Appl. Polym. Sci.* **2015**, *132*, DOI: 10.1002/APP.42096.
[2] M. A. Mintzer, E. E. Simanek, *Chem. Rev.* **2009**, *109*, 259.
[3] S. Zhao, Z. Wang, *J. Membr. Sci.* **2017**, *524*, 214.
[4] Y. Uludag, H. Ö. Özbelge, L. Yilmaz, *J. Membr. Sci.* **1997**, *129*, 93.
[5] S. Ponnurangam, I. V. Chernyshova, P. Somasundaran, *Adv. Colloid Interface Sci.* **2016**, https://doi.org/10.1016/j.cis.2016.09.002.
[6] D. Baskaran, A. H. E. Müller, *Prog. Polym. Sci.* **2007**, *32*, 173.
[7] J. Herzberger, K. Niederer, H. Pohlit, J. Seiwert, M. Worm, F. R. Wurm, H. Frey, *Chem. Rev.* **2016**, *116*, 2170.
[8] T. Ishizone, T. Takata, M. Kobayashi, *J. Polym. Sci.* **2003**, *41*, 1335.
[9] D. Luo, P. Li, Y. Li, M. Yang, *J. Appl. Polym. Sci.* **2010**, *118*, 1527.
[10] A. Alkan, L. Thomi, T. Gleede, F. R. Wurm, *Polym. Chem.* **2015**, *6*, 3617.
[11] A. Alkan, F. R. Wurm, *Macromol. Rapid Commun.* **2016**, *37*, 1482.
[12] R. Pietschnig, *Chem. Soc. Rev.* **2016**, *45*, 5216.
[13] C. Kunszt, N. Loew, T. Farwick, B. Feldmann, Patent US 20160137876 A1, **2016**.
[14] N. Suemura, K. Yoshitake, T. Takeyama, Patent US 20160145110 A1, **2016**.
[15] S. A. Bencherif, N. V. Tsarevsky, K. Matyjaszewski, *Macromolecules* **2007**, *40*, 4439.
[16] J. Majer, P. Krajnc, *Macromol. Symp.* **2010**, *296*, 5.
[17] A. Bhattacharya, *Prog. Polym. Sci.* **2004**, *29*, 767.
[18] E. Rieger, A. Manhart, F. R. Wurm, *ACS Macro Lett.* **2016**, *5*, 195.
[19] A. B. Lowe, *Polym. Chem.* **2010**, *1*, 17.
[20] M. J. Kade, D. J. Burke, C. J. Hawker, *J. Polym. Sci., Part A: Polym. Chem.* **2010**, *48*, 743.
[21] T. Homann-Müller, E. Rieger, A. Alkan, F. R. Wurm, *Polym. Chem.* **2016**, *7*, 5501.
[22] E. Rieger, A. Alkan, A. Manhart, M. Wagner, F. R. Wurm, *Macromol. Rapid Commun.* **2016**, *37*, 833.
[23] I. C. Stewart, C. C. Lee, R. G. Bergman, F. D. Toste, *J. Am. Chem. Soc.* **2005**, *127*, 17616.
[24] J. C. Brendel, F. Liu, A. S. Lang, T. P. Russell, M. Thelakkat, *ACS Nano* **2013**, *7*, 6069.
[25] C. Bakkali-Hassani, E. Rieger, J. Vignolle, F. R. Wurm, S. Carlotti, D. Taton, *Chem. Commun.* **2016**, *52*, 9719.
[26] L. Reisman, C. P. Mbarushimana, S. J. Cassidy, P. A. Rupar, *ACS Macro Lett.* **2016**, *5*, 1137.
[27] X. E. Hu, *Tetrahedron* **2004**, *60*, 2701.
[28] H.-J. Jang, J. T. Lee, H. J. Yoon, *Polym. Chem.* **2015**, *6*, 3387.
[29] H. K. Moon, S. Kang, H. J. Yoon, *Polym. Chem.* **2017**, *8*, 2287.
[30] R. Barbey, H. A. Klok, *Langmuir* **2010**, *26*, 18219.
[31] A. Apicella, L. Nicolais, *Ind. Eng. Chem. Prod. Res. Dev.* **1984**, *23*, 288.
[32] M. Kobayashi, K. Uchino, T. Ishizone, *J. Polym. Sci., Part A: Polym. Chem.* **2005**, *43*, 4126.

Supporting Information

for *Macromol. Chem. Phys.*, DOI: 10.1002/macp.201700145

4-Styrenesulfonyl-(2-methyl)aziridine: The First Bivalent Aziridine-Monomer for Anionic and Radical Polymerization

Tassilo Gleede, Elisabeth Rieger, Tatjana Homann-Müller, and Frederik R. Wurm*

Supporting Information for *Macromol. Chem. Phys*, DOI: 10.1002/macp.201700145

4-Styrenesulfonyl-(2-methyl)aziridine the first bivalent aziridine-monomer for anionic and radical polymerization.

*Tassilo. Gleede, Elisabeth. Rieger, Tatjana. Homann-Müller, Frederik R. Wurm**

Max Planck Institute for Polymer Research (MPIP), Ackermannweg 10, 55128 Mainz, Germany. E-mail: wurm@mpip-mainz.mpg.de

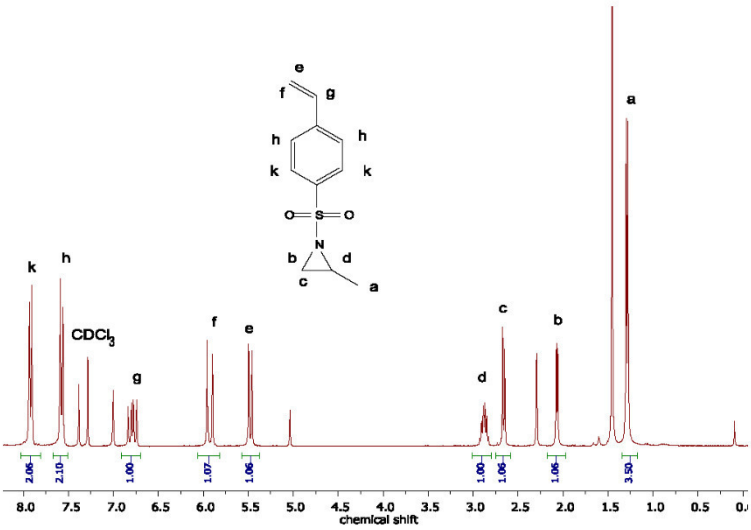

Fig. SI 1 ^{1}H NMR (300 MHz, 298 K, $CDCl_3$) of StMAz

^{1}H NMR (300 MHz, $CDCl_3$): δ [ppm] = 7.92 (d, 2H, k), 7.58 (d, 2H, h), 6.84-6.73 ppm (dd, 1H, g), 5.94 (d, 1H, f), 5.43 ppm (d, 1H, e), 2.95-2.78 (m, 1H, d), 2.66 (d, 1H, c), 2.07 (d, 1H, b), 1.29 (d, 3H, a).

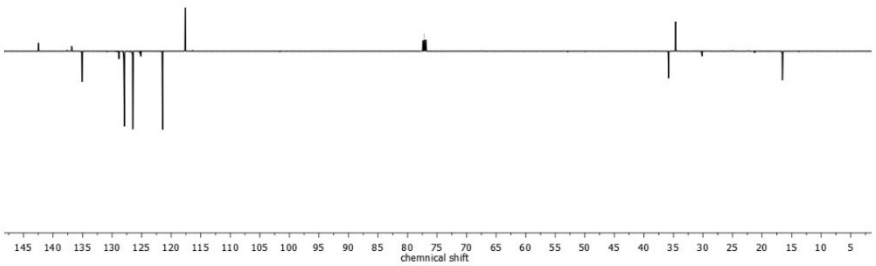

Fig. SI 2: ^{13}C NMR (101 MHz, $CDCl_3$) of StMAz

^{13}C NMR (101 MHz, 298 K, $CDCl_3$): δ [ppm] = 135.76, 128.14, 126.69, 117.79, 36.01, 34.85, 16.81.

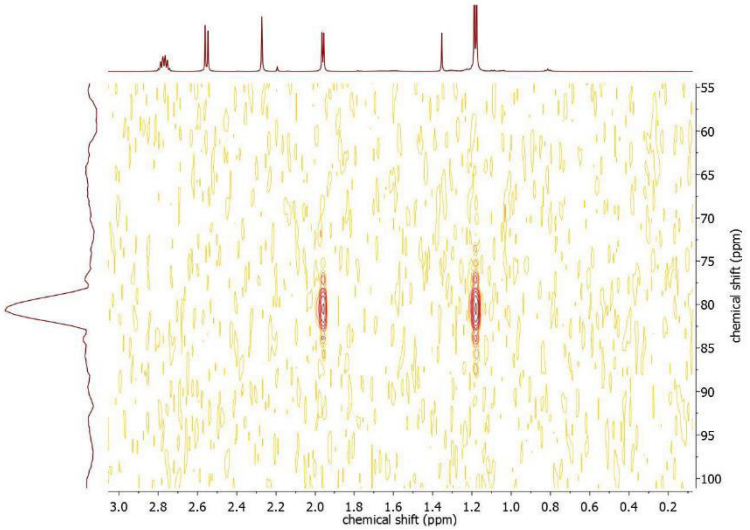

Fig. SI 3: $^{1}H\,^{15}N$-HMBC (71 MHz, 298 K, $CDCl_3$) of StMAz

$^{1}H\,^{15}N$ HMBC (71 MHz, 298 K, $CDCl_3$): δ [ppm] = 80.51.

3

Analytical Data / ^{1}H NMR Data of homo-polymers

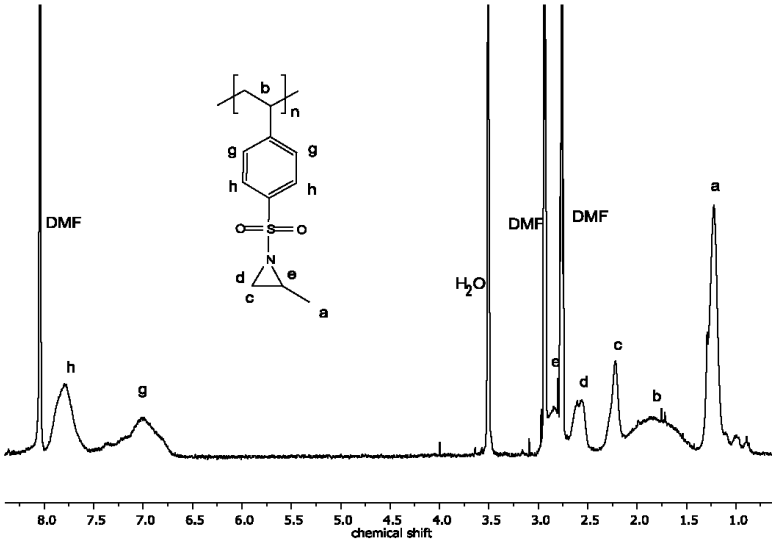

Fig. SI 4: H-NMR (300 MHz, $CDCl_3$) spectrum of P(StMAz). polymerized vinolog.

^{1}H NMR (300 MHz, $CDCl_3$): δ [ppm] = 8.00-7.5 (br, h), 7.50-6.65 (br, g), 3.02-2.72 (br, e), 2.69-2.43 (br, d), 2.38-2.13 (br, c), 2.11-1.41 (br, b), 1.40-1.04 (br, a).

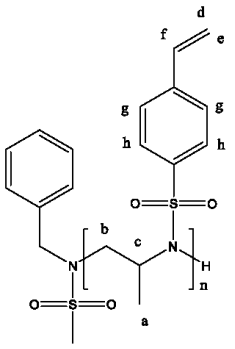

^{1}H NMR (300 MHz, $CDCl_3$): δ [ppm] = 8.16-7.70 (br, h), 7.70-7.35 (br, g), 6.90-6.52 (br, f), 6.00-5.68 (br, e), 5.50-5.24 (br, d), 4.61-3.67 (br, c), 3.67-2.96 (br, b), 1.42-0.55 (br, a). (For spectrum see Fig. SI 9)

4

NMR Data of copolymers with StMAz

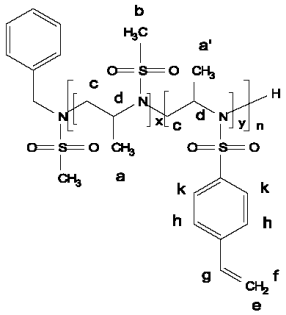

^{1}H NMR (300 MHz, $CDCl_3$): δ [ppm] = 8.13-7.71 (br, k), 7.71-7.34 (br, h), 6.89-6.62 (br, g), 6.03-5.71 (br, f), 5.55-5.28 (br, e), 4.53-3.69 (br, d), 3.69-3.09 (br, c), 3.09-2.62 (br, b), 1.55-0.67 (br, a, a‘).(For spectrum see Fig. SI 7)

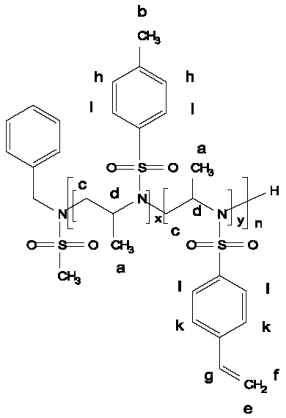

^{1}H NMR (300 MHz, $CDCl_3$): δ [ppm] = 8.17-7.66 (br, l), 7.66-7.39 (br, k), 7.39-7.17 (br, h), 6.87-6.57 (br, g), 5.98-5.71 (br, f), 5.54-5.28 (br, e), 4.62-3.84 ppm (br, d), 3.84-2.99 (br, c), 2.50-2.11 (br, b), 1.44-0.55 (br, a). (For spectrum see Fig. SI 8)

5

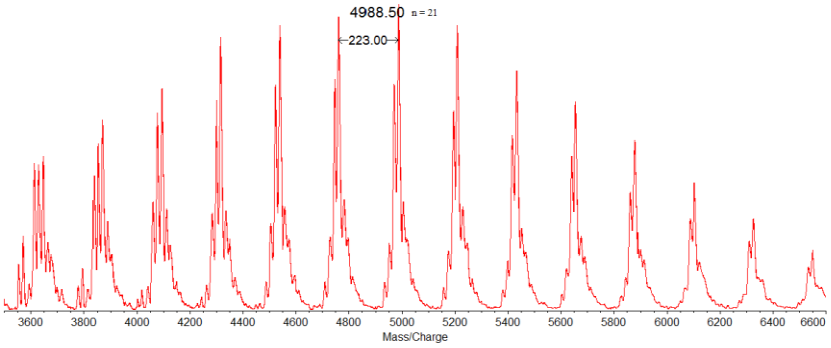

Fig. SI 5: MALDI-ToF MS von P(StMAz)$_{30}$

MALDI-TOF mass spectrometry proves the formation of the envisioned StMAz. The main distribution can be calculated to contain the mass of the initiator and the monomer mass with a distance of 223 g mol^{-1}, the molar mass of StMAz, up to a detectable molecular weight of ca. 7500 g mol^{-1}. The maximum of the distribution corresponds to the molecular weight of 21 repeating units, the initiator and potassium as a counter ion.

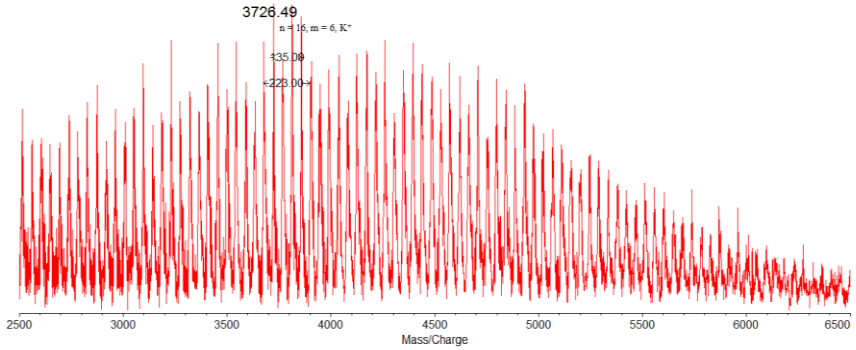

Fig. SI 6: Zoom into the MALDI ToF mass spectrum of P(MsMAz-co-StMAz).

Analytic of Polymers and thiol-ene functionalization

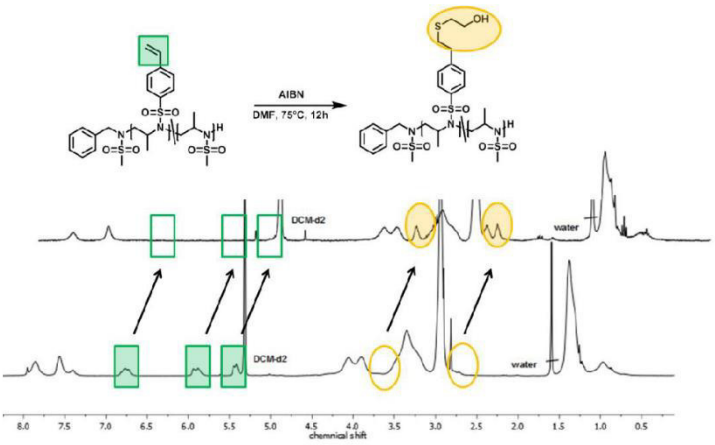

Fig. SI 7: ^{1}H NMR (DCM-d_2, 300 MHz, 298 K) spectra of P6 (unmodified) and P6-1 (after thiol-ene addition with 2-mercaptoethanol).

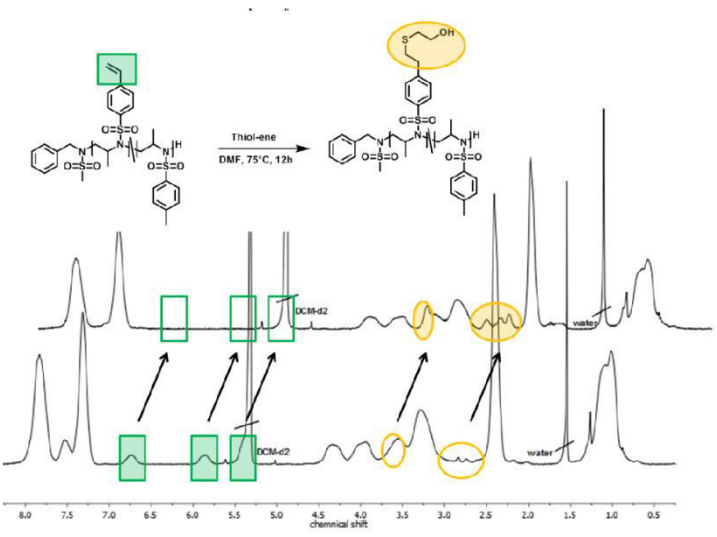

Fig. SI 8: ^{1}H NMR (DCM-d_2, 300 MHz, 298 K) spectra of P4 (unmodified) and P4-1 (after thiol-ene addition with 2-mercaptoethanol).

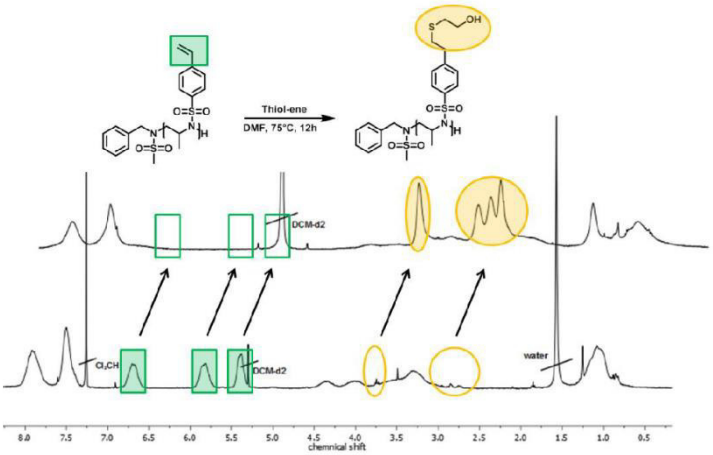

Fig. SI 9: ^{1}H NMR (DCM-d_2, 300 MHz, 298 K) spectra of P1 (unmodified) and P1-1 (after thiol-ene addition with 2-mercaptoethanol).

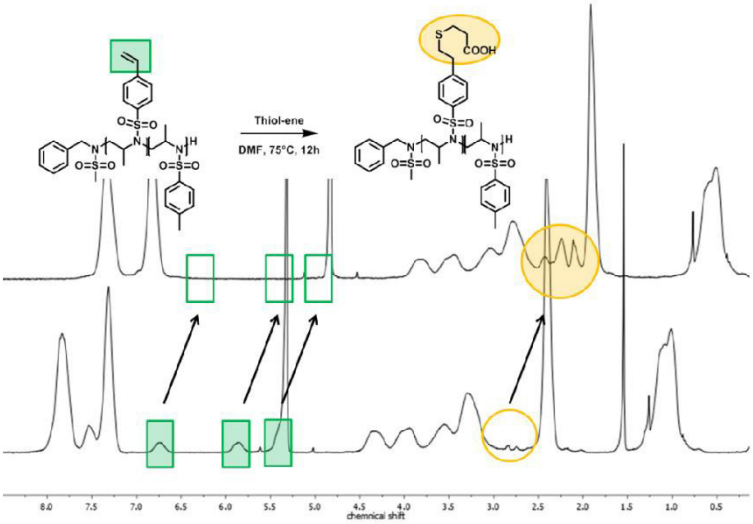

Fig. SI 10: ^{1}H NMR (DCM-d_2, 300 MHz, 298 K) spectra of P4 (unmodified) and P4-2 (after thiol-ene addition with 3-mercaptopropionic acid).

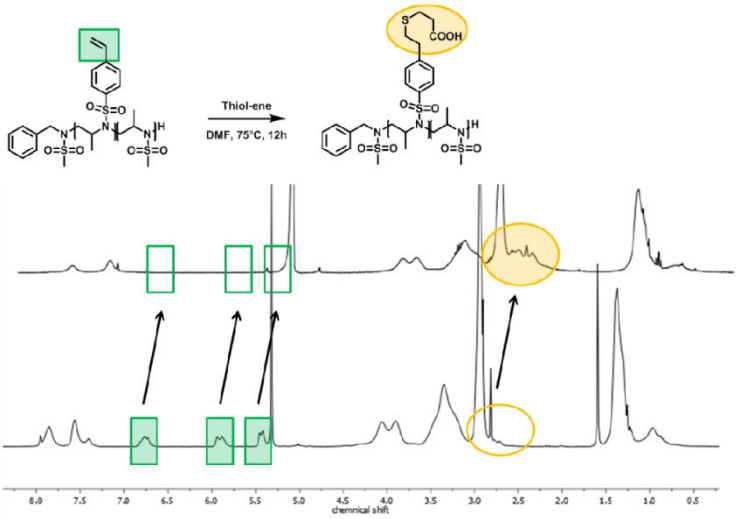

Fig. SI 11: ^{1}H NMR (DCM-d_2, 300 MHz, 298 K) spectra of P6 (unmodified) and P6-2 (after thiol-ene addition with 3-mercaptopropionic acid).

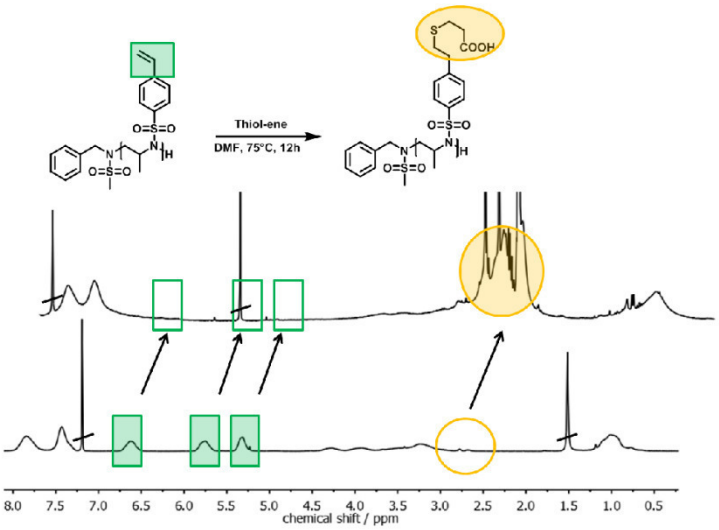

Fig. SI 12: ^{1}H NMR ($CDCl_3$ /DMSO-d_6, 300 MHz, 298 K) spectra of P1 (unmodified) and P1-2 (after thiol-ene addition with 3-mercaptopropionic acid).

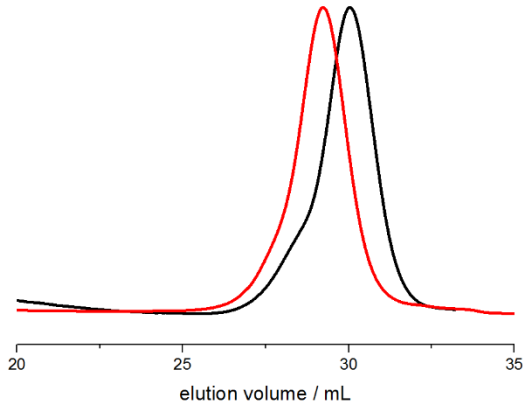

Fig. SI 13: SEC traces of P1 (black) and P1-1 (red) in DMF (RI signal)

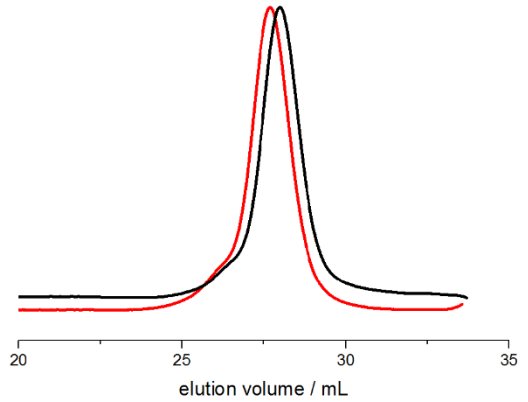

Fig. SI 14: SEC traces of P4 (black) and P4-1 (red) in DMF (RI signal)

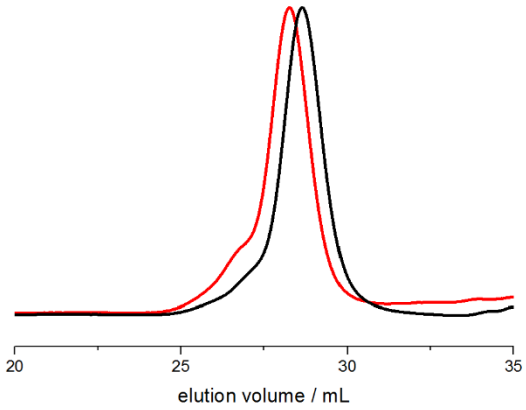

Fig. SI 15: SEC traces of P6 (black) and P6-1 (red) in DMF (RI signal)

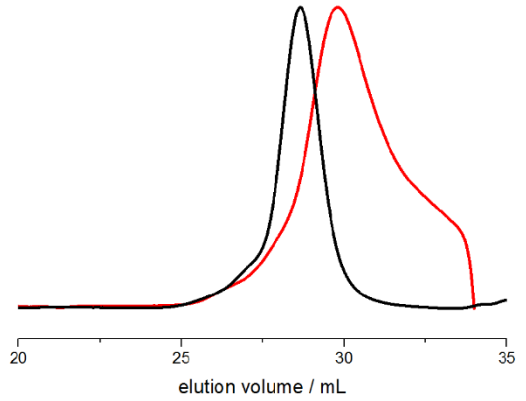

Fig. SI 16: SEC traces of P6 (black) and P6-2 (red) in DMF (RI signal)

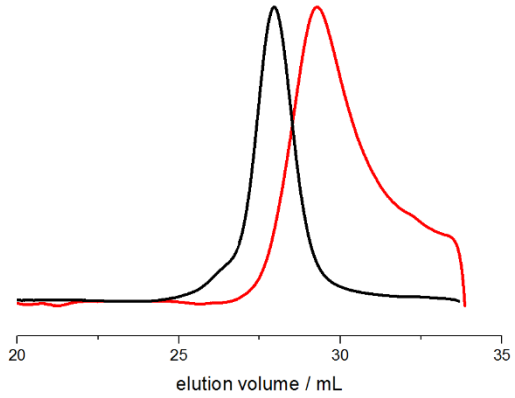

Fig. SI 17: SEC traces of P4 (black) and P4-2 (red) in DMF (RI signal)

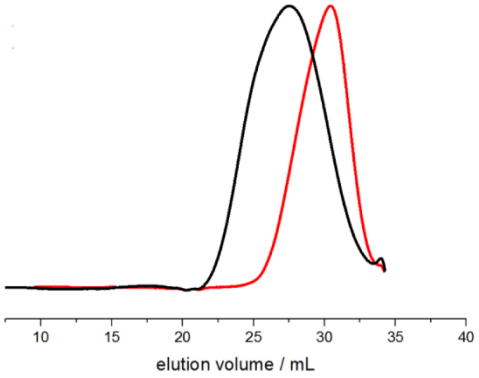

Fig. SI 18: SEC traces of P7 and P8 (free radical polymerization)

12

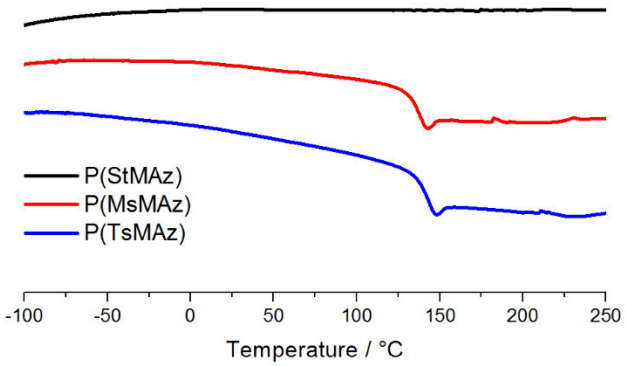

Fig. SI 19: DSC curves (second heating) of P(StMAz) (P2) and other homo poly(aziridine)s from MsMAz and TsMAz for comparison. P2: T_G=not observed, $P(MsMAz)_{50}$: T_G=140 °C, $P(MsMAz)_{50}$: T_G=142 °C

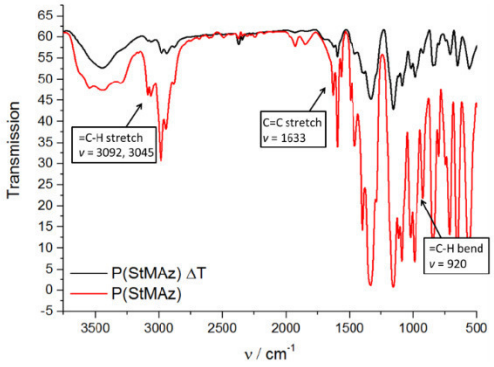

Fig. SI 20: IR Spectra of Poly(StMAz) (P1) (red) and P1 after heating to 250°C. Temperature program corresponded to DSC Measurement.

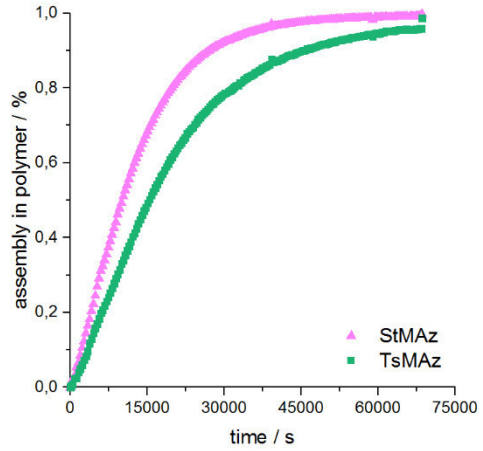

Fig. SI 21: Assembly of the monomer in the polymer versus reaction time.

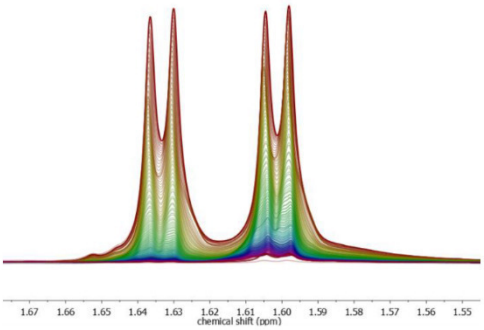

Fig. SI 22: Zoom-in of the relevant signals of the monomer ring-protons, showing the consumption of the monomer.

A.2 List of Publications

Journal Articles

- Controlling the Polymer Microstructure in Anionic Polymerization by Compartmentalization.
  Rieger, E.; Blankenburg, J.; Grune, E.; Wagner, M.; Landfester, K.; Wurm, F. R.
  Angewandte Chemie Int. Ed. **2018**, *57*, DOI:10.1002/anie.201710417

- Expanding the scope of *N*-heterolytic carbene-organocatalyzed ring-opening polymerization of *N*-tosyl aziridines using functional and non-activated amine initiators.
  Bakkali-Hassani, C.; Rieger, E.; Vignolle, J.; Wurm, F. R.; Carlotti, S.; Taton, D.
  European Polymer Journal **2017**, *95*, 746-755.

- 4-Styrenesulfonyl-(2-methyl)aziridine: The First Bivalent Aziridine-Monomer for Anionic and Radical Polymerization.
  Gleede, T.; Rieger, E.; Homann-Müller, T.; Wurm, F. R.
  Macromol. Chem. Phys. **2017**, 1700145.

- The living anionic polymerization of activated aziridines: a systematic study of reaction conditions and kinetics.
  Rieger, E.; Gleede, T.; Weber, K.; Manhart, A.; Wagner, M.; Wurm, F. R.
  Polym. Chem. **2017**, *8* (18), 2824-2832.

- *N*-Ferrocenylsulfonyl-2-methylaziridine: the first ferrocene monomer for the anionic (co)polymerization of aziridines.
  Homann-Müller, T.; Rieger, E.; Alkan, A.; Wurm, F. R.
  Polym. Chem. **2016**, *7*, 5501-5506.

- The organocatalytic ring-opening polymerization of *N*-tosyl-aziridine by an *N*-heterolytic carbene.
  Bakkali-Hassani, C.; Rieger, E.; Vignolle, J.; Wurm, F. R.; Carlotti, S.; Taton, D.
  Chem. Commun. **2016**, *52*, 9719-9722.

- Sequence-Controlled Polymers via Simultaneous Living Anionic Copolymerization of Competing Monomers.
  Rieger, E.; Alkan, A.; Manhart, A.; Wagner, M.; Wurm, F. R.
  Macromol. Rapid Commun. **2016**, *37*, 833-839.

- Multihydroxy Polyamines by Living Anionic Polymerization of Aziridines.
  Rieger, E.; Manhart, A.; Wurm, F. R.
  ACS Macro Lett. **2016**, *5* (2), 195-198.

Conference Contributions

- *Let's Get Things in Order: Sequence-Controlled Anionic Polymerization of Activated Aziridines*
  Rieger, E.; Gleede, T.; Manhart, A.; Thomi, L.; Wagner, M.; Wurm, F. R.
  253rd ACS National Meeting, San Francisco (CA), USA, April 2017 (**Oral**)
- *Let's Get Things in Order: Sequence-Controlled Anionic Polymerization of Activated Aziridines*
  Rieger, E.; Gleede, T.; Manhart, A.; Thomi, L.; Wagner, M.; Wurm, F. R.
  Makromolekulares Kolloquium, Freiburg, Februar 2017 (**Poster**)
- *New Insights in the Anionic Polymerization of Activated Aziridines*
  Rieger, E.; Manhart, A.; Alkan, A.; Wagner, M.; Wurm, F. R.
  Highlight Postersession, Max-Planck-Institut für Polymerforschung, Mainz, September 2015 (**Poster**)
- *New Insights in the Anionic Polymerization of Activated Aziridines*
  Rieger, E.; Manhart, A.; Alkan, A.; Wagner, M.; Wurm, F. R.
  11th International Symposium on Ionic Polymerization, Bordeaux, Frankreich. Juli 2015 (**Poster**)

A.3 Curriculum Vitae

Persönliches

Geburtsdatum: 22. Mai 1985

Geburtsort: Rosenheim

Nationalität: Deutsch

Berufserfahrung

12/2014 – 02/2018 **Promotion** zum Thema **„Anionic Polymerization of Activated Aziridines“** am **Max-Planck-Institut für Polymerforschung (Mainz)**
Arbeitskreis: Prof. Dr. Katharina Landfester
Projektgruppe: Dr. habil. Frederik R. Wurm

- Etablierung als neuartige Monomerklasse für anionische Polymerisation
- Erfolgreiche Herstellung und Charakterisierung sequenz-kontrollierter (Co)Polymere
- Entwicklung von NMR-Kinetiken als Hauptanalysemethode
- Konferenzvorträge und Publikationen in Fachzeitschriften
- Einarbeitung und Betreuung von Bachelor-Studenten und Laboranten
- Betreuung des Praktikums „Physikalische Chemie für Pharmazeuten"

08/2012 – 12/2012 **Studentische Hilfskraft** am **Max-Planck-Institut für Polymerforschung**
Arbeitskreis: Prof. Dr. Klaus Müllen

- Organische Synthese von Polyphenylen Dendrimeren
- Herstellung und Aufreinigung verschiedener Vorstufen und Endprodukten

Akademische und schulische Ausbildung

10/2007 – 09/2014 **Johannes Gutenberg-Universität Mainz**
Diplom in Biomedizinischer Chemie (Abschluss: 1,6)

- Schwerpunkte: Organische Chemie, Biochemie, Radiopharmazeutische Chemie und Makromolekulare Chemie

Diplomarbeit zum Thema **„Sequence-controlled Anionic Polymerization of Aziridines“** an der **Johannes Gutenberg-Universität Mainz** und am **Max-Planck-Institut für Polymerforschung**

- Erfolgreiche Herstellung und Charakterisierung neuartiger Monomere und (Co)Polymere

06/2011 – 12/2011 **Brookhaven National Laboratory, Long Island, USA**
Summer School und Forschungssemester in Radiopharmazeutischer Chemie (DAAD-gefördert)

- Erforschung einer externen Hormonbehandlung an Maispflanzen mittels [^{11}C]Isotopenmarkierung und radiochemischer Analyse
- Radiosynthese von [^{11}C]Methylsalicylat

10/2004 – 09/2005 **Universität Regensburg**
Magisterstudium in Archäologie, Geschichte und Vergleichende Kulturwissenschaften (2 Semester)

09/1995 – 06/2004 **Abitur** am **Ignaz-Günther-Gymnasium Rosenheim**

Besondere Qualifikationen und Interessen

Soft Skill Kurse	Scientific Writing; Projektmanagement; Presenting in English; Gekonnt präsentieren; Intercultural Communications; Kommunikation, Überzeugungskompetenz, Mikropolitik; organisiert vom Allgemeinen Promotionskolleg der Johannes Gutenberg-Universität Mainz
Sprachen	Deutsch (Muttersprache), Englisch (verhandlungssicher), Italienisch, Spanisch (Grundkenntnisse), Graecum, Latinum
PC-Kenntnisse	MS-Office (sehr gut), ChemBioDraw 14.0 (sehr gut), Origin 9.1 (gut), MestReNova 10.0.2 (sehr gut), TopSpin 3.0 (gut), Blender 2.76 (Grundkenntnisse)
Analytische Methoden	Magnetische Kernresonanzspektroskopie (NMR), Gel-Permeations-Chromatographie (GPC), Hochleistungsflüssigkeitschromatographie (HPLC), Dynamische Differenz-kalorimetrie (DSC), Thermogravimetrische Analyse (TGA), Massenspektrometrie (MS), Infrarot-, UV/VIS-Spektroskopie, Dynamische Lichtstreuung (DLS).
Studentische Nebenjobs	2005 - 2012: Diverse Tätigkeiten als Promoterin (u. a. als Hostess und im Verkauf) 2005 – 2007: Dialog Direct: Fundraising für Amnesty International und Save the Children, unter anderem als Teamleiterin 12/2005 – 02/2006: Pflegepraktikum im Klinikum Vogtareuth
Sonstiges	2001 - 2004: Jugendbetreuung im Rahmen einer christlichen Einrichtung 2016: Musikvideoproduktion „Lady Nano – Bad project“ und Live-Auftritt im Rahmen der wissenschaftlichen Weihnachtsshow des Max-Planck-Instituts für Polymerforschung https://www.youtube.com/watch?v=gPjAScbXi8c
Hobbys und Interessen	Meine freizeit-sportlichen Aktivitäten liegen im Bereich Laufen (u. a. für Halbmarathons), Bergwandern und Skifahren. Meine große Leidenschaft gehört der Musik unterschiedlichster Stilrichtungen, ich spiele selbst Klavier und Klarinette und singe gerne in verschiedenen Chören. Ich lese, reise und photographiere gerne, um andere Kulturen, ihre Menschen und Geschichten, zu entdecken.